



THERMEC'2025

**International Conference on
PROCESSING & MANUFACTURING OF
ADVANCED MATERIALS**

Processing, Properties, Fabrication and Applications



**June 30-July 4, 2025
Tours, France**

ABSTRACT BOOK

Contents

1.	Microstructural and mechanical characterisation of additively manufactured S235 and 430L steel components by cold spraying.....	27
2.	Co-sintering of LTCC-gold system: Coupled experimental, analytical and numerical approaches	28
3.	Towards new high-strength and heat-resistant Al alloy design enabled by additive manufacturing.....	29
6.	Tribological Properties of STS316L Sintered Body and Cu/STS316L Composite Using Binder Jetting Process	32
7.	Towards the defect-tolerant design of laser powder bed-fused metal parts: example of Ti64 alloy	32
8.	Effect of additive manufacturing-induced metastable retained austenite and austenite reversion on the mechanical properties of Corrax® stainless steel.....	33
9.	Improving High-Temperature Performance of Inconel 718 Using Ceramic Particle-Coated Superalloy Powders in Laser Additive Manufacturing	34
10.	Minimum ductility at intermediate temperatures of Al-Fe-Cr-X alloys processed by L-PBF ..	35
11.	Influence of a modulated laser irradiation on the LPBF process stability, induced microstructures and mechanical properties of Al10SiMg alloy	36
12.	Elastic properties of laser powder bed fusion processed β -phase Ti alloys	37
13.	Microstructure control of TiAl alloys using peculiar thermal history of additive manufacturing	38
14.	Design of high entropy alloy with suppressed elemental segregation for laser powder bed fusion process	39
15.	Effect of Surface Conditions on Mechanical Properties of IN718 and IN625 Manufactured by Additive/Subtractive Laser Powder Bed Fusion Technology	40
16.	Electron Microscopy Studies on Orientation-Controlled 316L Austenitic Stainless Steel Produced by Laser Powder Bed Fusion.....	41
17.	Substrate tubing heater suitable for large volume 3D printing with extrusion of thermo-reversible hydrogel	42
18.	Development of Material-Based Process Simulation Technology for BAAM and Composite AM.....	43
19.	Graphitic carbon nitride (g-C ₃ N ₄) as a Filler in the Photocuring 3D Printing Process for Enhanced Mechanical Properties	44
20.	A Novel Strategy for the Control of Crystallographic Texture of Metals with Non-Cubic Crystal System via Powder Bed Fusion using a Laser-Beam of Metals	45
21.	Additive Manufacturing of Cell-Based 3D Bone-Mimetic Collagen/Apatite Structures.....	46
22.	Effect of building conditions on high-temperature tensile properties of IN738LC fabricated by laser powder bed fusion.....	47
23.	Growth of Antiphase Domain in Laser-Irradiated Region and Superelasticity of Single-Crystal-Like Fe ₃ Al Fabricated by Laser Powder Bed Fusion Process	48
24.	Innovative design of crystallographic textures and macroscopic shapes via metal additive manufacturing.....	49

25.	Microstructures and Hardness of WC-Co and WC-HEA Cemented Carbides Additively Manufactured by the Multi-Beam Laser Directed Energy Deposition.....	50
26.	Development of an environmentally friendly and low-cost binder for 17-4PH metal part printing via Fused Deposition Modeling	51
27.	3D Volume Construction Methodology for Cold Spray Additive Manufacturing.....	52
28.	Effect of heat treatment on the microstructure and impact toughness of PBF-LB manufactured 17-4 PH stainless steel.....	53
29.	Generating a Digital Twin of the Laser Powder Bed Fusion Process	54
30.	Low Cycle Fatigue Response of Additive Manufactured Advanced Structural Alloys: Insights into high performance alloy fatigue life	55
31.	Microstructure, Mechanical and Thermal Conductivity Properties of Pure Copper Fabricated by Metal Material Extrusion Additive Manufacturing Process	56
32.	A Study on Monitoring of Large-Scale Composite Material Additive Manufacturing Processes Using Sensor Fusion.....	57
33.	Characterization and Effects of Anodized Aluminum Oxide Film on Additively Manufactured AlSi10Mg Alloy	58
34.	Advanced Laser Scanning Strategies for Minimizing Thermal Residual Stress in Additively Manufactured Topologically Optimized Automotive Parts	59
35.	Advancing Energy Absorption Through Hybrid Lattice Structures Fabricated via Powder Bed Fusion.....	60
36.	Influence of increasing chromium content on additively manufactured tool steels: microstructural and mechanical evolution before and after heat treatment.....	61
37.	Enhancing fatigue performance of additively manufactured H13 tool steel through surface finishing processes.....	62
38.	Development and optimization of metastable beta titanium-based alloys by laser powder bed fusion for biomedical applications	63
39.	Optimizing thermal cycles in Wire-Arc Additive Manufacturing: Investigating inter-pass time and the use of an external cooling system	64
40.	Combinatorial design of lightweight steels using multi-nozzle direct energy deposition (DED)	65
41.	Influence of hierarchical structure on mechanical properties of additive manufactured IN718 alloys	66
42.	Nano-scaled solidification microstructure characteristics in additively manufactured 316L stainless steel	67
43.	NiTi shape memory alloy by laser powder bed fusion : how manufacturing parameters influence the nature of the alloy and its mechanical properties.....	68
44.	Effect of Scanning Rotation Angle on the Properties of IN939 Fabricated by Laser Powder Bed Fusion.....	69
45.	Unique hierarchical structural features introduced by laser powder bed fusion and their contribution to mechanical function in IN718.....	70
46.	Additive Manufacturing and Post-Processing to Produce Microstructure Electrodes and Application Potentials	71

47.	Characteristics of Solidification by Super-Thermal Field in Powder Bed Fusion: Comparison with Conventional Rapid Solidification Processes.....	72
48.	Effect of Build Orientation on Crystallographic Texture and Fatigue Performance of Selective Laser Melted Ti-6Al-4V ELI Parts.....	73
49.	In-Situ Synthesis and Ex-Situ Addition Reinforced 3D Printing Aluminum Matrix Composites	74
50.	Microstructural Control of Unstable Beta-Type Titanium Alloy through Powder Bed Fusion using a Laser-Beam of Metals	75
51.	Spinodal Decomposition and Magnetic Properties of Single-Crystal-Like Fe-Cr-Co Alloy Fabricated by Laser-Powder Bed Fusion Type Additive Manufacturing.....	76
52.	Applications of CALPHAD-based tools for welding and additive manufacturing	77
53.	Multi-phase Flow System Study for Mixed N ₂ +CO ₂ Gas Separation and Pipeline Transport	78
54.	Electropolishing of NiTi cardiovascular stents produced via laser powder bed fusion technique	79
55.	La compensation des erreurs geometriques lors de la phase de conception.....	80
56.	LPBF processing of a metastable Ti-42Nb alloy for bone implant applications.....	81
57.	Evaluation of Porosity and Hardness in Aerospace-Grade Aluminium Alloys Processed by Friction Surfacing.....	82
58.	Novel cellular structure with phase-separation induced dislocation-network in Ti-Zr-Nb-Ta-Zr high entropy alloy fabricated by laser powder bed fusion.....	83
59.	Simulation based estimation of local heat build up during Laser Powder Bed Fusion processing	84
60.	Effect of chemical surface post-processing on the surface roughness of Niti fabricated by laser powder bed fusion	85
61.	Microstructure engineering of ultra-high strength martensitic steel produced by advanced manufacturing processes	86
62.	Effect of microstructural heterogeneity on slip localization in L-PBF processed AlFeCrX alloys	87
63.	Overview of advanced materials for the FCC-ee vacuum system.....	88
64.	Microstructural Evolution and Performance of LPBF Ti-6Al-4V Lattice Structures upon Hot Isostatic Pressing	89
65.	A layer-by-layer FEM curing model for binder jetting of 316L	90
66.	Additive manufacturing of recycled Ti-6Al-4V powder by Fused Granular Fabrication (FGF)	91
67.	Towards controlling 4D printing for developing innovative architected microstructures	92
68.	Gelation, Vitrification and Shrinkage of Thermoset Polymers Methods for Investigation and Modelling	93
69.	In vitro response of bioabsorbable zinc-based composites for implantology.....	94
70.	Widening the scope for non-noble metal initiation of electroless copper deposition.....	95
71.	Elastomer patterning and stacking process for stretchable multilayer electronic circuit based on laser-induced photo-thermal effect.....	96
72.	Biodegradable zinc matrix composites for bone implant materials.....	97

73.	Breakthrough of strength and ductility trade-off in biodegradable Mg alloys by drawing at elevated temperatures for bone implants	98
74.	Effect of Surface Modifications on the Biological Response of Additively Manufactured Metallic Implants.....	99
75.	Functional Coatings by Low Vacuum Plasma for the Innovation in Regenerative and Reparative Medicine.....	100
76.	Bioresorbable ultrafine-grained Zn stabilized with nanometric ZnO dispersoids	101
77.	Influence of Si and process parameters on the microstructure and properties of continuously annealed low C-Nb-Ti strip steel.....	102
78.	Microstructure development of a Zn-based biodegradable alloy during laser shock peening	103
79.	Coated biodegradable Zn-0.8Mg-0.2Sr alloy	104
80.	Design and Mechanical Evaluation of Ti-6Al-4V Lattice Structures for Biomedical Implants	105
81.	Surface Modification of Zn-0.8Mg-0.2Sr: Insights into Nitrogen Ion Implantation and Microstructural Evolution	106
82.	Enhanced Polyp Adhesion on Chemically Modified Titanium Nonwoven Fabric	107
83.	Hot deformation behaviour and microstructure evolution of degradable Zn-0.8Mn alloy.....	108
84.	High plasticity Zn-Mn alloy and effects of further alloying.....	109
85.	Deposition of nanoparticles in lattice structures: example of antibacterial ZnO nanowires ...	110
86.	Nanotopographical Surface Engineering and Corrosion Resistance Enhancement of Ti-based Bulk Metallic Glass through Alkaline Chemical Treatment	111
87.	Investigation of Microstructure Evolution and Cytocompatibilities of ODS Modified Ti64 Alloy: A Comparative Study of Y-Zr-O and Y-Hf-O Oxides.....	112
88.	Experimental and computational investigation on the anisotropy of BCC and HCP metals by distortional evolution of yield surfaces	113
89.	Impact of Rare Gas Addition on Fabrication of a-C:H Films via C ₂ H ₂ /Ar/Ne/He Plasma-Enhanced Chemical Vapor Deposition.....	114
90.	Masking Effect of Phosphate Pretreatment on Surface Defects of Auto Steel Sheets	115
91.	A robust solid-liquid composite superlubricity strategy toward high temperatures.....	116
92.	Revealing fretting wear resistance mechanism under liquid lead-bismuth eutectic of Cr-Al-C composite coatings fabricated by laser cladding	116
93.	What can be gained and what is lost from the perspective of properties, when modifying the structural design of thin films.....	117
94.	Electrical properties of large area perovskite type oxide epitaxial thin films transferred onto polymer sheets.....	118
95.	Modification of Microstructures and Cyclic Oxidation Behavior of Electron Beam Physical Vapor Deposition Processed Thermal Barrier Coatings.....	119
96.	Compositionally Complex Refractory Metal Nitride Coatings: The Effects of V, Nb and Ta On Their Structure and Mechanical Properties	120
97.	New Physics Informed Machine Learning Prediction of SiO ₂ Film Property from Optical Emission Spectroscopy in TEOS /O ₂ /Ar Plasma Enhanced CVD.....	121

98.	Laser surface hardening of AISI 431 martensitic stainless steel by using different laser sources 122	
99.	Long-Term Corrosion Resistant Thin Films Prepared by Plasma Enhanced Chemical Vapor Deposition	123
100.	Development of an intumescent inorganic coating on steel substrates	124
101.	Optimized Potential Distribution Enhancing Corrosion Resistance of C/Metal Coated Bipolar Plates Used in Proton Exchange Membrane Fuel Cells	125
102.	Effect of Cr content on oxidation layer of hot-dip galvanized high-strength steel: molecular dynamics simulation	126
103.	Unravelling precipitation kinetics in nanosteels using Small Angle Neutron Scattering	127
104.	Relation between low elastic limit and mobile dislocation density in as-quenched martensitic steel	128
105.	Carbides in Ferritic Steels : Defects and Atomic Diffusion from Ab-Initio Based Studies ...	129
106.	Heterogeneous deformation behavior of pre-strained 18%Ni martensitic steel	130
107.	Impact of Non-Metallic Inclusions and Grain Structures Modified by Fast Heating Annealing on Tensile Properties and Fracture Modes in a V-microalloyed High-Mn TWIP Steel	131
108.	Effect of Annealing Process on Microstructures and Mechanical Properties of Cold-Rolled Martensitic Steels for Automotive Structural Parts	132
109.	Revealing the Mechanisms of Austenitisation in Low-Alloy Steels Using In-situ EBSD	133
110.	Effect of intercritical annealing temperature and holding time to mechanical performance of hot-rolled medium manganese steel	134
111.	Solution nitriding of 304 stainless steel for hydrogen embrittlement resistance	135
112.	Nanoprecipitates-strengthened ultrastrong stainless steel with excellent work hardening	136
113.	Uncovering the interplay between thermo-mechanical processing parameters and microstructure of V, Cr-microalloyed steels	137
114.	Investigation of metal embrittlement in galvanized quenching and partitioning steels	138
115.	Inverse steel design	139
116.	Three-dimensional analysis of microstructure formation in the initial stage during martensitic transformation in low-carbon steel	140
117.	Mechanism of pearlite colony formation via various orientation relationships between ferrite and cementite	141
118.	Austenite Plasticity and Martensite Microstructures	142
119.	Evaluating LME susceptibility in third-generation AHSS: The role of testing methodologies and silicon concentration	143
120.	Modeling the effect of prior martensite on the kinetics of bainite formation	144
121.	Effect of nitrogen in yielding behavior of austenitic stainless steels	145
122.	Thermal stabilization by prior deformation in metastable austenitic steel undergoing gamma → epsilon → alpha' transformation	146
123.	Enhancing Cryogenic Strength of Austenitic Stainless Steels Through Thermo-Mechanical Controlled Processing and Nitrogen Alloying	147
124.	Evaluation of dislocation morphology in nitrogen-bearing austenitic stainless steel	148

125.	Microstructure and impact wear behavior of a V-Ti microalloyed carbide-containing high manganese steel.....	149
126.	Effect of Cold-Forming on Mechanical Properties of AHSS Steel.....	150
127.	Influence of Mo and N Additions on the Precipitation and Tensile Properties Behaviors in Austenitic Stainless Steel during Aging	151
128.	Effect of EAF impurities on microstructure and mechanical properties of low-carbon steels	152
129.	Enhancing the hydrogen embrittlement resistance in warm-rolled medium-Mn steels through nano-sandwich microstructure.....	153
130.	Thermomechanical rolling of thick Nb-Ti-V-Ni high strength structural steel plate	154
131.	Hydrogen-related effects in austenitic steels: Contribution to deformation behavior and hydrogen embrittlement resistance.....	155
132.	Multi-scale and multi-modal microstructure imaging for in-situ studying creep damage and healing in ferritic steels at ID11/ESRF	156
133.	Evolution of the microstructure and properties of a steel subjected to a Q&P treatment including a galvanizing step	157
134.	Discovery of nano-scaled promising strengthening factor in 316L stainless steel fabricated by laser powder bed fusion.....	158
135.	Analysis of white strip defects in the galvanized coating surface of hot -dip galvanized DP steel.....	159
136.	Assessing the Origins of Autogeneous Recrystallisation During the Austenitisation of Low-Alloy Steels: Comparing In-Situ EBSD and In-Situ Synchrotron XRD	160
137.	On the static recrystallization characteristics and kinetics of austenitic stainless steels under development for LH2 storage applications.....	161
138.	Formation mechanism of detrimental grain boundary kappa-carbide during age hardening of austenitic high manganese lightweight steel	162
139.	Effect of Mn concentration in Cementite on austenitization behavior of Fe-C-Mn Alloy	163
140.	Exploring Carbon Partitioning, Carbide Precipitation, and Bainite Formation During Q&P Processing in Medium-Carbon Steel Using In-Situ Synchrotron XRD	164
141.	On the Chemical Boundary Engineering of Hot-Rolled Medium Mn Steel	165
142.	Thermomechanical processing of 0.17C-4Mn-0.8Al-0.5Si QP-treated steels based on deformation-continuous-cooling-transformation diagrams	166
143.	Towards a comprehensive understanding of the effect of continuous annealing process conditions on the microstructure development of cold-rolled dual-phase (DP) steels and their correlations with mechanical and magnetic properties.....	167
144.	Influence of intermittent friction cycles on tribocorrosion behavior of 316L stainless steel in 5% NaHCO ₃	168
145.	A Novel Approach to Predict Martensitic Transformations in High-carbon Bearing Steels ..	169
146.	Influence of the phase state variations on the impact toughness of lean alloyed 19-22 wt% Cr ferritic-austenitic stainless steels	170
147.	Recent Development of Hot-rolled 780 and 980MPa AHSS for Automotive Lightweight Chassis.....	171
148.	Constructing high-density dislocations by primary (Nb,Ti)(C,N) to induce massive secondary precipitations in austenitic heat-resistant cast steel	172

149.	Detecting iron in vanadium carbide nanoprecipitates by atomic-resolution scanning transmission electron microscopy techniques	173
150.	Evolution of inclusions in physically simulated heat-affected zones of a weld metal used with a 500 MPa offshore steel.....	174
151.	Special Steels for the Hydrogen Society	175
152.	Thermodynamic and Algorithmic Optimization of Medium Manganese Steel Composition Design, Non-Metallic Inclusion Analysis, and Microstructural Insights	176
153.	High temperature crystal structure of beta-uranium from neutron diffraction.....	177
154.	On the conditions of pearlitic cementite nucleation at a migrating austenite-ferrite interface	178
155.	Impact of Aluminium in comparison to Silicon on Liquid Metal Embrittlement of 3rd Generation AHSS	179
156.	Effect of heat treatment and rolling process on microstructure and deformation behavior in Al-Si alloy.....	180
157.	Evolution of Microstructure and Mechanical Properties in Cold-Rolled 7050 Aluminum Alloy During Annealing	181
158.	The relationship between precipitates and mechanical properties in Al-Zn-Mg alloy with high and low Zn/Mg	182
159.	Effect of Er on the stability of precipitates in AlCuMgSiSc alloys after different homogenization treatment	183
160.	On the order-disorder transformation within a main hardening precipitate in Al-Mg-Si alloys	184
161.	Modeling precipitation evolution and intermetallics fragmentation in 6xxx Series Aluminum Alloys during industrial hot rolling.....	185
162.	Five-fold symmetry structure inhibiting the growth of an otherwise perfect η_2 phase in Al-Zn-Mg-Cu alloys	186
163.	Effect of microalloying on precipitation strengthening and mechanical properties of Al-Mg-Si alloys	187
164.	Evaluation of slip behavior of mobile dislocations during in-situ tensile-testing TEM observation of Al-Mg-Si alloys	187
165.	Ultrasonic Bonding Process of Al	188
166.	Mechanical properties of aluminum clad sheets fabricated by roll bonding process for automotive application	189
167.	Impact of Microstructure of Aluminum Electrodes on the Performance of Aluminum-Based Batteries.....	190
168.	In-situ nanometallurgy in transmission electron microscopy.....	191
169.	Interfacial Structure of Mg_2Si in Al-Mg-Si Alloy	192
170.	The influence of continuous retrogression and re-ageing treatment on the mechanical properties, corrosion behaviour and microstructure of an Al-Zn-Mg-Cu alloy	193
171.	Linking 3D grain and elastic strain mapping with the development of damage in 2050 Al alloys during high-temperature loading by synchrotron diffraction and tomography	194
172.	The effect of intensification pressure on the microstructure of non-heat treated HPDC AlSi9MnVZr alloy.....	195

173.	Investigation on friction surfacing layers of AA2024 studs produced via friction extrusion..	196
174.	Design of easier separable Fe-containing intermetallics in Al-Si alloy by thermodynamic properties prediction and three dimensional morphology regulation	197
175.	Study on grain refinement of high-purity aluminium by intermittent permanent magnet stirring technique	198
176.	Synthesis and characterization of an (Al-10Si-3Zn-2Cu)/Ti-6Al-4V interpenetrating phase composite with enhanced mechanical properties	199
177.	The combined effects of trace element Sn/Cu and double-step pre-aging on the precipitation kinetics of Al-Mg-Si alloys	200
178.	Insights for the design of high-performance secondary cast aluminium alloys.	201
179.	Competitive Nucleation of α -Al(MnFeCr)Si Dispersoids in Al-Mg-Si 6xxx Alloys By Adding Indium	202
180.	An assessment of the brazing performance of cast Al-Mn-Ni aluminum alloy	203
181.	A Novel Modelling Framework for the Portevin-Le Chatelier Effect in AA5182 Alloy.....	204
182.	CALPHAD-based modelling of microstructural evolution during D.C. casting and homogenization of AA3003 aluminium alloy	205
183.	Formation mechanism of dense and uniform structure during tailor welding of Aluminum Foam Structure preform	206
184.	Simulation of self-healing in Al-Cu alloys.....	207
185.	Thermomechanical Testing and Precipitation Modelling of Al-Mg-Si Alloys for Hot Forming Applications.....	208
186.	A novel model for of cluster nucleation during quenching of 6xxx Al alloys	209
187.	Application of Artificial Neural Networks for Microstructure Models ALFLOW and ALSOFT 210	
188.	Precipitation Kinetics of Aluminum Alloys During SPD Processes Investigated by SAXS/WAXS.....	211
189.	Structure and dissolution behavior of ZnO-containing phosphate invert glasses prepared by liquid phase method.....	212
190.	Structure of Ta2O5 containing phosphate invert glasses prepared by liquid phase method ...	213
191.	Fabrication of Co-Cr-W-Ni alloys with a unique heterogeneous microstructure utilizing carbide precipitation.....	214
192.	Hybrid organic/inorganic materials for drug release systems as new generation of biomaterials: a molecular dynamics study	215
193.	Pulsed anodization process to form a biocompatible layer on superelastic NiTi alloy surface	216
194.	Biodegradable zinc alloys with potent osteogenicity, antibacterial ability, and antitumor efficacy for bone-implant applications	217
195.	Electrochemical Bio-Interface Devices for Advanced Medical Applications via Ion Transport	218
196.	Synthesis of Inorganic Semiconductor Films with Narrow Bandgap Responsive to Visible LEDs and Their Photo-Response	219
197.	Enhancing Non-Viral Gene Delivery: Strategies for Improved Efficiency and Performance.	220

198.	Novel prospective in design of Mg alloys for implantology: in vitro and in vivo assessment of degradation of Mg-Zn-Ca-Y-Mn alloys	221
199.	Development of a realistic brain phantom for medical training: an ethical and technical alternative to animal testing.....	222
200.	Enhancing wear resistance and biological performance of the biomedical Ti-6Al-4V alloy through PEO Treatment in TMO-rich electrolyte	223
201.	A novel low-cost multicomponent biocompatible alloy for potential application as bone fixation devices.....	224
202.	Control of Bone Microstructure Formation: Role of Soluble Proteins Secreted by Osteocytes	225
203.	New aspects of production Mg-Zn-Ca alloys via Laser Powder Bed Fusion.....	226
204.	Contact-free Micro- and Nano-Deformation in inorganic and organic systems via Electronic Speckle Pattern Interferometry	227
205.	Desalination Membrane Strategy Using Ion-Exchange Membranes for Marine Farms.....	228
206.	Waterproof Polyelectrolyte for Implantable Medical Devices	229
207.	Identification and Optimization of Geometric Features Significant for Nozzle Design in Cold Spray Additive Manufacturing using CFD and Artificial Neural Networks	230
208.	Enhancing the thermal cycling lifetime of YSZ thermal barrier coatings with air plasma sprayed NiCrAlY bond coat	231
209.	Copper-nickel alloy coating on cast iron by cold spray: microstructure and thermal analysis	232
210.	Sustainability Efforts in Cold Spray Processing.....	233
211.	Application of the Thermal Spraying technology in Hot-dip galvanizing line zinc pot roll ...	234
212.	Effect of the interface between coarse and fine grains on strength-ductility balance in dispersion-strengthened bimodal Al-Y ₂ O ₃ nanocomposite fabricated via powder metallurgical route.....	235
213.	Design, fabrication, and understanding the heat transfer behaviors of the high-thermal conductive copper-matrix composite materials.....	236
214.	Global Reactive Synthesis and Additive Manufacturing: in-situ synthesis of near net-shape Aluminium Matrix Composites.....	237
215.	Synthesis of zirconium carbide and zirconium diboride particles and fibers as building blocks for ultra-high Temperature ceramic matrix composites	238
216.	Nanoscale engineering of low-misfit TiB ₂ /Al ₃ (Sc,Zr)/ α -Al multi-interface to improve strength-ductility synergy for direct energy deposited aluminum alloy	239
217.	Development of high-performance laser devices using room-temperature bonding.....	240
218.	Sintering process analysis of aluminum matrix composites using machine learning.....	241
219.	Microstructural characterization and analysis of the mechanical properties of composite materials based on epoxy resin and glass fiber for their application in blades manufacturing	242
220.	Fabrication, architecture design, and characterization of a new Al/graphite flakes-carbon fibre composite used for thermal management	243
221.	Femtosecond laser polishing of pure copper and copper/diamond composites surfaces.....	244
222.	Effect of Al ₂ O ₃ Particle Size of Al ₂ O ₃ /Al Composites Fabricated by ARB Process on Microstructure and Mechanical Properties.....	245

223.	Microstructural and Morphological Evolution of Novel In-Situ Al-15%Mg ₂ Si-4.5%Si Composite with Strontium Addition	246
224.	Thermal properties of carbon-reinforced copper matrix composites produced by powder metallurgy route.....	247
225.	Thermal Conductivity of Functionally Graded Aluminum-Alumina Composites: Experimental Study and Micro-XCT-based Numerical Simulations.....	248
226.	In-situ synthesis of AlN-reinforced hypereutectic Al-Si matrix composites by arc plasma melting for thermal management applications	249
227.	Composite Anion Exchange Membranes containing a long-side chain ionomer and exfoliated Lamellar Double Hydroxides	250
228.	Self-healing electrolytes for stretchable Li-ion microbatteries	251
229.	Sulfonated Poly(phenylene sulfone)s Ionomers	252
230.	Hydrogen absorption characteristics of lithium-cobalt oxide ceramics soaked in water at room temperature.....	253
231.	Research on Ammonia Synthesis by Alkali Metal compounds.....	254
232.	Preparation and application in oxygen reduction reactions of covalently linked MOF-PSU..	255
233.	Carbonaceous electrocatalytic materials for the oxygen reduction reaction	256
234.	Improving the Thermoelectric Performance of Bi ₂ Te ₃ via Cobalt Doping	257
235.	Thermoelectric Properties of Zn-Sb Thin Films Deposited by High-Power Impulse Magnetron Sputtering	258
236.	Lithium concentration dependence on water absorption characteristics of lithium-rich zirconates.....	259
237.	Enhancing the Electrochemical Stability of Aluminum Current Collectors for High-Voltage Lithium-Ion Batteries	260
238.	Electrochemical Synthesis of Ni-Co-W-Zr(P) Quinary Medium Entropy Alloy for Enhanced Hydrogen Evolution Reaction	261
239.	High-speed dry cutting performances of Ti(C, N)-(Ti, W, Re)(C, N)-(W-Re) cermet tools with core-rim microstructure against super stainless steel bars.....	262
240.	Comparison of practical properties of various practical TiAl alloys for jet engine blades	263
241.	Finite Element Analysis of the nanoindentation tests for evaluating Al ₂ O ₃ /Ni-base substrate interfacial failure stress.....	264
242.	Fabrication and Bonding Properties of Joints Formed by Transient Liquid Phase Diffusion Bonding Using Electroplated Films	265
243.	Approach of the Spark Plasma Sintering mechanisms for boron phosphides-based ceramics	266
244.	Exploring Nb-based alloys for high-temperature structural applications.....	267
245.	Removal and Immobilization of Impurities in Direct and Complete Recycling Method for Advanced Ni-base Single Crystal Superalloys.....	268
246.	TLP Bonding of dissimilar materials.....	269
247.	Harnessing Nanostructure Control: Strategies for Enhanced Performance in Ni-based Superalloys	270
248.	Thermodynamic assessment and calculations of Mo-Si-B-Ti-C system for ultra-high temperature materials	271

249.	Improvement of High Temperature Strength of Cr-Co-Ni Medium Entropy Alloy By Precipitation of Gamma-Prime Particles	272
250.	Microstructures and Mechanical Properties of Directionally Solidified $\text{TMSi}_2/\text{TM}_5\text{Si}_3$ (TM = Mo, Nb)-Based Eutectic Composites	273
251.	Grain boundary engineering in the cast & wrought Ni-based superalloy Rene 41 with microalloying additions	274
252.	Plastic deformation property of $\mu\text{-Fe}_7\text{Ta}_6$ topologically close-packed intermetallic compound	275
253.	Hot deformation capability and processing window of powder-HIPed TNM alloy with full lamellar microstructure.....	276
254.	Influence of grain boundary serration on creep properties in Nickel based superalloy Nimonic 80A	277
255.	Synthesis, characterization and physical properties of a $\text{Ti}_2\text{NbAlC}_{1.82}$ ternary nanolaminated carbide	278
256.	Novel spray-pyrolysis-based synthetic strategy for uniformly distributed oxide nanoparticles-dispersion-strengthened refractory alloy	279
257.	Age-hardening behavior of Ni rich high entropy conventional alloy after cold rolling and flash annealing	280
258.	Diffusion in high-entropy alloys: sluggish or anti-sluggish? Lattice structure vs. chemical complexity	281
259.	Novel FeNiMnAlCr Multi-Principal Component Alloys	282
260.	Hierarchical Nanotwin-Driven Mechanism in Cryogenically-Deformed CoCrFeNi HEA Alloys	283
261.	High Entropy Alloys for Applications in Hydrogen and Cryogenic Environments.....	284
262.	Advancements in high-entropy alloys through the liquid metal dealloying process	285
263.	Heterogeneous Structured High Entropy Alloys	286
264.	Application APT to Understand High-Entropy Alloy and Materials	287
265.	Development of Non-Equimolar CoCrCuFeNi High Entropy Alloys for Aerospace Brazing	288
266.	Rotational Deformation Twins in a Refractory High Entropy Alloy	289
267.	Characterization of a $\text{CoCrFeMnNi}(\text{Al}_x)$ alloy produced from ferroalloys and scraps with an industrial foundry process	290
268.	Creep Strength of AlCoCrFeNi High-Entropy Alloy Fabricated by Spark Plasma Sintering.	291
269.	Elevated Temperature Mechanical Properties of Harmonic Structure Designed AlCoCrFeNi High Entropy Alloy by MM/SPS Process	292
270.	Analyses of Oxidation Behaviours with Alloy Components in High Entropy Alloys with Pack Cementation Coatings at High Temperatures.....	293
271.	Enhanced ductility via high-density nanoprecipitates driven by chemical supersaturation in a flash-heated precipitation-strengthened high-entropy alloy	294
272.	Kinetics of Chemical Order Formation and Its Influence on Diffusivity in CrCoNi Medium Entropy Alloy	295
273.	High Hardness Nanotwinned High Entropy Alloys CoCrFeNi Thin Films with radiation resistance.	296

274.	The power and beauty of Cantor's First Experiment A 20 year retrospective.....	297
275.	Nanoprecipitate-strengthened high entropy alloys	298
276.	High Entropy Nonlinear Dielectric System.....	299
277.	What role might high entropy alloys play in a circular economy?	299
278.	Machine Learning-Assisted Design of Advanced Bilayer TBC Systems Using Multicomponent R2TiO5	300
279.	Development of Bimodal-Grained Microstructure in Metastable Multicomponent Alloys via Reversion of Strain-Induced BCC Phase.....	301
280.	Effect of Stacking Fault Energy on Deformation Mechanism and Low-Cycle Fatigue Property in Co-Cr-Mo-Ni Medium Entropy Alloys.....	302
281.	Plastic deformation behavior of single crystals of the equiatomic high- and medium-entropy alloys of the Cr-Mn-Fe-Co-Ni system.....	303
282.	Creep behavior of a precipitation-strengthened A2-B2 refractory high entropy alloy	304
283.	Effect of Re and Ru on two-phase A2+B2 Ta-Mo-Ti-Cr-Al refractory high entropy alloys..	305
284.	Elucidating the microstructural formation pathways in Refractory Metal High Entropy Alloys using in situ high energy diffraction.....	306
285.	Strengthening multicomponent alloys with ordered precipitates: the role of partitioning and site occupancy	307
286.	High-Entropy Alloys as Advanced Metal Hydrides for Efficient Hydrogen Storage	308
287.	Development of high entropy alloy thin films for energy-related research.....	309
288.	Transformation pathways and deformation mechanisms in refractory high entropy alloys....	310
289.	Characteristic Dislocation Slips in Polycrystalline HfNbTiZr Medium Entropy Alloy.....	311
290.	ICME and Microstructure Informatics framework for the development of multicomponent alloys	312
291.	The microstructural evolution of FCC high-entropy alloy after gas tungsten arc weld and friction stirring weld	313
292.	Enhancing strength and hydrogen embrittlement resistance by discontinuous L12 precipitation in high-entropy alloy	314
293.	Hierarchical structures of submicron and nanoscale blocks evolved through deformation twinning in CrCoNiSi0.3 medium entropy alloy under ballistic impact.....	315
294.	In-situ hydrogen embrittlement of CrCoNi medium-entropy alloy.....	316
295.	Great compositional discovery in materials history	317
296.	Shape memory effect in CrMnFeCoNi high-entropy alloys with high Co/Ni ratio	318
297.	Achieving remarkable strength and ductility through via nano-twinning enabled by L12 nano-precipitates in CoNiMoAl medium-entropy alloys	319
298.	Development of Ti based bio-high entropy alloys	320
299.	An Assessment of the Viability of the Refractory Metal High Entropy Alloy AlMo0.5NbTa0.5TiZr for High Temperature Structural Applications.....	321
300.	Deciphering the operative mechanisms affecting the strain rate sensitivity in (FeCrNi)99Si1 medium entropy alloy during high-pressure torsion.....	322
301.	In-vivo bone implantation study of TiZrNbTaFe high entropy alloy thin films	323

302.	Optimizing Al content to eliminate the brittle phase in lightweight TiZrNbTa _{0.1} Al _x refractory high-entropy alloys	324
303.	Shape memory effect in CrMnFeCoNi high-entropy alloys with high Co/Ni ratio	325
304.	Towards multifunctionality in novel high entropy alloy by compositional variation and thermo-mechanical processing.....	326
305.	Investigation of a Spinel Oxide Coating based on CoCuFeMnNi High-Entropy Alloy for SOFC application	327
306.	Microstructures and Properties of CoCrFeMn High Entropy Shape Memory Alloys Produced by Laser Direct Energy Deposition	328
307.	Shift and delete effect on aluminum twist grain boundary energy	329
308.	A Systematic Study of Grain Boundary Segregation in Nanocrystalline Alloys	330
309.	Comparison of Pd-42Cu-10Ni and Pd-30Cu-29.5Ag-0.5Zn as Probe Material in Interfacial Reaction with Sn.....	331
310.	Precipitation and growth behavior of β_0 phase in the α_2/r lamellar colonies of an intermetallic Ti-43.5Al-4Nb-1Mo-0.1B alloy	332
311.	Microstructural characterization and analyses of the of the damage in a Ti-based alloy by X-ray computed microtomography.....	333
312.	Deformation behavior of magnesium bicrystals with $90^\circ\langle 10\bar{1}0 \rangle$ and $90^\circ\langle 11\bar{2}0 \rangle$ grain boundaries: Changing grain boundary character and boundary proximity.....	334
313.	Assessment of Adhesion Degradation in A1050/Epoxy Resin Interface Under High-Humidity and High-Temperature Aging Conditions	335
314.	Degradation Behaviour of Sn-Ag-Cu Lead-free Solder Joint with Electrolytic Ni Plated Electrode due to Electromigration.....	336
315.	Evaluation of Joining Properties Between Potential-Controlled Ni-Cu Alloy Plating Film and Pb-Free Solder.....	337
316.	Effect of Thermal Cycle Profile on Thermal Fatigue Life of Sn-3.0Ag-0.5Cu Solder Joints for Wafer-Level Chip Scale Package	338
317.	Investigation of Degradation Behavior of Adhesion between Sealing Resin and Copper by Aging Treatment.....	339
318.	Plastic deformation propagation across grain boundaries in Fe-3%Si bicrystals: A comparative study of twist and tilt grain boundaries	340
319.	Structural change of Ga ₂ O ₃ layer formed on GaN(0001) substrate under various fabrication conditions	341
320.	Effect of low-angle grain boundary network on high cycle fatigue in grain boundary engineered 409L type ferritic heat resistant steel	342
321.	Structure-dependent electrical properties of grain boundaries	343
322.	Spintronic technologies for germanium devices	344
323.	Quantification of the grain boundary structure and determination of migration mechanisms	345
324.	Atom-Resolved Observations of Grain Boundary Dynamics in Oxides	346
325.	Gradient B2-BCT Transition and Interface Introduced by Deformation in Eutectic High-Entropy Alloy	347
326.	Atomistic Modelling and Design of Mechanical Properties of Grain Boundaries in Alloys ..	348

327.	Plasmon loss imaging at grain boundaries obtained by STEM-EELS and the grain boundary dependence	349
328.	Grain boundary precipitation behavior of Ni-Cr phase in γ -Ni matrix in Ni-Cr binary alloys	350
329.	Interfacial Mechanisms of Iron-Oxide Reduction: From Direct Microstructural Observations to Atomistic Simulations	351
330.	Graphite Crystallization in Austenitic Ductile Iron: Insights from TKD and TEM Diffraction	352
331.	Improved Indexing of Electron Backscatter Diffraction Patterns using Forward Modelling..	353
332.	Recrystallization mechanisms activated during multi-pass forging of austenitic stainless steels	354
333.	Recrystallization in ferritic stainless steels: experimental and modeling approaches	355
334.	A Computational Approach to Design Thermally Stable Metal-Metal Interfaces	356
335.	Effect of deformation twinning on the strength anisotropy in textured Ti: Insights from atomic simulations and slip transfer theory.....	357
336.	Anisotropy in high temperature deformation and oxidation behavior in textured Ti ₃ SiC ₂ MAX phase ceramics.....	358
337.	Disclination and cooperative deformation at intersection of kink interface and slip deformation	359
338.	Geometrical modeling of bent kinks: energy reduction and shape transition mechanisms.....	360
339.	Kink deformed microstructure in mille-feuille structured materials	360
340.	Kink Boundary Migrations in LPSO-structured Mg Alloys.....	361
341.	Numerical Evaluation of Kink Band Formation in Anisotropic Solids.....	362
342.	Anisotropic mechanical property-induced ductilization (AMID) A new mechanism to simultaneously improve the strength and ductility of multiphase alloys	363
343.	Effects of strain components on effective kink band formation in Mg-Y-Zn alloys.....	364
344.	Effects of microstructural factors on high temperature deformation behavior of Ti-based MAX phase ceramics.....	365
345.	Strength-ductility balanced by bimodal microstructures composed of kink-strengthening grains in a mille-feuille structured Mg-Al-Y Alloy	366
346.	Microstructure evolution of twin-roll cast and hot-rolled WZ73 alloy during the finishing heat-treatment.....	367
347.	Processing Strategies for Tailoring Strength and Ductility in Mg-Y-Zn Alloy	368
348.	Ignition characteristics and mechanical properties of Mg-Al-Ca-X alloys for electric vehicle applications.....	369
349.	Microstructural observation of high mechanical strengthened Nb ₃ Sn superconducting wires via the internal matrix reinforcements.....	370
350.	Re-design of low-activation vanadium alloys based on impurity control for fusion reactor applications.....	371
351.	DTT Bolometry and Soft X-Rays Diagnostics Design Facing Engineering and Physics Requirements.....	372
352.	Microstructures and Irradiation Hardening in Low-activation Fe-Mn-Cr-Al-V-C Alloys.....	373
353.	Helium concentration dependence of retarded recrystallization in tungsten.....	374

354.	Development of NDE Infrastructure for Fusion Device Relevant Materials and Components at EPRI	375
355.	In-situ EBSD phase transition analysis in ODS martensitic steels.....	376
356.	Evolution of dislocation microstructure in cyclically deformed [001], [011], and [111] oriented copper single crystals	377
357.	Production of Fe-6.5 %wtSi electrical steels sheets by conventional metallurgy for high-performance electric motors	378
358.	Investigating the Influence of Trace Tantalum on the Microstructure and Mechanical Properties of Niobium Microalloyed Steels	379
359.	Crystal orientation change during simple shear deformation of Fe-3%Si.....	380
360.	Evaluation method for Mode II crack growth rates under rolling contact conditions based on fracture mechanics in railway wheel steels	381
361.	Effect of precipitation phase on high cycle fatigue behavior of Ti-2Al-9.2Mo-2Fe alloy	382
362.	Wear Behavior Analysis of Nitrided Ti-12.1Mo-1Fe Alloy after Shot Peening Pre-treatment	383
363.	Analysis of Generation and Propagation of Fatigue Crack in Oxygen-free Copper Using Electron Backscattered Diffraction Method.....	384
364.	Analysis of Wear Properties and Mechanism Changes According to Fe Content in Metastable β Titanium Alloys.....	385
365.	Effects of Changes in Crystal Structure by Plastic Deformation on Corrosion Resistance of Magnesium Alloys.....	386
366.	Study of Adhesion Strength Degradation and Fracture Behaviour of Copper/Epoxy Resin Joints under Hygrothermal Conditions.....	387
367.	Effects of Prior Deformation at Cryogenic Temperature on Tensile Deformation Behavior of Heterogeneous Nano-Structured Austenitic Stainless Steel.....	388
368.	The Stress Field Dependency of Martensitic Transformation in Metastable Austenitic Stainless Steel	389
369.	Effect of heat treatment process on microstructure and toughness at cryogenic temperature for 9%Ni steel	390
370.	Evaluation of a Low-Cost System for Measuring Thermal Conductivity in 3D-Printed Metallic Structures.....	391
371.	Influence of Process Parameters Variation on Microstructure and Mechanical Properties of SLM-Printed 316L Stainless Steel	392
372.	The effect of zinc content on the acoustic properties of brass percussion.....	393
373.	The impact of surface properties on strain distribution in air-bending	394
374.	Application of bi-modal milling process to fabricate harmonic structure materials	395
375.	Environment-Assisted Cracking of Mg-Al-Zn Alloys in pH-Controlled Carbonate Buffer Solutions.....	396
376.	Mechanical and Thermal Properties of Harmonic Structure Composites with Ti-Ni Alloy and Copper	397
377.	Micro-mechanical characterisation of hydrogen-enhanced fatigue crack growth in 100Cr6 bearing steel under mixed-mode loading.....	398

378.	Phase-field modelling of hydrogen embrittlement in metals.....	399
379.	The effect of Cu and Sn contents on the microstructure and mechanical properties of eutectoid steel.....	400
380.	Effect of Ni on Low Temperature Impact Toughness of V-Nb Microalloying Non-quenched and Tempered Forged Steel.....	401
381.	Microstructural refinement enhances hydrogen embrittlement resistance in high-strength martensitic steel.....	402
382.	Synthesis and characterization of an (Al-10Si-3Zn-2Cu)/Ti-6Al-4V interpenetrating phase composite with enhanced mechanical properties	403
383.	Tailoring Biodegradable Zinc Alloys: A Powder Metallurgy Approach	404
384.	A unique high-temperature deformation mechanism in a CrMnFeCoNi alloy	405
385.	Creep properties of P92 pipe weld after annealing at 600 and 650°C	406
386.	Microstructure, texture and magnetic properties of warm thermomechanical processed carbon free Fe-1.5% Si (Wt.%) non-oriented electrical steels	407
387.	Numerical investigation of fatigue crack propagation in additively manufactured AA5087 sheets	408
388.	Corrosion-fatigue performance of friction-welded dissimilar joints	409
389.	Interfacial Plasticity of Proton-Irradiated Nanotwinned Metals.....	410
390.	Superior tensile and impact properties of a novel high-Mn austenitic steel at extremely low temperatures	411
391.	Micro-mechanical characterisation of resistances to hydrogen embrittlement and fatigue crack growth in type 304 stainless steel with nanotwin bundles.....	412
392.	Peltier-Induced Thermal Fatigue Testing for Reliability Evaluation of Thermoelectric Devices	413
393.	Lead-free KNN-based piezoelectric ceramics: Design and mechanical characterization	414
394.	Relationship between Maximum Bending Stress and Surface Roughness of AZ31 Magnesium Alloy Fully Corroded in Salt-water Environment	415
395.	Prediction of Hardness in the Heat-Affected Zone of Multilayer Welded Stainless Steel Based on Dislocation Density Change Behavior	416
396.	Sintering Characteristics of Mo-Ta Alloys via Spark Plasma Sintering Process	417
397.	An Innovative Grain Refinement Strategy on Biomedical Ti-6Al-4V Alloy for Texture Annihilation.....	418
398.	Synchrotron X-ray characterization of gradient microstructure and residual stress anisotropy in high-pressure torsion processed Inconel 718.....	419
399.	Application of Digital Image Correlation (DIC) at Cryogenic temperature: Deformation and Fracture Behavior of Metallic Materials (Al, Welding)	420
400.	Development of a New Mn and N Alloyed Austenitic Stainless Steel and Its Weldability Evaluation for Cryogenic Applications	421
401.	High pressure Spark Plasma Sintering of boron based nano-structured hard boron phosphide (BP, B12P2) for ballistic applications	422
402.	Correlation between microstrain and hydrogen embrittlement in high strength quenching and partitioning (QP) steel	423

403.	Effects of alloying elements on marine corrosion resistance of structural steel.....	424
404.	High Pressure Synthesis and Compression Behaviour of Multicomponent Transition metal Nitrides and Phosphides	425
405.	CALPHAD methodology for high-pressure synthesis: Phase diagram of Mg-C system by in-situ X-ray diffraction and phenomenological thermodynamics	426
406.	Damage evolution in nanostructured ferritic alloys produced via various methods under high dose ion irradiations	427
407.	Can accelerated neutron irradiations replicate historical microstructural characteristics in U-Zr fuels?	428
408.	Atomic cooperativity at deformation of metallic glasses	429
409.	Processing of a Zr-based bulk metallic glass.....	430
410.	Development of Biocompatible, Toxic-Free Zr-Based Metallic Glass Alloys for Long-Term Biomedical Applications	431
411.	Fabrication of Zr-based Bulk Metallic Glasses Lattice Structures by L-PBF process	432
412.	Insights on the heterogeneous to homogenous flow transition in a Zr-based metallic glass...	433
413.	From nano-patterned Pt-based metallic glass to copper oxide foam formation	434
414.	Identification of Deformation Elements in Metallic Glasses through Frozen Atom Analysis	435
415.	Influence of Strain Rate on the Deformation Behavior of Pt-Cu-Ni-P Bulk Metallic Glass...	436
416.	Relevance of the Structure and Dynamics of High Temperature Metallic Liquids to Glass Formation	437
417.	Cryogenic Thermal Cycling of Metallic Glasses: From Concept to Applications.....	438
418.	Surface designs to improve the biocompatibility of Ti-based bulk metallic glasses.....	439
419.	Rapidly Annealed High-Bs Soft Magnetic FeCo-Based Amorphous and Nanocrystalline Ribbons for High Temperature Applications	440
420.	The Crystal-Melt Interface in the Hard Sphere System.....	441
421.	Formation of gradient rejuvenation structure in Zr-based bulk metallic glass and its effect on ductility improvement	442
422.	SPD as a tool to improve the plasticity of Bulk Metallic Glasses	443
423.	On the design of biocompatible β -Ti-based alloys for bone implants by ab initio and cellular potts model	444
424.	Neutralization of impurity elements of Cu and Ni in Mg-Zn alloy by dissolution into $MgZn_{2/3}$ phase.....	445
425.	Effect of Grain Size on the Behavior of Exfoliation Corrosion in Cold-rolled Mg-14mass%Li-3mass%Al alloy.....	446
426.	Anisotropy in Microstructural Evolution in Pre-deformed AZ31 under directional EPT: A quasi in situ EBSD Analysis.....	447
427.	Enhancing Energy-Based Fatigue Life Model for Wrought Mg Alloys through Machine Learning Integration	448
428.	Microstructure changes due to additional elements and processability at room temperature in Mg-In alloy systems	449
429.	Atomistic Insights into Grain Boundary-Solute Interactions and Texture Formation in Mg Alloys	450

430.	Development of corrosion resistance Mg alloy for Die casting component.....	451
431.	Towards Green Magnesium - Environmental Aspects of Magnesium Materials for the Transportation Industry	452
432.	Ignition characteristics and mechanical properties of Mg-Al-Ca-X alloys for electric vehicle applications.....	453
433.	Electropulsing Treatment for Mg alloys: Acceleration and Anisotropy	454
434.	Research on the microstructural evolution of injection molded AZ91 and ultralight LAZ561Ca magnesium alloys during solidification and heat treatment: multiscale characterizations and multiphase field modeling	455
435.	Combined 3DATP and HADDF studies of the microstructures of new generation magnesium alloys developed Magnesium Research Centre, Kumamoto	456
436.	A Comparative Investigation of the Formation Mechanism and Corrosion Behavior of Micro-Arc Oxidation-Treated AZ31 and AC84 Kumadai Magnesium Alloys.....	457
437.	Development of Advanced Magnesium Alloys.....	458
438.	Effects of strain states induced by different wrought processes on microstructure evolution of AZ31 magnesium alloy	459
439.	Plastic deformation of fine-grained pure magnesium and AZ series Mg alloys between 298K and 4K	460
440.	Synergistic effects of Rolling and Mixed rare earth (Er+Yb) additions on mechanical, corrosion and biocompatibility properties of Mg-Zn-Ca alloys for orthopedic applications ..	461
441.	Development of biodegradable magnesium implants from an engineer's perspective.....	462
442.	Specific resistance measurements for the development of Mg based alloys.....	463
443.	A deep-learning based surrogate model for the numerical simulation of casting process	464
444.	Multiscale Modeling and Simulation of Manufacturing Process for Ni-Based Single-Crystal Superalloys	465
445.	Stochastic scaling of time step in a full-scale Monte Carlo Potts model.....	466
446.	Application of Thermodynamic Extremal Principle to the Sintering of Irregular Powder Particles	467
447.	Simple flow rules for three-phase viscoplastic materials	468
448.	Verification of a novel mathematical model for determination of the biomass specific growth rate in bioprocesses.....	469
449.	Generalized stacking fault energy in multi-component Co-based L12 precipitates.....	470
450.	Thermodynamics properties of Ti2Al-M-ternary V-VIB groups O-phase alloys from first-principles calculations	471
451.	The effect of precipitate chemistry on hydrogen-enhanced decohesion in Ni-based alloys: An ab initio study	472
452.	Generation of morphology-controlled three-dimensional microstructures in dual-phase steels using SliceGAN-AdaIN.....	473
453.	Data-driven estimation of tensile properties of alloys using instrumented indentation method	474
454.	Finite element modelling of electromagnetic heating	475
455.	Numerical modelling of precipitation kinetics in Al alloys during solid-state processing.....	476

456.	Experimental Studies and Simulation of TRIP-TWIP Roll Bonding.....	477
457.	Finite element simulation strategies for cold pilgering process	478
458.	Identification of the stochastic hot forming model based on the inverse analysis for the four types of compression tests	479
459.	Dissecting physics of carbon ordering in bcc iron	480
460.	Representing texture in surrogate models of crystal plasticity to predict material behaviour and quantify uncertainty.....	481
461.	Utilizing Automated Workflows and Thermodynamic Models to Compute Ab Initio Bulk and Defect Phase Diagrams.....	482
462.	Deep Generative Model to extract process-structure-property linkage in low-carbon steel ...	483
463.	Multiscale Finite Element Simulation on Effect of Groove Shape on Strain Distribution in Caliver Rolling	484
464.	Phase field model of modification of microstructure of Novel Al-15Mg2Si-4.5Si composite by addition of Strontium during semi-solid processing.....	485
465.	Testing Theories and Simulations on Phase Coarsening by Experiments.....	486
466.	Microstructure-Based Fatigue Life Prediction Approaches for Hypo-Eutectoid Steels: Uniaxial and Non-Uniaxial Fatigues Lives, and Their Variabilities.....	487
467.	A computational framework for modeling and predicting the mechanical behavior of materials applied to martensitic steels.....	488
468.	A meso-scale model to predict flow stress and microstructure during hot deformation of IN718WP	489
469.	Modelling combined hardening mechanisms in alloys through the analysis of dislocation percolation.	490
470.	Application of an Activation-function modified Norton law to predict the two-step minima creep deformation observed in Incoloy 800H	491
471.	Concept of a module for water treatment with plasmonically active nanoparticles, to extend a multivalent modular prototype system for adaptable water treatment and analysis.....	492
472.	Control of osteoblast cell behavior by titanium alloys' microstructure	493
473.	Argon plasma etching process to fabricate the antibacterial nanopillar on stainless steel surface	494
474.	Safe-by-design conception and synthesis of metallic nanoparticles for biomedical applications	495
475.	Self-Assembled Growth of 3D Nanostructures for High Electrochemical Performance by RF Magnetron Sputtering.....	496
476.	A Novel Understanding for Plastic Deformation and Mechanical Amorphization of Amorphous and Crystalline Silica under Electron-Beam Irradiation.....	497
477.	Employing Shear Punch Testing to Investigate Thermomechanical Properties of Nanocrystalline Brass.....	498
478.	Optimization of Hydrogen Alarm Sensor on Semiconductor Basis.....	499
479.	Low-temperature synthesis of graphene usable in the harsh environment of liquids for energy applications.....	500

480.	Nanocomposites of reduced graphene oxide for 2D symmetric micro-supercapacitor with high energy storage performances	501
481.	Some Issues Related to the Formation of GaN-based Nanopillar LEDs on Multicrystalline Si Substrates.....	502
482.	Plasma Synthesis of 3D Graphene-Based Materials and their Applications	503
483.	Superatom Like b-FeSi ₂ Core/Si Shell Quantum Dots via Self-Assembly and Self-Alignment Processes	504
484.	Growth and Magnetic Characteristics of Iron-filled Carbon Nanotubes.....	505
485.	Data-driven analysis and control of plasma-enhanced deposition of functional carbon materials	506
486.	Amorphous Gallium Oxide Memristor for High-temperature Electronics.....	507
487.	In situ XAFS study on chemical states of transition-metal catalyst during single-walled carbon nanotube growth under conventional CVD conditions with ethanol and C ₂ H ₂ feedstock	508
488.	Hydrogen desorption from GeH nanosheets under ultrahigh vacuum ambient towards germanene synthesizing.....	509
489.	Monolithic Integration of Eu-doped GaN/InGaN Quantum Wells for Full-color Micro-LEDs with Enhanced Red Emission	510
490.	Precision metal patterning via femtosecond laser-induced thermochemical reaction without excessive precipitation from glyoxylic acid metal complex solution.....	511
491.	Robust high-capacity all-solid-state Lithium-ion batteries enabled with nanoparticulate anodes produced by plasma spraying	512
492.	Surface Chemical Modification of BaTiO ₃ Nanocubes for Controlling Physical-Chemical Functions	513
493.	Transient phenomena in additive manufacturing of Ni-base alloys investigated by synchrotron X-ray scattering	514
494.	Accuracy Study on X-ray Stress Measurement using Fourier Analysis of Debye-Scherrer Ring	515
495.	Observation of Impact Fracture on Heterogeneous Nanostructured Stainless Steel and Titanium by Using Synchrotron Radiation	516
496.	How rapid quenching and reheating influences phase transformations in advanced gamma-TiAl alloys	517
497.	In-Operando Analysis of Carbide Formation and Stress Generation during Low Pressure Carburizing by High-Energy Synchrotron X-ray Diffraction	518
498.	Structure and dynamics in densified silica glasses.....	519
499.	Per-Grain behaviour in polycrystalline alloys during stress induced phase transformations ..	520
500.	Observation of a zirconium oxide crystal nucleus in the initial nucleation stage in aluminosilicate glass by X-ray multiscale analysis	521
501.	Quantitative Analysis of Complex Defect Structures created by Advanced Manufacturing using X-Ray Diffraction.....	522
502.	X-ray fluorescence Holography Study on Ferroelectric Materials under an Electric Field	523
503.	Development of Acoustic Device using Giant Magnetostrictive Material: Consideration on Acoustic Characteristics of Sound Generated by Wall Surface Vibration	524

504.	Effect of grain size on shape memory properties of Cr20Mn20Fe20Co35Ni5 high-entropy alloy	525
505.	Microstructures and Properties of Diffusion Layer Formed at Laminated Interface of Alumina-Particle Dispersed Magnesium Laminated Compacts Fabricated by MM/SPS Method	526
506.	Machine learning multi-objective optimization design multi performances of Zn alloys and Mg alloys	527
507.	Relationship between deformability and crystalline system of martensite phase in Au-Cu-Al	528
508.	Formulation of chitosan-based resists for an optimized eco-efficient photolithography process: focus on the ToF-SIMS characterization.....	529
509.	Thermal, Mechanical, and Materials Aspects of a Shape Memory Alloy Stirling Heat Engine	530
510.	Mechanical Properties of Au-Cu-Al Dual Phase Alloys for Biomedical Applications.....	531
511.	Application of electron beam welding in the production of TEMPALLOY AA1 and T92 butt joints of pipes assigned for the energy industry	532
512.	Evaluation of Strain Distribution of Perforated Sheet in Circular Cup Deep Drawing.....	533
513.	Enhancing Mechanical Properties of Mg-Zn-Ca Alloys via Texture Modification in Multi-Pass Constrained Friction Processing.....	534
514.	Microstructure evolution in two-step friction extrusion of aluminium alloys.....	535
515.	Low temperature sintering of ink-spray BST layers for fabrication of an electromagnetic shutter	536
516.	Forming of Multifunctional Corrugated Cup using Roller Ball Die	537
517.	In-situ observation and quantitative evaluation of dendritic silver precipitates growth inside borosilicate glass substrate	538
518.	Eliminating the Need for Post-Forming Annealing: Advancements in NSF Technology for Austenitic Stainless Steels.....	539
519.	Development of advanced tool pin geometries for Friction Stir Spot Welding (FSSW) by means of Selective Laser Melting (SLM).....	540
520.	Improving sintering ability of alumina through gel casting process	541
521.	Processing of Amorphous Oxide Semiconductors and Future Prospects.....	542
522.	Experimental Study on the Behavior and Emissions of Methane/Hydrogen Diffusion Flames Under DC Electric Field.....	543
523.	N ₂ O and NF ₃ Reduction and NO _x Emission Characteristics in Methane/Hydrogen Diffusion Flames	544
524.	Thermal Deformation Analysis and Flashback Prevention in Aluminum Body Portable Butane Gas Burners	545
525.	Phase diagram of Ni-Si-Mn precipitates in reactor pressure vessel steels	546
526.	Phase diagram of Ni-Si-Mn precipitates causing irradiation-induced embrittlement of nuclear reactors	547
527.	Downselection of Cladding Materials for Hydride Moderators	548
528.	Thermo-mechanical properties evaluation in chromium-doped UO ₂	549
529.	Electropulsing effects on microstructural evolution in cold-rolled Grade 2 titanium sheet....	550

530.	Fretting damage mechanisms mediated by α precipitates and β crystallographic textures in a metastable β titanium alloy.....	551
531.	Effects of heat treatments on the microstructure, phase development and mechanical properties of PMD additively manufactured ternary and quaternary Ti-Cu-based alloys with Fe and Cr additions	552
532.	Heterogeneous Beta structure significantly improves work hardening properties of metastable Beta titanium alloy	553
533.	Stability and segregation study of alphagenic and betagenic addition elements in pure titanium by atomistic approach.....	554
534.	Revealing the Mechanism Behind the Strength-Plasticity Dependence on Lamellar Orientation in Polycrystalline TiAl Alloys.....	555
535.	Enhancement of Mechanical Properties of Titanium Alloys through Innovative Thermomechanical Processing.....	556
536.	In situ assessment of the influence of omega on the properties of metastable beta Ti alloys .	557
537.	Fabrication and Thermomechanical Processing of Titanium-Based Laminates for Enhanced Performance under High Dynamic Impact.....	558
538.	Fabrication and Thermomechanical Processing of Titanium-Based Laminates for Enhanced Performance under High Dynamic Impact.....	559
539.	High temperature oxidation behavior of lightweight and formable high entropy alloys.....	560
540.	Effect of Subgrain Boundary Distributions on Extra-Hardening of SPD-processed Al-3%Mg alloy	561
541.	Strengthening Mechanisms of Heterogeneous Nano-Structured Stainless Steels and Copper Alloys	562
542.	Suppressing diffusion with the Schwarz crystal structure in Al alloys	563
543.	Prevention of hydrogen embrittlement of HPT-processed ultra-high strength aluminium alloys by hydrogen-absorbing nanoparticles.....	564
544.	Advancing High-Entropy Alloys Through Nanostructuring: Enhancing Mechanical Properties and Thermomechanical Behavior.....	565
545.	Applying ultra-high shear strains to aluminium-graphene composites to achieve an exceptional strength-ductility combination.....	566
546.	Fabrication and Characterization of Insulation-Type Thermal Interface Materials Using Conformal SiO ₂ -Coated Copper Dendritic Particles	567
547.	Effect of friction between bonding tool and workpiece on bond microstructure in ultrasonic bonding of Aluminum alloys.....	568
548.	Development of Advanced Orbital TIG welding for Utility pipe in Semiconductor factory.	569
549.	Ultrasonic Bonding of Aluminum alloys to carbon fiber reinforced thermoplastic	570
550.	Friction Behaviour and Microstructure in Ultrasonic Bonding using Complex Vibrations....	571
551.	Microstructure and Property of Aluminum/Iron Non-Uniform Heat Input Laser Welded Joints	572
552.	Finite Element Modelling and Microstructural Analysis of Laser-Welded AM Inconel 718 Joints.....	573
553.	Impact of post-weld heat treatment on microstructure, mechanical properties, and corrosion behavior of laser-welded Nb-microalloyed ferritic stainless steel	574

554.	Application of electron beam welding in the production of TEMPALLOY AA1 and T92 butt joints of pipes assigned for the energy industry	575
555.	Effects of Factors on Deformation-Induced Martensitic Transformation of Metastable Austenitic Weld Metals at Cryogenic Temperature	576
556.	Improved mechanical properties of Al-Cu laser lap joints by optimization of laser beam wobbling.....	577
557.	Effect of atmospheric condition in Electron beam welding of advanced high strength steel..	578
558.	Reinforcing FSW joints with mechanical interlock utilizing stamping holes	579
559.	Effect of Magnesium and Silicon on the Temperature Evolution and Mechanical Properties in Refill Friction Stir Spot Welding of Aluminum to Titanium	580
560.	Prediction and control of welding distorsion in the aluminium basic element of vehicle structures	581
561.	Porosity suppression Using a Combination of Quasi-continuous and Oscillating Lasers in HPDC Al-Si Alloy Welds	582
562.	Lap friction stir welding of a TRIP steel grade with a Ni filler.....	583
563.	Friction Stir Technologies Evolution of a Disruptive Process over 30 Years	584
564.	Corrosion Fatigue Property of Steel/Aluminum Alloy Weld-Bonded Lap Joint in High Temperature and High Humidity.....	585
565.	Microstructure and Mechanical Properties in Al-Cu Lap Joint by Dual Beam Laser Welding	586
566.	TLP Bonding of dissimilar materials.....	587
567.	Thermodynamical and experimental verification on the enhancement of tensile and impact properties of high strength low alloys steels and their welds	588
568.	The Role of Interstitials on Phase Metastability and Dislocation Pathways in BCC Refractory Multi-Principal Element Alloys	589
569.	Amorphous Materials Examined with a Multifaceted Approach	590
570.	Spintronic technologies for room-temperature germanium devices.....	591
571.	Effect of friction stir welding on the microstructure and precipitation behaviour of new generation cast (Al-Zn-Mg)-Fe alloys.....	592
572.	Impact of Grain Size on Strain-Induced Phase Transformation in a CrCoNi Multi-Principal Element Alloy.....	593
573.	Experimental and computational studies on delamination-induced loosening behavior of acetabular cup by cyclic load	594
574.	Biomimetic 3D printed polymer-ceramic composite scaffold for vascularized bone defect repair.....	595
575.	Internal Friction and Hydrogen Embrittlement of Steel	596
576.	Modification by heat treatment of powders for the cold spray process.....	597
577.	Unraveling the Dynamics of Eutectic Melting an Insitu Study of CBr ₄ -C ₂ Cl ₆ Microstructures	598
578.	Design and development of a novel Mg-Zn-Ca bulk metallic glass for biomedical applications	599
579.	Anti-oxidation UHTC coatings obtained by plasma spraying.....	600

580.	Multi-Physics, Multi-Scale Modeling Of A Plasma Jet Facility With Dsmc Technique: Methods For Continuous To Transitional Regimes And Evaluation Results.....	601
581.	Instrumented indentation studies on the hydrogenated high- and medium-entropy alloys	602
582.	High strength and high elongation of die-casting aluminium alloys.....	603
583.	High strength and high elongation of die-casting aluminium alloys.....	604
584.	Functionally graded materials by multi-layer friction stir (MLFS) deposition	605
585.	Microstructure and mechanical properties of Mg and Mg / Nb alloys after severe plastic deformation by accumulative fold-forging.....	606
586.	Deformation behavior of a 3D-printed high-entropy alloy	607
587.	Grains ain't misbehaving or going wild? A spontaneous activation of grain boundaries initiating abnormal grain growth!.....	608
588.	Asymmetric Rolling To Improve Sheet Formability of AM30 Mg Alloy	609
589.	Overlap-Bonding between Aluminium and Copper through Friction Stir Processing.....	610

1. Microstructural and mechanical characterisation of additively manufactured S235 and 430L steel components by cold spraying

Jiangnan Chen

Chair Of Steel Structures, Helmut Schmidt University, Hamburg, 22043, Germany.

With the growing importance of resource efficiency in the construction industry, additive manufacturing is becoming increasingly significant. Cold spray technology stands out in steel construction thanks to its high deposition rate and capability to produce large-scale components. In this study, deposits made of 430L stainless steel and S235 structural steel were additively manufactured and analysed to investigate the influence of spray parameters on material properties. The microstructure was examined using scanning electron microscopy (SEM) and optical microscopy. Mechanical properties were evaluated through quasi-static tensile testing and hardness measurements. The results for both materials are compared and discussed.

2. Co-sintering of LTCC-gold system: Coupled experimental, analytical and numerical approaches

Antou Guy ¹, Pradeilles Nicolas ², Delhote Nicolas ³, Maitre Alexandre ²

1 - Univ. Limoges, CNRS, IRCER, UMR 7315, F-87000, Limoges, France (France), 2 - Univ. Limoges, CNRS, IRCER, UMR 7315, F-87000, Limoges, France (France), 3 - Univ Limoges, CNRS, XLIM, UMR 7252, F-87000, Limoges, France (France)

LTCC (Low Temperature Co-fired Ceramic) and gold multilayers systems are extensively used in the development of multi-materials components for civil and military radio-frequency applications. This technology presents a high potential of development because it provides a packaging solution for electronic chips. During the additive manufacturing process of these multi-materials components (ceramic-metal), the co-sintering step is a key and critical one. Indeed, it leads to damages because of potential mismatches in thermal expansion coefficients as well as shrinkage kinetics. Thus in this work, a methodology combining experiments to analytical and numerical calculations is applied to investigate co-sintering behavior of a ceramic-metal layered structure. The sintering and thermomechanical behavior of the selected ceramic and metal materials have been carefully characterized. The constitutive laws so-identified have been implemented in a finite element code. The numerical model robustness has been analyzed by confrontation with experimental tests conducted thanks to the development of an original ombroscopy apparatus, which allows the in situ curvature monitoring. The approach conducted here, combining experiments to analytical and numerical modeling, allowed establishing a robust numerical model, reliably simulating the thermomechanical behavior of the ceramic-metal bilayer during co-sintering process. Numerical simulation is a key tool for adapting the co-sintering heating program (heating rate, temperature and dwell time) as well as bi-material geometry in order to optimize their densification and limit involved distortion.

Keywords : Multimaterials, LTCC, Co, sintering, Numerical simulation, Thermomechanical behavior

3. Towards new high-strength and heat-resistant Al alloy design enabled by additive manufacturing

Ji Gang , Ma Siming, Addad Ahmed, Chen Zhe

1 - Unite Materiaux et Transformations (UMET UMR CNRS8207) (France)

Softening due to severe strength degradation is inevitable in metallic materials at elevated temperatures especially at $T > 0.5T_m$. For instance, at 300 °C, most Al alloys exhibit a low yield strength of only several tens of MPa, merely 10~40 % of that at room temperature. The popular pathways to enhance high-temperature strength have been realized by integrating second-phase reinforcements, such as micro-/nanosized intermetallics, precipitates or ceramic particles in the alloy matrix. In this regard, the most efforts have been made to maintain high volume fraction of the evenly-distributed second-phase particles, while improving their coarsening-resistance. The recent thriving additive manufacturing (AM) technology has shown not only its massive industrial application prospects in rapid prototyping of complex-shaped metallic component with unprecedented freedom, but also highly potential to achieve novel metastable and ultrafine microstructures exploiting its inherent rapid solidification process. In particular, a specific 3D ultrafine cellular-like architecture, consisting of one phase/domain in cells enclosed by the other phase/domain as 3D interconnected network as cell boundaries, has been extensively reported in AM Al, Fe, Cu, and other alloys. In this work, we proposed a new architecture design strategy for developing high-strength and heat-resistant Al alloys using AM. We demonstrated that a thermally stable nano eutectic cellular network can be engineered in a novel near-eutectic AlLaScZr alloy during laser powder bed fusion (LPBF) process. The LPBFed alloy exhibits exceptional strength above $\sim 0.6 T_m$ of Al, where the tensile yield strength reaches ~ 250 MPa at 300 °C, two to five folds of the conventionally fabricated Al alloys.

Keywords : Additive manufacturing, laser powder bed fusion (LPBF), heat resistant aluminium alloys, high temperature strength

4. Enhancement of Mechanical Properties and Hydrogen Embrittlement Resistance of SUS 316L fabricated by DED through Laser Shock Peening

Ha Jeonghong ¹

1 - Korea Institute of Industrial Technology (South Korea)

316L stainless steel is widely recognized for its excellent corrosion resistance and formability, making it suitable for various industries including automotive, aviation, and medical applications. However, its relatively low strength and susceptibility to hydrogen embrittlement (HE) under extreme environments limit its broader use, particularly in hydrogen-rich settings. This study explores the combined application of Laser-Directed Energy Deposition (L-DED) and Laser Shock Peening (LSP) to enhance both the mechanical properties and hydrogen embrittlement resistance of 316L stainless steel. The L-DED process was optimized to fabricate 316L stainless steel components, followed by the application of multiple LSP treatments to induce plastic deformation and introduce compressive residual stress. Microstructural analyses using EBSD and SEM/EDS revealed grain refinement and an increase in dislocation density, which contributed to improved mechanical performance. Vickers hardness, slow strain rate tensile tests (SSRT), and hydrogen thermal desorption analyses were performed to assess the enhanced tensile strength and reduced hydrogen embrittlement susceptibility. The results demonstrated a significant improvement in both yield strength and wear resistance, as well as a notable reduction in hydrogen embrittlement susceptibility, confirming the effectiveness of LSP in improving the structural integrity of 316L stainless steel in harsh environments.

Keywords : 316L Stainless Steel, Laser, Directed Energy Deposition, Laser Shock Peening, Hydrogen Embrittlement Resistance, Mechanical Properties

5. Microstructure Evolution and Mechanical Characterization of SUS 316L-VCr Tool Steel Fabricated by DED

Ha Jeonghong ¹

¹ - Korea Institute of Industrial Technology (South Korea)

Stainless steel, known for its excellent corrosion resistance, oxidation resistance, and formability, is widely used in industries such as automotive, aviation, and medical care. However, its relatively low hardness and tensile strength limit its use in extreme environments. To overcome these limitations, studies have explored mechanical property enhancements through methods such as laser shock peening and high-pressure torsion. Recently, multi-materials, particularly those fabricated via Directed Energy Deposition (DED), have gained significant attention for their ability to combine the strengths of different materials, such as stainless steel and tool steel, to achieve superior multifunctionality. This study focuses on the fabrication and optimization of multi-materials composed of stainless steel and vanadium tool steel using DED. Process optimization was performed for both materials by adjusting key parameters, and three types of multi-materials were created by varying the powder feed rate of tool steel while maintaining a constant stainless steel feed rate. Microstructural analysis was conducted using optical microscopy and SEM/EDS to examine bonding characteristics. Mechanical properties were evaluated through Vickers hardness testing, tensile testing, and linear reciprocation abrasion testing. The results confirmed significant improvements in the tensile strength and wear resistance of stainless steel, along with enhanced elongation in vanadium tool steel, demonstrating the potential of multi-materials for extreme environment applications.

Keywords : Additive Manufacturing, Directed Energy Deposition, Stainless Steel, Tool Steel, Multi Materials

6. Tribological Properties of STS316L Sintered Body and Cu/STS316L Composite Using Binder Jetting Process

Kim Kyung Il ¹

1 - Korea Institute of Industrial Technology (South Korea)

The binder jetting (BJT) process offers high material selectivity and shape realization compared to other AM processes and enables the production of porous and composite materials through sintering and impregnation, common in powder metallurgy. STS316L powder, widely used in BJT, has excellent weldability, corrosion resistance, and tribological properties, yet studies on its tribological behavior remain limited. In this study, tribological tests were conducted on STS316L sintered bodies and Cu/STS316L composites fabricated via BJT. Sintering was done at three temperatures (1100, 1200, and 1300,°f), and tribological tendencies were analyzed using the Pin-on-disc method. The friction coefficients and microstructures of the tribological traces were examined with scanning electron microscopy (SEM) and energy-dispersive X-ray spectroscopy (EDS). The results showed that for STS316L, both friction coefficient and tribological mark size increased with sintering temperature. In contrast, Cu/STS316L composites exhibited stable friction coefficients and smoother wear marks under all conditions. The tribological mechanisms were identified through microstructure analysis of the wear marks

Keywords : Binder jetting, Tribology, Friction coefficient, Sintering

7. Towards the defect-tolerant design of laser powder bed-fused metal parts: example of Ti64 alloy

Brailovski Vladimir ¹

1 - Ecole de Technologie Supérieure (1100, rue Notre-Dame Ouest, Montreal (Quebec) H3C 1K3 Canada)

To establish the basics for defect-tolerant design of laser powder bed-fused (LPBF) parts, it is imperative to assess the evolution of fatigue resistance of printed material as a function of the maximum size of LPBF-induced flaws. To this end, three groups of Ti64 specimens were printed by modifying the printing conditions: the first with the lowest level of porosity

Keywords : Laser Powder Bed Fusion, Ti, 6Al, 4V alloy, Fatigue, Defect, Tolerant Design

8. Effect of additive manufacturing-induced metastable retained austenite and austenite reversion on the mechanical properties of Corrax® stainless steel

Tsai Chuan ¹, Yen Hung-Wei ², Wu Ming-Wei ³

1 - Department of Materials Science & Engineering, National Taiwan University (Taiwan), 2 - Department of Materials Science & Engineering, National Taiwan University (No. 1, Sec. 4, Roosevelt Road Taiwan), 3 - National Taipei University of technology [Taipei] (Taiwan)

This study investigates the role of retained austenite in mechanical properties of Corrax® maraging steel fabricated via laser powder bed fusion (LPBF). Advanced nano/microstructural characterizations by electron backscattering diffraction, transmission electron microscopy, and atom probe tomography are conducted to elucidate the microstructure-property relationships in the Corrax® maraging steels subjected to various printing directions and aging treatments. Moreover, cryogenic treatments and pre-straining tests were employed to reveal the impacts of austenite stability on the yield strengths. Here, nano/microstructural results showed that the retained austenite in as-built samples originates from incomplete martensitic transformation during rapid cooling. Such retained austenite has low stability and undergoes stress-assisted martensitic transformation, leading to early onset of yielding. During aging at 525 °, NiAl precipitation and austenite reversion occur simultaneously. The precipitation of NiAl intermetallic compound largely increase the strength. Besides, unexpected fraction of high-stability retained austenite forms during aging. Hence, transformation-induced plasticity (TRIP) effect help keep pace with the high flow stress during plastic deformation. This study provides comprehensive insights into the importance of austenite metastability in additively manufactured steels with retained austenite.

Keywords : Additive manufacturing, Metastable retained austenite, Austenite reversion, TRIP, Atom probe tomography

9.Improving High-Temperature Performance of Inconel 718 Using Ceramic Particle-Coated Superalloy Powders in Laser Additive Manufacturing

Jeong Wonjong , Kim Chaerin , Ryu Ho Jin ¹

1 - Korea Advanced Institute of Science and Technology (291 Daehakro, Yuseong, Daejeon South Korea)

Laser-based powder directed energy deposition (LP-DED) has emerged as a promising additive manufacturing (AM) method for fabricating large-scale, high-performance metallic components, particularly for aerospace applications. In this study, Inconel 718 superalloy powder was reinforced with various ceramic particles, including carbides (TiC, HfC), nitrides (TiN, BN), and borides (TiB₂), and processed using LP-DED. The ceramic particles were incorporated through a core-shell coating on spherical Ni-based superalloy powders, enhancing laser absorption and promoting efficient melting and solidification. The dissolution of ceramic particles in the matrix resulted in refined and equiaxed microstructures due to enhanced nucleation, thereby improving mechanical properties. Tensile testing revealed significant increases in both yield strength and elongation at room and elevated temperatures. Additionally, the distribution of dissolved elements such as Hf and B along grain boundaries strengthened these regions, mitigating intergranular cracking. These findings highlight the potential of ceramic additives to enhance the mechanical performance and manufacturability of Ni-based superalloy components produced via laser-based AM methods.

Keywords : Metal Additive Manufacturing, Powder Processing, Metal Matrix Composite, Superalloys, Mechanical Properties

10. Minimum ductility at intermediate temperatures of Al-Fe-Cr-X alloys processed by L-PBF

CarrenO Fernando ¹, Bahari-Sambran Farid ^{1 2}, Orozco-Caballero Alberto ², Cepeda-JimeNez Carmen M. ¹

1 - Consejo Superior de Investigaciones Cientificas (CENIM, CSIC) (Spain), 2 - Universidad Politecnica de Madrid (Spain)

The development of AM of metals opens new possible applications and new solutions for complex geometries which can be further optimized with digital tools. However, this new technology requires the melting of powders or wires to solidify additively layer by layer, which makes the processing alloys containing volatile elements difficult. In the particular case of aluminum alloys, the well-developed high-strength wrought alloys are quite difficult to process by AM. Thus, significant worldwide research is being carried out to obtain suitable new Al alloys for AM processing. Usually, this implies the use of transition elements with low volatility. Additionally, the low diffusivity in the aluminum matrix of these alloying elements decreases the need of post-processing thermal treatments. In this work, transition metal elements such as Fe, Cr and Ti have been chosen for the production by laser-powder bed fusion (L-PBF) of high resistant Al alloys at both, room and high temperatures. Their mechanical properties have been studied and a region of minimum ductility has been observed around 200 °C in all cases, which is an undesired behavior when targeting structural responsibility. Variations in strain rate sensibility have been observed by performing strain rate change tests, related to the dynamic strain aging (DSA) effect. Additionally, static strain aging (SSA) peaks have been observed in some testing conditions. Therefore, solutes play an important role in the medium to high temperature behavior, which effects are discussed taking into account the metastability and the expected excess of solutes in the as-processed alloys.

Keywords : Aluminum alloys, transition elements, laser powder bed fusion (LPBF), mechanical properties, minimum ductility, dynamic strain aging (DSA)

11. Influence of a modulated laser irradiation on the LPBF process stability, induced microstructures and mechanical properties of Al10SiMg alloy

Peyre Patrice ¹, Hebrard Pierre ¹, Barkia Bassem ², Leguen Emilie ³,
Demir Ali Gokhan ⁴, Galbusera Francesco ⁴, Caprio Leonardo ⁴

1 - PIMM Lab., Arts et Metiers Science & Technology, 75013 Paris (France), 2 - PIMM Lab., Arts et Metiers Science & Technology, 75013 Paris (France), 3 - I2M (France), 4 - Politecnico di Milano (Italy)

A modulated (or pulsed wave PW) LPBF laser regime was tested and compared with the classical CW (continuous wave) mode on an Al10SiMg aluminum alloy. Two frequencies (5 kHz and 50 kHz) were used for a large range of (power, scan speed) conditions, and with duty cycles DC (= laser time-on / laser period) comprised between 0.5 and 0.8. Their influence was considered on the following aspects: ¹ (P, V) process stability windows on single LPBF tracks, ² induced microstructures on 3D parts analyzed with optical and scanning microscopy and EBSD, ³ mechanical resistance during tensile testing. On single LPBF tracks, smaller process windows were obtained in PW mode, especially for the lower frequency of 5 kHz and the lower DC values inducing longer interruptions of the laser irradiation. More spatters and stronger oscillations of the melt-pool were also shown in PW regime, inducing deleterious build surface finishes. On 3D parts, nearly similar densities (99.9 %) could be obtained with both CW and PW conditions, but grain orientations on (X, Y) build planes were different with continuous lines oriented //BD for the CW regime versus islands of //BD areas for the PW regime. At a lower scale, no clear refinement of solidification cells was evidenced despite an increase of cooling rates at low DC. Finally, tensile tests parallel to BD (build direction) exhibited moderate differences between PW and CW specimens.

Keywords : Additive manufacturing, Laser, LPBF, pulsed wave, Aluminum

12. Elastic properties of laser powder bed fusion processed β -phase Ti alloys

Tane Masakazu ¹, Higashino Shota ², Miyoshi Eisuke ², Ishimoto Takuya ^{1 3}, Nakano Takayoshi ¹

1 - Osaka University (Japan), 2 - Osaka Metropolitan University (Japan), 3 - University of Toyama (Japan)

β -phase Ti alloys with a body-centered cubic (bcc) lattice have attracted considerable attention as biomedical implants such as artificial hip joints and dental implants. This is because β -phase Ti alloys have a low Young's modulus, which is required to prevent bone degradation and absorption caused by the difference between the Young's moduli of the implants and natural human bone. Recently, it has gathered much interest that the Young's modulus of β -phase Ti alloys can be reduced by controlling the crystallographic texture achieved by the laser powder bed fusion (LPBF) process. However, the effects of the texture and microstructure formed by the LPBF process on the elastic properties have not been revealed in detail. In the present work, the elastic properties of β -phase Ti alloys prepared by the LPBF process were studied. In order to reveal the effects of the anisotropic texture and microstructure formed by the LPBF process on the elastic properties, the anisotropic elastic properties were measured using resonance ultrasound spectroscopy. In addition, the correlation between the anisotropic elastic properties and the microstructures was analysed using micromechanics models. These analyses revealed a potential strategy for the design of LPBF-processed β -phase Ti alloys with low Young's modulus.

Keywords : Elastic properties, laser powder bed fusion process, Biomedical materials

13. Microstructure control of TiAl alloys using peculiar thermal history of additive manufacturing

Cho Ken ¹, Yasuda Hiroyuki Y. ², Takeyama Masao ³, Nakano Takayoshi ²

1 - Osaka University (Japan), 2 - Osaka University (Japan), 3 - Institute of Science Tokyo (Japan)

TiAl alloys are expected to become key materials for achieving carbon neutrality due to their light weight and high strength at high temperatures. We found that unique microstructures can be obtained in TiAl alloys fabricated by electron beam powder bed fusion (EB-PBF) process via ultra-fast cooling and repeated thermal effect from melt pool, which are phenomena peculiar to this process. In particular, it was revealed that nano lamellar structure with a lamellar spacing of a dozen nm is formed in β -containing TiAl alloys. The nano lamellar structure is formed through massive α transformations induced by the ultra-fast cooling. In addition, we also found that the strength of the alloys is improved significantly by the nano lamellar structure.

Keywords : Additive manufacturing, Electron beam powder bed fusion, TiAl, Microstructure, Mechanical properties

14. Design of high entropy alloy with suppressed elemental segregation for laser powder bed fusion process

Gokcekaya Ozkan ¹, Kim Yong Seong , Nakano Takayoshi

¹ - Division of Materials and Manufacturing Science, Osaka University (Osaka, 565-0871 Japan)

High entropy alloys (HEAs) are attracting attention as next-generation biomaterials due to their exceptional mechanical properties and corrosion resistance; however, casting, which is a commonly used method for HEA fabrication, results in severe compositional segregation at slow cooling rates and lacks shape customizability. In this context, this study demonstrates the superior potential of laser power bed fusion (LPBF) in overcoming these issues by enabling simultaneous suppression of segregation through supercooling, shape customization, and control of crystallographic texture. Nonetheless, challenges related to the segregation of high melting point elements at the melt pool boundary and the high time and cost associated with producing pre-alloyed powder still need to be addressed during the LPBF process. To overcome the segregation at the melt pool boundary during the LPBF process, this study developed a new non-equiatomic HEA using thermodynamic calculations and CALPHAD and conducted in-situ alloying using mixed powder to address the limitations associated with pre-alloyed powder in LPBF. The results showed that the HEA manufactured through arc melting exhibited a single-phase solid solution with suppressed component segregation despite the slow cooling speed owing to the novel alloy design approach. At the same time, the in-situ alloyed HEA produced through LPBF achieved single-phase super solid solutions with less segregation compared to casting. Additionally, the new non-equiatomic HEA exhibited biocompatibility similar to that of CP-Ti, higher mechanical strength than CP-Ti, and lower Young's modulus than CP-Ti through control of crystallographic texture, indicating its potential as a next-generation metallic biomaterial and cost-efficient in-situ alloying process.

Keywords : High, entropy alloy, Laser powder bed fusion, Segregation, Texture

15. Effect of Surface Conditions on Mechanical Properties of IN718 and IN625 Manufactured by Additive/Subtractive Laser Powder Bed Fusion Technology

Sarafan Sheida ¹, Wanjara Priti ¹, Gholipour Javad ¹, Atabay Sila ¹,
Soost Josh ²

1 - National Research Council Canada (Canada), 2 - Matsuura USA (United States)

Additive/subtractive hybrid manufacturing (ASHM) leverages the advantages of laser powder bed fusion (LPBF) with high-speed milling to produce parts that have intricate geometries, high surface quality and accurate dimensional tolerances in one setup (in-envelope process). Development of this ASHM process, however, entails thorough understanding of the synergies of the additive and subtractive sequences that influence the heating/cooling cycles and, in turn, affect the resulting microstructure, defects, distortion, dimensional integrity of un/machined surfaces, and mechanical properties of the final part. An overview of the ASHM research on two superalloy materials Inconel 718 and Inconel 625 (hereinafter IN718 and IN625) is provided to bridge key knowledge gaps and establish the process-microstructure-property relationships. The results examine the tensile properties of 3D printed vertical tensile samples manufactured by three different manufacturing paths: LPBF only (as-built, no machining), LPBF + dry micro-milling (ASHM, in-envelope) and machining performed after 3D printing and separating the tensile samples from the base plate (post-machined). The influence of the surface quality, resulting from various paths, was examined before and after various heat treatments by tensile testing at room and high temperature (650°C). Moreover, the density, porosity, microstructure, and hardness were also evaluated and linked to the mechanical performance of the materials built by the different manufacturing paths. Based on the findings, the presentation will discuss future areas for research and technology advancement vis-à-vis application of ASHM in the automotive and aerospace industrial sectors.

Keywords : Additive/Subtractive Hybrid Manufacturing, Laser Powder Bed Fusion, Superalloys, IN718, IN625, Tensile Properties

16. Electron Microscopy Studies on Orientation-Controlled 316L Austenitic Stainless Steel Produced by Laser Powder Bed Fusion

Sato Kazuhisa ¹, Takagi Shunya ¹, Ichikawa Satoshi ¹, Ishimoto Takuya ^{2 3 4}, Nakano Takayoshi ^{2 3}

1 - Research Center for Ultra-High Voltage Electron Microscopy, The University of Osaka, Ibaraki, 567-0047 (Japan), 2 - Division of Materials and Manufacturing Science, Graduate School of Engineering, The University of Osaka, Suita, 565-0871 (Japan), 3 - Anisotropic Design and Additive Manufacturing Research Center, The University of Osaka, Suita, 565-0871 (Japan), 4 - Aluminium Research Center, University of Toyama, Toyama, 930-8555 (Japan)

We have studied the microstructure and solute segregation around the melt-pool boundary (MPB) of orientation-controlled 316L austenitic stainless steel produced by laser powder-bed fusion (LPBF) using transmission electron microscopy and associated spectrometry. We found that the solidification cellular microstructures were visualized with the aid of solute segregation (Cr and Mo). Mn-Si-O inclusions (10-15-nm in diameter) were distributed along the lamellar boundaries, as well as in the dislocation cell walls. It is considered that grain growth of the inclusions can be effectively suppressed by rapid quenching during the LPBF process. The cellular spacing widened near the bottom of the MPB. A thin region without cellular microstructures was observed at the MPB, possibly a planar solidification zone. The low mobility of the solid/liquid interface will stabilize the planar solidification [1]. Local valence analysis of the LPBF-produced 316L by electron energy-loss spectroscopy revealed no obvious changes in the energy-loss near-edge structures of Cr and Fe measured within the solidification cellular microstructure, at the cell boundary, or at the MPB. This result indicates that solidification segregation in the LPBF-produced 316L is unlikely to affect the corrosion resistance of the material [2]. This study was supported by Grant-in-Aid for Transformative Research Area (A) (Grant No. 21H05196) from the MEXT, Japan. [1] K. Sato, S. Takagi, S. Ichikawa, T. Ishimoto, T. Nakano, *Materials*, 16, 218 (2023), [2] K. Sato, S. Takagi, S. Ichikawa, T. Ishimoto, T. Nakano, *Materials Letters*, 372, (2024) 136978.

Keywords : Additive Manufacturing, Laser Powder Bed Fusion, Crystallographic Lamellar Microstructure, Solute Segregation, Electron Energy Loss Spectroscopy

17. Substrate tubing heater suitable for large volume 3D printing with extrusion of thermo-reversible hydrogel

Engels Andreas ¹, Speck Sandy ², Schlegel Volker ¹, Jacobs Hannes ¹, Krenz-Baath Rene ¹, Boehme Andrea ¹

1 - Technical University of Applied Sciences Wildau (Germany), 2 - Technical University of Applied Sciences Wildau (Germany)

The advancement of 3-dimensional printing technology over the past ten years has raised interest in and accessibility to these devices. Due to its consistent growth and demand, 3D printing is becoming a consumer-friendly, reasonably priced craft. Due to technological advancements, it is becoming more and more integrated into broader fields of science and research, as well as the manufacturing sector as a whole. The need for customized solutions is constantly growing across several industries.

The 3D extrusion of hydrogels is advancing in the field of biomaterials with a broad spectrum of biomedical applications. Extrusion print heads often use stepper motors or pneumatic pressure systems to push the substrate onto a surface. These techniques are well-suited for materials with high viscosity. While these systems are usually bound to the syringe volume, a refillable reservoir enables to print above the syringe's limitations.

We developed a low-cost standalone heating system for silicon tubes to control the temperature, hence avoiding jellification and clogging of the tubing system leading to the nozzle of the print head. The system connects to an in-house made peristaltic pump, which forces the e.g. gelatin through the nozzle with low pulsation, enabling us to extrude multiple layers of precise tempered gelatin. The heating system is based on easily available materials and electronic components and does not require expensive tools.

Keywords : biomaterial printing, 3D printing, hydrogel, gelatin processing, low cost

18. Development of Material-Based Process Simulation Technology for BAAM and Composite AM

Ko Jong Wan ¹

1 - Korea Institute of Industrial Technology (South Korea)

As 3D printing technology advances, the demand for its industrial applications is increasing. Many efforts are being made to apply it to products that were previously impossible to manufacture using traditional processes. BAAM (Big Area Additive Manufacturing) and plastic-based composite 3D printing technologies are drawing attention for their potential to overcome technical limitations inherent in conventional manufacturing techniques like vacuum forming, injection molding, and CFRP molding, which include shape and size restrictions and the anisotropy of materials used. Recent studies have demonstrated that simulating the layering process can allow for the preemptive identification of potential issues, such as layer bonding, pores/cavities formation, material inhomogeneity, and warping, enabling the setting of process conditions that compensate for these problems. However, there are still discrepancies between simulation results and the actual quality of printed products, indicating challenges in achieving consistent outcomes. Additionally, a material validation platform is needed to drive innovation in BAAM and composite AM (Additive Manufacturing) processes through the development of new materials. This study aims to introduce high-accuracy BAAM and composite AM process prediction models by simulating material flow and its AM process. By utilizing simulation tools for new material development and collecting case studies of real applications, the study seeks to validate both materials and processes. Furthermore, it will present trends in the application of high-performance engineering plastics, such as PEEK, PEKK, and ULTEM (PEI), which extend beyond conventional engineering plastics and are suitable for use in aerospace, defense, and space sectors.

Keywords : Additive Manufacturing, Composite AM, Engineering Plastic, Simulation, BAAM, Process Optimization

19. Graphitic carbon nitride (g-C₃N₄) as a Filler in the Photocuring 3D Printing Process for Enhanced Mechanical Properties

Ko Jong Wan ¹, Ha Jeonghong ¹, Nam Jungsoo , Park Daegeun , Park Jiyong , Kim Kyung Il , Lee Seungmin

¹ - Korea Institute of Industrial Technology (South Korea)

3D printing or additive manufacturing (AM) technology is an emerging advanced manufacturing technology that offers a high degree of design freedom to manufacture complex-shaped products that were previously unattainable with conventional manufacturing methods. In particular, this technology is actively being researched in the polymer industry, which requires the fabrication of complex-shaped products. Several polymer 3D printing methods exist, such as fused deposition modeling (FDM), stereolithography (SLA), selective laser sintering (SLS), and digital light processing (DLP). DLP 3D printing, a representative photocuring 3D printing method and one of the most widely used techniques, has a very fast printing speed compared to other 3D printing processes due to its ability to solidify and laminate each layer simultaneously using a planar light source. It provides exceptional precision and surface smoothness in the printed product. However, DLP 3D printing has limitations, particularly in the low mechanical strength of the printed products, which is attributed to the inherent characteristics of photocurable resins, such as low crosslinking density. In this study, we propose graphitic carbon nitride (g-C₃N₄), a novel filler containing multiple hydrogen bonding motifs (-NH₂, -NH functional groups), to enhance the mechanical strength of general DLP acrylic resin. It was demonstrated that g-C₃N₄ can facilitate hydrogen bonding between the matrix and g-C₃N₄ molecules, thereby increasing intermolecular interactions and resulting in improved mechanical properties. Consequently, it was confirmed that the tensile strength of the DLP printed composite material increased by 22%, and the elastic modulus improved by 34% compared to the neat DLP polymer specimen.

Keywords : Additive Manufacturing, Composite AM, Graphitic Carbon Nitride, Mechanical Strength, Tensile Strength, Filler, Matrix

20. A Novel Strategy for the Control of Crystallographic Texture of Metals with Non-Cubic Crystal System via Powder Bed Fusion using a Laser-Beam of Metals

Ozasa Ryosuke ^{1 2}, Hagihara Koji ^{2 3}, Nakano Takayoshi ^{1 2}

1 - Division of Materials and Manufacturing Science, Graduate School of Engineering, The University of Osaka (Japan), 2 - Anisotropic Design and Additive Manufacturing Research Center, The University of Osaka (Japan), 3 - Department of Physical Science and Engineering, Nagoya Institute of Technology (Japan)

Crystallographic texture is one of the determinants of physical, chemical and biological properties in metallic materials. Despite the validity of conventional techniques for controlling the texture, the shape of the obtained products is limited. This study focused on powder bed fusion using a laser-beam of metals (PBF-LB/M), one of the additive manufacturing (AM) techniques, as a method for controlling crystallographic texture. Our group previously achieved the control of crystallographic texture in metals with cubic crystal system such as Ti-based alloys but not in metals with non-cubic crystal system such as a Mg-relating materials with a hexagonal close-packed (hcp) structure using PBF-LB/M. The purpose of this study is to develop single-crystalline-like texture and control mechanical functions in Mg alloy. The PBF-LB process using spherical Mg alloy powder was conducted by the EOS M290 (EOS, Germany) system. Microstructural observations were performed using SEM-EBSD and STEM. Compression test was conducted to determine mechanical properties. Thermal diffusion simulation was carried out by finite element method. Numerical simulations revealed the heat flux directionality occurred in Mg-alloy. Notably, this study, for the first time, succeeded to develop single-crystalline-like texture through AM by employing the scanning strategy inspired by the calculated heat flux directionality and symmetry of hcp structure. The PBF-LB/M-fabricated products exhibited anisotropic mechanical properties that is the same trend in single crystals of Mg. This is the first study to develop single-crystalline-like texture in metals with non-cubic crystal system through AM.

Keywords : Additive Manufacturing (AM), Powder Bed Fusion using a Laser, Beam of Metals (PBF, LB/M), Magnesium, Hexagonal Close, Packed (hcp) Structure, Crystallographic Texture

21. Additive Manufacturing of Cell-Based 3D Bone-Mimetic Collagen/Apatite Structures

Matsugaki Aira ^{1 2}, Nakano Takayoshi ^{2 1}

1 - Division of Materials and Manufacturing Science, Graduate School of Engineering, The University of Osaka (Japan), 2 - Anisotropic Design and Additive Manufacturing Research Center, The University of Osaka (Japan)

The formation of the bone matrix texture is primarily regulated by the unidirectional arrangement of osteoblasts, which is governed by three-dimensional communication among the cells. The replacement of damaged tissues or organs with bio-mimetic structures facilitates the rapid restoration of their intrinsic functions. Our recent findings demonstrate the significant effects of cellular activation using metal additive manufacturing materials. We aim to achieve an artificially ordered collagen/apatite bone matrix, mediated by aligned osteoblasts, using additive manufacturing techniques such as laser powder bed fusion (PBF-LB) and bio-3D printing. Titanium surface topography was successfully controlled using PBF-LB, enabling unidirectional cellular alignment and promoting ordered bone matrix formation. Human mesenchymal stem cells were cultured on the fabricated substrates. Additionally, we successfully created a 3D bone-mimetic anisotropic microstructure using the bio-additive manufacturing method with a laminated layer technique to orient the collagen scaffold. The unidirectional arrangement of osteoblasts was artificially controlled through scaffold design, which activated integrin signaling. Remarkably, the surface structure directed the mesenchymal stem cells toward the osteogenic lineage without the need for additional stimuli. Extended culture led to the differentiation of osteoblasts into osteocytes, accompanied by the formation of the ordered bone matrix texture. As the cells and matrix matured, they further established a network of osteocytes within the bone matrix, demonstrating that the bioprinting process replicated the biological processes of bone differentiation and functionalization outside the body. These results offer promising prospects for the development of customized bone medical devices and contribute to the advancement of bone organoid research.

Keywords : Additive manufacturing, Bone matrix microstructure, Artificial control of 3D Cell arrangement

22. Effect of building conditions on high-temperature tensile properties of IN738LC fabricated by laser powder bed fusion

Kusano Masahiro ¹, Osada Toshio ², Watanabe Makoto ³

1 - National Institute for Materials Science (Japan), 2 - National Institute for Materials Science, Tsukuba, Ibaraki, 305-0047, Japan. (Japan), 3 - National Institute for Materials Science (Japan)

Laser powder bed fusion (L-PBF), one of additive manufacturing processes, enables the fabrication of near-net-shape products and shows promise for producing engine components of nickel-based superalloys in the aerospace industries. On the other hand, the poor processability of nickel-based superalloys, which are prone to cracking during the additive manufacturing process, remains a significant challenge for their practical application. In our previous study on Inconel 738LC (IN738LC) fabricated by L-PBF, we empirically identified optimal laser scanning conditions that effectively prevent solidification cracking during processing. In this study, we further investigate the effects of these optimal laser scanning conditions as well as building directions and post-heat treatment conditions, on the high-temperature tensile properties of IN738LC. The results indicate that IN738LC fabricated with the optimal conditions exhibits excellent strength and ductility from room temperature to 600°C, while its properties above 800°C were comparable to those of precision-cast material. In the presentation, we will discuss the factors affecting these mechanical properties based on the microscopic analyses of fracture surfaces and crystal orientations.

Keywords : Additive manufacturing, Laser powder bed fusion, IN738LC, High, temperature tensile properties, building conditions

23. Growth of Antiphase Domain in Laser-Irradiated Region and Superelasticity of Single-Crystal-Like Fe₃Al Fabricated by Laser Powder Bed Fusion Process

Liu Yuheng^{1,2}, Sato Tsubasa¹, Okugawa Masayuki^{1,2}, Sato Kazuhisa³,
Yasuda Hiroyuki Y.^{1,2}, Nakano Takayoshi^{1,2}, Koizumi Yuichiro,^{1,2}

1 - Graduate School of Engineering, Division of Materials and Manufacturing Science, Osaka University (Japan), 2 - Anisotropic Design and Additive Manufacturing Center, Osaka University (Japan), 3 - Research Center for UHVEM, Osaka University (Japan)

Superelasticity in Fe₃Al intermetallic single crystals is attributed to interactions between antiphase domain (APD) boundaries and dislocations. Recent progress in additive manufacturing, particularly the laser powder bed fusion (L-PBF) process, enables the fabrication of single-crystal-like parts by employing optimized scanning strategies. Here we demonstrate the effects of excess vacancies generated during the rapid cooling inherent to the L-PBF process on APD growth in Fe₃Al alloys, with the aim of achieving superelasticity in L-PBF-fabricated Fe₃Al. Diffraction analysis revealed D0₃-type ordered structure in as-fabricated samples, although the APDs were too fine to measure directly. APD growth was significantly enhanced in laser-melted regions compared to bulk samples subjected to conventional water quenching. This enhancement is likely driven by the high concentrations of excess vacancies introduced during rapid solidification. However, the mobility of APD boundary was lower than expected by phase-field method based on calculated vacancy concentrations at the solidus temperature. This suggests that dislocations within the laser-irradiated regions act as sinks for vacancies, mitigating the effects of supersaturation. Microstructural analysis using SEM-EBSD demonstrated the formation of single-crystal-like textures with crystallographic orientation along the X, Y, and Z directions. In addition, SEM-EDS detected no solute segregation, indicating solidification under conditions of absolute stability. These findings indicates the potential of L-PBF for the precise control of microstructures in Fe₃Al. Moreover, preliminary tensile test experiments further suggest the emergence of superelastic behavior.

Keywords : Additive Manufacturing, Processing, Microstructure, Superelasticity

24. Innovative design of crystallographic textures and macroscopic shapes via metal additive manufacturing

Nakano Takayoshi ¹

1 - Osaka University (Japan)

Metal additive manufacturing (AM) has allowed a wide range of control over metallurgical microstructures as a unique manufacturing method of stacking powders layer-by-layer to fabricate products with complex shapes and high precision. In metal AM, the metal microstructure can be controlled by specific solidification directions and steep cooling, which enables the control of the metallurgical microstructure. In my talk, I will present some of the results of my research group on the control of crystallographic texture by laser powder bed fusion (LPBF). In cubic crystal system, we succeeded in artificially producing the oriented single-crystalline-like textured microstructures representing three directions, , , and parallel to the build direction (BD), by LPBF. Such successful control of crystal orientation, together with 3D control of shape, has the potential to trigger novel and innovative designs via AM.

Keywords : Laser Powder Bed Fusion, Crystallographic Texture Control, Mechanical Property

25. Microstructures and Hardness of WC-Co and WC-HEA Cemented Carbides Additively Manufactured by the Multi-Beam Laser Directed Energy Deposition

Kunimine Takahiro ¹, Guo Wenheng ¹, Ebihara Kaito ¹, Yamashita Yorihiro ², Yasui Shintaro ³

1 - Kanazawa University (Japan), 2 - University of Fukui (Japan), 3 - Institute of Science Tokyo (Japan)

The WC-Co cemented carbide is one of the metal-matrix composites produced by sintering hard WC carbide with Co as metallic binder at high temperatures, and has excellent hardness and wear properties. In recent years, the high-entropy alloys (HEAs), which contain at least five elements with equiatomic or near-equiatomic ratio, have gained significant attention. The HEAs possess unique properties, which cannot be achieved by conventional alloying approaches based on only one alloying element, such as enhanced mechanical properties at high temperatures induced by severe lattice distortion effect and sluggish diffusion effect. In this study, HEAs was applied to an alternative binder for the WC-Co cemented carbide as an attempt to seek enhanced mechanical properties. In the experiment, HEA powders such as the CrMnFeCoNi and CrFeCoNiMo HEAs were used as binder to fabricate WC-HEA cemented carbides by the multi-beam laser directed energy deposition (L-DED). WC-Co cemented carbide powder was also used for a comparative study. The multi-beam L-DED is one of the additive manufacturing (AM) processes. The WC-HEA cemented carbide powders were processed as single beads and square-shaped samples. Phase identification of the samples was performed by the X-ray diffraction (XRD). Microstructural observations were performed by a scanning electron microscope (SEM). The experimental results suggested the possibility for controlling hardness by tailoring formed carbides easily by laser processing condition and alloying elements than the conventional processing routes.

Keywords : Additive Manufacturing, Directed Energy Deposition (DED), Cemented Carbides, High Entropy Alloys (HEAs), Binder

26. Development of an environmentally friendly and low-cost binder for 17-4PH metal part printing via Fused Deposition Modeling

Khazaei Sheyda ¹, Martin Etienne ¹, Boukhili Rachid ¹, Bitar-Nehme Elie ¹, Kostenov Jovan ², Regnaud William ²

1 - Polytechnique Montreal (Canada), 2 - Dyze Design (Canada)

Using wax as a binder in metal fused deposition modeling (mFDM) offers benefits like easy removal, environmental friendliness, and lower costs compared to other polymers. However, wax-based binders usually lead to structural instability during heat treatment. This study aims to optimize a feedstock consisting of 17-4PH stainless steel powder (< 95.5wt.%), paraffin wax (< 5.3wt.%), and stearic acid (< 0.69wt.%) for FDM. Rheology analysis showed that increasing the metal content from 93 to 95.5wt.% significantly raises viscosity but retains printability by adjusting the temperature. Mechanical, physical, and structural properties of the green and/or sintered specimens were evaluated through bending tests, density measurements, debinding, and sintering. Higher metal content improved green parts' flexural strength from 3.34 to 4.45 MPa and relative green density from 0.65 to 0.74. Components with at least 95wt.% metal powder exhibited full structural stability post-sintering, achieving densities over 0.97.

Keywords : Wax binder, Additive manufacturing, FDM, Stainless steel, 17, 4PH, Rheology, 3Point, Bending, Density, Sintering

27. 3D Volume Construction Methodology for Cold Spray Additive Manufacturing

Wu Hongjian ¹, Gaertner Frank ¹, Klassen Thomas ¹

¹ - Helmut Schmidt University, University of the Armed Forces Hamburg (Germany)

Cold spraying has proved as an attractive and rapidly developing solid-state material deposition process that allows for fast formation of high quality, large 3D volume objects. Low risks of undesirable heat effects lead to increased interest in cold spraying based rapid additive manufacturing. However, by continuous powder spraying and high-pressure gas operation, cold spray additive manufacturing in terms of shape building is sensitive to operating parameters and imposes high requirements on the control of process conditions and locally needed kinematics. Every step of the manufacturing process therefore needs to be meticulously conceived and planned, especially the toolpath planning and implementation. This study presents a new implementation method for cold spray additive manufacturing to improve manufacturing accuracy and flexibility. The workflow and principles of the proposed method are explained. The developed algorithms for 3D applications can be well integrated into the cold spray additive manufacturing process for toolpath planning and path parameter determination. Toolpath planning and robot programming are supported and performed by applying virtual cells to simulate the automation process for the real scenario. Applied benchmarking tests prove acceptable shape accuracy and demonstrate that the current method can enhance the capabilities of cold spray additive manufacturing for near-net shape construction.

Keywords : Additive Manufacturing, Cold Spray, Toolpath, Robot, Simulation

28. Effect of heat treatment on the microstructure and impact toughness of PBF-LB manufactured 17-4 PH stainless steel

De Oliveira Melo Renata ¹, Ji Gang ², Nivet Eric ³, Grosjean Christophe ³, Baustert Eric ⁴, Tran Nhu-Cuong ⁵, Villaret Flore ⁶, Bouquerel Jeremie ⁷

1 - Unite Materiaux et Transformations - UMR 8207 (France), 2 - Unite Materiaux et Transformations (UMET UMR CNRS8207) (France), 3 - CEntre Technique des Industries Mecaniques (France), 4 - Volum-e (France), 5 - EDF R&D, EDF Lab des Renardieres, MMC, F-77818 Moret-sur-Loing Cedex, France. EDF (France), 6 - Materiaux et Mecanique des Composants (France), 7 - Unite Materiaux et Transformations - UMR 8207 (France)

17-4 PH is a stainless steel grade widely used in nuclear, chemical, and aerospace industries. In recent years, there has been significant interest in this reliable engineering alloy, particularly when produced through additive manufacturing (AM) methods like Laser Beam Powder Bed Fusion (PBF-LB), due to its design flexibility, customization, and rapid prototyping. However, despite the potential of AM for industrial component production, AM parts for certain alloys such as the 17-4 PH still tend to exhibit lower dynamic properties, such as impact toughness, compared to their conventionally manufactured counterparts, which limits their widespread adoption. This work aims to elucidate the mechanisms underlying the behaviour under high-strain rate loading (impact toughness) in PBF-LB 17-4 PH steel subjected to various heat treatment processes. A range of advanced characterization techniques was employed to analyse microstructural features across multiple scales. X-ray diffraction (XRD) was used to determine global phase compositions, while electron backscatter diffraction (EBSD) and electron channelling contrast imaging (ECCI) were combined associated with scanning electron microscopy (SEM) to assess local plasticity and the way each mesoscopic constituent accommodates plastic deformation. Crack propagation pathways were studied and correlated with the microstructure's capacity to deflect cracks. Transmission Electron Microscopy (TEM) was utilized to examine nanoscale Cu-rich precipitates and Si-rich oxide inclusions. Prospects for improving the impact toughness properties of PBF-LB 17-4 PH steel were also discussed.

Keywords : 17, 4 PH stainless steel, Additive Manufacturing, Laser Beam Powder Bed Fusion (PBF, LB), Impact Toughness

29. Generating a Digital Twin of the Laser Powder Bed Fusion Process

Brabazon Dermot^{1 2 3}

1 - I-Form Advanced Manufacturing Research Centre, Dublin City University, Dublin (Ireland), 2 - Advanced Processing Technology Research Centre, Dublin City University, Dublin (Ireland), 3 - School of Mechanical and Manufacturing Engineering, Dublin City University, Dublin (Ireland)

Metal additive manufacturing, which uses a layer-by-layer approach to fabricate parts, has many potential advantages over conventional techniques, including the ability to produce complex geometries, fast new design part production, personalised production, have lower cost and produce less material waste. While these advantages make AM an attractive option for industry, determining process parameters which result in specific properties, such as the level of porosity and tensile strength, can be a long and costly endeavour. In this review, the state-of-the-art in the control of part properties in AM is examined, including the effect of microstructure on part properties. The simulation of microstructure formation via numerical simulation and machine learning is examined which can provide process quality control and has the potential to aid in rapid process optimization via closed loop control. In-situ monitoring of the AM process couple with modelling and AI technologies, are discussed as a route to enable first time right production in the AM process, along with the hybrid approach of AM fabrication with post-processing steps such as shock peening, heat treatment and rolling. At the end of the presentation, an outlook is presented with a view towards potential avenues for further research required in the field of metal AM.

Keywords : Digital Twin, Additive Manufacturing, Powder Bed Fusion, Thermec'2025, Advance Manufacturing, Processing

30. Low Cycle Fatigue Response of Additive Manufactured Advanced Structural Alloys: Insights into high performance alloy fatigue life

N C Santhi Srinivas ¹, K Chattopadhyay ¹, Shreyasi Vasu ¹, R. Pavan Kumar ¹, Vishwakarma Jaydeep ²

IIT BHU - India

Additive Manufacturing enables the production of intricate geometries and products with improved strength-to-weight ratios, driving its applications in defence, aerospace and advanced engineering sectors. Maraging steel and Inconel 625, renowned for their excellent mechanical properties, are important structural materials for strategic applications. It is essential to study the fatigue behaviour of additively manufactured alloys prior to their deployment in actual working environments, as their fatigue performance differ from those of conventionally manufactured materials. In the present study, low cycle fatigue (LCF) behaviour of Maraging steel and Inconel 625 processed by powder bed fusion, at different strain amplitudes and heat treatment conditions studied and compared with the conventional samples. Build orientation (0° and 90°) significantly affected the fatigue life of additive manufactured maraging steel samples. The LCF testing at different strain amplitudes ($\pm 0.2\%$ to 0.8%) depicted drastic decrease in fatigue life at higher strain amplitude. Microstructural characterization revealed that defects introduced due to layer wise processing of additive samples had adverse effect on fatigue life. Ultrasonic shot peening was applied to the additively manufactured fatigue samples in an effort to enhance their fatigue life, resulted in a slight improvement in the fatigue life of the treated samples. Inconel 625 superalloy demonstrated initial cyclic hardening at room temperature before reaching peak stress in both additive manufactured and heat treated conditions. The fracture analysis revealed numerous crack initiation sites in both Inconel 625 and maraging steel samples. Heat treatment was found to be effective in improving the fatigue life in both alloys.

Keywords : Additive Manufacturing, Maraging Steel, Inconel 625, Powder Bed Fusion, Low Cycle Fatigue, Ultrasonic shot peening

31. Microstructure, Mechanical and Thermal Conductivity Properties of Pure Copper Fabricated by Metal Material Extrusion Additive Manufacturing Process

Lee Kee-Ahn ¹, Park So-Yeon ¹, Yee Na-Yoon ¹, Baek Michelle ²

1 - Inha University (South Korea), 2 - Markforged Korea (South Korea)

Pure copper was fabricated by using metal material extrusion additive manufacturing (M-MEX) process, and its microstructure, mechanical properties and thermal conductivity properties were investigated and compared with conventionally processed (Hot-Rolled) copper. Microstructure observation of M-MEX processed copper showed that it was composed of equiaxed grains with an average grain size of 79.87 μm (LD) / 91.74 μm (WD) / 82.11 μm (BD), and annealing twins existed inside the grains. The Hot-Rolled specimen consisted of elliptical grains along the rolling direction, inside which a large amount of shear bands and slip bands were developed. Room temperature tensile results showed that UTS was 299.8 MPa (Hot-Rolled) / 200.2 MPa (M-MEX WD) / 197.6 MPa (M-MEX BD), respectively, and (El) was 16.6% (Hot-Rolled) / 56.4% (M-MEX WD) / 57.7% (M-MEX BD). The mechanical properties of Hot-Rolled and M-MEX showed a typical strength-ductility trade-off. Furthermore, when comparing the properties with other AM-built coppers, the present M-MEX specimens exhibited good strength and excellent ductility. In the case of M-MEX, dimple fracturing inside the grain occurred throughout the specimen, and the initial stress concentration appeared in the interlayer region where printing voids and high angle grain boundaries were present in high fraction. The deformation behavior of M-MEX processed copper was found to be affected by the extrusion strategy. Thermal conductivity results showed that the TC of the M-MEX material was 329.45 Wm⁻¹K⁻¹, which was comparable to the value of the Hot-Rolled specimen (331.82 Wm⁻¹K⁻¹). The TC value of M-MEX specimens in this study was superior to that of coppers prepared by L-PBF (laser-powder bed fusion) and BJ (binder jetting) AM processes. Based on these, the microstructure and defect formation mechanism of M-MEX built copper and its deformation mechanism and thermal conductivity behavior were also discussed.

Keywords : Metal material extrusion additive manufacturing, Pure copper, Microstructure, Mechanical properties, Thermal conductivity

32. A Study on Monitoring of Large-Scale Composite Material Additive Manufacturing Processes Using Sensor Fusion

Nam Jungsoo, Ru Hangeol, Ju Song Hyeon, Jung Jiwon

Korea Institute of Industrial Technology (South Korea)

Additive manufacturing technology has been gaining increasing attention in both industry and academia due to its versatility and potential. Among the various additive manufacturing methods, screw-based material extrusion is widely regarded as an ideal process for producing large-scale components. In particular, the integration of thermoplastic polymers with fiber-reinforced composites has recently emerged as a focal point of research and development. Despite its advantages, composite material additive manufacturing is highly sensitive to material properties and process conditions. This sensitivity often results in challenges such as mechanical property degradation and quality defects, which necessitate additional time and cost to achieve satisfactory final product quality. These challenges underscore the critical need for effective process monitoring strategies. To address these issues, this study utilized a Thermwood 55AP system to monitor the additive manufacturing process of large-scale composite components and tooling. A sensor fusion approach was adopted, integrating vision cameras, infrared (IR) cameras, and depth cameras to enable comprehensive monitoring. The findings demonstrated that both temperature and geometric quality can be effectively tracked during the manufacturing process, providing valuable insights for process optimization. Building on these results, future research will aim to implement real-time monitoring and feedback control mechanisms, further enhancing the quality and reliability of the additive manufacturing process.

Keywords : Additive Manufacturing, Large scale, Composite, Sensor Fusion

33. Characterization and Effects of Anodized Aluminum Oxide Film on Additively Manufactured AlSi10Mg Alloy

Hamada Atef¹, Rautio Timo¹, Jaskari Matias¹, Nyo Tun Tun²,
JaRvenpaa Antti¹, Abdelghany Ahmed¹

1 - Future Manufacturing Technologies (FMT), Kerttu Saalasti Institute, University of Oulu, Pajatie 5, 85500 Nivala (Finland), 2 - Materials and Mechanical Engineering, Centre for Advanced Steels Research (CASR), University of Oulu, P.O. Box 4200, 90014 Oulu (Finland)

An anodized aluminum oxide film (AnAl-OF) was applied to an additively manufactured (AM) AlSi10Mg alloy using a chemical oxidation method to enhance its electrical conductivity and electrochemical performance. The AnAl-OF was characterized using a scanning electron microscope equipped with an in-lens detector and energy-dispersive X-ray spectroscopy (EDS) to analyze its microstructural features. Surface microindentation hardness testing was conducted to evaluate the coating's strength. Electrochemical behavior was assessed through immersion tests lasting up to 72 hours and potentiodynamic polarization tests in a 3.5% NaCl solution. The results demonstrated that the ~2 µm thick AnAl-OF effectively mitigated critical surface defects such as pores and flaws. The surface hardness of the AM alloy was significantly enhanced due to the presence of the hard aluminum oxide layer. Immersion corrosion tests showed delayed corrosion initiation compared to the as-built alloy. Polarization measurements revealed a marked reduction in anodic dissolution rates and an increase in pitting corrosion resistance for the AnAl-OF-coated surfaces compared to the bare AM AlSi10Mg alloy. This improvement was attributed to the stability of the AnAl-OF layer under anodic overpotential. Moreover, the AnAl-OF reduced the electrical resistance of the AM alloy by 40%, leading to a notable improvement in surface electrical conductivity. These findings highlight the potential of AnAl-OF to enhance both the electrochemical and electrical properties of AM AlSi10Mg alloys.

Keywords : Anodized oxide film, additively manufactured AlSi10Mg alloy, surface hardness, corrosion resistance, electrical conductivity

34. Advanced Laser Scanning Strategies for Minimizing Thermal Residual Stress in Additively Manufactured Topologically Optimized Automotive Parts

Park Jiyong

1 - Korea Institute of Industrial Technology (South Korea), 2 - University of Science and Technology [Daejeon] (South Korea)

This study addresses thermal residual stress reduction during Powder Bed Fusion (PBF) of topologically optimized, lightweight automotive brake calipers. While topology optimization enhances strength and reduces weight, it introduces challenges like thermal deformation due to uneven melting area ratios. To mitigate this, an advanced laser scanning strategy was developed to minimize anisotropy and residual stress, enabling successful manufacturing. Validation through JASO C406-compliant brake dynamometer tests confirms the redesigned caliper's superior performance compared to conventional models, particularly under lightweight conditions. This work provides key insights into overcoming manufacturing challenges for optimized automotive components.

Keywords : Additive Manufacturing, Powder Bed Fusion, Thermal Residual Stress, Ti, 6Al, 4V, Laser Scanning Strategy

35. Advancing Energy Absorption Through Hybrid Lattice Structures Fabricated via Powder Bed Fusion

Park Jiyong

1 - Korea Institute of Industrial Technology (South Korea), 2 - University of Science and Technology [Daejeon] (South Korea)

This study investigates the enhanced energy absorption performance of hybrid lattice structures fabricated using Ti-6Al-4V alloy and powder bed fusion (PBF) technology, emphasizing their potential across energy-intensive industrial applications. Three lattice geometries-octet truss (OT), diamond (DM), and diagonal (DG)-were designed and fabricated at varying densities. By strategically combining these geometries, hybrid lattice structures were developed to address the limitations of single-lattice designs. Experimental results revealed that the OT-DM hybrid structure achieved nearly twice the energy absorption compared to the single-lattice OT structure under equivalent density conditions. These findings highlight the promise of hybrid lattice architectures in applications requiring effective energy dissipation, such as shock absorption and protective components. The integration of diverse lattice geometries within hybrid structures offers a transformative pathway for overcoming energy absorption challenges across multiple industrial sectors.

Keywords : Additive Manufacturing, Powder Bed Fusion, Lattice Structures, Ti, 6Al, 4V, Fabrication, Energy Absorption

36. Influence of increasing chromium content on additively manufactured tool steels: microstructural and mechanical evolution before and after heat treatment

Ofner Nicole ¹, Bodner Sabine Carmen ¹, Kunnas Peter ¹, Asci Atacan ¹, Kutlesa Kevin ¹, Stark Andreas ², Hoebenreich Philipp ³, Aumayr Christin ⁴, Wu Liang ⁵, Turk Christoph ⁴, Keckes Jozef ¹, Meindlhumer Michael ^{1 6}

1 - Montanuniversitat Leoben (Austria), 2 - Helmholtz- Zentrum Hereon (Germany), 3 - Österreichische Akademie der Wissenschaften (Austria), 4 - voestalpine BÄHLER Edelstahl GmbH & Co KG (Austria), 5 - voestalpine Additive Manufacturing Center GmbH (Germany), 6 - CD Laboratory for Knowledge-based Design of Advanced Steels (Austria)

Given the growing interest in additively manufactured stainless martensitic chromium tool steels, this study investigates the effect of increasing Cr content on the microstructure and mechanical properties of these steels. The analysis covers both the as-built (AB) condition and the condition after a typical heat treatment, which includes austenitization, quenching and multiple tempering steps. Thus, three Cr-alloyed tool steels, named Alloy A (20 wt.% Cr), Alloy B (22 wt.% Cr), and Alloy C (24 wt.% Cr), were analyzed in the AB and heat-treated (HT) conditions. Comprehensive microstructural characterization techniques, including light microscopy, scanning electron microscopy, electron backscatter diffraction, and transmission electron microscopy unveiled a clear correlation between the Cr content and the resulting microstructural features as well as phase occurrences. Moreover, an in-situ synchrotron experiment identified the body-centered-cubic Fe-phase in the alloys exclusively as delta-ferrite. Increasing Cr content resulted in a higher amount of delta-ferrite in both AB and HT conditions, which consequently reduced the amount of martensite after heat treatment. Mechanical properties, evaluated through Vickers hardness and tensile testing, revealed a decrease in hardness and tensile strength with increasing Cr content and thus the delta-ferrite content. In addition, changes in deformation behavior from brittle to ductile were observed. This study thus contributes to a deeper understanding of the effects of increasing Cr content on the microstructural characteristics, phase occurrence and mechanical properties of high Cr-alloyed tool steels produced via additive manufacturing.

Keywords : additive manufacturing, tool steels, chromium content, microstructure, phase occurrence, mechanical properties

37. Enhancing fatigue performance of additively manufactured H13 tool steel through surface finishing processes

Hosseiniou Hassan ¹, Shakeri Mohsen ¹, Jaskari Matias ², Abdelghany Ahmed ², JaRvenpaa Antti ², Hamada Atef ²

1 - Mechanical Engineering Faculty, Babol Noshirvani University of Technology, Babol (Iran), 2 - Future Manufacturing Technologies (FMT), Kerttu Saalasti Institute, University of Oulu, Nivala, 85500, Finland. (Finland)

This study investigates the fatigue performance of additively manufactured H13 hot work tool steel (AM-H13 TS) produced using the laser powder bed fusion (L-PBF) process with two distinct build orientations: vertical and diagonal (45°). A fixed volumetric energy density of 57.3 J/mm³ was employed for fabrication. The study compares the as-built AM-H13 TS to its surface-finished counterpart, focusing on fatigue life and damage under fully reversed tension-compression loading conditions. The surface finishing processes involved electropolishing using commercial DLYte 100HF+ equipment, followed by mechanical surface refinement. Surface topography and roughness characteristics of the as-built and post-polished specimens were comprehensively analyzed using laser confocal scanning microscopy (LCSM), while scanning electron microscopy (SEM) was utilized to examine microstructural features and fatigue mechanisms. The as-built AM-H13 TS exhibited high surface roughness due to the presence of satellites and partially melted particles, which are inherent to the L-PBF process. Surface-finishing approach substantially mitigated these surface imperfections, leading to significantly improved surface quality and reduced roughness. As a result, the fatigue performance of surface-finished AM-H13 TS showed remarkable enhancement. The fatigue limit increased fivefold, from 100 MPa in the as-built condition to 500 MPa after surface-finishing. SEM analysis revealed that the improved fatigue strength was primarily attributed to the reduced surface roughness and elimination of surface flaws, which acted as crack initiation sites in the as-built condition.

Keywords : Additively manufacturing, H13 tool steel, Laser, Powder Bed Fusion (L, PBF), fatigue performance, post, processing.

38. Development and optimization of metastable beta titanium-based alloys by laser powder bed fusion for biomedical applications

Rince Nolwenn ¹, Castany Philippe ¹, Gloriant Thierry ¹

¹ - Institut National des Sciences Appliquees - Rennes (France)

Perfect biocompatible alloys are essential for the manufacture of biomedical devices. However, alloys currently used are composed of toxic or allergenic elements, such as V, Co or Ni. Moreover, mechanical properties of implants are often very different from those of bones, which can lead to loss of bone mass due to the stress-shielding effect, reducing their durability in service. Low modulus metastable beta titanium alloys made with biocompatible elements are thus promising for biomedical devices. These alloys can also exhibit a stress-induced martensite (SIM) transformation which can lead to superelastic behavior, properties required for self-expandable stents or surgical orthopaedic staples. Although metastable beta titanium-based alloy made by conventional melting techniques have been intensively studied, their elaboration by additive manufacturing remains unexplored. Additive manufacturing allows more complex part and customized devices for patients. Therefore, these processes, especially, laser powder bed fusion (LPBF), are of great interest for medical fields. However, fabrication of original beta titanium alloy is very challenging due to the poor diversity of pre-alloyed powder available for sale. Therefore, in situ elaboration using a blend of elemental powders instead of pre-alloyed powders was used in the frame of this study. In this communication, preliminary results on biocompatible metastable beta Ti-based alloys made from the Ti-Zr-Nb-Sn system will be presented. Design of experiments was used to optimize the LPBF manufacturing parameters aiming to create dense part with low unmolten particles and enhanced mechanical properties. The microstructures were characterized by X-ray diffraction and electron microscopy and the mechanical properties were evaluated by tensile tests.

Keywords : Additive manufacturing, In situ elaboration, Titanium alloys, Microstructure, Mechanical properties

39. Optimizing thermal cycles in Wire-Arc Additive Manufacturing: Investigating inter-pass time and the use of an external cooling system

Rassane Anas

1 - Institut de Recherche Technologique Jules Verne [Bouguenais] (France), 2 - Institut de Recherche en Genie Civil et Mecanique (France), 3 - Institut des Materiaux de Nantes Jean Rouxel (France)

The Wire-Arc Additive Manufacturing (WAAM) process is an additive manufacturing process, allowing the production of metal components layer-by-layer using an arc welding process. This operation leads to thermal, mechanical, and metallurgical phenomena responsible for forming residual strains and stresses. Inter-pass time management is a key strategy in WAAM, as it directly impacts various aspects such as inter-pass temperature control, the dimensions of the molten pool, the microstructure formation (affected by solidification and solid-state transformations), and ultimately, the development of residual stresses and strains. Adding external cooling during inter-pass delay is essential for controlling the part's temperature and the microstructure, ensuring desired mechanical properties, avoiding geometrical collapse due to heat accumulation, and maintaining a good manufacturing rate. Using an external cooling system for duplex stainless steel can offer a suitable compromise by controlling the austenite precipitation with reduced inter-pass time. The proposed cooling method involves spraying water with a spray gun after each bead deposition. Preliminary microstructural investigations of duplex stainless steel reveal the potential to limit solid phase transformation driven by heat accumulation, thereby facilitating the re-establishment of a proper phase balance. The geometric analysis indicates that producing wall shapes with a reduced interpass delay is possible under the new cooling conditions. This study encompasses experimental methods, including metallurgical and mechanical characterization, and numerical approach.

Keywords : Duplex stainless steel, Wire Arc Additive Manufacturing, Thermal Cycles, Inter, pass time, Cooling Systems.

40. Combinatorial design of lightweight steels using multi-nozzle direct energy deposition (DED)

Jung Chahee ¹, Nam Seungjin ¹, Chung Hyun ¹, Jeong Heechan ¹,
Choi Hyunjoo ², Sohn Seok Su ¹

1 - Korea University (South Korea), 2 - Kookmin University (South Korea)

With the increasing need to address the effects of global warming, lightweight materials have attracted significant attention for reducing environmental impact. Among these, Fe-C-Mn-Al alloys stand out for their exceptional combination of lightweight and high strength. Therefore, it is crucial to control the composition of these alloys over a wide range to find the optimal combination of strength and ductility. This study utilizes additive manufacturing, specifically the Direct Energy Deposition (DED) method with a multi-nozzle system, to effectively explore a wide compositional range of Fe-C-Mn-Al lightweight steels compared to conventional methods. Process parameters, such as laser power and scan speed, were optimized to ensure reliable printing quality. These optimized conditions were applied to combinatorial design to evaluate the effects of compositional changes on microstructure and mechanical properties. This study discusses the observed microstructures and mechanical properties across various compositions.

Keywords : Additive manufacturing, Direct energy deposition, Lightweight steel, Combinatorial design

41. Influence of hierarchical structure on mechanical properties of additive manufactured IN718 alloys

Yamashita Kippei ¹, Cho Ken ¹, Yasuda Hiroyuki Y. ¹, Saito Takuma ², Sasaki Taisuke ², Katsuhiko Sawaizumi ¹, Okugawa Masayuki ¹, Yuichiro Koizumi ¹, Nakano Takayoshi ¹

1 - Division of Materials and Manufacturing Science (Japan), 2 - National Institute for Materials Science (Japan)

Ni-based superalloys are used for aircraft engines due to its excellent high-temperature properties. In recent years, laser beam powder bed fusion (LB-PBF) has attracted significant attention as one of the new manufacturing processes for the alloys. A recent study reported the formation of a unique hierarchical structure in IN718 alloys fabricated by LB-PBF. The hierarchical structure is composed of microscale crystallographic lamellar microstructure (CLM) and nano-scale cellular structure. It is also reported that the hierarchical structure improves tensile strength of the alloy. However, the influence of energy density in the LB-PBF process on the morphology of the hierarchical structure has not been investigated, nor has the relationship between the morphology of the hierarchical structure and mechanical properties been established. We found that the cell boundary is a low angle grain boundary with dislocation cell and solute segregation. This suggests that the cellular structure is formed by a cellular crystal growth along direction, accompanied by Nb segregation between the cells. This process is followed by numerous dislocations accumulating in the vicinity of the cell boundaries, which is introduced to decrease a residual stress associated with LB-PBF process. Moreover, it was also clarified the cell spacing increases with increasing energy density. the cell boundaries act as a strong barrier to the dislocation motion, though the misorientation angle between the cells is less than 5 degrees. This results in a huge increase in yield stress.

Keywords : Metal Additive Manufacturing, Ni based Superalloy, Mechanical Property, in situ Neutron Diffraction Analysis

42. Nano-scaled solidification microstructure characteristics in additively manufactured 316L stainless steel

Sun Fei ¹, Adachi Yoshitaka ¹, Sato Kazuhisa ², Ishimoto Takuya ³,
Nakano Takayoshi ², Koizumi Yuichiro ²

1 - Nagoya University (Japan), 2 - Osaka University (Japan), 3 - University of Toyama (Japan)

Laser powder bed fusion (LPBF) generates large thermal gradients and rapid cooling rates, making it challenging to fully understand the relationship between nano-scaled solidification microstructure and process parameters. Most studies have focused on characterizing microstructures from macro to sub-micrometer scales, with few investigating features at the nano or atomic levels. This study aims to explore these nano/atomic scale microstructural features of 316L stainless steel (SS) produced through LPBF to better understand the relationship between solidification microstructure and process parameters. 316L stainless steel was manufactured by the LPBF method. All the microstructural analyses were performed in the as-built samples. Novel nano-scaled modulated structures were first observed in the dislocation cells parallel to the laser scan direction, which was considered an undiscovered strengthening factor and mainly caused by the elastic strain involving the thermal gradient inside the melt pool and across adjacent melt pools as well as the effective strain field in the dislocation cell interiors. A novel method has been proposed to clarify the segregation behavior of melt pool boundary (MPB) by controlling the crystallographic texture of 316L SS through unique LPBF processing parameters. The accurate location of the track-track MPB is distinguishable and its edge-on state makes the quantitative concentration analysis precisely using HAADF-STEM with EDS mapping, which is in good agreement with the Scheil-Gulliver solidification simulations.

Keywords : Laser power bed fusion, 316L stainless steel, Solidification structure, Modulated structure, Melt pool boundary, Segregation

43. NiTi shape memory alloy by laser powder bed fusion : how manufacturing parameters influence the nature of the alloy and its mechanical properties

Yang Yang ¹, Gloriant Thierry ²

1 - Guangdong University of Technology, State Key Laboratory for High-Performance Tools, Guangzhou, 510006, China (China), 2 - University of Rennes, INSA Rennes, UMR CNRS 6226 ISCR, F35000 Rennes, France (France)

In a near-equiatomic NiTi alloy manufactured by laser powder bed fusion, the effects of laser power and scanning speed on the tensile properties and characteristic transformation temperatures were investigated. Since the shape memory NiTi alloy can be characterized by its martensitic start transformation temperature (M_s temperature) and by its critical stress inducing martensitic transformation (σ_c), the evolution of these two parameters was investigated as the function of the delivered laser beam energy by differential scanning calorimetry and tensile tests. It was observed that the increase of the scanning speed under a certain laser power and the increase of the laser power under a certain laser beam energy density promote an increase of the critical stress (σ_c) and a decrease of the M_s temperature. Consequently, high laser beam energy suppresses the formation of the martensitic B19' phase and therefore stabilizes the austenitic B2 phase, which is confirmed by XRD and TEM observations. Two new coefficients called Energy Dependence Coefficient of martensitic transformation Temperature (EDCT) and Energy Dependence Coefficient of critical Stress (EDCS) were defined and calculated to describe the laser beam energy dependence of the martensitic phase transformation. These two new thermodynamic coefficients are thus very suitable to establish a link between the manufacturing parameters (through the delivered laser beam energy) and the nature of the alloy (through the martensitic transformation). On the other hand, we have employed a repetitive laser scanning strategy to fabricate a functionally graded NiTi alloy. Unlike conventional NiTi, an unusual mechanical behavior showing large plasticity and exceptional strain-hardening was obtained.

Keywords : additive manufacturing, NiTi alloy, martensitic transformation, mechanical properties

44. Effect of Scanning Rotation Angle on the Properties of IN939 Fabricated by Laser Powder Bed Fusion

Dogu Merve Nur ^{1 2 3}, Ozer Seren ⁴, Yalcin Mustafa Alp ⁵, Davut Kemal ⁶, Gu Hengfeng ⁷, Brabazon Dermot ^{1 2 3}

1 - I-Form Advanced Manufacturing Research Centre, Dublin City University, Dublin (Ireland), 2 - Advanced Processing Technology Research Centre, Dublin City University, Dublin (Ireland), 3 - School of Mechanical and Manufacturing Engineering, Dublin City University, Dublin (Ireland), 4 - Middle East Technical University [Ankara] (Turkey), 5 - Atilim University (Turkey), 6 - Izmir Institute of Technology (Turkey), 7 - ANSYS (United States)

IN939 is a Ni-based superalloy extensively used in land-based gas turbine engines due to its exceptional high-temperature stability, mechanical strength, and corrosion resistance. While traditional manufacturing techniques such as casting and forging are limited in achieving complex geometries in a single step, the laser powder bed fusion (L-PBF) process allows for the fabrication of intricate designs with minimal material waste. Recently, L-PBF has been employed to produce components using IN939; however, further research is required to fully understand how process parameters, particularly scanning strategies, affect its material properties. This study explores the influence of various scanning rotation angles on the relative density, microstructure, surface roughness, cracking behaviour, and residual stress of L-PBF-fabricated IN939. The findings offer valuable insights into optimizing L-PBF process parameters for IN939, paving the way for producing high-performance components with tailored properties for demanding applications, such as gas turbines.

Keywords :Laser powder bed fusion (L, PBF), IN939, Electron backscatter diffraction (EBSD), Microstructure, Scanning strategy, Residual stress

45. Unique hierarchical structural features introduced by laser powder bed fusion and their contribution to mechanical function in IN718

Kikukawa Taichi ¹, Ishimoto Takuya ², Mayama Tsuyoshi ³, Ozasa Ryosuke ¹, Nakano Takayoshi ¹

1 - Graduate School of Engineering, The University of Osaka, Osaka, 565-0871 (Japan), 2 - Aluminium Research Center, University of Toyama, Toyama, 930-8555 (Japan), 3 - Faculty of Advanced Science and Technology, Kumamoto University, Kumamoto, 860-8555 (Japan)

Laser powder bed fusion (L-PBF) has garnered significant attention in recent years because of its ability not only to manufacture complex three-dimensional shapes but also to introduce unique hierarchical structures that manipulate the mechanical properties of products. For example, we have successfully fabricated near-single-crystal textures with //BD (build direction) and //BD orientations, and a unique crystallographic lamellar microstructure with a periodicity of approximately 100 μm consisting of two layers with distinct crystal orientations [1]. These textured matrices have a submicron-scale cellular microstructure. In addition, adjacent compartments with different textures can form artificial crystallographic interfaces [2]. The presence or absence of these L-PBF-specific features can be controlled by the manufacturing conditions and application of post-processing. The presence of these hierarchical structures enabled the as-built specimens to exhibit extraordinarily high strength, comparable to that of cast specimens that were precipitation-strengthened by aging. We successfully identified the relative mechanical contribution of each microstructural feature. This work was supported by CREST-Nanomechanics: Elucidation of macroscale mechanical properties based on understanding nanoscale dynamics of innovative mechanical materials (Grant Number: JPMJCR2194) from the Japan Science and Technology Agency (JST). [1] O. Gokcekaya, T. Nakano et al., *Acta Materialia*, 212, (2021), 116876. [2] T. Mayama, T. Nakano et al., *Additive Manufacturing*, 93, (2024), 104412.

Keywords :Laser powder bed fusion, In718, Crystallographic texture, Mechanical function

46. Additive Manufacturing and Post-Processing to Produce Microstructure Electrodes and Application Potentials

Dr. Boehme Andrea ¹, Doehler Torsten

1 - Technical University of Applied Science Wildau (Hochschulring 1 15745 Wildau Germany)

Additive manufacturing (AM) is gaining prominence for its capacity to produce customized and intricate geometries. However, a significant limitation of AM is the rough surface finish of the produced parts, necessitating post-processing to achieve the surface quality required for various applications. This study examines the monolithic production of (micro) electrodes from stainless steel, specifically 316L, known for its high corrosion resistance due to its composition of 18% chromium, 10% nickel, and 2€“2.5% molybdenum [1]. This material offers a sustainable and cost-effective alternative to noble electrode materials used in electroplating, water treatment, and other applications. Stainless steel 1.4404 provides significant corrosion resistance and mechanical stability at a lower cost compared to noble metals like platinum [2]. The use of additive manufacturing techniques for metals allows for the creation of complex microstructures with high aspect ratios and predefined edge geometries, enhancing material efficiency and sustainability in electrode production. To meet surface quality standards, targeted post-processing through milling and eroding is necessary to achieve the desired roughness and precise micro topographies [3]. This research explores these methods to reduce surface roughness while maintaining intricate structural features. The findings reveal that a combination of various post-processing techniques enables the production of functional microelectrodes with precise geometry and improved surface quality [4]. The integration of additive and subtractive processes allows producing electrodes with optimized properties at reasonable costs, reducing the need for resource-intensive traditional manufacturing steps. This sustainable approach expands application possibilities and positions stainless steel 1.4404 as a viable, cost-effective alternative to conventional electrode materials.

Keywords :Additive Manufacturing, Microstructure, Post Processing, Fabrication, Electrodes

47. Characteristics of Solidification by Super-Thermal Field in Powder Bed Fusion: Comparison with Conventional Rapid Solidification Processes

Koizumi Yuichiro ^{1 2}, Okugawa Masayuki ^{1 2}, Liu Yuheng ^{1 2}

1 - Graduate School of Engineering, Division of Materials and Manufacturing Science, Osaka University (Japan), 2 - Anisotropic Design and Additive Manufacturing Center, Osaka University (Japan)

The project "Creation of Materials by Super-Thermal Field" focuses on controlling crystal orientation and microstructure using the large temperature gradients (G) generated in PBF-type AM processes. The "super-thermal field (STF)" is defined as a temperature gradient exceeding 10^7 K/m, surpassing the upper limit in traditional solidification maps. Rapid cooling and solidification characterize the crystal growth in STF. However, rapid cooling and solidification are not necessarily unique to the solidification in STF. Here, we discuss the characteristic of solidification microstructures obtained in STF by comparing the crystal growth under large temperature gradients with those in conventional rapid cooling processes, such as gas-atomization (GA) and melt-spinning (MS) processes. In GA, the G is approximately 10^5 K/m, and the resultant solidification structures are equiaxed-dendritic. In MS, cooling rate is controlled mainly by heat transfer between material and cooling wheel rather than heat conduction within solid phase. The values of G , which are not explicitly stated in general, were derived from the temperature distribution, to be approximately 10^6 K/m while R is around 10^{-1} m/s. MS forms cellular structures similar to those produced in PBF. MS is commonly used for creating amorphous materials with excellent soft magnetic properties. Attempts have been made to obtain bulk amorphous materials in PBF utilizing its large cooling rates comparable to or exceeding MS. The solidification in the STF of PBF, despite similar or greater cooling rate, effectively promotes unidirectional solidification and crystal growth with large temperature gradients, enabling the production of single crystal bulk as a major feature.

Keywords :Solidification, Additive Manufacturing, Crystal Growth, Segregation

48. Effect of Build Orientation on Crystallographic Texture and Fatigue Performance of Selective Laser Melted Ti-6Al-4V ELI Parts

Pal Mintu ¹, Meena Anil ¹, Polishetty Ashwin ²

1 - Indian Institute of Technology Madras (India), 2 - Auckland University of Technology (New Zealand)

Additive manufacturing techniques are cutting-edge technologies for aerospace and other industries due to their ability to fabricate lightweight parts with complex geometries. However, a challenge exists in the variation of crystallographic texture and mechanical properties in components produced via Selective Laser Melting (SLM) process with different build orientations. Therefore, this study focuses on the experimental investigation of the effect of build orientations on crystallographic grain orientation and fatigue performance at room temperature. Furthermore, a detailed examination of the fracture surfaces was carried out to determine crack initiation sites, and the influence of build orientation on failures modes. Optical and Scanning Electron Microscopy (SEM) were employed to analyze the microstructural features and examine the fracture surfaces. The Electron Backscatter Diffraction (EBSD) technique was used to study the grain orientation which can lead to the variation in mechanical properties. The results indicate that the α -laths and prior BETA-grains exhibit a preferred grain orientation with respect to the build orientation and contribute significantly to the anisotropy in fatigue performance.

Keywords :Selective Laser Melting, Build Orientation, Ti64 ELI, High Cycle Fatigue, Crystallographic Texture

49. In-Situ Synthesis and Ex-Situ Addition Reinforced 3D Printing Aluminum Matrix Composites

Kuo Che-Nan ¹

1 - Department of Materials and Optoelectronic Science, National Sun Yat-sen University (Taiwan)

3D printing technology is good at fabricating products with complex shapes. Hence, lightweight design is easier to be realized through the 3D printing process. To achieve lightweight, it is also important to introduce high-specific strength materials. Hence, the development of high specific strength materials, such as further improving the strength of Aluminum alloys, is an important topic. However, it is hard to achieve strain hardening on the complex shape product fabricated by 3D printing. Hence, exploring an effective way to achieve precipitation or dispersion strengthening on the 3D printing Aluminum alloys is considered a promising solution. This study introduces in-situ synthesis and ex-situ addition to accomplish the simultaneous strengthening of precipitation and dispersion. In this study, Sc is added to the Al-Mg alloy to achieve precipitation strengthening through in-situ synthesis. SiC is also added as the reinforcement to achieve dispersion strengthening. The microstructure evolution and the mechanical response of such high-specific strength aluminum matrix composites are discussed in detail in this research.

Keywords :additive manufacturing, laser powder bed fusion, aluminum alloy

50. Microstructural Control of Unstable Beta-Type Titanium Alloy through Powder Bed Fusion using a Laser-Beam of Metals

Miyasawa Keitaro ¹, Ozasa Ryosuke ¹, Egusa Daisuke ², Abe Eiji ²,
Tane Masakazu ¹, Nakano Takayoshi ¹

1 - Division of Materials and Manufacturing Science, Graduate School of Engineering, The University of Osaka, Suita, Osaka 565-0871, Japan. (Japan), 2 - Department of Materials Science & Engineering, University of Tokyo, Tokyo 113-8656, Japan. (Japan)

Powder bed fusion using a laser-beam of metals (PBF-LB/M), one of the additive manufacturing techniques, generally attracts attention for fabricating three-dimensional metallic products. Recently, our research group proposed that PBF-LB/M can control material properties such as microstructures, suppression of elemental segregation, crystallographic texture. This unique control of material properties is originated from directional thermal field with an extremely high cooling rate. Therefore, this unique thermal field has a great potential for controlling material functionality. The focus here was the formation behaviour of metastable phases under extremely high cooling rate condition in unstable beta-type Ti-Nb alloy. This study purposed to investigate the behaviour of microstructure formation, phase transformation and their contributions to mechanical properties. The PBF-LB/M process was conducted by EOS M290 (EOS, Germany). Microstructural observations using SEM-EBSD, TEM, STEM and tensile test were performed. The PBF-LB/M-fabricated specimen was mainly composed of beta, omega and alpha phases, which was the same trend in the specimen fabricated by arc melting. However, the size of metastable omega and alpha phases were finer within about 3 nm in the PBF-LB/M-fabricated specimen. In addition, crystallographic texture and its orientation were successfully controlled by employing a different scanning strategy. As a result of simultaneous control of metastable phases formation and crystal orientation, the specimen exhibited relatively high yield stress despite low Young's modulus. This study found that PBF-LB/M effectively disperses omega and alpha phases in unstable beta-type Ti alloys under extremely high cooling rate, leading to the increase of yield stress with the same Young's modulus.

Keywords :Additive Manufacturing (AM), Powder Bed Fusion using a Laser, Beam of Metals (PBF, LB/M), Titanium, Based Alloy, Metastable Phase, Microstructure

51. Spinodal Decomposition and Magnetic Properties of Single-Crystal-Like Fe-Cr-Co Alloy Fabricated by Laser-Powder Bed Fusion Type Additive Manufacturing

Saito Takato¹, Liu Yuheng^{1,2}, Okugawa Masayuki^{1,2}, Sato Kazuhisa³, Nakano Takayoshi^{1,2}, Koizumi Yuichiro^{1,2}

1 - Graduate School of Engineering, Division of Materials and Manufacturing Science, Osaka University (Japan), 2 - Anisotropic Design and Additive Manufacturing Center, Osaka University (Japan), 3 - Research Center for Ultra-High Voltage Electron Microscopy, The University of Osaka (Japan)

Fe-Cr-Co alloys are widely used as permanent magnets and hysteresis materials for non-contact brakes due to their well-balanced magnetic properties, which can be tuned through the control of spinodal decomposition. Recently, the applications of laser powder bed fusion (L-PBF) type additive manufacturing to Fe-Cr-Co alloys have been reported. However, the effects of the rapid cooling conditions inherent to the L-PBF process on the spinodal decomposition behavior and magnetic properties remain unclear. In this study, we have investigated Fe-Cr-Co alloys fabricated by L-PBF to reveal the relationship among solidification microstructure, spinodal decomposition, and magnetic properties. Gas-atomized Fe-25Cr-12Co (mass%) powder was used to fabricate blocks via an L-PBF machine (EOS M 290). The SEM-EBSD analysis confirmed the single-crystal-like texture oriented along in the X, Y, and Z directions except at the bottoms of the blocks. Furthermore, no solute segregation was detected by SEM-EDS analysis. The samples were subjected to multi-step aging to induce spinodal decomposition. The magnetic properties of the samples after aging were significantly improved compared to the as-built samples although the values of magnetization and coercive force were slightly lower than those for the samples fabricated using conventional casting and plastic deformation processes. The presence of a large amount of sub-grain boundaries introduced during L-PBF process may have disrupted the spinodal decomposition structure, resulting in a slight decrease in magnetic properties. Nevertheless, the findings suggest that the L-PBF process can fabricate Fe-Cr-Co magnetic components with their final geometry, eliminating the need for solution heat treatment.

Keywords : Laser Powder Bed Fusion, Spinodal Decomposition

52. Applications of CALPHAD-based tools for welding and additive manufacturing

Kwiatkowski Da Silva Alisson ¹, Markstroem Andreas ¹, Malik Amer ¹, Minh Do Quang ¹, Jeppsson Johan ¹

¹ - Thermo-Calc Software AB (Sweden)

During welding and additive manufacturing methods, the material experiences a moderately fast cooling rate after melting, resulting in out-of-equilibrium solidification, with solute segregation and consequent undercooling. The Scheil-Gulliver method obtained by Computational Thermodynamics is a powerful tool to simulate the segregation of solutes during solidification and to predict which phases appear as a result of the segregation. Segregation affects important aspects of manufacturing: it may require post-processing, as well as impacting the moldability, weldability, and printability of the alloy. In addition, Scheil segregation results in a delay at the end of solidification, extending the solidification window, with consequences for the tendency of the material to heat crack. If the solidification rate increases beyond the diffusivity of the solutes, as happens in AM, solute trapping occurs, which can be modeled using the Scheil model with solute trapping. The Scheil simulation also allows you to pre-generate a solidification profile, now also including evaporation properties, which can be saved in your own material library or used directly as input to the new Additive Manufacturing (AM) module. Most of today's finite element simulation (FEM) tools tend to use a simplified description of material properties, often manual values, which may have little dependence on the chemical composition of the material or even temperature. The AM module offers a unique possibility to solve the solidification problem during AM, where we obtain a unified treatment of process parameters and thermophysical properties to solve the multiphysics problem of a moving heat source that melts and solidifies the metallic material. Examples of the AM module applied to different material classes are shown. In this presentation, examples of Scheil's and AM's modules applied to different classes of materials will be shown.

Keywords : Additive Manufacturing, Calphad, Solidification, FEM simulation, segregation

53. Multi-phase Flow System Study for Mixed N₂+CO₂ Gas Separation and Pipeline Transport

Lee Seungmin ¹, Park Jiyu ¹

¹ - Korea Institute of Industrial Technology (South Korea)

According to the UN Climate Change Report, global warming is currently a severe crisis, and countries around the world are making significant efforts in technology development and infrastructure to expand CCUS, a key component in achieving Net-Zero. The recent commercialization of CO₂ offshore storage technology has garnered attention as an efficient alternative for substantial CO₂ reduction and processing. In this study, we designed a multiphase flow system to investigate the flow stability of CO₂ transportation in pipes, a fundamental technology for offshore storage, and examined the characteristics of flow properties within pipes based on transportation conditions (water, pressure, temperature, etc.). Additionally, thermodynamic studies predict CO₂ hydrate formation and dissociation behavior, measuring the thermodynamic phase equilibria of mixed CO₂+N₂ gas hydrates, and exploring the enthalpy characteristics of mixed CO₂+N₂ gas hydrates. In addition, the corrosion effect was also examined for reliability testing of the pipe material of the CO₂ delivery pipe. The fundamental research data obtained from this study is anticipated to provide valuable information for optimizing the design of multiphase flow systems for CO₂ transfer, fluid dynamics modeling, and simulations.

Keywords : Gas hydrate, CO₂ offshore storage technology, corrosion, transfer, fluid dynamics modeling

54. Electropolishing of NiTi cardiovascular stents produced via laser powder bed fusion technique

Agarwal Neha, Obeidi Muhannad Ahmed, Brabazon Dermot

1 - I-Form Advanced Manufacturing Centre, Dublin City University, Dublin, Ireland (Ireland), 2 - Advanced Processing Technology Research Centre, Dublin City University, Dublin, Ireland (Ireland), 3 - School of Mechanical and Manufacturing Engineering, Dublin City University, Dublin, Ireland (Ireland)

Nitinol, an alloy known for its exceptional properties such as shape memory effect and superelasticity, is widely used in stent manufacturing. The performance of stents is significantly influenced by their surface properties, which are directly impacted by the manufacturing technique. Laser Powder Bed Fusion (L-PBF), a popular method for fabricating Nitinol components, presents challenges such as high surface roughness. Surface roughness can affect the mechanical and functional behavior of stents, making post-processing crucial for enhancing their quality. This study investigates surface modification of L-PBF-manufactured NiTi parts using electropolishing, a process that smooths and refines surfaces by selectively removing material. Several parameters, including voltage, flow rate, time, and the type of electrolyte, were studied to optimize the process. Electropolishing experiments were conducted under varying conditions, with voltage ranging from 15-40V and processing times between 20-30 seconds, using two different electrolytes. The optimized electropolishing parameters were identified as 18V for 20 seconds using electrolyte A2 and 40V for 30 seconds using electrolyte A3. These conditions effectively reduced surface roughness, improved the weight and thickness uniformity, and enhanced the overall surface quality of the NiTi parts. The results highlight the potential of electropolishing as a reliable surface enhancement technique for NiTi stents produced via L-PBF. This advancement could contribute to improved stent performance, particularly in biomedical applications where surface quality is critical for functionality and biocompatibility.

Keywords :Nitinol, electropolishing, biomaterials, characterization, stents

55. La compensation des erreurs geometriques lors de la phase de conception

El-Qemary Anass ¹, Kabbouri Ikram , Boutahari Said , Chahbouni Mouhssine

1 - Universite Sidi Mohamed Ben Abdellah - Fes [Universite de Taza] (Morocco)

Maitriser les processus de fabrication additive est essentiel pour garantir la production de pieces avec une qualite geometrique optimale tout en evitant les ecarts entre le modele CAO et la piece finale apres fabrication. Pour cette raison, il est crucial de se concentrer sur la compensation des erreurs, la correction et les ecarts des la phase de conception. Cela garantit que le modele CAO s'aligne parfaitement avec le produit fabrique, notamment les ecarts indesirables et ameliore la precision globale du processus de fabrication.

Keywords : Deviations geometriques, Fabrication additive, Compensation

56. LPBF processing of a metastable Ti-42Nb alloy for bone implant applications

Gebert Annett ¹, Pilz Stefan ¹, GuNther Fabian ², Akman Adnan ¹,
Ter-Ovanessian Benoit ³, Calin Mariana ¹, Boenisch Matthias ⁴,
Zimmermann Martina ²

1 - Institute for Materials Chemistry, Leibniz Institute for Solid State and Materials Research (IFW) Dresden (Germany), 2 - Institut für Werkstoffwissenschaft, Technische Universität Dresden (Germany), 3 - University of Lyon (France), 4 - Dpt. of Materials Engineering, KU Leuven (Belgium)

Current requirements for load-bearing bone implants are patient-specific designs and new materials for improved mechanical and biological compatibility. Laser Powder Bed Fusion (LPBF) of Ti alloys facilitates not only near-net shape implant production but also defined microstructural states yielding unique mechanical performances. For beta-type Ti-42Nb, the control of LPBF parameters can lead to a strong anisotropy in the stiffness of bulk specimens. By using a non-standard top hat laser source, a unique microstructure with strong texture parallel to the building direction (BD) was generated. Tensile tests along selected loading directions revealed a strong mechanical anisotropy with the lowest Young's modulus of 44 GPa parallel to BD. Suitable post heat treatment strategies for LPBF-produced Ti-42Nb cause substantial materials strengthening effects. Heat treatments within the alpha+beta phase range at 723 K for different durations led to increasing fractions of the metastable orthorhombic alpha"iso phase, acting as an intermediate to the stable alpha phase. The beta grain boundaries are primary sites for early alpha"iso precipitation. Tensile tests demonstrated significant strength enhancements through treatments up to 30 h compared to the as-built state, i.e. a yield strength of up to 1060 MPa and ultimate tensile strength of up to 1125 MPa. The impact of different LPBF states of Ti-42Nb on tribocorrosion properties in a simulated body fluid (PBS) will be presented. Funding is acknowledged by the German Research Foundation DFG, project no 419952351 and by the European Commission, H2020-MSCA grant agreement No. 861046 (BIOREMIA-ITN).

Keywords : LPBF, Ti alloy, microstructure, mechanical properties

57. Evaluation of Porosity and Hardness in Aerospace-Grade Aluminium Alloys Processed by Friction Surfacing

Erol Halil Ibrahim ¹, Gulletutan Umut Can ¹, Gunaydin Ahmet Can ¹, Altinok Sertac ¹

¹ - Turkish Aerospace Industries (Turkey)

Aerospace companies prioritize materials with optimal mechanical properties and lightweight characteristics to enhance fuel efficiency and overall performance. In other words, the materials with high specific strength are preferred in aerospace applications. Traditionally, bulk materials in billet form undergo subtractive manufacturing methods, such as machining, to meet design specifications. However, in certain cases, a significant portion of the material—potentially exceeding 70%—may be removed, leading to substantial waste. This loss can be reduced to approximately 10% or less by employing additive manufacturing (AM) techniques, which offer a more material-efficient approach. Among these, Direct Energy Deposition (DED) enables the production of near-net-shape geometries, requiring only minimal machining for final processing. However, high-strength aluminium alloys, which are widely used in the aerospace industry, cannot be welded, limiting their application in DED-based manufacturing. As an alternative, solid-state processing techniques, particularly friction-based additive manufacturing (FBAM) methods, have emerged as a promising solution. Maintaining structural integrity without phase transformation is crucial in aerospace applications, where mechanical performance and material reliability are paramount. In this study, friction surfacing was employed to process AA7050 and AA7075 alloys. Their porosity and hardness values were evaluated and compared using optical microscopy and microhardness testing, respectively.

Keywords : Additive Manufacturing, Friction Surfacing, Microhardness, Porosity analysis, Aerospace Materials

Acknowledgements: The authors acknowledge the support of the European Union's Horizon Europe Research and Innovation Program under Grant Agreement Number: 101177422

58. Novel cellular structure with phase-separation induced dislocation-network in Ti-Zr-Nb-Ta-Zr high entropy alloy fabricated by laser powder bed fusion

Egusa Daisuke ¹, Chen Han ¹, Ozasa Ryosuke ², Okugawa Masayuki ², Sasaki Taisuke ³, Ishimoto Takuya ², Yuichiro Koizumi ², Nakano Takayashi ², Abe Eiji ¹

1 - Department of Materials Science & Engineering, University of Tokyo (Japan), 2 - Division of Materials and Manufacturing Science, Graduate School of Engineering, The University of Osaka (Japan), 3 - Research Center for Magnetic and Spintronic Materials, National Institute for Materials Science (Japan)

High-entropy alloys (HEAs) have gathering wide attention as a novel class of structural materials, primarily due to their exceptional mechanical properties. Notably, Ti-Zr-Nb-Ta-Zr alloys have been interested as biomedical HEA (BioHEA), owing to their superior mechanical properties and biocompatibility than the conventional Ti alloys. In this study, we present a novel cellular structure in Ti-Zr-Nb-Ta-Zr HEA fabricated by L-PBF process, originating from phase-separation induced dislocation-network. Microstructural observations revealed that this unique cellular structure is composed of Zr-rich and Ta-rich body-centered cubic (BCC) phases with slightly different compositions. Detailed analyses indicate that boundaries between these BCC phases were decorated by distinct dislocation networks, whose dislocation density is higher than that in typical AM-processed alloys. With the aid of thermodynamic simulations, we propose a formation mechanism of this cellular structure, in which rapid cooling leads to solid-state phase separation with semi-coherent phase boundaries with geometrically necessary dislocation-network. Strengthening effect of this cellular structure is higher than the amount of individual strengthening effects by phase-separation and dislocation-network in previous studies, providing valuable insights for developing high-performance AM materials.

Keywords : high entropy alloys (HEA), laser powder bed fusion (L, PBF), cellular structure, phase separation, dislocation network

59. Simulation based estimation of local heat build up during Laser Powder Bed Fusion processing

Schlenger Lucas ¹, Depond Philip ², Guss Gabe ², Loge Roland ³

1 - Thermomechanical Metallurgy Laboratory, PX Group Chair, Ecole polytechnique federale de Lausanne (EPFL), CH-2002 NeuchÂtél, Switzerland (Switzerland), 2 - Lawrence Livermore National Laboratory (United States), 3 - Laboratory of Thermomechanical Metallurgy - PX Group Chair, Ecole Polytechnique Federale de Lausanne (EPFL) (Switzerland)

Laser Powder Bed Fusion (LPBF) is an additive manufacturing technique that utilizes a laser heat source to locally melt and solidify metallic powder particles. While many strategies exist to translate processing conditions across LPBF systems, part geometries, and materials, many of them do not account for changes in local heat accumulation patterns. We elucidate the severe magnitude of heat build-up present during the printing of one layer and correlate the preheating to laser power, laser velocity, scan vector length and scanning strategy (unidirectional/bidirectional). This is achieved by in-situ forward-looking infrared (FLIR) observations of a total of 510 layers printed with a total of 51 different processing conditions. We then illustrate the ability of highly efficient Finite Element Method (FEM) based models to correctly predict the intra layer heating. The high efficiency of the models is achieved by relying on a time averaged energy deposition strategy. We subsequently identify the boundary of validity of such approaches and demonstrate their systematic failing under specific circumstances. Overall, we present a critical evaluation of FEM based prediction of local heat build-up and validate our claims against extensive FLIR observations. These considerations further highlight the significance of intra-layer heat build-up and present efficient means to predict the preheating under specific circumstances.

Keywords : Additive Manufacturing, Laser Powder Bed Fusion, local Heat Accumulation, Thermal Imaging, Numerical Modelling

60. Effect of chemical surface post-processing on the surface roughness of Niti fabricated by laser powder bed fusion

Ikiz Meris Meric

1 - Meris Ikiz (Ireland), 2 - Merve Nur Dogu a b, (Ireland), 3 - Dermot Brabazon a b (Ireland)

Laser powder bed fusion (L-PBF) is one of the most popular methods in additive manufacturing (AM) which is known as layer-by-layer production for complex geometries. It has many advantages which its design flexibility, material efficiency, and customization capabilities, particularly in comparison to conventional manufacturing methods. Despite its many benefits, certain drawbacks, including high surface roughness, spatters, and balling effects create imperfections that need to be addressed to make the components suitable for engineering applications. Surface roughness is a critical parameter in additive manufacturing (AM), as it has a profound impact on the mechanical properties of the final product. Chemical polishing is one of the most widely employed post-processing techniques for surface, effectively mitigating surface roughness and improving overall surface quality. This process works by dissolving irregularities and eliminating contaminants, resulting in a much smoother, more uniform finish that enhances the component's aesthetic and functional performance. In this experiment, a chemical polishing process was applied to the samples produced using the LPBF method, where the samples were treated with three different acids, each applied for varying durations, to assess their effectiveness in reducing surface roughness and improving surface quality. Surface roughness, relative density, and SEM and optical microscope analyses were conducted before and after surface treatment. These characterization techniques enabled a comprehensive comparison of the topographical features and provided valuable insights into the effectiveness of the chemical polishing process in enhancing and refining the surface characteristics of the samples.

Keywords : Nitinol (NiTi), Additive manufacturing (AM), post, processing techniques, surface roughness, mechanical properties, Laser Powder Bed Fusion (L, PBF)

61. Microstructure engineering of ultra-high strength martensitic steel produced by advanced manufacturing processes

Mozumder Yahya H., Taylor Mark, Prangnell Philip B., Pickering Ed J., Scenini Fabio

1 - Department of Materials, University of Manchester, Manchester M13 9PL (United Kingdom)

Advanced manufacturing processes like hot isostatic pressing (HIP) and wire-arc additive manufacturing (WAAM) enable efficient production of near-net-shaped high performance steel components. Compared to traditional manufacturing methods, these advanced processes offer significant advantages, including faster fabrication, lower machining costs, and reduced defects like macrosegregation and casting porosity. However, the microstructures of high strength steels produced by these advanced techniques often feature large columnar grains, chemical inhomogeneities, unwanted precipitations and oxides, potentially compromising mechanical properties. Hence, optimising processing parameters and heat treatments to control the microstructure is essential. This study explores the effect of advanced manufacturing processes and post-build heat treatments on the microstructure and mechanical properties of ultra-high strength martensitic steel, with comparative analysis of the same material produced by a conventional process. Although, the HIP microstructure exhibited finer grains than the forged material, networks of stable oxide particles were observed along the prior particle boundaries (PPBs), originating from the oxide layer at the powder particle edges. These oxides network created an easy fracture pathway, resulting in poor ductility. Tailoring HIP processing parameters was found to influence the oxide distribution, grain size and mechanical properties of the steel. In contrast, WAAM high strength steel microstructure exhibited coarse columnar grains, micro-segregation as well as intermetallic precipitation. Homogenisation and cyclic austenitisation treatments were performed on the WAAM samples to achieve chemical homogeneity and grain refinement, respectively. These findings highlight the critical need for innovative methodologies to enhance HIP powder cleanliness and optimise WAAM post-build processing to improve overall material performance.

Keywords : Hot Isostatic Pressing, Wire Arc Additive Manufacturing, Ultra High Strength Martensitic Steel, Prior Particle Boundaries, Oxide Particles, Microsegregation

62. Effect of microstructural heterogeneity on slip localization in L-PBF processed AlFeCrX alloys

Cepeda-Jimenez Carmen ¹, Bahari-Sambran Farid ^{1 2}, CarrenO Fernando ¹, Orozco Alberto ²

1 - National Center for Metallurgical Research [Madrid] (Spain), 2 - Universidad Politecnica de Madrid (Spain)

Laser-Powder Bed Fusion (L-PBF) is one of the most widely used metal additive manufacturing (AM) technologies, capable of producing complex and intricate geometries [1]. However, many existing alloys are not optimized for L-PBF, as they were originally designed for conventional thermomechanical processing. In particular, high-strength wrought Al alloys (7xxx and 2xxx series) exhibit limited mechanical properties and a high susceptibility to hot cracking (HCS) during the AM process due to the volatility of their alloying elements. Recent studies [2] have shown that the L-PBF processability of high-strength Al alloys can be significantly enhanced by alloying with transition elements (such as Fe, Cr, Ti, etc.) that possess: i) a low maximum solid-solubility limit in aluminum, facilitating the formation of precipitates and intermetallic compounds, and ii) low diffusion coefficients in aluminum alloys, contributing to improved high-temperature stability. This presentation will review recent advancements in the effect of transition alloying elements in AlFeCrX (X = Ti, Si) alloys, specifically developed for L-PBF. The review will focus on their impact on microstructure (grain size, precipitates, melt pool characteristics, etc.) and mechanical properties (strength and ductility) at room temperature. Additionally, slip localization behaviors have been analyzed using electron backscatter diffraction (EBSD) and high-resolution digital image correlation (HR-DIC) [3]. Significant heterogeneous slip localization is observed in the L-PBF AlFeCrX alloys, which varies with the initial composition, correlating with differences in grain size and precipitate distribution within the melt pool. Keywords: Laser-powder bed fusion (L-PBF); aluminium alloys; transition elements; High-resolution digital image correlation (HR-DIC); microstructure; slip localization. [1] R.S. Mishra, S. Thapliyal, Materials and Design 204 (2021) 109640. [2] M. Perez-Prado, A. Martin, D. Shi, S. Milenkovic, C. Cepeda-Jimenez, Addit. Manuf. 55 (2022) 102828. [3] A. Orozco-Caballero, D. Lunt, J.D. Robson et al, Acta Mater. 133 (2017) 357-379.

Keywords : Laser, powder bed fusion (L, PBF), aluminium alloys, transition elements, High, resolution digital image correlation (HR, DIC), microstructure, slip localization.

63. Overview of advanced materials for the FCC-ee vacuum system

Garion Cedric

1 - European Organization for Nuclear Research (Route de Meyrin 385, 1217 Meyrin Switzerland)

With the Future Circular Collider study, CERN has initiated the feasibility study of new particle physics accelerators at the energy frontier. Located in a 90.7 km circumference, 200 m underground tunnel, it aims, in a first phase (FCC-ee), at electrons-positrons collisions with beam energy up to 182.5 GeV. At such energy, high synchrotron radiation flux and power are generated and need to be managed by the vacuum system. The FCC-ee leads to challenging requirements for the vacuum system and calls for advanced materials and manufacturing process to get reliable and affordable and cost-effective technical solutions. The FCC-ee storage ring vacuum system is based on a copper vacuum chamber. Several technologies are being developed to integrate different functionalities and are presented in the paper. Synchrotron radiation absorbers, intercepting up to 3.5 kW power, are produced by selective laser melting 3D printing. Interfaces for beam position monitors are obtained by cold spray additive manufacturing. To reach the vacuum performance, an in-situ thermal cycle at 230 ° is required. The radiation hard heating system is based on Joule's effect and produced by the thermal spraying of a biomaterial ceramic/metal heating track. Flanges are joined to the vacuum chamber by friction stir welding. Finally, chambers are connected together with shape memory alloy leak tight rings.

64. Microstructural Evolution and Performance of LPBF Ti-6Al-4V Lattice Structures upon Hot Isostatic Pressing

Kavunkara Thadayil Ajai Sankar ^{1 2}, Farhadi Ahmad ^{2 3}, Keaveney Shane ³, Dowling Denis ¹, Celikin Mert ^{1 2}

1 - I-Form Advanced Manufacturing Research Centre, University College Dublin, Dublin (Ireland), 2 - School of Mechanical and Materials Engineering, University College Dublin, Dublin (Ireland), 3 - Croom Medical, Co. Limerick, Ireland, V35 YD39 (Ireland)

Additive manufacturing (AM), particularly Laser Powder Bed Fusion (LPBF), has become a transformative method for fabricating complex structures such as lattice components using materials like Ti-6Al-4V. This study investigates the synergistic effects of LPBF and Hot Isostatic Pressing (HIP) on porosity control, microstructural characteristics and structural integrity of Ti-6Al-4V components with a shell/core lattice design. Compared with bulk AM parts without internal lattice structure, X-ray CT and SEM analyses reveal similar porosity levels upon HIP which was achieved with significantly reduced production time. HIP effectively densifies the material, eliminating detrimental porosity while ensuring strong bonding at the powder-shell interface. Microstructural examination via Electron Backscatter Diffraction (EBSD) shows columnar grains in the shell region and equiaxed grains in the powder region, with seamless integration ensuring mechanical integrity. X-ray diffraction (XRD) patterns analysis revealed variations in crystallographic orientation and micro-strain, with anisotropic features observed between longitudinal and cross-sectional samples. These findings highlight the potential of this hybrid approach to optimize fatigue performance by controlling detrimental porosity and improving microstructural properties. This method offers sustainable and economic benefits for biomedical applications by reducing manufacturing lead times while delivering high-performance components with properties comparable to conventionally manufactured parts.

Keywords : Laser powder Bed Fusion, microstructure, Hot Isostatic Pressing, lattice structures, Ti, 6Al, 4V

65. A layer-by-layer FEM curing model for binder jetting of 316L

Desgagnes Leon ¹, Tangestani Reza ¹, Miao Hongyan ¹, Pendurti Srinivas ², Natarajan Arunkumar ², Martin Etienne ¹

1 - Polytechnique Montreal (Canada), 2 - Colibrium Additive (United States)

Binder jetting is faster than laser-based AM technologies, which enables the required throughput for the mass production of metal components. However, binder jetting requires several post-processing steps, such as curing and de-binding, which increase production costs. This study aims to establish an in-process curing method to reduce the production time of binder jetting printed parts using heat sources. Three different models based on FEM were developed to thermally simulate in-process curing during binder jetting. In the first model, the heat source moves incrementally over the powder bed. The second model integrates the heat input over each deposited powder layer, reducing computational time. In the third model, a lumped approach is employed, allowing for the grouping of several layers, thereby improving computational efficiency. The three models are compared with experimental measurements, their accuracy and computation times are also evaluated.

Keywords : Additive Manufacturing, Binder jetting, FEM, Metal powder, Simulation and Modeling

66. Additive manufacturing of recycled Ti-6Al-4V powder by Fused Granular Fabrication (FGF)

Pyczak Florian, Rackel Marcus, Limberg Wolfgang, Ebel Thomas

1 - Helmholtz-Zentrum hereon GmbH (Germany)

Powder based additive manufacturing processes are hampered by the high costs of powder and microstructures and properties differing significantly from those of more conventional processes like casting or forging. The latter is due to the fact, that powder based additive manufacturing processes as Laser Powder Bed Fusion and Electron Beam Melting induce extremely high cooling rates and complex heat treatment histories. In the talk a titanium powder recycling route from scrap from machining and finishing processes is presented. By cleaning this scrap and compacting it to pre-material for powder atomization it was possible to produce Ti-6Al-4V powder which met the impurity level specifications. The impurity level is extremely sensitive to the cleaning process, the mixture ratio of chips from machining and finishing steps and the powder handling. Thus, it is necessary to control the entirety of the process to produce recycling powder which exhibits equal properties as primary material. The recycling powder is used to produce specimens and prototype parts with Fused Granular Fabrication (FGF). In this process a powder polymer binder mixture is printed to a green part which is subsequently consolidated by sintering. The microstructure formation takes place during the sintering and is comparable with established processes like metal injection molding (MIM). The properties are comparable with those of MIM samples and meet the mechanical specifications for grade five titanium. In addition, the combination of FGF and MIM allows to economically produce parts over the complete range of quantities using FGF for small and MIM for large batches.

Keywords : Recycling, Additive Manufacturing, Titanium, Fused Granular Fabrication

67. Towards controlling 4D printing for developing innovative architected microstructures

Perrin Laura Rose, Esmaeilzadeh Reza, Jhabvala Jamasp, Schlenger Lucas, Banait Shruti, Van Der Meer Mathijs, Loge Roland

1 - Laboratory of Thermomechanical Metallurgy - PX Group Chair, Ecole Polytechnique Federale de Lausanne (EPFL) (Switzerland)

Developing architected microstructures in Laser Powder Bed Fusion (LPBF) requires modifying microstructures during the process. A cutting-edge approach leverages the laser in LPBF as a heat source for in-situ laser heat treatment (SLHT). Due to the high cooling rates (10 000 to 100 000 °C/s) in LPBF, a martensitic α' microstructure typically forms. However, Finite Element Method (FEM) simulations were used to optimize SLHT parameters, allowing a cooling rate between 3 000 to 8 000 °C/s while maintaining a sub-transus heat treatment temperature. This enables the decomposition of martensitic α' in Ti-6Al-4V (Ti64), creating a composite microstructure with alternating α' and (α + BETA) layers. The resulting fatigue properties surpass those of homogeneous microstructures. These innovative 4D printing strategies offer new opportunities for biomedical applications by enabling localized property tuning.

Keywords : advanced additive manufacturing, laser powder bed fusion, in, situ laser heat treatment, thermal simulation, microstructure composite

68. Gelation, Vitrification and Shrinkage of Thermoset Polymers Methods for Investigation and Modelling

Geiss Paul Ludwig ¹, Schumann Melanie

¹ - Rheinland-Pfalzische Technische Universität Kaiserslautern Landau (Germany)

Thermosets play an important role in composite processing, adhesive bonding and coating. In all these applications, shrinkage can introduce a significant amount of residual stress leading to distortion, reduced load carrying capacity and cracking. Total shrinkage can be caused by thermal shrinkage, chemical shrinkage and shrinkage due to physical ageing. As curing progresses, the viscosity of the resin increases as chemical reactions increase the average length and degree of cross-linking between the constituent oligomers. Gelation occurs when a continuous 3-dimensional network of oligomer chains is formed. After gelation, the microstructure of the polymer solidifies and vitrification occurs when the glass transition temperature exceeds the cure temperature. Further cure is then governed by diffusion limitations. In the viscous state prior to gelation, the flow behaviour prevents the development of mechanical stress. After gelation, the amount of stress caused by chemical shrinkage depends on the reaction rate and relaxation time. If curing is carried out at elevated temperature, thermal stress is likely to occur upon cooling to ambient service conditions due to differences in thermal expansion. In the cured state at service conditions below the glass transition temperature, physical ageing may lead to time-dependent shrinkage and release of relaxation enthalpy upon subsequent heating. A variety of methods are available to measure shrinkage in the liquid, viscoelastic and vitrified states of the polymer, including optical volume measurement, refractometry, confined and unconfined oscillatory rheology, dilatometry and dielectric analysis. This paper discusses various experimental methods for measuring shrinkage and viscoelastic properties of curing thermosets and modelling their evolution in relation to time and temperature induced transformations.

Keywords : Shrinkage, Gelation, Vitrification, Thermoset

69. In vitro response of bioabsorbable zinc-based composites for implantology

Seabra Francisca M.^{1,2}, Marques De Castro Moara³, Balog Martin^{1,3},
Krizik Peter^{1, 3}, Takacova Martina⁴, Lapinova Jana⁴, Svastova
Eliska^{3,4}, Hybasek Vojtech⁵, Kubasek Jiri⁵

1 - Institute of Materials and Machine Mechanics, Slovak Academy of Sciences (Slovakia), 2 - Faculty of Materials Science and Technology in Trnava, Slovak University of Technology (Slovakia), 3 - Centre of Excellence for Advanced Materials Application, Slovak Academy of Sciences (Slovakia), 4 - Biomedical Research Center, Institute of Virology, Slovak Academy of Sciences (Slovakia), 5 - Department of Metals and Corrosion Engineering, University of Chemistry and Technology (Czech Republic)

Certain implants, such as endovascular stents (ES) and orthopaedic internal fixators (OIF), are only required for a certain amount of time, with long-term implantation leading to health complications and removal implying additional surgery. Bioresorbable metallic implants could be an exciting solution for these situations, combining metals' good mechanic properties with limited permanence in the body. Zinc (Zn) is a bioresorbable metal with a corrosion rate that has been shown to be close to ideal for these applications, but that presents microstructural instability at human body temperature. To solve this, a Zn-based composite was developed with an ultrafine-grained Zn matrix stabilised by nanometric zinc oxide (ZnO) dispersoids formed in situ, providing the material with good mechanical performance. In this work, the influence of grain size and ZnO content on the material biocompatibility was evaluated by accessing in vitro corrosion and biological response. Corrosion was studied by analysing weight loss and electrochemical behaviour after immersion in cell culture medium. The material cytotoxic response was evaluated through cell viability and proliferation assays. ZnO is a known antibacterial and anti-inflammatory agent, thus assays to access such potential properties of the material were also conducted. All assays were performed for three Zn-based composites with different grain sizes and ZnO content and compared with control samples of cast and hydro-extruded Zn. The obtained results support that the concept of Zn stabilisation with ZnO can be applied to implantology, being a path to fabricate Zn-based resorbable implants that meet the requirements for ES and OIF applications. Acknowledgements: This work was supported by the VAIA 09I03-03-V04-00718, APVV-20-0417, VEGA 2/0157/24 and ITMS 313021T081 ERDF projects.

Keywords : Biomaterial, Zinc (Zn), Zinc oxide (ZnO), Metal matrix composite (MMC), Bioabsorbable, In vitro, Corrosion, Biocompatibility

70. Widening the scope for non-noble metal initiation of electroless copper deposition

Cobley Andrew ¹

1 - Coventry University (UK) (Coventry CV1 5FB United Kingdom)

The traditional approach to initiation of electroless copper deposition involves decorating the substrate with a precious metal catalyst which initiates the electroless copper reaction by catalysing the oxidation of formaldehyde[1]. Since this is a catalytic initiation, it is perhaps not surprising that the type of catalyst utilised is largely limited to noble metals. Most commonly Pd is employed as a Pd-Sn colloid, but the efficacy of Au[2], Ag[3] and others has been demonstrated. However, the cost of some of these materials, issues with supply and sustainability has meant that non-noble initiation of electroless copper has become critical. Although there has been important research on the use of Cu nanoparticles[4, 5] to initiate the electroless copper reaction this again is a catalytic process. In this paper a mechanism for the initiation of the electroless copper deposition reaction will be elucidated which involves an initial in situ electrolyte displacement (or immersion) step. Since this initial step is non-catalytic it widens the field for potential non-noble metals to be employed in the initiation process. The paper will describe some of the key factors that influence this mechanism and show how the optimised initiation process can produce electroless copper deposits that are equivalent to those obtained with a traditional Pd-Sn catalyst. 1. Deckert, C.A., Plating and Surface Finishing, 1995. 82³: p. 58-64. 2. Ma, H., et al., Thin Solid Films, 2011. 519(22): p. 7860-7863. 3. Wills, K.A., et al., The Journal of The Textile Institute, 2017: p. 1-10. 4. Taghavi Pourian Azar, G., et al., Surface and Coatings Technology, 2020. 396. 5. Cobley, A.J., et al.. Circuit World, 2010. 36³: p. 9-13.

Keywords : electroless, copper, non, noble, catalyst, initiation, palladium

71. Elastomer patterning and stacking process for stretchable multilayer electronic circuit based on laser-induced photo-thermal effect

Jeon Hojeong¹

1 - Korea Institute of Science and Technology (Hwarangro 14 gil 5, Seoungbuk-gu, Seoul 02792 South Korea)

Photothermal lithography is a new technique for fabricating intrinsically stretchable multilayer electronic circuits entirely composed of elastomeric matrices. Traditional photolithography struggles with the opacity of thick stretchable nanocomposite conductors, impeding their use in such applications. This study introduces photothermal lithography, utilizing pulsed lasers to pattern elastomeric conductors and create via holes. The resulting stretchable nanocomposite conductor shows three times higher conductivity (5940 S cm^{-1}) and five orders of magnitude lower resistance change ($R/R_0 = 40$) under 30% strain after 5000 cycles, compared to screen-printed conductors. This is attributed to a unique percolation network formed by spatial heating of the laser. Additionally, stretchable via holes with $50 \text{ }\mu\text{m}$ resolution can be created without material ablation or degradation. This method allows for seamless stacking of highly conductive and durable multilayer circuits. Demonstrations include a stretchable wireless pressure sensor and a passive matrix LED array, underscoring the potential for durable, high-density, multifunctional stretchable electronic circuits.

Keywords : Photo, thermal lithography, Laser fabrication, Stretchable electronics, Nanocomposites, Multilayer electronic circuit

72. Biodegradable zinc matrix composites for bone implant materials

Li Yuncang ¹

1 - School of Engineering, RMIT University (Melbourne, 3001 Australia)

Zinc-based alloys and composites are gaining increasing interest as promising biodegradable implant materials due to their appropriate biodegradation rates and biological functionalities. However, the inadequate mechanical strength and ductility of pure Zinc have restricted its application. This study investigated the zinc matrix composites (ZMCs) reinforced with graphene nanoplatelet (GNP) fabricated via powder metallurgy as potential biodegradable implant materials. The microstructural study revealed that the GNP was uniformly dispersed in the ZMCs after ball milling and sintering at 420 °C for 6 h. The microhardness, compressive yield strength, ultimate compressive strength, and compressive strain of ZMC€“0.2GNP were 68.7 HV, 123 MPa, 247 MPa, and 22.9 %, respectively, with improvements of ~ 18 %, 50 %, ~ 28 %, and ~ 15 % compared to pure Zn. The corrosion rate of the ZMCs was lower than that of pure Zn, and the ZMC-0.2GNP composite exhibited the lowest corrosion rate of 0.09 mm/y as measured by electrochemical testing. Furthermore, pure Zn was reinforced with 0.2 wt.% graphene nanoplatelets (GNP) and alloyed with different magnesium (Mg) content (0.5, 1.0, 1.5, and 2.0 wt.%) using hot-pressing sintering of Zn, Mg, and GNP powder mixtures. The hot-pressing sintered (HPS) Zn€“0.5Mg€“0.2GNP composite exhibited a compressive yield strength of 169 ± 18 MPa, an ultimate compressive strength of 270 ± 39 MPa, a compressive strain of $17 \pm 6\%$, and a microhardness of 86 ± 2 HV. The degradation rate increased from 0.032 to 0.141 mm/y by increasing Mg content from 0 to 2.0 wt.%.

Keywords : Biodegradable zinc composite, corrosion and mechanical property, graphene nanoplatelet.

73. Breakthrough of strength and ductility trade-off in biodegradable Mg alloys by drawing at elevated temperatures for bone implants

Yuan Guangyin ¹

1 - Shanghai Jiao Tong University (school of Materials Science & Engineering, 800 Dongchuan Road, Shanghai 200240 China)

Mg alloys possess great potentials in the biomedical fields due to their biodegradation, medium strength and good biocompatibility. However, there is always a concomitant decrease in ductility during strengthening in Mg alloys, resulting in an undesirable strength-ductility trade-off. Therefore, the development of Mg alloys with high strength-ductility synergy is highly demanded for their wider applications. In this study, the as-extruded biodegradable Mg-Nd-Zn-Zr (JDBM) alloy rod was subjected to single-pass drawing over a range of temperature 200 ~ 600 °C to enhance the properties. After drawing, a more homogeneous and refined microstructure developed because of dynamic recrystallization (DRX) and dynamic precipitation (DP). With the increase of drawing temperature, grain sizes increased first and then decreased due to the competition of grain nucleation and growth, while the sizes of the secondary phase particles varied in the same way. And a nearly basal texture evolved from a rare earth texture of the as-extruded sample. The yield strength of the as-drawn samples increased by ~2.2 times with a sacrifice of elongation to fracture at different level. The high yield strength mainly originated from grain boundary and dislocation strengthening. An optimal combination of high yield strength (~301 MPa) and good ductility (elongation to fracture of ~19% and improved strain hardening capacity) was obtained after drawing at 500 °C. The yield strength enhancement was mainly derived from texture and dislocation strengthening. Grain and secondary phase particle refinement, large volume fraction of low angle grain boundaries and reduced geometrically necessary dislocations are considered to be beneficial to the good ductility. In addition, a novel method has been proposed to fabricate materials with superior strength-ductility synergy by deformation with large strain at high temperatures to activate severe DP. JDBM magnesium alloy bone screws prepared by the above process have successfully carried out more than 150 multi-center clinical trials.

Keywords : Biodegradable Mg alloy, bone implants, Hot drawing, Strength and ductility synergy

74. Effect of Surface Modifications on the Biological Response of Additively Manufactured Metallic Implants

Echeverry-Rendon Monica ¹, OrdonO Jesus ¹, Contreras-Almengor Oscar ¹, Mollaei Nafiseh ^{1 2}, Llorca Javier ^{1 2}, Sket Federico ¹, Molina-Aldareguia Jon ^{3 4}

1 - Institute IMDEA Materials [Madrid] (Spain), 2 - Universidad Politecnica de Madrid (Spain), 3 - IMDEA Materials (Spain), 4 - Universidad Politecnica de Madrid (Spain)

Recent advances in additive manufacturing (AM) of metals offer significant potential to enhance both functionality and fabrication efficiency. This is particularly relevant to the biomedical industry, where personalized implants with complex geometries can be manufactured to meet patient-specific needs. A wide range of medical applications, including cardiovascular stents, bone fixation plates, and dental implants, can benefit from AM by allowing for greater customization and control over material composition and microstructural properties. For this conference, we want to present in a summarized way the results obtained in different studies where samples of Nitinol (NiTi), zinc (Zn), and magnesium (Mg) were manufactured by laser powder bed fusion (LPBF). To optimize their performance, these materials were subjected to various surface treatments, including chemical etching, electropolishing, and plasma electrolytic oxidation. These treatments altered surface characteristics such as roughness, composition, corrosion resistance, and surface energy, which are crucial factors for biomedical applications. To evaluate their suitability for implant applications, we conducted corrosion resistance assessments and biological compatibility tests. Hemocompatibility, cell proliferation, cell-material interaction, and molecular assays were performed to determine the impact of surface modifications on biological behavior. The results provide valuable insights into how surface treatments influence the integration of metallic implants with biological tissues. This study highlights the potential of tailored surface modifications to improve the biocompatibility and functional performance of AM-fabricated implants, paving the way for their broader clinical adoption.

Keywords : laser powder bed fusion (LPBF), metals, biomedical implants, surface modification

75. Functional Coatings by Low Vacuum Plasma for the Innovation in Regenerative and Reparative Medicine

Chevallier Pascale , Paternoster Carlo , Copes Francesco , Sarkissian Andranik , Mantovani Diego ¹

1 - Laval University (Pav Pouliot, 1745E Ave de la Medecine Quebec G1A 0V6 Canada)

Over the last 50 years, biomaterials, prostheses and implants saved and prolonged the life of millions of humans around the globe. Today, nano-biotechnology, nanomaterials and surface modifications provide a new insight to the current problem of biomaterial complications, and even allows us to envisage strategies for the organ shortage. In this talk, creative strategies for modifying and engineering the surface and the interface of biomaterials, including metals, polymers from natural and synthetic sources, will be discussed. The unique potential of low-pressure low-temperature plasma surface modification will be detailed with the overall aim to envisage today how far innovation can bring tomorrow solutions for reparative and regenerative medicine. Applications for health will be emphasized, including biologically active-based, biomimetic, low-fouling, bactericidal, and antiviral coatings. References M. Shekargoftar, S. Ravanbakhsh, V. Sales de Oliveira, J. Buhagiar, N. Brodusch, S. Bessette, C. Paternoster, F. Witte, A. Sarkissian, R. Gauvin, D. Mantovani. Effects of Plasma Surface Modification of Mg-2Y-2Zn-1Mn for Biomedical Applications, *Materialia*, 102285, 2024. S.H. Um, J. Lee, M. Chae, C. Paternoster, F. Copes, P. Chevallier, D.H. Lee, S.W. Hwang, Y.C. Kim, H.S. Han, K.S. Lee, D. Mantovani, H. Jeon. Biomedical Device Surface Treatment by Laser-Driven Hydroxyapatite Penetration-Synthesis Technique for Gapless PEEK-to-Bone Integration. *Adv Healthcare Mater*, 13, 26, 2401260, 2024. M.E. Lombardo, V. Mariscotti, P. Chevallier, F. Copes, F. Boccafroschi, A. Sarkissian, D. Mantovani. Effects of cold plasma treatment on the biological performances of decellularized bovine pericardium extracellular matrix-based films for biomedical applications. *Exploration of BioMat-X*, 1, 2, 84-99, 2024. L. Bonilla-Gameros, P. Chevallier, X. Delvaux, L.A. Yáñez-Hernández, L. Houssiau, X. Minne, V.P. Houde, A. Sarkissian, D. Mantovani. *Nanomaterials*, 14, 7, 609, 2024. L. Marin de Andrade, C. Paternoster, P. Chevallier, S. Gambaro, P. Mengucci, D. Mantovani. *Bioactive Materials*, 11, 166, 2022.

Keywords : Low vacuum plasma | Biomaterials | Implants | Regenerative Medicine

76. Bioresorbable ultrafine-grained Zn stabilized with nanometric ZnO dispersoids

Balog Martin^{1 2}, Krzik Peter¹, Marques De Castro Moara², Skolakova Andrea³, Pinc Jan³, Kubasek Jiri⁴, Seabra Francisca M.^{1 5}, Zhao Yujie^{1 5}, Figueiredo Roberto⁶

1 - Institute of Materials and Machine Mechanics, Slovak Academy of Sciences (Slovakia), 2 - Centre of Excellence for Advanced Materials Application, Slovak Academy of Sciences (Slovakia), 3 - Institute of Physics of the Czech Academy of Sciences (Czech Republic), 4 - Department of Metals and Corrosion Engineering, University of Chemistry and Technology (Czech Republic), 5 - Faculty of Materials Science and Technology in Trnava, Slovak University of Technology (Slovakia), 6 - Department of Metallurgical and Materials Engineering, Universidade Federal de Minas Gerais (Brazil)

After the time necessary to support a recovering tissue, endovascular stents and orthopedic fixators become redundant; their long-term retention becomes problematic and they must be removed. However, a secondary operation is stressful to a patient and brings economic burdens. This motivates research on bioabsorbable implants. Owing to their unique properties, that cannot be adequately achieved with polymers, metals are an attractive material option for bioabsorbable implants. Zn as a bioabsorbable metal attracted considerable scientific interest in the last decade because it solves the main problems related to the utilization of other bioabsorbable metals. Though, as a result of a low recrystallization temperature of Zn and an intense overaging of the present precipitates, the post-processing/deformation microstructural instability i.e., instability of the mechanical properties of high-strength alloyed and/or grain-refined Zn biometals remains insufficiently resolved. In this paper, we present a new concept of stabilization of refined Zn microstructures by a small fraction of nontoxic nanometric ZnO dispersoids. Zener pinning action induced by the ZnO allows the formation of ultrafine-grained Zn structures, with a high strength, and its long-term retention at high homologous temperatures. At the same time the utilized stabilization concept does not compromise in-vitro corrosion and biological responses. Actually, the presence of ZnO brings up an advantage of more homogeneous corrosion, enhanced bacteriostatic effect and it improves antiphlogistic response. The effect of the ZnO on post-processing microstructural stability (as a function of the strain and temperature), deformation and strengthening mechanisms, and creep endurance of the various Zn+ZnO composites is systematically pursued. Acknowledgements: This work was supported by the VAIA 09I03-03-V04-00718, APVV-20-0417, VEGA 2/0157/24 and ITMS 313021T081 ERDF projects.

Keywords : bioresorbable, metal matrix composite (MMC), zinc (Zn), zinc oxide (ZnO)

77. Influence of Si and process parameters on the microstructure and properties of continuously annealed low C-Nb-Ti strip steel

Banks Kevin ¹, Maubane Dannis ¹, Netshilema Muthoiwa ¹

¹ - Department of Material Sciences and Engineering, University of Pretoria (South Africa)

The influence of 0.4% Si addition and continuous annealing (CA) parameters on the microstructure and mechanical properties of low C-Nb-Ti steels for the automotive industry was investigated. Si-containing and Si-free steels were subjected to CA simulations varying annealing temperature (T_{max}), line speed (LS) and the amount of cold work (CW). During CA, recrystallisation of the cold-rolled polygonal ferrite and spheroidal pearlite microstructure initiated near 650 Celsius, progressing fully above 780 Celsius and was retarded by Si addition, fast LS and small CW. Although enhancing recrystallisation, large CW increased the dislocation density and promoted very fine NbTi(C,N) precipitation between 700 and 750 Celsius which retarded softening in Si-steel and restricted the final ferrite grain size to 4-5 microns. The Si addition increased strength by 7-15% which, besides solid solution strengthening, depended on processing parameters. In the above temperature range, strength was preserved in Si-steel subjected to small CW and fast LS because of restricted recrystallisation, whilst larger CW reduced strength due to increased recrystallisation. In both cases, strength reduction was counterbalanced by precipitation strengthening. Elongation improved marginally with higher T_{max} and slower LS. At least 80% recrystallisation was attained at a T_{max} of 750 Celsius and a LS of 60 m/min, ensuring balanced strength and elongation with acceptable variability. Surface oxides in Si-steel after hot rolling were predominantly wustite and magnetite, with no harmful hematite or fayalite detected. These findings underscore the role of Si and CA parameters in optimizing microstructural stability and mechanical performance of low C-Nb-Ti steels.

Keywords : Continuous annealing, Nb, Ti, Si steel, line speed, cold work, recrystallisation, mechanical properties, precipitation

78. Microstructure development of a Zn-based biodegradable alloy during laser shock peening

Capek Jaroslav ¹, Pinc Jan ¹, Kaufman Jan ², Brajer Jan ², Studecky Tomas ³, Kubasek Jiri ⁴

1 - Institute of Physics of the Czech Academy of Sciences (Czech Republic), 2 - HiLASE Centre, Institute of Physics of the Czech Academy of Sciences (Czech Republic), 3 - COMTES FHT a.s. (Czech Republic), 4 - Department of Metals and Corrosion Engineering, University of Chemistry and Technology Prague (Czech Republic)

Selected Zn-based materials are investigated as promising candidates for fabricating biodegradable, temporary, implants. As implants, materials are exposed not only to a corrosive environment, namely to various body fluids but also to various mechanical loading, including cyclic loading, which introduces the risk of damage by fatigue corrosion and stress-corrosion cracking. Those issues can be, at least partially, prevented by the grain refinement and implementation of residual compressive stress in the surface and subsurface layer. Laser shock peening is a novel, very effective, method allowing the modification of layers with a thickness of up to approximately 2 mm, which is significantly more than achievable by conventional techniques. In this study, we focused on the microstructural evolution of a hot forged ZnMgSr biodegradable alloy possessing a relatively strong texture and coarse grain size. Keywords: Zn-based biodegradable materials, surface treatment, laser shock peening, microstructure

Keywords : Zn, based biodegradable materials, surface treatment, laser shock peening, microstructure

79. Coated biodegradable Zn-0.8Mg-0.2Sr alloy

Skolakova Andrea¹, Pinc Jan ², Jablonska Eva ³, Skolakova Tereza ⁴,
Vlcak Petr ¹, Janebova Barbora ³, Kutova Anna ⁵, Capek Jaroslav ²,
Hosova Klara ⁶, Vojtech Dalibor ⁶, Kubasek Jiri- ⁶

1 - Institute of Physics of the Czech Academy of Sciences (Czech Republic), 2 - Institute of Physics of the Czech Academy of Sciences (Czech Republic), 3 - Department of Biochemistry and Microbiology, University of Chemistry and Technology Prague (Czech Republic), 4 - Department of Organic Technology, University of Chemistry and Technology Prague (Czech Republic), 5 - Department of Solid State Engineering, University Chemistry and Technology Prague (Czech Republic), 6 - Department of Metals and Corrosion Engineering, University of Chemistry and Technology Prague (Czech Republic)

Research on biodegradable metallic materials currently focuses on improving implant surfaces to promote faster bone healing. Biodegradable materials gradually degrade within the human body, necessitating the exclusion of toxic metals from potential implants. For this reason, magnesium (Mg), zinc (Zn), and iron (Fe) are the most commonly used elements in the preparation of biodegradable materials. However, challenges related to degradation rate and biocompatibility remain, which could potentially be addressed through surface modification of the implants. This study comprehensively describes the mechanism of hopeite formation on the biodegradable Zn-0.8Mg-0.2Sr alloy, which is considered a promising material for biomedical applications. The research focuses on the chemical composition of the coating bath, exposure time, and temperature, all of which influence the structure, quality, distribution, phase composition, thickness, and roughness of the resulting layer. Optimal coating conditions were identified under which a smooth and uniformly distributed hopeite layer was formed. Additionally, the study demonstrates the effect of the hopeite layer on the alloy's interactions with cells and bacteria. The presence of the hopeite layer significantly enhanced cell viability during direct cytotoxicity testing. Moreover, the formation of a smoother layer positively influenced the antibacterial properties of the alloy. These findings are promising for the use of the coated Zn-0.8Mg-0.2Sr biodegradable alloy as a temporary implant material.

Keywords : Conversion coatings, Surface properties, In vitro tests

80. Design and Mechanical Evaluation of Ti-6Al-4V Lattice Structures for Biomedical Implants

Najera Maria ¹, Araya Miguel ¹, Rautio Timo ², GuilleN Teodolito ¹, Jarvenpaa Antti ²

1 - Bio-inspired Materials and Processes, Instituto Tecnológico de Costa Rica, 30101 Cartago (Costa Rica), 2
- Future Manufacturing Technologies (FMT), Kerttu Saalasti Institute, University of Oulu, Pajatie 5, 85500 Nivala (Finland)

Additive Manufacturing of porous titanium alloys presents a promising approach for developing biomedical implants with tailored mechanical properties, offering precise control over stiffness and strength to better match human bone. This study investigates the morphological and mechanical properties of Ti-6Al-4V reticular structures manufactured using a Powder Bed Fusion Laser Beam. Three triply periodic minimal surface designs (diamond, primitive, and split P) were analyzed with constant and radial density gradients. Surface treatments included electropolishing and chemical etching to improve surface quality. Key findings reveal that the split P structures exhibited the highest yield strength (274.93-288.95 MPa) and moderate Young's modulus values (7.16-7.76 GPa), making them the most promising candidates for load-bearing biomedical implants. In contrast, the diamond structures demonstrated the highest stiffness (Young's modulus: 6.95-8.65 GPa) but exhibited brittle behavior, limiting their suitability for applications requiring energy absorption or flexibility. The primitive structures displayed the lowest modulus and yield strength, indicating their ductile mechanical performance. It might be advantageous in applications requiring flexibility but is less ideal for load-bearing scenarios. This research highlights the potential of optimized TPMS lattice designs in addressing challenges such as stress shielding and mechanical compatibility, paving the way for advanced implant solutions with improved durability and load-bearing capacity.

Keywords : PBF, LB, TPMS lattices, Ti, 6Al, 4V, Biomedical Implants, Surface Treatments

81. Surface Modification of Zn-0.8Mg-0.2Sr: Insights into Nitrogen Ion Implantation and Microstructural Evolution

Pinc Jan ¹, Vlak Petr ², Lebeda Miroslav ¹, Fojt Jaroslav ³, Bartunek Vilem ⁴, Smola Vojtech ², Vronka Marek ¹, Drahokoupil Jan ¹, Weiss Zdeněk ¹, Kubasek Jiri ³, Capek Jaroslav ¹, Skolakova Andrea ¹

1 - FZU - Institute of Physics of the Czech Academy of Sciences, Na Slovance 1999/2, Prague 8, 182 00, Czech Republic (Czech Republic), 2 - Department of Physics, Faculty of Mechanical Engineering, Czech Technical University in Prague (Czech Republic), 3 - Department of Metals and Corrosion Engineering, University of Chemistry and Technology, Technická 5, Prague 6, 166 28, Czech Republic (Czech Republic), 4 - Department of Inorganic Chemistry, University of Chemistry and Technology Prague, Technická 5, 166 28, Prague 6, Czech Republic (Czech Republic)

Biodegradable materials are increasingly valued for their potential to enhance patient comfort, with surface modification emerging as a key strategy to improve implant-tissue interactions. This study examined the effects of nitrogen ion (N⁺) implantation on the microstructure of a Zn, Mg₂Zn₁₁ and Zn-0.8Mg-0.2Sr alloy. Implantation at a fluence of $17\text{Å} \cdot 10^{18} \cdot \text{ions/cm}^2$ resulted in significant microstructural changes. Nanopores formed on pure Zn surfaces, while cracks appeared in the Mg₂Zn₁₁ intermetallic phase. In the alloy, both effects were observed, along with regions of varying height identified via AFM. Ion implantation caused oversaturation in pure Zn and Mg₂Zn₁₁, producing nano- and micro-porous layers up to 400 nm thick. The surface composition of the alloy shifted, with Mg content increasing from 0.8 to 15 wt.% due to the breakdown of Mg₂Zn₁₁ and subsequent Mg diffusion. A limited formation of MgO and Mg₃N₂ was detected, confirmed by XRD and TEM, but nitrides were unstable in humid environments, degrading within hours. Notably, Zn₃N₂ was absent, likely due to thermodynamic instability and low Zn-N affinity. However, GD-OES identified 10 at.% nitrogen in pure Zn, suggesting nitrogen incorporation into interstitial sites. Sputtering analysis using the TRIM code linked sputtering to increased surface roughness. These findings highlight the complexity of N⁺ implantation in modifying Zn-based materials and suggest its potential for engineering active, functional surfaces, paving the way for improved biomedical applications.

Keywords : Biodegradable zinc alloys, ion implantation, magnesium nitride, characterization

82. Enhanced Polyp Adhesion on Chemically Modified Titanium Nonwoven Fabric

Inoue Minami¹, Ueda Masato²

1 - Graduate School of Science and Engineering, Kansai University, Osaka, 564-8680 (Japan), 2 - Faculty of Chemistry, Materials and Bioengineering, Kansai University, Osaka, 564-8680 (Japan)

Coral reefs face significant damage from factors such as climate change, pollution, and careless tourism. In vertebrates like mammals, osteoblasts form bone composed of hydroxyapatite ($\text{Ca}_{10}(\text{PO}_4)_6(\text{OH})_2$). Similarly, in hard corals, polyps possess osteoblast-like cells that produce calcium carbonate (CaCO_3), with skeletal formation mechanisms being almost identical to those in vertebrates. Titanium (Ti) and its alloys are widely utilised as biomedical materials for orthopaedic and dental implants due to their excellent mechanical properties, biocompatibility, and corrosion resistance. Various surface modifications have been developed to enhance cell adhesion and bone formation. This study aimed to investigate polyp adhesion and skeletal formation on Ti nonwoven materials after chemical surface modifications. Polyps were isolated by increasing the salinity of artificial seawater (RED SEA SALT, Red Sea) in which coral fragments were immersed. Ti nonwoven fabrics were chemically treated with an $\text{H}_2\text{O}_2/\text{HNO}_3$ aqueous solution at 353 K for 20 minutes. This process resulted in a TiO_2 gel film with a sponge-like morphology forming on the Ti fibres. Polyps adhered to the nonwoven fabric within 70 hours, but surface modification reduced the adhesion time to 50 hours. TiO_2 gel has been reported to promote cell adhesion, and a similar trend was observed with coral polyps. We hypothesise that the functional OH groups on the titanium oxide surface and the three-dimensional morphology contribute significantly to the enhanced adhesion and skeletal formation of polyps on treated titanium surfaces.

Keywords : TiO_2 , Osteoblasts, Functional OH groups, Bone, Regenerative Medicine Technology

83. Hot deformation behaviour and microstructure evolution of degradable Zn-0.8Mn alloy

Li Meng¹, Shi Zhang-Zhi¹, Wang Lu-Ning¹

¹ - School of Materials Science and Engineering, University of Science and Technology Beijing, Beijing, 100083, China (China)

Zn-0.8Mn alloy is highly ductile, providing a foundation for developing high-performance Zn-Mn-based alloys. However, constitutive equation for this alloy is unknown, and its dynamic recrystallization (DRX) behaviour remains unclear, making the optimization of hot processing parameters largely reliant on trial and error. In this work, the constitutive equation and processing map of this alloy are obtained for the first time, which show that it has excellent hot formability with narrow instability zones. Volume fraction of DRX grains increases with temperature and decreases with strain rate. Discontinuous DRX, continuous DRX, twinning-induced DRX, and particle stimulated nucleation are activated during hot compressions. Mn addition promotes activation of non-basal slip in Zn grains and formation of a bimodal grain structure. This structure generates a hetero-deformation-induced strengthening effect, resulting in elevated-temperature strengths superior to those of pure Zn.

Keywords : Zn alloys, hot deformation, DRX, microstructure

84. High plasticity Zn-Mn alloy and effects of further alloying

Shi Zhang-Zhi^{1 2}, Li Meng^{1 2}, Li Xiang-Min^{1 2}, Wang Lu-Ning^{1 2}

1 - Beijing Advanced Innovation Center for Materials Genome Engineering, State Key Laboratory for Advanced Metals and Materials, School of Materials Science and Engineering, University of Science and Technology Beijing, Beijing 100083, PR China (China), 2 - Institute of Materials Intelligent Technology, Liaoning Academy of Materials, Shenyang 110004, China (China)

Improving plasticity has been an eternal theme of developing metallic materials. Good plasticity can improve formability of materials, which plays a critical role in processing them into parts. Zn-based materials have attracted growing attention as biodegradable metallic materials. However, as-cast pure Zn is very brittle with elongation (EL) < 5%. Herein, Zn-0.4/0.8Mn alloys, developed through a combination of rolling and heat treatment, exhibit high EL of 89% and 94%, respectively. Surface-roughness-induced plasticity is discovered in Zn-0.4Mn alloy. From unground to 5000# sandpaper ground states, its EL increases from 74% to 143% without sacrificing strength. Zn-Mn-x (x = Ag, Cu, Mg or Ca) alloys are designed, hot extrusion and then warm caliber rolling eliminate brittleness of the as-cast alloys. Ductility of Zn-Mn-Fe alloy is sensitive to Fe content. High plasticity Zn-Mn based alloys are promising candidates for fabrication of vascular stents and orthopaedic implants.

TRANSLATE with x English ArabicHebrewPolish BulgarianHindiPortuguese CatalanHmong DawRomanian Chinese SimplifiedHungarianRussian Chinese TraditionalIndonesianSlovak CzechItalianSlovenian DanishJapaneseSpanish DutchKlingonSwedish EnglishKoreanThai EstonianLatvianTurkish FinnishLithuanianUkrainian FrenchMalayUrdu GermanMalteseVietnamese GreekNorwegianWelsh Haitian CreolePersian

TRANSLATE with COPY THE URL BELOW Back EMBED THE SNIPPET BELOW IN YOUR SITE Enable collaborative features and customize widget: Bing Webmaster Portal Back

Keywords : Zn alloys, high plasticity, alloying, microstructure, plastic deformation

85. Deposition of nanoparticles in lattice structures: example of antibacterial ZnO nanowires

Weiss Laurent ¹, Seth Malobi ^{2 3}, Soule Samantha ³

1 - Laboratoire d'Etude des Microstructures et de Mecanique des Materiaux (F-57070 Metz France), 2 - Laboratoire d'Etude des Microstructures et de Mecanique des Materiaux (France), 3 - Laboratoire de Chimie Physique et Microbiologie pour les Materiaux et l'Environnement (France)

It's important to know that surgical site infections in trauma surgery are infrequent (3% for scheduled surgery), but lead to severe complications in 50% of cases (bone necrosis, generalized infection, etc.), and, a mortality rate of almost 5% (in France). Therapeutic responses most often require revision surgery with removal of infected material, massive use of antibiotics and longer hospital stays. Against this backdrop, it is vital to develop preventive solutions to reduce the rate of infection on prostheses. Today, additive manufacturing makes it possible to manufacture prostheses with lattice structures, either to reduce weight or to promote osseointegration. In both cases, lattices offer controlled apparent Young's modulus in order to reduce stress shielding with the bones. The problem with these prostheses is that bacteria can lodge and proliferate in them, leading to post-operative infection. In order to make Ti-6Al-4V lattices antibacterial, we have, for the first time, developed a protocol for achieving quasi-homogenous nanoparticle deposition. Various lattice structures were fabricated by PBF (powder bed fusion) and the unmelted particles at the surface were removed by acid etching. ZnO coating was carried out by seed dip coating for subsequent nanowire growth using the hydrothermal method. Several parameters such as precursor composition, deposition/growth time and temperature were adjusted to obtain an optimized coating. Characterization by scanning electron microscopy showed that the nanowires grew perpendicular to the surface, everywhere in the volume of the part (even in centrally located lattices), and ZnO formation was confirmed by Raman spectroscopy and X-ray diffraction.

Keywords : Additive manufacturing, lattice structure, Nanowires deposition, antibacterial activity, Ti, 6Al, 4V

86. Nanotopographical Surface Engineering and Corrosion Resistance Enhancement of Ti-based Bulk Metallic Glass through Alkaline Chemical Treatment

Douest Yohan¹, Tiwari Kirti², Ter-Ovanessian Benoit¹, Rizzi Paola³, Fabregue Damien¹, Chevalier Jerome¹, Courtois Nicolas⁴

1 - Universite de Lyon, INSA de Lyon, MATEIS CNRS UMR5510, 20 Avenue Albert Einstein, F-69621 Villeurbanne Cedex, France (France), 2 - Università di Torino, Dipartimento di Chimica e Centro Interdipartimentale NIS (Nanostructured Surfaces and Interfaces) (Italy), 3 - Università di Torino, Dipartimento di Chimica e Centro Interdipartimentale NIS (Nanostructured Surfaces and Interfaces) (Italy), 4 - Anthogyr SAS (France)

Due to their exceptional properties, Ti-based bulk metallic glasses (Ti-BMGs) have emerged as promising materials for minimally invasive dental implant devices. However, their relatively high copper content poses a significant challenge by compromising corrosion resistance and promoting localised corrosion. This study introduces a rapid and straightforward surface modification technique, termed chemical pseudo-dealloying, to address this limitation. This method selectively reduces copper content in the top surface layer, inducing palladium enrichment and significantly enhancing corrosion resistance. Furthermore, the selective etching of copper during the process generates nanoscale surface features, creating a Pd-rich nanoporous layer with tailored topographical characteristics. The modified surfaces were comprehensively characterized to evaluate their topography, chemical composition, electrochemical behavior, and biocompatibility. The nanoscale surface features and Pd-rich composition contribute to improved corrosion resistance while maintaining biocompatibility—critical attributes for biomedical applications. This study demonstrates the potential of chemical pseudo-dealloying as an effective approach to overcome the limitations of Cu-containing Ti-BMGs, combining improved functional properties with surface designs suitable for integration into biomedical devices. These findings open new avenues for optimizing metallic amorphous alloys' surface properties and topography, advancing their application in dental implants and broader biomedical contexts.

Keywords : Surface modification, bulk metallic glass

87. Investigation of Microstructure Evolution and Cytocompatibilities of ODS Modified Ti64 Alloy: A Comparative Study of Y-Zr-O and Y-Hf-O Oxides

Yalcin Merve Yesim^{1 2}, Dogu Merve Nur^{3 4 5}, Govercin Betul⁶,
Brabazon Dermot^{3 4 5}, Celikin Mert^{1 2}

1 - I-Form Advanced Manufacturing Research Centre, University College Dublin, Dublin (Ireland), 2 - School of Mechanical and Materials Engineering, University College Dublin, Dublin (Ireland), 3 - I-Form Advanced Manufacturing Research Centre, Dublin City University, Dublin (Ireland), 4 - Advanced Processing Technology Research Centre, Dublin City University, Dublin (Ireland), 5 - School of Mechanical and Manufacturing Engineering, Dublin City University, Dublin (Ireland), 6 - Simultura Material Technologies - R&D Engineering Software and Production Consultancy (Turkey)

Ti6Al4V(Ti64) alloy is one of the most common alloys used in biomedical implant production. To compensate for the stress shielding effect obtained in the use of bulk implants and to promote tissue growth, lattice structures were developed. Having complex shapes, lattice structures are produced via additive manufacturing techniques, in which columnar prior beta grains are formed at elevated temperatures, that transform into acicular alpha prime laths during rapid solidification. Columnar prior beta grains result in texture/anisotropy and alpha prime laths create stress concentration points under mechanical loading, that degrades the mechanical stability of implants. To overcome these problems, the microstructure needs to be refined. Oxide dispersoids are known for their effects on grain refinement and microstructure stabilization. For refining microstructure, in this study, three different nano-oxide-modified Ti64 alloys are designed and produced via the powder metallurgy (PM) route; their microstructure evolution and cytocompatibility responses are investigated. Nano-sized and submicron-sized Y₂O₃, ZrO₂, and HfO₂ oxides were mixed with gas-atomized Ti64 powders to form Y-Zr-O and Y-Hf-O oxide dispersoids in the matrix. The modified alloys are designated as Ti64-YZ (Ti64-Y₂O₃-ZrO₂) and Ti64-YH (Ti64-Y₂O₃-HfO₂). A heat treatment process was optimized to maximize dispersoid number density; the influence of each ternary oxide on the microstructure and texture evolution is investigated. Moreover, cytotoxicity tests were performed on MG63 cells to determine and compare the impact of nano-oxides on the cytocompatibility of Ti64 alloy.

Keywords : Ti64, ODS, Powder Metallurgy, Biomaterials, Microstructure Refinement.

88. Experimental and computational investigation on the anisotropy of BCC and HCP metals by distortional evolution of yield surfaces

Baodong Shi¹, Yang Xuejian ²

1 - National Engineering Research Center for Magnesium Alloys, School of Materials Science and Engineering, Chongqing University (Chongqing, 400044, PR China China), 2 - State Key Laboratory of Crane Technology, Yanshan University (Qinhuangdao, 066004, PR China China)

Focusing on non-proportional loading condition during forming process of BCC and HCP metals, the distortional evolution of yield surfaces of DP780 and AZ31 alloy are investigated experimentally in the complete σ_{11} - σ_{22} space. Strong anisotropy including initial strength differential effect and subsequent distortional hardening are detected. The underlying deformation mechanisms are discussed based on microstructure observation. For AZ31, it is found that the number of twinning decrease with pre-axial tension stress increasing, resulting from the restricted activity of twinning with c/a ratio decreasing. Furthermore, the subdivision of twin boundaries leads to large strain hardening rate. Therefore, the strain hardening rate and flow stress under pure torsion are much higher than other loading paths. For DP780, a high curvature of yield surfaces has been detected in the first quadrant of the σ_{11} - σ_{22} stress space. Compared with tension-tension and compression-compression biaxial loading, the yield strength is lower under compression-tension and tension-compression loading. The reason is that more low angle grain boundarys are formed and stress is concentrated at the grain boundary under compression-tension and tension-compression, resulting in grains to slip earlier.

89. Impact of Rare Gas Addition on Fabrication of a-C:H Films via C₂H₂/Ar/Ne/He Plasma-Enhanced Chemical Vapor Deposition

Nagamine Kazuki¹, Ikada Kizuku¹, Wakita Daichi¹, Kamataki Kunihiro¹, Shiratani Masaharu¹

¹ - Graduate School of Information Science and Electrical Engineering, Kyushu University (Japan)

Hydrogenated amorphous carbon (a-C:H) films have various applications, such as hard masks in semiconductor manufacturing. A-C:H films used as hard masks are required to have high film mass density and low film stress. Previous research using magnetron sputtering plasma showed that harder a-C:H films are obtained by adding Ne to Ar. So far, few studies have reported on effects of Ne and He addition on the quality of a-C:H films deposited by plasma-enhanced chemical vapor deposition (PECVD) of Ar+C₂H₂. In this study, we investigated such effects. Experiments were performed using a capacitively coupled plasma reactor. Plasma was generated by applying an RF voltage at 13.56MHz between two parallel plate electrodes. Total gas flow rate was 6 sccm, with 1 sccm of C₂H₂ and 5 sccm of Ar, Ar+Ne, or Ar+He. The mixing ratio of Ne and He was varied from 0 to 95%. The pressure was 5 mTorr. Under both Ne and He addition conditions, the film mass density is nearly constant (~2.2 g/cm³) regardless of the gas mixing ratio. While the film stress is 4.8 GPa without Ne and He addition, the film stress reduces to 3.5 GPa for 24-50% Ne addition. Moreover, the deposition rate increases from 1.5 nm/min to 3.5 nm/min with He addition. These results suggest that Ne and He addition to C₂H₂+Ar plasma is a potentially good tuning knob to control properties of a-C:H films.

Keywords : Diamond Like Carbon, Film stress, Plasma CVD, Rare gas

90. Masking Effect of Phosphate Pretreatment on Surface Defects of Auto Steel Sheets

Fang Baiyou

1 - Baosteel-NSC Automotive Steel Sheets Co., Ltd (Cold Rolling Comprehensive Building, Wei Wu Road, Baosteel, Baoshan District, Shanghai, 200941 China)

The proportion of hot-dip galvanized sheet in the automotive industry is on the rise, and the quality of its surface has become a pivotal determinant influencing the subsequent quality of painting. In order to investigate the impact of diverse plating defects on subsequent painting performance, this paper compares and analyses the typical defect characteristics of three automotive plate types: cold rolled plate, hot-dip galvanised plate and alloyed hot-dip galvanized plate. This study examines the masking ability of phosphate treatment on different types of defects and establishes a relationship between the transferability of small defects on the surface of various substrates and their phosphate grain sizes. The findings provide a theoretical basis for enhancing the surface quality of automotive plates after painting.

Keywords : phosphate conversion coating, cold, rolled sheet, galvanized steel, masking effect

91. A robust solid-liquid composite superlubricity strategy toward high temperatures

Zhang Yixuan¹, Wu Hongxing², Li Hang¹, Wang Lin¹, Shi Junqin¹, Hua Ke¹, Wang Haifeng¹

1 - Northwestern Polytechnical University (China), 2 - Northwestern Polytechnical University (127 West Youyi Road, Beilin District, Xi'an, Shaanxi China)

Superlubricity materials and technologies have received widespread attention in achieving near-zero friction (COF

Keywords : Lubrication, Superlubricity, Boronizing, Wide temperature range, anti, friction and anti, wear, tribology design, Lubrication mechanism

92. Revealing fretting wear resistance mechanism under liquid lead-bismuth eutectic of Cr-Al-C composite coatings fabricated by laser cladding

Cao Yue¹, Ke Hua¹, Haifeng Wang¹

1 - Northwestern Polytechnical University [Xi'An] (China)

Laser cladding technology was utilized to construct Cr-Al-C coatings on the surfaces of service materials. Through the fretting wear test in liquid LBE, the fretting wear behaviour of Cr-Al-C composite coatings under different fretting working conditions was studied to elucidate the characteristics of the coating's sub-surface components, chemical composition distribution, morphology, crystalline orientation, and micro-structure after the fretting wear, so as to reveal the protection mechanism of coatings against fretting wear in liquid LBE. Results show that the coating mainly consists of diffuse Cr₂AlC phase, interdendritic Cr₇C₃ phase and dendritic Cr-based solid solution. The wear resistance of the coating is 4.25 times that of the 316 stainless steel substrate at a test temperature of 320 °C, the wear resistance of the coating was 33 times that of the 316 stainless steel substrate at a test temperature of 450 °C. The oxidized layer can block the direct contact between the material and the friction partner and reduce the wear, while also preventing the infiltration of LBE and the dissolution of the base metal elements. In addition, the Cr₂AlC in the coating possesses good self-lubricating properties, which can also effectively reduce wear; the coating's Schmidt factor is statistically distributed between 0.41-0.5, with a high capacity for plastic deformation, which effectively improves the resistance to fretting wear damage of materials. The presence of carbide effectively impedes the movement of dislocations, dislocations stacked around it and can not make it fracture or deformation, thus

playing a certain role in strengthening. This study provides a theoretical basis and foundation for the protection design of heat transfer tubes in steam generators.

Keywords : MAX phase, Lead bismuth eutectic alloy, Fretting wear, Laser cladding

93. What can be gained and what is lost from the perspective of properties, when modifying the structural design of thin films

Munteanu Daniel¹, Lopes Claudia , Rodrigues Marco , Ferreira Armando , Macedo Francisco , Gabor Camelia , Alves Eduardo , Barradas Nuno , Vaz Filipe

1 - Transilvania University of Brasov (29 Eroilor blvd., 500036 Brasov Romania)

The thin films are frequently present in the case of various applications related to fields such as mechanical engineering, optics and optoelectronics, energy, sensors, biomedicine, etc. For certain compositions favorable for different applications, the modification of the properties can be achieved by changing the structural design of the layer. A deposition process associated with achieving this is GLancing Angle Deposition (GLAD) within the general Physical Vapour Deposition (PVD) method. The paper shows how the properties of a compound, in the form of a thin film, extremely well-known in practice - TiN, vary when changing the structural design (inclined aspect with different angles, zig-zag aspect with different angles) and maintaining the composition. The obtained results clearly show that, from different application perspectives, the modification of the porosity and roughness, of the thermal and electrical properties, of the optical ones, can be a real advantage, in extremely efficient conditions.

Keywords : GLAD, thin film, TiN, structural design, properties

94. Electrical properties of large area perovskite type oxide epitaxial thin films transferred onto polymer sheets

Nishikawa Hiroaki ¹

¹ - Kindai University (Japan)

Since the pioneering work by Nomura et al. on transparent flexible thin-film transistors using oxide materials, research on flexible oxide devices has advanced rapidly. Most studies in this field employ polymer films as flexible substrates, which requires low-temperature processing due to their limited heat resistance. A common approach has been the exploration of amorphous oxide materials, which can be deposited at room temperature and exhibit properties such as high carrier mobility. This has led to significant progress in applying amorphous oxide semiconductors to various flexible devices. Conversely, traditional applications of oxide materials often rely on their ability to integrate diverse electronic functions, which requires epitaxial thin films due to their strong anisotropy. However, the high process temperatures required for epitaxial growth have thus far precluded their use with flexible polymer substrates. This underscores the need for novel processes to enable traditional oxide material applications in flexible devices. In this study, we propose a transfer process for epitaxially grown functional oxide thin films, initially deposited on suitable substrates, to flexible polymer films. The process was demonstrated using a perovskite-type ferroelectric thin film transferred onto a polymer sheet. The results of this approach and its implications for flexible device applications are discussed.

Keywords : Flexible Oxide, Epitaxial Thin Film, Transfer Process, Large“Area

95. Modification of Microstructures and Cyclic Oxidation Behavior of Electron Beam Physical Vapor Deposition Processed Thermal Barrier Coatings

Seo Dongyi¹, Park Ihho², Pankov Vladimir¹, Lee Sunghun², Yang Wonjon²

1 - Aerospace Research Centre, National Research Council of Canada (NRC), Ottawa, Ontario (Canada), 2 - Korea Institute of Materials Science (KIMS), Changwon, Gyeongnam (South Korea)

In the hot section of gas turbine engines, thermal barrier coatings (TBCs) are used to provide protective layers for safe operation of the engines at elevated temperatures. The TBC system consists of a ceramic top coat deposited on a metallic bond coat. The purpose of the bond coat is to provide protection layers against oxidation and hot corrosion of a metal substrate caused by combustion gases while improving adhesion of the top coat to the metallic substrate. The ceramic top coat is to provide a temperature drop across its thickness due to its low thermal conductivity. The typical material for the top coat is yttria-partially stabilized zirconia (YSZ). In this study, TBCs with YSZ based ceramics were fabricated and optimized as ceramic top coats on NiCrAlY bond coats by electron beam physical vapor deposition (EB-PVD) processes. Thermally grown oxides (TGO) layers between YSZ TBCs and NiCrAlY bond coats were controlled at various coating processes such as substrate temperatures, oxygen pressures and pre-oxidation processes. To assess the coating durability, cyclic furnace tests were carried out at 1100 degree C. Microstructures of selected coated and tested samples were characterized by optical microscopy, scanning electron microscopy and x-ray diffraction. Especially, the characteristics of the TGOs are analyzed by transmission electron microscopy. The effect of modified coating structures on coating performance was elucidated in terms of coating microstructures including TGOs and degradation of the coatings.

Keywords : Thermal barrier coatings, thermally grown oxides (TGO), cyclic oxidation behaviour, electron beam physical vapor deposition, and yttria, partially stabilized zirconia (YSZ).

96. Compositionally Complex Refractory Metal Nitride Coatings: The Effects of V, Nb and Ta On Their Structure and Mechanical Properties

Lofaj Frantisek¹, Kvetkova Lenka¹, Petra Hviscova¹, Mikula Marian², Fiantok Tomas², Roch Tomas², Dmitry Albov¹

1 - Institute of Materials Research of the Slovak Academy of Sciences (Slovakia), 2 - Faculty of Mathematics, Physics and Informatics, Comenius University in Bratislava (Slovakia)

The work investigates structure evolution and mechanical behavior of the reactively sputtered multi-element nitride coatings based on TiZrHf alloyed by V, Nb, and Ta with variable stoichiometry. The characteristics of the studied (TiHfZr-V)-Ny, (TiHfZr-Nb)-Ny, (TiHfZr-Ta)-Ny, and (TiHfZr-VNbTa)-Ny coatings were compared with those of the reference (TiHfZr)-Ny coatings over the entire range of nitrogen concentrations from the metallic alloys up to the stoichiometric compositions. Homogeneous solid solutions with very similar cubic structures observed in all coatings classified these coatings as compositionally complex nitrides with the metallic sub-lattice stabilized by high entropy. Their mechanical properties depended on nitrogen concentration and refractory metals present in the corresponding system. The maximum values of hardness (~43 GPa) and indentation modulus (~530 GPa) were achieved in the reference TiZrHf-Ny coatings deposited by reactive DC magnetron sputtering with (near-)stoichiometric composition. DFT modeling suggested the lowest energy of formation in the bcc TiHfZr with Nb in the entire nitrogen stoichiometry range. However, the experimental observations revealed that the mechanical properties of the coatings containing additional V, Nb, or Ta were ~10 % lower than in the reference, and the differences among them were within the scatter of measurements. Moreover, the properties of TiZrHfVNbTa-Ny coatings were at the lower boundary of the range in the previous coating containing three or four refractory metals. Thus, the synergy effect from incorporating the additional refractory metals into TiZrHf sub-lattice on mechanical properties was not confirmed.

Keywords : compositionally complex nitrides, high entropy nitride coatings, reactive sputtering, mechanical properties

97. New Physics Informed Machine Learning Prediction of SiO₂ Film Property from Optical Emission Spectroscopy in TEOS /O₂/Ar Plasma Enhanced CVD

Kamataki Kunihiro¹, Fitrianni Sukma¹, Sato Yushi¹, Yamamoto Yuma¹, Kurosaki Yosei¹, Yamashita Daisuke¹, Okumura Takamasa¹, Itagaki Naho¹, Koga Kazunori¹, Shiratani Masaharu¹

¹ - Kyushu University (Japan)

To address the challenges posed by the increasing complexity of semiconductor devices and nanostructures, advanced plasma processes require a deep understanding of non-equilibrium and non-linear plasma dynamics. In this study, machine learning was used to predict the deposition rate of SiO₂ thin films using optical emission spectroscopy (OES) data from TEOS+O₂+Ar plasma. Experiments were conducted with a capacitively coupled plasma CVD system by varying RF power, pressure, and gas flow ratios to generate about 30 samples. Gradient Boosting Regression Tree (GBRT) was applied as the machine learning model, with Bayesian optimization used for hyperparameter tuning. The model demonstrated high predictive accuracy with an R² of 0.8 and RMSE of 8.5%. Analysis using SHAP (Shapley Additive Explanations) identified key spectral emissions, such as CO, OI (844.1 nm), and H α (656.5 nm), as significant contributors to predicting deposition rates. This indicates a strong correlation between these emissions and the film growth process. Based on these findings, a predictive model for the SiO₂ deposition rate was constructed, which showed good agreement with experimental results. The findings suggest that machine learning-based, non-invasive approaches can effectively optimize plasma processes by linking spectral data to process outcomes, offering a promising direction for further research in nanofabrication.

Keywords : Physics Informed Machine Learning, OES, Film properties, PECVD

98. Laser surface hardening of AISI 431 martensitic stainless steel by using different laser sources

Aroubi Oumaima¹, Bourahima Fazati ¹, Lafarge Christophe ¹, Ardid Renaud ¹, Brisset Francois ²

1 - CHPOLANSKY (France), 2 - Universite Paris Saclay (France)

Laser surface hardening process is an advanced technology used to enhance metal surface properties through phase transformation. In recent decades, it has gained significant attention for its efficiency and precision. The glassmaking industry has shown interest in this technology as an alternative to laser cladding process, which causes environmental risks and machining challenges. This study aims to enhance AISI 431 stainless steel mold hardness without molten powder deposition. Surface hardening of AISI 431 stainless steel was carried out using continuous wave diode (940-1020 nm), Nd:YAG (1030 nm), and fiber (1070 nm) 4 kW laser sources. The influence of process parameters such as laser power (500-3040 W), scanning speed (4.5-8.5 mm/s) and number of laser head passes (1-4) were investigated on the hardened zone's geometry, microhardness, and microstructure. Microstructural analysis was conducted using optical microscopy, scanning electron microscopy (SEM), and electron backscatter diffraction (EBSD). The current findings revealed a significant increase in microhardness due to martensite formation, which decreased with depth as martensite content reduced. Results showed that beyond a certain limit, the hardness reaches a maximum value that, regardless of the parameters, can no longer increase. This mainly depends on several factors, such as material properties, processing parameters, and cooling conditions. Achieving a target hardness is possible by adjusting the number of passes, while the desired depth will primarily depend on the power, scanning speed, and spot diameter.

Keywords : laser hardening, martensitic stainless steel, microhardness

99. Long-Term Corrosion Resistant Thin Films Prepared by Plasma Enhanced Chemical Vapor Deposition

Wang Meng-Jiy ¹

¹ - National Taiwan University of Science and Technology (Taiwan)

Metal alloys are widely employed in orthopedic implants, such as artificial bones and joints. However, significant challenges remain, including limited tissue integration and the risk of corrosion. Corrosion, primarily driven by the presence of chloride ions and dissolved oxygen in the physiological environment, degrades implant mechanical properties and releases potentially toxic metallic ions. Consequently, developing corrosion-resistant biocompatible implants is crucial for clinical success. Surface modification techniques including surface coating, passivation, electrochemical polishing, sol-gel methods, and chemical vapor deposition (CVD), have been explored to enhance the corrosion resistance of metallic implants. However, these methods often suffer from limitations such as lengthy processing times, high costs, and potential toxicity. This study proposes the utilization of plasma enhanced chemical vopro deposition (PECVD) method to deposit thin films onto metallic substrates to improve their surface properties. PECVD offers several advantages, including the ability to rapidly produce homogeneous and dense coatings at relatively low temperatures through a dry process . The chemical composition of the resulting organic/inorganic hybrid films can be precisely controlled by carefully selecting the precursor gases used in the PECVD process. Corrosion behavior was evaluated using potentiodynamic polarization tests in Hank's solution to simulate physiological conditions. The results demonstrated that the corrosion resistance of the PECVD-coated implants was significantly influenced by the thickness and density of the plasma polymer film. Finally, the biocompatibility and osteoinductive potential of the plasma polymer-protected metal constructs were assessed by culturing human osteoblast cells (hFOB1.19) to evaluate their suitability for bone tissue engineering applications. Furthermore, long-term accelerating corrosion experiments were conducted to evaluate the effectiveness of the PECVD deposited thin films on protecting metallic substrates for up to 2 years.

Keywords : Plasma Enhanced Chemical Vapor Deposition (PECVD), Thin Film, Surface Modification, Metallic Substrates, Anti, corrosion.

100. Development of an intumescent inorganic coating on steel substrates

N'Cho Wilfried Cyrille^{1 2}, Gharzouni Ameni^{2 3}, Rossignol Sylvie^{2 4}

1 - IRCER (France), 2 - IRCER - Axe 3 : organisation structurale multiechelle des materiaux (France), 3 - Institut de Recherche sur les CERamiques (France), 4 - Science des Procedes Ceramiques et de Traitements de Surface (SPCTS, Centre Europeen de la Ceramique, 12 Rue Atlantis, 87068 LIMOGES CEDEX France)

The challenge of environmental protection is a fundamental issue in all industries (nuclear, civil engineering, aeronautics). Organic polymers are used in many safety-related applications and in large quantities to fight corrosion and fire. However, they are less durable and require a lot of energy to maintain. The development of new environmentally-friendly fireproof materials is a challenge. Geopolymer-based coatings are a promising alternative due to their thermal stability (up to 1700 °C). The aim of this work is to produce a high-temperature resistant and intumescent geopolymer-based coating on steel plates. Geopolymer coatings were prepared with several expandable additives and submitted to heat treatments at 800°C for 30 min in the furnace. SEM observations were carried out in situ during the heat treatment, as well as thermal analysis measurements and X-ray diffraction measurements on the heat-treated samples. Results showed that, it is possible to produce intumescent coatings based geopolymer with proportions of aluminum less than or equal to 24% with potassium percentage greater than 17%. The intumescent samples have an expansion rate of up to 400%. The SEM shows the formation of bubbles from 700 °C associated to the viscous flow with temperature increasing. Thermal analysis shows that the rate of gas release is around 5% for intumescent samples and the phases formed at 800°C by XRD are essentially leucite and some borate alumina phases. Finally, it is possible to predict the quantity of geopolymer required to produce intumescent coatings.

Keywords : Geopolymer, intumescent, coating, expansion, additives

101. Optimized Potential Distribution Enhancing Corrosion Resistance of C/Metal Coated Bipolar Plates Used in Proton Exchange Membrane Fuel Cells

Hu Qian¹, Wang Xian-Zong ¹

1 - Northwestern Polytechnical University (China)

Developing a conductive and corrosion-resistant coating is essential to promote the application of metal bipolar plates in proton exchange membrane fuel cells (PEMFCs). For the purpose of optimizing the interfacial potential distribution, a multilayer coating that C and Ti/Cr alternatively dominated the sublayers is fabricated on SS316L (C/Ti(Cr)/SS). Multiple diffusional interfaces optimize the potential distribution across the coating and improve significantly transpassive potential to 1.6 V of C/Ti/SS, and thus offers full protection within the entire working potential range of fuel cells. After cyclic polarizations simulated the high cathodic transient potentials, a conductive TiO₂ nanofilm forms on the surface to mitigating the continuous dissolution. And C/Ti/SS achieves a noticeable interfacial contact resistance (ICR) of 9.43 mΩ.cm², highlighting the remarkable commercial application. Correspondingly, the long-term cyclic dynamic potential polarizations based on New European Driving Cycle (NEDC) are investigated on the C/Cr/SS. As a result of Cr dissolution at the heterogeneous interface, mild local corrosion occurs at 1.16 V and accelerates at 1.22 V, experiencing stages of pitting initiation, cavity, delamination, and finally collapse. Nonetheless, C/Cr/SS achieves superior small ICRs and low corrosion rate with E_{peak} up to 1.12 V. Accordingly, the optimized structure of alternatively dominated the sublayers effectively increases the internal potential drop of the coating and enhances the corrosion resistance within the noble potentials. These works offer the multilayer coating structure and combine the actual conditions potential experienced by the bipolar plate, promoting the application for metal bipolar plates used in PEMFCs.

Keywords : Corrosion Resistance, Conductivity, Metal Bipolar Plates, Metal Protective Coating, Proton Exchange Membrane Fuel Cells

102. Effect of Cr content on oxidation layer of hot-dip galvanized high-strength steel: molecular dynamics simulation

Zhang Shaoshuang, Song Renbo

1 - University of Science and Technology Beijing [Beijing] (China)

This study employs experimental and molecular dynamics simulation methods to analyze the micro-mechanisms of the influence of Cr content and temperature on the surface oxides of hot-dip high-strength steel. The simulation results indicate that the presence of Cr significantly affects the formation of the oxide layer, especially under high-temperature conditions, where the preferential reaction between Cr and O atoms promotes the formation of a Cr oxide layer, effectively enhancing the substrate's oxidation resistance. When the Cr content is less than 0.156 at.%, an increase in Cr content leads to a gradual reaction between Cr and O to form a Cr₂O₃ oxide layer, resulting in an initial increase followed by a decrease in the diffusion layer thickness, an increase in the Cr-O radial distribution function, and a decrease in the atomic diffusion coefficient. At a Cr content of 0.156 at.%, the oxide layer is the thinnest, with Cr forming a dense protective film that effectively blocks further penetration of oxygen. When the Cr content exceeds 0.156 at.%, excess Cr promotes the movement of Fe atoms and forms iron oxides on the substrate surface. An increase in oxygen partial pressure promotes the linear thickening of the oxide layer, affecting the atomic diffusion coefficient. This research provides guidance for understanding substrate surface oxidation and improving coating performance.

Keywords : Hot dip galvanizing, Cr element, oxide layer, molecular dynamics simulation, diffusion coefficient

103. Unravelling precipitation kinetics in nanosteels using Small Angle Neutron Scattering

Khan Zamran Zahoor¹, Van Dijk Niels¹, Offerman Sven Erik¹,
Parnell Steven R.²

1 - Delft University of Technology (Netherlands), 2 - ISIS Neutron and Muon Source (United Kingdom)

The formation of nanoscale vanadium carbide (VC) precipitates is studied in steels subjected to two different thermal cycles. The thermal cycling leads to either interphase precipitation (IP) or random precipitation (RP) mechanisms. Small-Angle Neutron Scattering (SANS) measurements coupled with Transmission Electron Microscopy (TEM) analysis are employed to determine the differences between these two precipitation processes. Specimens exhibiting interphase precipitation show a higher volume fraction and number density of VC precipitates compared to those undergoing random precipitation. Moreover, a broader size distribution of the precipitate radii is observed in specimens with random precipitation, where lens-shaped nanoscale precipitates are found predominantly at grain boundaries and sub-grain boundaries, with smaller precipitates dispersed within the matrix. The effect of varying carbon and vanadium concentrations on the VC precipitation strengthening is found to be more pronounced in RP in comparison with IP for samples annealed for 20 min at 650 °C. These findings shed light on the distinct characteristics of VC precipitation under different thermal cycles, offering valuable insights for the design and optimization of steel microstructures.

Keywords : AHSS, Interphase Precipitation, Random Precipitation, Small Angle Neutron Scattering, Kinetics

104. Relation between low elastic limit and mobile dislocation density in as-quenched martensitic steel

Tsuchiyama Toshihiro^{1 2}, Takenouchi Yushi³, Wada Shuhei³, Ochiai Yuto³, Masumura Takuro^{1 2}, Okano Hiroshi⁴

1 - Department of Materials, Kyushu University (Japan), 2 - Research Center for Steel, Kyushu University (Japan), 3 - Graduate School of Engineering, Kyushu University (Japan), 4 - JFE Steel Corporation (Japan)

Various factors have been considered as reasons for the low elastic limit of as-quenched martensitic steels, one of which is the high density of mobile dislocations. Dislocations introduced during martensitic transformation that are neither entangled with each other nor pinned by solute atoms are thought to produce plastic strain through their movement at a relatively low stress, probably also affected by internal stresses. In this study, using a carbon-free martensitic steel, the amount of mobile dislocations that moved was estimated by interrupting a tensile test in the macroscopic elastic deformation region and measuring the stress relaxation after the crosshead was fixed (relaxation test). The relationship between the elastic limit and the density of mobile dislocations was then discussed. In the relaxation test results, it was found that the specimens subjected to stress loading at higher stresses exhibited greater stress relaxation. This indicates that more mobile dislocations moved at a higher stress. Subsequent tensile testing of the relaxation-tested specimens showed an increase in the elastic limit. The increase was more pronounced for the specimens with a larger amount of stress relaxation. In other words, the mobile dislocations that moved during stress relaxation interacted with other dislocations and grain boundaries to become immobile dislocations, which may have increased the elastic limit during subsequent tensile testing. In addition to the above experiments, the effects of pre-cold rolling and trace carbon addition, as well as heterogeneous dislocation motion on a block-by-block basis were also investigated.

Keywords : martensite, dislocation density, strengthening mechanism, mechanical property

105. Carbides in Ferritic Steels : Defects and Atomic Diffusion from Ab-Initio Based Studies

Lemercier Adrien¹, Fu Chu-Chun², Soisson Frederic³, Bechade Jean-Luc⁴

1 - SRMP (France), 2 - SRMP, CEA Saclay (SRMP, CEA Saclay, 91191 Gif-sur-Yvette, France), 3 - Service de recherches de metallurgie physique (France), 4 - Universite Paris-Saclay, CEA, Service de recherche en Corrosion et Comportement des Materiaux, SRMP (France)

Carbides are generally present in steels like ferritic steels. Many of their properties are still unclear, especially the atomic-scale driving forces and mechanisms. Among the elementary properties, atomic diffusion is crucial in controlling various kinetic processes including the growth, dissolution, and amorphization of carbides. We start by focusing on cementite, appearing in Fe-C and dilute Fe-Cr-C alloys, in which carbon and metal elements migrate via points defects, such as vacancy, self-interstitial atom and Frenkel pair. We perform density functional theory (DFT) calculations to determine energetic properties for the point-defects formation and migration. Then, we determine the diffusion coefficients through DFT-parameterized kinetic Monte Carlo simulations. We consider not only the stoichiometric but also off-stoichiometric cementite. Concerning the diffusion of carbon, various mechanisms are identified, some of them being highly anisotropic. The computed energetic barriers range from 2.0 to 2.4 eV, which is much larger than the carbon migration energy in bcc iron. The dominant mechanism depends strongly on the concentration of carbon in cementite as well as the direction of diffusion. On the other hand, the metallic elements mainly migrate via the vacancy mechanism. The orthorhombic structure and the arrangement of the intrinsic C atoms induces very different energy barriers, from 0.5 to 1.7 eV for iron. Finally, as shown experimentally, the M₇C₃ and M₂₃C₆ carbides tend to form, instead of cementite, with increasing concentration of Cr in Fe-Cr-C alloys, we investigate the relative energetic and mechanical stability of these carbides with respect to cementite, as a function of Cr content.

Keywords : Carbides, ferritic steel, diffusion, DFT, Monte Carlo

106. Heterogeneous deformation behavior of pre-strained 18%Ni martensitic steel

Yamada Ayumu¹, Masumura Takuro², Tsuchiyama Toshihiro², Shimoda Eriko³

1 - Graduate School of Engineering, Kyushu University, Motoooka, Nishi-ku, Fukuoka 819-0395, Japan (Japan), 2 - Department of Materials, Kyushu University, Japan (Japan), 3 - Steel Research Laboratories, Nippon Steel Corporation, 20-1 Shintomi Futtsu, Chiba 293-8511, Japan (Japan)

It is well known that as-quenched martensite exhibits heterogeneous deformation on a block-by-block basis during tensile testing, and it causes the unique stress-strain curves characterized by a low elastic limit and a high work hardening rate in the early stage of deformation. Two main factors for the heterogeneous deformation in as-quenched martensite are proposed: ¹ the anisotropy of microscopic internal stress (Type-...*i*) and ² preferential activation of ϵ -in-lath plane slip system'. However, it is not yet clear which factor is dominant in the heterogeneous deformation. In this study, the effect of internal stress on the heterogeneous deformation was investigated by pre-straining 18%Ni martensitic steel to reduce the internal stress, and the heterogeneous deformation behavior was analyzed before and after pre-straining by using the digital image correlation method. Regardless of the pre-strain, the same blocks were preferentially strained during tensile deformation, and the in-lath plane slip system was activated in these blocks. Therefore, it was concluded that the preferential activation of in-lath plane slip system should be the more dominant factor for the heterogeneous deformation compared to the anisotropy of microscopic internal stress.

*Keywords : Martensite, Internal stress (Type...*i*), in lath plane slip system, Heterogeneous, Deformation behavior*

107. Impact of Non-Metallic Inclusions and Grain Structures Modified by Fast Heating Annealing on Tensile Properties and Fracture Modes in a V-microalloyed High-Mn TWIP Steel

Hamada Atef¹, Alatarvas Tuomas², Jaskari Matias¹, Abdelaal Walaa³, Allam Tarek⁴, Jarvenpaa Antti¹, Karjalainen Pentti⁵

1 - Future Manufacturing Technologies (FMT), Kerttu Saalasti Institute, University of Oulu, Pajatie 5, 85500 Nivala (Finland), 2 - Process Metallurgy Research Unit, Centre for Advanced Steel Research, University of Oulu, P.O. Box 4300, FI-90014 Oulu (Finland), 3 - Department of Mechanical Design and Production Engineering, Faculty of Engineering, Zagazig University, P.O.Box 44519 (Egypt), 4 - Institute of Energy and Climate Research: Structure and Function of Materials (IEK-2), Forschungszentrum Julich GmbH, 52425, Julich (Germany), 5 - Materials and Mechanical Engineering, Centre for Advanced Steels Research, University of Oulu, FI-90014 (Finland)

Characterization, classification, and size distribution of non-metallic inclusions (NMIs) in a cast high-Mn TWIP steel (Fe-20Mn-0.6C-1.5Al-0.3V, in wt.%), were studied to explore their interplay with the fracture mode during tensile deformation. NMIs were separated by electrochemical extraction, and subsequent X-ray dispersive analysis was performed to characterize their compositions. Subsequently, 70 % cold rolled TWIP sheets were processed and undergone fast heating (FH) treatment at a heating rate of 200°C/s to anneal at temperatures 700 - 900 °C for 30 s. The grain structures achieved by FH were evaluated by EBSD. The mechanical properties were determined by tensile testing. Distinct categories of NMIs, including Al₂O₃ and Mn(S,Se), and (Ti,V)N nitrides, and intricate combinations of inclusions, were identified. FH process at low temperatures, 700-800 °C, promoted partially recrystallized microstructures. Fully recrystallized structures were obtained at 850-900 °C characterized by an average grain size of 2 µm at 850 °C. The structure promoted at FA 850 °C displayed noteworthy elongation of 60% with a yield strength (YS) and tensile strength (TS) of 415 and 850 MPa, respectively. This structure revealed the highest product of (TS x TE) vs YS with a value of 50700 MPa%. Comparing literature data, mechanical properties achieved by FA indicated an enhancement in the mechanical strength and the product (TS x TE). A minimal effect of NMIs in TWIP steel was observed due to activating mechanical twinning mechanism, which overcomes the detrimental effect of NMIs and retard the necking induced by void formation related to NMIs.

Keywords : High, Mn TWIP steel, non, metallic inclusions, fast annealing, microstructure, mechanical properties

108. Effect of Annealing Process on Microstructures and Mechanical Properties of Cold-Rolled Martensitic Steels for Automotive Structural Parts

Yang K.C.¹, Tu J.F.¹, Wu T.F.², Hsieh P.C.³, Liu P. H.¹

1 - Iron & Steel Research & Development Department, China Steel Corporation (Taiwan), 2 - Metallurgical Department, China Steel Corporation, (Taiwan), 3 - Rolling Mill Department III-Cold Rolled Products, China Steel Corporation (Taiwan)

Recently, light-weight and energy-saving requirements for the automobile industry are extremely important in order to protect the environment by a reduction of the emission of CO₂. One of this ways to attain the aim is the reduction of steel thickness, but maintaining safety must be the prerequisite. In order to simultaneously satisfy these requirements, high-strength steels, even ultrahigh strength steels with tensile strength larger than 1GPa are used. Among these, martensitic steels have attracted much attention due to their superior strength due to owing the hardest microstructure of full martensite in steel. Martensitic steels are manufactured by hot stamping in a tradition way. However, the hot stamping process requires additional equipment and the steel is necessarily reheating. As a result, the hot stamping has high manufacturing costs and high energy losses. Therefore, it is urgent to provide cold-rolled martensitic steels for direct cold forming to automotive structural parts to save cost and energy. In this research, the influence of different annealing treatments on the phase transformation further affecting the mechanical properties and microstructure was investigated. These microstructures were analyzed via Optical Microscope (OM), Scanning Electron Microscope (SEM) and Electron Backscatter Diffraction (EBSD). The suitable chemical composition combined with annealing process has been developed to provide martensitic steels with tensile strength over 1300MPa. These martensitic steels can meet the requirement of automotive structure parts after performing cold forming of the reinforcement of bumper.

Keywords : Martensitic steel, High Strength Steel, Annealing Process

109. Revealing the Mechanisms of Austenitisation in Low-Alloy Steels Using In-situ EBSD

Pickering Ed^{1 2}, Taylor Mark³, Smith Albert⁴, Donoghue Jack⁵, Thomas Rhys⁶, Hutchinson Christopher, Prangnell Philip¹, Scenini Fabio³

1 - University of Manchester [Manchester] (United Kingdom), 2 - Henry Royce Institute (United Kingdom), 3 - Department of Materials, University of Manchester, Manchester M13 9PL (United Kingdom), 4 - Tescan UK Ltd. (United Kingdom), 5 - Henry Royce Institute and Department of Materials, The University of Manchester, Manchester, M13 9PL, UK (United Kingdom), 6 - The University of Manchester (United Kingdom)

It has been recognised for many years that the mechanism of austenitisation in martensitic steels can proceed via a two-step mechanism. The first step is a 'memory effect', whereby the ferrite-austenite transformation reforms the old prior-austenite grain structure. The second step is a recrystallisation of the austenite, which results in an entirely new grain structure being formed. These phenomena can be seen even at relatively slow heating rates, without applied loads. It appears that the memory effect step always occurs, but the extent of the recrystallisation step is more variable. Interestingly, there has been some debate about the mechanisms at work in these steps e.g., there remain questions regarding the precise mechanism of the memory effect, and regarding the origin of the strain driving the recrystallisation of the austenite. In this work, we have used automated high-temperature in-situ electron backscatter diffraction (EBSD) to analyse the process of austenitisation in two low-alloy steels. The grain morphologies, crystallographic orientations, and internal strains (kernel-average misorientations) of both ferrite and austenite were tracked in real time at high spatial and temporal resolution. This has allowed us to comment on the validity of theories offered in the literature for the memory effect, and also propose mechanisms for the creation of strain in the austenite prior to austenite recrystallisation.

Keywords : Steels, austenitisation, in situ EBSD, processing.

110. Effect of intercritical annealing temperature and holding time to mechanical performance of hot-rolled medium manganese steel

Perkioe Tuomas¹, Kantanen Pekka¹, Kaijalainen Antti¹

1 - Materials and Mechanical Engineering, Centre for Advanced Steels Research, University of Oulu, Oulu, 90570, Finland (Finland)

In order to find optimal IAT parameters and alloy composition for simple process route of hot rolling followed by single-step IAT, the effects of intercritical annealing treatment (IAT) on three different medium-manganese steels were investigated. Nominal chemical compositions in wt.% were 1) 6Mn-0.3C, 2) 6Mn-0.4C and 3) 8Mn-0.4C(0.2Al-1Si-0.05Nb-Fe). Materials were laboratory hot rolled to a thickness of 6 mm, and IAT was simulated with Gleeble 3800 and Linseis DIL L78 DQT / RITA dilatometer. Different variations of IAT included annealing temperatures of 650 °C, 675 °C, 700 °C and 725 °C, and holding times of 3, 10 and 30 minutes with a heating rate of 50 °C/s and cooling rate of 10 °C/s. Quasi-static tensile tests were performed parallel to rolling direction. XRD and EBSD phase mappings were performed to assess IAT parameters effect on volume fraction of retained austenite. Most promising mechanical properties were obtained with material 6Mn-0.4C annealed at 700 °C. Holding time was found to be of minor importance for material in question, with tested holding time range. Product of strength and elongation well exceeded 40 000 MPa% for above-mentioned IAT-material variation, being distinguishable higher compared to other variations. However, investigated materials, especially 6Mn-0.4C, seems to be very sensitive to IAT temperature, which could inflict some challenges in industrial scale production. Also, all materials experienced some level of serrations during tensile testing, which is frequently encountered phenomena with medium-manganese steels. Further research is required, to evaluate the role of austenite stability on mechanical behavior of these materials and to determine effects of heating and cooling rates.

Keywords : Medium Manganese Steel, Intercritical annealing, Retained Austenite, Tensile Properties

111. Solution nitriding of 304 stainless steel for hydrogen embrittlement resistance

Kwon Young-Je¹, Kang Jee-Hyun¹

¹ - Yeungnam University (South Korea)

As the transition to hydrogen economy is imminent for carbon neutrality, the development of materials for hydrogen infrastructure is necessary. Austenitic stainless steels, with a face-centered cubic(FCC) structure are gaining attention as the materials for hydrogen infrastructure due to its superior resistance to hydrogen embrittlement in comparison with the materials with body-centered cubic(BCC) or body-centered tetragonal(BCT) structures. Due to a lower nickel content than 316L stainless steel(STS), 304L STS has a lower stability of an FCC phase, austenite, which transforms to a BCT phase, martensite. Although this resulted in higher strength than 316L STS, the resistance to hydrogen embrittlement was severely impaired. In this study, we aimed to improve hydrogen embrittlement resistance of 304L STS by increasing the austenite stability through high-temperature solution nitriding. A 0.8 mm thick commercial 304L STS sheet was subjected to the high-temperature nitriding, and evolutions of microstructure, hardness, and tensile properties were analyzed, and hydrogen embrittlement resistance was assessed by slow-strain-rate testing. When subjected to high-temperature nitriding at 1200°C for more than 3 hours, nitrogen was saturated in the sample, which resulted in an increase in yield and tensile strengths by 120 MPa, and hardness by 40HV0.05 despite grain coarsening. Hydrogen embrittlement resistance could effectively be improved after 1 hour of high-temperature nitriding; relative elongation loss decreased from 50% to 9%.

Keywords : Austenitic Stainless Steel, High Temperature Nitriding Treatment, Austenite Stability, Strengthening, Hydrogen Embrittlement

112. Nanoprecipitates-strengthened ultrastrong stainless steel with excellent work hardening

Zhang Zhongwu¹, Li Junpeng¹, Jiang Weiguo¹

¹ - Harbin Engineering University (China)

In ultrahigh-strength maraging steels, nanoprecipitates contribute significant yield strength increments with low work hardening. The low work hardening is detrimental to their applications. In this study, core-shell nanoprecipitates are introduced to modulate strength, ductility, and work hardening in ultrahigh-strength stainless steels. The formation of core-shell nanoprecipitates and their effects on the work hardening of the steels are systematically investigated. The formation of various nanoprecipitates, including Ni₃Ti, Mo-rich precipitates, alpha prime Cr-rich precipitates and Ni₃Ti/Mn-rich core-shell precipitates, etc are characterized carefully by using transmission electron microscopy and atom probe tomography. The precipitation sequence and their effects on the multiplication of dislocations, evolution of reversed austenite, thereby on the work hardening are studied extensively. The nanoscale core-shell precipitates with Ni₃Ti core encapsulated by a Mn-enriched shell promote the multiplication of dislocations, thereby significantly improving work hardening and uniform elongation. The interface (e.g., grain or lath boundaries) segregation of Ni and Mn atoms induces transformation to form reversed austenite, where multiple nanoprecipitates are present inside. This reversed austenite accompanied by its interior nanoprecipitates facilitate the transformation induced plasticity effect and improves mechanical properties of the maraging stainless steels.

Keywords : nanoprecipitates, stainless steel, multiplication of dislocations, work hardening, reversed austenite

113. Uncovering the interplay between thermo-mechanical processing parameters and microstructure of V, Cr-microalloyed steels

Pereloma Elena^{1 2}, Baqeri Gholam^{1 2}, Singh Navjeet^{1 2}, Kostryzhev Andrii³, Killmore Chris^{2 4}

1 - University of Wollongong (Australia), 2 - ARC Research Hub for Australian Steel Innovation (Australia), 3 - ARC Research HUB for Australian Steel Manufacturing (Australia), 4 - BlueScope Steel Limited (Australia)

There are continuing efforts to improve mechanical properties of high strength low alloyed (HSLA) steels by modification of thermo-mechanical processing (TMP) parameters. However, the effects of TMP parameters are complex, as while the increase in the amount of deformation refines the final microstructure, it influences the phase transformation temperatures. Furthermore, a higher strain in the non-recrystallisation region accelerates formation of strain-induced precipitates in austenite leaving less solute available for formation of precipitates at later stages of the processing. This presentation will provide some insights into these issues using as an example the HSLA steel containing $\sim(0.08\pm0.003)\text{C}$, 1.5Mn, 0.3Si, 0.2Ni, 0.03Al, 0.003S, 0.015P, $(0.0131\pm0.0002)\text{N}$, and 0.73 (Cr + V + Nb) (wt. %) subjected to laboratory-simulated TMP using a Gleeble 3500 simulator. Results on the effects of deformation during roughing and finishing temperatures of hot rolling, as well as coiling temperatures and times on the microstructure and interphase precipitation formation will be presented and discussed.

Keywords : High strength low alloy steel, Thermomechanical processing, Microstructure, Precipitation, Electron microscopy

114. Investigation of metal embrittlement in galvanized quenching and partitioning steels

Sommitsch Christof¹, Wallner Matthias , Steineder Katharina ,
Schneider Reinhold

1 - Institute of Materials Science, Joining and Forming, Graz University of Technology (Austria)

Third-generation advanced high-strength steels, such as quenching and partitioning steels, offer enhanced crash safety and enable lightweight designs due to their exceptional combination of high strength and ductility. These properties contribute to increased fuel efficiency and reduced environmental impact. These benefits are achieved through a refined, homogeneous microstructure comprising tempered martensite and retained austenite, which facilitates the Transformation-Induced Plasticity effect. To stabilize high levels of retained austenite during the Q&P process, significant amounts of silicon are typically added. Silicon effectively suppresses carbide precipitation, but its high content poses challenges, including poor galvanizability and an increased risk of liquid metal embrittlement during spot welding of galvanized steels. Aluminum has been identified as an alternative to Si for suppressing carbide precipitation, while also improving Zn wettability during galvanizing. However, the effects of fully or partially substituting Si with Al on the microstructure-property relationships and LME sensitivity of Q&P steels remain insufficiently understood, and this study aimed to address these gaps. Microstructural characterization techniques such as electron backscatter diffraction, X-ray diffraction, transmission electron microscopy, dilatometry, and differential scanning calorimetry were employed, alongside tensile testing to evaluate mechanical properties. Hot tensile tests and spot-welding experiments were conducted to assess LME behavior in laboratory-produced steels with varying Si:Al ratios. The findings reveal that Al has a markedly weaker effect than Si on inhibiting the precipitation of transitional carbides during martensite tempering. While this leads to lower levels of retained austenite, Al-alloyed steels exhibit greater mechanical and thermal stability of the retained austenite. Additionally, substituting Si with Al significantly reduced the occurrence of LME cracks during spot welding, attributed to Al's distinct influence on Zn-Fe phase formation and austenite formation compared to Si. In conclusion, replacing Si with Al in Q&P steels can substantially improve LME resistance while offering moderate global formability and enhanced local formability.

Keywords : Steel, LME, Q&P

115. Inverse steel design

Adachi Yoshitaka ¹

¹ - Nagoya University (Furo-cho, Chikusa-ku, Nagoya, 464-8603, Japan Japan)

In data science-driven steel materials design, the analysis has been limited to forward and inverse analyses of the process–microstructure, microstructure–properties, and process–properties correlations, without fully establishing the true process–microstructure–properties relationships. This presentation will focus on several proposed coupled models aimed at illustrating these correlations among the three entities.

The first model is a coupled framework involving image regression using Convolutional Neural Networks (CNN) to relate microstructure and properties, and a multi-output Artificial Neural Network (ANN) that connects the convolutional features obtained in the intermediate steps to the process. The second model involves the generation of virtual microstructures through a Generative Adversarial Network (GAN) based on latent variables optimized through Bayesian optimization, which are then linked to properties using Finite Element Method (FEM) or CNN image regression in the BO-GAN-FEM (or CNN) model. Additionally, this model is coupled with a Conditional Generative Adversarial Network (CGAN), which can generate microstructure images based on process conditions. The third model focuses on Multi-Objective Optimization (MOO) for balancing multiple properties that are in trade-off with each other, and the MOO-experimental observation coupled model, which experimentally implements the proposed processes to verify the microstructure. Finally, a parallelized model for sequential and inverse analyses of the correlations between process conditions, microstructure features, and properties will be discussed.

In the presentation, we will also discuss the characteristics and challenges of these models, the integration with microstructure and property simulations, and how surrogate models can be used to improve computational efficiency.

Keywords : inverse analysis, process, microstructure, property linkage, GAN, CNN, Bayesian optimization

116. Three-dimensional analysis of microstructure formation in the initial stage during martensitic transformation in low-carbon steel

Nambu Shoichi ¹

¹ - Department of Materials Engineering, The University of Tokyo (7-3-1 Hongo, Bunkyo, Tokyo 113-8656 Japan)

In this study, three-dimensional development of lath martensite in a low-carbon steel was investigated by combining serial sectioning method mainly based on optical microscopy to build three-dimensional image of microstructure and crystallographic analysis with electron back scattering diffraction (EBSD), especially in the initial stage of the martensitic transformation. A steel containing 0.15 mass pct. carbon was prepared. It was austenitized and quenched just below the martensite start temperature, and subsequently heated up to tempering temperature in order to distinguish the martensite blocks formed in the initial stage of transformation from those formed later. To obtain three-dimensional microstructure, the optical microscopy-based serial sectioning was conducted with a polishing interval of about 1 micron, the crystal orientation analysis by EBSD was performed every 5 steps and then the three-dimensional images were constructed by the Avizo software. From the results of the three-dimensional image of martensite and prior austenite grain boundary, many of the blocks that are considered to have formed first form near the grain boundary, and it was found that the close-packed direction of the blocks is close to parallel to one grain boundary plane. By investigating which grain boundaries are most likely to form, the martensite blocks are likely to form from grain boundaries where the close-packed direction is close to parallel to the grain boundary, and also have a small misorientation with the Kurdjumov-Sachs relationship with the adjacent austenite grain.

Keywords : Martensite, Transformation, Three, dimensional observation, Crystal orientation, Steel

117. Mechanism of pearlite colony formation via various orientation relationships between ferrite and cementite

Shiori Endo¹, Nakada Nobuo¹, Toshihiko Teshima², Makoto Kosaka²

1 - Institute of Science Tokyo (Japan), 2 - Nippon Steel Corporation (Japan)

To better understand the formation mechanism of lamellar pearlite, the orientation relationship (OR) between ferrite and cementite in spheroidized pearlite was analyzed using electron backscattered diffraction (EBSD) over a wide area with high precision. Cementite lamellae were sufficiently spheroidized and coarsened, yet the substructures of lamellar pearlite—specifically, block and colony boundaries—were preserved even after extended spheroidizing annealing. This spheroidization facilitated the accurate indexing of the cementite orientation in the EBSD analysis. It was found that three different ORs—Bagaryatsky, Isaichev, and Pitsch-Petch—coexisted in the pearlite, with each OR deviating from the theoretical orientation. Notably, the deviation was most significant in the Pitsch-Petch OR. Furthermore, the ferrite/cementite boundaries corresponding to each OR were unevenly distributed, and OR transitions generally aligned with colony boundaries characterized by low angle misorientations. Based on these observations, pearlite colony boundaries were classified into three types: ¹ boundaries maintaining an orientation relationship with different cementite variants, ² boundaries defined by two different ORs with low-angle misorientation, corresponding to the transition between Bagaryatsky and Isaichev ORs, and ³ boundaries with high-angle misorientation, representing the transition between Isaichev and Pitsch-Petch ORs. In addition to the multiple variant formation, the coexistence of multiple ORs contributed to changes in lamellar alignment, leading to a high degree of freedom in the pearlitic transformation.

Keywords : Steel, Pearlite, Orientation relationship, EBSD, Phase transformation

118. Austenite Plasticity and Martensite Microstructures

Samajdar Indradev¹, Kumar Saurabh², Pai Namit³, Akhtar Junaid

1 - Department of metallurgical Engineering and materials science, IIT Bombay (India), 2 - Department of Metallurgical Engineering and Materials Science, IIT Bombay, Mumbai, 400076 (India), 3 - Department of Metallurgical and Materials science IIT Bombay (India)

Elastic-plastic deformation in the austenite phase is expected to affect the martensitic transformation and the martensite microstructure. This hypothesis has been tested under (i) controlled thermomechanical processing in the austenite phase and its effects on martensite variant selection and (ii) hydrogen embrittlement under the so-called transformation induced plasticity (TRIP). In (i), high resolution electron backscattered diffraction (HR-EBSD) plus dynamical simulations of HR-EBSD patterns established the state of residual stresses in the reconstructed austenite phase. This was then used in bring out the martensite variant selection in an interaction energy-based approach. In (ii), the role of hydrogen on the interfacial and austenite stacking fault energies were explored to establish the basis of hydrogen-induced accelerated TRIP effect.

Keywords : Residual Stress, Austenite, Martensite, Microstructure, Variant Selection, Hydrogen.

119. Evaluating LME susceptibility in third-generation AHSS: The role of testing methodologies and silicon concentration

Katharina Steineder , Martin Gruber, Simone Kaar-Schickinger, Matthias Wallner, Korbinian Högerv, Martin Arndt, Reinhold Schneiderv

Department for Materials Technology, University of Applied Sciences Upper Austria, Wels, Austria

The automotive industry's push for lightweight, high-strength materials has led to the advancement of third-generation advanced high-strength steels (AHSS). Known for their blend of ultra-high tensile strength and ductility, these steels are ideal for structural applications. However, their adoption has faced obstacles, notably due to Zinc (Zn)-assisted liquid metal embrittlement (LME), particularly in cases where Zn-based corrosion-resistant coatings are used during resistance spot welding (RSW). This study explores testing methodologies for evaluating LME susceptibility and examines the impact of silicon (Si) concentration, specifically between 0.5 and 1.4 wt.-%, on Zn-LME vulnerability in AHSS. This research introduces two primary testing approaches: spot welding tests and hot tensile tests, each designed to quantify LME susceptibility. Both methods show that higher Si levels correlate with increased LME vulnerability, evidenced by greater ductility loss and the formation of longer critical cracks during welding. Thermodynamic modeling further demonstrates that Si affects phase stability in the Fe-Zn system, broadening the liquid Zn range. The findings highlight Si's significant role in Zn-LME susceptibility and underscore the importance of robust testing methods to facilitate the safer application of AHSS in automotive manufacturing.

120. Modeling the effect of prior martensite on the kinetics of bainite formation

Dos Santos Avila Daniel¹, Van Bohemen Stefan², Offerman Sven Erik¹, Santofimia Navarro Maria³

1 - Delft University of Technology (Netherlands), 2 - Tata Steel (Netherlands), 3 - Delft University of Technology (Netherlands)

The presence of prior martensite accelerates the kinetics of bainite formation. The reported magnitude of such an acceleration in the rate of bainite nucleation ranges from the same magnitude as the autocatalytic effect of bainite to two orders of magnitude higher. However, the mechanisms behind the acceleration and the factors controlling the magnitude of the acceleration are unknown. In this work, a kinetic model based on the diffusionless theory of bainite formation is expanded to include the nucleation of bainite sub-units at the interface between prior martensite and austenite (M/A interface). The expanded model captures the accelerating effect of prior martensite and, by comparison against experimental measurements, indicates that the acceleration originates from the large number of potential nucleation sites created at the M/A interfaces. The magnitude of the acceleration is shown to be stronger at higher temperatures. However, the two order of magnitude increase in the rate of bainite nucleation is likely an overestimation due to measuring artifacts caused by thermal gradients in the dilatometry samples. The finding that M/A interfaces are the dominant site for bainite nucleation allows to increase the hardenability of steels without slowing down the kinetics of bainite formation in the presence of martensite by alloying the steels with elements that strongly segregate to austenite grain boundaries, such as boron.

Keywords : bainite, martensite, kinetics, modeling

121. Effect of nitrogen in yielding behavior of austenitic stainless steels

Hani Kento¹, Shigesato Genichi¹, Tsuchiyama Toshihiro², Maeda Takuya³, Nakamura Shuichi³

1 - Research Center for Steel, Kyushu University, Fukuoka, Japan (Japan), 2 - Department of Materials Science and Engineering, Kyushu University, Fukuoka, Japan (Japan), 3 - Steel Research Laboratories, Nippon Steel Corporation, Chiba, Japan (Japan)

Nitrogen (N) is recognized as an effective alloying element for strengthening austenitic stainless steels. This is because N not only contributes solid solution strengthening but also enhances grain refinement strengthening by increasing the Hall-Petch coefficient k . However, the mechanism for the rise of k by N has been unclear. It has been reported that carbon addition in ferritic steel brought an increase of k . Takaki et al. suggested the possibility that segregation of C atoms on grain boundaries raises the threshold stress for dislocation emission from the grain boundaries resulting in the augmentation of k . However, N has not been reported as a grain boundary segregation element so that the same mechanism as C might not be applicable. In this study, we focused on the effect of the distribution of dislocations. Fe-20mass%Cr-10mass%Ni-0.2mass%N alloy and -0.5mass%N were used in this study. The 0.5N steel was prepared by nitrogen absorption treatment. These were cold rolled and solution-treated at 1473 K for 1.8ks. Pile-up dislocations at a grain boundary were observed by means of in-situ SEM tensile tests with an applied stress lower than the yield stress. Increasing the applied stress, strain contrast was observed near the boundary in the adjacent grain. At the same time, slip lines appeared in the former grain, which is considered to be so-called micro-yielding. The critical stress for dislocation emission at the boundary was estimated from the result. The influence of N content on the number of pile-up dislocations and the critical stress of micro-yielding is discussed.

Keywords : austenitic stainless steel, high nitrogen steel, micro yielding, yield strength

122. Thermal stabilization by prior deformation in metastable austenitic steel undergoing gamma → epsilon → alpha' transformation

Otaki Manato¹, Masumura Takuro², Tsuchiyama Toshihiro²,
Yamasaki Shota³

1 - Department of Materials, Graduate School of Engineering, Kyushu University, Fukuoka (Japan), 2 - Department of Materials, Faculty of Engineering, Kyushu University, Fukuoka (Japan), 3 - Nippon Steel Stainless Steel, Hikari, Yamaguchi (Japan)

Metastable austenitic stainless steels such as type 304 are known to undergo a two-step martensitic transformation through epsilon martensite during cooling to cryogenic temperatures. alpha'-martensite is characterized by high strength, while also exhibiting magnetism and susceptibility of hydrogen embrittlement. Therefore, it is important to control the thermal stability of austenite depending on its use. However, the stabilization behavior in metastable austenitic stainless steel (Fe-Cr-Ni alloys) undergoing the two-step martensitic transformation remains unclear. In this study, we investigated the effect of prior deformation above the Md temperature on the thermal stability of austenite in metastable austenitic stainless steel. Type 304 (Fe-18%Cr-8%Ni alloy) was used in this study. The specimen was solution-treated at 1273 K for 1.8 ks, followed by water cooling and subzero treatment by liquid nitrogen (77 K). The specimens water-cooled after solution treatment were then 5–30% warm-rolled at 973 K, where recrystallization and deformation-induced alpha'-martensitic transformation do not occur. Subsequently, the prior-deformed specimens were water-cooled and subzero treated. As a result, the Ms temperature decreased as the thickness reduction by warm rolling increased. The ECCI shows the tangled dislocations introduced by warm rolling around the plate-like microstructures (thin epsilon-martensite or stacking faults) formed during sub-zero treatment, which suggests that the dislocations should inhibit the growth of epsilon-martensite because epsilon-martensite is formed via the movement of partial dislocations. Because epsilon-martensite is preferential nucleation sites for alpha'-martensite, the thermal stability of austenite for alpha'-martensitic transformation is also improved by prior deformation.

Keywords : Austenite stability, Stainless steel, Two step martensitic transformation, Prior deformation, Epsilon martensite

123. Enhancing Cryogenic Strength of Austenitic Stainless Steels Through Thermo-Mechanical Controlled Processing and Nitrogen Alloying

Smith Ali ¹, Hoffmann Frank ², Somani Mahesh ³, Abdelghany Ahmed ^{3 4}, Muratori Marta ⁵

1 - RINA Consulting - Centro Sviluppo Materiali SpA (Italy), 2 - Institut für Metallformung, TU Bergakademie Freiberg (Germany), 3 - Materials and Mechanical Engineering, Centre for Advanced Steels Research, University of Oulu (Finland), 4 - Future Manufacturing Technologies (FMT), Kerttu Saalasti Institute, University of Oulu, Nivala, 85500, Finland. (Finland), 5 - Acerinox Europa S.A.U., Acerinox Europa, Los Barrios (Spain)

In the last years there has been renewed interest in the mechanical properties of metallic materials at cryogenic temperatures. This has been driven by demands for strong and tough alloys in liquid hydrogen storage (20 K) and nuclear fusion applications (4 K). Austenitic stainless steels represent an attractive candidate material for such applications, due to their high toughness at low temperatures. However, a potential drawback is their low to modest yield strength at room and low temperatures. A potential solution to this issue is the use of TMCP which can greatly increase the strength of austenitic stainless steels. For the current contribution, several austenitic stainless steels were investigated with different nitrogen contents. TMCP processed plates and solution annealed plates were then manufactured on a pilot mill. The plates were examined to determine the microstructure at room temperature. Tensile tests were carried out from room temperature down to -180°C (in liquid nitrogen), to determine the cryogenic yield and tensile strength of the plates. From the results obtained, the roles of TMCP and alloy chemistry on the realised cryogenic strength at -180°C were determined. An attempt was also made extrapolate the measured yield strength to lower temperatures based on a physically based formulation. Finally, the roles of TMCP and nitrogen level were estimated also at 20K.

Keywords : Austenitic stainless steel, liquid hydrogen, TMCP, strength, nuclear fusion

124. Evaluation of dislocation morphology in nitrogen-bearing austenitic stainless steel

Kubo Shotaro¹, Ma Tianze¹, Masumura Takuro², Tsuchiyama Toshihiro²

1 - Department of Materials, Graduate School of Engineering, Kyushu University, Fukuoka (Japan), 2 - Department of Materials, Faculty of Engineering, Kyushu University, Fukuoka (Japan)

It is well known that the addition of nitrogen to austenitic stainless steels increases the work-hardening rate owing to the formation of a planar dislocation array in which dislocations are aligned in a straight line on the same slip planes. The moving dislocations are back-stressed by leading planar dislocations, resulting in the prevention of dislocation movement. The frequency of planar dislocation formation should be related to the work-hardening rate, but there has been no quantitative evaluation of this relationship. In this study, we evaluated the planarity of dislocations in nitrogen-bearing austenitic stainless steels (Fe-25%Cr-20%Ni-N alloy) using various techniques and investigated the nitrogen content dependence and relationship with the work hardening rate. In the direct observation by the SEM/ECCI method, planar dislocations were defined as parallel dislocations aligned within 200 nm on the slip planes, and planarity was defined as the number of planar dislocations divided by the total number of dislocations. For the 0.15%N and 0.47%N steels, the rates of planar dislocation were 56% and 73%, respectively, quantitatively indicating that the planarity increased with increasing nitrogen content. It is also expected that the undulations of the slip lines appearing on the specimen surface become larger when more planar dislocations are formed. Laser microscopy measurements of the surface roughness revealed that the surface undulations increased with increasing nitrogen content. In addition, X-ray line profile analysis and the EBSD-Wilkinson method were used to evaluate the planarity and estimate the work-hardening rate in nitrogen-bearing austenitic stainless steel.

Keywords : Austenitic stainless steel, Planar dislocation array, Nitrogen, ECCI

125. Microstructure and impact wear behavior of a V-Ti microalloyed carbide-containing high manganese steel

Wang Yongjin¹, Song Renbo¹, Bi Siyao¹

¹ - University of Science and Technology Beijing (China)

In this study, an new V-Ti microalloyed high manganese steel (Hadfield steel) with carbide precipitations was designed and fabricated to improve the initial hardness and wear resistance of conventional high manganese steel. Microstructure evolution and impact wear behavior was investigated. The wear performance under different impact energies was tested using MLD-10 dynamic load abrasive wear tester. The microstructure of newly developed carbide-containing high manganese steel was composed of austenite and granular M₇C₃ carbides distributed inside the grain. The hardness of carbide-containing steel could reach 240.8 HBW with impact toughness of 117.2 J. The impact wear performance of carbide-containing high manganese steel was higher than that of conventional pure austenitic high manganese steel. As the impact energy increases, the thickness of the work hardening layer and the surface hardness increased gradually. A work hardening layer with thickness higher than 3500 μm could be formed for the carbide-containing steel. The hardening behavior was due to the combination of dislocation, stacking faults, and deformation twinning strengthening mechanisms. The wear resistance showed a trend of increasing first and then decreasing with the increase of impact energy. The wear mechanism of carbide-containing steel changed from plastic deformation mechanism to chiseling mechanism and fatigue wear mechanism during the impact wear process. The carbides played an important role in strengthening the austenite matrix and work as high hardness particles to hinder plow cutting under medium or low impact energy. Under high impact energy, cracks nucleated near the carbides, which led to the decrease of wear resistance.

Keywords : High manganese steel, Carbides, Impact wear, Hardening

126. Effect of Cold-Forming on Mechanical Properties of AHSS Steel

Nyo Tun Tun¹, Autio Laura¹, Tulonen Juha², Kajjalainen Antti¹

1 - Materials and Mechanical Engineering, Centre for Advanced Steels Research (CASR), University of Oulu, P.O. Box 4200, 90014 Oulu (Finland), 2 - SSAB Europe Oy, Hameenlinna, 13300 (Finland)

Advanced high strength steels (AHSS) can offer an excellent combination of high strength and light weight for applications including cold forming. These steels may be used in press braking, profile- and section manufacturing. The aim of this work is to study mechanical properties and microstructure of steel used in the manufacturing of roll formed profiles with decreased radii. In this study, ferritic feed stock steel in 450 N/mm² yield strength, coiled at room temperature, and the sections with wall thicknesses 7.1 mm and 12.5 mm are studied with middle line radii 7.5 mm and 13 mm respectively. Mechanical properties and impact toughness, especially considering the corners of cold formed profiles, with and without aging (250 °C for 1 h), are studied. Cold deformation on corners has an effect on thickness and tensile strength in aged condition. Impact energies are at a high level at -40 °C and aging does not have a major effect on the toughness and hardness.

Keywords : Cold forming, ferrite, high strength steel, mechanical properties.

127. Influence of Mo and N Additions on the Precipitation and Tensile Properties Behaviors in Austenitic Stainless Steel during Aging

Bang Seungkook¹, Shin Jongho¹, Jung Geunsu¹, Cha Dojin¹, Ma Youngwha¹

¹ - Doosan Enerbility (South Korea)

Seungkook Bang[^]—, Jongho Shin^V, Geunsu Jung⁺, Dojin Cha⁺, Youngwha ma^{+ ^}— Doosan Enerbility, Materials Technology Development Team, Changwon, 51711, Republic of Korea. Email: seungkook.bang@doosan.com ^V Doosan Enerbility, Materials Technology Development Team, Changwon, 51711, Republic of Korea. Email: jongho.shin@doosan.com ⁺ Doosan Enerbility, Materials Technology Development Team, Changwon, 51711, Republic of Korea. Email: geunsu.jung@doosan.com

⁺ Doosan Enerbility, Materials Technology Development Team, Changwon, 51711, Republic of Korea. Email: dojin.cha@doosan.com ⁺ Doosan Enerbility, Materials Technology Development Team, Changwon, 51711, Republic of Korea. Email: youngwha.ma@doosan.com
Corresponding Author : jongho.shin@doosan.com The study investigates the precipitation behavior and tensile properties of austenitic stainless steel designed to stabilize the austenite phase through the addition of Mn, N, and C. Aging processes were conducted at temperatures of 300 °C, 400°C, 500°C, 600°C, 700°C, and 800°C for durations of 100, 300, 500, and 1000 hours. The materials used in this study contain varying levels of Mo and N. The addition of these alloying elements resulted in distinct precipitation behaviors. This study provides valuable insights into the role of Mo and N additions on the microstructural evolution during aging and its consequent influence on mechanical properties. These findings are important for the development and optimization of high-performance stainless steels. Keywords: Stainless Steel, Precipitation Behavior, Aging, Tensile Properties

Keywords : Stainless Steel, Precipitation Behavior, Aging, Tensile Properties

128. Effect of EAF impurities on microstructure and mechanical properties of low-carbon steels

Hoikkaniemi Anttu¹, Haiko Oskari¹, Kajjalainen Antti¹

¹ - Materials and Mechanical Engineering, Centre for Advanced Steels Research, University of Oulu, Oulu, 90570 (Finland)

The effects of common electric arc furnace (EAF) impurities, including copper (Cu), nickel (Ni), molybdenum (Mo), and chromium (Cr), were investigated in low-carbon steels. These steel scrap originating tramp elements can influence the microstructures and mechanical properties of steel. Tramp elements containing test materials were thermo-mechanically rolled to achieve yield strengths between 355-450 MPa with different cooling routes. Various methods of microstructure characterization and mechanical testing were utilized to study the resulting steels. Additionally, thermo-mechanical simulations were conducted using Gleeble 3800 equipment to gather information about flow stress and static recrystallization properties. The results indicate that with a lower cooling rate, the microstructure is not significantly affected by tramp elements, however strength levels can be increased and elongation properties decreased, mostly due to the solid solution strengthening effect of impurities. In the water-quenched steels, the addition of tramp elements can alter the final microstructure morphology, increasing the strength levels but simultaneously improving the ductility. Flow stress and static recrystallization are not significantly affected by tramp elements in the temperature range of 950-1050 degrees Celsius.

Keywords : EAF impurities, microstructure, mechanical properties, steel

129. Enhancing the hydrogen embrittlement resistance in warm-rolled medium-Mn steels through nano-sandwich microstructure

Jeong Mun Sik¹, Song Geon Ho¹, Han Jeongho¹

¹ - Hanyang University (South Korea)

Here, we attempted to improve the resistance to hydrogen embrittlement (HE) of medium-Mn steels through implementation of nano-sandwich microstructure via warm-rolling. The hot-rolled and annealed (HRA) specimen shows the martensite and retained austenite with a multi-variant laminate morphology (average lath widths: ~0.82 μm) and the cold-rolled and annealed (CRA) specimen exhibits the ferrite and retained austenite with a globular morphology (average grain size: ~0.61 μm). The warm-rolled (WR) specimen shows a similar microstructure to HRA, however, it reveals a single directional laminate structure aligned to the rolling direction as well as much finer grain size (~0.45 μm) than HRA. This resulting microstructure is called nano-sandwich structure. The resistance to HE of WR is higher than that of HRA and CRA. H-induced cracks in HRA propagate rapidly along the coarse prior austenite grain boundaries (PAGBs) (~30 μm) weakened by Mn segregation, resulting in the largest elongation loss (EL) (~92.9%). The HE resistance of CRA (EL: ~63.3%) is higher than that of HRA, because H-induced cracks propagate by frequently changing their path along the interface between fine ferrite and austenite. The WR shows the highest HE resistance (EL: ~49.1%), because the cracking is suppressed by the breaking of PAGBs during warm deformation. Additionally, the crack could propagate in a direction perpendicular to the crack propagation, reducing the propagation energy and delaying H-induced fracture; this phenomenon is called delamination. Therefore, it is suggested that simple warm-rolling can serve as a novel route for enhancing the HE resistance of medium-Mn steels.

Keywords : Medium Mn steel, Warm rolling, Nano sandwich microstructure, Hydrogen embrittlement, Prior austenite grain boundary, Delamination

130. Thermomechanical rolling of thick Nb-Ti-V-Ni high strength structural steel plate

Maubane Dannis Rorisang Nkarapa¹, Banks Kevin Mark², Luthuli Nonkululeko Tracy³

1 - Department of Materials Science & Metallurgical Engineering, University of Pretoria (South Africa), 2 - Department of Materials Science and Metallurgical Engineering, University of Pretoria (South Africa), 3 - Quality management, ArcelorMittal South Africa (South Africa)

The influence of applied pass strain, thermomechanical controlled processing (TMCP) strain and finishing temperature on the microstructure of TMCP rolled 50mm thick Nb-Ti-V-Ni microalloyed steel plate was investigated. Laboratory simulations were performed that included reheating, roughing followed by an extended air-cooling delay and finishing in the low temperature austenite region. Larger TMCP strains promoted sub-grain formation and increased the nucleation site density for grain refinement. Recrystallisation was completely suppressed at the commencement of finishing in all TMCP schedules. The progress of recrystallisation during finishing passes depended on the TMCP start temperature: i) above 950 Celsius, softening alternated between complete and partial, ii) below 950 Celsius, gradual strain accumulation in the earlier passes culminated in complete softening at the end of rolling. Finer polygonal ferrite and pearlite microstructures were obtained after finishing below 900 Celsius. Decreasing the amount of applied pass strain during finishing significantly reduced the rolling loads but led to coarser microstructures due to under-developed sub-structure and lower ferrite nucleation site density. Similar microstructures were observed in schedules subjected to the same finishing temperatures and total TMCP strains but applied over different temperature ranges: i) 1000-860 Celsius, that included inter-pass water cooling and ii) 900-860 Celsius, only air-cooled that indicated that both schedules were conducted entirely below the so-called no-recrystallisation temperature, T_{nr} . The microstructure after commencing finishing at 950 Celsius produced comparable microstructures in laboratory simulations and industrial plate trials where yield strength in excess of 500MPa was achieved.

Keywords : Thermomechanical rolling, NbTiVNi steel, finishing temperature, TMCP strain, applied strain, thick plate

131. Hydrogen-related effects in austenitic steels: Contribution to deformation behavior and hydrogen embrittlement resistance

Gutierrez-Urrutia Ivan¹, Ogawa Yuhei¹, Shibata Akinobu¹

¹ - National Institute for Materials Science (NIMS) (Japan)

The influence of hydrogen on the deformation behavior of structural materials is still a controversial topic due to the limited understanding of the role of hydrogen-induced effects on plasticity. In austenitic steels, this effect has been mainly associated with slip localization, ascribed to the locking of dislocations by hydrogen atmospheres and the hydrogen-induced reduction of dislocation cross-slip. According to these processes, hydrogen tends to localize the emitted dislocations into a narrow slip band formed by unrelaxed pileups. When interacting with GBs can result in the initiation of a microcrack via void nucleation at GBs (hydrogen embrittlement, HE). In this presentation, we present unrevealed hydrogen-induced effects on plasticity in austenitic steels that evidence the complex influence of hydrogen on the collective behavior of dislocation plasticity. The analysis of the hydrogen-related deformation structure by several electron microscopy techniques, such as electron channeling contrast imaging (ECCI), electron backscatter diffraction (EBSD), and scanning transmission electron microscopy (STEM), reveal that hydrogen-induced effects on plasticity have a considerable impact on the HE resistance and deformation behavior of an austenitic Fe₃₀Mn_{6.5}Al_{0.3}C low-density steel and a 310S steel. Hydrogen accelerates the plastic deformation of these steels by promoting dislocation structures associated with inhomogeneous plasticity (deformation bands), strain localization (microbands), and coarsening slip bands in specific grain orientations. The contribution of these effects to the deformation behavior and hydrogen embrittlement resistance are analyzed and discussed. In particular, we present novel dislocation-based mechanisms of plastic relaxation that contribute to the high HE exhibited by these steels.

Keywords : Hydrogen embrittlement, Austenitic steels, Materials Performance, Deformation behavior, Dislocation structure, Strain hardening

132. Multi-scale and multi-modal microstructure imaging for in-situ studying creep damage and healing in ferritic steels at ID11/ESRF

Fang Haixing^{1 2}, Hussein Abdelrahman³, Ludwig Wolfgang²,
Wright Jonathan², Van Der Zwaag Sybrand⁴, Van Dijk Niels⁴

1 - European Synchrotron Radiation Facility (France), 2 - European Synchrotron Radiation Facility (France),
3 - university of Oulu (Finland), 4 - Delft University of Technology (Netherlands)

A suite of diffraction microstructure imaging (DMI) techniques, including near-field diffraction contrast tomography (DCT) and far-field 3DXRD, have been developed at ID11 of the European Synchrotron Radiation Facility (ESRF) to map grain shapes, strains and local orientations from spotty diffraction patterns. Combining with phase contrast tomography, these techniques can offer multi-modalities for characterizing the microstructure from atomic to mm length scales. Recent efforts in large amount of developments in the reconstruction methods have been made to i) extend the applicability of DCT for mapping grains in more deformed materials with a forward model based reconstruction and ii) reconstructing intragranular strains in highly deformed samples with scanning 3DXRD. To benefit from these non-destructive multi-scale DMI techniques, we have performed in-situ creep experiments on Fe-Au alloys, which combines creep damage formation in ferritic steels with a subsequent healing potential, at 550 °C and 3 different constant loading conditions. With DCT and s3DXRD providing grain maps in the initial and final state of the creep experiments, the evolutions of creep voids and cavities and the Au precipitation at the locations of these damage sites were characterized by phase contrast tomography and the strain state of individual grains were determined by 3DXRD. These results provide inputs for a micromechanical model that takes into account the connection between crystal plasticity and the local transport of Au atoms and vacancies. The combined work gives a much better and a more quantitative insight into the mechanisms of damage evolution and potential healing in ferritic steels.

Keywords : Diffraction contrast tomography, 3DXRD, Creep damage, Grain mapping, Strain mapping

133. Evolution of the microstructure and properties of a steel subjected to a Q&P treatment including a galvanizing step

Calvo Jessica^{1 2}, Carpio Marcel³, Garca Omar⁴, Pedraza Juan Pablo⁴, Cabrera Jose Maria^{1 2}

1 - Universitat Politècnica de Catalunya (Spain), 2 - Fundació Centre CIM (Spain), 3 - Eurecat, Centre Tecnològic de Catalunya (Spain), 4 - TERNIUM Mexico (Mexico)

Quenching and Partitioning (Q&P) steels belong to the third generation of Advanced High-Strength Steels (AHSS) and offer an exceptional combination of high tensile strength and good ductility at a reduced cost. These properties are particularly attractive for automotive and structural applications where both strength and formability are critical. The properties of Q&P steels are based on two-step thermal cycles designed to optimize the microstructure of the steel by retaining austenite at room temperature. For sheet metal applications in the automotive industry, galvanizing is widely used to enhance the corrosion resistance of steels. In this work, the Q&P treatment has been designed to include a third step corresponding galvanizing. Conventional Q&P treatment has been compared to cycles including the galvanizing stage to assess the effect of this surface treatment on the evolution of the microstructural constituents, as well as the mechanical properties of a medium C and Mn steel.

Keywords : Q&P steel, galvanizing, retained austenite, microstructural evolution

134. Discovery of nano-scaled promising strengthening factor in 316L stainless steel fabricated by laser powder bed fusion

Sun Fei¹, Adachi Yoshitaka, Sato Kazuhisa, Ishimoto Takuya, Nakano Takayoshi, Koizumi Yuichiro

1 - Nagoya University (Japan)

Laser powder bed fusion (LPBF) generates large thermal gradients and rapid cooling rates, making it challenging to fully understand the relationship between nano-scaled solidification microstructure and process parameters. Most studies have focused on characterizing microstructures from macro to sub-micrometer scales, with few investigating features at the nano or atomic levels. This study aims to explore these nano/atomic scale microstructural features of 316L stainless steel (SS) produced through LPBF to better understand the relationship between solidification microstructure and process parameters. 316L stainless steel was manufactured by the LPBF method. Novel nano-scaled modulated structures have been observed in the dislocation cells parallel to the laser scan direction, which was mainly caused by the elastic strain involving the thermal gradient inside the melt pool and the accumulated strain by dislocation accommodation at the cell boundaries during the heating-cooling cycles in the melt pool [1]. Compared to the as-built sample, the microstructure after aging at 650°C for 1 hour shows a slight increase in the size of the dislocation cells. After further aging at 1050°C for 1 hour, the dislocation cells disappear, leaving only a few random dislocation segments. Interestingly, the modulated structure persists, demonstrating stability at high temperatures. Hardness test results show a decrease in hardness, resulting from the increase in dislocation cell size and their eventual disappearance. Most interestingly, even after the dislocation cells disappear after aging at 1050°C for 1 hour, the hardness remains higher than that of the as-cast samples.

Keywords : Laser power bed fusion, 316L stainless steel, Solidification structure, Modulated structure, Melt pool boundary, Segregation

135. Analysis of white strip defects in the galvanized coating surface of hot -dip galvanized DP steel

Guang Chen^{1 2}, Min Zhu^{2 3}, Weichen Mao^{2 4}

1 - CHEN Guang (China), 2 - Baoshan Iron & Steel Co.,Ltd, Shanghai (China), 3 - ZHU min (China), 4 - MAO Weichen (China)

The microstructure and characteristics of two types of white stripe defects in hot -dip galvanized DP steel were studied and the relevant processes were analyzed and discussed. The results show that both types of white strip defects originate from the surface defects of the substrate before galvanizing and one originates from iron scale of finishing roller with its microstructure characterized by characteristic elements Mo V Cr Ni etc; Another type originates from microcracks in the casting slab whose microscopic characteristics are mainly secondary oxides. Based on the above analysis the paper clarifies the impact of hot rolling and slab casting processes on white strip defects.

Keywords : hot dip galvanneal dual phase steel, white stripe defects in iron scale of finishing roller secondary oxides

136. Assessing the Origins of Autogeneous Recrystallisation During the Austenitisation of Low-Alloy Steels: Comparing In-Situ EBSD and In-Situ Synchrotron XRD

Taylor Mark¹, Thomas Rhys², Smith Albert³, Mozumder Yahya H.¹, Donoghue Jack⁴, Prangnell Phil⁵, Scenini Fabio¹, Hutchinson Christopher, Pickering Ed^{6 7}

1 - Department of Materials, University of Manchester, Manchester M13 9PL (United Kingdom), 2 - The University of Manchester (United Kingdom), 3 - Tescan UK Ltd. (United Kingdom), 4 - Henry Royce Institute and Department of Materials, The University of Manchester, Manchester, M13 9PL, UK (United Kingdom), 5 - Department of materials, Manchester University, Manchester, M13 9PL (United Kingdom), 6 - University of Manchester [Manchester] (United Kingdom), 7 - Henry Royce Institute (United Kingdom)

The austenitisation of martensitic or bainitic low-alloy steels is known to proceed via a two-step mechanism. The first step is a 'memory effect', which involves the formation of the old prior-austenite grain structure. The second step is recrystallisation (RX), in which new austenite grains nucleate and grow, which occurs without any externally-applied deformation. The extent of this RX step appears to vary according to both alloy composition and the austenitisation heat treatment applied (e.g., the heating rate used). It is reasonable to assume that the driving force for the recrystallisation originates from the strain associated with the ferrite austenite (BCC to FCC) transition. However, precisely how dislocation density arises in the austenite during the preceding 'memory effect' step are unclear. In this work, automated in-situ EBSD was used to observe austenitisation via the memory effect in two different low alloy steels. The first steel, Super CMV, underwent only a memory effect, while the second, SA505 grade 4N, underwent a memory effect followed by recrystallisation. The austenitisation experiments were repeated using in-situ synchrotron X-ray Diffraction (SXRD), enabling the measurement of dislocation density in both phases during austenitisation. Corroborating the microstructural evolution observed using in-situ EBSD, with bulk SXRD dislocation density measurements, has enabled us comment on the origins of the austenite dislocations that drive the RX step.

Keywords : Low Alloy Steels, High Temperature In, situ EBSD, Synchrotron XRD, Memory Effect

137. On the static recrystallization characteristics and kinetics of austenitic stainless steels under development for LH2 storage applications

Somani Mahesh ¹, Abdelghany Ahmed ^{2 3}, Ghosh Sumit ⁴, Smith Ali ⁵, Muratori Marta ⁶, Hoffmann Frank ⁷

1 - Faculty of Technology, Centre for Advanced Steels Research, University of Oulu, PL 4200, 90014 Oulu (Finland), 2 - Materials and Mechanical Engineering, Centre for Advanced Steels Research, University of Oulu (Finland), 3 - Future Manufacturing Technologies (FMT), Kerttu Saalasti Institute, University of Oulu, Nivala, 85500, Finland. (Finland), 4 - Materials and Mechanical Engineering, Centre for Advanced Steels Research, University of Oulu, 90014 Oulun yliopisto, Finland. (Finland), 5 - RINA Consulting - Centro Sviluppo Materiali SpA (Italy), 6 - Acerinox Europa S.A.U., Acerinox Europa, Los Barrios (Spain), 7 - Institut für Metallformung, TU Bergakademie Freiberg (Germany)

With ever increasing demand for strong and tough alloys for liquid hydrogen (LH2) storage, renewed efforts have been made to design new stainless steels with varying nitrogen and alloying contents that are amenable for TMCP processing in order to impart improved yield strength at room and sub-zero temperatures with adequate toughness and austenite stability. In order to design appropriate thermomechanical rolling processes, the static recrystallization characteristics and kinetics of three austenitic stainless steels were determined using the double-hit compression technique on a Gleeble 3800 thermomechanical simulator and modelled in terms of the effects of temperature, strain, strain rate and initial grain size using a fractional softening approach. A comprehensive analysis of the recrystallization data enabled estimation of material parameters for the three stainless steels, including the powers of strain (~ -3.1) and strain rate (~ -0.3), and estimation of apparent activation energies of recrystallization that clearly depicted the effects of alloying with 0.1 wt.% Nb (273 kJ/mol) in one steel and 7.0 wt.% Mn (298 kJ/mol) in another steel compared to the reference 304L steel (251 kJ/mol). The influence of nitrogen, if any, could not be clearly established. The presence of Nb and Mn in the two austenitic stainless steels retarded their static recrystallization rates compared to the reference steel. Together with detailed metallography, confirmation experiments suggested reasonability of the developed fractional softening equations. This paper presents a detailed account of the static recrystallization behaviour and kinetics of the three austenitic stainless steels intended for TMCP processing for LH2 storage applications.

Keywords : Static recrystallization, Activation energy of recrystallization, Austenitic stainless steel, Double hit compression, TMCP, Liquid hydrogen storage

138. Formation mechanism of detrimental grain boundary kappa-carbide during age hardening of austenitic high manganese lightweight steel

Ponge Dirk¹, Elkot Mohamed N.¹, Sun Binhao², Raabe Dierk¹

1 - Max Planck Institute for Sustainable Materials (Germany), 2 - Key Laboratory of Pressure Systems and Safety, (China)

The age hardening of austenitic high-Mn, high-Al lightweight steel leads to beneficial increases in yield strength and tensile stress due to a homogeneous distribution of fine kappa-carbide precipitates inside the grains. However, by employing high resolution microstructure characterization by atom probe tomography we observe the formation of detrimental kappa-carbides at the grain boundaries already in under-aged samples. During these early stages of age hardening, tensile tests at room temperature still show a ductile fracture mode. But impact tests or tensile tests at lower temperatures reveal a loss of toughness and ductility due to intercrystalline fracture. In this contribution we will discuss the mechanism of the early formation of grain boundary kappa-carbides during age hardening in such steels.

Keywords : Intergranular Failure, Lightweight steel, High Manganese steel, Impact toughness, Precipitation hardening, Grain Boundary embrittlement

139. Effect of Mn concentration in Cementite on austenitization behavior of Fe-C-Mn Alloy

Fujikura Kai, Nakada Nobuo ¹, Nagashima Ryota , Yabu Shohei

1 - Institute of Science Tokyo (Japan)

To achieve a sustainable society, it is necessary to develop advanced high-strength steels without rare elements. This study investigated Mn enrichment in cementite during pearlitic transformation and subsequent annealing using near-eutectoid Fe-0.6%C-3.0Mn alloys (mass%). And its effect on austenitization behavior was discussed in terms of thermodynamics and kinetics. The cementite, which initially had a lamellar morphology after the completion of pearlitic transformation, was spheroidized by prolonged annealing, with Mn enrichment reaching near-equilibrium levels. This Mn enrichment locally stabilized austenite after cementite dissolved into the austenite matrix during austenitization, resulting in the formation of retained austenite on quenching. The retained austenite fraction in the reversed material increased monotonically with annealing time and saturated after annealing exceeding 72 ks. The annealing time dependent variation in composition of Mn within cementite was analyzed, showing a steady increase toward the equilibrium composition of 19.2% at 923 K. Moreover, composition of Mn increased from 7.0% to 10.5% between 7.2 ks to 18 ks of annealing, corresponding to a rapid increase in the retained austenite fraction. This level of Mn enrichment was sufficient to lower Ms temperature below room temperature. Furthermore, the kinetics simulation by DICTRA demonstrated that Mn had concentrated in cementite remained locally within reversed austenite matrix because of the slow diffusion of Mn. As a result, austenite stabilized locally by Mn remaining was left as retained austenite after quenching. From these results, it can be concluded that the Mn concentration in cementite, whether before and after pearlitic transformation, complicates austenitization behavior.

Keywords : Steel, Austenitization, Martensitic, transformation, Pearlite

140. Exploring Carbon Partitioning, Carbide Precipitation, and Bainite Formation During Q&P Processing in Medium-Carbon Steel Using In-Situ Synchrotron XRD

Aalipour Hafshejani Zeynab¹, Ghosh Sumit ¹, Koemi Jukka ¹, Javaheri Vahid ¹

¹ - Materials and Mechanical Engineering, Centre for Advanced Steels Research, University of Oulu (Finland)

Quenching and partitioning (Q&P) treatment enable the development of microstructures comprising mainly tempered martensite and retained austenite, thereby significantly enhancing mechanical properties. However, most existing Q&P processing strategies presume complete suppression of carbide precipitation in martensite and the austenite-to-bainite transformation. In practice, these reactions are not fully eliminated, particularly in medium carbon steels. In this study, the effects of carbon partitioning, carbide precipitation, and carbide-free bainite formation on austenite stabilization during Q&P processing were investigated. Experiments were performed on novel 0.4C€“1.5Si€“2Mn€“1Cr€“0.3Mo€“0.2V (wt.%) steel at quench stop temperatures of 200°C and 240°C, followed by a partitioning temperature of 300°C and a holding time of 1000 s. In-situ synchrotron X-ray diffraction (XRD) was employed to monitor the entire process, with particular focus on carbon partitioning. The results revealed that lower quench temperature, which yield a higher fraction of primary martensite, accelerates carbon partitioning from martensite to austenite, effectively suppressing austenite decomposition. Consequently, a higher fraction of austenite is stabilized through carbon enrichment, preventing its transformation into bainite. Moreover, lower quench stop temperature promote a greater volume fraction of stabilized austenite and correspondingly reduce bainite formation. In addition, the in-situ XRD approach provides real-time monitoring of phase evolution, offering insights into the mechanisms governing microstructural development during quench and partitioning process.

Keywords : Quenching and partitioning, Retained Austenite, Insitu synchrotron XRD, Carbon partitioning, Advanced high strength steel

141. On the Chemical Boundary Engineering of Hot-Rolled Medium Mn Steel

Sadeghpour Saeed¹, Javaheri Vahid ¹, Koemi Jukka ¹, Karjalainen Pentti ¹

¹ - Materials and Mechanical Engineering, Centre for Advanced Steels Research, University of Oulu, FI-90014 (Finland)

In the pursuit of novel microstructures with enhanced mechanical properties in medium Mn steels, various processing routes have been explored beyond conventional intercritical annealing treatment (IAT). Among these approaches, chemical boundary engineering (CBE) stands out for its ability to produce materials with ultrafine hierarchically heterogeneous microstructures, even after exposure to high temperatures. Unlike conventional IAT, CBE yields higher strengths without compromising material ductility. However, despite its promise, CBE remains a complex process with multiple steps and retains certain drawbacks of IAT, including the yield point and dynamic strain ageing phenomena in cold-rolled samples. In this study, we applied the CBE process to a hot-rolled medium Mn steel and observed significant improvements in tensile properties compared to its IAT-treated counterpart. Notably, stress-strain curves revealed the absence of both the yield point phenomenon and dynamic strain ageing. Comprehensive investigations of the microstructural evolution and resulting tensile properties further elucidate the efficacy of the CBE approach in achieving a heterogeneous microstructure with enhanced mechanical properties.

Keywords : Medium Mn steel, Chemical boundary engineering, Heterogenous microstructure, tensile properties

142. Thermomechanical processing of 0.17C-4Mn-0.8Al-0.5Si QP-treated steels based on deformation-continuous-cooling-transformation diagrams

Grajcar Adam¹, Skowronek Adam, Kassaye Firew Tullu, Gulbay Oguz, Gramlich Alexander, Krupp Ulrich

1 - Silesian University of Technology (Poland)

Three 0.17C-4Mn-0.8Al-0.5Si medium-Mn steels alloyed with molybdenum and copper were subjected to different thermomechanical scenarios including continuous compression tests in a temperature range of 900-1100°C at different strain rates of 0.05, 0.5 and 5 s⁻¹ and double-hit compression tests at 900 and 1100°C with interval times from 1 to 60s using the Gleeble 3800 machine. Next, the samples were subjected to different quenching and partitioning (QP) treatments directly from the finishing deformation temperature and compared to the undeformed samples. The microstructures were assessed by using light microscopy and SEM, whereas a fraction of retained austenite was determined based on X-ray quantitative calculations. The QP parameters were selected on the basis of continuous-cooling-transformation (CCT) and deformation-cooling-transformation (DCTT) diagrams. The effects of Mo and Cu additions and plastic deformation on the phase transformations of undercooled plastically deformed and undeformed austenite, microstructure and retained austenite amounts were investigated. The assumptions of the thermomechanical processing of high-hardenability steel forgings with tailored strength and ductility were finally formulated. Acknowledgement The study was funded by National Science Centre, Poland under the OPUS call in the Weave programme, grant no. 2021/43/I/ST5/02658 and by the Deutsche Forschungsgemeinschaft (DFG, German Research Foundation) 504849602.

Keywords : Thermomechanical Processing, Medium, Mn Steel, QP Treatment, DCTT diagram, Retained Austenite

143. Towards a comprehensive understanding of the effect of continuous annealing process conditions on the microstructure development of cold-rolled dual-phase (DP) steels and their correlations with mechanical and magnetic properties

Iza-Mendia Amaia^{1 2}, Jorge-Badiola Denis^{1 2}, Fernandez-Sanchez Sergio^{1 2}, Aramendi Iosu^{1 2}, Cuenca-Ariza Mikel^{1 2}, Martinez-de Guerenú Ane^{1 2}, Valcarcel Luis Vitores^{1 2}

1 - 1 Ceit-Member of Basque Research & Technology Alliance (BRTA), Manuel Lardizabal 15, 20018 Donostia / San Sebastián, Spain (Spain), 2 - 2 Universidad de Navarra, Tecnun, Manuel Lardizabal 13, 20018 Donostia / San Sebastián, Spain (Spain)

The complexity of continuous annealing (CA) cycles applied to Advanced High Strength Steels (AHSS) is transferred to microstructure development and final mechanical properties (MP). In addition, the characterisation of these grades through the application of ND (non-destructive) techniques, especially those based on magnetism, shows an overwhelming potential to reduce the workload associated with the application of the time-consuming and costly characterisation techniques. Currently, the relationship between processing parameters and microstructure with mechanical/magnetic properties is an active area of research. In the present work, cold-rolled DP steels are subjected in a dilatometer to thermal cycles based on variations of CA and continuous cooling cycles to produce a range of multiphase microstructures (ferrite, bainite, martensite) and dissimilar MP. A thorough microstructural, mechanical and magnetic (BH hysteresis loops) characterisation of the samples has been carried out accordingly. The analysis of the results shows that both the MP and the magnetic parameters (MGP), such as the coercive field (H_c), the induction field B at certain applied magnetic fields or the hysteresis losses (W_h) estimated from BH loops, are sensitive not only to the microstructure but also to the processing conditions. Some correlations of MP and MGP with thermal conditions and microstructure, or among themselves can be found. The latter may be useful for the development of microstructure-based classification models. However, the complexity of establishing generalised relationships between mechanical/magnetic properties-thermal processing parameters-microstructure becomes apparent when attempting to develop numerical predictive models.

Keywords : Advanced High, Strength Steel (AHSS), Continuous annealing, Mechanical Properties, Magnetic hysteresis BH loops, NDT, Multiphase microstructures, Modelling

144. Influence of intermittent friction cycles on tribocorrosion behavior of 316L stainless steel in 5% NaHCO₃

Bouguerra Kaouthar , Richard Caroline, Chen Yan-Ming , Ducommun Nadege , Romaine Alexandre , Cardey Pierre Francois

1 - GREMAN (matériaux, microélectronique, acoustique et nanotechnologies) (France)

The food processing industry requires durable stainless steel equipment resistant to repeated friction and corrosion cycles. Cleaning and maintenance procedures introduce periodic interruptions that may affect the passivation and depassivation mechanisms of these materials. This study investigates the tribocorrosion behavior of 316L stainless steel under extended experimental conditions, simulating industrial interruptions. The primary objective is to assess the robustness of the passive film and its ability to sustain protective properties over time. The study follows ASTM G-133 tribological testing standards in a 5% NaHCO₃ solution over 14 hours, incorporating alternating friction phases and rest periods. Open circuit potential is continuously monitored, and surface characterization employs profilometry, SEM-EDS, Raman spectroscopy, and XPS. Results show an initial drop in the coefficient of friction due to passive film formation, with stability maintained despite intermittent rest. A transient CoF drop occurs after overnight pauses, indicating temporary film weakening before repassivation. Wear analysis confirms film stability, with corrosion product characterization revealing iron-based oxides, hydroxides, and carbonates. XPS analysis highlights a multilayered passive film dominated by Fe₂O₃, Fe₃O₄, Cr₂O₃, and Cr(OH)₃. The findings confirm that 316L stainless steel maintains stable tribocorrosion performance in 5% NaHCO₃ despite long-term cyclic friction, supporting its industrial applicability in aggressive environments.

145. A Novel Approach to Predict Martensitic Transformations in High-carbon Bearing Steels

Catal-Isik Aysel Aysu¹, Galindo-Nava Enrique¹, Sanchez-Camacho Lizeth Johana², Bedekar Vikram², Pantawane Mangesh Vyankat²

1 - Department of Mechanical Engineering [University College London] (United Kingdom), 2 - Timken Company (United States)

Understanding and predicting martensitic transformations is crucial for improving the rolling contact fatigue performance of high-carbon bearing steels. Existing martensite models for high-carbon steels cannot accurately predict the variant selection process, along with the autocatalytic nature of plate martensite nucleation, and ignore the connection between nucleation and growth of individual martensite plates. This work proposes a novel modelling approach to predict plate martensite evolution in high-carbon steels. The analytical model couples a new martensite nucleation equation with individual variant growth and volume fraction evolution. The plate boundary mobility of individual variants is defined by calculating the change in length of a martensite plate from the martensite volume fraction evolution using the Koistinen-Marburger equation. The nucleation rate is defined by a nucleation probability equation that depends on the local retained austenite fraction and Thermodynamic driving force. We validate the model predictions in a high carbon bearing steel by measuring the area fraction of each martensite variant using a new automated method in the SEM-EBSD; the method consists of identifying individual martensite variants and classifying martensite plates in terms of their area, length, and aspect ratios. We observe an exponential decrease in the area fraction of subsequent variants, confirming a hierarchical variant selection process and cascade-like nucleation behaviour, both phenomena consistent with our model predictions. The present results provide more compelling insights of the interplay between martensite nucleation, growth and variant selection kinetics that will help in the design and optimisation of high-carbon martensitic steels.

Keywords : Martensite nucleation, high carbon steel, modelling, heat treatments, characterisation

146. Influence of the phase state variations on the impact toughness of lean alloyed 19-22 wt% Cr ferritic-austenitic stainless steels

Uusikallio Sampo¹, Moallemi Mohammad , Koemi Jukka

1 - University of Oulu [Finland] = Oulun yliopisto [Suomi] = Universite d'Oulu [Finlande] (Finland)

A set of laboratory-manufactured lean alloyed ferritic-austenitic stainless steels containing 19-22 wt% Cr were investigated in their annealed hot-band condition to assess impact toughness. The austenite-to-ferrite phase ratio varied from 60:40 to 15:85, leading to differences in phase morphology and banding intensity. Charpy-V impact toughness tests were conducted using sub-sized (3.5 mm) specimens over a temperature range of -80 to 160 °C to evaluate ductile-to-brittle transition behavior. The T28J temperature was observed to increase with the ferrite content. Microstructural features were analyzed using laser confocal, scanning electron microscopy and electron backscatter diffraction. Multiple linear regression analysis was performed to identify factors influencing impact toughness. The results showed that toughness deteriorated with increasing ferrite volume fraction and ferrite grain size, particularly the 90th percentile ferrite grain size. Inclusions and grain orientation were found to have no statistically significant effect on impact toughness.

Keywords : Hot, band, Impact toughness, Lean alloyed, Ferritic, austenitic, Stainless steel

147. Recent Development of Hot-rolled 780 and 980MPa AHSS for Automotive Lightweight Chassis

Lee Jewoong¹, Song Taejin¹, Kim Sungil¹, Im Youngroc¹

POSCO, KOREA

From a materials perspective, developing ultra-high-strength automotive steel sheets remains an effective strategy for achieving lightweight vehicles. While cold-rolled steels for Body In White (BIW) applications have long surpassed the commercialization of steels with ultimate tensile strengths (UTS) of 980 MPa or more, and the adoption of 1.2 GPa and 1.5 GPa cold-rolled steels is on the rise, the advancement in strength for hot-rolled steels used in chassis applications has not progressed as rapidly. This slower pace is primarily due to the chassis's role as the vehicle's lower structure, where durability is of paramount importance. However, due to the rapid expansion of the electric vehicle market, efforts are being made to lighten these chassis components through thinning and ultra-high strength to offset the heavy battery weight. In response to these changes, POSCO has developed hot-rolled and hot dip galvanized 780 and 980MPa grade steels for automotive chassis.

Keywords : Hot rolled AHSS, CP steels, HB Steels, lightweight chassis

148. Constructing high-density dislocations by primary (Nb,Ti)(C,N) to induce massive secondary precipitations in austenitic heat-resistant cast steel

Mu Rong , Wang Yongjin , Song Renbo ¹

¹ - University of Science and Technology Beijing [Beijing] (China)

The microstructural evolution and the high-temperature tensile properties of a novel Nb-Ti-N alloyed austenitic heat-resistant cast steel were investigated during the isothermal aging at 900° for up to 1000 h. The mechanisms of enhancing strength-ductility synergy and the high-temperature tensile fracture behaviors after the aging process were analyzed in detail through tensile tests at 900°. Obtained results show that the high-density dislocation regions and the Cr segregation, formed around the intragranular primary (Nb,Ti)(C,N), provided numerous nucleation sites for submicron-sized secondary M₂₃C₆ precipitates. The density of secondary M₂₃C₆ significantly increased, while the coarsening rate was notably reduced during the aging process. Simultaneously, the uniform dispersed precipitation of nano-sized secondary (Nb,Ti)C was promoted by massive dislocations, which exhibited high resistance to coarsening during long-term aging. The improvement of high-temperature strength is attributed to the precipitation strengthening effects induced by the submicron-sized M₂₃C₆ and nano-sized (Nb,Ti)C particles. Additionally, the enhancement of ductility during aging was mainly due to the more effective stress transmission and the ameliorated interface relationship between primary (Nb,Ti)(C,N) and austenitic matrix, which was facilitated by the abundant precipitation of secondary phases. The current findings indicate that high-density dislocations constructed by the intragranular primary (Nb,Ti)(C,N) induce the extensive dispersion of secondary strengthening phases, which enhanced both ultimate tensile strength of 158 MPa and elongation of 45.3% at 900 ° after isothermal aging for 1000 h.

Keywords : Isothermal aging, Microstructural evolution, Precipitation strengthening, High, temperature tensile properties, Austenitic steel

149. Detecting iron in vanadium carbide nanoprecipitates by atomic-resolution scanning transmission electron microscopy techniques

Sabet Ghorabaei Amir ¹, Kooi Bart J. ¹

¹ - Zernike Institute of Advanced Materials (Netherlands)

Microalloyed low-carbon steels strengthened by vanadium carbide (VC) nanoprecipitates are receiving increasing attention for use in automotive industry. Recent analyses of small-angle neutron scattering (SANS) and atom probe tomography (APT) data suggest that interphase-precipitated VC nanoprecipitates are enriched in iron in the initial stages of their nucleation and growth during the austenite-to-ferrite phase transformation. Iron may reduce the coherency strain resulting from the lattice mismatch between the precipitate and the matrix, thereby lowering the nucleation barrier during the interphase precipitation. However, it is not yet clear whether the iron is present as a shell or in the core of the nanoprecipitates and whether the iron also plays a role in random precipitation of VC nanoprecipitates during aging of bainitic/martensitic microstructures. Here a model vanadium-microalloyed low-carbon steel with interphase and random nanoprecipitates was studied through detailed (scanning) transmission electron microscopy (S/TEM) of carbon extraction replicas. Energy-dispersive X-ray spectroscopy (EDS) spectrum imaging combined with experimental and simulated high-angle annular dark-field (HAADF) and integrated differential phase contrast (iDPC) microscopy by STEM was employed for detection of iron in the VC crystal structure. The VC nanoprecipitates formed by the interphase precipitation mechanism indicated the presence of iron in their crystal structure whereas the VC nanoprecipitates formed by the random precipitation mechanism were almost iron-free. These results are supported by thermodynamic and kinetic evaluations of the precipitation mechanisms, improving our understanding of the evolution of VC nanoprecipitates in microalloyed low-carbon steels.

Keywords : vanadium carbide precipitation, transmission electron microscopy, energy dispersive X ray spectroscopy, integrated differential phase contrast microscopy, carbon extraction replica, microalloyed steels

150. Evolution of inclusions in physically simulated heat-affected zones of a weld metal used with a 500 MPa offshore steel

Tervo Henri¹, Gaspar Marcell², Kovacs Judit², Kaijalainen Antti¹,
Javaheri Vahid¹, Sainio Johannes³, Alatarvas Tuomas⁴, Koemi Jukka¹

1 - Materials and Mechanical Engineering, Centre for Advanced Steel Research, University of Oulu (Finland), 2 - Institute of Material Science and Technology, University of Miskolc (Hungary), 3 - SSAB Europe (Finland), 4 - Process Metallurgy, Centre for Advanced Steel Research, University of Oulu (Finland)

Non-metallic inclusions in weld metals often have a role inducing the formation of acicular ferrite, which is known to improve the toughness and other properties of the weld metal. The ability of the inclusions to promote the acicular ferrite formation depends on various factors such as chemical composition, morphology and size of the inclusions. In multipass welding, additional thermal cycles affect the inclusions in the pre-existing weld passes, potentially causing compositional and morphological changes in the inclusions. These changes may have an effect on the inclusions' ability to promote the formation of acicular ferrite. In the current study, the thermal cycles of multipass welding were produced on a single pass weld by physical simulation. Intercritical (ICHAZ), coarse-grained (CGHAZ) and intercritically reheated coarse-grained heat-affected zones (ICCGHAZ) in weld metal were simulated using three different cooling times from 800 °C to 500 °C (t_{8/5}). Inclusions in the heat-affected zones of the weld were analyzed using field emission scanning electron microscope equipped with energy dispersive spectroscope (FESEM-EDS), after which they were classified according to their chemical composition. The results showed that the inclusion content in the weld metal was affected by the thermal cycles. In the CGHAZ simulation the number of Mn-bearing inclusions increased compared to the unaffected single-pass weld metal, whereas in ICHAZ such phenomenon was not observed. The increase of these inclusions was seen to affect the microstructure by refining the acicular ferrite laths.

Keywords : Welding, Offshore steel, Inclusions, Acicular ferrite, HAZ

151. Special Steels for the Hydrogen Society

Nguyen Dong¹, Tervo Henri¹, Paavola Jussi¹, Koemi Jukka¹

¹ - Materials and Mechanical Engineering, Centre for Advanced Steel Research, University of Oulu (Finland)

The transition to hydrogen-based energy systems presents a critical need for materials capable of withstanding the harsh conditions of hydrogen storage. Our project addresses this challenge by developing a multilayer steel designed specifically for hydrogen environments. This material combines austenitic steel, known for its resistance to hydrogen embrittlement, with carbon steel, which provides strength and cost efficiency. Hydrogen embrittlement poses a well-known issue in the storage and transport of hydrogen, often degrading various metals. Although many stainless steels provide superior resistance, its high-cost limits widespread application. Our solution involves a multilayer approach, where austenitic layer serves as the primary barrier against hydrogen-induced degradation, and the carbon steel layer ensures the material's structural strength under high pressure. The manufacturing process involves hot roll bonding, where the surfaces of the two materials are cleaned of oxides, welded together, heated up to 1200 °C, and then hot rolled to form a strong bond. This method not only strengthens the material but also making it a potential solution for large-scale hydrogen storage applications.

Keywords : hydrogen embrittlement, multilayer steel, hot roll bonding, hydrogen storage, advanced materials

152. Thermodynamic and Algorithmic Optimization of Medium Manganese Steel Composition Design, Non-Metallic Inclusion Analysis, and Microstructural Insights

Elaraby Mahmoud^{1 2}, Ali Mohammed^{1 2}, Eissa Mamdouh², Koemi Jukka¹, Karjalaine Pentti¹, Tervo Henri¹, Alatarvas Tuomas¹, Ghassemali Ehsan³, Steggo Jacob³, Javaheri Vahid¹

1 - University of Oulu (Finland), 2 - Central Metallurgical Research and Development Institute (Egypt), 3 - Jankaping University [Sweden] (Sweden)

High-throughput computational screening based on CALPHAD (CALculation of Phase Diagram) was employed to investigate potential chemical compositions within the medium manganese steel system for optimizing austenite phase fraction and stacking fault energy (SFE). The primary objective was to identify optimal alloy compositions that balance the complex effects of various alloying elements on phase stability and mechanical properties. Utilizing thermodynamic software coupled with a custom-developed algorithm, two optimized compositions were determined: 0.35, 9Mn, 1Mo, 3Al, 1Si, 0.05Nb, 0.3V (353), and 0.35C, 9Mn, 1Mo, 3Al, 1Si, 0.1Nb (310) in wt.%. Comprehensive quantitative and qualitative analyses of NMIs were conducted for both as-cast and as-forged conditions. For alloy 353, 80% of the NMI area was below 5 μm^2 , and 86.6% of NMIs had an equivalent circular diameter below 3 μm . In addition, alloy 310 exhibited 70% of the NMI area below 5 μm^2 and 88.7% of NMIs below 5 μm in equivalent circular diameter. Non-metallic inclusions were identified as MnS, AlN, MnO, and Al₂O₃.

Keywords : medium manganese steel, computational design, thermodynamic modeling, alloy optimization, non metallic inclusions, stacking fault energy.

153. High temperature crystal structure of beta-uranium from neutron diffraction

Sven Vogel¹, Yi Xie², Michael T. Benson³, Jason M. Harp⁴, Sven P. Rudin⁵

1 : Los Alamos National Laboratory (LANL), *P.O. Box 1663, Los Alamos, NM, 87545 - United States*

2 : Purdue University [West Lafayette]

3 : Idaho National Laboratory

4 : Oak Ridge National Laboratory

5 : Los Alamos National Laboratory

Beta-uranium may occur in metallic nuclear fuels such as U-10wt.%Zr, a leading fuel candidates for sodium-cooled fast reactor due to high fissile density, high thermal conductivity, ease of fabrication, and good compatibility with coolants. In the Zr-lean part of the phase diagram, the occurrence of beta-uranium, with its large tetragonal unit cell containing 30 atoms, is reported. However, experimental characterizations of such alloys with diffraction methods are very rare. Here, we present results on thermal cycling of U-2Zr and U-0.5Ti characterized by time-of-flight neutron powder diffraction, during which the beta-uranium phase was observed. The data for thermal motion parameters of the beta phase is compared with results from atomistic modeling.

Keywords : Uranium, Neutron Diffraction

154. On the conditions of pearlitic cementite nucleation at a migrating austenite-ferrite interface

Ogris Daniel Marian¹, Kreyca Johannes², GamsjaGer Ernst³,
Zamberger Sabine¹

1 - voestalpine Forschungsservicegesellschaft Donawitz GmbH (Austria), 2 - Independent Researcher (Austria), 3 - Chair of Mechanics, Montanuniversitat Leoben (Austria)

Understanding the kinetics of the pearlite transformation is a key success factor for efficient heat treatment of commercial steel grades. The usually applied global Hultgren extrapolation concept for predicting the pearlite formation is not sufficient to explain all experimentally observed phenomena. As an example, the influence of the austenite grain size on the amounts of microstructural constituents after an isothermal heat treatment cannot be predicted by means of the Hultgren approach. A deeper understanding of the pearlitic cementite nucleation at a moving austenite-ferrite interface is thus of great importance. In this work, the role of the kinetics of the austenite-ferrite transformation on the nucleation conditions of cementite is investigated by means of local equilibrium and mixed-mode models to gain deeper insights into the early stages of pearlite formation. Thereby, degenerate forms of eutectoid transformations as well as other experimentally observed phenomena not in line with the concept of a global Hultgren extrapolation can be explained.

Keywords : thermodynamic modelling, phase transformations, nucleation and growth, steel, proeutectoid ferrite, pearlite

155. Impact of Aluminium in comparison to Silicon on Liquid Metal Embrittlement of 3rd Generation AHSS

Hoeger Korbinian^{1 2}, Kaar-Schickinger Simone³, Wallner Matthias³,
Schneider Reinhold², Steineder Katharina³, Gruber Martin³,
Sommitsch Christof¹

1 - Graz University of Technology [Graz] (Austria), 2 - University of Applied Sciences Upper Austria (Austria), 3 - voestalpine Steel GmbH (Austria)

The impact of Si on Zn-induced Liquid Metal Embrittlement (LME) in 3rd Generation Advanced High-Strength Steels (AHSS) has been widely studied, but the effect of Al is rather unknown. This study investigates the substitution of Si with Al by analysing six steel compositions with fixed C (0.2 wt.%) and Mn (3 wt.%) contents. Three variants contain Si (0.5, 0.8, and 1.4 wt.%), while the others contain Al (0.5, 1.0, and 1.4 wt.%). To minimize microstructural effects, all steels were quenched and tempered before electro-galvanizing. The effects of alloying were examined using hot tensile testing (600-900 °C), resistance spot welding with prolonged welding times, dilatometry, and annealing (700 and 800 °C for 1 s), combined with EDX to study Fe-Zn phase formation. Results indicate that the use of either Si or Al increases susceptibility to LME but substituting Si with Al significantly reduces Zn-induced LME cracking. In hot tensile tests, higher testing temperatures generally increase the steel's vulnerability to LME. Increasing Si content consistently raises LME susceptibility across all testing conditions. The LME response of Al-alloyed steels is more complex. In hot tensile tests, the influence of Al varies with temperature, with both the highest and lowest Al concentrations showing specific temperature ranges where they exhibit the greatest and least susceptibility to LME. In welding tests, initial LME susceptibility rises with Al content but diminishes at higher Al concentrations. Based on these findings, the study proposes a hypothesis regarding the mechanisms by which Al affects LME behavior in AHSS.

Keywords : Liquid Metal Embrittlement, Galvanized AHSS, Silicon, Aluminium, Spot Welding, Hot Tensile Testing

156. Effect of heat treatment and rolling process on microstructure and deformation behavior in Al-Si alloy

Tokunaga Toko¹, Reiji Hirono¹, Mayama Tsuyoshi², Hagihara Koji

1 - Nagoya Institute of Technology (Japan), 2 - Kumamoto University (Japan)

The strength of currently-used Al alloys is strongly depend on strengthening by fine precipitates and grain refinement. Thus, their strength exhibits a rapid decrease at temperature at above 150 °. Recently, it has been shown that the high strength at high temperature can be achieved by inducing kink-bands formation in alloys having aligned lamellar microstructure. However, the kink-bands formation has been confirmed only in lamellar microstructures, where slip surface is limited to the lamellar plane, and not in rod-like or Chinese script microstructure. In this study, we clarified the contribution of Si and Mg₂Si phase on the mechanical properties, which are main secondary phase in Al-Si-Mg alloys, and focused on the feasibility of introduction of kink bands in the alloys with hard phase having rod-like or Chinese script morphology. We prepared Al-Si eutectic alloy and Al-Mg₂Si alloy with directional solidification by Bridgman technique at 850°. Then, the alloys were subjected to rolling process at 340°. The mechanical properties of the alloys were investigated with compression tests and tensile tests, and deformation microstructures were observed. With the directional solidification and rolling process, the Si and Mg₂Si phases were aligned to the heat flow and rolling directions. After the compression tests at room temperature, although directionally-solidified Al-Si alloy exhibited buckling, rolled Al-Si alloy exhibited shear bands formation and homogeneous deformation was achieved. This result implied that the formation of the shear bands relaxed the stress concentration and improved ductility of the alloy.

Keywords : Al Si alloy, mechanical property, deformation microstructure, directional solidification, rolling

157. Evolution of Microstructure and Mechanical Properties in Cold-Rolled 7050 Aluminum Alloy During Annealing

Jie He¹, Guangjie Huang¹, Shuaibo Zhang¹

¹ - School of Materials Science and Engineering, Chongqing University, Chongqing 400044, China (China)

This study investigates the microstructural evolution in 7050 aluminum alloy during annealing at varying temperatures following solid solution treatment and significant cold rolling. Key processes include recovery, recrystallization, second-phase precipitation, and re-dissolution. Microstructural characterization was performed using optical microscopy (OM), scanning electron microscopy (SEM), and electron backscatter diffraction (EBSD). Changes in alloy properties during annealing were evaluated via electrical conductivity and tensile strength tests. Annealing at 320°C and 350°C resulted in second-phase precipitation before recrystallization, which pinned grain and sub-grain boundaries, thereby inhibiting recrystallization. At annealing temperatures above 380°C, precipitated phase content decreased progressively prior to recrystallization as the temperature rose. Preferential precipitation of second-phase particles at specific sites within the alloy inhibited recrystallization, leading to non-recrystallized regions. The results indicate that at annealing temperatures below 380°C, alloy strength decreases gradually with extended annealing and holding time. At 380°C, however, strength remains stable over time. Above 380°C, prolonged annealing enhances alloy strength, an effect resulting from the interplay of annealing softening, fine-grain strengthening, and solid-solution strengthening mechanisms.

Keywords : 7050 Aluminum alloy, Thermomechanical Processing, Annealing, Induced Strengthening

158. The relationship between precipitates and mechanical properties in Al-Zn-Mg alloy with high and low Zn/Mg

Sanphiboon Wanlalak¹, Matsuda Kenji²

1 - Graduate School of Science and Engineering, University of Toyama, Toyama (Japan), 2 - Faculty of Sustainable Design, University of Toyama, Toyama (Japan)

Al-Zn-Mg alloys are well-known as high-strength, age hardenable aluminum alloys with excellent strength-to-weight ratios. The heat treatment process enhances their mechanical properties, such as hardness and tensile strength. Alloys with different Zn/Mg ratios produce different precipitate phases: high Zn/Mg alloys are primarily strengthened by metastable $\hat{\eta}'$ precipitates, while the T' phase is dominant in low Zn/Mg alloys. In this research, we studied the effects of η' and T' phases on the mechanical properties of Al-Zn-Mg alloys with high and low Zn/Mg ratios. Al-4.83at%Zn-1.93at%Mg (ZM52) as high Zn/Mg alloy and Al-1.45at%Zn-5.76at%Mg (ZM16) as low Zn/Mg alloy, both with a combined Zn and Mg content of approximately 7 at%. Each alloy was aged to peak hardness at 120° and 200 °, and the microstructure was analyzed using Transmission Electron Microscope (TEM). TEM observations showed that in ZM52, the main precipitates were $\eta'/\hat{\eta}'$ phases, while in ZM16, T/T' phases were dominant. For ZM52, aging at 120° and 200° produced precipitates of similar size but with high and low number densities respectively. In contrast, ZM16 exhibited significantly different results at the two temperatures: aging at 120°,f resulted in a higher number density and smaller precipitate size. Additionally, long rod-shaped η' phase precipitates were observed under this condition.

Keywords : Al, Zn, Mg alloy, Heat treatment, Precipitates, TEM, microstructure

159. Effect of Er on the stability of precipitates in AlCuMgSiSc alloys after different homogenization treatment

Hou Xingkai¹, Wen Shengping¹, Wei Wu¹, Wu Xiaolan¹, Huang Hui¹, Gao Kunyuan¹, Xiong Xiangyuan¹, Li Bolong¹, Nie Zuoren¹, Liang Shangshang², Qi Peng³

1 - College of Materials Science & Engineering, Beijing University of Technology, Beijing 100124 (China),

2 - School of Materials Science and Engineering, Taiyuan University of Science and Technology, Taiyuan 030024 (China), 3 - Chinalco Science and Technology Institute Co., LTD, Beijing 102209 (China)

Micro-alloying may provide a strategy for increasing the service temperature of Al-Cu series alloys. The introduction of additional thermally-stable precipitates and interface segregation of slowly diffusing solute atoms are two different mechanisms. In this work, one-stage (540°C/8h) and two-stage (400°C/10h+540/0.5h) homogenization treatments were designed to investigate the effect of Er addition on the thermal stability of AlCuMgSiSc alloys. The electron backscattered diffraction (EBSD) technique and transmission electron microscopy (TEM) were used to study the microstructure of the AlCuMgSiSc alloys after solid solution treatment and the coarsening of precipitates after aging. The results show that two-stage (400°C/10h+540/0.5h) homogenization treatment provides a greater nucleation driving force for the precipitation of Al₃(Sc, Zr) dispersoids. Moreover, the addition of Er results in a more uniform distribution of Al₃(Sc, Zr) dispersoids and refinement of grain structure. After artificial aging at 175°C, Al₃(Sc, Zr) dispersoids can serve as heterogeneous nucleation sites for the theta precipitates to improve the hardness value of the alloy. One-stage homogenization treatment is more beneficial for the long-term stability of alloys. The enrichment of Er solute atoms and the segregation of Sc solute atoms at the interface of theta precipitates have been observed, which contribute to stabilizing the coarsening of the theta precipitates. In contrast, the precipitation of Al₃(Sc,Zr) dispersoids consumes Er and Sc atoms in the Al matrix during the two-stage homogenization, leading to a weakening of solute atom segregation.

Keywords : Micro alloying, Homogenization treatment, Thermal stability, Al₃(Sc, Zr), Solute segregation

160. On the order-disorder transformation within a main hardening precipitate in Al-Mg-Si alloys

Ding Lipeng¹, Flemming Ehlers¹, Zhihong Jia¹

¹ - Nanjing Tech University (China)

The earliest stages of solid-state precipitation in age hardenable alloys, before the first ordered phase formation, are notoriously elusive, yet often of central importance to material properties quantification. The order-disorder precipitate transformations are currently accepted to proceed by long-range chemical ordering on a substructure extending through the particle, with the Al-Mg-Si alloy Guinier-Preston (GP) zone $\rightarrow \beta''$ transformation representing the most well-documented example. It is shown here that the structurally distinct β'' -phase arises directly from solute diffusion-controlled precipitation within a precipitate, providing an alternative pathway for the transformation of one precipitate to a more thermodynamically stable precipitate. The emergence of dispersed β'' nuclei in the otherwise fcc-based particle is revealed by structural and chemical signs of a significant spatial solute variation. Furthermore, upon reduced aging temperature, heavily structurally flawed final particles result from increasingly challenging nucleus coalescence. The highly localized origin of this process suggests that early-stage precipitate transformation mechanisms be revisited for other age hardenable alloys.

Keywords : Aluminum, Precipitation, Phase transformation, Scanning transmission electron microscopy

161. Modeling precipitation evolution and intermetallics fragmentation in 6xxx Series Aluminum Alloys during industrial hot rolling

Moosavi Seyyed Ezzatollah¹, Cayron Cyril¹, Friedli Jonathan², Aron Loic², Liang Zeqin², Cantergiani Elisa^{2 3}, Loge Roland¹

1 - Laboratory of Thermomechanical Metallurgy - PX Group Chair, Ecole Polytechnique Federale de Lausanne (EPFL) (Switzerland), 2 - Novelis Switzerland (Switzerland), 3 - Monash university (Australia)

The automotive industry relies on 6xxx series aluminum alloys for car body components due to their lightweight, corrosion resistance, and formability. A critical stage in automotive sheet production is hot rolling, a complex thermomechanical process where phenomena such as precipitation, recrystallization, and texture change occur simultaneously, shaping final material properties like formability and surface quality. Improving these properties thus requires a robust precipitation model. In this study, a precipitation model was developed for prime-based and recycled AA6014 using classical nucleation and growth theories with thermodynamic and kinetic computations. The model simulates the nucleation, growth, and coarsening of β -Mg₂Si precipitates at different sites, such as grain boundaries, sub-grain boundaries, dislocations, intermetallics, and dispersoids, each with distinct kinetics. Simulation outputs include the number density, volume fraction, and size distribution of the precipitates. In addition to the precipitation model, a statistical approach was used to estimate the fragmentation of the intermetallics during hot rolling. Laboratory experiments were conducted to progressively calibrate the precipitation and fragmentation models, while industrial samples were used to validate them. Calibration samples were prepared either by exposing them to various thermal profiles or performing Gleeble tests mimicking the intermediate stages of industrial hot rolling. Meanwhile, an advanced image analysis method combining Backscatter Electron (BSE) imaging and Electron Backscatter Diffraction (EBSD) was developed to statistically differentiate the β -Mg₂Si precipitates, the Si precipitates and the (Fe,Mn) rich intermetallics at different nucleation sites. This method, applied to the experimental samples, enabled us to adjust the model parameters and assess its predicting capabilities.

Keywords : 6xxx Aluminum Alloys, Hot Rolling, Precipitation Model, β , Mg₂Si Precipitates, Image Analysis

162. Five-fold symmetry structure inhibiting the growth of an otherwise perfect η_2 phase in Al-Zn-Mg-Cu alloys

Ehlers Flemming¹, Xiang Kaiyun¹, Ding Lipeng¹, Jia Zhihong¹

¹ - Key laboratory for Light-weight Materials, Nanjing Tech University, Nanjing, 211816 (China)

In order to circumvent stress-corrosion cracking issues, the age-hardenable 7xxx Al alloys typically employ a precipitate microstructure dominated by the equilibrium phase η , with these precipitates however displaying faster growth than their precursors in the precipitation sequence as a result of reduced coherency with the Al matrix. Given this necessary compromise, there is an interest in finding ways to limit η growth, via modification of the main alloying element concentrations and/or micro-alloying. The present combined experimental and theoretical study discusses the formation of a five-fold symmetry structure, referred to in the present work as the “Pentagon Structure”, at the semi-coherent (1100)//(110) η /Al interface of otherwise defect-free η_2 precipitates in the Al-Zn-Mg-Cu alloy system. High-angle annular dark-field scanning transmission electron microscopy imaging supports a growth-limiting influence of this quasi-crystalline entity, while density functional theory calculations link its formation to Zn-rich conditions at the interface. This theoretical conclusion finds direct support by experimental investigations of the influence of alloy Zn/Mg ratio on Pentagon Structure occurrence. The implications of these findings are discussed.

Keywords : Al Zn Mg Cu alloy, Precipitates, Interfaces, High angle annular dark field transmission electron microscopy, Density functional theory

163. Effect of microalloying on precipitation strengthening and mechanical properties of Al-Mg-Si alloys

Weng Yaoyao¹, Ding Lipeng², Jia Zhihong²

1 - Nanjing Institute of Technology (China), 2 - Nanjing Tech University (China)

Microalloying is an effective method to regulate the precipitation strengthening and mechanical properties of Al-Mg-Si alloys. There are two main influencing mechanisms of microalloying elements, the first mechanism: microalloying elements change the atomic structure of the precipitate, such as Ag and Cu. Cu element can promote the formation of Cu-containing precipitates. Compared with Cu, Ag element is better in enhancing the precipitation strengthening of Al-Mg-Si alloy. While Ag is not ideal in inhibiting the harmful effect of natural aging. The second mechanism: microalloying elements regulate the diffusion of vacancy during aging, such as Sn, Cd, In elements. These elements have strong binding energy with vacancy, which can trap free vacancy in natural aging and inhibit the formation of clusters, while release vacancy and promote the precipitation strengthening under artificial aging at high temperature.

Keywords : Aluminium alloy, microalloying, microstructure, mechanical property

164. Evaluation of slip behavior of mobile dislocations during in-situ tensile-testing TEM observation of Al-Mg-Si alloys

Hirosawa Shoichi¹, Inoue Daiki²

1 - Yokohama National University (Yokohama 240-8501 Japan), 2 - Graduate student, Yokohama National University (Japan)

In general, slip, multi-slip and accumulation behaviors of dislocations occur on the micrometer scale, whereas cutting and Orowan mechanisms involving interactions between dislocations and precipitates are formulated on the nanometer scale. In this study, mobile dislocations within commercial-purity aluminum and an Al-Mg-Si alloy with fine beta precipitates were dynamically observed by in-situ tensile-testing transmission electron microscopy (TEM), and correlated with their deformation and strengthening mechanisms. Homogeneous dislocation movement along the primary slip systems was observed in commercial-purity aluminum, whereas a localized slip of mobile dislocations due to the dispersed beta precipitates was

followed by the expansion of deformation region with many slip traces as a result of rotation of segmented beta precipitates.

Keywords : Dislocation, Slip behaviour, Aluminum alloy, Deformation, Precipitates, Strengthening mechanism

165. Ultrasonic Bonding Process of Al

Iwamoto Chihiro¹

1 - Graduate School of Science and Engineering, Ibaraki University (Japan)

Ultrasonic bonding is one of the methods of joining two metal plates by applying ultrasonic vibration and pressure. During ultrasonic bonding, the friction by ultrasonic vibration breaks an oxide film existing on the metal surface, allowing bonding at contact between clean surfaces. However, due to experimental difficulties, microstructural variation in the metals during the bonding is not clear enough. Our recent development of a new TEM sample holder has allowed us to observe the ultrasonic bonding process at the nanoscale. This study will show the ultrasonic bonding process of Al foils and an Al and a Cu foil at the nanoscale. When an Al foil with ultrasonic vibration was brought into contact with a fixed Al foil, the fixed Al was cut into the uneven shape of the Al foil with ultrasonic vibration. Many nanoparticles were generated at the contact region and grew around the interface. Depending on the vibration and contact conditions, dislocations were observed to be generated at the contact point and propagated through the Al. Near the contact point, a decrease in the number of lattice defects was also observed. In contrast, when an Al foil with ultrasonic vibration was brought into contact with a Cu foil, the generated nanoparticles merged, and the Cu foil deformed smoothly. We will compare these joining processes and discuss the differences.

Keywords : Ultrasonic bonding, In situ TEM, Al, Cu, nanoparticle, interface

166. Mechanical properties of aluminum clad sheets fabricated by roll bonding process for automotive application

Kim Hyoungwook¹, Jeong Dea-Han¹, Euh Kwangjun¹, Kim Won-Kyeong¹

¹ - Korea Institute of Materials Science (South Korea)

Aluminum alloys have high specific strength, excellent corrosion resistance, and thermal conductivity, making them suitable not only as structural materials but also for electrical and electronic applications. However, the use of a large quantity of alloying elements to enhance specific strength makes it challenging to meet various required chemical and physical properties. To achieve additional characteristics in high-strength aluminum alloys, techniques have been developed that involve cladding aluminum alloys with different alloy compositions. Recently, roll bonding technology has been utilized to produce aluminum clad sheets by joining thin aluminum sheets during the rolling process. This method is employed for manufacturing brazing aluminum clad materials as well as multilayer sheets with superior corrosion resistance and surface treatment properties. This paper aims to introduce the technology for producing aluminum clad sheets using roll bonding techniques, along with the properties of aluminum multilayer clad materials manufactured by this method, and to discuss on their application. In particular, the results of roll bonding for 4343/3003/4343 clad sheets used in automotive heat exchanger and the strategies for controlling microstructure to enhance the performance of heat exchangers after brazing will be presented.

Keywords : Aluminum alloy sheet, Clad, Roll bonding, Brazing, Microstructure

167. Impact of Microstructure of Aluminum Electrodes on the Performance of Aluminum-Based Batteries

Weissensteiner Irmgard ¹, Razaz Ghadir

¹ - Montanuniversitat Leoben (Austria)

Aluminum-based batteries are emerging as promising candidates for sustainable energy storage. To date, the use of high-purity aluminum as an anode material has been common and costly. Studies have shown that there is some potential to use alloys as anode materials. Therefore, this study investigates the effects and interactions of solute element content, intermetallic particles, chemical inhomogeneity, and annealing conditions in binary Al alloys on the resulting microstructure, crystallographic texture, and grain boundary structures using advanced electron microscopy. Correlative electrochemical tests were used to analyze electrochemical performance and correlate effects on the plating-stripping behavior of an alloy. The presence of solutes and intermetallic particles, along with changes in microstructure and defects, could significantly affect plating and stripping operations. This highlights the importance of considering multiple microstructural and compositional factors when optimizing materials for plating and stripping processes. However, the interactions between these factors are complex and further analysis is required to fully understand their contributions to overall electrochemical performance. The results demonstrate the potential for using lower purity aluminum alloys in battery applications, providing a more sustainable alternative to high purity metals without compromising electrochemical efficiency.

Keywords : Al, batteries, alloyed anodes, microstructure, plating, stripping behavior

168. In-situ nanometallurgy in transmission electron microscopy

Pogatscher Stefan¹, Kremmer Thomas¹, Tunes Matheus A.¹,
Dumitraschkewitz Phillip¹

¹ - Montanuniversitat Leoben (Austria)

Transmission electron microscopes are becoming increasingly versatile instruments with enhanced capabilities for in situ experimentation. The technique can be used as a chemical reactor to study classical metallurgical processes and reactions at the nanoscale. The presentation will show a link to processes such as heat treatments, sublimation, alloying, irradiation and solidification. While Cu and Au nanoparticles and nanowires are used for sublimation and in-situ alloying experiments, Al and Al alloys in the form of lamellae/thin foils have been used to study phase precipitation and dissolution or recrystallisation and irradiation phenomena. Even irradiation effects that can occur in alloys in deep space can be mimicked and studied. In addition to these solid-state reactions, we show that melting and solidification can be studied in detail directly in a transmission electron microscope. This is based on a sample preparation method that avoids focused ion beam preparation but still uses a low-drift micro-electro-mechanical system. We show that intermetallic phases can be studied as they form from the melt at rates ranging from rapid solidification to large-scale industrial casting processes. As iron-containing intermetallic phases are gaining attention due to their importance in the recycling of aluminium alloys, we take them as an example here. Their morphology can have a strong influence on mechanical properties, and we show that direct observation of their formation by transmission electron microscopy can provide a better understanding of their evolution.

Keywords : Metallurgy, Alloys, Transmission electron microscopy, In, Situ

169. Interfacial Structure of Mg₂Si in Al-Mg-Si Alloy

Matsuda Kenji¹, Ahmed Abrar², Taiki Tsuchiya², Lee Seungwon²,
Ikeno Susumu²

1 - Faculty of Sustainable Design, University of Toyama (Japan), 2 - University of Toyama (Japan)

The typical precipitation sequence in Al-Mg-Si alloys is shown below. Supersaturated solid solution → G.P. zones → metastable β'' phase → metastable β' phase → equilibrium β(Mg₂Si)-phase + Si. The equilibrium phase in over-aged Al-Mg-Si alloys is the β-phase(Mg₂Si), which forms as a truncated octagonal plate with a cubic anti-CaF₂ structure and a lattice parameter of $a = 6.35 \text{ \AA}$ In our previous study, the β-phase in a homogenized ingot (heated at 723 K for four days without solution heat treatment, cold-rolling, or aging) shows a hexagonal tabular morphology in Al-Mg-Si alloys containing Cu. This hexagonal tabular β-phase (hex. β) has the same crystal structure and chemical composition as the conventional truncated octagonal β-phase (con. β), but its shape and orientation relationship differ. The orientation relationships of both con. β and hex. β are as follows: {001}Al // {001}con. β, Al // con. β {111}Al // {111}hex. β, Al // hex. β. In this study, we would like to introduce our recent studies about the different shapes of 2 types of β-phase in the Al-Mg-Si alloy and their orientation relationship with Al-matrix, misfit, interfacial condition, and the segregation of additional elements, such as Ag.

Keywords : Al, Mg, Si Alloy, β(Mg₂Si), High Resolution Transmission Electron Microscopy, Interface, Orientation Relationship

170. The influence of continuous retrogression and re-ageing treatment on the mechanical properties, corrosion behaviour and microstructure of an Al-Zn-Mg-Cu alloy

Wu Xiaodong¹, Lingfei Cao^{2 3}, Guangjie Huang⁴

1 - International Joint Laboratory for Light Alloys (Ministry of Education), College of Materials Science and Engineering, Chongqing University, Chongqing (China), 2 - International Joint Laboratory for Light Alloys (Ministry of Education), College of Materials Science and Engineering, Chongqing University (China), 3 - Electron Microscopy Center of Chongqing University, Chongqing University (China), 4 - School of Materials Science and Engineering, Chongqing University, Chongqing 400044, China (China)

7xxx series Al - Zn - Mg - Cu aluminum alloys are widely used in the aerospace and automotive industries due to their high specific strength and processability. RRA treatment (retrogression and re-aging treatment) can achieve an optimal strength - corrosion resistance balance in 7xxx series alloys. RRA treatment, consisting of three aging treatments, is generally carried out in a DRRA (discontinuous RRA) manner, i.e., the sample is cooled down to room temperature after each aging treatment. The CRRA (continuous RRA) treatment, wherein the three aging treatments are linked by either slow heating or cooling, can be accomplished in a single step. The DRRA treatment has been well studied, while the CRRA treatment hasn't been studied much. This paper aims to systematically study the properties, microstructure, and corrosion resistance of Al - Zn - Mg - Cu alloy during CRRA treatment. The results reveal that the partial dissolution of pre-existing precipitates (GP I zone and η' phase), the growth of remaining precipitates, as well as the formation of new η' phase occur in the retrogression heating process, which are similar to the phase transformation in the retrogression stage of the DRRA treatment. The higher the retrogression treatment temperature, the better the comprehensive performance of the alloy. The microstructure observation suggests that intergranular corrosion predominantly affects the T6 sample, with extensive propagation into the bulk resulting in delamination and intergranular cracking. In contrast, crystallographic pitting dominates in the CRRA-treated sample, which effectively mitigates exfoliation corrosion and suppresses intergranular cracking. The different corrosion resistance between the T6 sample and the CRRA-treated sample is attributed to the disparate distribution of Cu in the alloy, which influences the corrosion rate, the types of corrosion and the corrosion propagation path.

Aluminium alloy, Continuous retrogression and reaging treatment, Corrosion properties, mechanical property

171. Linking 3D grain and elastic strain mapping with the development of damage in 2050 Al alloys during high-temperature loading by synchrotron diffraction and tomography

Fernandes Chaves Macieira Gisele^{1 2}, Lhuissier Pierre², Wright Jonathan¹, Fang Haixing¹, Villanova Julie¹, Salvo Luc²

1 - European Synchrotron Radiation Facility [Grenoble] (France), 2 - Science et Ingenierie des Materiaux et Procedes (France)

The formability of Al2050 alloy is critical for manufacturing large and thick components while maintaining its outstanding performance. Previous studies showed that pores and cracks occur during the hot deformation of this alloy and the pore growth follows three different paths (exponential, decelerated, mixed). To link the damage development during high-temperature loading with the alloy microstructure evolution, an in-situ tensile loading at 480 °C was performed on this alloy using synchrotron diffraction and tomography, i.e. diffraction contrast tomography (DCT) to provide 3D grain maps at ~1.1 µm resolution, phase contrast tomography (PCT) and holo-tomography to characterize pores and intermetallic phases down to 35 nm per voxel and scanning 3DXRD (s3DXRD) to obtain 2D/3D grain and elastic strain maps at 0.5 µm resolution. The pore density and volume fraction were quantified as a function of macroscopic strain up to 12% and three pore formation mechanisms were identified: growth from pre-existing pores, fracture of the intermetallic particles, and nucleation of new pores. The characteristics of the pore evolution are then linked with the grain structure (grain boundaries, orientations and strains) characterized by DCT and s3DXRD. Additionally, the grain maps show newly recrystallized grains, suggesting the presence of dynamic recrystallization. To exclude the possible explanation by annealing recrystallization, an in-situ annealing experiment at 480 °C without external loading was performed and the results confirmed no recrystallized grains. This study demonstrates that correlating synchrotron grain mapping techniques with tomography offers comprehensive insight in linking the damage development with the microstructure evolution under high-temperature deformation.

Keywords : Damage formation, Diffraction contrast tomography, Scanning 3DXRD, Holo tomography, Grain and Strain mapping

172. The effect of intensification pressure on the microstructure of non-heat treated HPDC AlSi9MnVZr alloy

Akhtar Saria¹, Xiong Shou-Mei^{1 2}

1 - School of Materials Science and Engineering, Tsinghua University, Beijing 100084, China (China), 2 - Key Laboratory for Advanced Materials Processing Technology, Ministry of Education, Beijing 100084, China (China)

The microstructural characteristics of externally solidified crystals (ESCs) and porosities in a non-heat-treated high-pressure die-cast AlSi9MnVZr alloy are investigated under two distinct process conditions: one with the application of intensification pressure and the other without it. Optical microscopy (OM), scanning electron microscopy (SEM), and computed tomography (CT) are employed to analyze the ESCs and porosity distribution. The alloy's microstructure primarily consists of primary α -Al, ESCs, Al-Si eutectic, and iron-rich phases. ESCs nucleate in the shot sleeve, while α -Al forms within the die cavity. In the absence of intensification pressure, larger dendritic ESCs are observed, along with significant gas porosity, shrinkage pores, and numerous smaller dispersed pores, resulting in a high porosity fraction. Conversely, the application of intensification pressure results in a notable refinement in ESCs morphology, with a significant reduction in their diameter and area fraction. Additionally, the size and fraction of porosity decrease substantially, indicating a marked improvement in casting quality

Keywords : High pressure die cast, Al Si alloy, ESCs, Porosity

173. Investigation on friction surfacing layers of AA2024 studs produced via friction extrusion

Aspes Pietro¹, Kallien Zina^{1 2}, Rath Lars¹, Suhuddin Uceu¹, Klusemann Benjamin^{1 2}

1 - Helmholtz- Zentrum Hereon (Germany), 2 - Leuphana Universitat Luneburg (Germany)

Friction surfacing (FS) is a solid-state layer deposition process able to act as a coating or additive manufacturing technique. Operating at low temperatures with respect to other fusion-based techniques, FS exploits high friction and severe plastic deformations to obtain a microstructure characterized by micron-sized equiaxed grains and to avoid common additive manufacturing defects affecting aluminum alloys such as hot cracks and volatilization of alloying elements. Most of the research is focused on the processing of common hot-extruded studs characterized by elongated grains; however, few attempts have been made to deposit materials with different microstructures. Friction extrusion is a solid-state process, based on similar principles to FS, able to produce fine-grained wires, starting from bulk, recycled, or powder material. These wires can be of importance as they can come from recycled material or feature new alloy compositions via mechanical alloying. In this investigation, FS was used to maintain the microstructure characteristics of friction-extruded AA2024 wires. These have been compared with the commercially available hot-extruded AA2024-T3 material. The comparison was based on the FS process behavior, the geometric characteristics, and the microstructure of the deposits and showed significant differences and similarities. These analyses proved the necessity of process parameter adaptations.

Keywords : Solid state layer deposition, Friction surfacing, Microstructure

174. Design of easier separable Fe-containing intermetallics in Al-Si alloy by thermodynamic properties prediction and three dimensional morphology regulation

Zhang Xiaozu¹, Wang Dongtao¹, Nagaumi Hiromi¹

¹ - Soochow University (China)

As a common detrimental element in Al-Si cast alloy, Fe can be effectively removed by Fe-containing intermetallics separation in the alloy melt. However, the formation temperature and three dimensional morphology of Fe-containing intermetallics can be further improved for higher removal efficiency of Fe element. In this paper, the crystal characteristics, thermal stability, thermophysical properties and mechanical behavior of multicomponent α -Al(FeMn)Si and α -Al(FeMnCr)Si phases are investigated by first-principles calculations and experimental verification. The results showed that α -Al(FeMnCr)Si phase shows the higher thermal stability, modulus, intrinsic hardness and the lower volumetric thermal expansion coefficient at different temperatures due to strong chemical bonding of Si-Fe and Si-Cr. The enhanced thermodynamic stability, theoretical melting point and mechanical modulus of α -Al(FeMnCr)Si phase were validated by the experimental results. Moreover, the addition of Mn and Cr significantly changes the morphology of Fe-containing intermetallics from plate-like to cubic shapes. First principles calculation results showed that the final 3D morphology of α -Al(FeMn)Si and α -Al(FeMnCr)Si phase are determined by the surface stability and growth competition of (100), (110) and (111) surfaces. These results provide a new strategy for designing the easy separable Fe-containing intermetallics, which contributes to guiding the development of high performance recycled Al-Si alloys.

Keywords : Fe containing intermetallics, thermodynamic stability, three dimensional morphology, electronic structure, surface stability.

175. Study on grain refinement of high-purity aluminium by intermittent permanent magnet stirring technique

Zou Jing ¹, Haitao Zhang ², Nagaumi Hiromi ¹

1 - High-Performance Metal Structural Materials Research Institute, Soochow University, Suzhou, Jiangsu, 215021, China (China), 2 - Key Laboratory of Electromagnetic Processing of Materials, Ministry of Education, Northeastern University, Shenyang, 110819, China (China)

High-purity aluminum plays an irreplaceable role in many high-end industrial fields, and the improvement of its mechanical and functional properties is crucial for expanding its application scope. Grain refinement holds the key to achieving the goal of high-purity aluminum. However, traditional approaches encounter numerous hurdles in grain refinement of high-purity aluminum owing to the limited heterogeneous nucleation sites. This study focuses on the grain structure evolution of high-purity aluminum through the application of novel intermittent permanent magnet stirring technique, and deeply deliberates its grain refinement mechanism and practical consequences. The outcomes demonstrated that compared with the untreated samples, the high-purity aluminum grains subjected to intermittent permanent magnet stirring were significantly refined, with the average size being significantly reduced, and the shape being more rounded and uniform. This is because the repeated scouring effect of forced convection can promote dendrite fragmentation or remelting, achieve the multiplication of crystal nuclei during the stirring process. In addition, forced convection intensifies the temperature fluctuations in the melt, increases local undercooling, and thus improves the nucleation rate of crystal nuclei. Simultaneously, the swirling flow also disrupts the growth of new grains, impeding their unrestrained expansion. This work imparts valuable understandings into the grain refinement mechanism of high-purity aluminum, and furnishes a theoretical basis for the development of high-performance aluminum materials, which possess prospective applications in the aerospace, electronics, and automotive industries.

Keywords : High, purity aluminum, Grain refinement, permanent magnet stirring, refinement mechanism

176. Synthesis and characterization of an (Al-10Si-3Zn-2Cu)/Ti-6Al-4V interpenetrating phase composite with enhanced mechanical properties

Mohanta Debashish¹, Suman Ravisankar¹, Punera Devesh²,
Gollapudi Srikant³

IIT Bhubaneswar, India

Metal-metal interpenetrating phase composites (MMIPCs) are a new type of composite material where one phase forms a continuous network, while the other has a lattice structure. The lattice structure ensures structural integrity and carries the load effectively. In this work, an interpenetrating phase composite is successfully fabricated by infiltrating Al-10Si-3Zn-2Cu aluminum alloy (A383) into an additively manufactured Ti-6Al-4V lattice. XRD and SEM-EDS characterizations were performed on the A383/Ti-6Al-4V composite. The hardness values of the A383 and Ti-6Al-4V phases were found to be approximately 90 VHN and 390 VHN, respectively. The composite demonstrates excellent load-bearing capabilities under compression, with a yield strength of around 300 MPa which is 200% higher than pure A383 (100 MPa). Additionally, the observation of a plateau in the compressive stress-strain curve highlights its enhanced energy absorption capability. The corrosion behavior of the Ti-6Al-4V/A383 composite in a 3.5 wt.% NaCl aqueous solution is evaluated using open circuit potential (OCP), potentiodynamic polarization curves and electrochemical impedance spectroscopy (EIS). The composite exhibited a corrosion potential (E_{corr}) of -0.66 volts and a current (i_{corr}) of 26.16 micro-A/cm², compared to -0.76 volts and 2.56 micro-A/cm² for A383. Additionally, the compressive and corrosion behavior of the composite was analyzed using finite element modeling to develop insights into the material behavior.

Keywords : Interpenetrating phase composites (IPC), Mechanical properties, Additive manufacturing, Corrosion, Simulation, Finite element analysis.

177. The combined effects of trace element Sn/Cu and double-step pre-aging on the precipitation kinetics of Al-Mg-Si alloys

Jingwei Zhao¹, Pizhi Zhao¹

1 - Chinalco Materials Application Research Institute Co., Ltd. (China)

The effect of trace element Sn, Cu composite double-stage pre-aging process on the microstructure and mechanical property of Al-Mg-Si alloy automotive sheet was systematically investigated. The paint baking strength can be increased by up to approximately 70% without compromising other properties. To interpret this phenomenon, Positron Annihilation Lifetime Spectroscopy, Differential Scanning Calorimetry, Transmission Electron Microscopy, and MatCalc calculations were applied to identify the microstructural changes in different aging stages. Compared with conventional single-step pre-aging process, double-step pre-aging process can promote the formation of more beneficial clusters which can be transformed easily to β'' precipitates during paint baking owing to their similar chemistry. The Sn/Cu elements help capture supersaturated vacancies during quenching and pre-aging stage. During the paint baking process, a large number of vacancies are released, effectively accelerating the transformation of pre-aging clusters into β'' precipitates, thereby significantly increasing the paint baking strength increment.

Keywords : AlMgSi alloy, trace element, double steps preaging, vacancy, paint baking strength

178. Insights for the design of high-performance secondary cast aluminium alloys.

Poletti Maria Cecilia^{1 2}, FortmuLler Stefan^{2 1}, Stauder Bernhard³,
Letofsky-Papst Ilse⁴, Arrabal Raul⁵, Povoden-Karadeniz Erwin⁶

1 - Institute of Materials Science, Joining and Forming (Austria), 2 - CD Laboratory for Design of high-performance alloys by thermomechanical processing (Austria), 3 - Nematik Linz GmbH, ZeppelinstraÅŸe 24, A-4030 Linz (Austria), 4 - FELMI-ZFE. Steyrergasse 17 | A-8010 Graz, Austria (Austria), 5 - Universidad Complutense de Madrid = Complutense University of Madrid [Madrid] (Spain), 6 - Institute of Materials Science and Technology (TU Wien, A-1060 Vienna Austria)

Recycling aluminium alloys increases the percentage of some alloying elements, which may form phases detrimental to mechanical properties and corrosion resistance. Although secondary wrought aluminium alloys are state-of-the-art, this cannot be said for cast aluminium alloys for two reasons. Firstly, there is a high percentage of alloying elements in cast alloys. Secondly, there is the ability to change and reshape unfavourable intermetallic phases during thermomechanical treatments in wrought alloys. In this study, we examined a variety of primary and secondary AlSi7/10Mg0.3Cu0.1-2.0 alloys to determine how chemical composition and heat treatments affect mechanical properties and corrosion resistance. We specifically investigated the effects of Fe, Cu, and Ti on forming primary phases after casting and precipitating following T5 and T6 heat treatments. We produced alloys with controlled chemical composition and grain size in laboratory conditions and characterised the microstructure with microscopy, differential scanning calorimetry, and dilatometry. CalPhad-based models supported by experimental data connected the phase occurrence with thermal history. The presence of Cu-rich (θ , -Al₂Cu) and Cu-enriched phases reduced corrosion resistance. Copper segregated in the solid state at iron-intermetallic phases and the primary Si. Finally, we determined that adding titanium-based grain refiners reduces the ageing potential if the heating rate is not high enough.

Keywords : secondary aluminium alloys, corrosion, precipitates, heat treatments

179. Competitive Nucleation of α -Al(MnFeCr)Si Dispersoids in Al-Mg-Si 6xxx Alloys By Adding Indium

Li Zhen, Gao Kang , Qin Jian , Nagaumi Hiromi

Weiqiao Lightweight Research Center at Soochow (China)

Improving precipitation of α -Al(MnFeCr)Si dispersoids has been proved to be an effective approach to control recovery and recrystallization behaviors during hot deformation. In the present investigation, influences of Indium addition to Al-Mg-Si 6xxx alloys on nucleation and coarsening behaviors of dispersoids were studied using state-of-the-art Transmission Electron Microscope (TEM). In the alloy with Indium addition, both β' precipitates and In-rich phases were observed to be the heterogeneous nucleation sites for dispersoids. These two nucleation mechanisms coexisted and competed with each other in the same temperature range during the heating process of homogenization heat-treatment. At the beginning stage of dispersoid precipitation, equivalent diameter of dispersoids in In-modified alloy is smaller than base alloy but exhibited two different morphologies in size. This is due to that In-rich phases provide more heterogeneous nucleation sites, however, the initial larger size of In-rich particles leads to rapid coarsening of the dispersoids nucleated on In-rich phase because of Ostwald ripening. Indium addition promotes the nucleation of dispersoids by providing more heterogeneous nucleation sites but has a limited effect on the final size of dispersoids.

Keywords : Dispersoid, Indium addition, Nucleation, 6xxx alloy, Transmission Electron Microscope

180. An assessment of the brazing performance of cast Al-Mn-Ni aluminum alloy

Jin Xiaojie¹, Zhu Huiying¹, Chen Lai¹, Zhu Guanglei¹, Wang Xueyang¹, Nagaumi Hiromi^{1 2}

1 - Weiqiao Lightweight Research Center at Soochow (China), 2 - Soochow University (China)

As a cost effective, safe and clean technology, aluminum brazing has been widely used in automotive industry, electronic products and other fields. The aluminum brazing cycle is usually operated at elevated temperature (~600°C), and a Si-rich AA4XXX alloy would be completely molten and act as a brazing material to achieve a metallic bond between the components. Due to the limitation of brazing temperature, the commonly used cast aluminum alloys like Al-Si, Al-Cu and Al-Zn series, cannot be used as the components for aluminum brazing. In recent years, the alloy systems with high melting point, such as Al-Mn and Al-Mn-Ni, are chose to develop braze-able cast aluminum alloy. In this work, a squeeze cast Al-Mn-Ni aluminum alloy is vacuum brazed with the aluminum brazing sheet, and the brazing performance is assessed by comparing with wrought AA6061. It shows that, a metallurgical bonding is achieved between Al-Mn-Ni aluminum alloy and aluminum brazing sheet. Meanwhile, an obvious penetration behavior of the molten clad alloy in the matrix can be observed in Al-Mn-Ni aluminum alloy, which may be due to the smaller grain size. The micro-hardness test shows that, both the Vickers microhardnesses of Al-Mn-Ni aluminum alloy and AA6061 after brazing fall in the range of 46~50 HV. Hence, it is suggested that cast Al-Mn-Ni aluminum alloy is a promising candidate for aluminum brazing.

Keywords : aluminum brazing, cast aluminum alloy, Al, Mn, Ni, brazing performance

181. A Novel Modelling Framework for the Portevin-Le Chatelier Effect in AA5182 Alloy

Xu Jianbin¹, Holmedal Bjorn¹, Hopperstad Odd Sture², Manik Tomas¹, Marthinsen Knut¹

1 - Department of Materials Science and Engineering, NTNU Norwegian University of Science and Technology (Norway), 2 - Structural Impact Laboratory (SIMLab), Department of Structural Engineering, NTNU-Norwegian University of Science and Technology (Norway)

Commercial Al-Mg alloys possess an exceptional balance of strength and ductility, rendering them highly suitable for automotive applications. However, these alloys are prone to inhomogeneous deformation, a phenomenon referred to as the Portevin-Le Chatelier (PLC) effect. This poses challenges to the reliability and performance of these materials in engineering applications, necessitating a deeper understanding and more accurate modeling of the underlying mechanisms. Various factors, including strain accumulation, temperature, strain rate, and intrinsic material properties, strongly influence this localization behaviour. It is now widely accepted that these instabilities and strain localizations arise from negative strain rate sensitivity (nSRS). Traditionally, nSRS is believed to become more pronounced as strain accumulates. However, experimental evidence has shown that, in some cases, instability may diminish with continued deformation. To address these complexities, a new phenomenological framework for constitutive modelling of the PLC effect is proposed. This model provides a more realistic description of strain localization and instability induced by dynamic strain aging.

182. CALPHAD-based modelling of microstructural evolution during D.C. casting and homogenization of AA3003 aluminium alloy

Tsiolis Fotios^{1 2}, Papaefthymiou Spyros¹

1 - National Technical University of Athens, School of Mining and Metallurgical Engineering, Heroon Polytechniou 9, 15780 Zografou, Athens (Greece), 2 - ²ELKEME, 61st km of Athens-Lamia National Road, 32011 Oinofyta, Viotia (Greece)

Microstructural evolution during D.C. casting and subsequent homogenization of non-heat-treatable aluminium alloys involves complex phenomena, including micro-segregation of alloying elements and intermetallic phase selection during solidification as well as phase transformations of both primary (constituents - intergranular) and secondary (dispersoids - intragranular) intermetallic phases. In this study, we simulated the microstructural evolution of AA3003 using a CALPHAD-based modelling framework implemented in ThermoCalc®. The framework integrates a Scheil-Gulliver solidification model with a 1-D micro-segregation alleviation and diffusional phase transformation model (DICTRA®) and a Kampmann-Wagner Numerical (KWN) model for dispersoid precipitation (TC-PRISMA®). According to this approach the development of a robust computational methodology is aimed to accurately predict the influence of homogenization cycles on dispersoid precipitation, which in turn affects recrystallization behaviour via the well-known Zener drag phenomenon. Additionally, these CALPHAD-based simulations facilitate the assessment of impurity content effects on dispersoid precipitation, considering the increasing use of scrap in the fabrication of non-heat-treatable aluminium alloys. Furthermore, they provide precise estimates of Zener pinning forces as inputs for downstream mesoscale process models, contributing to a holistic through-process modelling approach.

Keywords : Aluminium alloys, AA3003, CALPHAD, based modelling, D.C. Casting, Homogenization, Micro, segregation, Constituent Phases, Dispersoids, Zener Drag, Recrystallization.

183. Formation mechanism of dense and uniform structure during tailor welding of Aluminum Foam Structure preform

Tan Ming-Jen ¹

1 - Nanyang Technological University [Singapour] (Singapore)

Due to the long process cycle, high cost, and low efficiency of the traditional preparation of Aluminum foam sandwich (AFS) preform, in this work AFS preform with high, density and uniform powder mixing was prepared by FSW. The three-dimensional temperature field and flow field model of AFS preform plate powder composite structure FSW are established by using SolidWorks and Fluent software to analyze temperature field and flow field in the process of AFS preform welding and reveal the formation mechanism of dense structure and uniform structure in the process of AFS preform welding, and establish the regulation method of high density and uniform structure of AFS preform. The microstructure of AFS preforms and the distribution of TiH₂ and Al₂O₃ powder in the matrix and tensile fracture were analyzed by optical metallographic microscope (OM) and scanning electron microscope (SEM) respectively. The results revealed that the quality of three-pass welded joint with the rotation speed of 2000r/min, welding speed of 50mm/min, weld spacing of 3mm, and reduction of 0.1mm is the best.

Keywords : Aluminum Foam Structure, Formation mechanism, Friction Stir Welding

184. Simulation of self-healing in Al-Cu alloys

Doesinger Christoph¹, Wiebogen Anika², Eichlseder Marlene²,
Poletti Cecilia², Romaner Lorenz¹

1 - Montanuniversitat Leoben (Austria), 2 - Technische Universitat Graz (Austria)

The investigation of self-healing mechanisms in metals has attracted considerable attention in recent years to extend the durability of components and reduce waste. In general, self-healing reduces the size of defects like cracks or voids based on different strategies. One of them relies on the transport of matter by diffusion and the formation of precipitates inside the voids. This requires the presence of a supersaturated solid-solution phase in the material from which the solute-rich precipitates can easily form. In the Al Cu alloying system, self-healing of voids has already been reported. We present atomistic simulations to explore self-healing phenomena in Al-Cu alloys. First we analyse ab-initio predictions of segregation at surfaces and grain boundaries of Cu in Al, which is a necessary prerequisite for the formation of precipitates. Then, to show the filling of the voids directly, we use molecular dynamics (MD) simulations of polycrystalline Al with varying Cu-contents. We show that voids remain stable in pure Al and in the intermetallic phases Al₂Cu and AlCu. In contrast, at low alloying contents of Cu in Al, the voids are filled and the empty space is dissolved in the materials. We show that this behaviour reflects experimental results. Finally, the relevance of our findings for achieving self-healing in Al alloys will be discussed.

Keywords : Self, healing, atomistics, grain, boundary segregation, molecular dynamics

185. Thermomechanical Testing and Precipitation Modelling of Al-Mg-Si Alloys for Hot Forming Applications

Myhr Ole Runar^{1 2}, Tomstad Asle J. , Marioara Calin D.³, Borvik Tore⁴, Hopperstad Odd Sture⁴

1 - Hydro Aluminium, R&D SunndalsØra (Norway), 2 - NTNU-Norwegian University of Science and Technology, Department of Structural Engineering (Norway), 3 - Sintef Industry, Materials and Nanotechnology (Norway), 4 - Structural Impact Laboratory (SIMLab), Department of Structural Engineering, NTNU-Norwegian University of Science and Technology (Norway)

Thermomechanical tension tests were conducted on an AlMgSi alloy at temperatures of 250°C, 350°C, and 450°C, with displacement rates of 2, 20, and 200 mm/s. The tests utilized an axisymmetric specimen with a diameter of 6 mm and a parallel length of 91 mm. Net axial stress versus logarithmic strain curves beyond diffuse necking were generated from the force measurements combined with edge tracing using synchronized images captured by a digital camera. Transmission electron microscopy (TEM) analysis was conducted on selected samples extracted near the fracture surface after testing and cooling to room temperature. After testing at 450°C, overaged needle precipitates were nucleated in bulk and on dispersoids. The dislocation density was low, but subgrains of one to a few micrometres were observed. In contrast, after testing at 250°C, fine needle precipitates were nucleated in the bulk and on dislocations. A high dislocation density was found, with no subgrain formation. A combined precipitation, yield strength, and work hardening model for AlMgSi alloys, known as NaMo, was employed to simulate the evolution of the precipitate structure and the stress-strain behavior in the thermomechanical tension tests. In the model, parameters representing the instantaneous state of the precipitate structure are predicted and used to calculate the corresponding yield strength and work hardening rate incorporating the effects of strain rate and temperature. A comparison between the calculated and measured yield stresses for small plastic strains showed good agreement. Additionally, the model explained the qualitative observations of the TEM investigation regarding the resulting dislocation sub-structure.

Keywords : AlMgSi alloys, precipitation modelling, thermomechanical testing, elevated temperatures, high strain rates

186. A novel model for of cluster nucleation during quenching of 6xxx Al alloys

Kozeschnik Ernst^{1 2}, Li Ya³, Robert Kahlenberg⁴

1 - Institute of Materials Science and -Technology TU-Wien (TU Wien, Vienna, 1060 Austria), 2 - MatCalc Engineering GmbH (Getreidemarkt 9, A-1060 Vienna Austria), 3 - Institute of Materials Science and Technology, TU Wien (Austria), 4 - Materials Center Leoben Forschung GmbH, Leoben (Austria)

During quenching of 6xxx-series aluminium alloys and subsequent holding at room temperature (natural aging), sub-nano meter-sized Mg- and Si-rich clusters form in the Al matrix. The nucleation process can be modelled by consideration of two mechanisms: First, the conventional mechanism of single atom attachment to the nucleus as described by classical nucleation theory, and second, the stabilization of pre-existing clusters by increasing supersaturation and reduction of the critical radius of the nucleus accompanying the decrease of temperature during cooling. The corresponding nucleation model is introduced and discussed. The results are compared to several experimental data reported in literature, where good agreement is achieved both in the prediction of number densities of the clusters as well as the observed wide range of cluster chemical composition.

Keywords : Al, alloys, solid, state nucleation, nucleation theory, atomic clusters

187. Application of Artificial Neural Networks for Microstructure Models ALFLOW and ALSOFT

Marthinsen Knut¹, Preminger Daniel, Manik Tomas

1 - Department of Materials Science and Engineering, Norwegian University of Science and Technology, NO-7491, Trondheim (Norway)

The Al industries are working on green transitions by adopting new technologies and/or recycling based feedstocks, to reduce their carbon footprint and cost. This green shift challenges their existing process and operations and their ability to reach required final part properties and performance, governed by the microstructure features (grain structure, texture, precipitate properties, etc.), which again are determined by both alloy composition and thermo-mechanical processing conditions. To handle the wide compositional range that may be involved with recycling and the complexity of industrial processing conditions, adequate modelling tools to predict the evolution of microstructure and associated mechanical properties, including a full integration between forming simulations (i.e. FE-simulations for forging and extrusion) are needed. This will enable better prediction of their final mechanical properties, leading to improved sustainability and product quality. However, available adequate physics-based microstructure models for Al-alloys to predict the flow stress during the plastic deformation (ALFLOW), and the softening behavior after a thermo-mechanical processing (ALSOFT) are too computationally demanding to be directly embedded in FE simulations. In the present work artificial neural networks (ANN) were therefore designed and trained as surrogate models to replicate the ALFLOW's and ALSOFT's outputs. Accuracy and efficiency were tested for different ANN architectures. It is demonstrated that fully connected feed-forward neural network architectures with ~3 hidden layers are suitable as surrogate models for both ALFLOW and ALSOFT, with a potential speed-up of ~100x for ALFLOW and ~10x for ALSOFT.

Keywords : Aluminium alloys, microstructure modelling, sub, structure evolution, recovery and recrystallization, mechanical properties, machine learning, neural networks

188. Precipitation Kinetics of Aluminum Alloys During SPD Processes Investigated by SAXS/WAXS

Mathew Elizabeth¹, Markmann JuRgen^{1 2}, Chan Chang Yin-Cheng¹, Ovri Henry¹, Suhuddin Uceu Fuad Hasan¹, Ivanisenko Julia³, Staron Peter¹, Klusemann Benjamin^{1 4}

1 - Helmholtz- Zentrum Hereon (Germany), 2 - Hamburg University of Technology (Germany), 3 - Karlsruhe Institute of Technology (Germany), 4 - Leuphana University Luneburg (Germany)

Modifying the microstructure and characteristics of aluminium alloys during severe plastic deformation (SPD) requires an understanding of precipitation kinetics [1]. Using Small-Angle X-ray Scattering (SAXS) and Wide-Angle X-ray Scattering (WAXS), this work examines the precipitation behavior in 7075 and Al-Cu-Li alloys under SPD. A thorough examination of precipitate size, distribution, and phase evolution throughout the deformation process is made possible by the combined SAXS/WAXS technique. The study shows the relevance of deformation-induced changes in precipitation evolution is highlighted by in situ measurements that show the interaction of dislocations with nanoscale precipitates. Initial results show that SPD accelerates the precipitation kinetics. Grain size is seen to rise throughout the procedure. The volume fraction of precipitate, however, decreases as the temperature rises. There is also a rise in the volume of the precipitate after cooling, which significantly affects the mechanical properties and thermal stability of these alloys. The insights gained from this study aim to optimize SPD techniques for high-performance aluminum alloys, advancing their applications in aerospace and other industries requiring superior mechanical and thermal properties. Acknowledgement This project has received funding from the European Research Council (ERC) under the European Union's Horizon 2020 research and innovation programme (grant agreement No 101001567). References 1. Sabirov, I., Murashkin, M. Y. & Valiev, R. Nanostructured aluminium alloys produced by severe plastic deformation: New horizons in development. Materials science and engineering: A 560, 1€“24 (2013).

Keywords : Al alloys, SPD, SAXS, WAXS, precipitation kinetics

189. Structure and dissolution behavior of ZnO-containing phosphate invert glasses prepared by liquid phase method

Lee Sungho¹, Obata Akiko²

1 - National Institute of Advanced Industrial Science and technology (Japan), 2 - Nagoya Institute of Technology (Japan)

Phosphate invert glasses are mainly composed of ortho- and pyro-phosphate groups, and stimulate cellular functions by releasing inorganic ions. Our group has succeeded in the synthesis of titanium-containing phosphate invert glasses with the liquid phase method at room temperature. The glasses were mainly composed of pyrophosphate groups, and titania were crosslinked pyrophosphate groups to form a chain-like structure of $(-O-P-O-P-O-Ti-O-)_n$. The structure may be unique to liquid-phase-derived glasses and was not observed in melt-derived phosphate invert glasses. On the other hand, ZnO is an amphoteric oxide, which can dissolve in acidic and basic conditions, and has been reported to exhibit a wide range of antibacterial ability. In addition, ZnO is classified as an intermediate oxide in the glass network structure and improves the chemical durability of phosphate invert glasses. However, excess amounts of zinc ions can be toxic to cells. Hence, the dissolution behavior of zinc ions must be controlled for biomedical applications. In this work, ZnO-containing phosphate invert glasses (PIG-Zn) were prepared using the liquid phase method, and their structure and ion-releasing behavior were evaluated. PIG-Zn showed a halo peak from XRD patterns, indicating that the glasses containing higher ZnO were partially crystallized with $Zn_2P_2O_7$. The P_2O_5 content in PIG-Zn had no significant difference regardless of the ZnO content. The phosphate groups of PIG-Zn were composed of ortho- and pyro-phosphate groups, and the peaks were blue-shifted with increasing the ZnO content due to the field strength of Zn^{2+} being larger than that of Ca^{2+} . Thus, phosphate groups may be cross-linked by Zn^{2+} to form P-O-Zn bonds. Meanwhile, ion-releasing amounts from PIG-Zn were decreased with increasing ZnO content. This is because the formation of P-O-Zn bonds can increase the chemical durability of PIG-Zn. Therefore, PIG-Zn is expected to exhibit antibacterial ability with controlled Zn^{2+} ion-releasing behavior for biomedical applications.

Keywords : Bioactive glass, phosphate glass, Zinc, antibacterial ability, glass structure

190. Structure of Ta₂O₅ containing phosphate invert glasses prepared by liquid phase method

Asano Hayato^{1 2}, Takahashi Minori³, Obata Akiko³, Sakurai Makoto², Nagata Fukue¹, Lee Sungho¹

1 - National Institute of Advanced Industrial Science and Technology (Japan), 2 - Chubu University (Japan),
3 - Nagoya Institute of Technology (Japan)

Phosphate glasses can contain various metal ions in a wide range of compositions, and their biological properties can be controlled by controlling the glass structure. Our group has been focusing on the liquid-phase method to prepare phosphate glasses, which can operate at room temperature and normal pressure. In our previous work, the ion dissolution behavior (chemical durability) of phosphate glasses prepared by the liquid phase method was controlled by the amount of intermediate oxides incorporated into the glasses. In this work, tantalum (Ta), which is one of intermediate oxides, was used for the glass preparation and the structure of the resulting materials was characterized. XRD patterns of all samples showed halo peaks, indicating amorphous status. The amounts of P₂O₅ in the materials increased with increasing Ta₂O₅ content, while the amount of CaO decreased. The P : Ta molar ratio of the sample prepared with the nominal ratio of 2 : 1 was 1.87 : 1. Thus, almost all the Ta was incorporated into the glass. Raman spectra showed the peaks corresponding to QP0 and QP1. The P-O-P (QP1) peak was blue shifted with increasing Ta₂O₅ content. The shift originated from higher field strength (valence/A²) of Ta compared with Ca. Ta more strongly bonded to the non-bridging oxygen in the phosphate groups than Ca, and the P-O bond length elongated. The oxygen density, which is an indicator of the density of the glass network structure, increased with the addition of Ta. This indicates that Ta forms strong bonds with the phosphate groups.

Keywords : Bioactive glass, Phosphate glass, Tantalum, Liquid method, Glass structure

191. Fabrication of Co-Cr-W-Ni alloys with a unique heterogeneous microstructure utilizing carbide precipitation

Ueki Kosuke¹, Nakajima Tomoki², Ueda Kyosuke², Nakai Masaaki¹, Narushima Takayuki²

1 - Department of Mechanical Engineering, Graduate school of Science and Engineering, Kindai University (Japan), 2 - Department of Materials Processing, Graduate school of Engineering, Tohoku University (Japan)

Two types of Co-Cr-W-Ni alloy powders with different carbon concentrations were mechanically milled and then sintered by spark plasma sintering to fabricate a microstructure with a non-uniform grain size distribution. In addition, by annealing the sintered specimens at 1423 to 1473 K for 0.6 ks, we succeeded in fabricating an unusual microstructure with a grain size distribution ranging from several hundred nanometers to about 30 micrometers. The carbides formed in the high-carbon region suppressed grain size growth during heat treatment, while in the low-carbon region where no carbides were formed, grains grew during heat treatment, resulting in the formation of a microstructure with a very wide grain size distribution. The heat-treated specimens showed superior strength and ductility balance compared to the untreated specimens. Therefore, a microstructure with a broad grain size distribution was considered to exhibit superior mechanical properties compared to a microstructure with uniform grain size. Plastic deformation caused strain-induced martensitic transformation (SIMT) in the coarse grain region, but not in the fine grain region. On the other hand, strain was concentrated in the fine-grain regions. Since the larger the grain size, the lower the apparent stacking fault energy, SIMT is considered to have occurred even if there was no strain concentration in the coarse grain region. In a microstructure with a broad grain size distribution, extreme strain concentration in the fine grain region was suppressed. As a result, the initiation of fracture in the fine grain region was considered to have been delayed.

Keywords : Biomedical Co alloy, Heterogeneous structure, powder metallurgy, precipitation, Mechanical properties

192. Hybrid organic/inorganic materials for drug release systems as new generation of biomaterials: a molecular dynamics study

Raffaini Giuseppina ¹

1 - Department of Chemistry, Materials and Chemical Engineering , Politecnico di Milano (via Mancinelli 7 - 20131 - Milano Italy)

Biomaterial-based drug delivery systems for controlled drug release are drawing increasing attention due to their possible pharmaceutical and biomedical applications. It is important to control the local administration of drugs, especially when the drug exhibits problems to diffuse in a human body. Thus, in appropriate concentration, it would be released in situ reducing side effects due to interactions with the biological environment after implantation. In recent years, theoretical studies based on molecular mechanics (MM) and molecular dynamics (MD) methods have been performed to investigate the adhesion and surface intermolecular interactions between the amorphous SiO₂ surface and the drug molecules ketoprofen and quercetin, anti-inflammatory drugs, considering the role of drug concentration. Interestingly, these theoretical results are in good agreement with experimental data obtained by analyzing, through Fourier Transform Infrared Spectroscopy (FT-IR), the intermolecular interaction between the amorphous silica surface obtained via sol-gel method and the dried SiO₂ materials, considering two percentages of these drugs entrapped in silica matrix. Drugs loaded into these amorphous bioactive materials form hydrogen bonds with the silica surface, as found in this theoretical study. Surface interactions in these organic/inorganic materials are essential to have a new generation of biomaterials not only important for biocompatibility, with specific structural and functional properties, but also capable of incorporating anti-inflammatory agents to be released into the human body.

Keywords : hybrid organic/inorganic materials, silica surface, drug delivery, modeling

193. Pulsed anodization process to form a biocompatible layer on superelastic NiTi alloy surface

Hirano Mitsuhiro¹, Kawakami Ryota ², Ohtsu Naofumi ¹

1 - Kitami Institute of Technology (Japan), 2 - Hokkaido Research Organization (Japan)

A fatal disadvantage of superelastic NiTi alloy when considering as biomaterial application is the Ni as the constituent element. Ni ion releases in the human body often induces cytotoxicity as well as allergic reaction, and medical doctors hesitate to use NiTi devices due to such risks. This presentation introduces a surface modification process that forms an almost Ni-free oxide layer improving the alloy's biocompatibility. The process is an electrochemical process being similar with anodization adopting a pulsed waveform voltage including voltage-off period. During the voltage-off period, anodic reaction is suspended but chemical reaction is highlighted, thereby enabling to remove Ni content from the alloy. As result, an oxide layer without Ni, corresponding to TiO₂, is formed on the alloy.

Actually, an almost Ni-free TiO₂ layer with a Ni content below a few percent was grown up to ~50 nm in thickness when anodized a NiTi alloy using a pulsed voltage in a nitric acid electrolyte. Such layer formation hydrophilized the surface, thereby activating cell extension and migration thereon. Also, forming surface region without Ni contributes the reduction of Ni ion release. As a result, cell proliferation rate on the pulsed-anodized NiTi alloy was superior to that on an untreated surface significantly.

The process does not raise the alloy's temperature; thus, metallographical change is negligible. The layer thickness is ultrathin; thus, the risk of peeling off is minimized. Based on above, the process is likely to be applicable as the industrial process.

Keywords : NiTi alloy, Anodization, Ni, free layer, Cell activation

194. Biodegradable zinc alloys with potent osteogenicity, antibacterial ability, and antitumor efficacy for bone-implant applications

Wen Cuie ¹

1 - School of Engineering, RMIT University (Melbourne, 3001, Australia Australia)

Biodegradable zinc-selenium (Zn-Se) alloys are projected to become a competitive material for implantation into hard tissues due to Se's antitumor effect in cancer prevention and treatment. However, adding Se to Zn to fabricate Zn-Se alloys is challenging due to the substantial volatilization of the monomeric Zn and Se components, as well as their immiscibility. In this study, we have successfully prepared biodegradable Zn-xSe ($x = 0, 1, 3, \text{ and } 5, \text{ at.}\%$) alloys using ultrahigh pressure sintering, which effectively suppressed the volatilization of monomeric Zn and Se elements, and increased the solid solubility of Se in Zn. The microstructure characteristics, mechanical properties, degradation rate, anticoagulant, and antitumor properties of the ultrahigh pressure sintered (UPS) Zn-Se alloys were systematically evaluated. The microstructure of the UPS Zn-Se alloys consisted of Zn matrix phases, Zn(Se) solid solution, and ZnSe second phases. The UPS Zn-1Se showed the highest compressive yield strength of $\sim 206 \text{ MPa}$, a fracture strain of 16.4%, a degradation rate of $27.2 \mu\text{m/y}$, effective antibacterial ability against *S. aureus*, effective antitumor activity against Cal-27 carcinoma cells, and excellent biocompatibility toward pre-osteoblast MC3T3-E1 cells. Overall, the addition of 1 at.% Se to Zn does not affect the growth of normal cells, but effectively inhibits the growth and reproduction of tumor cells and the Zn-1Se alloy is promising for orthopedic applications due to its unique combination of mechanical and biological properties.

Keywords : Antibacterial ability, Antitumor activity, Biodegradability, Osteogenicity, Ultrahigh pressure sintering, Zn, Se alloy.

195. Electrochemical Bio-Interface Devices for Advanced Medical Applications via Ion Transport

Kang Seung-Kyun ¹

1 - Department of Materials Science and Engineering, Seoul National University (South Korea)

The flow of ions and molecules is fundamental to a range of biological processes, including neural signal transmission and drug delivery. However, natural biological barriers-such as the stratum corneum in skin or the blood-brain barrier-often obstruct these flows, posing challenges for treatments that depend on effective ion or molecular transport. This research introduces innovative electrochemical bio-interfacing devices that overcome such barriers by utilizing ion electrophoresis and electroosmotic mechanisms to facilitate efficient drug delivery. By leveraging ion exchange membranes, the study demonstrates a cutting-edge anticancer therapy that employs electric fields to precisely regulate drug release and target delivery to cancerous tissues. This approach not only enhances therapeutic efficacy by directing minimal drug quantities to the intended site but also minimizes systemic side effects. Furthermore, the research showcases a biodegradable electronic patch designed for cosmetic applications. Operating in harmony with a biodegradable battery, this wearable device utilizes ion electrophoresis to enhance the penetration of cosmetic agents into the dermis while ensuring environmentally sustainable degradation of all components. This dual focus on precision delivery and eco-friendly design represents a significant advancement in both therapeutic and cosmetic care technologies.

Keywords : drug delivery, implantable device, iontophoresis, cancer, medical device

196. Synthesis of Inorganic Semiconductor Films with Narrow Bandgap Responsive to Visible LEDs and Their Photo-Response

Ueda Masato^{1 2 3}, Jinsoo Lee⁴

1 - Faculty of Chemistry, Materials and Bioengineering, Kansai University (3-3-35 Yamate-cho, Suita, Osaka, 564-8680 Japan), 2 - Kansai Univ. Carbon Neutrality Research Centre, Kansai University (Japan), 3 - Innoqua Inc. (Japan), 4 - Faculty of Chemistry, Materials and Bioengineering, Kansai University (Japan)

Anatase-type TiO₂ films synthesised on quartz glass demonstrated cell adhesion control when illuminated from the backside with a 150 W Xe lamp emitting white light. The UV component was fully absorbed by the TiO₂ film, preventing cell exposure to it. By selectively applying localised light, non-contact control of cell adhesion areas was achieved. If non-toxic films responsive to conventional LED panels could be used, this would enable precise and easy control of cell adhesion areas. The purpose of this study was to synthesise inorganic semiconductor films with a narrower bandgap than TiO₂, responding to visible light from LED, and to investigate their photo-responsive properties. Two types of oxide films were deposited on borosilicate glass or ITO-coated quartz glass using RF sputtering with the corresponding metallic targets under an Ar-O₂ atmosphere. XRD analysis showed sharp diffraction peaks, confirming the successful synthesis of the target oxide films. The absorption edges of both oxides shifted to longer wavelengths compared to that of TiO₂, corresponding to their bandgap differences. When a tablet device (HUAWEI MediaPad M3 Lite 10wp) displaying a white image was used as a light source, both oxide films showed a noticeable photocurrent. In the photocurrent profile during the on/off cycle of the light, a phenomenon of current flowing in the reverse direction when the light was turned off was observed. Moreover, this current reversal was more pronounced when the grains were fine. This suggests that the grain boundaries acted like a capacitor and induced polarisation behaviour.

Keywords : Photocatalytic reaction, Visible light, Cell printer, Sputtering, Microstructure

197. Enhancing Non-Viral Gene Delivery: Strategies for Improved Efficiency and Performance

Candiani Gabriele ¹

¹ - Politecnico di Milano (Italy)

Gene delivery involves transferring genetic material into cells to control their functions, but naked nucleic acids are ineffective at entering cells. Thus, gene delivery vectors are crucial for both basic research and medical applications. Viral vectors offer high transduction efficiency and long-lasting effects but have significant limitations. Non-viral delivery systems, such as cationic lipids and polymers, form nano- and micro-particles (lipoplexes and polyplexes) through self-assembly with nucleic acids. These particles are endocytosed but exhibit lower transfection efficiency and cytotoxicity, despite being safer than viral systems. This presentation outlines strategies to optimize gene delivery systems, focusing on key challenges: shaping delivery complexes at the nano/microscale, improving interactions with biological fluids, and incorporating cell-targeting and antimicrobial properties to enhance performance. Additionally, the talk will explore the emerging use of physical forces to disrupt cell membranes and boost non-viral delivery efficiency. To accelerate optimization, new tools are essential for unbiased and quantitative assessment of transfection efficiency and cytotoxicity. A promising solution is the development of miniaturized, user-friendly devices. Lab-on-chip (LoC) platforms enable streamlined transfection assays, facilitating the selection of effective gene delivery vectors.

Keywords : Gene delivery applications, Cell behavior control, Nanostructured biomaterials, Cationic polymers, Cationic lipids

198. Novel prospective in design of Mg alloys for implantology: in vitro and in vivo assessment of degradation of Mg-Zn-Ca-Y-Mn alloys

Dobkowska Anna¹, Martinez Diana , Inoue Shinichi , Kawamura Yoshihito , Swieszkowski Wojciech¹

¹ - Warsaw University of Technology [Warsaw] (Poland)

Mg and its alloys, due to their unique properties, are of great interest for use as temporary orthopaedic implants. In this study Mg-1.0Ca-0.5Zn-0.1Y-0.03Mn at.% produced using different methods: traditional ingot metallurgy and rapid solidification with subsequent extrusion, are investigated. Pure Mg was taken as a reference sample. To assess the degradation performance of the samples, in vitro immersion and electrochemical tests were performed under cell culture conditions. The morphology of the corroded surfaces and distribution of elements was also investigated on the cross sections of samples prepared by focus ion beam (FIB)/SEM. Male Wistar rats were used for in vivo evaluation. After 7 and 28 days, the animals were euthanized, and specimens, with and without surrounding tissues, were collected for further characterization. As per results of this research, the manufacturing method has significant influence on the degradation parameters of the alloys. In vitro research clearly show the potential of application of rapidly solidified and extruded alloy. During in vivo the corrosion products formed consisted primarily of Mg(OH)₂, with homogeneous Ca and P distribution and higher concentrations in the outer and middle regions of the corrosion layers for both materials after 28 days of implantation. Histological analysis revealed gas cavities, larger in the pure Mg group, surrounded by fibrous tissue. New bone formation was observed in both groups, with no adverse tissue reactions, confirming for the first time the biocompatibility of the Mg-1.0Ca-0.5Zn-0.1Y-0.03Mn at.% in vivo.

Keywords : magnesium, in vitro tests, in vivo tests, biocompatibility

199. Development of a realistic brain phantom for medical training: an ethical and technical alternative to animal testing

Speck Sandy ¹, Claudio Verona , Boehme Andrea ², Foitzik Andreas ³

1 - Technische Hochschule Wildau (Germany), 2 - Technical University of Applied Sciences, Wildau, 15745 Wildau, Germany (Germany), 3 - Technical University Wildau (Hochschulring 1, 15745 Wildau Germany)

The present study is concerned with the development of realistic organ models, particularly brain phantoms, as human alternatives for medical training. The use of these models not only leads to a reduction in the need for animal testing, but also offers practical advantages such as cost efficiency, reusability and an improvement in training opportunities for complex medical procedures, such as ultrasound diagnostics. The research focuses on the design of an anatomically accurate brain phantom that simulates human brain tissue for ultrasound diagnostics. The phantom is made of gelatin with additives such as glycerin and potassium sorbate, which ensure sufficient durability and elasticity. An essential feature is the imitation of functional ventricles, which can be filled and emptied with fluid. This allows for a realistic simulation of invasive procedures. Furthermore, a tumor model is integrated to simulate advanced diagnostic and therapeutic training scenarios. The study shows that the phantom can be considered a valuable teaching tool both in terms of its structural accuracy and its ultrasound compatibility. However, limitations in terms of the durability of the animal gelatine can be deduced, so that in the future, the investigation of synthetic alternatives is recommended to optimize longevity and reusability. The research represents a significant advance in medical education, providing an ethical and practice-oriented solution for training without the use of animals.

Keywords : Advance Manufacturing, Fabrication, Applications, Gelatin, Medical Science, Education

200. Enhancing wear resistance and biological performance of the biomedical Ti-6Al-4V alloy through PEO Treatment in TMO-rich electrolyte

Diego Correa¹, Coan Karine¹, Grandini Carlos Roberto¹, Barbaro Katia², Fosca Marco³, Rau Julietta^{3 4}, Tsipas Sophia⁵

1 - Sao Paulo State University (UNESP), School of Sciences, Campus Bauru, Laboratory of Anelasticity and Biomaterials, 17.033-360, Bauru, SP, (Brazil), 2 - Istituto Zooprofilattico Sperimentale Lazio e Toscana M. Aleandri, Via Appia Nuova 1411, 00178 Rome (Italy), 3 - Istituto di Struttura della Materia, Consiglio Nazionale delle Ricerche (ISM-CNR), Via del Fosso del Cavaliere 100, 00133 Rome (Italy), 4 - Department of Analytical, Physical and Colloid Chemistry, Institute of Pharmacy, Sechenov First Moscow State Medical University, Trubetskaya 8, Build. 2, 119048 Moscow (Russia), 5 - University Carlos III of Madrid, Department of Materials Science and Engineering and Chemical Engineering, IAAB, Avda. de la Universidad, 30, 28911 Leganes, Madrid (Spain)

In this study, we developed a new approach to modify the surface of biomedical Ti alloys using plasma electrolytic oxidation (PEO). Our goal was to create a coating composed of multiple transition metallic oxides (TMO; Fe, Mo, Mn, Ti, and Al) and bioactive elements (Ca, P) on the surface of the Ti-6Al-4V alloy. After the surface treatment, the samples were characterized by diverse techniques such as scanning and transmission electron microscopy (SEM and TEM), X-ray diffraction (XRD), and X-ray photoelectron spectroscopy (XPS). The results suggested that the chemical, phase, and topological aspects positively influenced the wear and biological responses of the samples and indicated promising properties to be used as biofunctional coatings on biomedical implants. (Financial support: FAPESP grant #2024/03148-3 and CNPq 404020/2023-2)

Keywords : biomaterial, Ti, 6Al, 4V, PEO, TMO, biofunctionalization

201. A novel low-cost multicomponent biocompatible alloy for potential application as bone fixation devices

Torrento Jhulienne¹, Afonso Conrado², Grandini Carlos¹, Diego Correa¹

1 - Sao Paulo State University (Brazil), 2 - Federal University of Sao Carlos (Brazil)

High entropy alloys (HEAs) have been considered for biomedical applications due to their unique combination of single crystalline structure, e.g., HCP, BCC, or FCC, low elastic modulus, and superior mechanical strength. Even though the current HEAs do not fully reproduce the complex biomechanical loads of the human body neither possess adequate interaction with the biological host, the design of novel HEAs for use as biomaterials is an emerging focus of research. This study aimed to create a novel Bio-HEA based on non-toxic, low-cost, and non-refractory alloying elements, including Ti, Zr, Mn, Al, Nb, and Fe. The as-cast ingots were later subjected to a homogenization heat treatment. The chemical composition was verified using density, XRF, and EDS measurements. Structural and microstructural analyses were carried out using XRD, optical microscopy, and SEM. Finally, Vickers microhardness and elastic modulus measurements were taken to evaluate the selected mechanical properties. The samples demonstrated a complete mixture of all alloying elements in a non-equiatomic solid solution, with an overall density of around $6.0 \text{ g}\cdot\text{cm}^{-3}$ and a dendritic microstructure. The XRD profiles exhibited the formation of a dual-phase composition (BCC and HCP). Vickers microhardness measurements showed an average value above 450 HV, higher than some commercial metallic biomaterials. Besides that, the elastic modulus values remained close to 95 GPa, lower than the commercially pure Ti (CP-Ti). The results indicated that the obtained Bio-HEA grouped promising characteristics for potential use in biomedical applications, especially as implants and fixation devices. (Financial support: FAPESP grant #2023/15812-2 and #2021/13921-3)

Keywords : Biomaterials, High entropy alloy, Phase, Microstructure, Mechanical properties

202. Control of Bone Microstructure Formation: Role of Soluble Proteins Secreted by Osteocytes

Matsuzaka Tadaaki¹, Matsugaki Aira¹, Nakano Takayoshi¹

¹ - Graduate School of Engineering, The University of Osaka (Japan)

The hierarchical microstructure of the collagen/apatite bone matrix plays a crucial role in determining its mechanical properties and functionality. Understanding the mechanisms underlying the anisotropic organization of the bone matrix is essential for designing biomimetic materials for bone tissue engineering. However, the direct link between mechanical stimuli and the microstructural organization of bone matrix remains elusive. Here, we propose a novel materials-focused approach utilizing a co-culture device to investigate the interplay between mechanical stimuli and bone matrix organization. A novel co-culture system was developed to integrate stress-responsive osteocytes with osteoblasts seeded on collagen scaffolds featuring controlled molecular orientation. The two kinds of cells were cultured via nanopore membrane which enables intercellular communication via soluble factors. The dynamics of fluid flow stimuli to osteocytes were regulated using Particle Image Velocimetry (PIV). Gene expression changes in osteocytes were analysed to identify the molecules determining bone matrix organization in response to mechanical stimuli. Mechanical stimuli with oscillatory flow modulated osteocyte regulation of osteoblast arrangement. Specifically, the release of cytokines from osteocytes in response to oscillatory stimuli promoted the degree of osteoblasts alignment along the scaffold arrangement. Moreover, we successfully determined the dominant factor Prostaglandin E2 (PGE2) that controls the oriented microstructure of the bone matrix under mechanical stimuli. PGE2 controlled the cytoskeletal regulation of osteoblasts and further determined the microstructure organization of bone matrix. By linking the anisotropic architecture of bone matrix with cellular behaviour, our research lays the foundation for the development of advanced bone graft materials with customizable mechanical properties.

Keywords : Bone matrix microstructure, Mechanosensing, Functional adaptation, Osteocyte, Osteoblast arrangement

203. New aspects of production Mg-Zn-Ca alloys via Laser Powder Bed Fusion

Dobkowska Anna¹, Ciftci Jakub^{1 2}, Zrodowski Lukasz²,
Swieszkowski Wojciech¹

1 - Warsaw University of Technology [Warsaw] (Poland), 2 - AMAZEMET Sp.z o.o. (Poland)

Within this research we produced ZXX Mg alloys showing novel aspects of production for biocompatible alloys. After Laser Powder Bed Fusion (LPBF) optimization it is expected to produce a material with a unique microstructure with improved mechanical properties (i.e. ductility), controlled degradation rate and enhanced antibacterial properties with a special focus for application in implantology. The cast rods of ZX00, ZX50, and ZX50 with Ag addition were atomized via ultrasonic atomization using a rePowder device (AMAZEMET, Poland). The alloy was melted in a graphite crucible with a 400 cm³ volume at a heating rate of 150 K/min up to 1023 K and kept for 2 min at this temperature under an Ar atmosphere with oxygen content below 40 ppm as firstly chamber was evacuated using vacuum pump. Subsequently, the molten alloy was poured using pressure differential pressure through nozzle with 1,2 mm orifice diameter on a plate-type sonotrode, which vibrated at 40 kHz frequency. As a result of a atomization process, the powder with high sphericity was produced. The particle size distribution of as-atomized powders is suitable for alloy development for additive manufacturing as most of the particles were below 100 microns. The powder was collected under an inert atmosphere and sieved to obtain particles with the desired size. Afterwards, samples were printed using Acconity Midi 3D printer. The microstructure and corrosion properties were evaluated. The results of this work show wide perspective to be the accurate way to improve the properties of Mg-based alloys for biomedical applications.

Keywords : magnesium, additive manufacturing, biocompatibility

204. Contact-free Micro- and Nano- Deformation in inorganic and organic systems via Electronic Speckle Pattern Interferometry

Foitzik Andreas¹, Lietzau Kai-Henning, Stollfuss Carsten,
Gottschalk Josefine, Krumnow Erik, Vogt Thomas, Sixt Willi,
Arkipov Serguei

¹ - University of Applied Sciences Wildau (Germany)

Electronic Speckle Pattern Interferometry (ESPI) was customized to determine the three-dimensional deformation in micro-sized technical objects as well as in fluidic and (micro-)biological samples on physical or chemical stresses. An appropriate Micro Electronic Speckle Pattern Interferometer (Micro-ESPI) was developed and applied to MEMS as well as micro-sized fluidic microstructures to prove the suitability of the device and the method. Subsequently the influence of ultrasonic sound and the resulting mechanical interaction with fluidic and organic microstructures was determined. Such measurements were carried out on micro-sized transparent biological samples in terms of (i) static Micro-ESPI as well as (ii) dynamic Micro-ESPI (iii) down to the optical resolution limit. The results were transferred to cancer cells and their equivalent interaction with mechanical stress as well as their interaction with cytostatic chemical treatment. Single biological cells could be observed (i) under periodic mechanical stress, (ii) on chemical influence and (iii) during chemical attack. Micro-ESPI finally allowed to determine the 3D change in the morphology of the biological cells (i) at high magnifications up to 1000x, (ii) contact free, (iii) in fluidic environment in vitro, (iv) statically and dynamically, (v) without alteration due to any staining and (vi) during additional interaction with electro-mechanical vibrations. The deformation and the death of healthy and cancer cells being treated with cytostatic drugs could be determined, aiming for the correlation of treatment, mechanical deformation and death of cancer cells. This opens new perspectives for an improved physical and chemical treatment of cancer and other diseases on a single cell level, while microbiology and genetics aim for a molecular understanding and treatment.

Keywords : ESPI, micro, nano, deformation, contact, free, in, vitro, high magnification, static, dynamic, cancer, cells

205. Desalination Membrane Strategy Using Ion-Exchange Membranes for Marine Farms

Choi Myung-Kyun¹, Han Jieun¹, Kang Seung-Kyun¹

¹ - Department of Materials Science and Engineering, Seoul National University (South Korea)

The growing shortage of farmland caused by climate change and population growth led to efforts to cultivate crops on wastelands through urban agriculture and film farming. However, these approaches faced significant challenges, such as limited space and high irrigation costs. On the other hand, marine farming, which eliminates the need for farmland and directly utilizes seawater, was largely impractical due to salt stress, which inhibited plant growth and reduced crop yields. Here we developed an ion-selective membrane-based ion filter inspired by the salt-tolerant roots of mangroves, allowing plants to filter salt through root pressure. The nanoporous ionized membrane demonstrated excellent biocompatibility and mechanical durability, effectively filtering sodium ions using a high negative zeta potential based on the Donnan mechanism. By adjusting the membrane's surface potential and nanoporosity, we controlled desalination rates and water supply to make the system suitable for a wide variety of plants. This study showed that high-surface-potential membrane filters enabled energy-free marine farming, providing a sustainable and innovative solution to agricultural challenges.

Keywords : Desalination, Marine farm, Ion, filter, Membrane, Polyelectrolyte

206. Waterproof Polyelectrolyte for Implantable Medical Devices

Choi Myung-Kyun¹, Choi Yi-Jeong¹, Kang Seung-Kyun¹

¹ - Department of Materials Science and Engineering, Seoul National University (South Korea)

Ensuring the prolonged functionality of electronic implants is crucial for the accurate diagnosis of chronic disease such as brain tumors, meningitis, and hydrocephalus. Encapsulation is crucial in ensuring the sustained functionality of devices exposed to biological fluids, effectively shielding them from biofouling, electrical leakage, corrosion, and performance deviations. However, encapsulating soft electronic implants presents significant challenges, as conventional methods require certain organic thicknesses and involve complex fabrication processes for inorganic materials. Herein, we propose a novel active encapsulation system inspired by the active transport of ions and water molecules in alveolar membranes. Unlike conventional barriers that passively block water diffusion, Our active waterproofing barrier possesses enhanced waterproofing properties. Additionally, integrating conventional encapsulation with active barrier layer enhances the waterproofing ability while maintaining their excellent passive water barrier properties. In vivo studies involving pressure monitoring in living animal models using actively encapsulated pressure sensors showcase reliable monitoring of chronic diseases.

Keywords : Waterproof, Implantable device, Polyelectrolyte, Osmosis, Membrane

207. Identification and Optimization of Geometric Features Significant for Nozzle Design in Cold Spray Additive Manufacturing using CFD and Artificial Neural Networks

Ozdemir Ozan¹, Cura Ege

1 - Department of Mechanical and Industrial Engineering, Northeastern University (United States)

In cold spray additive manufacturing (CSAM), high kinetic impact velocity of particles enables solid-state material deposition opening avenues for materials development, surface coatings, repair of industrial components facing obsolescence, and additive manufacturing (AM). Supersonic spray nozzle design is one of the most significant factors dictating the particle impact velocity and temperature, which are the primary parameters of control in CSAM. In this study, varying fidelity computational fluid dynamics (CFD) models validated via particle image velocimetry and schlieren imaging are used for identifying supersonic region geometric features significant for CSAM. To this end, diverging section of a spray nozzle is parameterized with 50 nodes by fixing other geometric features. A Monte Carlo approach is used for studying the influence of the internal topological features and also for generating an extensive data set for training an artificial neural network (ANN). A correlation is also made between nozzle geometry and gas pressure, gas temperature, particle size, and particle material properties. The current neural network achieves over 95% accuracy on more straightforward cases when compared to 1D model results. This provides an effective model for generating baseline geometries, which can be further optimized using 2D and 3D CFD models. While reducing computational cost, this workflow allows for rapid prototyping. In this talk, primary attention is given to the spray nozzle internal geometry. However, further insights are provided in the design of the nozzle material and internal surface conditions to maximize particle velocity and reduce nozzle clogging.

Keywords : Cold Spray Additive Manufacturing, Nozzle Design, Nozzle Optimization, Artificial Neural Networks

208. Enhancing the thermal cycling lifetime of YSZ thermal barrier coatings with air plasma sprayed NiCrAlY bond coat

Zhu Yong-Sheng¹, Luo Xiao-Tao², Li Chang-Jiu²

1 - School of Materials Science and Engineering, Xi'an Jiaotong University (China), 2 - State Key Laboratory for Mechanical Behavior of Materials, School of Materials Science and Engineering, Xi'an Jiaotong University (China)

MCrAlY coatings have been widely used as a bond coat for thermal barrier coatings (TBCs) due to their excellent high temperature oxidation resistance and the ability to minimize the mismatch in the coefficient of thermal expansion (CTE) between the ceramic top coat and the superalloy substrate. The high oxide content introduced into MCrAlY during air plasma spraying (APS) leads to low thermal cycle life of the TBCs. In the present work, using a deoxidizer-diamond-containing NiCrAlY composite powder the NiCrAlY coating with a low oxide content was successfully deposited by APS. The thermal cycling lifetime of TBCs with an APS NiCrAlY bond coat was examined by the isothermal thermal cycling test. The NiCrAlY coatings deposited by APS exhibit low oxide inclusions and dense microstructure as a result of the in-flight in-situ deoxidation effect contributed by the sacrificial oxidation of diamond. The results show that the residual carbon within NiCrAlY coating can be transformed into chromium carbide at high temperature, which effectively reduces the CTE of the NiCrAlY coating, to further reduce CTE mismatching between superalloy and ceramic top coat. The thermal cycling test results demonstrate that the TBCs with the present APS NiCrAlY bond coat show an enhanced thermal cycling life time than TBCs with the conventional vacuum plasma spraying (VPS) NiCrAlY bond coat. The present results demonstrate the novel approach to deposit high performance MCrAlY bond coats for TBCs using APS. The results also reveal that it becomes possible to substitute the VPS by APS when using carbon-containing MCrAlY powders.

Keywords : Air plasma spraying, Coatings, NiCrAlY, Bond coat, Thermal Barrier Coatings, Thermal cycling behavior

209. Copper-nickel alloy coating on cast iron by cold spray: microstructure and thermal analysis

Lauridant Timothee¹, Rostom Aya¹, Brisset Francois², Bourahima Fazati¹

1 - Chpolsansky (France), 2 - Institut de Chimie Moleculaire et des Materiaux d'Orsay (France)

Glass containers are manufactured by pressing or blowing a hot glass gob (700-1200°C) onto a metallic mold. Beside forming the glass, molds are heat exchangers for cooling down the glass final product. To this goal, molds are made of cast iron or cupro-nickel alloy due to their thermal properties. If copper-nickel (bronze) is the most efficient material, cast iron is mainly used for economic purposes. To enhance the properties of the cast iron mold, cold spray coating of a copper-nickel alloy is investigated. Optimization of the parameters process such as spraying temperature (800-1000°C), pressure (40-50bar) and gun's travel speed (200-400mm/s) lead to a dense and well-bonded bronze coating on cast iron. Microstructural analysis is performed thanks to Optical Microscope, Scanning Electron Microscope, Electron BackScatter Diffraction, X-Rays Diffraction and microhardness tests on two coatings made with two different batches of powder of distinct granulometry. Flat coated samples underwent thermal experiment (heated to 400°C then air cooled) to be closer to the glass production conditions. In comparison with cast iron and copper-nickel alloy reference, the coatings showed better thermal conductivity than cast iron, as desired. As this thermal experiment can be seen as an aging treatment, microstructural study (based on Grain Size, Kernel Average Misorientation and Grain Orientation Spread) is also described after the test, showing stress relieving or recrystallization.

Keywords : cold spray, cast iron, copper nickel alloy, microstructure, thermal conductivity

210. Sustainability Efforts in Cold Spray Processing

Cote Danielle¹, Tsaknopoulos Kyle , Lyon Ashton

1 - Worcester Polytechnic Institute (100 Institute Road; Worcester, MA 01609 United States)

Cold spray processing is a solid state additive manufacturing technique which has inherent benefits, including a reduction in material waste compared to more traditional manufacturing techniques. This effort identifies additional ways in which cold spray processing can lead towards further sustainability, including recovery of unbonded feedstock powder, production of new feedstock powder from recycled metal, more efficient development of process parameters for novel materials, recycled and recovered processing gasses, and more. Computational thermodynamic and kinetic modelling and simulations are used in conjunction with machine learning techniques to increase the effectiveness and efficiency of these efforts.

Keywords : Cold spray, recycling, recovery, sustainability, powder metallurgy, computational thermodynamics

211. Application of the Thermal Spraying technology in Hot-dip galvanizing line zinc pot roll

Lu Wang ¹

1 - Baosteel Nova Automotive Steel Sheets Co.LTD,Shanghai,201900 (China)

With the continuous improvement demand for galvanized automotive sheet quality, and the zinc pot equipment corrosion resistance and dross adhesion resistance requirements are also increasing, thermal spraying has played an important role. The failure forms of zinc pot hardware in continuous hot-dip galvanizing lines (CGLs) are Zn corrosion, abrasion and dross build-up. Enhancing the life of the pot hardware will not only upgrade the quality of sheet plate product but also increase the efficiency of CGLs with cost decreasing and energy saving. The paper introduces the current research and development of thermal spray coating in pot rolls sleeves & bushings pointed out sealing treatment after thermal spraying can greatly improve the ability of coating layer anti-corrosion and anti-zinc dross adhesion. The article also introduces a newer surface treatment technology, a special surface treatment called CDC-ZAC. This treatment liquid is a chromium (Cr_2O_3) as the main component, the ceramic composite coating film forming by chemical reaction. have excellent characteristics of high-density, high hardness coatings, high adhesion and low friction coefficient. especially suitable for non-contact with the strip zinc pot hardware. it gives the prospect of application and developing trend of thermal spray coating and surface treatment technology in pot hardware.

*Keywords : Hot, dip galvanizing line automotive sheet WC composite thermal spraying Sink roll
Surface treatment*

212. Effect of the interface between coarse and fine grains on strength-ductility balance in dispersion-strengthened bimodal Al-Y₂O₃ nanocomposite fabricated via powder metallurgical route

Sakamoto Tatsuaki¹, Yamasaki Taichi¹, Jinno Yusuke¹, Shiga Shinya², Takebe Hiromichi¹

1 - Ehime University (Japan), 2 - National Institute of Technology, Niihama College (Japan)

The strength-ductility balance of dispersion-strengthened Al-Y₂O₃ was improved by incorporating bimodal microstructures (BMs) in the matrix through powder metallurgy. The fine-grained and the coarse-grained raw powders for BM were Al-Y₂O₃ alloy and pure Al powders, respectively. The former powder was prepared by mechanical alloying (MA); supersaturated solid solution (SSS) and particle dispersion (PD) powders were prepared depending on the oxygen content in the MA atmosphere; both sintered SSS and PD powders were dispersion-strengthened, but exhibited low ductility. BMs were prepared by spark plasma sintering of the powder mixture (the SSS powder as the fine grain component and pure Al powder as the coarse grain component) with two different volume ratios of the SSS powder to the pure Al powder: 5 and 1. The specimen with the ratio of 5 showed simultaneous enhancement of yield strength and uniform strain as compared to that with the ratio of 1. The yield strength increased due to the rule of mixture, i.e. because there were more SSS powder consisting of particle-dispersed fine grains. The uniform strain increased because the amount of boundaries between fine and coarse grains increased, and thus geometrically necessary dislocations accumulated at the boundaries during deformation, resulting in the increase in work hardening.

Keywords : Strength, ductility synergy, Heterogeneous nanostructure, Bimodal microstructure, Powder metallurgy, Mechanical alloying

213. Design, fabrication, and understanding the heat transfer behaviors of the high-thermal conductive copper-matrix composite materials

Yang Fei ¹

1 - University of Waikato (School of Engineering, University of Waikato, Hamilton 3240 New Zealand)

The technical capabilities of modern electronic devices increasingly demand higher frequencies, more power, and greater miniaturization. Rapid heat dissipation is critical to ensuring these high-power devices maintain function and avoid overheating. Developing advanced thermal management materials with high thermal conductivity and cost-effective manufacturing technology is of significant global interest. In this presentation, I will present a cost-effective route to fabricate advanced copper-matrix composite heat-sink materials, which have potential to be used in high-power electronic components; and discuss the key affecting factors that influence the composite's heat transfer behaviours and their underlying mechanisms from micro- and atomic-scales. This will help design required copper matrix composites to meet varied practical applications.

Keywords : Copper matrix composites, heat sink materials, hot processing, interface formation, heat transfer behaviours.

214. Global Reactive Synthesis and Additive Manufacturing: in-situ synthesis of near net-shape Aluminium Matrix Composites

Andrieux Jerome¹, Forget Baptiste², Gardiola Bruno¹, Flament Camille², Soulier Mathieu², Chaffron Laurent³, Baffie Thierry², Dezellus Olivier¹

1 - Laboratoire des Multimateriaux et Interfaces (France), 2 - Departement des Technologies des Nouveaux Materiaux (Ex Departement des Technologies des NanoMateriaux) (France), 3 - Service de Recherche en Materiaux et procedes Avances (France)

The in-situ synthesis of Aluminium Matrix Composites (AMC) via the Global Reactive Synthesis (GRS) has been demonstrated in the recent years as a promising approach to control reinforcement size and distribution, as well as to obtain sharp matrix/reinforcement interface. Based on the use of chemical precursors, the GRS is driven by controlled reactivity and thermodynamics to in-situ form both the matrix and the reinforcement under basic geometries (cylinders or plates). It has been applied successfully to conventional AMCs like Al-TiC and Al-TiB₂. It also opens the field of new class of AMCs and the most advanced studies have been focused on Al-Tau₃ AMC, where Tau₃ is a ternary borocarbide (Al₃B₄SiC₂). We will first detail the rules and conditions for AMCs to be obtained by the GRS route, as well as a comparison in terms of mechanical properties and microstructure with conventional AMCs. More recently, the GRS route of Al-Tau₃ AMC was adapted to the Laser Powder Bed Fusion (LPBF) Additive Manufacturing technique to get near net shape and complex geometries. The main challenges were to adapt the precursors powder to the criteria of LPBF in terms of flowability and spreading and to achieve the in-situ chemical reaction, given the high rate of heating and cooling and the very small time in temperature imposed by the LPBF process. The talk will present dense AMCs from Al-Tau₃ to Al-nano(AlB₂) with promising mechanical properties. We will also discuss the influence of different heat treatment parameters on the final phases and microstructures.

Keywords : MMC, Aluminium Matrix Composites, Additive Manufacturing, Laser Powder Bed Fusion, Global Reactive Synthesis

215. Synthesis of zirconium carbide and zirconium diboride particles and fibers as building blocks for ultra-high Temperature ceramic matrix composites

Maillard Mathieu¹, Juvin Manon¹, Prum Sovannara Frederic¹, El Bouzidi Zineb¹, Andrieux Jerome¹, Reynaud Pascal²

1 - Laboratoire des Multimateriaux et Interfaces (France), 2 - laboratoire MATEIS (France)

In the present work, we developed building blocks for ultra-high temperature composite matrix ceramics as particles and fibers made of ZrC and ZrB₂. Fibres were synthesised by electrospinning before being heat-treated under 'mild' conditions. Particles are synthesized using molten salts processes. Their size, composition and morphology were studied in order to obtain continuous, non-oxide ZrC fibres. These fibres were then assembled with a ZrC matrix to obtain a composite material, again at relatively low processing temperatures. The microscopy methods used and the XRD enabled us to characterise the fibres and ceramics obtained, supporting our results.

Keywords : UHTC, zirconium carbide, zirconium diboride, electrospinning, CMC

216. Nanoscale engineering of low-misfit TiB₂/Al₃(Sc,Zr)/ α -Al multi-interface to improve strength-ductility synergy for direct energy deposited aluminum alloy

Li Yang^{1 2}, Ji Gang³, Zhe Chen²

1 - SJTU-Paris Elite Institute of Technology, Shanghai Jiao Tong University (China), 2 - School of Materials Science and Engineering, Shanghai Jiao Tong University (China), 3 - CNRS, INRAE, Centrale Lille, UMR 8207 - UMET - Unite Materiaux et Transformations, Universite de Lille (France)

The nature of the interface between ceramic particle (CP) and metal matrix is critical to obtain solidification microstructures with optimal mechanical properties of CP-reinforced Al alloys in additive manufacturing. Generally, when the lattice misfit between the CP (e.g., TiB₂) and the α -Al matrix is higher than 4 %, the interfacial coherency reduces, lowering the effectiveness of CPs. Here, we demonstrate that an L12 three-dimensional compound (3DC), which possesses lattice misfit with α -Al lower than 1 %, can be introduced in between TiB₂ and α -Al via properly regulating the solidification cooling rate. In the 5TiB₂/Al-4.5Mg-0.7Sc-0.2Zr (wt.%) as a model system, the lattice coherence of the TiB₂/ α -Al interface is tailored by introducing a 10-30 nm thick Al₃(Sc,Zr) 3DC interphase when the cooling rate is increased to ~1000°C/s. But, further increasing the cooling rate to ~6800°C/s, only Al₃(Sc,Zr) two-dimensional compound (2DC) with an apparent lattice strain forms at the interface. Taking advantage of the cooling rate (102-103 °C/s) provided by laser direct energy deposition (L-DED), the low-misfit TiB₂/Al₃(Sc,Zr) 3DC/ α -Al multi-structural interfaces are acquired, enabling the 3.56TiB₂/Al-4.36Mg-0.72Sc-0.22Zr alloy as fabricated with L-DED to achieved improved strength-ductility synergy (yield strength 257 MPa, elongation 13.8%) due to the isotropically fine Al grain structure and the homogenous TiB₂ particle dispersion. The outcome of this study provides fundamental knowledge on designing ceramic/coherent primary interphase/metal matrix multi-structural interfaces to improve the mechanical properties of engineering metallic materials manufactured by rapid solidification techniques, such as DED additive manufacturing (AM).

Keywords : Aluminum alloys, Nucleation and growth, Interface, Rapid solidification, Additive manufacturing

217. Development of high-performance laser devices using room-temperature bonding

Shoji Ichiro ¹

¹ - Department of Electrical, Electronic, and Communication Engineering, Chuo University (Japan)

Composite structures composed of different materials or the same material with different orientations are crucial for developing high-performance laser devices. High-quality bonding of materials is essential in such composite structures, as laser light must pass through the bonded interfaces with minimal scattering loss. We employ room-temperature bonding (RTB) to develop these composite laser devices. RTB is performed at room temperature under vacuum, where the surfaces of the materials to be bonded are irradiated with argon atom beams to activate them chemically. These activated surfaces are then atomically bonded by bringing them into contact and applying pressure. We have fabricated Nd:YAG/diamond composite lasers with anti-reflection coatings at the bonded interface. The diamond crystal effectively dissipates the heat generated in the Nd:YAG crystal, resulting in a significant increase in output laser power. We have also fabricated wavelength-conversion devices by alternating the crystal orientation, a critical factor for enhancing conversion efficiency. In this paper, we will present new devices developed using the RTB technique. The first is a Yb:YAG/undoped YAG composite microchip laser capable of single-longitudinal-mode oscillation with high power. The second is a quasi-phase-matched wavelength-conversion device utilizing GaAs and ZnSe plates to generate mid-infrared light.

Keywords : Room, temperature bonding, Composite lasers, Microchip lasers, Wavelength, conversion devices, Quasi, phase matching

218. Sintering process analysis of aluminum matrix composites using machine learning

Sugio Kenjiro¹, Shinohara Yuuki, Hayashi Yoshikazu, Sasaki Gen

¹ - Hiroshima University (Japan)

Materials informatics is a field in which materials development is carried out using information processing technology, including technology based on statistical mathematics, etc., and has attracted attention in recent years as an epoch-making method that will significantly change the materials development process. The conventional materials development process is strongly dependent on the knowledge, experience and ability of researchers, and requires a lot of time and effort as the process of sample preparation and property evaluation is repeated. If information science and technology methods such as machine learning can be applied, it will be possible to propose preparation conditions for materials with the desired properties, thereby reducing the aforementioned trial-and-error process. In this study, the sintering behavior of spark plasma sintering was analyzed by extracting features from process data obtained during the fabrication of aluminum matrix composites, and machine learning with the obtained features was performed to predict the relative density of composites. Seventy-five samples were sintered with different types of reinforcements, and different temperature and pressure conditions. Regression methods include linear regression such as Ridge, Lasso and Elastic Net, and nonlinear regression such as random forest, gradient boosting and XGBoost were tested. XGBoost had the highest prediction accuracy and the trained model was used for Shapley additive explanations value analysis and inverse analysis. The process parameters that could achieve the desired relative density were proposed by inverse analysis and used for sample preparation. The relative density of the prepared samples showed the target relative density.

Keywords : Spark plasma sintering, Aluminum matrix composites, Machine learning, SHAP, Inverse analysis

219. Microstructural characterization and analysis of the mechanical properties of composite materials based on epoxy resin and glass fiber for their application in blades manufacturing

Avila-Davila Erika O.¹, Castillo-Hernandez Jorge A.¹, Hernandez-Demesa Yuri S.¹, Vera-Cardenas Edgar E.¹, Martinez-Perez Armando I.¹, Lopez-Hirata Victor M.², Dorantes-Rosales Hector J.

1 - Tecnológico Nacional de México-Pachuca, DEPI, Pachuca de Soto, Hgo., C.P. 42080 (México), 2 - Instituto Politécnico Nacional (ESIQIE), UPALM, Edif.7, Ciudad de México. C.P. 07738 (México)

It is known that the energetic demand has increased considerably in the past years. This situation has motivated the development of devices to generate electric power, such as wind turbines (WT). It is well known that one of the more important components in WT are the blades. These components require periodical maintenance. In some cases, the manufacturing cost of the wind turbine blades is approximately 20% of the WT production cost, depending on the type of the WT, of the materials and process to produce them. This work shows an analysis of the manufacturing (vacuum assisted resin infusion process), mechanical properties and the chemical and microstructural characterization of three composite materials based on glass fiber and epoxy resin as the matrix. Information regarding to identify the internal structure of each composite material was obtained by mean of X-ray diffraction. Also, it was carried out the microstructural characterization of each composite by using scanning electron microscopy (SEM), before and after of carried out mechanical tests. The purpose of this study was to identify the critical parameters that promote high structural homogeneity and high mechanical stability in the composite material for use it in blades manufacturing of a vertical axis wind turbine (VAWT). It was obtained a good structural homogeneity consistent with the mechanical properties of the composite material, in correlation with the study of a post-cure process at three different temperatures during manufacturing stage.

Keywords : Composites, structural characterization techniques, vacuum assisted resin infusion process

220. Fabrication, architecture design, and characterization of a new Al/graphite flakes-carbon fibre composite used for thermal management

Silvain Jean-Francois ¹

¹ - Institut de Chimie de la Matière Condensée de Bordeaux (87 Avenue du Docteur Albert Schweitzer, 33608 Pessac, France France)

In the microelectronic industry, the ever increase in power density due to miniaturization of electronic components requires heat sink materials with a high thermal conductivity (TC), a low coefficient of thermal expansion (CTE). Pure metals, such as Al and Cu, have been previously used. However, they have limited TCs and their CTEs are too high being incompatible with those of electronic components leading to failures in service due to thermal fatigue. Regarding this, metal matrix composites have been proven to be promising material where carbon materials, such as graphite, diamond, and carbon fibres, have been introduced as reinforcements because of their excellent thermal properties. In this work, Al matrix composites reinforced with low-cost and easily machinable graphite flakes (hereafter called Al/GF composite) and graphite flakes + carbon fibres (hereafter called Al/GF+CF composite) were developed with the aim to maximize TCs and tailor CTEs close to $6 \times 10^{-6}/K$. The intrinsic TCs of GFs and CFs are highly anisotropic, e.g., in-plane TC of 1000 W/mK for GFs and 600 W/mK for the CFs and out-of-plane TC of 5-10 W/mK, respectively. In this study, a new approach to combining flake powder/powder metallurgy with a step-by-step powder filling process was successfully applied to achieve this conventional 1D/2D arrangement. As such, the highest TC values theoretically predicted can be achieved experimentally. Further, the 2D and 3D arrangements of GFs were made using specifically designed punches in order to tailor the anisotropic CTEs of GFs (e.g., in-plane CTE of $-1 \times 10^{-6}/K$ and out-of-plane CTE of $28 \times 10^{-6}/K$), being unavailable in the 1D arrangement. The 2D arrangement allows to achieve the reduced CTEs being compatible with those of the substrate materials while maintaining a high TCs, demonstrating the strong potential for applications.

Keywords : Metal Matrix Composites, Carbon, Al, Architecture, Physical and microstructural properties

221. Femtosecond laser polishing of pure copper and copper/diamond composites surfaces

Veillere Amelie¹, Silvain Jean-Francois^{1 2}, Lu Yongfeng³, LoubeRe Emmanuel⁴

1 - Institut de Chimie de la Matiere Condensee de Bordeaux (France), 2 - University of Nebraska - Lincoln (United States), 3 - University of Nebraska-Lincoln (University of Nebraska-Lincoln, Lincoln, Nebraska 68588-0511, United States United States), 4 - Institut de Chimie de la Matiere Condensee de Bordeaux (France)

In recent years, femtosecond (fs) laser processing has attracted increasing interest in a wide range of applications, as it offers the possibility to process the surface morphologies of metals and semiconductors. In contrast to other polishing techniques, laser polishing offers a flexible and non-contact solution, thereby avoiding potential external contamination, while enabling a precise selection of processing areas. For pure copper (Cu), we investigated the influence of fs laser parameters on surface roughness and ablation thickness, focusing on the importance of pulse energy and scanning overlap. Using a two-step processing strategy, surfaces with $S_a < 400$ nm were achieved for pure Cu representing a 98 % reduction from the high roughness of 15 μm on initial surfaces. In the case of copper/diamond composite materials (Cu/D) a sidewall polishing method was investigated in order to overcome the difference in ablation threshold between Cu and D. This approach achieved submicronic roughness, reducing the initial roughness of 95%. This research demonstrated the feasibility of directly polishing rough parts using a fs laser, whether with perpendicular and parallel incidence.

Keywords : Femtosecond laser, Laser polishing, Copper, Metal matrix composites, Diamond

222. Effect of Al₂O₃ Particle Size of Al₂O₃/Al Composites Fabricated by ARB Process on Microstructure and Mechanical Properties

Sasaki Gen ¹

1 - Hiroshima University (Japan)

Alumina (Al₂O₃) powders of different sizes (diameters 1.0 micrometer and 0.3 micrometer) were sandwiched between pure aluminum (Al) foils with 0.5 mm in thickness, and then cold-rolled with 50-67% in rolling rate, cut in half, annealed, stacked, and rolled again. This process was repeated up to 10 times to produce 2 vol. % Al₂O₃ particle-dispersed pure Al composites. The particle size and number of repeated rolling cycles were used as parameters to investigate these effects on the Al grain size, and Al₂O₃ particle dispersibility using SEM, EBSD, and X-ray diffraction. And hardness, and tensile properties were investigated. the results showed that the use of finer Al₂O₃ particles improved dispersibility and refined the Al grains with fewer rolling cycles. Accordingly, improvements in hardness and strength were also observed.

Keywords : Accumulative Roll, Bonding Process, Alumina, Aluminium Sheet, Composites, Microstructure, Mechanical Properties

223. Microstructural and Morphological Evolution of Novel In-Situ Al-15%Mg₂Si-4.5%Si Composite with Strontium Addition

Kedir Mohammed¹, Das Prosenjit²

1 - 1Advanced Manufacturing and Materials Processing Laboratory (AMMPL), Department of Materials Engineering, Indian Institute of Science (India), 2 - Advanced Manufacturing and Materials Processing Laboratory, Department of Materials Engineering, Indian Institute of Science (India)

This study investigates the effect of Sr (0.1, 0.15 and 0.2wt.%) modification on the microstructure and morphological evolution of the novel in-situ Al-15%Mg₂Si-4.5%Si composite. The composites were fabricated by gravity assisted low superheat casting technique and characterized via Optical microscope, Xray Diffractogram (XRD), Scanning Electron Microscope (SEM), Electron Probe Microprobe Analyser (EPMA) and XRD texture based equipment. It was found that with the increase of Sr content in the Al-15%Mg₂Si-4.5%Si composite, the morphology of primary Mg₂Si particles changed from irregular dendritic and hopper structure to nearly perfect cubic morphology. The addition of 0.2wt.% Sr reduced the average primary magnesium silicide (Mg₂Si) particle size from ~44μm to 36 μm and the Al grain size from ~58μm to ~45μm, indicating significant grain refinement. The XRD texture analysis through Orientation Distribution Function (ODF) revealed that the cubic texture and the rotated cubic texture are a predominant orientation for Al and Mg₂Si phases, respectively. However, the composite modified with 0.2wt.% Sr exhibited a weak texture and more random grain distribution, highlighting the role of Sr in reducing grain size and promoting uniformity. These findings underscore the potential of Sr addition to improve the microstructural attributes and thereby mechanical properties of the Al-15Mg₂Si-4.5Si composite for advanced applications.

Keywords : Morphology, Magnesium silicide, In, situ composite, Microstructure

224. Thermal properties of carbon-reinforced copper matrix composites produced by powder metallurgy route

Gauthier-Brunet Veronique¹, Charteau MeLanie², Silvain Jean-Francois³, Audurier Valerie², Joulain Anne²

1 - Institut Pprime (Institut PPRIME : Recherche et Ingenierie en Materiaux, Mecanique et Energetique) SP2MI Teleport 2 Boulevard Pierre et Marie Curie BP 30179 86962 FUTUROSCOPE CEDEX France), 2 - Institut Pprime (France), 3 - Institut de Chimie de la Matiere Condensee de Bordeaux (France)

Today, the microelectronics industry uses higher functioning frequencies in commercialized components. These frequencies result in higher functioning temperatures and, therefore, limit the component's integrity and lifetime. Until now, heat-sink materials were composed of metals which exhibit high thermal conductivities. However, these metals often induce large coefficient of thermal expansion (CTE) mismatches between the heat sink and the nonmetallic components of the device. Such differences in CTEs cause thermomechanical stresses at the interfaces and result in component failure after several on/off cycles. Carbon fiber-reinforced copper matrix composites with optimal thermo-mechanical properties are materials of choice for replacing the metallic heat sink materials. However, proper transfer of properties is compromised by the absence of effective interfaces, in the nonreactive Cu/C system. The goal of this work was to synthesize carbon fiber-reinforced copper matrix composites by hot pressing using a solid-liquid coexistent phase process to produce in-situ a ZrC interphase at the Cu/C interface. The addition of zirconium enabled the composite's integrity to be optimized in order to obtain thermally efficient assemblies. The microstructure and chemistry of the matrix, and those of the interphase, were analysed by transmission and scanning electron microscopies. Finally, the thermal properties of the composites were measured at room temperature, both from an experimental point of view (measurement of thermal conductivity) and from a theoretical point of view, thanks to an analytical study of the thermal behavior of the samples.

Keywords : metal matrix composites, powder metallurgy, microstructure, thermal properties, heat, sink.

225. Thermal Conductivity of Functionally Graded Aluminum-Alumina Composites: Experimental Study and Micro-XCT-based Numerical Simulations

Basista Michal, ¹, Sequeira Anil ¹, Weglewski Witold ¹, Bochenek Kamil ¹, Jain Amrita ¹, Hutsch Thomas ², Weissgaerber Thomas ^{2 3}

1 - Institute of Fundamental Technological Research, Polish Academy of Sciences (Poland), 2 - Fraunhofer Institute for Manufacturing Technology and Advanced Materials (Germany), 3 - Institute of Material Science, Dresden University of Technology (Germany)

This research on aluminum matrix FGMs was driven by an application to brake disks, which require advanced materials with improved wear resistance on the outer surface and effective heat dissipation of the graded disk. The AlSi12/Al₂O₃ composite layers with a stepwise gradient in the volume fraction of alumina reinforcement were prepared by hot pressing (HP) and spark plasma sintering (SPS) techniques. The thermal conductivities of the individual composite layers and the FGM specimens were evaluated experimentally and by numerical simulations using finite element models based on micro-computed X-ray tomography (micro-XCT) images of actual AlSi12/Al₂O₃ microstructures. An incongruity was identified between the thermal conductivity of the pure AlSi12 samples consolidated by hot pressing and spark plasma sintering. The primary reason for the disparity in thermal conductivity between the SPS and HP samples was ascertained to be the difference in grain size, as revealed by SEM analysis. The micro-XCT-based FEM simulations incorporated the effects of porosity, thermal resistance, and imperfect interfaces between the AlSi12 matrix and the alumina particles. The simulation results align well with the experimental data for various compositions and FGM structures.

Keywords : Aluminum, alumina FGMs, powder metallurgy, thermal conductivity, micro, XCT, finite element analysis

226. In-situ synthesis of AlN-reinforced hypereutectic Al-Si matrix composites by arc plasma melting for thermal management applications

Choi Jeongwon¹, Lee Je In¹

¹ - Pusan National University (South Korea)

As high-power electronic devices become lighter and smaller, extensive research on the development of Al alloys or Al matrix composites (AMC) has been conducted for heat sink materials due to their excellent thermal properties and high specific strength. Aluminum nitride (AlN) is one of the reinforcements used in AMCs due to its high thermal conductivity and low coefficient of thermal expansion (CTE) similar to that of semiconductors, which are essential for thermal management applications. Here, we report hypereutectic Al-Si matrix composites (20, 30, 40 at.% Si) reinforced with a unique combination of lamellar-structured AlN and discontinuous primary Si. AlN was in situ formed up to 30 vol.% by spontaneous nitridation of molten Al with nitrogen gas by arc melting process within 150 seconds. High compressive strengths were achieved by lamellar-structured AlN. Low coefficient of thermal expansion down to 10 ppm/K was obtained by primary Si and lamellar AlN. These in-situ formed AMCs by arc melting were much different from those by conventional powder metallurgy/stir casting process in that high-fraction AMCs with a unique lamella structure were produced. In this study, we present a design strategy for Al-Si/AlN composites that can be applied for lightweight heat sink materials which satisfy both excellent thermal and mechanical properties.

Keywords : metal matrix composites, aluminum matrix composites, lamellar structure, aluminum nitride, in situ process

227. Composite Anion Exchange Membranes containing a long-side chain ionomer and exfoliated Lamellar Double Hydroxides

Pasquini Luca^{1 2}, Narducci Riccardo^{3 4}

1 - Aix Marseille University, CNRS (MADIREL, SITE ST JÉRÔME, 13397 Marseille France), 2 - International Laboratory (LIME) (France), 3 - University of Rome Tor Vergata (Department of Industrial Engineering, University of Rome Tor Vergata, Rome, Via del Politecnico 1, 00133 Italy), 4 - International Laboratory (LIME) (France)

The low alkaline stability is the main drawback for the large use of anion exchange membranes in fuel cells and other electrochemical energy storage and conversion devices including water electrolyzers.

In this work we report the study of composite anion exchange membranes made from poly(2,6-dimethyl-1,4-phenylene oxide) with quaternary ammonium groups on long side chains (PPO-LC) and exfoliated Mg/Al lamellar double hydroxide as inorganic filler. The composite membranes are fully characterized from different aspects as an application in alkaline based devices, including alkaline fuel cells. The mechanical stiffness of the membranes increases significantly by addition of exfoliated LDH, up to 5%. The ionic conductivity was measured as function of the temperature in fully humidified conditions and also as function of relative humidity. The maximum of conductivity was also observed for 5% LDH. The average activation energy for conductivity amounts to (0.20 ± 0.01) eV in fully humidified conditions and $> 50\%$ RH. The accelerated degradation of the anion exchange membrane in 2 M NaOH at 80°C was investigated measuring the ionic conductivity, water uptake and also by thermogravimetric analysis. A protecting effect by LDH on the alkaline degradation of TMA groups is clearly evidenced making these composite membranes promising for alkaline energy storage and conversion devices.

Keywords : Exfoliated LDH, anion exchange membranes, poly(2, 6, dimethyl, 1, 4, phenylene oxide), alkaline stability.

228. Self-healing electrolytes for stretchable Li-ion microbatteries

Maria Sebastien¹, Chambrial CleMent¹, Rollet Marion¹, Ramuz Marc², Djenizian Thierry², Gigmes Didier¹

1 - Institut de Chimie Radicalaire UMR 7273 (France), 2 - Center of Microelectronics in Provence, Department of Flexible Electronics (France)

Energy storage microsystems composed of thin films have attracted attention to ensure autonomy of complex devices for wearable microelectronics. Recently, we have developed flexible systems as deformation and integration of rigid micropower sources cannot be achieved (Fig.1) (M. Nasreldin et al Energy Stor. Mater. 2020, 33, 108). The technological challenge is to design energy storage devices showing high electrochemical performance with advanced mechanical properties to prevent crack issues during electrochemical and mechanical tests. But in simple flexible micropower sources, the strains experienced by the active materials during bending usually remain well below the typical levels required leading to multiple fractures and subsequent loss of electrical contact. Considering that classical battery elements composed of solid thin films are not suitable, new stretchable electrodes and smart electrolytes bearing mechanical failures must be investigated. Self-healing polymers are a new class of smart materials with the ability to repair themselves after a mechanical damage. This feature is highly interesting for batteries since their lifetime is shortened by mechanical fractures generated during the electrochemical cycling processes. One promising method to obtain spontaneous self-healing is based on supramolecular assembly through dynamic reversible hydrogen bonding. In this context, we have synthesized self-healing electrolytes based on block copolymers for the fabrication of a stretchable lithium-ion microbattery for wearable applications. Indeed, smart thermoplastic elastomers have been developed with a first block composed of ionic conducting poly(ethylene glycol) and monomers that enable quadrupolar hydrogen bonding. Mechanical properties have been provided by a second block, notably with anions covalently attached to backbone to form single-ion conductor copolymers (R. Bouchet et al. Nat. Mater. 2013, 12, 452), ensuring a lithium transference number close to unity. These materials have been achieved in a controlled manner using Reversible Addition-Fragmentation Chain-Transfer (RAFT) in solution and by polymerization-induced self-assembly (PISA).

Keywords : Batteries, Smart materials, Self healing, Polymers

229. Sulfonated Poly(phenylene sulfone)s Ionomers

Kim Jedeok ¹

1 - Jedeok KIM (Japan)

Aiming to achieve carbon neutrality by 2050, safe electricity storage and utilization technologies using renewable energy are required. To achieve these technological developments, each component needs to have high performance. In particular, high performance catalysts and ion exchange polymer materials are key for fuel cells, water electrolysis, and redox flow batteries. Fluorine-based electrolytes such as Nafion are used as ion exchange polymer electrolytes, but the development of alternative electrolytes has attracted attention due to PFAS regulations. We are researching hydrocarbon-based SPPSU ionomers as non-fluorine-based electrolytes. Several SPPSU ionomers with high IEC were synthesized from PPSU polymer and monomer. The SPPSU ionomers from PPSU polymer had a high IEC value of 3.6 meq/g. The SPPSU ionomers synthesized from monomers had an even higher IEC value of 5.6 meq/g. These IEC values are higher than the IEC of Nafion ionomer (approximately 1.0 meq/g), and they are expected to be used as hydrocarbon ionomers. The mechanical properties of the SPPSU ionomer synthesized from the polymer (IEC=3.6 meq/g) were more rigid than those of the SPPSU ionomer synthesized from the monomer (IEC=5.6 meq/g). The mechanical properties of the SPPSU ionomer synthesized from the monomer were similar to those of Nafion, but the young's modulus was two times higher. The conductivity of the SPPSU ionomer synthesized from the monomer at 120°C and RH40% was about four times higher than that of Nafion. In this presentation, we will report on the physicochemical properties of the SPPSU ionomers with high IEC values.

Keywords : Hydrocarbon ionomers, PPSU, Sulfonated poly(phenylene sulfone)s, Electrolytes, High IEC, Membranes, Energy devices

230. Hydrogen absorption characteristics of lithium-cobalt oxide ceramics soaked in water at room temperature

Tsuchiya Bun¹, Kataoka Keisuke, Terasawa Ryosuke, Suzuki Kohtaku, Sasaki Tomoko

¹ - Department of General Education, Faculty of Science and Technology, Meijo University (Japan)

The production of hydrogen molecules (H₂) by splitting water (H₂O), which is a renewable resource, using electrolysis, photo-catalysis, solar energy, and other such methods, is one of the most attractive processes, involving zero emission of carbon dioxide (CO₂). It is important to split H₂O at low temperatures and electric powers and, in addition, to store and release significant amounts of the produced H₂ by spending minimal energy in order to reduce the cost of this H₂ production process. The aim of this work was to investigate the H absorption and desorption characteristics of LiCoO₂ materials soaked in H₂O at room temperature. Thus, the H concentration of LiCoO₂ materials exhibiting H₂O-uptake was investigated in air using weight gain (WG) measurement and ion beam surface analysis, which was combined with high-energy elastic recoil detection (ERD) with 5.1 MeV He²⁺ ion-probe beams. In addition, the release of hydrogen molecules (H₂) and the dissociation temperature were characterized using gas chromatography (GC). In addition, first-principles calculations performed using a density functional theory (DFT) code were also examined to elucidate the most stable sites for trapping H in LiCoO₂ after H₂O uptake. In the present study, the results by WG, ERD, GC, and DFT revealed that the release of H₂ was clearly confirmed by heating the H₂O-soaked LiCoO₂ up to the lower temperatures less than 523 K and, in addition, the production of H₂ might occur owing to the desorption of H atoms from the Li substitutional sites and the recombination of activated H atoms.

Keywords : Water, Hydrogen, Absorption, Desorption, Lithium, cobalt oxides, Elastic recoil detection

231. Research on Ammonia Synthesis by Alkali Metal compounds

Miyaoka Hiroki¹, Tsunematsu Koki, Ichikawa Takayuki²

1 - Natural Science Center for Basic Research and Development, Hiroshima university (Japan), 2 - Graduate School of Integrated Arts and Sciences, Hiroshima University (Japan)

Ammonia (NH₃) is an attractive energy or hydrogen carrier because of the high gravimetric and volumetric energy density. In this work, the NH₃ synthesis processes via catalytic and chemical looping processes by using Li and Na compounds are investigated. To systematically understand the N₂ dissociation properties, the N₂ dissociation temperature and the chemical state of alkali elements were evaluated and compared. As a result, for the Li systems, correlation between the reaction temperature and metallic feature of Li in the compounds was clarified. The compounds with more metallic Li dissociate N₂ molecule at lower temperature. On the other hand, the alloys with more metallic Na showed the higher NH₃ generation rate, and the N₂ dissociation temperature is related to their thermal stability. The chemical looping processes of Li alloys are composed of three step reactions, and NH₃ can be synthesized under atmospheric pressure below 500 °C. By using the chemical looping of LiH, NH₃ is synthesized by two step reactions under atmospheric pressure below 400 °C as well. Furthermore, it was clarified that scaffold materials drastically improved the reaction kinetics by preventing the condensation of reaction products. Since Na nitrides are unstable phases, the Na alloys are not suitable as reactant in the chemical looping processes. However, the Na alloys showed catalysis for the NH₃ synthesis around atmospheric pressure. This work was supported by JSPS KAKENHI, Grant-in-Aid for Scientific Research (B): 20H02465 and (A): 24H00386.

Keywords : Ammonia, Chemical looping, Synthesis, Lithium, Sodium

232. Preparation and application in oxygen reduction reactions of covalently linked MOF-PSU

Di Vona Maria Luisa ¹

¹ - Department of Industrial Engineering, University of Rome Tor Vergeta (Via del Politecnico 1, 00133, Rome Italy)

Metal-organic frameworks (MOFs) have received significant attention as porous materials formed by inorganic metal nodes connected by organic ligands; they nowadays represent one of the most developed families of solid-state materials. The synthesis of Zr-MOF and Fe-MOF covalently bonded with polysulfone trimethylammonium (PSU) anion conductor for electrocatalytic applications will be presented. The synthesis involves anchoring a synthon molecule onto PSU, followed by MOF assembly and subsequent quaternization with a tertiary amine. The samples were characterized by NMR, FTIR, XPS spectroscopies, and thermogravimetric analysis. The resulting electrocatalyst demonstrated high efficiency for the oxygen reduction reaction (ORR). The ORR in acidic conditions requires a potent electrocatalyst, generally from expensive Pt-group metals. Replacing noble metal-based electrocatalysts with highly efficient and inexpensive non-metallic ones is critical for practical applications. In alkaline conditions, where the ORR is less energetically demanding than in acidic media, carbon materials, are available. However, high catalytic activity, high stability and durability, large availability, and low cost are needed. A high amount of 4-electron reduction is revealed with a high onset ($\gg 0.9$ V vs. RHE). We assume this efficiency is due to the high electrochemically active surface area, related to the simultaneous presence of catalytic transition metal ions (Zr or Fe) and ion conducting groups. This work presents a novel strategy for enhancing MOF processability through polymer integration and introduces a pioneering MOF-ionomer electrocatalyst with promising applications in fuel cells.

Keywords : Zr, MOF, ionomer, Fe, MOF, ionomer, electrochemistry, polysulfone, fuel cells.

233. Carbonaceous electrocatalytic materials for the oxygen reduction reaction

Knauth Philippe ¹

¹ - Aix Marseille University, CNRS (France)

The oxygen reduction reaction (ORR) is the main source of overpotential in fuel cells and critical raw and expensive materials, such as platinum are necessary as electrocatalyst in acidic solution. In alkaline media, the oxygen reduction reaction has a faster kinetics and non-noble metal electrocatalysts can be used. In this keynote, we will present some examples of doped and defective carbonaceous material-based electrocatalysts for the ORR. We will discuss the effect of co-doping by nitrogen and other main elements, such as boron, sulfur and silicon 1. The influence of the nitrogen site (graphitic vs pyrrolic/pyridinic) will also be discussed 2. Furthermore, we will investigate the role of an anion-conducting ionomer on the electrocatalytic performance 3. A.R. Nallayagari, E. Sgreccia, L. Pasquini, F. Vacandio, S. Kaciulis, M. L. Di Vona, P. Knauth, Catalytic electrodes for the oxygen reduction reaction based on co-doped (B-N, Si-N, S-N) carbon quantum dots and anion exchange ionomer, *Electrochim. Acta*, 427, 140861 (2022) S. Syahputra, E. Sgreccia, A. R. Nallayagari, F. Vacandio, S. Kaciulis, M. L. Di Vona and P. Knauth, Influence of Nitrogen Position on the Electrocatalytic Performance of B,N-Codoped Carbon Quantum Dots for the Oxygen Reduction Reaction, *J. Electrochem. Soc.* 171, 066510 (2024). A. R. Nallayagari, E. Sgreccia, L. Pasquini, M. Sette, P. Knauth, M. L. Di Vona, Impact of Anion Exchange Ionomers on the Electrocatalytic Performance for the Oxygen Reduction Reaction of B,N Co-doped Carbon Quantum Dots on Activated Carbon, *ACS Applied Materials and Interfaces*, 14, 46537-46547 (2022).

Keywords : Anion Exchange Membranes Fuel Cells, catalytic electrodes, electrochemistry

234. Improving the Thermoelectric Performance of Bi₂Te₃ via Cobalt Doping

Chuang Min-Chen¹, Chen Cheng-Lung², Sheng-Chi Chen^{1 3}, Chou Shang-Wei⁴, Sun Hui⁵

1 - Ming Chi University of Technology (Taiwan), 2 - National Chung Hsing University (Taiwan), 3 - Chang Gung University [Taiwan] (Taiwan), 4 - National Taiwan University (Taiwan), 5 - Shandong University at Weihai [Weihai] (China)

Achieving net zero emissions by 2050 demands substantial advancements in energy efficiency, with thermoelectric materials playing a critical role in waste heat recovery. As global demand for low-carbon technologies grows, recent research has extensively explored bismuth telluride (Bi₂Te₃), known for its topological insulator properties. Studies have shown that magnetic doping significantly enhances the electrical and thermal transport properties of Bi₂Te₃, making it an attractive candidate for thermoelectric applications. This study investigates the effects of cobalt (Co) magnetic doping on the growth and enhanced thermoelectric performance of sputtered Bi₂Te₃ films. Initially, Bi₂Te₃ thin films were fabricated using a co-sputtering technique, with Bi and Te sputtering powers set at 12 W and 20 W, respectively, resulting in films with large grains, precise stoichiometry, and favorable thermoelectric properties. We then varied the Co target power while keeping Bi and Te powers constant to produce Co-doped Bi₂Te₃ films with doping concentrations ranging from 0 to 8.2 at.%. Increasing Co content led to denser films with finer grain structures. While higher Co levels generally raised carrier concentration, films with Co doping levels between 1.9% and 4.7% showed only a modest increase in carrier concentration. The optimal Co concentration was found to be 2.5%, at which the electrical conductivity significantly improved without compromising the Seebeck coefficient, thereby enhancing the power factor. These results demonstrate the ability to precisely control carrier concentration in Bi₂Te₃ thin films through magnetic Co doping, achieving a substantial 26% increase in Power Factor. This research highlights the potential of magnetic doping to optimize thermoelectric materials, establishing a strong foundation for the use of Bi₂Te₃ in high-efficiency waste heat recovery applications. Such advancements may play a pivotal role in achieving future net zero emission goals.

Keywords : Thermoelectric Materials, Thin Films, Sustainable Energy, Bismuth telluride

235. Thermoelectric Properties of Zn-Sb Thin Films Deposited by High-Power Impulse Magnetron Sputtering

Chuang Min-Chen¹, Chen Cheng-Lung², Enzlberger Ludwig³,
BuHler-Paschen Silke³, Heinz Mayrhofer Paul³, Sheng-Chi Chen^{1 4}

1 - Ming Chi University of Technology (Taiwan), 2 - National Chung Hsing University (Taiwan), 3 - Vienna University of Technology = Technische Universitat Wien (Austria), 4 - Chang Gung University [Taiwan] (Taiwan)

Thermoelectric (TE) technology, which can convert heat into electricity and vice versa, is particularly well-suited for applications such as waste heat recovery and thermal management. With the rise of the Internet of Things (IoT), there is an increasing demand for lightweight, thin, and compact devices, including microsensors, processors, and wearables. The zinc antimony (Zn-Sb) alloy, known for its thermoelectric properties at mid-range temperatures, has attracted significant interest. While various methods have been employed for Zn-Sb thin film fabrication, the use of High Power Impulse Magnetron Sputtering (HiPIMS) remains largely unexplored. This study investigates Zn-Sb alloy thin films deposited under different duty cycles using a Zn₄Sb₃ target, with duty cycles ranging from 1 to 100 %. The deposited films were confirmed to have a ZnSb phase crystal structure. Hall measurements revealed that lower duty cycles reduced carrier concentration in the thin films, influenced by controlled pulse parameters. Additionally, lower duty cycles resulted in smoother surfaces and improved the Seebeck coefficient and power factor. The highest power factor, 1.26 mW/mK², was achieved in the sample with a 1% duty cycle at 570K. Integrating Zn-Sb with HiPIMS offers a novel approach to thin-film deposition technology, paving the way for further research and exploration.

Keywords : Thermoelectric Materials, Thin Films, Sustainable Energy, HiPIMS, Zinc Antimony

236. Lithium concentration dependence on water absorption characteristics of lithium-rich zirconates

Tsuchiya Bun¹, Kataoka Keisuke, Terasawa Ryosuke, Busabok Chumphol

¹ - Department of General Education, Faculty of Science and Technology, Meijo University (Japan)

Fuel cell vehicles are environmentally friendly because they utilize hydrogen molecules (H₂) as fuels and emit only water (H₂O). the best method for H₂ production with CO₂ zero-emission must be established in the near future. Given that H₂O is an inexhaustible resource on Earth, H₂O splitting is one of the most ideal and attractive methods for H₂ production. However, the decomposition of H₂O into H and OH requires a large amount of energy. Our group has been investigating a technology to produce H atoms by H₂O splitting at room temperature and subsequently storing the H atoms to realize a H-energy society. Our efforts have revealed that the weight of lithium-zirconium oxide ceramics (Li₂ZrO₃) with a high diffusion coefficient for H increases when left in the atmosphere at room temperature. In addition, a small amount of H₂ is released from air-exposed Li₂ZrO₃ upon heating to temperatures below 523 K using gas chromatography. The reaction of Li, which is segregated to the topmost surface of Li₂ZrO₃ materials, with H₂O may enhance H₂O absorption. To clarify the Li segregation effect in the H₂O absorption of Li₂ZrO₃ materials, the dependence of the H absorption characteristics of Li-rich Li₂xZrO_{2+x} (x = 1.00 and 1.25) €” fabricated at sintering temperatures of 1473 K and 1573 K and subsequently exposed to normal air including H₂O at room temperature €” was investigated. The investigation involved the use of weight gain (WG) measurements, field emission-scanning electron microscopy (FE-SEM), and X-ray diffraction (XRD), Rutherford backscattering spectrometry (RBS), and elastic recoil detection (ERD).

Keywords : Lithium, zirconate materials, Water, Hydrogen, Surface analysis, Rutherford backscattering spectrometry, Elastic recoil detection

237. Enhancing the Electrochemical Stability of Aluminum Current Collectors for High-Voltage Lithium-Ion Batteries

Mahe Leo¹, Richard Caroline¹, Tran Van Francois²

1 - GREMAN (matériaux, microélectronique, acoustique et nanotechnologies) (France), 2 - Physico-chimie des Matériaux et des Electrolytes pour l'Energie (France)

Aluminum foils are widely applied as cathode current collectors for lithium-ion batteries, they still face many challenges, such as weak adhesion with electrode materials and localized corrosion by electrolytes during long-term cycling, which will lead to the degradation of electrochemical performances. Here we investigated the electrochemical behaviors of aluminum current collector compared with graphene and chromium conversion as protective coating in high voltage electrolytes. In our case, we used spin-coating method and a chromium conversion to coat respectively graphene oxide and chromium onto aluminum, creating a thin protective film on the surface of the aluminum current collector. Raman spectra and SEM images were recorded in order to demonstrate the presence and the quality of graphene oxide coating and chromium conversion. Electrochemical characterizations were carried out by linear sweep voltammetry, Tafel plot and chrono-coulometry. The results show that large oxidation current of the aluminum foil in carbonate solutions, while a much smaller current on aluminum with graphene oxide coating and chromium conversion decrease gradually. Consequently, both graphene oxide coating and chromium conversion can inhibit the corrosion of the current collector. All these results indicate that the use of graphene coating and chromium conversion can improve drastically the electrochemical stability of aluminum foil for current collector in high voltage lithium ion batteries.

Keywords : Aluminum foil, Cathode current collector, Lithium ion batteries, Corrosion resistance, Protective film

238. Electrochemical Synthesis of Ni-Co-W-Zr(P) Quinary Medium Entropy Alloy for Enhanced Hydrogen Evolution Reaction

Unni Megha¹, P Nageena¹, Dasaradha Ramarao S¹, Muniyandi Muneeswaran¹, Sha Wei², Jothi Sudagar¹

1 - Vellore Institute of Technology-Andhra Pradesh (VIT-AP) University (India), 2 - Queen's University [Belfast] (Ireland)

Over the course of history, the principles of alloying have evolved, with the past fifteen years witnessing the emergence of high-entropy alloying theory, which has fundamentally transformed our approach to alloy design. Developing cost-effective and efficient electrocatalysts is critical for large-scale hydrogen production via water splitting. The Ni-Co-W-Zr-P alloy coating offers a promising alternative to noble metal-based electrocatalysts. In this study, we developed a Co-W-Zr-incorporated NiP coating using the electroless plating method. By optimizing the composition of Co, W, Zr, Ni, and P, significant charge delocalization was achieved on the surface of the coating. The integration of Co-W-Zr into the NiP matrix notably enhances the number of active sites during the hydrogen evolution reaction. Electrochemical studies revealed that the coating exhibits a low overpotential of 791.9 mV at a current density of 62.8 mA cm⁻². Kinetic parameters were analyzed using Tafel plots and EIS measurements, and a potential mechanism for the hydrogen evolution reaction (HER) was proposed. The coating demonstrated exceptional stability, with no surface degradation even after prolonged electrochemical testing, making it suitable for large or irregularly shaped electrodes required in industrial applications.

Keywords : Electrocatalysts, Water splitting, Electroless method, Charge delocalization, Hydrogen evolution reaction, Electrochemical study

239. High-speed dry cutting performances of Ti(C, N)-(Ti, W, Re)(C, N)-(W-Re) cermet tools with core-rim microstructure against super stainless steel bars

Murakami Takashi¹, Herwan Jonny², Ogura Ichiro²

1 - National Institute of Advanced Industrial Science and Technology (Tsukuba, Ibaraki 305-8564 Japan), 2 - National Institute of Advanced Industrial Science and Technology (Japan)

Super stainless steels have high corrosion resistance and strength, and are used in chemical plants. When these steels are cut at high cutting speeds under dry conditions, the tool tip temperature easily exceeds 1000°C. Therefore, conventional tools such as cemented carbide, which have inferior high-temperature strength, cannot be used for a long time. In our study, we found that the Ti(C, N)-(Ti, W, Re)(C, N)-(W-Re) cermet specimens prepared by blending and hot pressing Ti(C, N), W, and Re submicron powders have a Ti(C, N) core-(Ti, W)(C, N) rim microstructure, and that the cermet specimens exhibit much higher strength at room temperature than the Ti(C, N)-(Ti, W)(C, N)-W cermet specimens prepared by blending and hot pressing Ti(C, N) and W submicron powders. In contrast, the Ti(C, N)-(Ti, W, Re)(C, N)-(W-Re) cermet specimens exhibited the fracture toughness as high as the Ti(C, N)-(Ti, W)(C, N)-W cermet specimens. Furthermore, the Ti(C, N)-(Ti, W, Re)(C, N)-(W-Re) cermet cutting tools showed a lifetime approximately twice that of conventional tools when high-speed dry cutting super stainless steel bars.

Keywords : high, temperature resistant tool material, cermet, cutting performance, powder metallurgy, spark plasma sintering

240. Comparison of practical properties of various practical TiAl alloys for jet engine blades

Tetsui Toshimitsu¹, Mizuta Kazuhiro²

1 - National Institute for Materials Science (Japan), 2 - AeroEdge Co., Ltd. (Japan)

The intermetallic compound-based TiAl alloys TiAl4822 (Ti-48Al-2Nb-2Cr (at.%)) and TNM alloy (Ti-43.5Al-4Nb-1Mo-0.1B) have been used to fabricate last-stage turbine blades for commercial aircraft engines, with 45XD (Ti-45Al-2Nb-2Mn+0.8 vol.% TiB₂) also considered for practical use in the past. TiAl4822 is still widely used today without any major problems. On the other hand, TNM alloy blades have been discontinued due to frequent impact fractures caused by high-speed debris collisions during operation. The main reason for this difference in results is believed to be the difference in operating environment for both alloys, such as engine rotational speed, but the details are not known. It cannot be ruled out that differences in the material properties also played a role. In this study, the practical properties of the aforementioned alloys, required for jet engine blades, were investigated. Impact resistance, which is related to reliability, was evaluated using the Charpy impact test at various temperatures. In particular, the impact resistance of the TNM alloy after oxidation at 700 °C, which is similar to the practical environment, was less than half that of TiAl4822. In addition, since all TiAl blades are manufactured via machining, the machinability, which significantly affects cost and quality, was evaluated. The results revealed that the machinability of TiAl4822 was significantly superior to that of the TNM alloy and 45XD. Based on these results and a comparison of various related material properties, TiAl4822 was determined to be the most suitable TiAl alloy for jet engine blade applications.

Keywords : Titanium aluminides, Impact resistance, Machinability, Jet engine blades

241. Finite Element Analysis of the nanoindentation tests for evaluating Al₂O₃/Ni-base substrate interfacial failure stress

Tabata Chihiro^{1 2}, Maeda Taiyo³, Osada Toshio¹, Ozaki Shingo⁴,
Kawagishi Kyoko¹, Suzuki Shinsuke^{2 5 6}

1 - National Institute for Materials Science, Tsukuba, Ibaraki, 305-0047, Japan. (Japan), 2 - Department of Materials Science, Graduate School of Fundamental Science and Engineering, Waseda University, Okubo, Shinjuku, Tokyo, 169-8555, Japan. (Japan), 3 - Graduate School of Engineering Science, Yokohama National University, Yokohama, Kanagawa, 240-0067, Japan. (Japan), 4 - Division of System Research, Faculty of Engineering, Yokohama National University, Yokohama, Kanagawa, 240-0067, Japan. (Japan), 5 - Department of Applied Mechanics and Aerospace Engineering, Waseda University, 3-4-1 Okubo, Shinjuku, Tokyo 169-8555, Japan. (Japan), 6 - Kagami Memorial Institute for Materials Science and Technology, Waseda University, 2-8-26 Nishiwaseda, Tokyo 169-0051, Japan. (Japan)

Ni-base alloys have excellent high temperature oxidation resistance. However, oxide spallation is observed by the existence of S at a ppm level, caused by the segregation of these impurities at the Al₂O₃/substrate interface. Previous study assessed the changes in interfacial strength using nanoindentation, by comparing the load required to form cracks along the interface. However, how the cracks had formed during the nanoindentation tests was unclear. Therefore, the objectives of this study are to clarify the crack formation mechanism and assess the validity of the nanoindentation technique using the finite element analysis (FEA). The nanoindentation tests were simulated using the commercial software package, LS-DYNA, with the material properties of Ni-9.8 wt.% Al alloy obtained using nanoindentation. The analysis results were compared with the nanoindentation tests to clarify where the interfacial crack propagation had initiated. The maximum principal and shear stresses at the Al₂O₃/substrate interface were obtained, and two-parameter Weibull distributions of interfacial stresses obtained from the FEA were created. Results showed about 0.11 GPa increase in the interfacial stress by the suppression of S segregation by 1.5 at.%. The value of maximum stresses on the interface and its location in relation to the location of the indenter were obtained, which indicated a movement of the indenter from the oxide to the substrate after the crack initiation. The calculated interfacial stresses were the same order of magnitude as the thermal stress between the Al₂O₃ layer and Ni-base substrate at 1100 °C, proving the validity of the nanoindentation testing method and FEA.

Keywords : High temperature materials, FEA, oxidation, nanoindentation, interfaces

242. Fabrication and Bonding Properties of Joints Formed by Transient Liquid Phase Diffusion Bonding Using Electroplated Films

Totsuka Shunsuke ¹

1 - Graduate School of Science and Technology, Gunma University (Japan)

This study investigates the bonding properties of joints fabricated via transient liquid phase diffusion bonding using electroplated films, specifically examining the effects of bonding time on microstructural development and shear strength. Cu and Ni plates were employed as substrates, with Cu electroplating performed initially, followed by Sn electroplating. In the bonding process, a Ni plate was placed onto a Cu plate layered with Cu/Sn electroplating, and joints were formed on a hot plate. Cross-sectional analyses of the fabricated joints were conducted using an Electron Probe X-ray Microanalyzer to evaluate microstructural characteristics. Shear tests were subsequently performed to assess bonding strength. The experimental findings revealed the formation of a reaction layer at the joint interface for bonding times of 3 and 30 minutes. Elemental mapping identified this layer as a Cu-Ni-Sn compound, and the reaction area was observed to expand as bonding time increased. However, with a bonding time of 60 minutes, cracks emerged within the bonded region, resulting in a near-complete loss of bonding integrity. Shear test results showed significant variability in joint strength, which was attributed to void formation within the joint interface.

Keywords : Transient liquid phase diffusion bonding, Cu/Sn electroplating, Bonding strength, Cu, Ni, Sn compound

243. Approach of the Spark Plasma Sintering mechanisms for boron phosphides-based ceramics

Maitre Alexandre¹, Tahan Yves , Pradeilles Nicolas , Rapaud Olivier ,
Le Godec Yann , Moutaabbid Hicham , Rojas Oscar , Durand Olivier ,
Genevois CeCile , Allix Mathieu

1 - Institute of Research for Ceramics (France)

Boron phosphides exhibit exceptional mechanical properties, including high hardness (BP: Hv ~30 GPa, B12P2: Hv ~35 GPa), Young's modulus (> 360 GPa), and remarkably low density (BP: 2.9 g.cm⁻³, B12P2: 2.5 g.cm⁻³). They also present a high thermal conductivity (> 400 W.m⁻¹.K⁻¹ at room temperature). Due to these outstanding properties, these phases are considered promising candidates for various

thermo-structural applications. The understanding of these phases is largely limited in the literature, mainly due to the technical challenges associated with their synthesis and sintering. As a result, their use in industrial applications currently remains limited. More recently, in order to facilitate large-scale production without compromising high purity, innovative synthesis methods such as mechanochemical processes have been developed to produce BP and B12P2. The Spark Plasma Sintering (SPS) behavior of these nanopowders and their microstructural evolution were examined as a function of the physicochemical features of raw powders and the thermal stability of the main compounds. As an example, the mechanism of thermal destabilization for the low temperature boron phosphide phase (BP) has been deeply investigated by coupling TEM and XRD characterizations. This information has been relevant to establish the optimized SPS treatment for manufacturing fully dense specimens. Therefore, SPS mechanisms of boron phosphide-based ceramics were investigated using an analytical model, the densification kinetic obtained under isothermal and isobaric conditions, and TEM characterizations. In addition, mechanical characterizations were carried out on the SPSed parts and yielded promising results, particularly in terms of Vickers hardness, with values close to 35-40 GPa.

Keywords : Boron phosphides, thermal stability, Spark Plasma Sintering, Densification, mechanism

244. Exploring Nb-based alloys for high-temperature structural applications

Park Ki-Seong ¹, Thekkepat Krishnamohan ², Kim Du-Hyun ^{2 3}, Shim Jae-Hyeok ², Lee Seung-Cheol ², Sohn Seok Su ³, Suh Jin-Yoo ⁴, Choi Shi-Hoon ¹, Lee Geun Woo ⁵

1 - Sunchon National University (South Korea), 2 - Korea Institute of Science and Technology (South Korea), 3 - Korea University (South Korea), 4 - Korea Institute of Science and Technology (5, Hwarang-ro 14-gil, Seongbuk-gu, Seoul, Republic of Korea South Korea), 5 - Korea Research Institute of Standards and Science (South Korea)

Nickel-based superalloys are known for their excellent properties as structural metals with heat-resistant characteristics in high-temperature environments. However, they are limited by a melting point below 1300°C. Therefore, in cases where it is challenging to implement separate cooling using a coolant fluid or when the target high-temperature environment exceeds these limits, refractory metals having high melting temperatures can be used as structural materials instead of nickel-based superalloys. While refractory metals offer superior mechanical stability at elevated temperatures due to their high melting points, they also face technical challenges such as poor workability or ductility at room temperature, instability of oxides, and issues arising from high solubility of atmospheric elements like oxygen and nitrogen. Among these, niobium alloys exhibit relatively fewer technical difficulties, making them suitable for specific, limited applications. As a result, alloys for such specialized applications have been developed. This presentation aims to review and summarize existing literature on niobium alloys, discuss their mechanical properties at room and high temperatures through solid-solution strengthening, and explore the computational factors influencing the affinity of interstitial elements like oxygen and nitrogen. With this considered, this study builds a predictive model for the mechanical properties of Nb-based alloys using machine learning (ML) techniques, web-scraped scientific data, and customized feature engineering. Through this, the applicability of niobium alloys was assessed and some candidate alloys were tested experimentally.

Keywords : Nb, based alloy, Mechanical property, Machine learning

245. Removal and Immobilization of Impurities in Direct and Complete Recycling Method for Advanced Ni-base Single Crystal Superalloys

Kawagishi Kyoko¹, Tabata Chihiro^{1 2}, Utada Satoshi¹, Yokokawa Tadaharu¹, Suzuki Shinsuke^{2 3 4}, Harada Hiroshi¹

1 - National Institute for Materials Science, Tsukuba, Ibaraki, 305-0047, Japan. (Japan), 2 - Department of Materials Science, Graduate School of Fundamental Science and Engineering, Waseda University, Okubo, Shinjuku, Tokyo, 169-8555, Japan. (Japan), 3 - Department of Applied Mechanics and Aerospace Engineering, Waseda University, 3-4-1 Okubo, Shinjuku, Tokyo 169-8555, Japan. (Japan), 4 - Kagami Memorial Institute for Materials Science and Technology, Waseda University, 2-8-26 Nishiwaseda, Tokyo 169-0051, Japan. (Japan)

In order to improve the efficiency of gas turbine engines, increase of turbine inlet temperature is most effective. Ni-base single crystal superalloys are applied to the high-pressure turbine blades because of their excellent characteristics in high temperature mechanical and environmental properties, however, increase of the temperature capability of superalloys is still necessary. National Institute for Materials Science (NIMS) has been developing world-leading Ni-base superalloys for the turbine blades and discs. However, high-performance advanced single crystal superalloys contain Re and Ru, which hinder the practical application of the alloys due to their high cost. Therefore, direct and complete recycling" method was proposed with the aim of promoting the practical application of advanced alloys through efficient use of resources and cost reduction. This is a process where used turbine blades are melted in a CaO crucible and impurities such as S, Sb, and Pb contained in the alloy are removed. Ca reacts with the impurities and removes them as slag. It also has another effect of forming compounds with the remaining impurities to suppress segregation at the oxide scale/alloy substrate interface during oxidation. This technique is expected to contribute to reducing the manufacturing costs not only of advanced alloys, but of all other single crystal superalloys.

Keywords : superalloy, recycle, smelting, oxidation, interface

246. TLP Bonding of dissimilar materials

Lopez-Ferreno Inaki¹, Sanchez-Del Rio Laura¹, Cofre Gonzalo²,
Saugo Melisa², Sommadossi Silvana², Straumal Boris³, Poletti
Cecilia⁴, Lopez Gabriel A.¹

1 - Physics Department, University of the Basque Country UPV/EHU, Leioa, 48940, Spain (Spain), 2 - Research Institute of Engineering Sciences and Technologies IITCI CONICET-UNCo, Comahue National University, 8300-Neuquen, Argentina (Argentina), 3 - Institute Osipyan Institute of Solid State Physics, Russian Academy of Sciences, 142432-Chernogolovka, Rusia (Russia), 4 - Institute of Materials Science, Joining and Forming, Graz University of Technology, 8010-Graz, Austria (Austria)

Transient Liquid Phase bonding (TLP) is an innovative technique used to join identical or dissimilar materials. This method is based on the formation of a liquid interfacial layer promoting a diffusion-reaction process to produce the formation of a thin, high-quality bond using a filler layer between both substrates. However, the selection of the parameters of the process influence directly the mechanical properties and corrosion resistance of the joints, which are crucial in industrial high-temperature applications or in the medical field. The quality of the bonds relies on the different phases and/or intermetallics formed in the joint zone. Usually, it can be divided into three regions, namely, the isothermally solidified zone (ISZ), the athermally solidified zone (ASZ) and the diffusion-affected zone (DAZ). Using Al and Nickel_braze HTN2 as thin filler materials, we bonded dissimilar substrates, like stainless steel SS316, Ti-Al6-V4 and Inconel 718, at high temperatures using a Gleebe machine. We characterise the microstructure and analyse the formed phases to optimise the process variables and ensure the joints' integrity. We use high-resolution techniques such as TEM and SEM-EDS-EBSD to characterise the thin interfacial diffusion reaction. Therefore, preparation of selected lamellas by Focused Ion Beam (FIB) is mandatory. The results show that the ISZ forms at the early stages of joining and disappears at longer treatment times. This zone is critical for the corrosion resistance of the final joint.

Keywords : Transient Liquid Phase Bonding, Bonding of dissimilar materials, FIB, TEM, SEM

247. Harnessing Nanostructure Control: Strategies for Enhanced Performance in Ni-based Superalloys

Rielli Vitor ¹

1 - UNSW Sydney (Australia)

The performance of advanced high-temperature alloys is critically dependent on the interplay between their processing parameters, microstructural evolution, and resulting mechanical properties. This talk will explore cast-and-wrought materials alongside additively manufactured components of Ni-based superalloys, investigating phenomena such as nanoscale precipitation, phase transformations, and segregation at interphase boundaries. High-resolution characterisation techniques provide insights into the co-precipitation of strengthening phases, their morphological evolution, and chemical partitioning. Key findings demonstrate how variations in strain rate, deformation temperature, and cooling strategies influence the distribution and kinetics of nanoscale features. The role of geometrically necessary dislocations and grain boundary segregation further highlights the importance of optimising processing parameters to achieve desired performance. A collection of recent studies, covering alloys such as IN718, IN738, and Rene 65, contributes to refining predictive models for microstructural evolution and offers strategies to mitigate property heterogeneities[1€3]. These findings enable tailored processing techniques to enhance high-temperature capabilities, supporting the advancement of aerospace and other critical applications. By addressing challenges posed by demanding operational environments, this research underscores the potential for innovative alloy design and scalable manufacturing practices to meet emerging engineering needs. [1] V. V Rielli, E. Farabi, F. Godor, C. Gruber, A. Stanojevic, B. Oberwinkler, S. Primig, Mater Des 241 (2024) 112961. [2] V. V Rielli, T.D. Pham, F. Godor, C. Gruber, A. Stanojevic, B. Oberwinkler, S. Primig, Materials Science and Engineering: A 913 (2024) 147069. [3] V. V Rielli, M. Luo, E. Farabi, N. Haghdadi, S. Primig, Scr Mater 244 (2024) 116033.

Keywords : Ni, based superalloys, microstructural evolution, nanoscale precipitation, thermo, mechanical processing.

248. Thermodynamic assessment and calculations of Mo-Si-B-Ti-C system for ultra-high temperature materials

Oikawa Katsunari¹, Nobufumi Ueshima

1 - Tohoku University (Aoba 6-6-02, Aramaki, Aoba-ku, Sendai, 980-8579 Japan)

MoSiBTiC alloys are expected to be ultra-high temperature alloys. In this study, a thermodynamic assessment of the binary and ternary systems constituting the Mo-Si-B-Ti-C system was conducted based on the CALPHAD (Calculation of Phase Diagrams) approach and thermodynamic database was constructed to predict the phase equilibria of MoSiBTiC alloys. Liquid phase was approximated by the association model and bcc, fcc, hcp and intermetallic compounds were approximated by the compound energy model. The calculated phase equilibrium of binary and ternary can reproduce the previous experimental data. Thermodynamic calculations for MoSiBTiC alloys were also performed. As a result, the precipitation temperature and process during solidification could be reproduced the experimental results. The primary crystal surface was also reproduced. This database can be used for the development of MoSiBTiC alloys.

Keywords : CALPHAD, Phase diagram, Liquidus surface

249. Improvement of High Temperature Strength of Cr-Co-Ni Medium Entropy Alloy By Precipitation of Gamma-Prime Particles

Tanaka Katsushi¹, Yoshioka Keiki¹, Teramoto Takeshi¹

¹ - Kobe University (Japan)

Equiatomic Cr-Co-Ni medium entropy alloys have superior mechanical properties, especially for low temperatures, but the yield stress decreases significantly at high temperatures. One way to strengthen a material while minimizing the loss of elongation is to introduce inclusions into the material. In this study, gamma prime precipitates are introduced into a nearly equiatomic Cr-Co-Ni matrix by co-alloying with Al and Ti. The solvus temperature of gamma-prime precipitates is about 950°, and significant strengthening is observed below the solvus temperature. The introduction of gamma prime precipitates with the volume fraction of approximately 40% increases the yield stress at room temperature from 310 to 820MPa, and the strength is maintained up to 700°. At 1000°C, the gamma prime precipitates disappear and the yield stress becomes approximately the same as that of Cr-Co-Ni alloys. This alloy does not contain heavy elements such as Mo or W, making it suitable for use as a lightweight, high-temperature structural material.

Keywords : Multi, principal alloys, Precipitation hardening, L12 compound, Lightweight alloy, Yield stress anomaly.

250. Microstructures and Mechanical Properties of Directionally Solidified $\text{TM}_5\text{Si}_3/\text{TM}_2\text{Si}$ (TM = Mo, Nb)-Based Eutectic Composites

Kishida Kyosuke¹, Inui Haruyuki¹

¹ - Kyoto University (Japan)

Eutectic composites composed of intermetallics and/or ceramics with very high eutectic temperatures have been considered as attractive materials for ultra-high temperature structural applications because of their high melting temperature, high structural stability and good mechanical properties. Recently, we have systematically investigated microstructure-property relationship of directionally solidified (DS) ingots of $\text{Mo}_5\text{Si}_3/\text{C11b}$ eutectic composites with very high eutectic temperature ($\sim 1900^\circ\text{C}$) and have revealed that their high-temperature strength and room-temperature fracture toughness can be improved simultaneously by optimization of microstructure and interface properties through controlling growth condition and ternary/quaternary alloying. These results open a new possibility to develop novel structural materials endowed with excellent high-temperature strength and good room-temperature fracture toughness by utilizing interphase boundaries. As another example along this line, we have investigated microstructure variation of DS ingots of $\text{Nb}_5\text{Si}_3/\text{Nb}_2\text{Si}$ eutectic composites as a function of ternary Mo addition. When Mo is alloyed more than 2 at. %, we have successfully obtained DS eutectic composites of $\text{C40-(Nb,Mo)}_2\text{Si}$ and $\text{D8m-(Nb,Mo)}_5\text{Si}_3$ with a fine eutectic microstructure of the so-called script-lamellar type, which is similar to those observed in $\text{Mo}_5\text{Si}_3/\text{C11b}$ DS eutectic composites. Characteristics of microstructures (orientation relationships, interface structures etc.) and mechanical properties (high-temperature mechanical properties and room-temperature fracture toughness) of the $\text{C40-(Nb,Mo)}_2\text{Si}$ and $\text{D8m-(Nb,Mo)}_5\text{Si}_3$ DS eutectic composites will be presented.

Keywords : Transition metal silicides, Eutectic composites, Directional Solidification, Mechanical Properties, Fracture toughness

251. Grain boundary engineering in the cast & wrought Ni-based superalloy Rene 41 with microalloying additions

Primig Sophie¹, Theska Felix², Street Steven³, Lison-Pick Michael³

1 - School of Materials Science & Engineering, UNSW Sydney, NSW 2052 (Australia), 2 - School of Materials Science & Engineering, UNSW Sydney, NSW 2052 (Australia), 3 - Western Australian Specialty Alloys (Australia)

The excellent high-temperature properties of cast & wrought Ni-based superalloys are brought about by their complex microstructures of a γ -matrix, intra- and intergranular γ' precipitates, carbides, and borides. High-alloyed grades such as Rene 41 provide the high-temperature strength required for next generation gas turbine engines. Yet, their processability remains limited due to grain boundary (GB) cracking. A common mitigation approach is microalloying with B and C. However, the roles of microalloying elements in controlling the GB microstructure (segregation, precipitation) and properties (cracking, cohesion) remain largely unexplored. This talk summarizes recent results on GB microstructure engineering in microalloyed Rene 41. We show that B additions reduce ductility but slow down grain growth more effectively than C. GB-M₂B, carbides, and GB- γ' precipitates decorating GBs and differences in interfacial solute segregation are revealed via atom probe microscopy. B is captured by GB-M₂B, making it unavailable to improve GB cohesion. C depletion at interphase boundaries is shown to control GB cracking. We assess potential mechanisms for the onset of GB cracking via in-situ tensile testing and crystal plasticity, revealing no direct correlation between equivalent strains and stresses and cracking susceptibility. However, we find a correlation between low interfacial excess of B and Mo and severe decohesion at γ -matrix / GB-M₂B interfaces. In contrast, GB microstructures with GB- γ' encapsulating GB-M₂B preserve high interfacial excess of B and GB cohesion. We propose a precipitation-controlled GB engineering approach for Rene 41 and Ni-based superalloys with limited formability, via formation of GB serrations and precipitation upon slow cooling.

Keywords : Ni, based superalloys, processability, grain boundary engineering, gas turbine engines

252. Plastic deformation property of miu-Fe₇Ta₆ topologically close-packed intermetallic compound

Chen Zhenghao¹, Kishida Kyosuke¹, Inui Haruyuki¹

¹ - Kyoto University (Japan)

Heat-resistant steels are widely used in the energy production industry. Due to the ongoing demand to improve the creep properties further, adding more and more alloying elements is required. As a result, the topologically close-packed (TCP) phases inevitably precipitate in these heat-resistant steels during a long time of service. Recently, Takeyama et al. pointed out that these TCP phases could contribute to enhancing the grain boundaries and thus improving the creep properties by controlling the precipitation morphologies. Therefore, a new need to understand the deformation behaviors of these phases is arising nowadays. Among the category of TCP phase, the A₂B-type Laves phase with C₁₄, C₁₅, or C₃₆ structures and the A₇B₆-type miu phase are the most observed phases in long-served heat resistance steels. These TCP phases show a similarity in crystal structure in that they share the same unit layer, but the stacking consequence of these unit layers is different. For example, the crystalline structure of miu phase can be treated as an alternative stacking of a C₁₄-type laves unit and a Zr₄Al₃ unit. Hence, knowing the difference in the deformation behavior of these two phases concerning the structural similarity is of great interest, industrially and scientifically. In the present study, we investigate the room temperature deformation behavior of the miu-Fe₇Ta₆ phase and the C₁₄-Fe₂Ta phase via micropillar single-crystal compression. We identify the operative slip systems, their CRSS, and dislocation fine structures and discuss the effect of the crystal structure on the deformation behavior of these TCP phases.

Keywords : Heat resistant steel, Laves phase, micropillar, operative slip system, dislocation structure

253. Hot deformation capability and processing window of powder-HIPed TNM alloy with full lamellar microstructure

Xu Xiaoxuan¹, Yu Yonghao¹, Zhang Zilong¹, Wang Yarong¹, Wang Guodong¹, Kou Hongchao¹

¹ - State Key Laboratory of Solidification Processing, Northwestern Polytechnical University (China)

Due to the addition of beta stabilizing elements, the microstructure of TNM alloys retains beta phase and the hot workability was significantly improved. However, the beta phase will precipitate in alpha lamellae and transformed to the omega phase in the service, leading to the deterioration of lamellar stability and creep resistance. Preliminary studies shows that powder hot isostatics pressing can prepare the TNM alloy with less beta phase (~0.3%) and full lamellar microstructure. Therefore, the hot deformation capability and the processing method to refine the coarse initial lamellar colonies of powder-HIPed TNM alloy need to explore urgently. In this work, the hot compressions of powder-HIPed TNM alloy under the conditions of (1100~1250),,f deformation temperatures and (0.01~1)s-1 strain rates were conducted. The powder-HIPed TNM alloy exhibits greater deformation resistance than casting TNM alloys and has lower hot deformation activation energy. The flow instability will occur in the deformed specimens of TNM alloy when deformation temperature is selected lower than the temperature of eutectic reaction or the gamma phase volume fraction before deformation is higher than 65%. In the processing safety zone, the lamellar colonies are broken incompletely after hot compressions at 1100~1200 °, which seriously affects the homogeneity of microstructures; while the initial lamellar colonies can be completely broken and are refined about 50% after compression at 1250 °/0.1s-1 and 0.01s-1. Thus, the optimum hot processing window of powder-HIPed TNM alloy for obtaining a uniform deformed microstructure is (1210~1250),,f/(0.01~0.2)s-1.

Keywords : TiAl alloys, Hot Processing Window, Deformation capability, Dynamic softening

254. Influence of grain boundary serration on creep properties in Nickel based superalloy Nimonic 80A

Kim Ka Yeong¹, Lee Je In¹

1 - School of Materials Science and Engineering, Pusan National University (South Korea)

In the power generation industry, it is important to improve efficiency of power plant to reduce carbon dioxide emissions. Most of thermal power plants are being replaced by combined cycle power plant (CCPP), and its turbine inlet temperature has been increased to improve the efficiency. Currently, Ni-based superalloys have been used for steam turbine blades for CCPP. The materials used in the turbine blades should withstand higher temperatures, so their creep properties need to be improved. Because grain boundaries of Ni-based superalloys are the path for crack propagation at elevated temperatures, we tried to control the morphology of grain boundaries in the superalloys. The alloy used in this study is Nimonic 80A, which is one of the forged precipitation-hardening polycrystalline Ni-based superalloys. In this study, multi-stage heat treatment was designed to include high-temperature solution treatment followed by slow cooling and low-temperature aging treatment. During the slow cooling step, we found that M23C6 carbides precipitated at the grain boundaries and the particles resulted in the serration of the boundaries. Creep tests were conducted at 750 ° for 260 MPa to investigate the effect of grain boundary serration. The alloys with serrated boundaries showed 23 % increase in the creep life compared to conventional Nimonic 80A alloy. We found that the length of cracks under the fracture surface was much shorter in the alloys with grain boundary serration, which was responsible for the delay of crack propagation.

Keywords : Ni based superalloy, grain boundary serration, heat treatment

255. Synthesis, characterization and physical properties of a $\text{Ti}_2\text{NbAlC}_{1.82}$ ternary nanolaminated carbide

Dubois Sylvain¹, Berrabah Mohammed¹, Cabioch Thierry¹,
Gauthier-Brunet Veronique¹, Chartier Patrick¹

¹ - Institut Pprime (France)

We report on the synthesis of $[\text{Ti}_2\text{Nb}]\text{AlC}_{1.82}$ MAX phase by hot isostatic pressing starting with sub-stoichiometric titanium carbide, niobium and aluminum powders. In addition to a few TiC impurity, $\text{Ti}_2\text{NbAlC}_{1.82}$ is formed. It is demonstrated that the 312 phase is mainly formed at high temperature. The weight percent of $[\text{Ti}_2\text{Nb}]\text{AlC}_{1.82}$ is about 6% at 1450°C and reaches 98% at 1580°C. At low temperature, the main phases are $\text{Ti}_{0.3}\text{Nb}_{0.7}\text{Al}_3$, $\text{Ti}_{0.6}\text{Nb}_{0.4}\text{AlC}_{0.91}$, TiC, NbC and/or $\text{Ti}_{1-x}\text{Nb}_x\text{C}$. Mean lattice parameters ($a=0.310087[5]$ nm and $c=1.86138[4]$ nm) are deduced from Rietveld refinement of X-ray diffraction patterns. Standard deviations of the a and c parameters, respectively 0.00007 and 0.007 nm, allows demonstrating that $\text{Ti}_2\text{NbAlC}_{1.82}$ is not a line compound but a disordered solid solution. Nb, Ti and Al contents are determined from Energy Dispersive X-ray analysis. Thermal and Electrical conductivities, Seebeck coefficient are measure as a function of temperature. Hall measurements allows determining the charge carrier density and mobility. Magnetoresistance measurements allow demonstrating that the Kohler's rule is obeyed thus implying that magnetoresistance is proportional to the square of the charge carrier mobility.

Keywords : MAX phases, solid solution, electronic transport properties, X, ray diffraction, Rietveld refinement

256. Novel spray-pyrolysis-based synthetic strategy for uniformly distributed oxide nanoparticles-dispersion-strengthened refractory alloy

Jeong Hyun Kim¹, Hee Yeon Jeon¹, Jongmin Byun¹, Lee Young-In¹

¹ - Department of Materials Science and Engineering, Seoul National University of Science and Technology (South Korea)

Conventional mechanical alloying processes for oxide dispersion strengthened (ODS) refractory alloys have reached certain limits in further improving their properties. In this study, we successfully demonstrated the ultrasonic spray pyrolysis (USP) technique combined with hydrogen reduction to synthesize ODS W alloy powders with uniformly dispersed Y₂O₃ nanoparticles. The synthesized powders exhibited micro-sized secondary particles composed of primary particles with a size of about 30 nm. Thus, they secured both formability and sinterability, essential for producing high-quality sintered bodies. Sintered specimens were fabricated using conventional uniaxial compression and pressureless sintering to confirm the size and distribution of Y₂O₃ nanoparticles. After sintering, they exhibited a grain size of approximately 3 μ m and a relative density of more than 96%, and Y₂O₃ nanoparticles with a size of approximately 50 nm were uniformly dispersed. In addition, they show an excellent hardness of approximately 7.2 GPa. These results indicate the successful synthesis of ODS W powder with a desirable structure. They highlight its potential in various applications, particularly those requiring high-quality sintered bodies with enhanced mechanical properties.

Keywords : W, Y₂O₃ alloy, Ultrasonic spray pyrolysis, Microstructure, Sintering behavior, Mechanical properties

257. Age-hardening behavior of Ni rich high entropy conventional alloy after cold rolling and flash annealing

Jangra Pooja¹, Dutta Akshit¹, Nene Saurabh¹

¹ - Advanced Materials Design and Processing Group, Department of Metallurgical and Materials Engineering, Indian Institute of Technology Jodhpur, Karwar, Jodhpur, Rajasthan 342030, India (India)

Ni-based superalloys are known for good precipitation hardening ability due to the formation of γ' and γ'' precipitates at relatively higher temperature aging. Similar trend was seen in high entropy superalloys (HESA), however at the expense of higher density and cost. Thus, this work is an attempt to attain a similar precipitation-strengthening effect in novel Ni-rich compositionally lean but configurationally random high entropy conventional alloy (HECA). In line with that, we designed Ni-based Ni₇₀Fe_{12.5}Al_{7.5}Cr_{4.75}Mn_{4.75}Si_{0.5} (Ni-HECA), which exhibits a configurational entropy of $\sim 1R$ in spite of having compositionally lean contents of constituent elements in comparison with classical HESAs. Ni-HECA is successfully fabricated using arc melting followed by cold rolling (CR) to 90% reduction. The aging behavior of Ni-HECA is studied systematically at 700°C & 800 °C for varying times after flash annealing of CR specimen at 1100 °C for 2 mins. Ni-HECA showed excellent strength ductility synergy after aging 800 °C for 2 hrs, which is also confirmed by the peak hardening at the same condition in hardness vs aging time curve. Hence, this work confirms a similar precipitation strengthening effect in Ni-HECA due to the formation of Ni-Al-Si type precipitate as confirmed by XRD and thermodynamic modeling.

Keywords : High entropy conventional alloy, precipitation strengthening, Aging, flash annealing

258. Diffusion in high-entropy alloys: sluggish or anti-sluggish? Lattice structure vs. chemical complexity

Divinski Sergiy ¹

¹ - Institute of Materials Physics, University of Munster (Germany)

Single-phase multi-principal element alloys, termed as high-entropy alloys (HEAs), provide a new design concept for materials development. The sluggish diffusion concept, considered originally as one of the core effects of HEAs, boosted an interest from many diffusion groups and helped to generate an extensive data set. In this overview, the current state-of-the-art of diffusion research in the multi-principal element alloys is presented, with a focus on own results with respect to the radiotracer diffusion measurements. A geometric mean of the tracer diffusion coefficients in pure metals is proposed to use for a systematic comparison. Whereas tracer diffusion might be considered as sluggish when the diffusion rates in FCC CoCrFeMnNi HEA are analysed, the concept becomes ambiguous when the element diffusivities in the FCC (Ni)_x(CoCrFeMn)_{1-x} alloys are considered. In BCC HfTiZrNbTa and HfTiZrNbV HEAs, self-diffusion rates are not retarded with respect to the diffusivities in unary BCC elements. In HCP AlHfScTiZr HEAs, Ti diffusion is significantly enhanced with respect to that in pure HCP elements, even when considered at the same homologous temperatures. The interplay of crystalline structure, lattice distortions and diffusion rates in multi-principal element alloys is discussed. A novel augmented tracer-interdiffusion couple approach for high-throughput measurements of concentration-dependent atomic mobilities is presented and its application to multi-principal element alloys is exemplified.

Keywords : Thermec'2025, High, entropy alloys, diffusion, lattice distortions, point defects

259. Novel FeNiMnAlCr Multi-Principal Component Alloys

Baker Ian ¹

1 - Thayer School of Engineering (14 Engineering Drive, Hanover, NH 03755 United States)

FeNiMnAlCr multi-principal component alloys have been under development since 2004 with a focus on producing economical alloys for both high-temperature and cryogenic applications. Four different types of FeNiMnAl(Cr) microstructures have been developed: ¹ ultrastrong, ultrafine (5-50 nm) spinodally-formed microstructures in Fe₃₀Ni₂₀Mn₂₀Al₃₀, Fe₂₅Ni₂₅Mn₂₀Al₃₀ and Fe₃₅Ni₁₅Mn₂₅Al₂₅ consisting of (Fe, Mn)-rich B2-ordered (ordered b.c.c.), and (Ni, Al)-rich L21-ordered (Heusler) phases, and in Fe₃₀Ni₂₀Mn₂₅Al₂₅ consisting of (Ni,Al)-rich B2 and (Fe,Mn)-rich b.c.c. phases, aligned along ; ² strong but brittle fine eutectoid microstructures in Fe₃₀Ni₂₀Mn₃₀Al₂₀, Fe₂₅Ni₂₅Mn₃₀Al₂₀, and Fe₂₈Ni₁₈Mn₃₃Al₂₁ consisting of alternating (Fe, Mn)-rich f.c.c. and (Ni, Al)-rich B2 plates with an orientation relationship close to f.c.c.(002)//B2(002): f.c.c.(011)//B2(001); ³ strong, ductile lamellar eutectic microstructures present in Fe₃₀Ni₂₀Mn₃₅Al₁₅, Fe₂₉Ni₁₉Mn₃₈Al₁₄ and Fe₃₁Ni₁₈Mn₃₈Al₁₃ consisting of alternating (Fe, Mn)-rich f.c.c. and (Ni, Al)-rich B2 phases with a Kurdjumov-Sachs orientation relationship between the phases. Cr was also added to some alloys; and ⁴ a very-ductile single-phase f.c.c. alloy Fe_{40.4}Ni_{11.3}Mn_{34.8}Al_{7.5}Cr₆. The effects of temperature on the quasi-static mechanical properties have been studied at temperatures from 4.2 K to 1073 K. The creep behavior and dry sliding wear behavior have also been studied at a variety of temperatures The effects of nitriding; solute additions such as titanium or interstitials such as carbon or boron; recrystallization, and production by additive manufacturing have been explored. This paper will outline the microstructures (before and after mechanical testing) and mechanical properties of these alloys along with current applications that are being pursued in concentrated solar power and for cryogenic use.

Keywords : High entropy alloys, multi, principal component alloys, additive manufacturing, mechanical properties

260. Hierarchical Nanotwin-Driven Mechanism in Cryogenically-Deformed CoCrFeNi Hea Alloys

Chung Tsaifu¹, Chiu Po-Kai², Hsiao Chien-Nan², Yeh An-Chou³

1 - Department of Materials Science and Engineering, National Yang Ming Chiao Tung University, Hsinchu, Taiwan (Taiwan), 2 - National applied research laboratories, Taiwan Instrument Research Institute, Hsinchu, Taiwan (Taiwan), 3 - Department of Materials Science and Engineering, National Tsing Hua University, Hsinchu (Taiwan)

The cryogenic mechanical performance of face-centered cubic (FCC) high entropy alloys (HEAs) presents substantial promise for strategic applications. Herein, we employ transmission electron microscopy (TEM) to characterize the hierarchical nanotwin microstructural evolution in post-deformed FeCoNiCr HEA under true strain at cryogenic temperatures, contrasted with its room temperature response. Deformation at 25 °C initiates with wavy dislocation entanglement, transitioning to planar dislocation structures, dislocation walls, and deformation nanotwins. At -150 °C, in contrast, extensive nanotwin bundling occurs via deformation nanotwin coalescence, segmenting the matrix into microscale closed blocks. Increased true strain induces dense deformation nanotwins, refining annealing micro/nano twins to nanoscale closed blocks. Within these annealed twins, deformation twin variants interpenetrate, resulting in serrated, curved interfacial structures. These distinctive interfaces promote ultra-fine deformation nanotwins and closed blocks, enhancing strain accommodation at cryogenic temperatures. This work provides crucial insights and a framework for designing FCC HEAs with a hierarchical nanotwin-driven mechanism optimized for cryogenic applications.

261. High Entropy Alloys for Applications in Hydrogen and Cryogenic Environments

Na Young Sang¹, Kim Young-Kyun¹, Lee Jae-Ho¹, Jeon Seung-Min¹

¹ - Korea Institute of Materials Science (South Korea)

Extreme environments such as hydrogen and cryogenic conditions are gaining attention as application field for high-entropy multi-component alloys. The CoCrFeMnNi equiatomic alloy, also known as the Cantor alloy, is the most representative high-entropy alloy, with numerous studies reporting its excellent hydrogen embrittlement and cryogenic toughness. However, the high cost of elements like Co and Ni has always raised questions about the alloy's commercial viability. Additionally, the lack of experience in large-scale manufacturing technology for high-entropy alloys poses a barrier to commercialization. In this study, we aimed to design a cost-effective alloy based on the composition of the Cantor alloy, develop large-scale manufacturing process technology, and ultimately assess the feasibility of commercialization in hydrogen and cryogenic environments. Large-scale Cantor-alloy ingots, plates, tubes and wires could be successfully manufactured without any macro-scale compositional inhomogeneity, which can be occur in equiatomic alloy systems. In this presentation, our efforts to commercialize high-entropy alloys to hydrogen and cryogenic environments will be given in terms of low-cost alloy design, development of manufacturing process and property measurements in hydrogen or cryogenic environments.

Keywords : high entropy alloys, multicomponent alloys, Cantor alloy, hydrogen, cryogenic

262. Advancements in high-entropy alloys through the liquid metal dealloying process

Joo Soo-Hyun ¹

¹ - Dankook university (South Korea)

Liquid metal dealloying (LMD) is an innovative metal processing technique first reported in 2011, gaining significant attention for its unique phenomena and exceptional properties. Unlike traditional chemical dealloying, which is restricted to noble metals, the LMD process utilizes molten metal baths with low oxygen content, making it the only feasible approach for producing three-dimensional, nanoscale interconnected structures from non-noble metals. Through the LMD process, various materials—including C, Si, Nb, Fe, stainless steel, Ti, and Ti alloys—have been fabricated into 3D interconnected microstructures, which offer extensive interfacial surface areas suitable for applications in catalysis, capacitors, and sensors. To date, LMD research has predominantly focused on the development of 3D interconnected structures from simple metals or binary alloys. Future studies are anticipated to emphasize property enhancement and broadened application potential through the addition of alloying elements. This presentation provides recent insights into the fabrication processes and properties of various 3D interconnected nanostructured high-entropy alloys produced via the LMD process.

Keywords : high, entropy alloy, liquid metal dealloying, 3D interconnected microstructure

263. Heterogeneous Structured High Entropy Alloys

Kim Hyoungseop^{1 2}

1 - Pohang University of Science and Technology (South Korea), 2 - Tohoku University [Sendai] (Japan)

Recent decades have seen the development of innovative approaches to enhance the strength-ductility synergy through heterogeneous microstructures, including gradient, harmonic, lamellar, bimodal, hierarchical nanostructures, and partially recrystallized configurations, which have proven effective in addressing the strength-ductility trade-off. However, conventional alloy design principles constrain the discovery of new compositions with desirable strength-ductility combinations, even when advanced microstructural strategies are employed. The emergence of multi-principal element alloys, known as high entropy alloys (HEAs) and medium entropy alloys (MEAs), has significantly expanded the compositional landscape, creating new possibilities for alloys with exceptional properties. In this presentation, various heterostructuring strategies developed at POSTECH to enhance the strain hardening and strength of HEAs, including sequential deformation-induced martensitic transformation in MEAs, twinning-induced plasticity HEAs, immiscible multi-phase MEAs, surface nanostructuring, maraging MEAs, segregation-engineered HEAs, multi-scale gradient-structured HEAs, and partially recrystallized HEAs are demonstrated. Additionally, various processing methods for fabricating HEAs/MEAs and the properties of the resulting materials are introduced.

Keywords : High, entropy alloys, Heterogeneous microstructure, Hetero, deformation induced strengthening, Strain hardening, Tensile behavior

264. Application APT to Understand High-Entropy Alloy and Materials

Sha Gang ¹

1 - Nanjin University of Science and Technology (Xiaolingwei 200#, Nanjing 210094 China)

High-entropy alloys (HEAs) have garnered significant research interest due to their exceptional properties, including high strength, good ductility, superior thermal stability, corrosion resistance, and radiation resistance. These remarkable properties stem from the unique and complex microstructures of HEAs. Understanding these microstructures at the atomic level is crucial for guiding alloy design and optimizing processing parameters. Atom probe tomography (APT), with its high spatial resolution and chemical sensitivity, enabling the detection of individual atoms, has become an indispensable tool for characterizing the complex elemental distributions in HEAs. This presentation will highlight our recent work applying APT to investigate HEAs with excellent mechanical and physical properties. Specifically, I will discuss findings from new multi-phase HEAs with eutectic microstructures, selected nanoprecipitates, and nanoscale compositional undulations, focusing on how APT reveals the relationships between these microstructural features and the desirable combination of strength and ductility.

Keywords : APT, HEA, Nano, precipitates, Compositional Undulation, Multiphase

265. Development of Non-Equimolar CoCrCuFeNi High Entropy Alloys for Aerospace Brazing

Ross Samuel¹, Butcher Daniel¹, Mehraban Shahin¹, Goddard Caroline², Cookson Peter², Lavery Nicholas¹

1 - MACH 1, Swansea University, Faculty of Science and Engineer, Swansea, SA1 8EN, Wales, United Kingdom (United Kingdom), 2 - Reaction Engines Ltd, Building F5, Culham Science Centre, Abingdon, Oxon, OX14 3DB, United Kingdom (United Kingdom)

The manufacturing of high temperature heat exchangers and precoolers within the aerospace industry often requires the joining of thin-walled components through brazing. Existing commercially available brazing alloys are often relatively hard with brittle failure modes despite ductility and strength being desirable properties of a brazed joint. High entropy alloys have been demonstrated to have desirable material properties with equimolar CoCrCuFeNi such as high ductility and strength. Previous work on CoCrCuFeNi has demonstrated that the addition of melting point depressants such as Boron, [1], are able to beneficially reduce the brazing temperatures sufficiently to allow brazing of steel components while maintaining a strong and ductile joint. The current work has focussed on finding new, non-equimolar, HEA compositions with a lower targeted melting point for a wider range of brazed substrate materials. Alloy compositions were down-selected through empirical thermodynamic classification and CALPHAD simulations. Identified potential compositions were synthesised using induction casting, and solidus and liquidus measured using DSC. Phases were confirmed using a combination of microscopy, hardness and XRD analysis. The best alloy candidates were then modified with the addition of Boron to further reduce the melting point to meet the required manufacturing temperatures of the joint. Finally, shear strength measurements were carried out on the samples which met the brazing temperature requirements. [1] S. Ross et al. Design of High Entropy Alloys for Aerospace Brazing 9th International Brazing and Soldering Conference (IBSC) Charleston, South Carolina, USA, April 14-17, 2024.

Keywords : High Entropy Alloy, Brazing, Alloy design, Thermophysical Properties, Mechanical Properties

266. Rotational Deformation Twins in a Refractory High Entropy Alloy

Senkov Oleg N. ¹

¹ - Air Force Research Laboratory, Materials and Manufacturing Directorate, Wright-Patterson AFB, Ohio 45433, USA (United States)

Results of the analysis of deformation twins formed in a HfNbTaTiZr refractory high entropy alloy during compression deformation at 20 °C 600 °C are reported. All studied twins were formed by rotation of the matrix crystal lattice around a pole and have the common reciprocal twinning plane $K2 = \{001\}$ and reciprocal twinning direction $n2 =$. At the same time, the twinning plane $K1$ and twinning direction $n1$ depend on the degree of rotation of $K2$ and $n2$ around the common pole. The following rotational twinning modes have been identified: $\{1-14\}$ (38.94° rotation), $\{1-15\}$ (31.58°), $\{1-16\}$ (26.54°), $\{1-17\}$ (22.84°), and $\{1-18\}$ (20.04°). A rotational mechanism of twinning, with the rotation axis or , is proposed as an alternative to the commonly accepted shear twinning mechanism.

Keywords : Refractory alloy, Refractory high entropy alloy, HfNbTaTiZr, Microstructure, Deformation twinning

267. Characterization of a CoCrFeMnNi(Al_x) alloy produced from ferroalloys and scraps with an industrial foundry process

Vicario Iban¹, Villanueva Ester¹, Albizuri Joseba², Guraya Maria Teresa², Arruabarrena Gurutze³, Escauriza Borja⁴

1 - Fundacion Tecnia Research & Innovation (Spain), 2 - University of the Basque Country (Spain), 3 - Mondragon University (Spain), 4 - Sidenor (Spain)

A CoCrFeMnNi(Al_x) High Entropy Alloy (HEA) with high mechanical properties manufactured with semi-industrial equipment from Fe scrap and ferroalloys has been studied. To the CoCrFeMnNi base Cantor alloy different amounts of Al were added to promote a decrease in grain size and improve the final mechanical properties. With the XRD analysis results, a solubilization thermal treatment (TT) was defined at 1,100°C for 36 hours and immediately water-cooled. The obtained microstructures were composed of dendrites with eutectic precipitation with Mn, Ni, Al-rich elements in higher percentage in the eutectic, and low Al addition seems to act similar to a grain refiner in other alloys. Al addition decreases the hardness, and treatment slightly increases the hardness, with hardness values around 150 HRC. Obtained tensile (Y.S. 250 MPa; U.T.S. 550 MPa and 50% E) and compressive (Y.C.S 250 MPa and 60% Z) test values are like those of high-purity multi-melted vacuum Cantor alloys with similar ductility values in both tests. Jmatpro simulation was employed to determine the ductility dwells, showing promising good forging conditions that were confirmed by Geoble thermodynamic tests. The electrical conductivity was very low (0.87 MS/m) and decreased with the TT and the corrosion resistance of the CrMnFeCoNiAl_x alloy improved with higher Al addition. The obtained processes and alloys can have future use in automotive or energy applications, especially for H₂ applications.

Keywords : Cantor alloys, mechanical properties, low CO₂ alloy processing, scraps

268. Creep Strength of AlCoCrFeNi High-Entropy Alloy Fabricated by Spark Plasma Sintering

Ohgi Naoki¹, Honda Ryota¹, He Lei¹, Kawabata Mie¹, Kuno Tomoko¹, Ameyama Kei¹, Fujiwara Hiroshi¹, Itoh Takamoto¹

¹ - Ritsumeikan University (Japan)

In recent years, AlCoCrFeNi High-Entropy Alloy (HEA) has attracted attention because it is expected to be a next-generation aerospace engine material in that it is characterized by high strength from room temperature to high temperatures, excellent corrosion and wear resistance, and being lighter and more cost-effective than conventional alloys. However, the influence of microstructure of the material synthesized via spark plasma sintering (SPS), a powder metallurgy technique, on high-temperature mechanical properties, in particular, creep features, has rarely been reported. In the study, to investigate the abovementioned issue, the HEAs using powder mean size of 14.6, 41.9 and 82.4 μm synthesized via SPS at 1273 K and 1373 K were prepared. Creep tests were conducted at 973 K. The obtained results indicated that HEAs SPSed at 1373 K exhibited higher creep strength than those of synthesized at relatively low temperature, because the microstructure of the former is different from those of the latter. In addition, FCC/B2 phase boundary fracture was observed for HEA synthesized at 1373 K. By contrast, powder boundary fracture was observed for the remaining HEAs. Moreover, the Monkman-Grant law can be employed to predict creep rupture time for all types of HEAs on one master curve.

Keywords : Powder Metallurgy, Spark Plasma Sintering, Creep Strength

269. Elevated Temperature Mechanical Properties of Harmonic Structure Designed AlCoCrFeNi High Entropy Alloy by MM/SPS Process

Hori Ryohna¹, Honda Ryota¹, Kawabata Mie¹, Kuno Tomoko¹, He Lei¹, Ameyama Kei¹, Itoh Takamoto¹, Fujiwara Hiroshi¹

¹ - Ritsumeikan University (Japan)

AlCoCrFeNi high entropy alloys (HEA) have superior strength and corrosion resistance at both room and high temperatures and are expected to application in elevated temperature environments. However, it is not clear the relationship between the harmonic structure and the mechanical properties of this HEAs at elevated temperatures. The harmonic structure is composed of dispersed coarse grains and fine grains that are networked around them. In this study, the harmonic structure AlCoCrFeNi HEA was fabricated by mechanical milling (MM) / spark plasma sintering (SPS) process and the microstructure and elevated temperature mechanical properties of its HEA are investigated in detail. AlCoCrFeNi mixed powders with average particle sizes of 14.6 and 82.4 μm were treated with MM. The MM powders were consolidated by SPS at 1173 to 1373 K. Mechanical properties were evaluated by compression tests at room temperature to 1073 K. Microstructural observation was performed using a scanning electron microscope, electron back scattered diffraction and energy dispersive X-ray spectrometer. The conventional SPS compacts have modulated structure with BCC and B2 phase and grain boundary precipitates with FCC phase. While the MM-SPS compacts have a similar structure of the conventional compacts at dispersed region and an equiaxed nano grains including a σ phase at network region. MM compacts with harmonic microstructure demonstrate high compression strength compared to conventional compact at room temperature to 673 K. However, conventional microstructure compacts have higher strength than harmonic structure above 873 K. These results suggest that the harmonic structure have unique deformation behaviour at elevated temperatures.

Keywords : harmonic structure, heterogeneous, compression test, mechanical milling, spark plasma sintering

270. Analyses of Oxidation Behaviours with Alloy Components in High Entropy Alloys with Pack Cementation Coatings at High Temperatures

Oh Jeongseok¹, Park Jini¹, Park Joon Sik¹

¹ - Department of Materials Science & Eng., Hanbat National University (South Korea)

The Mo or Nb component, essential for high-entropy alloys, often experiences significant oxidation when exposed to high temperatures. For instance, molybdenum (Mo) in the alloy sublimates at approximately 500 °C, while niobium (Nb) forms porous oxides under similar conditions. This indicates that both components require protection during high-temperature exposure to air. In this study, we have selected pack cementation coatings to protect the surfaces of refractory high-temperature alloys containing Mo and/or Nb. When silicon (Si) or boron (B) powders are applied as coatings, silicides or borides form on the surface of the high-entropy alloys. We investigate several examples within high-entropy alloys, such as the AlMoNbTaTiZr system. New findings, including the presence of coating layers with nanograins, will be discussed. Additionally, we will compare the oxidation behaviors of Mo-Si-B systems with those of high-entropy alloy systems to develop effective protective coating strategies for high temperatures.

Keywords : Oxidation, high temperature, growth kinetics, high entropy alloys, pack cementation coatings

271. Enhanced ductility via high-density nanoprecipitates driven by chemical supersaturation in a flash-heated precipitation-strengthened high-entropy alloy

Zhang Yang¹, Liu Liyuan¹, Zhang Zhongwu¹

¹ - Harbin Engineering University (China)

Precipitation strengthening is an effective method to strengthen high-entropy alloys (HEAs); however, the incompatible plastic deformation caused by precipitates accelerates the initiation and development of cracks, reducing ductility. Therefore, it is necessary to spare no effort to overcome this strength–ductility trade-off. However, improving the ductility of HEAs without losing the precipitation-strengthening effect remains a daunting challenge. The strategy of this study is to increase chemical supersaturation without introducing other defects to drive the formation of high-density nanoprecipitates to share stress, reduce localization, and alleviate incompatible plastic deformation, thereby fully utilizing the strain-hardening ability to improve the ductility of HEAs without reducing their strength. Specifically, common Ni₃₅(CoCrFe)₅₅Al_{5.5}Ti_{4.5} (at.%) precipitation-strengthened HEAs were selected as the experimental object. Short-term high-temperature flash heating causes the dissolution of the initial nanoprecipitates, and the separated atoms form chemically supersaturated microregions in the matrix between the initial nanoprecipitates after insufficient short-range diffusion, resulting in the formation of high-density new nanoprecipitates. The density of the nanoprecipitates reaches $5.0 \times 10^{24} \text{ m}^{-3}$, representing a two-order increase in magnitude compared to the aging state ($1.9 \times 10^{22} \text{ m}^{-3}$). By increasing the density of nanoprecipitates, multiple nanoprecipitates share stress together. Sufficient slippage of dislocations maximizes the potential excellent strain-hardening ability, considerably improving the ductility of HEAs. Moreover, the strategy of improving the ductility by increasing the density of nanoprecipitates can be applied to many other precipitation-strengthened alloy systems.

Keywords : High entropy alloy, Precipitation strengthening, High density precipitates, Nucleation rate, Flash heating

272. Kinetics of Chemical Order Formation and Its Influence on Diffusivity in CrCoNi Medium Entropy Alloy

Ogata Shigenobu ¹

1 - Department of Mechanical Science and Bioengineering, Osaka University (Osaka, 560-8531 Japan)

This study employs neural network interatomic potentials and neural network activation energy predictions to explore the kinetics of chemical order formation and its effects on the diffusion behavior of interstitials and vacancies in CrCoNi medium entropy alloys. Kinetics are depicted through a time-temperature-degree of chemical order diagram that closely matches experimental electronic resistivity measurements. Our findings reveal that the degree of chemical ordering, which can be precisely manipulated through annealing at elevated temperatures, significantly impacts both interstitial and vacancy diffusion. This influence is primarily due to restricted diffusion pathways in areas with lower degrees of chemical ordering, elucidating the sluggish diffusion characteristic of CrCoNi.

Keywords : CrCoNi alloys, Atomic simulation, Chemical order formation kinetics, diffusivity

273. High Hardness Nanotwinned High Entropy Alloys CoCrFeNi Thin Films with radiation resistance.

Chang Wei-Cheng^{1 2}, Patel Maulik , Ouyang Fan-Yi

1 - University of Liverpool (United Kingdom), 2 - National Tsing Hua University [Hsinchu] (Taiwan)

High entropy alloy (HEA) and highly nanotwinned (NT) material with improved ductility and high strength demonstrate promising potential compared to nanocrystalline materials and traditional alloys. In this study, nanotwinned high entropy alloy material was synthesized by sputtering technology. The properties and microstructure of CoCrFeNi-based high entropy alloy (HEA) thin films with twin structures were investigated. In the view of microstructure, the NT- HEA thin films showed a simple Face Centered Cubic (FCC) structure with nearly 100% of (111) texture with high hardness (7.9 - 9.15 GPa). At the same time, the parallel-twin boundary with 1.8-2.8 nm twin thickness and the lattice images had been observed by high resolution transmission electron microscope (TEM). Radiation effects in High Entropy Alloys (HEA) have intrigued researchers for decades as well, with their unique material properties challenging conventional understanding. Utilizing the radiation damage experiment was investigated at room temperature under 275keV Helium ion radiation. Remarkably, the presence of small-sized helium bubbles and their distribution showed significant radiation resistance within this system. Moreover, TEM and x-ray diffraction analysis showed the retention of stable grain and twin microstructures after radiation damage. Notably, interactions between defects, grains, and nanotwinned boundaries were observed. The HEA-NT thin films exhibited a phase transformation from a face-centered cubic to a hexagonal closed-packed phase owing to radiation-induced local strain build-up, accompanied by substantial local strain-induced grain rotation within the thin film structure. Further explanation of the mechanism will be discussed comprehensively.

Keywords : High entropy alloy, nanotwinned structure, radiation damage, phase transformation

274. The power and beauty of Cantor's First Experiment A 20 year retrospective

Miracle Dan ¹

¹ - Air Force Research Laboratory (United States)

There is a hidden power and beauty in Cantor's first expedition into the centers of complex, multi-component phase spaces. In a single experiment, an equimolar alloy with 20 main elements probed over a million different alloy families. The multi-phase microstructures that were produced by casting and melt-spinning this remarkable alloy were both dominated by a solid solution of primarily five of the 20 elements, again in nearly equimolar proportions, with smaller dissolved quantities of other elements. This single experiment thus uncovered a solid solution phase with exceptional thermodynamic stability and compositional range. In the 20 years since this result was first published in the open literature, the Cantor alloy has been prodded, stretched, contracted, and measured in almost countless ways. This presentation revisits Cantor's initial work, with a fresh perspective made possible by 20 years of extensive work on multi-component materials that was not available when the paper was first published. Additional insights into the thermodynamics, phase stability and applicability to other elemental palettes and alloy families are explored.

Keywords : High, entropy alloys, Cantor alloy, phase stability

275. Nanoprecipitate-strengthened high entropy alloys

Zhang Zhongwu¹, Zhang Yang¹

¹ - Harbin Engineering University (China)

Introducing high-density nanoprecipitates into high entropy alloys is an effective strategy for designing high-performance structural and functional materials. However, while nanoprecipitates provide precipitation strengthening, they inevitably lead to a loss of plasticity. This trade-off is largely influenced by the intrinsic properties of the nanoprecipitates, such as their structures and coherence relationships with matrix. Therefore, our research group is investigating various nanoprecipitates, including L12 and B2 to D022 structures. A series of design strategies are proposed to improve the macroscopic deformation mechanisms and mechanical properties by regulating the nanoprecipitates properties. By changing the crystal structure of Ni₃Nb nanoprecipitate from D022 to L12 crystal structure, On one hand, high anti-phase boundary energy provides strong precipitation strengthening effects; on the other hand, by adjusting the matrix stacking fault energy through pre-cold deformation and two-stage aging, the continuous formation of deformation-activated stacking faults, twins, and L-C locks is promoted. The Zr-rich B2 nanoprecipitate and D022 nanoprecipitate in the heterogeneous grain structure promote the transformation of the alloy's deformation mode from strain localization dominated by dislocation plane slip to microband deformation dominated by dislocation cross-slip. Furthermore, Introducing nanoprecipitates is also an effective strategy to improve the irradiation resistance of structural materials. By controlling the lattice mismatch between the nanoprecipitates and the matrix, the processes of disordered dissolution and ordered reprecipitation of the nanoprecipitates during irradiation can be regulated. This enables the realization of irradiation-induced dissolution and precipitation, as well as reversible cycles of dissolution-precipitation for B2 and L12 nanoprecipitates in matrices with different mismatch degrees. The excess atoms significantly eliminate point defects generated during the cascade process through long-range diffusion, delaying their aggregation and evolution into complex defect clusters.

Keywords : High, entropy alloy, Precipitation strengthening, Nanoprecipitates, Deformation mechanism

276. High Entropy Nonlinear Dielectric System

Chu Ying-Hao ¹

1 - National Tsing Hua University (Taiwan)

A high configurational entropy, achieved through a proper design of compositions, can minimize the Gibbs free energy and stabilize the quasi-equilibrium phases in a solid-solution form. This leads to development of high-entropy materials with unique structural characteristics and excellent performance, which otherwise could not be achieved through conventional pathways. This work develops a high-entropy nonlinear dielectric system based on the expansion of lead magnesium niobate/lead titanate. A dense and uniform distribution of nano-polar regions is observed in the samples owing to the addition of Ba, Hf, and Zr ions, which lead to enhanced performance of nonlinear dielectrics. The fact that no structural phase transformation is detected up to 250 °C, and no noticeable change or a steep drop in structural and electrical characteristics is observed at high temperatures suggests a robust thermal stability of the dielectric systems developed. With these advantages, these materials hold vast potential for applications such as dielectric energy storage, dielectric tunability, and electrocaloric effect. Thus, this work offers a new high-entropy configuration with elemental modulation and enhanced dielectric material features.

Keywords : high entropy, dielectric

277. What role might high entropy alloys play in a circular economy?

Barnett Matthew ¹, Gorsse StePhane ²

1 - Deakin University, Geelong, VIC, Australia, Institute for Frontier Materials (Australia), 2 - University of Bordeaux (CNRS) (UPR 9048, F-33600 Pessac France)

Ideally, new materials should further sustainability. The circular economy is a much discussed path to a more sustainable use of materials. The current presentation will explore the role of high entropy alloys (HEAs) in a more circular economy. The Material Power Cost of Circularity (MPCC) is defined and used to direct the discussion. This term is the forecast net power expected to be expended over the use, replacement and re-use phases of an alloy component. It is proposed that if a new alloy enables a drop in the MPCC, it may prove to be a sustainable step forward. It is shown that, in some cases, the potentially large energy costs of high entropy alloy production, and the challenges they will present to open loop recycling, may be justified if the alloy mediates sufficient energy efficiencies in their use phase. Some examples are given and the topic of recyclability is discussed.

Keywords : high entropy alloy, sustainability, circular economy, recycling

278. Machine Learning-Assisted Design of Advanced Bilayer TBC Systems Using Multicomponent R2TiO5

Kitaoka Satoshi¹, Tanaka Makoto¹, Kawashima Naoki¹, Ogawa Takafumi², Ito Taishi², Nakayama Kei², Kato Takeharu², Yamaguchi Norio¹, Suzuki Hiroaki³, Shibata Haruo³, Kawasaki Akira³

1 - R&D Laboratory, Japan Fine Ceramics Center (Japan), 2 - Nanostructures Research Laboratory, Japan Fine Ceramics Center (Japan), 3 - Japan Aerospace Technology (Japan)

Increasing turbine inlet temperatures and reducing cooling air in airplane engines can significantly improve fuel efficiency, thereby reducing CO₂ and NO_x emissions. Conventional thermal barrier coatings (TBCs) use YSZ, but further advancements are necessary to enhance performance. Heat-transfer calculations considering the optical properties of TBC topcoats under burner heating suggest that improved TBCs require both lower thermal conductivity and higher emissivity. Yb₂TiO₅, with an oxygen-deficient fluorite structure, demonstrates extremely lower thermal conductivity than YSZ while maintaining comparable thermal expansion, making it a strong candidate for advanced TBCs. In this study, we developed a machine learning-based method to predict the crystal structure and emission performance of multicomponent R₂TiO₅ systems, which was validated experimentally. A bilayer TBC system was fabricated using multicomponent R₂TiO₅ with high emissivity on top of t'-YSZ layer, applied through double electron beam physical vapor deposition. Comparative evaluations under H₂-O₂ burner rig tests revealed that the bilayer TBC system reduced heat flux by 12% compared to the conventional YSZ-TBC system. Moreover, while the heat flux in the YSZ system increased with thermal cycling, the bilayer TBC system maintained consistent performance over 200 cycles, demonstrating superior thermal barrier properties and durability. These results highlight the potential of multicomponent R₂TiO₅ materials for next-generation TBCs.

Keywords : Machine, learning, R₂TiO₅, multicomponent, emissivity, TBC

279. Development of Bimodal-Grained Microstructure in Metastable Multicomponent Alloys via Reversion of Strain-Induced BCC Phase

Han Jeongho ¹

¹ - Hanyang University (South Korea)

During the past decade, multicomponent alloys (MCAs) with face-centered-cubic (FCC) structures have garnered significant attention due to their exceptional mechanical properties. Traditionally, MCAs consist of three to five multi-principal elements in near-equimolar compositions (e.g., CrMnFeCoNi, CrCoNi). Recently, however, non-equiatomic MCAs have emerged as a promising alloy design concept, offering enhanced mechanical properties through synergetic transformation-induced plasticity (TRIP) and twinning-induced plasticity (TWIP) effects. To maximize both strength and damage tolerance, prior studies have explored grain refinement through severe plastic deformation or cryogenic rolling followed by annealing. While these methods effectively improve strength, they face challenges in industrial scalability and often result in reduced ductility. In this study, we introduce a novel thermo-mechanical process involving the reversion of strain-induced body-centered-cubic (BCC) phases as an alternative approach, using V10Cr10Fe45Co35 alloy as a model system. During reversion annealing, the strain-induced BCC phase transformed into ultrafine FCC grains, with martensitic substructures serving as abundant nucleation sites. Simultaneously, the deformed FCC grains underwent recrystallization and grain growth, producing a bimodal grain structure. This unique microstructure achieved an exceptional combination of strength and ductility, exceeding 45,000 MPa%, alongside a high yield strength of nearly 1 GPa.

Keywords : Multicomponent alloys, martensite, reversion, transformation, induced plasticity

280. Effect of Stacking Fault Energy on Deformation Mechanism and Low-Cycle Fatigue Property in Co-Cr-Mo-Ni Medium Entropy Alloys

Tsuchiya Koichi ¹

¹ - National Institute for Materials Science (Tsukuba, 305-0047 Japan)

Co-based alloys, such as MP35N and L605, are most widely used for coronary stents due to their high-strength and corrosion resistance. However, relatively earlier fracture has been reported in 2~84 month after implantation when the stents receive unexpected deformation in the blood vessel. Aiming for the application to medical devices, Co_{51-x}Cr₂₃Mo₆Ni_{20+x} (x = 0-15) medium entropy alloys were designed based on the FCC-HCP phase stability using Calphad. Room temperature tensile tests revealed markedly high work-hardening rate and good strength-elongation balance of the alloys. X-ray diffraction (XRD) and Electron Backscattered Diffraction (EBSD) analysis revealed that the dominant deformation modes gradually shift from the FCC-HCP transformation to deformation twinning and dislocation slip with the Ni content, x. The observed good strength-elongation balance may be due to the TRIP and TWIP. In the tensile deformed samples of the x = 3~9 alloys, HCP phase and twins coexist. The low-cycle fatigue (LCF) behavior was investigated with a total strain amplitude of 0.01. The highest LCF lives were observed for the x = 6 alloy (6537 cycles). They are much higher than those of alloys currently used for coronary stents, such as L605 or MP35N. These findings suggests that the formation of epsilon-twin bundles may be an important factor to obtain high LCF resistance. Microstructures and mechanical properties of tubes and wires made of the MEA alloys, and the property of a proto-type stent will be reported.

Keywords : Co, Cr alloys, Mechanical Properties, TRIP, TWIP, Stent

281. Plastic deformation behavior of single crystals of the equiatomic high- and medium-entropy alloys of the Cr-Mn-Fe-Co-Ni system

Li Le¹, Chen Zhenghao¹, Kishida Kyosuke¹, Inui Haruyuki¹

¹ - Kyoto University (Japan)

The equiatomic quaternary and ternary medium-entropy alloys derived from the Cr-Mn-Fe-Co-Ni system serve as useful prototypes to scientifically investigate the variation in mechanical properties as a function of element combinations by experiments and theoretical calculations. They also help us to understand how expensive constituents may be substituted by less expensive elements to achieve specific properties and a better cost-performance balance for practical applications. These factors motivate us to establish a sound understanding of the roles of constituent elements through the study of the equiatomic quaternary and ternary MEAs derived from the Cr-Mn-Fe-Co-Ni system. Therefore, we investigate in compression and tension the plastic deformation behavior of single crystals of quaternary and ternary equiatomic FCC MEAs belonging to the Cr-Mn-Fe-Co-Ni system at temperatures from 9 K to 1373 K. The results of the present study can help establish a benchmark for the fundamental plastic deformation behavior of FCC high-and medium-entropy alloys (HEAs/MEAs). In the present study, it was found that the critical resolved shear stresses (CRSSs) of these high increase with decreasing temperature below room temperature. The CRSS at 0 K can be precisely predicted by some solid solution strengthening models of HEA/MEAs including the one based on the mean-square atomic displacement (MSAD). The element combinations lead to a wide range of SFE and substantially affect the tensile deformation behavior such as Stage I deformation and twinning stress.

Keywords : High entropy alloys, Single crystals, Critical resolved shear stress, Mean, square atomic displacement, Stacking fault energy.

282. Creep behavior of a precipitation-strengthened A2-B2 refractory high entropy alloy

Kauffmann Alexander¹, Yang Liu¹, Sen Sandipan¹, Schliephake Daniel¹, Vikram Raja J.¹, Laube Stephan¹, Pramanik Aparajita², Chauhan Ankur², Heilmaier Martin¹

1 - Karlsruhe Institute of Technology (Germany), 2 - Indian Institute of Science (India)

Refractory high entropy alloys (RHEA) consisting of a disordered A2 matrix and ordered B2 precipitates mimic the microstructures of state-of-the-art, Ni-based superalloys with A1 matrix and L12 precipitates. They are promising candidates for high-temperature applications because of their high melting points and mechanical strength at elevated temperatures. However, systematic studies on their creep behavior are still scarce. 27.3Ta-27.3Mo-27.3Ti-8Cr-10Al (in at. %) is a relevant example where the A2-B2, two-phase microstructure is formed by a precipitation reaction and remains stable even at temperatures close to the B2 solvus temperature TS of about 1070 °C. The present study systematically addresses the creep response of poly-crystalline 27.3Ta-27.3Mo-27.3Ti-8Cr-10Al at temperatures of 1000 °C and above. Compared to poly-crystalline, single-phase A2 and B2 RHEA, a substantially higher creep resistance is observed for the two-phase alloy while minimum creep rates comparable to those of state-of-the-art, single-crystalline A1-L12 CMSX-4 are found. This is specifically remarkable considering its poly-crystalline condition, the open matrix A2 crystal structure and extremely high homologous temperature of 0.98 TS compared to 0.85 TS for CMSX-4. Consistent with a positive lattice misfit, directional coarsening of precipitates is revealed in 27.3Ta-27.3Mo-27.3Ti-8Cr-10Al perpendicular to the compression direction after creep in grains with $\epsilon \approx 100\epsilon^a$ close to the compression direction.

Keywords : Refractory high entropy alloys, Compositionally complex alloys, Super alloys, Creep, High temperature deformation

283. Effect of Re and Ru on two-phase A2+B2 Ta-Mo-Ti-Cr-Al refractory high entropy alloys

Yang Liu ¹, Sen Sandipan ¹, Raja Vikram ¹, Schliephake Daniel ¹,
Heilmaier Martin ¹, Kauffmann Alexander ¹

¹ - Karlsruhe Institute of Technology (Germany)

Refractory high entropy alloys (RHEA), comprising a disordered A2 matrix and B2 ordered precipitates, exhibit microstructures analogous to $\gamma + \gamma'$ in state-of-the-art, Ni-based super alloys. They are promising candidates for high-temperature applications because of their high melting points. 27.3Ta-27.3Mo-27.3Ti-8Cr-10Al (in at. %) is a relevant example where this two-phase A2+B2 microstructure is formed by a precipitation reaction and remains stable even at temperatures close to the solvus temperature of B2 at around 1070 °C. This two-phase alloy in polycrystalline condition shows significantly better creep resistance than single phase A2 or B2 RHEA, with a minimum creep rate comparable to that of state-of-the-art, single-crystalline A1-L12 CMSX-4. However, the strengthening provided by B2 precipitates is limited due to their low solvus temperature, making it crucial to find strategies to increase the solvus temperature. Recently, Ru-containing B2 precipitates were proven to be stable between 1300 and 1900 °C in RHEA systems [Kube et al., Acta Mat. 265 (2024) 119628], suggesting that adding Ru can increase the solvus temperature of B2 precipitates. In the present study, Re (0.5 to 10 at%) and Ru (0.5 to 5 at%) were added to the aforementioned base alloy system to increase the solvus temperature of B2 precipitates. Thermal analyses and microstructural analyses of aged and quenched specimen confirm the enhancement of the solvus temperature by Re and Ru addition. As the temperature-dependent sequence of phase separation vs. ordering, determines the matrix character of the final microstructure, critical Re and Ru contents to preserve an A2 matrix are identified.

Keywords : Refractory high entropy alloys, Phase transformations, Solvus temperature, B2 precipitates, High temperature materials

284. Elucidating the microstructural formation pathways in Refractory Metal High Entropy Alloys using in situ high energy diffraction

Jones Nick ¹, Yang S-T ¹, Church N. L. ¹, Wise G. J. ¹, Thompson R. P. ¹, Mellor R. F. L. ¹, Stone H. J. ¹

¹ - University of Cambridge (United Kingdom)

Refractory metal high entropy alloys are one of the most promising candidates for structural applications at temperatures beyond the capability of Ni-base superalloys. Their suitability for such applications is derived from the high melting temperatures and intrinsically low diffusivities of their constituent elements. In addition, several systems can exhibit two phase A2-B2 microstructures in configurations that are visually similar to the γ - γ' assemblies of Ni-based superalloys. Yet, in most of these systems, the matrix is the ordered phase, whilst the precipitates are solid solutions. This leads to concerns around the ductility and toughness, particularly at lower temperatures. Many studies have sought to understand the microstructural formation pathways of these alloys, with an aim to modifying them to achieve an inverted microstructural configuration. However, despite these efforts, a definitive and unambiguous understanding has yet to be established. In this talk, we will present a series of in situ datasets acquired during heating and cooling experiments using high energy synchrotron radiation. These data provide direct evidence of the actual microstructural formation pathways and highlight interesting features that would likely be missed by other approaches. We have collected data from a number of model alloys, with varying compositional complexity, helping to assess the role of certain key elements, such as Al. In addition, by combining these data with those obtained from other advanced techniques, such as high-resolution electron microscopy, has enabled us to highlight how interphase misfit plays a crucial role in influencing the microstructural features observed.

Keywords : Refractory Metal, High Entropy Alloy, Phase transformation, Diffraction

285. Strengthening multicomponent alloys with ordered precipitates: the role of partitioning and site occupancy

Chattopadhyay Kamanio^{1 2}

1 - Indian Institute of Science [Bangalore] (Bangalore 560 012 India), 2 - National Science Chair (India)

The presentation celebrates the achievements of Professor Brian Cantor and the many facets of his contributions that have enriched our discipline. One of the authors was an early collaborator of Professor Cantor and saw first-hand the germination of many ideas, including the multicomponent alloys, initially popular with the names of high entropy alloys. However, our work on multicomponent alloys is of recent origin when the field is already well developed. We were working on cobalt-based lightweight superalloys and realized that some of the multicomponent alloys we are exploring qualify as multi-principal elements or high entropy alloys. These are also classified as precipitation-strengthened high entropy alloys or PSHEA. The strengthening of these depends on the nature of the precipitates and the partitioning of solutes in the multi-component matrix and the precipitate phases. In the first work, we showed the effect of Cr partitioning on the properties of these alloys. Subsequently, we discovered that site occupancy plays an important role in the development of alloy properties. We have highlighted it by comparing two alloys with different Fe content, 5 and 10%Fe. Both the alloys have identical distribution of the precipitate's sizes, shapes, volume fractions and γ/γ' lattice misfit (~ 0.56). However, the 5Fe alloys have higher strength due to a different site occupancy of Fe atoms in the precipitates. These open up newer possibilities for alloy development.

Keywords : multicomponent alloys, site occupancy, solute partitioning, PSHEA

286. High-Entropy Alloys as Advanced Metal Hydrides for Efficient Hydrogen Storage

Floriano Ricardo ¹

¹ - University of Campinas (Brazil)

High-entropy alloys (HEAs) are emerging as promising candidates for solid-state hydrogen storage due to their broad compositional range and unique properties. Composed of at least five principal elements in proportions of 5€“35 at%, HEAs stabilize single-phase solid solutions with diverse crystal structures, such as body-centered cubic (BCC), face-centered cubic (FCC), or hexagonal close-packed (HCP) with laves phase. This compositional diversity facilitates the design of new HEAs with optimized hydrogen storage capabilities. This study focuses on high-entropy hydrides with a predominant single C14-Laves phase, employing a design strategy based on semi-empirical parameters such as atomic radii ratios, mixing enthalpies, atomic size mismatches, electronegativity differences, and valence electron concentrations, combined with CALPHAD thermodynamic simulations. HEAs are synthesized via arc melting and characterized using SEM, TEM, and XRD. Hydrogen storage properties are evaluated through kinetics and pressure-composition-temperature (PCT) isotherms. Several HEAs, including TiZrCrMnFeNi, TiZrNbFeNi, and TiZrMnFeCo, achieve reversible hydrogen capacities of 1.70-1.90 wt% with fast kinetics at room to moderate temperatures (200 °C), often without activation. Others, such as Zr33(CrMnFeNi)67 and TiZrFeNiV, require simple activation procedures. Most HEAs exhibit a dominant C14 Laves phase and minimal BCC structures (

Keywords : High, entropy Alloys, Hydrogen Storage, CALPHAD, C14, Laves Phase

287. Development of high entropy alloy thin films for energy-related research

Lee Jyh-Wei¹, Lou Bih-Show

¹ - Ming Chi University of Technology (Taiwan)

The designs of multicomponent alloys and high entropy alloys (HEAs) proposed by Prof. Cantor and Prof. Yeh, respectively, in 2004 opened a new world in material discovery due to their unique properties. At the same time, the HEA thin films fabricated by the magnetron sputtering technique have been explored extensively. This work studied the refractory VNbMoTaWO HEA oxide films as a novel graphite felt (GF) electrode modification of vanadium redox flow batteries (VRFBs). A superior energy efficiency of 80.50 % at a current density of 100 mA/cm² was obtained on the HEAO film-modified GF electrode, outperforming the VRFB with the unmodified GF electrode by 9.49 %. The corrosion resistance of TiZrNbSiMoN and TiZrNbTaFe thin films in a 0.5 M sulfuric acid environment was examined. The excellent corrosion resistance of these HEA films can be deposited as corrosion-protective coatings on the surfaces of metallic bipolar plates in proton exchange membrane fuel cells. Lastly, AlCoCrFeNiN HEA thin films were synthesized via magnetron sputtering onto nickel foam and Si substrates under varying nitrogen gas flow rates. Electrochemical evaluations in a 1.0 M KOH + 3.5 wt.% NaCl electrolyte revealed that nitrogen doping significantly enhanced catalytic performance, yielding a high double-layer capacitance and a large electrochemically active surface area. Notably, the AlCoCrFeNiN HEA film exhibited the lowest overpotential of 329 mV at a current density of 10 mA.cm⁻² and exceptional stability after 300 hours of chronoamperometric testing at 100 mA.cm⁻² in combined alkaline and saline media. These findings indicate the AlCoCrFeNiN films are highly promising electrocatalysts for water-splitting applications. We demonstrated that functional HEA films can be fabricated and applied in energy-related research by properly designing the chemical compositions of HEA films and controlling magnetron sputtering parameters.

Keywords : high entropy alloy thin films, sputtering, vanadium redox flow batteries, proton exchange membrane fuel cell, electrocatalysts, water splitting

288. Transformation pathways and deformation mechanisms in refractory high entropy alloys

Fraser Hamish¹, Welk Brian, O'Kelly Paraic, Viswanathan Gopal

¹ - The Ohio State University (United States)

The advent of refractory high entropy alloys (RHEA) has afforded the materials community an opportunity regarding the development of new (and improved) high temperature alloys. For very high temperature applications, it is necessary to make use of alloying elements that will respond to such temperatures (e.g., usually elements with high atomic numbers), and combinations of these elements usually result in microstructures consisting of a bcc phase and a B2 ordered intermetallic phase. Either of these phases may be continuous. In this talk, the transformation pathways that produce attractive microstructures in these alloys will be described briefly. Thus, such microstructures are often the result of a spinodal transformation, and fairly refined microstructures may be formed. Of interest is the detailed characterization of the microstructures, such as the nature of the interfaces (coherent, semi-coherent, or incoherent), and the details of the ordering scheme in the B2 compound when consisting of a number of alloying elements. The deformation mechanisms operating in these B2/bcc alloys has been characterized and the results will be presented in this talk.

Keywords : High Entropy Alloys, Refractory HEAs, Deformation mechanisms of RHEAs

289. Characteristic Dislocation Slips in Polycrystalline HfNbTiZr Medium Entropy Alloy

Tsuji Nobuhiro¹, He Qian^{1 2}, Yoshida Shuhei¹, Okajyo Shinji³,
Tanaka Masaki³

1 - Kyoto University (Japan), 2 - Southern University of Science and Technology (China), 3 - Kyushu University (Japan)

Characteristics of dislocation slip behavior in an equi-atomic HfNbTiZr refractory medium entropy alloy (RMEA) having BCC single phase were studied, comparing with those of pure Nb. Fully-recrystallized specimens were fabricated by cold rolling and subsequent annealing, and uniaxial tensile tests at room temperature were conducted. Slip trace morphologies on the surfaces of the tensile-deformed specimens were quantitatively characterized, and the so-called $\bar{\Gamma}^*$ and $\bar{\Gamma}^\dagger$ relationships of the observed slip plane traces were evaluated. Wavy slip traces were observed in most grains in pure Nb. They consisted of low-indexed slip planes, such as $\{1\ 1\ 0\}$ and $\{1\ 1\ 2\}$, together with high-indexed (or undetermined) slip planes. Some straight slip traces persisting on the low-indexed slip planes were also found in pure Nb. In contrast, straight slip traces were dominant in the HfNbTiZr RMEA. The straight slip traces in the HfNbTiZr alloy were not parallel to particular slip planes but mostly distributed along the maximum shear stress plane (MSSP), indicating that frequent cross-slip in very short intervals occurred. Large deviations of slip planes from the MSSP found in several grains of the HfNbTiZr alloy were attributed to the slip transfer from neighboring grains as a characteristic of polycrystalline materials. Frequent cross-slip in short intervals, attributed to homogeneous slip resistance distribution for screw dislocations in the HfNbTiZr alloy originating from the chemical heterogeneity in atomic scale in high/medium entropy alloys composed of different elements, was proposed as a novel mechanism responsible for the unique slip behavior and macroscopic deformation behavior.

Keywords : BCC Metals and Alloys, Polycrystals, Dislocation Slip, Cross Slip, High/Medium Entropy Alloys

290. ICME and Microstructure Informatics framework for the development of multicomponent alloys

Rahul M R ¹

1 - Indian Institute of Technology (Indian School of Mines) Dhanbad (India)

Design and development of new materials for high-temperature applications is challenging. Several modifications in microstructures and properties of conventional alloys are reported. Recently, several potential compositions have been reported in the high entropy alloy (HEA) domain. The design and development of alloys from large compositional domains is challenging. The trial and error method requires a large number of experiments and resources. Several computational tools are available to accelerate and guide the HEA design. Recently, the application of machine learning (ML) and computer vision is getting wider attention in alloy design and development. The current study will be focused on the development of multiphase high entropy alloys using a combined framework of Integrated Computational Materials Engineering (ICME) and materials informatics tools. The ML + CALPHAD-based approach will be used to identify the potential compositions. Phase field modelling + computer vision-based approach will be used to identify the microstructures. Finally, potential compositions with experimental validation are proposed.

Keywords : ICME, Materials Informatics, Microstructure Informatics, High Entropy Alloys, Alloy Design

291. The microstructural evolution of FCC high-entropy alloy after gas tungsten arc weld and friction stirring weld

Chewei Tsai¹, Sato Yutaka S.², Yeh Jien-Wei³

1 - National Tsing Hua University [Hsinchu] (Taiwan), 2 - School of Engineering [Tohoku Univ] (Japan), 3
- National Tsing Hua University (101, Sec. 2, Kuang-Fu Road, Hsinchu 30013 Taiwan)

Welding technology plays a crucial role in the industrial use of high-entropy alloys (HEAs). This research examines the mechanical properties and microstructures of Al_{0.2}Co_{1.5}CrFeNi_{1.5}Ti_{0.3} following gas tungsten arc (GTA) welding and friction stir welding (FSW). The GTA welding of precipitated HEAs led to the development of dendrites in the fusion zone. In contrast, FSW demonstrated outstanding mechanical properties, maintaining over 94% of the hardness and tensile strength of the original material. The mechanical properties were evaluated through tensile tests using digital image correlation (DIC), while the microstructure was analyzed using electron backscatter diffraction (EBSD).

Keywords : welding, high, entropy alloy, mechanical properties

292. Enhancing strength and hydrogen embrittlement resistance by discontinuous L12 precipitation in high-entropy alloy

Song Sang Yoon¹, Jang Tae Jin¹, Lee Chang-Gi¹, Yang Dae Cheol¹,
Sung Min Young¹, Lee Gunjick¹, Han Jung Hun¹, Baek Ju-Hyun²,
Suh Jin-Yoo², Zargaran Alireza³, Saksena Aparna⁴, Gault Baptiste⁴,
Ko Won-Seok⁵, Kim Se-Ho

1 - Korea University (South Korea), 2 - Korea Institute of Science and Technology (South Korea), 3 - Pohang University of Science and Technology (South Korea), 4 - Max-Planck-Institut für Eisenforschung GmbH (Germany), 5 - Inha University (South Korea)

Hydrogen embrittlement (HE) presents a severe challenge to ultrahigh-strength alloys, as atomic hydrogen interacts with microstructural defects, causing brittle failure. This issue is further aggravated by stress-induced hydrogen diffusion near crack tips, particularly in high-strength materials. To address this, we introduce a CrFeCoNi-based high-entropy alloy (HEA) featuring discontinuous L12 precipitation (DP-L12) as a novel approach to achieving ultrahigh strength (~1600 MPa) while maintaining superior resistance to HE. The DP-L12 alloy, developed through cold-rolling and aging, exhibits coherent nano-lamellar L12 precipitates and serrated grain boundaries, which enhance hydrogen trapping and deflect crack propagation. Cryo-atom probe tomography confirmed the high hydrogen affinity of L12 precipitates, supported by density functional theory calculations. These microstructural features result in a 1.5-fold increase in elongation loss during hydrogen charging compared to a single-phase FCC reference alloy, while simultaneously enhancing strength. Our findings demonstrate that discontinuous L12 precipitation provides a promising strategy for designing ultrahigh-strength alloys with improved resistance to HE suitable for structural applications in hydrogen-related environments.

Keywords : Hydrogen embrittlement, High, entropy alloy, Discontinuous precipitation, Hydrogen, assisted crack, Atom probe tomography

293. Hierarchical structures of submicron and nanoscale blocks evolved through deformation twinning in CrCoNiSi0.3 medium entropy alloy under ballistic impact

Yang Jer-Ren¹, Chen Jia-Jun ¹, Chiu Po-Han ¹, Tsao Tzu-Ching ¹

¹ - Department of Materials Science and Engineering, National Taiwan University (Taiwan)

CrCoNiSi_x (x = 0, 0.15, 0.3) medium entropy alloys, processed through hot rolling to a 70% thickness reduction at 1000 °C followed by annealing at the same temperature, were tested under ballistic impact (strain rate > 10⁶ s⁻¹) using ultra-high-speed bullets (900 m/s, 9.8 g). Among the alloys, CrCoNiSi0.3 exhibited an exceptional energy absorption capacity of 82% during ballistic impact, outperforming CrCoNiSi0.15 (76.7%) and CrCoNi (68.9%). The targeted addition of silicon (Si) to the CoCrNi alloy significantly enhances its strength and provides a remarkable energy absorption capability, as evidenced by the superior performance of CrCoNiSi0.3. This study focuses on analysing the evolution of hierarchical deformation structures in CrCoNiSi0.3 under varying strain levels induced by ballistic impact. Deformation structures in the lightly deformed (Region I), medium deformed (Region II), and severely deformed (Region III) regions of the CrCoNiSi0.3 alloy plate after ballistic impact have been thoroughly analysed by TEM and STEM. In Region I, deformation is predominantly driven by dislocations, as the strain is insufficient for the formation of deformation twins. In Region II, the intersection of two variants of deformation bundles forms typical features of submicron blocks. In Region III, Numerous intersecting arrays of two variants of deformation bundles divide the matrix into a large number of closed blocks. The atomic resolution HAADF-STEM images of the deformation bundle have revealed the alternate mixing of HCP nano-lamellae and deformation nanotwins, indicating that during ballistic deformation the combination of high strain and high strain rate activates the TWIP and TRIP effects within the highly localized block regions, further enhancing the work-hardening. These intersecting deformation bundles contribute to dynamic refinement of deformation structures due to the continuous segmentation that occurs during high-speed deformation.

Keywords : FCC, type medium entropy alloy (MEA), Ballistic impact deformation, Deformation twin, Strain induced phase transformation, HCP phase, Hierarchical deformation structure

294. In-situ hydrogen embrittlement of CrCoNi medium-entropy alloy

Chung Yoonmoon¹, Song Geon Ho ¹, Han Jeongho ¹

¹ - Hanyang University (South Korea)

High-entropy alloys (HEAs) are innovative materials with unique mechanical properties, making them ideal for extreme environments. In hydrogen-rich conditions, conventional alloys face a notable challenge. They are prone to hydrogen embrittlement (HE), resulting in significant degradation of mechanical properties even with minimal hydrogen absorption. In contrast, FCC-based HEAs are generally recognized for their superior resistance to hydrogen embrittlement due to several key factors: the inherent characteristics of the FCC structure, such as high lattice symmetry and multiple slip systems; the complex interactions among various elemental atoms; and the solid solution strengthening effect, which hinders hydrogen penetration into defects. A prime example is the Cantor alloy (FeMnCrCoNi), with recent studies shifting focus to the more advanced CrCoNi medium-entropy alloy. Traditionally, research on hydrogen embrittlement relies heavily on pre-charging methods, where hydrogen is introduced into the material prior to mechanical testing, such as tensile testing. While this approach effectively assesses material susceptibility to embrittlement, it may not fully capture the behavior of materials under real-world service conditions. To bridge this gap, in-situ hydrogen charging methods have been developed. Unlike pre-charging, in-situ hydrogen charging continuously supplies hydrogen into the material during mechanical testing, offering a more precise simulation of actual service environments. This study introduces in-situ hydrogen charging of CrCoNi to provide a deeper understanding of its performance under realistic conditions. Surprisingly, this approach resulted in rapid fracture and severe embrittlement, uncovering critical insights into the material's behavior. The research seeks to elucidate the underlying mechanisms through comprehensive experiments, including post-mortem fracture surface analysis.

Keywords : High Entropy Alloy, Medium Entropy Alloy, Hydrogen Embrittlement, In situ charging

295. Great compositional discovery in materials history

Yeh Jien-Wei ¹

National Tsing Hua University, Taiwan

The new composition concept Multi-principal-element compositions was a breakthrough of alloy compositions. Professor Cantor and I independently explored this alloy field near the end of 20th century and published related papers in the beginning of this century. In order to emphasize the most importance of high mixing entropy in enhancing the formation of solid solution phases, I especially defined high-entropy alloys as those having at least five principal elements, medium-entropy alloys having 3 or 4 principal elements and low-entropy alloys having 1 or 2 elements. In addition to the high-entropy effect, I proposed other three core effects: lattice distortion, sluggish diffusion and cocktail, to help the understanding of high-entropy alloys. I also extended the concept of high entropy from alloys to ceramics, polymers and composite materials, and constructed the world of low-entropy, medium-entropy and high-entropy materials, which almost covers all possible compositions from the periodic table. In addition to the academic research, many new materials have been presented for overcoming the bottlenecks of traditional alloys in applications and even creating new applications. The high-entropy-related papers display an exponential growth in yearly numbers since 2004, which shows a broad and far-reaching influence. In recent years, I have led a team to industrialize green and healthy high-entropy material technology in both domestic and foreign industries.

Keywords : High Entropy Alloys, High, Entropy Materials, Medium, Entropy Alloys, Medium, Entropy Materials, Four Core Effects

296. Shape memory effect in CrMnFeCoNi high-entropy alloys with high Co/Ni ratio

Lee Je In¹, Lim Jinsurang ¹, Jeong Hwiyeun ¹

1 - Pusan National University (South Korea)

Designing novel materials in metal community has generated significant interest for the concept of high-entropy alloys (HEAs) or multi-principal element alloys to develop structural and/or functional materials with outstanding properties. In this study, we demonstrate reversible martensitic transformation between austenite fcc and martensite hcp phases in the CrMnFeCoNi quinary alloy systems. The phase transformation in the fcc-structured HEAs was predicted by calculating the difference in Gibbs free energy between fcc and hcp phases via CALPHAD simulation. It was found that initial microstructure, phase transformation temperature, and shape recovery strains were strongly affected by varying alloy composition in the quinary system. To improve the recovery strain of the novel HEAs, the effect of grain structure and alloying elements was systematically investigated. These results could suggest a new application of the multi-principal element alloys as low- and/or high-temperature shape memory materials.

Keywords : high, entropy alloy, shape memory alloy, martensitic transformation, CALPHAD

297. Achieving remarkable strength and ductility through via nano-twinning enabled by L12 nano-precipitates in CoNiMoAl medium-entropy alloys

Sung Minyoung¹, Jang Tae Jin¹, Song Sang Yoon¹, Lee Gunjick¹, Ryou Kenhee², Oh Sang-Ho³, Lee Byeong-Joo³, Choi Pyuck-Pa², Neugebauer Joerg⁴, Grabowski Blazej⁵, Koermann Fritz⁶, Ikeda Yuji⁴, Zargaran Alireza³, Sohn Se

1 - Korea University (South Korea), 2 - Korea Advanced Institute of Science and Technology (South Korea), 3 - Pohang university of science and technology (South Korea), 4 - Max€“Planck€“Strabe 1 (Germany), 5 - University of Stuttgart (Germany), 6 - Ruhr-Universitat Bochum (Germany)

Alloys with a single-phase FCC matrix containing L12 precipitates have demonstrated superior properties compared to conventional FCC alloys, garnering significant research attention. However, the increased stacking fault energy due to L12 precipitates often induces deformation via dislocations rather than twins, resulting in low work hardening capacity relative to their high yield strength in conventional FCC+L12 alloys. In this study, Al is added to a CoNiMo alloy, which inherently exhibits high yield strength through solid solution strengthening and grain boundary strengthening, coupled with low stacking fault energy that facilitates twin formation. The microstructure of the alloy comprises an FCC matrix with L12 and HCP+D019 precipitates. After cold rolling and short-term heat treatment at 1000 °C, a recrystallized microstructure with fine grain size is achieved, followed by aging treatment to form nano-sized spherical L12 precipitates within the grains and HCP+D019 precipitates along the grain boundaries. The L12 precipitates contribute to the formation of various stacking faults through interactions with dislocations and promoted nano-twin formation even in the early stages of deformation. Meanwhile, the HCP+D019 precipitates, which exhibited higher strength compared to the FCC matrix, facilitated dislocation accumulation. This synergistic effect of L12 and HCP+D019 precipitates enabled the design of an alloy with a yield strength of 1087 MPa, tensile strength of 1526 MPa, and elongation of 34%, demonstrating excellent strength-ductility-work hardening balance. The influence of each precipitate phase on dislocation behavior and mechanical properties is systematically analyzed.

Keywords : Medium entropy alloy, L12 nano, precipitate, Nano, twin, Strain, hardening capability, DFT calculation

298. Development of Ti based bio-high entropy alloys

Todai Mitsuharu^{1 2}, Takahashi Nagi¹, Tanaka Neiro¹, Tanaka Daisuke¹, Nagase Takeshi³, Matsugaki Aira⁴, Nakano Takayoshi⁴

1 - National Institute of Technology, Niihama College (Japan), 2 - Institute of Industrial Science [Tokyo] (Japan), 3 - University of Hyogo (Japan), 4 - Osaka University (Japan)

High-entropy alloys (HEAs) are solid solutions consisting of five components that have attracted a great deal of attention because of their high strength. We reported on the potential of high-entropy alloys as biomaterials on 2017 (Scripta Materialia 129 (2017) 65-68). A number of bio- HEAs have been reported since 2017. In this study, we report the history of the development of bio-HEAs and the microstructure, mechanical properties, and biotoxicity of new hcp-type titanium-based bio-HEAs. Specifically, TiZrHfAlx alloys, in which Al is added to the TiZrHf alloy, were prepared by vacuum arc melting, and their crystal structure, microstructure, mechanical properties, and biotoxicity were investigated. The results showed that TiZrHfAlx alloys exhibit an hcp structure, high strength comparable to that of fcc-based HEAs, and biocompatibility comparable to that of pure Ti.

Keywords : High entropy alloys, Metallic bio materials, microstructure, Strength

299. An Assessment of the Viability of the Refractory Metal High Entropy Alloy AlMo0.5NbTa0.5TiZr for High Temperature Structural Applications

Wise George¹, Church Nicole ¹, Pang Hon Tong ¹, Thompson Robert ¹, Stone Howard ¹, Jones Nicholas ²

1 - Department of Materials Science and Metallurgy, University of Cambridge, 27 Charles Babbage Road, Cambridge, CB3 0FS (United Kingdom), 2 - Department of Materials Science and Metallurgy, University of Cambridge, 27 Charles Babbage Road, Cambridge, CB3 0FS (United Kingdom)

There is a significant research effort to develop new structural materials for high temperature service, so that enhanced efficiencies can be realised in next-generation power and propulsion applications. High-Entropy or Multiple Principal Element alloys incorporating refractory elements have been shown to be a viable source of potential new materials for these applications, with significant increases in thermal capabilities compared to current commercially used alloys. Despite this, significant work is required in order to evaluate the suitability of these materials for operation in extreme environments of temperature and mechanical load. One alloy that has received considerable attention is AlMo0.5NbTa0.5TiZr, a multi-phase alloy comprising an ordered B2 matrix and disordered A2 precipitates. In this work, we report on studies of the phase equilibria and mechanical properties as function of temperature, for the first time providing an in-situ determination of the B2 solvus, correlated to the changes in mechanical properties. In addition, a low temperature (800°C) regime of catastrophic accelerated oxidation has been identified, which is discussed in context of the potential future applications for this alloy. These results highlight significant limitations in AlMo0.5NbTa0.5TiZr and related alloys, making them unsuitable for high temperature structural applications in their current form.

Keywords : Thermec'2025, High Entropy Alloys, Oxidation, Mechanical Properties, X, ray Diffraction

300. Deciphering the operative mechanisms affecting the strain rate sensitivity in (FeCrNi)99Si1 medium entropy alloy during high-pressure torsion

Mahato Swati¹, Biswas Krishanu , Gurao Nilesh Prakash ²

1 - Indian Institute of Technology [Kanpur] (India), 2 - Department of Materials Science and Engineering, Indian Institute of Technology Kanpur (India)

The primary objective of the present investigation is to decipher the operative micromechanisms influencing the strain rate sensitivity and activation volume in low stacking fault energy (FeCrNi)99Si1 medium entropy alloy. Nanoindentation techniques using different loading rates were employed to estimate the strain rate sensitivity and activation volume of the alloy subjected to high-pressure torsion samples at 300 K to study the effect of the strain. Unlike the general trend followed by FCC metals and alloys, with an increase in strain rate sensitivity with a decrease in grain sizes, (FeCrNi)99Si1 exhibits decreased strain rate sensitivity with decreasing grain size. The present study reveals an opposite trend followed by strain rate sensitivity concerning grain size in the current alloy. Furthermore, the alloy exhibits remarkably low activation volume in the microcrystalline grain size regime which decreases marginally with grain size reduction to the nanocrystalline regime. The present study explores the deviation from the reported trend by examining the evolution of dislocation structure and the synergetic operation of additional mechanisms like twinning, cluster strengthening, and short-range ordering due to the aperiodic energy landscape of the present medium entropy alloy.

Keywords : Medium entropy alloy, Strain rate sensitivity, Synchrotron, Activation volume, Twinning, short, range ordering

301. In-vivo bone implantation study of TiZrNbTaFe high entropy alloy thin films

Lou Bih-Show¹, Lee Jyh-Wei ², Hou Sen-You ³, Chen Po-Yu ⁴

1 - Chang Gung University (Taiwan), 2 - Ming Chi University of Technology (Taiwan), 3 - National Tsing Hua University (Taiwan), 4 - National Tsing Hua University [Hsinchu] (Taiwan)

With aging populations and increased rates of injury, the demand for orthopedic implants has grown significantly. Modifications to the implant surface have been developed to improve its longevity by boosting its mechanical and physiochemical properties. High entropy alloys (HEAs) represent a new class of metallic biomaterials that enable the synergistic combination of properties to tailor the resultant coatings for specific applications. Using a sputtering system, this work prepared two amorphous TiZrNbTaFe HEA films with different Ti concentrations on the surfaces of cp-Ti rods. These bare and coated cp-Ti rods were implanted into the distal rat femur to assess each implant's osseointegration through pull-out tests, histologic analysis, and micro-computed tomography imaging. There was no change in physical activity or delayed wound healing after implantation. The TiZrNbTaFe HEA-coated implants enhanced collagen synthesis and mineralization and improved bone-like tissue fixation at the implant surfaces compared to uncoated cp-Ti. The Ti-rich TiZrNbTaFe thin film showed a more noticeable improvement. This study suggested that TiZrNbTaFe HEA thin films can improve the quality and quantity of newly formed bone while promoting osseointegration, implying their potential and applicability for orthopedic applications.

Keywords : high entropy alloy thin film, TiZrNbTaFe, sputtering, bone implantation, osseointegration

302. Optimizing Al content to eliminate the brittle phase in lightweight TiZrNbTa0.1Alx refractory high-entropy alloys

Liao Wei-Bing ¹

¹ - Shenzhen University (China)

Body-centered cubic (BCC) lightweight refractory high-entropy alloys (LWRHEAs) with Al contents have attracted much attention due to their low density and excellent mechanical properties. However, these typical lightweight alloys often suffer from poor room-temperature plasticity. In this study, we prepared TiZrNbTa0.1Alx LWRHEAs by high-vacuum arc-melting technique, and investigated the Al content influence on the phase structures and mechanical properties. It was found that the TiZrNbTa0.1Al1 alloy showed a BCC solid solution matrix with some micron-sized Al₃Zr₅ precipitates, and exhibited a density of 6.110 ± 0.003 g/cm³. The TiZrNbTa0.1Al1 alloy had a low mixed enthalpy of -20.831 kJ/mol and a compressive yield strength of 1037 ± 178 MPa, and a fracture plasticity of ~ 6 %. As reducing the Al content, the TiZrNbTa0.1Al0.2 alloy showed a simple BCC phase structure without any precipitates, and maintained a low density of 6.743 ± 0.008 g/cm³. The TiZrNbTa0.1Al0.2 alloy had a relatively high mixed enthalpy of -4.5577 kJ/mol and a high yield strength of 1022 ± 51 MPa and a plasticity of > 70 %. The TEM analysis results demonstrated that the excellent mechanical properties of this LWRHEAs were mainly attributed to the reducing Al content, which could elevate the mixed enthalpy of the alloy to eliminate the brittle Al₃Zr₅ phase and induce the formation of a dense network dislocations at the grain boundaries.

Keywords : Lightweight refractory high, entropy alloy, Microstructure, Mechanical properties, Second phases

303. Shape memory effect in CrMnFeCoNi high-entropy alloys with high Co/Ni ratio

Lim Jinsurang¹, Jeong Hwiyun ¹, Lee Je In ²

1 - Pusan National University (South Korea), 2 - Pusan National University (South Korea)

Designing novel materials in metal community has generated significant interest for the concept of high-entropy alloys (HEAs) or multi-principal element alloys to develop structural and/or functional materials with outstanding properties. In this study, we demonstrate reversible martensitic transformation between austenite fcc and martensite hcp phases in the CrMnFeCoNi quinary alloy systems. The phase transformation in the fcc-structured HEAs was predicted by calculating the difference in Gibbs free energy between fcc and hcp phases via CALPHAD simulation. It was found that initial microstructure, phase transformation temperature, and shape recovery strains were strongly affected by varying alloy composition in the quinary system. To improve the recovery strain of the novel HEAs, the effect of grain structure and alloying elements was systematically investigated. These results could suggest a new application of the multi-principal element alloys as low- and/or high-temperature shape memory materials.

Keywords : high, entropy alloy, shape memory alloy, martensitic transformation, CALPHAD

304. Towards multifunctionality in novel high entropy alloy by compositional variation and thermo-mechanical processing

Dutta Akshit¹, Tsai Ming-Hung², Nene Saurabh¹

1 - Advanced Materials Design and Processing Group, Department of Metallurgical and Materials Engineering, Indian Institute of Technology Jodhpur, Karwar, Jodhpur, Rajasthan 342030, India (India), 2 - Department of Materials Science and Engineering, National Chung Hsing University, Taichung City 402, Taiwan (Taiwan)

High-entropy alloys (HEAs) exhibit a diverse range of functionalities, yet achieving a balance between multiple property profiles remains a significant challenge. In this study, we explore the multifunctionality in Fe(65-x-y-z)Mn20Cr15NixCoySiz (at. %) HEAs by leveraging alloy chemistry and thermo-mechanical processing (TMP) to integrate multiple property profiles within a single processed state. The hierarchical microstructure evolved through TMP dictates superior mechanical performance while simultaneously introducing microstructural complexities such as grain size heterogeneity and annealing twins that affect magnetic domain wall mobility and hence magnetic coercivity. Despite this trade-off, Fe44Mn20Cr15Ni7.5Co6Si7.5 HEA (M-HEA) demonstrates a unique convergence of key structural/functional properties, including strength-ductility synergy, corrosion resistance, fatigue resistance, and compressive superformability. However, achieving a balance between mechanical and magnetic performance is crucial to further expand its practical utility. Therefore, this work systematically examines the interplay between alloy composition (especially the role of Ni, Co, and Si), microstructural features, and multifunctional performance, demonstrating that strategic microstructural and compositional modifications can enhance both mechanical performance and magnetic efficiency. If M-HEA exhibits favourable magnetic response, it would further establish its potential as a multifunctional yet sustainable alternative to conventional structural materials.

Keywords : High Entropy Alloy, Thermo mechanical processing, Strength ductility synergy, Soft magnetic response, Multifunctionality

305. Investigation of a Spinel Oxide Coating based on CoCuFeMnNi High-Entropy Alloy for SOFC application

Yeh An-Chou¹, Tsai Cheng-Ju², Murakami Hideyuki³, Yoshiaki Toda³, Ouyang Fan-Yi⁴

1 - High Entropy Materials Center, National Tsing Hua University (Taiwan), 2 - Department of Materials Science and Engineering, National Tsing Hua University (Taiwan), 3 - National Institute for Materials Science (Japan), 4 - Department of Engineering and System Science, National Tsing Hua University (Taiwan)

The CoCrFeMnNi Cantor alloy is a symbolic system which has inspired research of fundamental science and potential applications. This study looks at the functional properties of oxide materials derived from the Cantor alloy, we aim to investigate their potential as coatings for the solid oxide fuel cell (SOFC) interconnector. Spinel oxide coatings were based on CoFeMn, CoCuFeMn, and CoCuFeMnNi alloys, these alloys were deposited by magnetron sputtering method onto an interconnector material - SUS441 stainless steel as the target substrate. To convert these alloys into oxide coatings, a 24-hour pre-oxidation treatment at 650°C was employed. The properties of different coating materials were evaluated by isothermal oxidation test at 650°C, area specific resistance (ASR) and Cr evaporation studies. The experimental results indicate that CoCuFeMnNi high entropy alloy appeared to form a single-phase spinel oxide, and its thermal stability, ASR and Cr evaporation resistance performances have significantly surpassed those based on CoFeMn and CoCuFeMn alloys. This study can serve as a guideline to develop coating technology for SOFC interconnector applications.

Keywords : High Entropy Alloys, Oxide Coating, Solid Oxide Fuel Cell, Thermal Stability, Oxidation Resistance, Area Specific Resistance, Cr Evaporation

306. Microstructures and Properties of CoCrFeMn High Entropy Shape Memory Alloys Produced by Laser Direct Energy Deposition

Wookjin Lee, Minsu Park V

School of Materials Science and Engineering, Pusan National University, Busan, 46241, Republic of Korea.

Laser direct energy deposition (L-DED) is an additive manufacturing process that utilizes a focused laser beam to melt and deposit metal powder onto a substrate, enabling precise and efficient metal 3D printing. This technique is widely used for repairing, coating, and fabricating complex 3D metal components with high deposition rates and good mechanical properties. On the other hand, Co-Cr-Fe-Mn high-entropy alloys (HEA) are a unique type of high-entropy alloys which shows shape memory properties due to the stress-induced fcc (face-centered cubic) to hcp (hexagonal closed packed) phase transformation and its reverse when heating. In this study, Co-20Fe-19Cr-18Mn (wt.%) HEAs, with and without carbon addition, were produced by the L-DED process. The effect of carbon addition on microstructure, mechanical properties and shape memory behavior of the HEA were investigated. It was shown that the L-DED processed HEA exhibited good shape memory performance.

Keywords : High Entropy Alloy, Shape Memory Alloy, Laser Direct Energy Deposition

307. Shift and delete effect on aluminum twist grain boundary energy

Nishitani Shigeto¹, Tamura Tomoyuki², Kobayashi Ryo²

1 - Kwansei Gakuin University (Japan), 2 - Nagoya Institute of Technology (Japan)

A widely accepted model for low-angle grain boundary is the Read-Shockley dislocation model [1]. For understanding high-angle grain boundaries, however, there is no unified model. The high degree of freedom in high-angle grain boundaries, in-plane translations and atom deletion at the grain boundary, makes it computationally expensive to explore the entire configuration space. In this study, we employed first-principles calculations to investigate these effects on low sigma symmetric twist boundaries in aluminum. We employed both VASP and QMAS [2] for first-principles calculations. While VASP is widely used in materials science, QMAS has a routine implemented to calculate the individual atomic energies. To select high-energy atoms for deletion, we compared an empirical potential of EAM (embedded atom method) and QMAS. Although EAM involves arbitrariness due to the parametrized interactions, QMAS provides a theoretically predicted energy based on electronic theory. The results showed that while the absolute values differed, the order of energies was consistent. The energy of the (011) \Sigma 3 model, which was applied the deletion process following this procedure, reproduced the experimentally obtained results [3]. The structure and the energy of this orientation can be interpreted as having collapsed from an ideal structure with energy extrapolated from the low-angle region of the Read-Shockley plot. As schematically drawn on Fig.1, while conventional high-angle models involve adding extra energy to a low-energy state, the collapse model suggests that the experimentally observed energy is obtained by relaxation from a higher-energy state.

References: [1] W. Shockley and W. T. Read, Phys. Rev., 75 (1949), p. 692. [2] S. Ishibashi, T. Tamura, S. Tanaka, M. Kohyama, and K. Terakura, Phys. Rev. B 76 (2007), 153310. [3] A. Otsuki, Research on boundary energy of Al, Ph.D. diss., (Kyoto Univ. 1990), pp.99-120.

Keywords : Grain Boundary, Read Shockley, Dislocation Theory, First Principles Calculation

308. A Systematic Study of Grain Boundary Segregation in Nanocrystalline Alloys

Chandross Michael¹, Winter Ian², Montes De Oca Zapiain David²,
Mahmood Yasir³, Abdeljawad Fadi⁴, Asta Mark⁵, Curry John²

1 - Sandia National Laboratories (New Mexico Sandia National Laboratories, New Mexico PO Box 5800 Albuquerque, NM 87185 United States), 2 - Sandia National Laboratories (United States), 3 - National Institute of Standards and Technology [Gaithersburg] (United States), 4 - Lehigh University [Bethlehem] (United States), 5 - University of California, Berkeley (United States)

Segregation of solute atoms to grain boundaries (GBs) in metallic alloys can often impart thermomechanical stability of nanocrystalline microstructures. This, in turn, can lead to desirable mechanical properties including increased hardness and corrosion resistance. While some efforts have been made to understand the propensity for GB segregation through thermodynamic and atomistic modelling, a detailed understanding of the general relationships between elements that lead to segregation is still lacking. We present the results of simulations of GB segregation using EAM-X, a newly developed atomistic model for metals that enables systematic studies of the links between elemental properties and structure. We show how the differences between the elements (e.g. difference in atomic radius, enthalpy of mixing, etc.) result in segregation using 35 GBs, including symmetric tilt, asymmetric tilt and symmetric twist boundaries. Our results are coupled with machine learning to both accurately predict the propensity for segregation as well as to identify the key properties with the strongest influence. We also examine the effects of segregation on GB mobility in order to develop an understanding of nanocrystalline stability in these alloys. SNL is managed and operated by NTESS under DOE NNSA contract DE-NA0003525 (SAND2022-1056 A).

Keywords : Grain Boundary Segregation, Molecular Dynamics, Nanocrystalline Alloys

309. Comparison of Pd-42Cu-10Ni and Pd-30Cu-29.5Ag-0.5Zn as Probe Material in Interfacial Reaction with Sn

Hashizume Rin¹, Kobayashi Tatsuya¹, Shohji Ikuo¹, Hoshino Tomohisa², Sato Kenichi², Kobayashi Shunsuke², Odani Naohito²

1 - Graduate School of Science and Technology, Gunma University (Japan), 2 - YOKOWO CORPORATION (Japan)

Semiconductor packages with solder balls such as a ball grid array are inspected for energization using the test probe. The probe material is often damaged due to solder adhesion on it by repeated test. The Pd-42Cu-10Ni (mass%) alloy has been developed as a substitute material for the conventional probe material, Pd-30Cu-29.5Ag-0.5Zn alloy (mass%). The alloy was confirmed to be effective to suppress the interfacial reaction with Sn-Bi system solder. It was also clarified that the Bi phase scarcely take part in the interfacial reaction and the reaction between the Sn phase and the constituent elements of the probe material causes the growth of the reaction layer. Thus the interfacial reaction between Pd-42Cu-10Ni and pure Sn was investigated under aging conditions in this study. Moreover, the growth rate of the reaction layer was compared with that in the interface between Pd-30Cu-29.5Ag-0.5Zn and pure Sn. As a result, it was confirmed that granular (Cu, Ni)₆Sn₅ forms near the interface with Sn in the reaction layer, and the reaction layer mainly consists of stacked layers of the PdSn₄+PdSn₃ layer and the (Cu, Ni)₆Sn₅+Cu₃Sn+PdSn layer. The reaction layer mainly grew toward the Sn side from the joint interface. The ratio of the thickness of the reaction layer grown in the Sn side and that in the probe side was approximately 4:1. Furthermore, the thickness of the reaction layer was reduced to approximately a quarter in comparison with conventional alloy.

Keywords : Pd, 42Cu, 10Ni, Pd, 30Cu, 29.5Ag, 0.5Zn, Sn, Aging Treatment, Reaction Layer

310. Precipitation and growth behavior of β_0 phase in the α_2 /r lamellar colonies of an intermetallic Ti-43.5Al-4Nb-1Mo-0.1B alloy

Cha Limei ¹

¹ - Guangdong Technion-Israel Institute of Technology (China)

The precipitation and growth behavior of $\beta(\beta_0)$ phases in an intermetallic Ti-43.5Al-4Nb-1Mo-0.1B (at.%) alloy were investigated using X-ray diffraction (XRD), focused ion beam-scanning electron microscopy (FIB-SEM) and transmission electron microscopy (TEM). The results show that the applied heat treatment changes the volume fraction of the constituting phases and thus the feature of the lamellar microstructure in the alloy. Furthermore, a three-dimensional (3D) reconstruction reveals that β_0 precipitates mainly form small rods within the α_2 lamellae. There, the rod-shaped β_0 precipitates grow in different well-defined directions, and some precipitates are interconnected along their growth paths. TEM investigations indicate that beside the Blackburn orientation relationship (OR): $(0001)\alpha_2 // \{111\}\gamma$, $\langle 11\bar{2}0 \rangle \alpha_2 // \langle 1\bar{1}0 \rangle \gamma$, the β_0 precipitates which emerge from the α_2 lamellae obey the following OR: $(0001)\alpha_2 // \{110\}\beta_0$, $\langle 11\bar{2}0 \rangle \alpha_2 // \langle 111 \rangle \beta_0$. In addition, the $\{110\}$ planes of β_0 have multiple variants. As a consequence, they can grow in different directions in the α_2 lamellae.

Keywords : Intermetallics, TiAl alloy, Heat treatment, Precipitation, 3D reconstruction, Transmission electron microscopy, Interface energy

311. Microstructural characterization and analyses of the of the damage in a Ti-based alloy by X-ray computed microtomography

Avila-Davila Erika O.¹, Monroy-Sanchez Ixchel¹, Moreno-Martinez Jesus D.¹, Moreno-Rios Marisa¹, Cayetano-Castro Nicolas², Lopez-Hirata Victor M.³, Resendiz-Hernandez Jose E.⁴

1 - Tecnológico Nacional de México-Pachuca, DEPI, Pachuca de Soto, Hgo., C.P. 42080 (Mexico), 2 - Instituto Politécnico Nacional (CNMN), UPALM, Ciudad de México. C.P. 07738 (Mexico), 3 - Instituto Politécnico Nacional (ESIQIE), UPALM, Edif.7, Ciudad de México. C.P. 07738 (Mexico), 4 - Tecnológico Nacional de México-Pachuca, DEPI, Pachuca de Soto, Hgo., C.P. 42080 (Mexico)

The microstructural characterization of a titanium-based alloy (Ti-based alloy) was carried out with the purpose to obtain an evaluation of the internal damage of this alloy, used in the fabrication of a blade located in the fan of an aeronautic turbine. It is important to mention that the blade studied was retired from in-service operation aeronautic. An analysis by X-ray computed microtomography and scanning electron microscopy of three specimens obtained of the tip and root of the blade and of its middle section, along its length, was carried out. These results were compared with those obtained from the microstructural characterization by optical microscopy of fifteen specimens of about 15 x 5 x 4 mm, all cut in the middle section of the blade, along its length. The results of this study show the occurrence of erosive wear in the surface of the blade and the deformation of grains in the longitudinal section of the component, which could be related to the mechanical stress direction during in-service operation of the element. They were not observed changes in the microstructure of the transversals sections images of the specimens obtained by optical and scanning electron microscopy, with respect to that reported in literature. The results obtained by X-ray computed microtomography do not show evidence of internal cracking sever. Finally, it was concluded that the deformation of grains along longitudinal section of the blade is a critical parameter to remove the component of its in-service operation.

Keywords : Structural characterization techniques, X ray computed microtomography, Ti based alloys.

312. Deformation behavior of magnesium bicrystals with $90^\circ\langle 10\text{-}10\rangle$ and $90^\circ\langle 11\text{-}20\rangle$ grain boundaries: Changing grain boundary character and boundary proximity

Bissa Kevin¹, Schreiber Marcel¹, Molodov Konstantin², Al-Samman Talal³, Molodov Dmitri^{1 4}

1 - Institute of Physical Metallurgy and Materials Physics, RWTH Aachen University (Germany), 2 - Department of Materials and Process Development, Salzgitter Mannesmann Forschung GmbH (Germany), 3 - Institute of Physical Metallurgy and Materials Physics, RWTH Aachen University (Germany), 4 - International Research Organization for Advanced Science and Technology (IROAST), Kumamoto University (Japan)

Grain boundaries play a significant role in the deformation of polycrystals. Their response to deformation is however not completely understood, particularly with respect to how they accommodate lattice rotation of adjoining crystallites. The current study thus investigates the deformation behaviour of Mg bicrystals with $90^\circ\langle 10\text{-}10\rangle$ and $90^\circ\langle 11\text{-}20\rangle$ tilt boundary strained in plane-strain compression up to different final strains. Due to the initial soft orientation of the two crystals, activation of basal slip in each crystal gave rise to lattice rotation around the transverse direction towards the compression direction of the channel-die. Orientation measurements showed that the initial character of the grain boundary changed significantly during plastic straining. This was interpreted in terms of the interaction between grain boundary and incoming lattice dislocations gliding on the basal planes, which caused a gradual annihilation of the grain boundary structural units. When deformation in the two grains became markedly non-uniform at larger strains of 0.3 and 0.4 due to the presence of the boundary, the adjacent regions of the latter underwent a pronounced lattice curvature of about $0.005\text{ deg}/\mu\text{m}$ persisting over a distance of 4 mm from the boundary. The reported observations demonstrated the excellent capability of the investigated grain boundary to accommodate strain-induced lattice rotation by substantially changing its structure, thereby preventing intercrystalline fracture of the material up to a certain level of deformation.

Keywords : Grain boundary, Bicrystal, Magnesium, Lattice rotation, Dislocation gliding

313. Assessment of Adhesion Degradation in A1050/Epoxy Resin Interface Under High-Humidity and High-Temperature Aging Conditions

Ryota Nakagawa¹, Shohji Ikuo ¹, Funatomi Fumiya ², Ohashi Kyohei ², Sakai Ryuki ², Kobayashi Tatsuya ¹

1 - Graduate School of Science and Technology, Gunma University (Japan), 2 - Test Consulting Service Headquarters, ESPEC CORP. (Japan)

In recent years, global environmental measures, energy conservation, and efficiency improvements through power electronics technology have gained considerable attention. A key issue is reducing power loss in power modules, which are critical components of power electronics. Epoxy resins, thermosetting resins, are widely used in semiconductor encapsulation because of their excellent heat resistance, chemical resistance, electrical insulation, and strength. However, the development of next-generation power semiconductor devices has led to power modules that are smaller, operate at higher temperatures, and handle higher current densities, necessitating even greater performance and functionality from epoxy resins. In this context, understanding the factors influencing adhesion at the metal-epoxy resin interface has become an important area of research. The purpose of this study was to develop an analytical approach to clarify the relationship between adhesion and deterioration at the metal/epoxy resin interface under high-temperature and high-humidity conditions. Evaluations were conducted through Fourier transform infrared spectrometer (FT-IR) analysis and adhesive strength tests. FT-IR analysis showed that hydrogen bonding gradually weakened as water absorption in the A1050/epoxy resin substrate increased, with this effect becoming more pronounced as the resin layer thickness decreased. Adhesive strength tests further revealed a decline in adhesive strength with prolonged aging time. Observations of the fracture surfaces confirmed a decrease in the cohesive fracture ratio as aging time increased, indicating a shift towards interfacial fracture.

Keywords : Epoxy Resin, A1050, Adhesion, Thermal Humidity Test, Water Absorption

314. Degradation Behaviour of Sn-Ag-Cu Lead-free Solder Joint with Electrolytic Ni Plated Electrode due to Electromigration

Kawaguchi Kenta¹, Oyama Marina ¹, Kobayashi Tatsuya ¹, Shohji Ikuro ¹, Nakamura Keishi ², Hirasawa Koichi ², Amemiya Hitoshi ²

1 - Graduate School of Science and Technology, Gunma University (Japan), 2 - KOA CORPORATION (Japan)

In recent years, the current density in the solder joint has been increasing due to the miniaturization of electronic components. Therefore, degradation of the solder joint due to electromigration (EM) has become a problem. Recently, Ni plating has been expected to suppress the growth of intermetallic compound formed in the joint interface, which is one of the degradation behaviours. However, the effects of Ni plating on the deterioration suppressant effect has not been yet understood well. In this study, EM tests were conducted on the solder joints with electrolytic Ni plated Cu electrodes to observe the microstructural change of the joint, and the effect of electrolytic Ni plating on EM was investigated. Three types of specimens with Ni plating thicknesses of 1 μm , 5 μm and without Ni plating were prepared. Sn-3.0Ag-0.5Cu (mass %) solder was used as the solder. EM tests were conducted with a current density of 15 kA/cm² at the solder joint interface. After the EM test, microstructural observation was conducted using an electron probe X-ray microanalyzer. It was clarified that the electrolytic Ni plating suppresses the growth of the reaction layer in the joint interface in the anode side by applying current. This is due to the fact that the Ni plating layer suppresses Cu diffusion to the anode side. Moreover, in most specimens, the formation of voids was observed in the solder side of the joint interface in the cathode side after applying current.

Keywords : Electromigration, Solder Joint, Sn, Ag, Cu Solder, Ni Electrolytic Plating

315. Evaluation of Joining Properties Between Potential-Controlled Ni-Cu Alloy Plating Film and Pb-Free Solder

Mori Sota¹, Shohji Ikuo ¹, Kobayashi Tatsuya ¹

¹ - Graduate School of Science and Technology, Gunma University (Japan)

In this study, the effect of potential on Ni-Cu alloy electroplating was investigated, and the solder joint properties of Cu plates with Ni-Cu alloy electroplating films were evaluated. Dendritic structures were observed to form on the Ni-Cu alloy electroplating films, with these structures growing larger and more numerous at higher negative potentials, independent of the Cu plate surface properties. On the rough surface, a smaller number of large dendritic structures were formed, suggesting that plating cores are preferentially generated on surface protrusions. Conversely, on the smooth surface, a high density of uniformly distributed dendritic structures formed, suggesting that plating nuclei were generated at various parts across the surface. In a solder joint using a Ni-Cu alloy plating film, cross-sectional observation of the joint showed that Ni-Cu and Cu were detected in dendritic form at the as-soldered joint interface that the Ni-Cu alloy plating film retained its three-dimensional structure even after joining. Cu, Ni, and Sn were detected in the same region at the joining interface under all conditions, and the region expanded with increased aging time, confirming that progressive growth of the Cu-Ni-Sn compound as a result of aging treatment. Shear tests of the joints showed lower strength compared to unplated joints, with a further decrease in shear strength observed after 25 hours of aging treatment. Fracture surface observations indicated that after 100 h of aging, fractures occurred within the solder and in the Cu-Ni-Sn and Cu-Sn intermetallic compounds.

Keywords : Ni, Cu Alloy, Electroplating, Electrochemical Method, Solder Joint

316. Effect of Thermal Cycle Profile on Thermal Fatigue Life of Sn-3.0Ag-0.5Cu Solder Joints for Wafer-Level Chip Scale Package

Sakagami Shun¹, Kawaguchi Kenta¹, Kobayashi Tatsuya¹, Shohji Ikuo¹, Funatomi Fumiya², Ohashi Kyohei², Sakai Ryuki²

1 - Graduate School of Science and Technology, Gunma University (Japan), 2 - Test Consulting Service Headquarters, ESPEC CORP. (Japan)

Thermal cycling tests were conducted on solder joints of wafer-level chip scale packages (CSPs) with Sn-3.0Ag-0.5Cu (mass%) to investigate the effect of difference in the thermal cycle profile by using various equipment on the thermal fatigue properties. The CSP with 10 x 10 rows of Cu post electrodes of 0.20 mm dia. and 0.05 mm height at 0.4 mm pitch on a Si chip was prepared. The CSP was bonded to the FR-4 substrate with Sn-3.0Ag-0.5Cu (mass%) solder balls. Thermal cycling tests were conducted using three types of equipment: liquid phase type, two zone type and sample stationary type. The temperature range for the thermal cycle tests was -40°C to 125°C, and the holding time at high and low temperatures were 15 min. The results showed that the thermal fatigue life tends to be shorter when the temperature change rate in the thermal cycle profile is slow. In the finite element analysis, it was also confirmed that the inelastic strain amplitude applied to the solder joint was the largest under the thermal cycle loading condition with a slow temperature change rate, and the thermal fatigue life tended to be shortened. From the results of microstructural analysis of the damaged solder joints, it was confirmed that the cracks generated by the thermal cycling test propagate along the grain boundaries of recrystallized grains generated on the CSP side in the solder joint, suggesting that the way of the generation of recrystallized grains in the solder joint may affect the thermal fatigue life.

Keywords : Lead, free solder, Sn, 3.0Ag, 0.5Cu, Thermal Cycle Profile, Thermal Fatigue Behaviour, Crystal Orientation Analysis, Finite Element Analysis

317. Investigation of Degradation Behavior of Adhesion between Sealing Resin and Copper by Aging Treatment

Tozaki Anzu¹, Kobayashi Tatsuya ¹, Shohji Ikuo ¹, Takenaka Hiroto ², Suzuki Hirose ², Ueshima Minoru ²

1 - Graduate School of Science and Technology, Gunma University (Japan), 2 - Daicel corporation (Japan)

In this study, we focused on alicyclic epoxy resin used for encapsulation of power modules and investigated the degradation behavior of the copper/resin interface under high temperature and high humidity conditions. As a specimen, the joint of two Cu rivets with the resin was prepared. Two aging treatments were conducted on the specimens. As a high temperature storage test, the specimens were aged at 175 °C for 1000 h. As a high temperature and high humidity storage test, they were aged at 85 °C in 85% R. H. for 1000 h. The aged copper/resin joints were analyzed by a tensile test and the fracture surface was observed by Fourier transform infrared spectroscopy (FT-IR). As a result, it was confirmed that the bond strength was retained after aging at 175 °C for 1000 h, while it decreased with an increase in the aging time under the high temperature and high humidity aging. Furthermore, it was found that the interfacial fracture increased with aging in the high temperature aging. On the other hand, cohesive fracture was the main fracture mode regardless of aging in the high temperature and high humidity aging. From the FT-IR analysis results, it was found that the peak intensity of the carbonyl group increased and that of the methylene group decreased due to the high temperature aging. Moreover, the peak intensities of carboxy and hydroxyl groups increased and that of ester groups decreased due to the high temperature and high humidity aging.

Keywords : Epoxy Resin, Cu, Bond Strength, High Temperature and High Humidity Storage Test

318. Plastic deformation propagation across grain boundaries in Fe-3%Si bicrystals: A comparative study of twist and tilt grain boundaries

Ichimura Yoshitake¹, Molodov Dmitri ^{2 3}, Ii Seiichiro ⁴, Tsurekawa Sadahiro ⁵

1 - Dept. of Materials Science and Applied Chemistry, Graduate School of Science and Technology, Kumamoto University, Kumamoto, 860-8555, Japan (Japan), 2 - Institute of Physical Metallurgy and Materials Physics, RWTH Aachen University, Aachen 52056, Germany (Germany), 3 - International Research Organization for Advanced Science and Technology (IROAST), Kumamoto University, Kumamoto 860-8555, Japan (Japan), 4 - Research Center for Structural Materials, National Institute for Materials Science (NIMS), Sengen 1-2-1, Tsukuba 305-0047, Japan (Japan), 5 - Division of Materials Science and Chemistry, Faculty of Advanced Science and Technology, Kumamoto University, 860-8555, Japan (Japan)

Grain boundaries (GBs) play a crucial role for the mechanical properties of polycrystals. Their behaviour depends on five degrees of freedom determining GB geometry. This study aims to investigate the local mechanical properties of GBs, with a particular focus on the propagation of plastic deformation across them. For this purpose, $\langle 110 \rangle$ twist GBs with different misorientations in Fe-3% Si bicrystals are examined and compared with symmetric tilt GBs (STGBs) of the same misorientation angles. Fe-3 mass%Si bicrystals with $\Sigma 3$, $\Sigma 9$, $\Sigma 27a$ and $\Sigma 33c$ $\langle 110 \rangle$ twist GBs, as well as $\{111\}\Sigma 3/\langle 110 \rangle$ and $\{221\}\Sigma 9/\langle 110 \rangle$ STGBs were prepared using the floating zone method and characterised by EBSD. Nanoindentation tests were conducted on and near the GBs to investigate the deformation mechanisms. A GB pop-in event, reflecting the propagation of plastic deformation across a GB, was observed at lower loads for $\Sigma 27a$ and $\Sigma 33c$ twist GBs compared to $\Sigma 3$ and $\Sigma 9$ twist GBs. A continuity factor m , derived from the geometric compatibility of the slip systems, was evaluated, and it was found that higher m values correlate with reduced GB pop-in loads. Moreover, twist GBs and STGBs with the same Σ value were compared. Twist GBs exhibited lower first pop-in loads compared to STGBs, indicating lower critical shear stress for dislocation generation. Conversely, the $\Sigma 9$ STGB with higher m value showed lower GB pop-in load than the $\Sigma 9$ twist GB. These results suggest that the propagation of plastic deformation across a GB is governed primarily by dislocation transmission rather than dislocation generation at GBs.

Keywords : grain boundary, dislocation, mechanical property, nanoindentation, Fe 3%Si alloy

319. Structural change of Ga₂O₃ layer formed on GaN(0001) substrate under various fabrication conditions

Nabatame Toshihide¹, Irokawa Yoshihiro ¹, Sawada Tomomi ¹, Miura Hiromi ¹, Miyamoto Manami ¹, Koide Yasuo ¹, Tsukagoshi Kazuhito ¹

¹ - National Institute for Materials Science (Japan)

Vertical GaN MOSFETs with gate dielectrics have been widely investigated. GaOx interfacial layer between gate dielectric and GaN substrate is well known to play an important role in the transistor performance. We recently found that modified-GaOx layer which formed on the surface of GaN substrate using the dummy-SiO₂ technique led to improve electrical properties of n-GaN/modified-GaOx/Al₂O₃/Pt capacitors. Therefore, to understand this behavior, GaOx layer formation on GaN substrate under various fabrication conditions intensively studied. The native oxides on GaN were observed on both n- and p-type GaN(0001) substrates using RHEED, cross-sectional ADF-STEM and 1D Fourier transform images. The native oxides with around 1nm were not amorphous but crystalline with lattice-matched structures to GaN. Considering to GaN/SiO₂ MOSFET, GaN/SiO₂ interface was evaluated after SiO₂ gate dielectric deposition on GaN(0001) via PE-ALD at 300 °C. The crystalline oxide layer similar to the native oxides on GaN(0001) was observed at GaN/SiO₂ interface. Furthermore, the structure of the crystalline oxide layer found to be gamma- and epsilon-Ga₂O₃ structures. The epsilon-Ga₂O₃/GaN interface was also atomically smooth and free from misfit dislocations. To understand Ga₂O₃ formation on the GaN surface, the direct oxidation at 800 °C in O₂ was performed. As a result, the gamma-Ga₂O₃ was found to be formed on GaN(0001) substrate, although beta-Ga₂O₃ is expected to form in the viewpoint of the thermal stabilization. This work was partially supported by the MEXT Program for Creation of Innovative Core Technology for Power Electronics Grant Number JPJ009777.

Keywords : Ga₂O₃ layer, GaN/SiO₂ interface, gamma, phase, epsilon, phase, beta, phase

320. Effect of low-angle grain boundary network on high cycle fatigue in grain boundary engineered 409L type ferritic heat resistant steel

Kobayashi Shigeaki¹, Kobori Daiju¹, Tsurekawa Sadahiro²

1 - Ashikaga University (Japan), 2 - Kumamoto University (Japan)

409L type ferritic heat resistant steel is applied mainly to automobile exhaust system parts owing to the excellent deep drawability. Improving tensile strength and fatigue strength in the steel will lead to weight reduction of machine and expanding the range of applications. Recently, we have demonstrated that introducing high fraction of low-angle grain boundaries (LAGBs) is useful for improving fatigue property in ferritic stainless steels. In this work, the effect of highly introducing of LAGBs which formed LAGB network on the high-cycle fatigue was investigated in detail.

The grain boundary control in 409L type steel was achieved by 2-step thermomechanical processing consisted of first process which develop sharp {111} texture by cold rolling at 70 % and annealing at 973 K for 3.6 ks and second process which introduce high fraction of LAGBs by cold rolling at 67 % and annealing for 973 K for 600s.

The LAGBEed 409L steel specimen possessing an average grain size of 1.0 micro meter and a high fraction of LAGBs of more than 80 % was produced accompanying with the development of sharp {111} texture. The LAGBEed specimen showed the higher fatigue strength than the commercially available 409L steel specimen. The microstructural change in LAGB engineered 409L type steel after high cycle fatigue tests which carried out at different stress amplitude range were quantitatively evaluated to reveal the cause of improvement of fatigue property in GBEed specimen.

Keywords : Ferritic Heat Resistant Steel, Thermomechanical Processing, Low, Angle Grain Boundary, High cycle fatigue, Grain Boundary Engineering

321. Structure-dependent electrical properties of grain boundaries

Tsurekawa Sadahiro ¹

¹ - Division of Materials Science and Chemistry, Faculty of Advanced Science and Technology, Kumamoto University, 860-8555, Japan (Japan)

Grain boundaries (GBs) play a crucial role in determining the mechanical and functional properties of polycrystalline materials. Extensive fundamental studies have revealed that the properties of GBs depend significantly on their character and structure. This talk will discuss the structure-dependent electrical properties of GBs in metallic and semiconductor materials, primarily based on our experimental findings. Key topics to be covered include: 1. Potential barriers at GBs in Si and 3C-SiC Kelvin probe force microscopy was employed to measure the potential barriers associated with grain boundaries in B-doped p-type polycrystalline silicon. The results showed that the potential barriers at clean GBs varied from approximately 5 to 90 meV, depending on the GB character. Random GBs exhibited higher potential barriers compared to CSL GBs. Furthermore, the potential barrier increased with the twist component of the GB when the misorientation angle between two adjoining grains was almost the same. Contamination with copper and iron significantly increased the GB potential barriers, further emphasizing their misorientation dependence, likely due to the anisotropy of grain-boundary segregation. 2. Electrical resistivity of GBs in Cu Using a 4-point nanoprobe technique, we investigated the effect of GB configuration on the electrical resistivity of Cu wires. Notably, when the current flowed across a random GB, the resistivity increased by 15.7% relative to the grain interior. In contrast, when the current flowed parallel to a random GB, the resistivity decreased by 28.5% compared to the grain interior.

Keywords : grain boundary, electrical conductivity, potential barrier, Kelvin probe force microscopy

322. Spintronic technologies for germanium devices

Hamaya Kohei^{1 2}

1 - Center for Spintronics Research Network, Graduate School of Engineering Science, Osaka University, 1-3 Machikaneyama, Toyonaka 560-8531, Japan (Japan), 2 - Spintronics Research Network Division, Institute for Open and Transdisciplinary Research Initiatives, Osaka University, Yamadaoka 2-1, Suita, Osaka 565-0871, Japan (Japan)

Semiconductor (SC) spintronic technologies are expected for novel logic and memory architectures with low power consumption in future electronics [1]. Thus far, we have developed highly efficient electrical spin injection and detection technologies in germanium (Ge) [2] at room temperature for CMOS- and Si-photon compatible spintronics. In this talk, we show an original technique for growing high-quality ferromagnetic Heusler alloys on Ge and for detecting large spin signals in Ge-based lateral spin-valve devices [3,4]. For getting the highest magnetoresistance (MR) ratio, we can reduce the resistance area (RA) product down to $\sim 0.1 \text{ k}\Omega\mu\text{m}^2$, several order of magnitude lower than that in Si-based devices with MgO tunnel barriers. Also, by using a strained Si_{0.1}Ge_{0.9} layer as a spin transport layer, we observe a long spin diffusion length of $\sim 0.9 \mu\text{m}$ [5], comparable to Si, at room temperature. The present Ge spintronics technologies will be paving the way to achieve high-performance electron-photon-spin integrated devices on the Si platform at room temperature. This work was supported in part by JSPS KAKENHI (Grant No. 19H05616, 24H00034), and MEXT X-NICS (Grant No. JPJ011438), and the Spintronics Research Network of Japan (Spin-RNJ). [1] M. Tanaka and S. Sugahara, IEEE Trans. Electron Devices 54, 961 (2007). [2] K. Hamaya et al., J. Phys. D: Appl. Phys. 51, 393001 (2018). [3] M. Yamada, KH et al., NPG Asia Mater. 12, 47 (2020). [4] K. Kudo, KH et al., Appl. Phys. Lett. 118, 162404 (2021). [5] T. Naito, KH et al., Phys. Rev. Applied 18, 024005 (2022).

323. Quantification of the grain boundary structure and determination of migration mechanisms

Barrales-Mora Luis¹, Bizana Gashaw ²

1 - George W. Woodruff School of Mechanical Engineering (2 Rue Marconi, 57070, Metz France), 2 - George W. Woodruff School of Mechanical Engineering (United States)

Grain boundary migration has been investigated for several decades. It is accepted that a grain boundary can move under the action of mechanical stresses and jumps in chemical potential. A jump in chemical potential occurs for example if a grain is curved or there is gradient of any intensive thermodynamic variable. Experiments and simulations have substantiated differences in the motion of grain boundaries depending on the acting driving force. In particular, different activation enthalpies have been determined to be different for crystallographically similar grain boundaries. The migration enthalpy is considered to be a fingerprint of the migration mechanisms, which in turn depends on the grain boundary structure. In the present contribution, persistent homology (PH) was utilized to quantify the structure of the grain boundaries during their migration. To this aim, more than 1200 MD simulations of GB migration were performed. In these simulations, mechanical stresses and a jump in chemical potential were used to drive the motion of the boundaries. We show that PH can be used to quantify the GB structure and that by association it is possible to discriminate the type of migration of a boundary.

Keywords : Grain boundaries, principal, component analysis, persistent homology

324. Atom-Resolved Observations of Grain Boundary Dynamics in Oxides

Ikuhara Yuichi ^{1 2 3}

1 - School of Engineering, The University of Tokyo (Japan), 2 - WPI-AIMR, Tohoku University (Japan), 3 - NSRL, Japan Fine Ceramics Center (Japan)

Material properties of oxides are strongly influenced by their dynamic behaviors under various conditions such as temperature, stress, and atmosphere. This study investigated the role of grain boundaries (GBs) in phenomena like fracture, deformation, and ion diffusion using SrTiO₃ and Al₂O₃ bicrystals as model systems. In-situ nanoindentation experiments conducted inside (S)TEM revealed dynamic GB-related processes such as dislocation pile-up, jog formation, jog-drag motion, deformation twinning, and crack propagation. On the other hand, electron irradiation was applied to enhance GB migration in Al₂O₃, and Ti-doped Al₂O₃ bicrystals were used to study atomic-scale diffusion mechanisms. In-situ STEM observations also showed a zigzag crack propagation path along segregated Zr atom layers in Zr-doped Al₂O₃, highlighting the relationship between atomic-scale crack behaviour and GB structures. Furthermore, high-energy electron beam irradiation enabled direct visualization of GB migration as stop-motion movies, revealing that GB migration occurs through a cooperative shuffling of atoms along GB ledges and structural transformations between low-energy GB states. These findings provide a deeper understanding of how GB dynamics influence key properties, such as sintering behavior, high-temperature mechanical performance, and oxide processing. By systematically analyzing these GB-related mechanisms, this study significantly advances the knowledge of atomic-scale processes in oxides and their dependence on GB structures, offering valuable insights for improving the design and processing of oxide materials.

Keywords : Grain Boundary, STEM, Dynamics, GB Migration, Dislocation

325. Gradient B2-BCT Transition and Interface Introduced by Deformation in Eutectic High-Entropy Alloy

Zhao Bingbing ¹, Shu Qingsong ², Dong Xianping ², Zhang Lanting ²

1 - School of Materials Science and Engineering, Shanghai Jiao Tong University (800 Dong Chuan Road, Shanghai China), 2 - School of Materials Science and Engineering, Shanghai Jiao Tong University (China)

Eutectic high-entropy alloys (EHEAs) demonstrate a compelling balance of high strength and ductility, attributed to their complex deformation mechanisms. In this study, a gradient B2-to-body-centered tetragonal (BCT) phase transformation was identified in a deformed Al19Fe20Co20Ni41 (at.%) EHEA. X-ray diffraction analysis revealed a strain-induced gradual transformation from the B2 to the BCT phase during tensile testing. Notably, the gradient transition occurs within a single grain, characterized by a stepwise variation in the lattice constants. The existence of a gradient interface was confirmed through electron backscatter diffraction (EBSD) Kikuchi patterns, displaying a progressively elongated quadrangle surrounded by four [110] poles. Furthermore, transmission electron microscopy (TEM) with nanobeam diffraction (NBD) confirmed the cubic symmetry of the B2 phase through {110}-type diffraction spots forming a symmetric circle, contrasting with the asymmetrical diffraction patterns of the BCT phase, where two {110}-type spots deviate outward. This strain-driven phase transformation in the thermomechanically processed sample led to a nearly threefold improvement in elongation during tensile testing compared to its as-cast counterpart, which exhibited no such transformation. These findings underline the transformative potential of strain-induced gradient phase transformations in optimizing the mechanical performance of EHEAs.

Keywords : Eutectic high, entropy alloys, Phase transformation, Gradient transition, Interfaces

326. Atomistic Modelling and Design of Mechanical Properties of Grain Boundaries in Alloys

Wakeda Masato ¹

¹ - National Institute for Materials Science (Japan)

The grain boundaries affect local deformation behaviours and macroscopic mechanical properties of metals and alloys. This study realizes the modelling and design of the deformation behaviors and mechanical properties of grain boundaries in metals and alloys using atomistic simulation methods. The energy barrier and dominant factors for dislocation nucleation from interfaces were evaluated for various metals and alloy systems. The activation energy and activation volume for dislocation nucleation depend on the grain boundary local structure, crystalline types such as FCC and BCC, and alloy composition. The necessary stress for dislocation nucleation was predicted and discussed by comparing experimental results for BCC iron. For atomistic models of multi-element FCC systems, I also demonstrated the simultaneous optimization of mechanical properties of grain boundaries, such as dislocation nucleation stress and surface nucleation energy, using machine learning techniques. A nonempirical evaluation scheme for the correlation between the local structure and local properties of grain boundary was also suggested using the data analysis scheme. Based on the local structure information obtained by atomistic modelling, atomistic potential energy and atomistic entropy information of random grain boundaries can be predicted within the simulation framework. These atomistic results provide fundamentals and new knowledge of the mechanical properties of grain boundaries for realizing the design of further excellent mechanical properties.

Keywords : Grain boundary, Dislocation, Free energy, Machine learning, Alloys

327. Plasmon loss imaging at grain boundaries obtained by STEM-EELS and the grain boundary dependence

Ii Seiichiro¹, Hara Toru ¹

¹ - National Institute for Materials Science (Japan)

The correlation between structures and energies of grain boundary (GB) is often discussed with computational calculations and experimental characterization of the GB structure. On the other hand, the GB energy has been experimentally and macroscopically estimated, particularly from a measurement of the dihedral angle on a thermally grooved surface at GB. In recent, Nandi et al. reported their interesting work, in which they evaluated an electron density around the GBs in Al bicrystals using plasmon loss in electron energy loss spectroscopy (EELS) equipped with scanning transmission electron microscopy (STEM), and they discussed the experimental results with the GB energy [1]. However, they evaluated it with the line profile. In this study, we present the results of attempting to acquire the two-dimensional spectrum imaging of plasmon loss by aberration-corrected STEM-EELS at an atomic resolution. Evaluating two kinds of $\Sigma 3$ GBs with different grain boundary planes in Si, we successfully imaged the plasmon loss at an atomic scale. In $\{111\}$ $\Sigma 3$ coherent boundary, almost no peak shift was seen, even at the GB. On the other hand, in $\{112\}$ $\Sigma 3$ incoherent boundary, the plasmon peak position was obviously shifted to the low energy at the GB, suggesting a decrease of the electron density locally. Also, it was irregularly changed even along the GB plane. Based on the results, we discussed the correlation between the GB energy and structure and the possibility of those experimental evaluations. [1] P. Nandi et al.: Phys. Rev. Mater., 3(2019), 053805.

Keywords : grain boundary energy, electron density, STEM, EELS, plasmon loss

328. Grain boundary precipitation behavior of Ni-Cr phase in γ -Ni matrix in Ni-Cr binary alloys

Nagashima Ryota¹, Nakada Nobuo²

1 - Institute of Science Tokyo (Japan), 2 - Institute of Science Tokyo (Japan)

Grain boundary precipitation strengthening has been demonstrated in austenitic heat-resistance steels, where 80% of the grain boundaries (GBs) are covered by Laves phase. However, large strain concentration occurs at GBs that lack Laves phase converge. To enhance creep resistance, it is thought that all GBs should be covered by precipitates. This study investigated the precipitation behavior of the α phase in Ni–Cr alloys, which have γ -Ni and α -Cr phases in their binary system. Ni–(44, 46, 48) at.%Cr alloys were prepared by arc melting, yielding 35 g button ingots. They were solution-treated at 1573 K, followed by aging at 1473–1073 K. The microstructure and the crystal orientation were analyzed using electron backscattered diffraction detectors attached to a field-emission scanning electron microscope. The GB coverage ratio ρ of α -Cr increased with higher levels of Cr supersaturation in γ -Ni matrix. However, ρ exhibited a wide scatter of approximately 40%, indicating a significant variation in GB coverage depending on the GB characteristics. Orientation analysis revealed the α phase at GBs could be categorized into three types: (1) Kurdjumov-Sachs (KS) relationship with one grain, (2) Nishiyama-Wasserman (NW) relationship with one grain, or (3) KS relationship with both grains (double KS). For a single KS or NW relationship, ρ increases as the angle θ between $\langle 111 \rangle \alpha$ and the intersection line of GB plane and $\{111\} \gamma$ of the matrix decreased. GBs with double KS showed high ρ values ($>95\%$). These findings indicate that the improving ρ requires tailoring GB characteristics to achieve a double KS relationship and minimize the angle θ .

Keywords : Microstructure, Grain boundary, Precipitation, Crystallography, EBSD

329. Interfacial Mechanisms of Iron-Oxide Reduction: From Direct Microstructural Observations to Atomistic Simulations

Chavan Vikram ¹, Pai Namit ¹, Bhattacharjee Debarna, Girish S. ²,
Nag Samik ², Kundu Saurabh ³, Basu Somanth, Panwar Ajay ⁴,
Samajdar Indradev ⁴

1 - Department of Metallurgical and Materials science IIT Bombay (India), 2 - Tata Steel, Jamshedpur (India), 3 - Research and Development Division, TATA steel, Jamshedpur, India (India), 4 - Department of metallurgical Engineering and materials science, IIT Bombay (India)

This study used direct microstructural observations and atomistic reaction force field molecular dynamics (ReaxFF MD) simulations to explore interfacial mechanisms of iron ore reduction. The combined experiments and atomistic simulations were used in conjunction with controlled thermogravimetric analysis, so that different stages of interfacial transformations were realistically captured. In particular, transformation of Hematite (Fe_2O_3) to Magnetite (Fe_3O_4) was clearly distinguished by a transition phase called Maghemite. The latter was responsible for the majority of atomic shear and controlled the transformation induced mesoscopic shear strains. The latter controlled the homo-epitaxial growth of Wüstite (FeO_{1-x}) into Magnetite grains, while a reverse phase transformation Metallic Iron (Fe) to Magnetite was also observed during the final reduction stage.

Keywords : Reduction, Iron Ore, Microstructure, Phase transformation, EBSD, MD Simulations, Interface.

330. Graphite Crystallization in Austenitic Ductile Iron: Insights from TKD and TEM Diffraction

Tokarski Tomasz¹, Wojciak Karolina , Gorny Marcin , Marosz Jan

1 - AGH University of Krakow (Poland)

Austenitic ductile iron (Ni-Resist) is a class of cast iron known for its exceptional mechanical properties, including high toughness, wear resistance, and corrosion resistance, making it highly suitable for demanding engineering applications. These superior properties are largely attributed to the presence of austenitic metallic matrix and graphite nodules, which play a crucial role in determining the material's strength, ductility, and fatigue resistance. The size, distribution, and morphology of these nodules significantly influence the alloy's overall performance. Despite extensive research, the mechanisms governing graphite crystallization, particularly the role of various nucleation sites, are not yet fully understood. One contributing factor is the difficulty of crystallographic analysis of nodular graphite due to its softness and low atomic number. Conventional local crystallinity analysis using Electron Backscatter Diffraction (EBSD) is ineffective in such cases. To address this challenge, Focused Ion Beam (FIB) techniques will be employed for the precise preparation of thin lamellae, enabling high-spatial-resolution examination of the internal graphite microstructure. This study aims to investigate the local microstructure of graphite nodules and its relationship with nucleation sites using advanced characterization techniques, including Transmission Kikuchi Diffraction (TKD) and Transmission Electron Microscopy (TEM) with local diffraction analysis. Special focus will be given to local crystallinity variations, ranging from amorphous regions to turbostratic structures and fully crystalline graphite. Acknowledgments: This research was conducted within Horizon Europe Project No. 101159771 €” NetCastPL4.0.

Keywords : Austenitic ductile iron, Nodular graphite, Transmission Kikuchi Diffraction, TEM diffraction

331. Improved Indexing of Electron Backscatter Diffraction Patterns using Forward Modelling

Wright Stuart¹, Lenthe William¹, Nowell Matthew¹, De Kloe Rene²

1 - EDAX/Gatan (United States), 2 - EDAX/Gatan (Netherlands)

Since the inception of fully automated Electron Backscatter Diffraction (EBSD) in the early 1990s, pattern indexing has relied on Hough transform based detection of diffraction bands. This approach has proven effective for most material systems. However, it tends to be noise sensitive, restricted to indexing only the Laue class of a crystal, and limited in angular precision. Realistic dynamical diffraction simulations have facilitated forward model-based indexing techniques where experimental patterns are indexed by direct comparison against a 'dictionary' of simulated patterns. A more efficient forward modelling approach based on cross-correlation using spherical harmonics has been developed. In addition to being more robust against noise and capable of resolving the full point group, results obtained using this technique can be refined to provide an order of magnitude improvement in angular precision. The implementation of spherical harmonic indexing and orientation refinement on a Graphical Processing Unit enables the practical application of forward model techniques to large datasets. An overview of spherical indexing will be presented along with application examples.

Keywords : Microstructure Characterization, Electron Backscatter Diffraction, EBSD

332. Recrystallization mechanisms activated during multi-pass forging of austenitic stainless steels

Latuner Hugo¹, Favre Julien ², Helstroffer AureLien ³, Inacio Da Rosa Gregory ¹, Plancher Emeric ¹, Joly Pierre ¹, Kermouche Guillaume ², Desrayaud Christophe ²

1 - Mechanical Engineering Division - Materials and Technology Department (La Defense) (France), 2 - PMM-ENSMSE- Departement Physique et Mecanique des Materiaux (France), 3 - Le Creusot - Forge shop - R&D (France)

Multi-pass forging is used to produce large components in austenitic stainless steels for Generation III and III+ nuclear reactors. Gaining a deeper comprehension of multi-pass forging is crucial for optimizing the end-process microstructure and mechanical properties of the materials. The primary objective of this study is to characterize and model the microstructural evolution occurring in multi-pass thermomechanical processing, with a particular emphasis on the dynamic and post-dynamic recrystallization mechanisms. To this end, an experimental simulation of multi-pass hot forging by uniaxial hot compression was performed under different thermomechanical conditions, with a specific focus on small strain increments. SEM-EBSD was employed to characterize the resulting microstructures. The processed EBSD data are used to develop a mean-field model combining dynamic and post-dynamic recrystallization. Further investigation into the microstructural effects of successive deformations helps to understand the contribution of the elastic stored energy to the recrystallization mechanisms and the resulting grain size distribution.

Keywords : Dynamic recrystallization, Austenitic stainless steels, Forging, Microstructure, Electron backscatter diffraction, Mean field modeling

333. Recrystallization in ferritic stainless steels: experimental and modeling approaches

Favre Julien¹, Louis Hennocque², Nicolas Meyer³, Thomas Sourisseau³, David Piot¹, Frank Montheillet¹, Laurence Latu-Romain⁴, Guillaume Kermouche¹

1 - Laboratoire Georges Friedel (France), 2 - SAFRAN [Paris] (France), 3 - Centre de recherche Ugitech (France), 4 - Science et Ingenierie des Materiaux et Procedes (France)

This study focuses on understanding and modeling the processes that occur during the hot rolling of ferritic steel to achieve a fine-grained microstructure. Laboratory thermomechanical tests, such as torsion and uniaxial compression, were performed on various ferritic stainless steel grades with different niobium contents, including a specially fabricated Nb-free grade. The purpose of these tests was to analyze microstructural evolution mechanisms such as recovery, recrystallization, and grain growth under varying strain rates and temperatures.

The main mechanisms investigated include continuous dynamic recrystallization (CDRX) and discontinuous dynamic recrystallization (DDRX). The research proposes a unified model for these mechanisms at the single grain level, integrating subgrain boundary formation, misorientation, and thermodynamic nucleation criteria. This model was tested under specific conditions (900°C, 60% deformation) and analyzed for dynamic and static microstructural changes. The results, including grain size distribution, recrystallized fractions, and subgrain boundary density evolution, demonstrated the potential for simplifying and unifying CDRX and DDRX mechanisms within a coherent framework.

Keywords : steels, recrystallization, microstructure, hot deformation, modeling

334. A Computational Approach to Design Thermally Stable Metal-Metal Interfaces

Gaskey Bernard¹, Hawk Cheryl¹, Hackenberg Robert¹, Adams Claire², Field David², Carpenter John¹

1 - Los Alamos National Laboratory (United States), 2 - Washington State University (United States)

New classes of high-performance metals provide extreme environment performance which is vital for the design of next-generation aerospace and power generation systems. However, these new materials also present new manufacturing challenges that are not easily solved with existing techniques. Diffusion bonding is one promising technique to produce joints with acceptable properties. Development of diffusion bonding processes lags behind the development of new materials. These interfaces can fail immediately due to residual stress from manufacturing, or they can fail later in service due to the formation of detrimental intermetallic phases. Here, we use the calculation of phase diagrams (CALPHAD) computation approach to understand the behavior of interfaces and gradients in composition. We show how this technique describes behavior at diffusion bonded interfaces between a variety of metals including complex alloys. We use the same approach predictively to develop new interface designs. By using computational tools to select experiments, we greatly reduce the time and cost of interface development. This technique is vital to reduce the time to market of new joint designs.

Keywords : CALPHAD, thermodynamics, dissimilar materials, diffusion bonding

335. Effect of deformation twinning on the strength anisotropy in textured Ti: Insights from atomic simulations and slip transfer theory

Shimokawa Tomotsugu ¹

¹ - Kanazawa University (Japan)

The commercially pure textured titanium (Ti), processed through multi-axial forging and cold rolling, exhibits excellent mechanical properties and significant mechanical anisotropy. The potential reasons for these mechanical characteristics are as follows: ¹ A strong texture, characterized by the prismatic plane being perpendicular to the rolling direction (RD) and the basal plane inclined at approximately 40 degrees from the normal direction (ND) toward the transverse direction (TD) of the rolled plate; and ² The formation of different deformation twins depending on the loading direction: {11-22} compression twins predominantly form during RD tension, while {10-12} tension twins primarily form during TD tension. It is suggested that the excellent mechanical properties and mechanical anisotropy of the textured Ti are closely related to its strong texture and deformation twins, though the detailed mechanisms remain unclear. Deformation twins, despite having crystallographically identical twin boundaries, exist in multiple variants, and each variant has a different crystal orientation in the specimen coordinate system. This indicates that the resistance to slip transfer across twin boundaries varies depending on the twin variant. In this study, molecular dynamics (MD) simulations are used to introduce {10-12} or {11-22} twins into textured Ti models and analyze tensile deformation in the RD and TD. Additionally, the slip transfer resistance, derived from crystal plasticity theory, is calculated. Through a comparison of MD simulations and slip transfer theory, the effects of twin variants on mechanical properties are investigated.

Keywords : Deformation twin, Slip transfer, Mechanical anisotropy, Ti, Molecular dynamics

336. Anisotropy in high temperature deformation and oxidation behavior in textured Ti₃SiC₂ MAX phase ceramics

Sei Eiichi¹, Ikeda Ken-Ichi², Miura Seiji², Morita Koji³, Suzuki Tohru³, Sakka Yoshio³

1 - Division of Materials Science and Engineering, Graduate School of Engineering, Hokkaido University (Japan), 2 - Division of Materials Science and Engineering, Faculty of Engineering, Hokkaido University (Japan), 3 - National Institute for Materials Science (Japan)

Ti₃SiC₂ is classified as a MAX phase, which is layered ternary compounds with a general formula of Mn+1AX_n (where n=1~3, M is an early transition metal, A is an A-group element, and X is carbon and/or nitrogen). Due to its hexagonal layered crystal structure and a high c/a ratio, Ti₃SiC₂ has anisotropic properties. Therefore, it is expected that crystal orientation control leads to further strengthening and anisotropy. In this study, the anisotropy in the high temperature compressive deformation behavior and oxidation behavior is investigated, using highly textured sintered bodies. First, green bodies with the c-axis parallel to the casting direction were prepared by a slip casting in a strong magnetic field. The textured bodies were sintered at 1300 ° using a spark plasma sintering machine. Then, the samples were cut into rectangular shapes with 0°, 45°, 90° between the compression axis and c-axis, and the compression tests were performed at 1200°C with a strain rate of 3 Å—10⁻⁴ s⁻¹. Oxidation tests were conducted at 1100,.,f for 24 hours in air. The deformation behavior was anisotropic, and the 90° sample showed the work-softening due to kink deformation. Oxide scales are thicker on the surface parallel to the c-axis than on the surface perpendicular to the c-axis. This shows that Ti₃SiC₂ also has an anisotropic oxidation behavior.

Keywords : Ti₃SiC₂, MAX phase, high temperature deformation, oxidation, anisotropy, textured

337. Disclination and cooperative deformation at intersection of kink interface and slip deformation

Matsumura Ryutaro¹, Inamura Tomonari¹

¹ - Laboratory for Materials and Structures, Institute of Science Tokyo (Japan)

Kink deformation is one of plastic deformation mode in layered structural materials with only one slip system. The slip deformation on the layered plane and rigid body rotation of the layer itself occur simultaneously in the kink deformation. Kink band and kink microstructure, which is aggregate of connected kink bands, are formed by the kink deformation. Long-period stacking ordered (LPSO) Mg alloy with a large amount of kink introduced by hot extrusion has high specific strength and ductility. This strengthening is called kink strengthening and has attracted attention as a new strengthening principle. This strengthening is attributed to the kink microstructure, however, the strengthening mechanism has not yet been clarified. In order to clarify one of the geometric aspects of the kink strengthening mechanism, we analyzed the geometry of the intersection between the kink interface and the slip deformation in a situation where the slip system is limited to one. This analysis was conducted using a rank-1 connection, which represents the continuity of deformation. The result shows the rotational lattice defects, i.e. disclination, are always formed at these intersections, and the migration of kink interface (cooperative deformation) is also required. These act as a strengthening mechanism to increase the deformation stress, as they require elastic energy and plastic work, respectively. The deformation behaviour occurring at the kink interface will be discussed based on the power of disclination and the amount of migration of the kink interface due to the cooperative deformation.

Keywords : kink strengthening, kink microstructure, LPSO Mg alloy, rank 1 connection

338. Geometrical modeling of bent kinks: energy reduction and shape transition mechanisms

Zhang Xueyu¹, Matsumura Ryutaro ¹, Shinohra Yuri ², Inamura Tomonari

1 - Institute of Science Tokyo (Japan), 2 - The University of Electro-Communications (Japan)

This study investigates the geometry of bent kinks by introducing sequences of ortho-connected kink bands into ridge-kinks, aiming to explore the reasons behind their bending and the resulting geometrical configurations. To achieve this, we derived the Frank angles and disclination coordinates within bent kinks and analyzed their impact on Gibbs energy using Romanov's disclination model. The analysis revealed that introducing ortho-kinks can alleviate elastic strain energy and reduce Gibbs energy under lower external compressive stresses. Conversely, at higher compressive stresses, the introduction of ortho-kinks leads to an increase in Gibbs energy, favoring the formation of sharp ridge-kinks under such conditions. This behavior aligns with experimental observations, which suggest that newly formed kinks transition from bent pre-kinks to sharp ridge-kinks as compression progresses.

Keywords : kink, compatibility, LPSO, Mg

339. Kink deformed microstructure in mille-feuille structured materials

Daisuke Egusa¹, Abe Eiji

1 - The University of Tokyo (Japan)

Kinking is a type of plastic deformation involving crystal rotation, which is confirmed in materials with structural anisotropy. Recently, it has been reported that kinking and related deformed microstructure can improve the mechanical properties of various materials with layered structures, termed as mille-feuille structure (MFS), leading to the expectation of its application to structural materials. In deformation with crystal rotation, the amount of deformation is not uniform within the material, so a microscopic deformation mechanism is required to achieve non-negligible volume transport, which is typically believed to be played by the collective motion of dislocations. However, the kink deformation microstructure varies with the materials, suggesting the activity of a micro-scale relaxation mechanism that is different from the conventional dislocation motion. In this paper, we report characteristic of

kink deformed microstructures in various MFS materials, such as Mg alloys, Al alloys, and intermetallic compounds, using electron microscope observations. Based on the atomic-scale investigation of the kink structure and strain distribution, we discuss the influence of the microscopic deformation mechanisms on the kink deformation.

Keywords : Kink deformation, mille feuille structure, electron microscopy, defects

340. Kink Boundary Migrations in LPSO-structured Mg Alloys

Abe Eiji ¹

¹ - Department of Materials Science & Engineering, University of Tokyo, Tokyo 113-8656, Japan. (Japan)

Dilute Mg alloys containing a few atomic percent of transition-metal and rare-earth element have attracted increasing attentions because of their excellent mechanical properties. The remarkable microstructural feature common for all of these Mg alloys is formation of a novel type of long-period stacking/order (LPSO) structures, which reveal a remarkable strength through the warm-extrusion process. During the process the LPSO crystals are deformed not by simple dislocation migrations but of kink-type that is the direct relevance to realize excellent properties of the alloys. From the extensive studies of the LPSO-structured Mg alloys, it has become apparent that the kink regions indeed play a critical role for effective strain storage of the alloys, but its detailed mechanism is not fully understood yet. In the present talk, I will describe the interesting kink boundary migrations, based on STEM experiments and MD simulations.

Mg alloys, LPSO structure, Kink deformation, Grain boundary migrations, Microstructure analysis, Molecular dynamics simulations

341. Numerical Evaluation of Kink Band Formation in Anisotropic Solids

Tsuyoshi Mayama ¹

¹ - Kumamoto University (Japan)

Kink band formations in various anisotropic solids under uniaxial compressive loading were numerically analysed by a crystal plasticity finite element method. Influences of elastic and plastic anisotropy on kink band formation were evaluated in details for both single-phase materials including LPSO single phase alloy and multi-phase materials with lamellar microstructure (MFS materials). The results showed significant intra-granular misorientations were developed with formation of kink bands in both single-phase and multi-phase materials. In multi-phase materials, larger difference in yield stresses for each phase lead to formation of more pronounced kink bands with larger angle of intra-granular misorientations. The contributions of shear deformation and lattice rotation to morphology of kink bands were also studied.

Keywords : Crystal plasticity, Finite element method, Non, uniform deformation, Anisotropy

342. Anisotropic mechanical property-induced ductilization (AMID) A new mechanism to simultaneously improve the strength and ductility of multiphase alloys

Koji Hagihara¹, Toko Tokunaga¹

¹ - Department of Physical Science and Engineering, Nagoya Institute of Technology (Japan)

We recently proposed a new mechanism to simultaneously improve the strength and ductility of multiphase alloys, named Anisotropic mechanical property-induced ductilization (AMID). In a composite material, if the slip system operating in the hard phase is limited to a single system with a low Schmid factor, the apparent work-hardening rate of the hard phase geometrically becomes high. This results in a significant increase in the overall work-hardening rate of the composite, and there is a possibility that leads to the increase in uniform elongation of the alloy. The validity of this idea was examined in the Mg/LPSO two-phase extruded alloys, by the tensile tests. In the Mg/LPSO two-phase alloy, the composite-like deformation behavior was enhanced, and the LPSO phase significantly contributed to the strengthening of the alloy. Moreover, the experimental results obtained by using neutron diffraction analysis suggested that the LPSO phase contributes not only to the alloy's strength but also to its elongation by increasing the work-hardening rate, as expected. The details on this, and the contribution of kink-band strengthening in the LPSO phase to the AMID mechanism will be discussed in the presentation.

Keywords : Mg alloys, LPSO, phase, extruded alloy, Anisotropic mechanical property, induced ductilization (AMID), kink, band strengthening

343. Effects of strain components on effective kink band formation in Mg-Y-Zn alloys

Yuasa Motohiro¹, Yoshizumi Hiromasa ¹, Miyamoto Hiroyuki ¹,
Somekawa Hidetoshi ²

1 - Doshisha University [Kyoto] (Japan), 2 - National Institute for Materials Science (Japan)

Magnesium alloys containing the long-period stacking order (LPSO) phase have been attracting attention because of their strength exceeding the high-strength aluminum alloys. It has been reported that this high strength is due to the formation of deformation kink bands by wrought-processing methods. It has reported the effects of wrought-processing methods on the formation of the kink bands and the hardness, and the strain introduced into the specimens by the wrought-processing methods affects the kink band formation. However, the effects of strain state introduced during the wrought-processing methods remain unclear. Thus, this study focused on the effects of strain components, specifically equivalent plastic strain and shear strain, on kink band formation in Mg-9at.%Y-6at.%Zn alloy. The unique shape specimens to change the introduced shear strain were subjected to simple compression tests at 623 K. The strain distributions during compression tests were calculated using finite element (FE) simulation. The microstructure of these deformed specimens was observed by laser microscopy. The correlation between the strain components computed by FE simulations and the number density of the kink band was discussed. The results showed that while the number density of the kink band exhibited correlations with both equivalent plastic strain and shear strain, a stronger correlation was observed with shear strain. This indicates that the degree of applied shear strain is one of the factors for the effective kink band formation in the LPSO phase.

Keywords : Magnesium alloys, LPSO, Microstructure, kink band, Finite element simulation

344. Effects of microstructural factors on high temperature deformation behavior of Ti-based MAX phase ceramics

Ikeda Ken-Ichi ¹, Sei Eiichi ², Muraoka Johtaro ², Miura Seiji ¹, Morita Koji ³, Suzuki Tohru S. ³, Sakka Yoshio ³

1 - Division of Materials Science and Engineering, Faculty of Engineering, Hokkaido University (Japan), 2 - Division of Materials Science and Engineering, Graduate School of Engineering, Hokkaido University (Japan), 3 - National Institute for Materials Science (Japan)

The MAX phase ceramics are classified as mille-feuille materials because of their hard-soft two-layered structure consisting of MX and A layers due to the difference in bonding strength. It is also known to be a novel material that combines ceramic and metallic properties due to the difference in its bonding strength. Focusing on plastic deformation, it has been reported that kink deformation occurs in many MAX phase ceramics during deformation and fracture. In this study, we prepared textured sintered compacts of Ti₂AlC and Ti₃SiC₂, which are classified as Ti-based MAX phase ceramics, using slip casting in a magnetic field and spark plasma sintering to clarify the microstructural factors affecting high temperature deformation behavior. In Ti₂AlC, mechanical properties under high temperature compression strongly depend on the compressive orientation. Furthermore, the results of compression tests on specimens with pre-introduced kink bands showed that in addition to an increase in work hardening exponent, the 0.2% proof stress was increased. In Ti₃SiC₂, compressive loading of the textured pressureless compacts by constraining the sides in the SPS showed that the densification increased despite the introduction of kink bands.

Keywords : MAX phase ceramics, kink deformation, high temperature deformation, orientation dependence

345. Strength-ductility balanced by bimodal microstructures composed of kink-strengthening grains in a mille-feuille structured Mg-Al-Y Alloy

Chen Han¹, Kubota Kakeru ¹, Egusa Daisuke ¹, Yamasaki Michiaki ²,
Abe Eiji ^{1 3}

1 - The University of Tokyo (Japan), 2 - Kumamoto University (Japan), 3 - National Institute for Materials Science (Japan)

Light-weight Mg alloys with high-strength remain an enduring pursuit as advanced structural materials. Conventional strengthening strategies for Mg alloys often come at the expense of ductility, exemplifying the well-known strength-ductility trade-off, which has long hindered the development of Mg alloys. In this study, we propose a novel approach to fabricate mille-feuille Mg-Al-Y alloys exhibiting excellent strength and ductility via bimodal microstructures composed of kink-strengthening grains. This unique bimodal structure comprises fine recrystallized grains and large deformed grains adorned with kink boundaries (KBs). The kink-strengthening effect enables the large deformed grains to significantly contribute to evident strengthening, resulting in exceptional strength. The superior ductility stems from the progressive work hardening ability, which is facilitated by two factors: first, the kink-strengthened large grains promote dislocation multiplication during deformation, as KBs act as dislocation storage sites; second, continuous dislocation storage is also maintained by the fine recrystallized grains. This KB-assisted bimodal strategy differs fundamentally from conventional bimodal approaches, where large grains and small grains are used primarily for toughening and strengthening, respectively. This study introduces a novel strengthening-toughening mechanism aimed at achieving a balanced strength-ductility synergy in light-weight Mg alloys.

Keywords : Mg alloys, strength, ductility, bimodal grains, kink boundary

346. Microstructure evolution of twin-roll cast and hot-rolled WZ73 alloy during the finishing heat-treatment

Ueberschar Franziska¹, Ullmann Madlen ², Prahl Ulrich ²

1 - Institute of Metal Forming, TU Bergakademie Freiberg, GERMANY (Germany), 2 - Institute of Metal Forming, TU Bergakademie Freiberg, GERMANY (Germany)

The microstructural evolution of the WZ73 magnesium alloy (Mg-7.38Y-3.8Zn-0.44Zr) was systematically investigated during finishing heat treatments following twin-roll casting and hot rolling at equivalent strain rates of 17 s^{-1} and 50 s^{-1} . Hot rolling at 500°C was performed to achieve a logarithmic strain of 0.7 (thickness reduction from 5.3 mm to 3 mm). Higher strain rates during hot rolling enhanced dynamic recrystallization (DRX), resulting in refined microstructures, whereas lower strain rates promoted the formation of lamellar long period stacking ordered (LPSO) phases. Subsequent heat treatments at 200°C to 550°C for up to 24 hours revealed temperature-dependent microstructural transformations. At 500°C , complete recrystallization occurred with minimal grain growth, while 550°C caused grain coarsening, partial grain boundary melting, and LPSO phase transitions from lamellar to spherical and rod-like morphologies. Notably, at temperatures above 500°C , prior hot rolling had limited influence on microstructure. Cooling strategies shaped LPSO morphology up to 500°C : air cooling retained lamellar structures, while water quenching at 550°C formed a networked 18R LPSO phase and a dispersed W-phase. Combined heat treatment strategy holding at 550°C for 4 hours, followed by aging at 400°C for 10 hours produced a homogeneous microstructure dominated by lamellar 14H LPSO phases, regardless of prior deformation or cooling method. The microstructure and phase evolution were characterized using optical and scanning electron microscopy (SEM), electron backscatter diffraction (EBSD), and energy-dispersive X-ray spectroscopy (EDS). Mechanical properties were evaluated to correlate the observed microstructural changes with performance improvements.

Keywords : microstructure, WZ73, LPSO phases, finishing heat, treatment

347. Processing Strategies for Tailoring Strength and Ductility in Mg-Y-Zn Alloy

Dvorsky Drahomir¹, Inoue Shin-Ichi², Nishimoto Soya², Yoshida Ayami², Kubasek Jiri³, Heller Ludek¹, Prado Esther De¹, Duchon Jan¹, Cavojsky Miroslav⁴, Vojtech Dalibor³, Kawamura Yoshihito²

1 - Institute of Physics, Czech Academy of Science (Czech Republic), 2 - Magnesium Research Center, Kumamoto University (Japan), 3 - Department of Metals and Corrosion Engineering, Faculty of Chemical Technology, University of Chemistry and Technology Prague (Czech Republic), 4 - Institute of Materials and Machine Mechanics, Slovak Academy of Sciences (Slovakia)

The Mg-Y-Zn magnesium alloy system is widely recognized for its exceptional combination of high strength and ductility, even with minimal alloying element content. This remarkable performance is attributed to its unique microstructure, which includes Long-Period Stacking Ordered (LPSO) phases and the distinctive Mille-Feuille Structure (MFS) derived from these phases. Kink strengthening, induced during thermomechanical processing, has emerged as a promising approach for achieving materials with superior strength and ductility. Additionally, dynamic recrystallization (DRX) during extrusion plays a critical role in tailoring mechanical properties. A higher DRX content enhances ductility, while non-DRX grains contribute to increased strength. The primary objective in optimizing processing conditions is to achieve a balance between strength and ductility. This can be accomplished by selecting suitable methods that maximize strengthening through kinks and non-DRX regions while maintaining limited DRX content to ensure adequate ductility.

Keywords : Magnesium, LPSO, kinking, mechanical properties, extrusion

348. Ignition characteristics and mechanical properties of Mg-Al-Ca-X alloys for electric vehicle applications

Jonghyun Kim^{*}, Yu Cao^a, Shuai Zhou^b, Bin Jiang^c, Fusheng Pan^d

* College of Materials Science & Engineering, Chongqing University, Chongqing, 400044, China

a, College of Materials Science & Engineering, Chongqing University, Chongqing, 400044, China,

b College of Materials Science & Engineering, Chongqing University, Chongqing, 400044, China

c College of Materials Science & Engineering, Chongqing University, Chongqing, 400044, China

d National Engineering Research Center for Magnesium Alloys, Chongqing University, Chongqing, 40045, China

Magnesium alloys have low strength and are easy to oxidize and burn at high temperatures. In the process of using magnesium alloys, the study of magnesium alloys with high ignition points is very important to ensure the safety of magnesium alloys. In particular, non-combustible magnesium alloys have low ductility and are difficult to apply in industry. Mg-Al-Ca alloys have very low elongation, which limits their application in industry. We studied the mechanism of the effect of adding small amounts of additive elements to Mg-Al-Ca magnesium alloy on the microstructure, mechanical properties, and ignition properties. The addition of X element makes the grains finer, improves the strength and elongation of Mg-Al-Ca-X alloy, and increases the ignition point of the alloy, which can be applied to the battery case of electric vehicles.

Keywords : Mg-Al-Ca, mechanical properties, ignition characteristics, non-combustible magnesium alloy

349. Microstructural observation of high mechanical strengthened Nb₃Sn superconducting wires via the internal matrix reinforcements

Yokoyama Hayato¹, Lee Seungwon², Tsuchiya Taiki², Hishinuma Yoshimitsu³, Aida Tetsuo², Ikeno Susumu⁴, Matsuda Kenji²

1 - Graduate School of Science and Engineering, University of Toyama (Japan), 2 - Faculty of Sustainable Design, University of Toyama (Japan), 3 - National Institute for Fusion Science, Gifu (Japan), 4 - Professor Emeritus, University of Toyama (Japan)

International Thermonuclear Experimental Reactor (ITER) project will become the milestone to realize the fusion power generation, and it is under progressing. The bronze processed Nb₃Sn superconducting wire has been adopted to the large current capacity conductor on the huge magnet for fusion plasma confinement because of its excellent high critical current density (J_c) property under high magnetic field and long workability. On the ITER procurement activity, J_c degradation by mechanical stress and strain based on the huge electromagnetic force was noted as critical research issue to the beyond ITER. We scoped the new internal matrix reinforcement using bronze based ternary alloy. In the general bronze process, the Cu-Sn bronze alloy as the wire matrix acts only as a Sn source to the Nb₃Sn phase formation during the Cu-Sn/Nb diffusion heat treatment. Thus, if the Sn-free Cu matrix after heat treatment is strengthened by solid solution strengthening, Nb₃Sn wire will be able to be strengthened without the reinforcement material. We fabricated to Nb₃Sn multifilamentary wire using Cu-Sn-In ternary alloy as the wire matrix. After the heat treatment, both Nb₃Sn phase formation and (Cu, In) solid solution transformation in the wire matrix were observed. In this study, the Nb₃Sn diffusion phase formation by Sn diffusion and the (Cu, In) solid solution formation mechanism into the matrix will be discussed based on microstructural observations, and the microstructural changes in the superconducting wire due to the addition of In, the amount of In added and the optimum heat treatment conditions were investigated.

Keywords : superconductor, Microstructure, Nb₃Sn

350. Re-design of low-activation vanadium alloys based on impurity control for fusion reactor applications

Nagasaka Takuya¹, Sugawara Takamasa², Sakurai Seiji³, Fukumoto Ken-Ichi⁴, Yamauchi Yuji⁵, Katayama Kazunari⁶, Watanabe Hideo⁷, Tsisar Valentyn⁸

1 - National Institute for Fusion Science (Japan), 2 - Institute for Materials Research, Tohoku University (Japan), 3 - Taiyo Koko Co., LTD. (Japan), 4 - Research Institute of Nuclear Engineering, University of Fukui (Japan), 5 - Faculty of Engineering, Hokkaido University (Japan), 6 - Interdisciplinary Graduate School of Engineering Sciences, Kyushu University (Japan), 7 - Research Institute for Applied Mechanics, Kyushu University (Japan), 8 - Belgian Nuclear Research Centre SCK-CEN (Belgium)

Vanadium alloys are promising for the structural material of fusion reactor blanket, due to their high-temperature strength, and good compatibility with liquid metal lithium serving both as a coolant and a fuel tritium breeder material. The vanadium-lithium blanket can provide sufficient tritium breeding from neutron-lithium reaction without any neutron multiplier Be and isotope tailoring for Li-6 enrichment. Chemical composition of V-4Cr-4Ti has been selected as the primary candidate after systematic investigations on its neutron irradiation properties. Since V and Cr never create long-lived radioactive isotopes emitting high-energy gamma ray even under the heavy neutron irradiation condition, low-activation characteristics are controlled by Ti and harmful high activation impurities, such as Co. The cooling time for radioactivity decay and material recycling would be only 10 years, if the impurity levels and Ti concentration are effectively reduced, maintaining similar mechanical and irradiation properties to the V-4Cr-4Ti alloy. The present paper reports recent progress in development of vanadium alloys, focusing on refining of vanadium alloys and re-design of their Cr and Ti concentration balance. In the present study, vanadium metal was purified by electron-beam melting and zone-melt refining in vacuum. It was revealed that removal of Co impurity is more efficient for vanadium melt than that from ferro-alloy melt, due to better vaporization coefficient and liquid-solid distribution coefficient. In other words, vanadium alloys are fortunately suitable for the impurity control. In the present paper, these mechanisms and directions of the alloy re-design concerning mechanical, irradiation and corrosion properties are discussed.

Keywords : Fusion blanket material, low, activation materials, refractory metals, electron, beam melting, zone refining

351. DTT Bolometry and Soft X-Rays Diagnostics Design Facing Engineering and Physics Requirements

Peluso Emmanuele^{1 2}, Belpane Andrea³, Noce Simone², Palomba Silvia⁴, D'Agostino Valentina¹, Apruzzese Gerarda², Boncagni Luca², Gabelleri Lori⁴, Gaudio Pasquale¹

1 - University of Rome Tor Vergata, Department of Industrial Engineering, Rome, Italy. (Italy), 2 - ENEA, Nuclear Department, via Enrico Fermi 45, 00044 Frascati (Italy), 3 - Consorzio RFX (CNR, ENEA, INFN, Università di Padova, Acciaierie Venete SpA), Corso Stati Uniti 4, 35127 Padova, Italy (Italy), 4 - DTT S.c.a.r.l., Via Enrico Fermi 45, 00044 Frascati, Italy (Italy)

The decision to equip the new Italian Divertor Tokamak Test (DTT) project, an experimental fusion reactor under construction in Frascati (Italy), with essential diagnostics from the first plasma necessitates a significant effort to integrate different systems. This has resulted in the development of specific optimized solutions aimed at reducing costs and potentially streamlining maintenance procedures. Currently, the Soft X-ray (SXR) and the bolometry diagnostics are housed in a compact modular support. While the metal foil bolometers and their surrounding box are expected to be actively cooled, the same is not yet assessed for the chemical-vapor-deposition (CVD) diamond-based SXR detectors. Both bolometers and diamonds detectors must be able to withstand high incident power fluxes of the order of 0.5 MW m^{-2} , which implies elevated thermo-mechanical stresses and significant expected neutron loads while maintaining their mechanical and electrical properties. This contribution aims to illustrate the ongoing studies, and the results already obtained with the objective of addressing the most relevant problems. Additionally, it will report the remaining issues to be addressed in the forthcoming years to optimize the final design of the diagnostics.

Keywords : Materials & Technologies in Fusion Reactors, DTT, Bolometry, SXR, Plasma Diagnostics, Nuclear Fusion

352. Microstructures and Irradiation Hardening in Low-activation Fe-Mn-Cr-Al-V-C Alloys

Furuya Kazuyuki¹, Tsuchiya Koichi², Eiichi Wakai³

1 - National Institute of Technology, Hachinohe College (Japan), 2 - National Institute for Materials Science (Tsukuba, 305-0047 Japan), 3 - Facility for Rare Isotope Beam, Michigan State University (United States)

Microstructures, mechanical properties and irradiation hardening were studied of Fe-(10 and 20)Mn-15Cr-2.0Al-0.7V-0.5C (at%). The alloys do not contain high activation elements, such as, Co, Ni and Mo. The alloy samples were processed by vacuum induction melting and hot-rolling. The final heat treatment was done at 1073 K for 0.5 h followed by water-quench. The Fe-10Mn-15Cr-2.0Al-0.7V-0.5C (10Mn) sample consisted mainly of BCC phases with two distinct microstructures, i.e., fine lath-like structures and recrystallized grains. Meanwhile, the Fe-20Mn-15Cr-2.0Al-0.7V-0.5C (20Mn) sample were a mixture of fine lath-like BCC phase and FCC phases. Fe-20Mn-15Cr-2.0Al-0.7V-0.5C had a good mechanical property with tensile strength of 620 MPa and total elongation of about 60 %. The 10Mn sample exhibits very high tensile strength of 961 MPa but low elongation, while the 20Mn sample exhibits lower tensile strength of 622 MPa but much improved elongation over 60%. The samples were simultaneously irradiated with 10.5 MeV Fe³⁺ ions, 1.05 MeV He⁺ ions and 0.38 MeV H⁺ ions to a depth of 1 μ m from the sample surface. The irradiation hardening in average was only about 1.5 GPa in the alloys irradiated with 10.5 MeV Fe³⁺ ions up to 30 dpa at 573 K at the damage peak, measured by nano-indentation. The irradiation hardening resistance of the alloys was better than that of fusion structural materials and fission reactor pressure vessel steels. It was revealed that the irradiation hardening is less significant in the lath BCC phase than in recrystallized BCC (10Mn) and in FCC (20Mn).

Keywords : medium entropy alloys, nanoindentation, EBSD, fusion reactor, fission reactor

353. Helium concentration dependence of retarded recrystallization in tungsten

Cheng Long¹, Peng Jiaguan ¹, Yuan Yue ¹, Lu Guang-Hong ¹

¹ - School of Physics, Beihang University (China)

Recrystallization is considered as one of the most important issues when using tungsten as plasma facing material (PFM) for fusion device like ITER. Helium exposure significantly impacts PFM properties, as helium could induce surface modifications, including pinholes, nanofiber fuzz, and orientation-dependent patterns. Recently, helium irradiation was found to enhance the recrystallization temperature and thermal shock resistance of tungsten, potentially expanding the operating temperature window. However, the effect of helium concentration on recrystallization remains unclear. In this work, tungsten samples were exposed to 40 keV helium ions at doses from $5\text{Å}^{-10^{21}}\text{ m}^{-2}$ to $1\text{Å}^{-10^{23}}\text{ m}^{-2}$, followed by recrystallization annealing. Surface morphology and microstructure were systematically studied. After annealing, the strongest retarding effect is observed at $5\text{Å}^{-10^{21}}\text{ m}^{-2}$ with the lowest recrystallization fraction, indicating the helium concentration dependence of the retarding effect on recrystallization. A new phenomenon of large protrusions formation termed thermal ridges near grain boundaries is observed. Furthermore, orientation-dependent helium bubble growth is observed during annealing. Oversized elliptical bubbles ($> 200\text{ nm}$ in diameter) were observed only in $\{110\}$ grains, while small bubbles ($< 10\text{ nm}$) were observed in other grains. This work helps enhance understanding of the helium effect on the surface morphology and microstructure evolution in tungsten materials, and provides insights for predicting helium-containing PFM performance in fusion devices.

Keywords : Helium bubble growth, Tungsten, Surface morphology, Recrystallization, Grain boundary grooving

354. Development of NDE Infrastructure for Fusion Device Relevant Materials and Components at EPRI

Wall James¹, Hohmann Brian ², Meyer Ryan ³, Panetta Paul ⁴

1 - Electric Power Research Institute (United States), 2 - Hohmann Engineering Associates (United States), 3 - Oak Ridge National Laboratory (United States), 4 - The Aerospace Corporation (United States)

The Electric Power Research Institute (EPRI) has become engaged in high level coordination of fusion Industry materials research, such as design and qualification of materials to be used in fusion devices. The EPRI Fusion Forum was established to facilitate information exchange among the nascent commercial fusion Industry, EPRI and other stakeholders such as the US Department of Energy. Recently, there has been a resurgence of interest in development of nuclear fusion as a commercial electric power source due to several recent significant technological achievements. This renewed interest, combined with global CO₂ emission goals, have made it apparent that now is an ideal time for EPRI to get more directly engaged in fusion R&D and technology transfer to support the Industry. The PI and collaborators envision that a critical area for hastening commercial fusion power generation is development of infrastructure to support nondestructive evaluation (NDE) method optimization, benchmarking studies and development of inspection procedures. The focus will be on magnetic plasma confinement fusion devices (tokamaks and stellarators) as they have unique advantages for industrial scale up and eventual electric power generation. The PI and Collaborators envision the establishment the Fusion NDE R&D and Benchmarking Laboratory at the EPRI NDE Center in Charlotte, NC USA. The Laboratory will house an evolving library of calibration blocks and component mock ups fabricated using fusion device relevant materials and manufacturing processes. The initial focus will be component manufacturing process optimization and device assembly. Longer term, the scope will expand to include operational degradation assessment techniques.

Keywords : Nondestructive Evaluation, Fusion, Process Optimization, Aging Management Inspections

355. In-situ EBSD phase transition analysis in ODS martensitic steels

Fekih Maissa¹, Sornin Denis ², Germain Lionel ¹, Guyon Julien ¹, Gey Nathalie ¹

1 - Universite de Lorraine, CNRS, Arts et Metiers Paris Tech, LEM3, F-57000 Metz, France (France), 2 - Universite Paris-Saclay, CEA, Service de Recherches en Materiaux et procedes Avances, 91191, Gif-sur-Yvette, France. (France)

Oxide Dispersion Strengthened (ODS) stainless steels are considered promising candidates for fuel cladding and plasma-facing materials in next-generation nuclear reactors. To enhance creep resistance, their body-centered cubic (BCC) matrix is reinforced with a fine dispersion of oxides. Following powder mechanical alloying with the oxide and subsequent hot consolidation, these materials are typically cold-formed into fuel cladding tubes or thin sheets. Martensitic grades with 9-11 wt% Cr undergo phase transformations at elevated temperatures. Usefully, this transformation promotes cold forming microstructure recovery during heat treatments. The martensitic ODS steels investigated in this study also exhibit an untransformed ferrite phase coexisting with austenite at high temperatures. This study employs Electron Backscatter Diffraction (EBSD) analysis to track the grain size and crystallographic texture evolution of both phases during an in-situ heating ramp from room temperature to 1050°C, and through subsequent cooling to martensitic transformation. The effects of ODS reinforcement on a 10 and 12 wt% Cr steels are compared, highlighting the distinctive high-temperature behavior of ODS martensitic grades. Various initial microstructures, obtained through hot isostatic pressing and hot extrusion, are also examined. The findings are compared with ex-situ characterizations available in the literature. At high temperatures, the study reveals a very fine austenite microstructure and, for the first time, explicitly documents the presence of residual ferrite at 1000°C in martensitic ODS steels.

Keywords : Martensitic ODS steel, MEB in, situ heating, EBSD, Phase transformations

356. Evolution of dislocation microstructure in cyclically deformed [001], [011], and [111] oriented copper single crystals

Fujii Toshiyuki¹, Miyazawa Tomotaka ¹, Lei Xiao-Wen ¹

¹ - School of Materials and Chemical Technology, Institute of Science Tokyo (Japan)

Copper single crystals with stress axes near the multiple slip orientations of [001], [011], and [111] were subjected to cyclic deformation under plastic strain control at room temperature, and the dislocation structures developed during deformation were observed using a scanning electron microscope and a scanning transmission electron microscope. The evolution of the dislocation structure strongly depends on the orientation of the stress axis, and a characteristic evolution of the structure was observed for each orientation. The deformation structure differed significantly depending on which secondary slip system was active and when it started to be active. When heterogeneous deformation occurred, macroscopic deformation bands were formed and within these bands, cell structures were formed along specific orientations. It was found that the orientation of the deformation bands and cell bands could be explained geometrically by the combination of the multiple slip systems that were activated depending on the stress axis. The cell boundaries that constitute the cell structure were found to consist of a network structure of screw dislocations. It was also found that cell boundaries with positive and negative rotation components were arranged alternately to offset the crystal rotation within the deformation band.

Keywords : Fatigue, Dislocation structure, Deformation band, Cell structure

357. Production of Fe-6.5 %wtSi electrical steels sheets by conventional metallurgy for high-performance electric motors

Badaoui Touria¹, Helbert Anne-Laure ¹, Ji Vincent ¹, BeRard Emilie ¹,
Betanda Yanick Ateba ², Waeckerle Thierry ²

1 - Institut de Chimie Moleculaire et des Materiaux d'Orsay (France), 2 - Aperam alloys Imphy (France)

Fe-6.5 wt%Si electrical steel has excellent soft magnetic properties compared to a Si content 3.5%: high permeability, low DC coercive field, low AC magnetic losses thanks to its high electrical resistivity, low magneto-crystalline anisotropy and almost zero magnetostriction. High Si content electrical steel promises a more efficient motor, it is the ideal material for electric motors. Nevertheless, the alloy with a high Si content is still very brittle at room temperature because of the appearance of minor phases below 760°C during its elaboration by hot-rolling: ordered B2 (FeSi) and DO3 (Fe₃Si) phases. In order to overcome the brittleness of this alloy and ensure its successful production by conventional metallurgy, less expensive and complex than the CVD currently used, the detection by DRX and TEM, the identification and quantification of these ordered B2 and DO3 phases is a crucial step. The results confirm the relationship between the percentage of ordered B2 and DO3 phases measured by the Rietveld method and the brittleness of the alloy, established by measurements of the mechanical properties. The amount of ordered phases is a function of the rolling temperature, the heat treatments carried out on the strip after hot rolling, the quenching rate, the initial thickness of the sheet and also the alloy addition elements. The aim of the study is to make the material more ductile at room temperature and to ensure that it can be rolled down to a thickness of 0.2 mm.

Keywords : Metallurgical, Fe-6.5 wt%Si, Order, microstructure, brittleness

358. Investigating the Influence of Trace Tantalum on the Microstructure and Mechanical Properties of Niobium Microalloyed Steels

Siqueira Borges De Carvalho Felipe Moreno¹, M. Lasmar Ronaldo²,
L. O. Goulart Livia², S. Carvalho Marcelo², V. Braga Ana Paola¹

1 - Instituto de Pesquisas Tecnologicas (Brazil), 2 - Mineracao Taboca (Brazil)

The global production of niobium-microalloyed steels is now a well-established industrial practice. Initially driven by experimental insights into niobium's ability to refine steel microstructures during thermomechanical processing, this technology has become especially prevalent in low-alloy steels. An important aspect of niobium's production is its natural association with tantalum, which often leads to the co-extraction of both elements. This paper investigates the impact of tantalum traces, present as a contaminant in FeNb, on the microstructure and mechanical properties of niobium-microalloyed steels. The study reveals that the presence of tantalum leads to a further refinement of austenitic grains without negatively affecting the yield strength of the alloys. Additionally, the tantalum contamination enhances the toughness of the steel samples. By exploring the subtle effects of tantalum contamination, this study provides new insights into its influence on microalloyed steels, particularly in terms of microstructural refinement and mechanical performance in two specific Nb-microalloyed steel compositions.

Keywords : Microalloyed Steels, Tantalum, Alloy Element, Thermomechanical Rolling

359. Crystal orientation change during simple shear deformation of Fe-3%Si

Wada Naoki¹, Tsukamoto Genki ¹, Kimura Ken ¹, Sugiura Natsuko ¹

¹ - Nippon Steel Corporation (Japan)

The changes in crystal orientation under simple shear deformation were investigated to clarify the mechanism of the {110} orientation (Goss orientation) formation near the surface due to shear deformation during hot rolling of Fe-3%Si steels. Columnar grains with //ND orientation rotated towards the vicinity of the {112} (Copper orientation) regardless of the initial orientation by applying simple shear deformation with a strain of 0.6 at room temperature. The slip lines of {100} (D-cube orientation) and {100} (Cube orientation) under simple shear deformation with a strain of 0.02 were analysed to investigate the active slip systems. Slip lines parallel to the traces of two types of {110} planes were clearly observed in the D-cube orientation, indicating that deformation occurred due to the activity of two types of {110} slips. On the other hand, more slip lines were observed indistinctly in the Cube orientation, suggesting the activation of multiple slip systems.

Keywords : Texture, Goss Orientation, Shear Deformation, Hot Rolling, Slip System

360. Evaluation method for Mode II crack growth rates under rolling contact conditions based on fracture mechanics in railway wheel steels

Kurosaka Ryuta¹, Kato Takanori ¹

1 - Nippon Steel Corporation (Japan)

This research aims to evaluate the rates of shear-mode crack growth under rolling contact fatigue (RCF) in railway wheel steels. At present, a standardized methodology for assessing shear-mode crack propagation in the context of RCF remains unestablished. In this study, twin-disc-type RCF tests were executed on railway wheel steels with artificial defects, complemented by finite element analyses (FEA) that simulated these experimental conditions. The outcomes of the RCF tests demonstrated that cracks originating from the leading side of the defects propagated inward, whereas those initiated from the trailing side progressed toward the surface. Calculations of the stress intensity factor (SIF) revealed that cracks initiated from the leading side propagated through a combination of modes I and II, in contrast to those from the trailing side, which propagated exclusively in Mode II. Moreover, the rates of crack propagation on the trailing side were observed to exceed those on the leading side, a phenomenon attributed to a more substantial Mode II equivalent SIF range on the trailing side compared to the leading side. These findings indicate a correspondence between the FEA results and the RCF test outcomes. Consequently, the relationship between the RCF crack propagation rate and the shear mode SIF range may be effectively evaluated through the integration of twin-disc-type RCF tests utilizing specimens with artificial defects alongside FEA.

Keywords : Rolling contact fatigue, Railway wheel, Artificial defect, Mode II fatigue crack propagation, Finite element analysis

361. Effect of precipitation phase on high cycle fatigue behavior of Ti-2Al-9.2Mo-2Fe alloy

Shin Su-Hong¹, Lee Dong-Geun ¹

1 - Department of Materials Science and Metallurgical Engineering, Sunchon National University (South Korea)

The Ti-2Al-9.2Mo-2Fe (2A2F) alloy is a low-cost beta-Ti alloy in which expensive beta-stabilizing elements (such as Ta, Nb, W, and Ni) are replaced by more affordable Mo and Fe, making it suitable for low-cost applications in various industries. High cycle fatigue properties are increasingly receiving attention as an important consideration when designing structural materials. Therefore, this study investigates the precipitation phase control and resulting high cycle fatigue fracture behavior of the Ti-2Al-9.2Mo-2Fe alloy. To control the precipitation phases, solution treatment was performed at 790°C for 1 hour, followed by aging treatments at 450°C, 500°C, and 550°C for 4 hours at each temperature to precipitate and control the alpha and omega phases. Vickers hardness and room-temperature tensile tests were conducted to analyze the basic mechanical properties. Subsequently, high cycle fatigue tests were carried out under various loading conditions, and the mechanisms of fatigue crack initiation and propagation, as well as failure modes, were analyzed in detail for each aging temperature.

Keywords : Ti, 2Al, 9.2Mo, 2Fe, aging treatment, precipitation, high cycle fatigue test

362. Wear Behavior Analysis of Nitrided Ti-12.1Mo-1Fe Alloy after Shot Peening Pre-treatment

Lee Seung-Woo¹, Lee Dong-Geun ¹

1 - Department of Materials Science and Metallurgical Engineering, Sunchon National University (South Korea)

Beta titanium alloys have excellent mechanical properties, but their application as structural materials is limited due to low wear resistance. Gas nitriding can improve the wear resistance of titanium, but it requires high temperature and long treatment, which can affect the internal microstructure. In this study, the nitriding efficiency was improved through shot peening pre-treatment of a metastable beta titanium Ti-12.1Mo-1Fe alloy, and the wear behavior thereof was investigated. Shot peening was performed for 1 min at 0.6 MPa in a vacuum atmosphere using an HSS (High-Speed Steel) ball, followed by nitriding at 800 °C for 1 hr. Through shot peening pre-treatment, the surface particle size was refined into nanocrystals, and it was confirmed that the surface nanocrystals served as sites for nitrogen atom diffusion, thereby increasing the diffusion depth. As a result of performing a ball-on-disc wear test, it was confirmed that the highest wear resistance was achieved under the condition of nitriding after shot peening due to the formation of a hard Ti_xN nitride layer.

Keywords : Metastable beta titanium alloy, shot peening, Ti_xN nitride layer, wear properties

363. Analysis of Generation and Propagation of Fatigue Crack in Oxygen-free Copper Using Electron Backscattered Diffraction Method

Yonekura Hiroki¹, Tatsuya Kobayashi¹, Ikuo Shohji¹

¹ - Gunma University (Japan)

These days, because of the performance of power equipment has improved, fatigue damage of conductor oxygen-free copper was increasing. But fatigue life prediction of copper is difficult because copper has no fatigue limit and not researched of fatigue failure well. It is said that fatigue cracks expand by slip deformation, and crystal grain is rotated. Thus, we investigated fatigue crack initiation and propagation processes by electron backscattered diffraction (EBSD) method to find indication of fatigue failure and figure out the mechanism of fatigue damage in oxygen-free copper for power equipment.

Heat-treated C1020 at 850°C was prepared as a specimen. The specimen was polished, buffed using and etched. After etching, observed of notch area by optical microscope and EBSD analysis. The specimen cycled triangle wave, under fully reversed($R=-1$), load-controlled and room temperature. The fatigue test was stopped as appropriate, and slip lines were observed by optical microscope. Then, the specimen was polished, buffed and etched. EBSD analysis was performed after etched. Time series observation was done by repeating fatigue test through EBSD analysis until the specimen brake.

Optical microscope image and the inverse pole figure (IPF) map showed that the fatigue crack in the grain was caused by slip deformation. The Schmid factor map showed that Schmid factor has no relation to crack initiation location. Grain orientation spread (GOS) and grain average misorientation (GAM) confirm the signs of fatigue crack initiation. Elastic strain analysis suggested that tensile axial strain concentrated at the crack tip promotes crack propagation.

Keywords : C1020, Fatigue Failure, EBSD, Elastic Strain

364. Analysis of Wear Properties and Mechanism Changes According to Fe Content in Metastable β Titanium Alloys

Jung Yeonghun¹, Lee Dong-Geun ¹

1 - Sunchon National University (South Korea)

Titanium alloys are widely used in applications such as aircraft and implants due to their high specific strength and excellent corrosion resistance. However, titanium alloys exhibit poor machinability because of the limited slip systems in their HCP structure. To address this issue, β titanium alloys have been developed, but they are associated with higher costs and increased density due to the use of expensive β -stabilizing elements. Consequently, there is a growing demand for research on metastable β titanium alloys that offer relatively lower costs while maintaining adequate machinability. In this study, Ti-5Mo-xFe (x = 2, 4 wt%) alloys were designed and fabricated using Mo and Fe, which are cost-effective and strong β -stabilizing elements. The wear resistance properties of Ti-5Mo-xFe alloys were evaluated using a tribometer, and the effects of varying Fe content on microstructural changes and wear mechanisms were analyzed. The Ti-5Mo-xFe alloys were compared with the Ti-6Al-4V ELI alloy. The results revealed that the Ti-5Mo-xFe alloys exhibited relatively lower wear resistance, attributed to increased adhesive wear resulting from the high-volume fraction of the β phase.

Keywords : Ti, 5Mo, xFe, tribometer, wear properties, adhesive wear

365. Effects of Changes in Crystal Structure by Plastic Deformation on Corrosion Resistance of Magnesium Alloys

Hayasaka Ryo¹, Yoshihara Shoihiro ¹, Mitome Riku ¹, Honma Yuki ¹,
Kishimoto Takuma ², Furushima Tsuyoshi ³

1 - Shibaura Institute of Technology (Japan), 2 - Nagoya Institute of Technology (Japan), 3 - University of Tokyo (Japan)

Magnesium alloys have excellent biocompatibility and biodegradability and might be expected to be bioabsorbable materials for medical device stents. A stent is used to expand and support blood vessels from the inside to treat diseases in which the heart's coronary arteries are narrowed or occluded, resulting in insufficient blood flow to the heart. Conventional stents are made of stainless steel and remain semi-permanently in the body, possibly leading to restenosis and thrombosis. Therefore, magnesium attracts attention as a material for bioabsorbable stents that can be gradually degraded and absorbed into the body. However, magnesium has low corrosion resistance, and the corrosion resistance must be improved. The crystal structure is one factor affecting the corrosion properties of metallic materials. Several studies have focused on the relationship between crystal structure and corrosion properties to improve magnesium's corrosion resistance. However, the relationship between crystallographic factors and corrosion mechanisms requires clarification. Especially in stents, plastic deformation during expansion leads to refined grains and twins forming. Therefore, the purpose of this study is to investigate the influence of refined grains and twinning on the corrosion properties of magnesium. In fact, hot rolling and compression is used to refine the crystal grains and form twinning in experiments. The crystal structure can be observed by optical microscopy and SEM-EBSD. After evaluation of the crystal structure, immersion tests in brine are conducted to measure the amount of mass loss and observe corrosion behavior.

Keywords : Magnesium alloys, Corrosion resistance, Crystal structure, Grain size, Twinning

366. Study of Adhesion Strength Degradation and Fracture Behaviour of Copper/Epoxy Resin Joints under Hygrothermal Conditions

Zhao Xinya, Kobayashi Tatsuya, Shohji Ikuo

Gunma University (Japan)

In this study, the degradation of the adhesion strength and the fracture behaviour of the metal/resin (alicyclic epoxy resin) interface, which is used for electronic packaging, were investigated by the reliability test. The adhesion strength of the copper/resin joints was investigated by the tensile test after high temperature and high humidity aging at 85, *f* in 85% R.H. for 1000 h. The change of its fracture surface was observed by optical microscopy. The results showed that the adhesion strength of the copper/resin joints gradually decreased with an increase in the aging time. The primary fracture mode gradually changed from interface fracture to cohesive fracture. To further investigate the cause of this change, the fracture surface characterization was analyzed by Fourier transform infrared spectroscopy (FT-IR). The FT-IR analysis results indicated that the penetration of water into the resin leads to the breaking of the ester bond in the resin and the formation of a significant amount of COOH, which contributed to the degradation of the resin material. Additionally, the elemental composition and chemical structure of the fracture surface were analyzed by X-ray photoelectron spectroscopy (XPS). The XPS analysis results indicated that the copper layer is oxidized by aging and the fracture easily occurs in the oxidized layer.

Keywords : Copper, Alicyclic Epoxy Resin, Adhesion Strength, Fracture mode

367. Effects of Prior Deformation at Cryogenic Temperature on Tensile Deformation Behavior of Heterogeneous Nano-Structured Austenitic Stainless Steel

Watanabe Chihiro¹, Koga Norimitsu¹, Miura Hiromi²

1 - Kanazawa University (Japan), 2 - Toyohashi University of Technology (Japan)

Recently, it was reported that heterogeneous nano-(HN-)structured SUS316LN austenitic stainless steel, fabricated by heavy cold rolling, exhibited an exceptional strength-ductility balance at 77 K by deformation-induced $\gamma \rightarrow \alpha'$ martensitic transformation (DIMIT) and transformation-induced plasticity (TRIP) effect. Even while the TRIP effect was impotent at room temperature (RT) in SUS316 type austenitic steels due to the high stability of the austenite phase, a recent report have suggested that α' -martensite nuclei formed by cryogenic deformation can grow by subsequent deformation at RT to enhance ductility. In the present study, the effects of prior tensile deformation at 77 K of HN-structured SUS316L steel on the mechanical properties during subsequent deformation at RT are investigated through detailed microstructural observations. The pre-deformation up to plastic strain of 4% at 77 K drastically improved the elongation to fracture by 1.5 times larger from 6% without pre-deformation to 9% with pre-deformation (i.e., $9 + 4 = 13\%$ in total). However, UTS of 1350 MPa was scarcely affected. Digital image correlation methods revealed that the specimen pre-deformed had a much wider necking region during tensile test at RT than that without pre-deformation. Microstructural observations and magnetization measurements directly demonstrated that α' -martensite nucleation occurred by pre-deformation at 77 K and grew during subsequent tensile deformation at RT. These findings strongly indicated that pre-deformation at cryogenic temperature promotes DIMIT at RT even in stable austenitic stainless steels, improving ductility due to the TRIP effect.

heterogeneous nano, structure, nucleation, martensitic transformation, transformation, induced plasticity

368. The Stress Field Dependency of Martensitic Transformation in Metastable Austenitic Stainless Steel

Morohoshi Ritsuki¹, Kawabata Tomoya¹, Hatano Masaharu²

1 - Systems innovation, The University of Tokyo, 7-3-1 Hongo Bunkyo-ku Tokyo, 113-8654 (Japan), 2 - Nippon Steel Stainless Steel Corporation, 3434 Ooaza-shimata Hikari-shi Yamaguchi 743-8550 (Japan)

Precise characterization of martensitic transformation under various stress fields is essential to assess fracture toughness of metastable austenitic stainless steel through finite element analysis. However, there are few previous studies[1,2,3] experimentally focusing on the topic because the methods to measure α' transformation are limited to mainly four, and each has pros and cons: Neutron diffraction, X-ray diffraction, Electron backscatter diffraction (EBSD), and Ferrite scope. To my knowledge, no previous experiments have given crystallographic insight into the stress field dependency. The objective of the study is to make the crystallographic insight by utilizing EBSD, the highest space resolution but only on the very surface. The method is to conduct tensile tests in an SEM chamber and observe EBSD for every certain load. The tests are done with three different specimens to analyze the stress field dependency: notched, flat plate, and pure shear. Then the sequential EBSD data along loading are analyzed by newly-made image registration techniques which enables to tracking of almost every individual crystal. In other words, the track system can automatically specify how a portion of a crystal becomes α' for the next loading increment. Fig. 1 shows parts of the sequential EBSD data of the notched specimen. The result showed the stress field dependency by EBSD is in almost good accordance with the previous experiments, indicating surface information is enough to substitute the inner property. Additionally, the Schmid factor, one promising factor explaining the stress field dependency, does not solely account for the dependency. References [1] Beese, M. Allison, Mohr Dirk (2011). Acta Materialia, 59, 7, 2589-2600, [2] Lebedev Anatoly. A., Kosarchuk, V. V. (2000). International Journal of Plasticity, 16, 7€“8, 749-767, [3] Polatidis, E. et al. (2021). Materials Science and Engineering: A, 800, 2021, 140321,

Keywords : insitu, Martensitic transformation, stress triaxiality, SEM, EBSD, metastable austenitic stainless steel

369. Effect of heat treatment process on microstructure and toughness at cryogenic temperature for 9%Ni steel

Madambashi Rikiya¹, Kawagoe Norino ¹, Umezawa Osamu ², Ono Yoshinori ³, Komatsu Masayuki ⁴

1 - Graduate School of Engineering Science, Yokohama National University, Yokohama, 240-8501, Japan. (Japan), 2 - Faculty of Engineering, Yokohama National University, Yokohama, 240-8501, Japan. (Japan), 3 - Research Center for Structural Materials, National Institute for Materials Science, Tsukuba, 305-0047, Japan. (Japan), 4 - Research Network and Facility Services Division, National Institute for Materials Science, Tsukuba, 305-0047, Japan. (Japan)

Quenched 9% Ni steel is mainly composed of martensite structure, and intermediate quenching (lamellarization) is applied to improve its toughness at cryogenic temperature, where the precipitated austenite phase and annealed martensite are stabilized. However, the role of the austenite phase and tempered martensite on the toughness at cryogenic temperature has not been clear. In this study, the austenitized and water quenched (Q-step) 9%Ni steel was isothermally heated at 923 K followed by intermediate quenching (L-step) and then tempered at 823, 838, 873, and 923 K (T-step). The volume fraction, distribution, morphology, precipitation sites, and phase stability of the austenite phase during the QT (quenching-tempering) and QLT (quenching-lamellarizing-tempering) processes were characterized and their Charpy impact absorbed energy at cryogenic temperature was evaluated. The austenite phase in the QLT sample was detected at the lath boundaries and its volume fraction was high as up to 10%. Although the austenite phase was detected at the large angle boundaries in the QT sample, it was non-uniformly distributed with a much lower volume. The more uniform distribution of the austenite phase in the QLT sample was attributed to dislocation rearrangement through the T-step. No clear ductile to brittle transition was detected in both QT and QLT samples, which maintained high Charpy impact absorbed energy even at cryogenic temperature. A higher volume fraction of austenite is not necessary to achieve higher toughness, and the stability of austenite affects the cryogenic toughness.

Keywords : quenching, Tempered martensite, Precipitated austenite, Stability of austenite, Cryogenic toughness

370. Evaluation of a Low-Cost System for Measuring Thermal Conductivity in 3D-Printed Metallic Structures

Friedo Maria Helene¹, Hauschultz Mike Thomas¹, Kallabis Conrad¹,
Richetta Maria², Boehme Andrea¹, Krenz-Baath Rene¹

1 - Technical University of Applied Sciences Wildau (Germany), 2 - Department of Industrial Engineering,
University of Rome Tor Vergata (Italy)

Novel injection moulding tools have been developed using metal 3D printing, particularly Selective Laser Melting (SLM). SLM allows for the creation of new designs, including the integration of lattice structures within the components. These structures, which are known for their lightweight and high-strength characteristics, are being employed in the aerospace and automotive industries. Lattice structures exhibiting enhanced thermal properties have the potential to optimize injection moulding tools, where effective thermal management is of importance. To achieve these innovative thermal characteristics, a thorough investigation of their thermal behaviour and conductivity is essential. A cost-effective test setup has been designed and built. The system employs a comparative method, whereby heat flow through a 3D-printed sample is measured in series with a reference body. By analysing the temperature gradients across both bodies, the thermal conductivity of the printed structure can be determined. BK7 glass is employed as the reference material, given its well-characterised thermal conductivity. A significant factor to be considered is interfacial thermal resistance, which occurs at the boundary between two contact materials and can impede the flow of heat. The properties of the materials in question, the surface finish and the contact pressure exerted exert influence on this resistance. The system ensures more accurate measurements of the thermal conductivity of the printed materials by conducting multiple measurements of the same structure with varying heights. This approach allows for the identification and compensation of thermal contact resistances.

Keywords : Selective Laser Melting, Thermal Conductivity, Lattice Structures, Low Cost, Injection Moulding

371. Influence of Process Parameters Variation on Microstructure and Mechanical Properties of SLM-Printed 316L Stainless Steel

Hauschultz Mike Thomas¹, Friedo Maria Helene¹, Palombi Alessandra², Varone Alessandra², Geissler Ute¹, Boehme Andrea¹, Richetta Maria², Krenz-Baath Rene¹

1 - Technical University of Applied Sciences Wildau (Germany), 2 - Department of Industrial Engineering, University of Rome Tor Vergata (Italy)

This study presents the characterization of 316L stainless steels fabricated by selective laser melting (SLM), focusing on the influence of printing parameters on microstructure and mechanical properties. The choice of process parameters is crucial for achieving desired material properties, as it directly affects the microstructure and mechanical behavior, which is important when optimizing for potential applications in several fields, such as aerospace and automotive. In this study, different scanning speeds were tested to identify optimal settings, followed by the evaluation of the effects of orientation relative to the building plate and hatching strategies to enhance performance. To assess the impact of these factors, tensile tests, microhardness measurements, and X-ray diffraction (XRD) analyses were conducted. Tensile tests revealed that higher laser scan speed generally reduces ultimate tensile strength and elongation, likely due to an increase in porosity and a less homogeneous fusion of layers. The analysis of samples printed with different orientation relative to the building plate highlighted a strong mechanical anisotropy, with the samples printed vertically exhibiting lower tensile strength and ductility compared to horizontally printed samples. Microhardness testing further confirmed an anisotropy in material properties. XRD analysis reveals a preferential orientation of austenitic grains depending on building direction. This, in turn, influences the anisotropic behavior. These findings highlight the critical role of process parameters in tailoring the microstructure and mechanical performance of SLM-produced parts, thereby providing insights into the optimization of additive manufacturing for specific applications.

Keywords : 316L, Additive Manufacturing, Selective Laser Melting, Parameter Optimization

372. The effect of zinc content on the acoustic properties of brass percussion

Naganuma Ryusei¹, Taro Kato², Mitsuaki Furui³

1 - Tokyo University of Technology, Sustainable Engineering Program, Graduate school of Engineering (Japan), 2 - Department of Mechanical Engineering, and Sustainable Engineering Program, Graduate school of Engineering (Japan), 3 - Department of Mechanical Engineering, and Sustainable Engineering Program, Graduate school of Engineering (Japan)

Tones emitted by metal materials change by the physical properties of metals, chemical composition, mechanical properties, and microstructure. However, there are very few studies on the influence of differences in the frequency of hitting the sound of the material and the color of the sound on human comfort. In this study, we consider the difference tones of materials by the physical properties, chemical composition, mechanical properties, and microstructure. Furthermore, we aim to evaluate the quality of the tone of the material by acoustic factors. In this paper, we quantitatively clarify the effects of differences in zinc content in brass on hitting sound using acoustic factors. In this experiment, we prepared brasses with different zinc contents and recorded their hitting sounds. Recordings were made in an anechoic chamber, and a pendulum was used to keep a constant hitting force when producing sound. We analyzed the recorded sounds for frequency and decay time. Moreover, we considered the difference of hitting sound by the physical properties and mechanical properties. From the result, we proved that the frequency changes to a lower value due to the decrease in Young's modulus caused by addition of zinc. The decay time increases with the increase in hardness due to the addition of zinc. In the future, we plan to investigate the relationship between the zinc content of brass and the hitting sound from microstructure of the material.

Keywords : Acoustic properties, Zinc content of brass, Frequency, Decay time, Hitting sound

373. The impact of surface properties on strain distribution in air-bending

Kajjalainen Antti¹, Pokka Aki-Petteri ¹, Jaskari Matias ², Huuki Juha ³

1 - Materials and Mechanical Engineering, University of Oulu (Finland), 2 - Kerttu Saalasti Institute, University of Oulu (Finland), 3 - Department of Mechanical Engineering, Aalto University (Finland)

Bending is the most used forming process for structural steels. However, the limited formability of ultra-high strength steels (UHSS) poses some challenges for the bending process in the form of strain localization, surface defects and pseudo-polygonal nut-like shape of the bend. Bendability is well known to be affected by surface quality. This study is a continuation of previous studies; therefore, the idea is to determine the influence of surface roughness, residual stress and dislocation density on the bendability of a UHSS grade, and it is investigated with 3-point bending tests, utilizing Digital Image Correlation (DIC) for measuring the strain distributions on the outer curvature. Investigated bending samples of a 4 mm thick commercial bainitic-martensitic steel sheet were tested in different surface conditions: ¹ as-rolled, ² dry electropolished, ³ ultrasonic burnishing and ⁴ a combination of dry electropolishing and ultrasonic burnishing. Ultrasonic burnishing strongly affects the surface quality, by increasing the surface hardness and decreasing the surface roughness. The main aim of the present paper is to establish an understanding of how bendability can be influenced by modifying the surface characteristics using the polishing and ultrasonic burnishing. Investigations revealed that coarser surface roughness and/or higher subsurface hardness reduced bending capacity, resulting in a lower maximum bending angle and critical strain. The differences in the extent of multi-breakage and bend forms are also investigated, and these findings are associated with the results of bending force, strain measurements, and roughness parameters.

Keywords : roughness, hardness, bendability, DIC, ultra, high strength steel, residual stress, dislocation density

374. Application of bi-modal milling process to fabricate harmonic structure materials

Suzuki Seitaro¹, Yagi Koki ², Kawabata Mie ¹, Fujiwara Hiroshi ¹,
Ameyama Kei ¹

1 - Ritsumeikan University (Japan), 2 - Kyocera Co (Japan)

The Harmonic Structure [1] represents a novel design concept that facilitates the engineering of metallic materials to achieve enhanced mechanical performance. The Harmonic Structure is comprised of soft, coarse-grained regions (the Core) surrounded in three dimensions by an interconnected network of hard, ultra-fine grain regions (the Shell). The interaction in these core/shell regions produces a synergistic effect during plastic deformation, resulting in superior mechanical properties that are of great significance. The distinctive network configuration of the Harmonic Structure enhances the dislocation density within the coarse-grain regions in contact with the interface through stress partitioning, thereby accelerating the work hardening rate and consequently enhancing the strength. This phenomenon is referred to as Hetero Deformation Induced (HDI) strengthening [2]. The fabrication of HS material is achieved through the application of mechanical milling (MM) to the powder, which results in the formation of a deformed layer on the surface of the powder and the creation of bimodal structured particles. However, one of the significant limitations of the MM process is that it requires a longer time frame to achieve the desired bimodal structure. In contrast, the bi-modal milling (BiM) technique involves the controlled mechanical milling of coarse and fine powders in conjunction with each other, with the objective of forming a layer of fine powders of a specified thickness over the coarse particles. The most advantageous aspect of bi-modal milling (BiM) is not only its shorter processing time, but also its superior ability to control the thickness of the surface deformation layer.

Keywords : Heterogeneous structure, Three, dimensional periodic structure, Coarse powder, Fine powder, martensitic transformation, High strength and high ductility

375. Environment-Assisted Cracking of Mg-Al-Zn Alloys in pH-Controlled Carbonate Buffer Solutions

Haruna Takumi ¹

1 - Kansai University (Japan)

In this study, the influence of solution pH on susceptibility to Environment-Assisted Cracking (EAC) of Mg-Al-Zn alloys in carbonate buffer solutions was investigated.

Carbonate buffer solutions were used as test solutions to maintain its pH during the test. The pH was adjusted from 8.3 to 11.2. A constant load EAC test device was employed and dead weights approximately 0.2% yield strength were applied to the specimen. During the EAC test, a strain, a corrosion potential, and a solution pH were spontaneously measured.

The specimen tested in solution at a pH between 8.0 and 10.5 showed typical creep curves of the first, second, and third stages, and then fractured due to EAC. The fracture time increased as the pH increased to 10.5, and no EAC was obtained at pH 11.2. The corrosion potential at which the third creep stage begins was defined as the EAC initiation potential, and the potential increased as the pH increased. The evidences suggest that higher pH promotes formation of hydroxide or oxide film on the specimen to suppress crack initiation.

Keywords : Mg, Al, Zn alloys, Environment, Assisted Cracking, Carbonate buffer solution, Constant load test, Corrosion potential

376. Mechanical and Thermal Properties of Harmonic Structure Composites with Ti-Ni Alloy and Copper

Miyauchi Kentaro¹, Kawabata Mie¹, Kuno Tomoko¹, Ameyama Kei¹, Fujiwara Hiroshi¹

¹ - Ritsumeikan University (Japan)

Heat dissipation materials are expected the thermal properties of low thermal expansion coefficient and high thermal conductivity. However, these two properties are a trade-off relationship. A harmonic structure control may solve such a trade-off problem. The harmonic structure is composed of dispersed coarse grains and fine grains that are networked around them. Harmonic structure composites have different metallic materials in network and dispersed region of the harmonic structure. It is reported that the Mo/Cu harmonic structure composites exhibit low thermal expansion and sufficient thermal conductivity, simultaneously. In addition, the harmonic structure composite indicates excellent mechanical properties. In this study, the harmonic structure composites with Ti-Ni alloy and Cu were fabricated by mechanical milling (MM) / spark plasma sintering (SPS) process and were investigated mechanical and thermal properties in detail. Fine Ti-Ni alloy powder and coarse Cu powder were mechanically milled using planetary ball mill equipment at cryogenic temperature. The MM powder was sintered by using the SPS apparatus at 1073 to 1273 K. Tensile tests carried out at 383 K as mechanical properties evaluation. Thermal expansion to 1073 K was evaluated using thermomechanical analyser equipment. The 0.2% proof stress of Ti-Ni/Cu harmonic structure composite sintered at 1073 K, 1173 K and 1273 K was 129 MPa, 173 MPa and 245 MPa, respectively. The harmonic structure composite exhibits unique mechanical properties with increase in 0.2% proof stress with increasing the sintering temperature. The coefficient of linear thermal expansion was lower than that of Cu and greater than that of Ti-Ni alloy.

Keywords : harmonic structure, spark plasma sintering, mechanical milling, mechanical property, thermal property

377. Micro-mechanical characterisation of hydrogen-enhanced fatigue crack growth in 100Cr6 bearing steel under mixed-mode loading

Kawaguchi Kurumi¹, Mine Yoji¹, Dienwiebel Martin^{2 3}

1 - Kumamoto University (Japan), 2 - Karlsruhe Institute of Technology (Germany), 3 - Fraunhofer Institute for Mechanics of Materials (Germany)

This study employed miniature compact-tension-shear specimens with different loading angles to reveal the effect of mixed-mode loading on the fatigue crack propagation in bearing steel. In-situ hydrogen charging micro-fatigue testing was also performed to elucidate the contribution of mixed-mode loading to hydrogen-enhanced crack propagation. In the uncharged state, the fatigue crack growth was retarded immediately after changing from mode I to mixed-mode loading at an angle of 60 and 80 degrees, whereas the crack growth rate remained unchanged under mixed-mode loading of 30 degrees. Debris appeared in the flank of slant pre-cracks with a loading angle of 60 and 80 degrees. These findings indicate that the roughness-induced crack closure reduces the effective driving force for crack propagation, which extends its incubation period under the high-angle mixed-mode loading. Hydrogen increased the crack growth rate by 1€“2 orders of magnitude. Unlike the uncharged specimen, no crack growth retardation occurred in hydrogen-charged state under the 60 degrees mixed-mode loading. In the uncharged state, the cracks in the mixed-mode loading were kinked at an angle slightly lower than that estimated from the maximum energy release rate criterion, whereas in the hydrogen-charged state, the crack propagated orthogonal to the applied normal stress. Transmission electron microscopy analyses showed that cracks tend to propagate along the nanotwin boundaries in martensite microstructures in the hydrogen-charged state. These findings suggest that hydrogen macroscopically increases the contribution of the normal stress to crack propagation, while the micro-mechanism of crack growth strongly depends on the orientation of nanotwins in the martensite microstructure.

Keywords : Bearing steel, Hydrogen embrittlement, Martensite, Micro mechanical testing, Mixed mode fatigue

378. Phase-field modelling of hydrogen embrittlement in metals

Ruffini Antoine¹, Bouobda Moladje Gabriel Frank ¹, Finel Alphonse ¹,
Le Bouar Yann ¹

1 - Universite Paris-Saclay, ONERA, CNRS, Laboratoire d'etude des microstructures (LEM) (France)

Hydrogen-enhanced decohesion (HEDE) is one of the Hydrogen Embrittlement (HE) mechanisms that consists in the lowering of the atomic bond strength due to the trapping of dissolved hydrogen atoms at the crack surface of a material. In the last few years, phase-field methods have emerged as a powerful tool to describe such a phenomenon at the continuous scale. Usually, the reduction in the cohesion properties is modelled by explicitly decreasing the critical energy release rate, as a function of the hydrogen coverage. In this work, to simulate the HEDE mechanism, we propose a new phase-field approach, based on the Kim-Kim-Suzuki (KKS) formalism, which is more rigorously connected to the segregation physics of the hydrogen atoms at the crack surface. This variational formulation accounts naturally for the decrease of the surface energy, in conjunction with the hydrogen atoms trapping, by minimization of the total free energy of the system. The model and some validation tests are first presented, followed by a systematic study of the HEDE mechanism in Al-based polycrystalline alloys, where intra- and intergranular regimes are characterized as a function of grain boundary density and the distribution of hydrogen trapping energy in these boundaries.

Keywords : Hydrogen Embrittlement (HE), Hydrogen, enhanced decohesion (HEDE), Grain boundaries, Phase field

379. The effect of Cu and Sn contents on the microstructure and mechanical properties of eutectoid steel

Kim Chae Young¹, Jeong Mun Sik¹, Ryou Kenhee², Choi Pyuck-Pa², Kang Minwoo³, Han Jeongho¹

1 - Hanyang University (South Korea), 2 - Korea Advanced Institute of Science and Technology (South Korea), 3 - Hyundai Motor Group (South Korea)

With the transition to a carbon-neutral society, the steel industry has faced increasing pressure to reduce greenhouse gas emissions. Electric arc furnace (EAF) steelmaking, which generates less than one-fifth of the greenhouse gas emissions of blast furnace steelmaking, has gained significant attention as a sustainable alternative for producing high-quality steel materials. However, EAF-produced steel often contained residual tramp elements such as Cu and Sn due to scrap recycling. These elements have been known to degrade mechanical properties through high-temperature segregation, but comprehensive studies examining the effects of tramp element types and concentrations on the microstructure and mechanical behaviour of specific steels have been insufficient. Eutectoid steels, widely used in the automotive industry, undergo repeated high-temperature deformation processes, such as casting and drawing. While they exhibit excellent formability, tramp elements lead to grain boundary segregation and liquid metal embrittlement (LME) at high temperatures, causing significant challenges in processing. To facilitate a successful transition to EAF-based steelmaking while maintaining high-quality steel, a comprehensive understanding of the microstructural and mechanical changes induced by tramp elements is essential. This study investigated the effects of Cu and Sn content on the microstructural evolution and mechanical properties of eutectoid steel. Alloys with varying Cu and Sn concentrations were fabricated using a vacuum induction melting (VIM) furnace, and atom probe tomography (APT) was employed to analyse segregation behaviour. The findings provided insights into mitigating tramp element-induced property degradation, contributing to the advancement of sustainable steel production.

Keywords : Tramp element, LME, Eutectoid steel, Segregation

380. Effect of Ni on Low Temperature Impact Toughness of V-Nb Microalloying Non-quenched and Tempered Forged Steel

Ren Shuhao¹, Song Renbo ¹, Sun Lican ¹, Zhao Shuai ¹

¹ - School of Materials Science and Engineering, University of Science and Technology Beijing (China)

In this study, non-quenched and tempered forged steels with V-Nb microalloying and V-Nb-Ni(wt.(Ni)%=0.15%) microalloying were designed. The microstructure, mechanical properties, and low-temperature impact fracture behavior at -28°C of the two steels were compared and analyzed. V-Nb microalloying can refine the grain size, with an average grain size of 17.1 micrometres. (V,Nb)(C,N) particles are formed to improve strength, with a tensile strength of 710MPa and yield strength of 521MPa. Fan shaped dissociation surfaces and river patterns were observed on the low-temperature(-28°C) impact fracture surface of V-Nb steel, which are typical characteristics of brittle cleavage fractures, with an impact energy of 14.3J. The average grain size of V-Nb-Ni steel is 10.2 micrometres, with a tensile strength of 731MPa and yield strength of 600MPa. The low-temperature(-28°C) impact fracture surface exists brittle dissociation features such as dissociation planes and river patterns. However, there are small ductile dimples on the dissociation plane, and tearing ridges where ductile dimples aggregate, demonstrating ductile fracture characteristics. The impact energy of V-Nb-Ni steel reaches 100.7J. The smaller average grain size results in less stress concentration caused by dislocation pile up, which is not conducive to crack propagation. SEM revealed that the pearlite interlayer spacing of V-Nb-Ni steel(171nm) is smaller than that of V-Nb steel(274nm), and the deformation of cementite flakes is more coordinated, which helps to improve low-temperature impact toughness. In addition, (V,Nb)(C,N) particles as local cleavage initiation points (CIS) in V-Nb steel leads to dissociation fracture, which decreases the low-temperature impact toughness.

Keywords : Non-quenched and tempered steel, Microalloying, Microstructure, Low temperature impact toughness

381. Microstructural refinement enhances hydrogen embrittlement resistance in high-strength martensitic steel

Lan Xiaodong¹, Okada Kazuho ¹, Gutierrez-Urrutia Ivan ¹, Shibata Akinobu ¹

¹ - National Institute for Materials Science (Japan)

The global pursuit of carbon neutrality and the growing adoption of hydrogen-based technologies have heightened the demand for advanced high-strength steels, particularly martensitic steels, with superior resistance to hydrogen embrittlement. However, the dilemma between strength and hydrogen embrittlement resistance remains a significant challenge. In this study, the effects of prior austenite grain (PAG) size on hydrogen embrittlement behavior in high-strength martensitic steel were systematically investigated using slow strain rate tensile tests combined with digital image correlation (DIC) and X-ray computed tomography analyses. The results demonstrated that PAG refinement significantly improved the hydrogen embrittlement resistance under a similar hydrogen level. DIC analysis revealed that the susceptibility to hydrogen embrittlement originated from the plastic deformation related with microstructure of lath martensite. The PAG refinement mitigated the microstructure-related strain localization, thereby enhancing the hydrogen embrittlement resistance. Moreover, PAG refinement increased the apparent fracture toughness, which was associated with a higher estimated ratio of the crack surface area to the projected surface area on the macroscopic crack plane. This suggested that enhanced crack meandering and branching contributed to increased fracture energy. We found that the improved resistance to hydrogen embrittlement is attributed to several factors: reduced strain localization, lower local hydrogen concentration at PAG boundaries, frequent deflection of intergranular cracks, and an increased density of high-angle boundaries that impede quasi-cleavage cracks—all facilitated by PAG refinement. These findings establish PAG refinement as an effective strategy for developing hydrogen-resistant high-strength martensitic steels.

Keywords : Hydrogen embrittlement, Martensitic steel, Prior austenite grain size, Crack morphology, Three dimensional analysis

382. Synthesis and characterization of an (Al-10Si-3Zn-2Cu)/Ti-6Al-4V interpenetrating phase composite with enhanced mechanical properties

Mohanta Debashish¹, Suman Ravishankar¹, Punera Devesh²,
Gollapudi Srikant³

IIT Bhubaneswar, India

Metal-metal interpenetrating phase composites (MMIPCs) are a new type of composite material where one phase forms a continuous network, while the other has a lattice structure. The lattice structure ensures structural integrity and carries the load effectively. In this work, an interpenetrating phase composite is successfully fabricated by infiltrating Al-10Si-3Zn-2Cu aluminum alloy (A383) into an additively manufactured Ti-6Al-4V lattice. XRD and SEM-EDS characterizations were performed on the A383/Ti-6Al-4V composite. The hardness values of the A383 and Ti-6Al-4V phases were found to be approximately 90 VHN and 390 VHN, respectively. The composite demonstrates excellent load-bearing capabilities under compression, with a yield strength of around 300 MPa which is 200% higher than pure A383 (100 MPa). Additionally, the observation of a plateau in the compressive stress-strain curve highlights its enhanced energy absorption capability. The corrosion behavior of the Ti-6Al-4V/A383 composite in a 3.5 wt.% NaCl aqueous solution is evaluated using open circuit potential (OCP), potentiodynamic polarization curves and electrochemical impedance spectroscopy (EIS). The composite exhibited a corrosion potential (E_{corr}) of -0.66 volts and a current (i_{corr}) of 26.16 micro-A/cm², compared to -0.76 volts and 2.56 micro-A/cm² for A383. Additionally, the compressive and corrosion behavior of the composite was analyzed using finite element modeling to develop insights into the material behavior.

Keywords : Interpenetrating phase composites (IPC), Mechanical properties, Additive manufacturing, Corrosion, Simulation, Finite element analysis

383. Tailoring Biodegradable Zinc Alloys: A Powder Metallurgy Approach

Kubasek Jiri¹, Boukalova Anna¹, Necas David¹, Minarik Peter²,
Dvorsky Drahomir³, Jablosnka Eva⁴

1 - Department of Metals and Corrosion Engineering, University of Chemistry and Technology, Prague, Praha, 166 28, Czech Republic (Czech Republic), 2 - Department of Physics of Materials, Charles University, Faculty of Mathematics and Physics, Prague, 121 16, Czech Republic (Czech Republic), 3 - Department of Functional Materials, Czech Academy of Sciences, Prague, 18200, Czech Republic (Czech Republic), 4 - Department of Biochemistry and Microbiology, University of Chemistry and Technology Prague, Praha, 166 28, Czech Republic. (Czech Republic)

Biodegradable zinc alloys are emerging as promising candidates for biomedical implants due to their biocompatibility and controlled degradation rates. However, achieving optimal mechanical, corrosion, and biological properties for orthopaedic applications remains a challenge. This study explores an innovative powder metallurgy-based approach to enhance the performance of zinc-based materials. By employing mechanical alloying, spark plasma sintering, and extrusion, we synthesized materials with tailored microstructures, achieving a balance between strength and ductility. The resultant composites exhibit ultrafine-grained microstructures with grain sizes below 1 μm and, in some cases, incorporate ultrafine-grained domains and coarse-grained zinc regions, forming a synergistic structure. The process utilizes the formation of fine $\text{Mg}_2\text{Zn}_{11}$ intermetallic phases to improve strength while addressing challenges such as oxide shell formation, which compromises mechanical performance. Hot extrusion disrupts these oxide layers, resulting in materials with superior homogeneity and enhanced mechanical properties. Standout materials with tensile strengths exceeding 350 MPa and elongation to fracture nearing 15% were developed, meeting key benchmarks for biomedical applications. Furthermore, the corrosion behavior of zinc-based materials produced via powder metallurgy differs from that of conventional alloys, with slightly higher corrosion rates, which may be advantageous for real-world applications. Results from indirect in-vitro cytotoxicity tests revealed no significant differences compared to conventionally prepared zinc-based alloys. While harmonic structure design is part of the broader methodology, the primary focus remains on advancing powder metallurgy techniques to produce alloys with improved performance, highlighting their potential in next-generation biomedical applications.

Keywords : Zinc, Biodegradable materials, Powder metallurgy, Microstructure, Mechanical properties

384. A unique high-temperature deformation mechanism in a CrMnFeCoNi alloy

Kawano Hibiki¹, Onoue Shuki ¹, Kawabata Mie ², Fujiwara Hiroshi ², Ameyama Kei ²

1 - Graduate School of Science and Engineering, Ritsumeikan University (Japan), 2 - College of Science and Engineering, Ritsumeikan University (Japan)

The Harmonic Structure (HS) design was implemented in a high-entropy CrMnFeCoNi alloy compact to study its deformation characteristics at elevated temperatures, with particular emphasis on comparison with the homogeneous (Homo) compacts. The HS compact was prepared by powder metallurgy using a mechanical grinding process with a planetary ball mill in an argon atmosphere. The rotational speed was set at 150 rpm and the milling time was either 180 ks or 360 ks. The resulting powders were then subjected to spark plasma sintering at 1223 K for 1.8 ks under 50 MPa, and the compacts were then subjected to high temperature compression tests at 1073 K or 1173 K, at varying initial strain rates over a range of temperatures after the sintering process was completed. The compression test piece had a cylindrical shape with a diameter of 4 mm and a height of 6 mm. The strain rate sensitivity coefficients (m-values) of the Homo compact were found to be 0.26, while that of the HS compact was 0.61, at 1173 K. In addition, the UFG fraction of the HS compacts had a significant influence on the softening during deformation. In-situ observation of the compression tests suggested that the observed softening during high-temperature deformation could be attributed to the dynamic recrystallization occurring in the shell region, followed by the rotation of the shell-core unit caused by the sliding of the grain boundaries of a UFG structure.

Keywords : Heterogeneous structure, two, step compression test, High temperature mechanical properties, pseudo, plasticity, Shell, Core unit rotation softening

385. Creep properties of P92 pipe weld after annealing at 600 and 650°C

Sowka Karol¹, Purzynska Hanna ¹, Zielinski Adam ¹, Sroka Marek ²

1 - Ąukaszewicz Upper Silesian Institute of Technology, ul. K. Miarki 12-14 44-100 Gliwice. (Poland), 2 - Division of Materials Processing Technology, Management and Computer Techniques in Materials Science, Institute of Engineering Materials and Biomaterials, Silesian University of Technology, Konarskiego 18a, 44-100 Gliwice, Poland (Poland)

Ensuring the reliability of modern power units operating at supercritical parameters requires a continuous expansion of knowledge about the condition of welded joint materials. The construction of such boilers necessitates detailed periodic inspections to accurately assess the strength of individual pressure components. This is particularly important for elements with the highest operational parameters, such as steam pipelines and collectors, which operate above the critical temperature. In the case of components not externally heated by exhaust gases, the creep process proves to be the dominant factor affecting the degradation of these components. P92 (X10CrWMoVNb9-2) steel, with a martensitic structure and 9% chromium content, is commonly used for high-pressure components in modern power units designed for supercritical steam parameters. This steel is characterized by good strength, as well as excellent corrosion and creep resistance at elevated temperatures. Welded joints of pressure elements in steam boilers are potentially the weakest points when assessing their service life. These joints are particularly susceptible to material continuity issues within the weld, often in the heat-affected zone, during long-term operation. Consequently, material studies of welded joints on the base material are crucial to understanding degradation processes. This paper presents creep testing procedures and results of a P92 welded joint material after annealing at 600°C and 650°C up to 10000h. Shortened and long-term creep tests were performed with the results of determination of creep strength and creep speed in steady state. Also the microstructure tests were conducted using a scanning electron microscope.

Keywords : creep properties, energy, steel, pipe weld, P92 steel, degradation, microstructure

386. Microstructure, texture and magnetic properties of warm thermomechanical processed carbon free Fe-1.5% Si (Wt.%) non-oriented electrical steels

Soni Ram Jee¹, Yasam Palguna ², Korla Rajesh ², Gervasyev Alexey ³, Kestens Leo A.I. ³, Gautam Jaiprakash ¹

1 - School of Engineering Sciences and Technology, University of Hyderabad, Telangana- India 500046. (India), 2 - Indian Institute of Technology, Hyderabad, Telangana- India 502284 (India), 3 - Materials Science and Technology Group, Department of Electromechanical, Systems and Metal Engineering, Ghent University, Tech Lane Ghent Science Park Campus A, Technologiepark 46, 9052 Gent, Belgium. (Belgium)

The present study focuses on the effect of heat treatment on microstructure, texture, magnetic and mechanical properties of the warm rolled carbon free Fe-1.5%Si electrical steel. The iron-silicon alloys are prepared using vacuum arc melting, homogenization, and warm rolling at 600°C. Warm rolled samples were subjected to different heat treatment temperatures such as 750, 900, and 1200°C for 5 min with 10°C/sec heating and cooling rates. Microstructure and texture were studied by using the SEM-EBSD, magnetic evaluation by Vibrating sample magnetometer (VSM), and the mechanical properties by using the Vickers hardness. The warm rolled microstructure shows that grains are aligned along the rolling direction and recrystallized dynamically. SEM-EBSD results showed that with increase in annealing temperatures the grain size increased from 20 to ~90 micrometres while promoting the development of cube, rotated cube, Goss and rotated Goss-texture. This can be attributed to the deformation characteristics of increasing grain size. The mechanical properties of the specimens are evaluated by using micro-Vickers hardness tester on the warm-rolled and heat-treated samples. Silicon addition influences the α -Fe to γ -Fe transformation kinetics and temperatures, while also forming solid solutions that significantly alter the alloy's mechanical and electrical properties, with solubility increasing at higher temperatures. The relation between the texture and magnetic properties is explained, and the possible mechanics are identified.

Keywords : FeSi alloy, Non, oriented electrical steel, Microstructure, Texture evolution, magnetic properties, Mechanical

387. Numerical investigation of fatigue crack propagation in additively manufactured AA5087 sheets

Poeltl Dominik¹, Kashaev Nikolai², Klusemann Benjamin^{3 4}

1 - Leuphana University of Luneburg (Germany), 2 - Helmholtz-Zentrum Hereon, Institute of Material and Process Design, Geesthacht (Germany), 3 - Institute of Materials Research, Materials Mechanics, Department Joining and Assessment, Helmholtz-Zentrum Geesthacht (Max-Planck-Str. 1, 21502 Geesthacht Germany), 4 - Institute of Product and Process Innovation, Leuphana University of Luneburg (Volgershall 1, 21339 Luneburg Germany)

This work implements a residual stress (RS) field mapping between an additively manufactured (AM) geometry and a standardised fatigue crack propagation (FCP) testing geometry in a finite element method (FEM) framework. The mapping enables an investigation of the influence of the initial introduced residual stresses on the FCP behavior. Direct energy deposition (DED) is an AM technique that promises near-final-shape processing. For this work, hollow cubes built from the aluminium alloy AA5087 with varying wall thickness and edge length are modelled. The thermo-mechanical simulation of the DED process results in a characteristic RS field. In practice, subtractive processing such as milling is applied to reduce the AM geometry to the standardised FCP specimen. Mimicking this, an orientation preserving mapping scheme is applied for transferring the simulated RS field between AM and FCP specimen. A quantitative metric is proposed to compare the potential for FCP for any combination of parameters, in particular the directional dependent RS field. The numerical simulation results will be compared with experimental findings. Finally, parameter studies of processing and geometry parameters add mechanical insight to the AM process and offer progress towards near-final-shape processing at no expense of the mechanical properties.

Keywords : finite element analysis, additive manufacturing, fatigue crack propagation

388. Corrosion-fatigue performance of friction-welded dissimilar joints

Rossi Stefano¹, Benedetti Matteo ², Fontanari Vigilio ²

1 - Department of Industrial Engineering, University of Trento (via Sommarive 9, 38123 Trento Italy), 2 - Department of Industrial Engineering, University of Trento (Italy)

Dissimilar joints allow for differentiation of properties, particularly considering mechanical and corrosion resistance properties, between two metallic component parts, often with cost reduction. However, there are some critical aspects, such as the joining method, difficulty in controlling the microstructure, and frequent corrosion phenomena in case of the presence of an aggressive environment. In aggressive environments, the situation can become critical when environmental factors influence the mechanical behavior. This can lead to phenomena like stress-corrosion cracking, hydrogen embrittlement, and ultimately, corrosion fatigue. This work focuses on the latter phenomenon, considering joints obtained through friction welding of carbon steel and stainless steel. The first part aimed to identify a testing setup suitable for studying the mutual influence of the corrosive phenomenon and cyclic loads. In the second part, the corrosion fatigue behavior of the dissimilar joint was studied in a 3.5% weight NaCl solution under various conditions: free immersion, cathodic protection with partial inhibition of the corrosive phenomenon, and the presence of hydrogen, developed through a cathodic reaction. Fracture analysis was conducted using optical and electron microscopy to identify the potential causes of damage nucleation and the different damage mechanisms produced under the various test conditions. The negative effect of the corrosive environment and the positive role of cathodic protection were highlighted. The fracture morphology was found to differ depending on the specific corrosion fatigue conditions.

Keywords : Dissimilar joint, Fatigue, corrosion, Hydrogen embrittlement, Friction welding, Aggressive Environment

389. Interfacial Plasticity of Proton-Irradiated Nanotwinned Metals

Jang Dongchan ¹

1 - Korea Advanced Institute of Science and Technology (South Korea)

Structural metals and alloys used in nuclear applications often experience significant reductions in plasticity due to high-dose ionizing radiation, leading to radiation-induced embrittlement—a major challenge in the design and operation of advanced nuclear energy systems. Efforts over the past few decades have focused on mitigating this issue by utilizing crystallographic interfaces, such as phase or grain boundaries, which effectively serve as sinks for irradiation-induced point defects. However, these boundaries can also impede dislocation glide, potentially causing embrittlement if present in excess. Thus, strategies that balance high plasticity with the ability to absorb radiation-induced defects are crucial for developing radiation-tolerant materials. This presentation highlights recent studies on the effects of proton irradiation on interfacial plasticity in nano-twinned copper focused on twin boundaries. Due to their perfect or near-perfect coherence, these interfaces accommodate various dislocation activities, such as transmission across boundaries or slip along interfacial planes. Nano-tension experiments on specimens containing these specific interfaces demonstrate their dual capability to absorb radiation damage while facilitating plasticity. These findings provide valuable insights for developing novel nuclear materials for advanced energy systems.

390. Superior tensile and impact properties of a novel high-Mn austenitic steel at extremely low temperatures

Qian Lihe¹, Wei Chaozhang ²

1 - Yanshan University (State Key Laboratory of Metastable Materials Science and Technology, Yanshan University, Qinhuangdao 066004 China), 2 - Yanshan University (YSU) (China)

Materials with ultrahigh strength, ductility and toughness are highly required for producing some key structural components applied at various temperatures ranging from room down to liquid helium temperature, such as for the storage and transportation of liquefied gas, exploration of outer space, construction of nuclear fusion devices, etc. However, such materials with ultra-high performance and low cost, especially for critical components used at extremely low temperatures, are currently very limited. Here, based on traditional Fe-Mn-C high manganese austenitic steel, a novel Fe-Mn-C-Al-Si high manganese steel was designed and prepared by adjusting the contents of C/Mn and adding Al/Si elements to regulate the stacking fault energy and low-temperature deformation mechanisms, and by optimizing the thermal mechanical processes. The microstructural features were characterized and mechanical properties were examined at room down to liquid helium temperature, and compared with those of two other control steels. The results demonstrate excellent tensile and impact properties of the designed steel. Especially at the liquid helium temperature of 4.2K, the yield strength, tensile strength and V-notch impact absorption energy of the steel reach over 1250 MPa, 1600 MPa and 200 J/cm², respectively. The strengthening and toughening mechanisms responsible for the superior mechanical properties of the steel at extremely-low temperatures are discussed.

Keywords : Cryogenic temperature, Mechanical properties, Strengthening, Toughening, Deformation mechanisms, Twinning, induced Plasticity

391. Micro-mechanical characterisation of resistances to hydrogen embrittlement and fatigue crack growth in type 304 stainless steel with nanotwin bundles

Mine Yoji¹, Kawaguchi Kurumi ¹, Ueki Shohei ², Takashima Kazuki ¹

1 - Kumamoto University (Japan), 2 - Kyushu University (Japan)

This study used micro-tensile testing to clarify the effect of twin boundary orientation on the hydrogen embrittlement of a nanotwinned type 304 austenitic stainless steel. The resistance to fatigue crack growth was also investigated using a miniature compact-tension specimen with a 0.05-mm thickness and 1-mm width to understand the relationship between the crack growth and microstructural evolution at the crack tip. In micro-tensile testing, nanotwinning increased the yield stress up to 540-760 MPa, which depended on the twin boundary orientation. In a single-variant nano-twinned specimen with a so-called soft orientation, hydrogen suppressed martensitic transformation and promoted deformation twinning parallel to the nanotwin boundaries, leading to moderate uniform elongation. In hard orientations, where the nanotwin boundaries were parallel and perpendicular to the loading axis, hydrogen-induced twin boundary separation had positive and negative effects, respectively, while hydrogen increased the tensile strength in both cases. These findings indicate that shear deformation parallel to the nanotwin boundaries has a significant effect on mitigating the hydrogen-induced ductility loss. The fatigue crack growth rate was reduced by the introduction of nanotwin bundles, regardless of the twin boundary orientation. This reduction is attributed to detwinning and martensitic transformation parallel to the nanotwin boundaries. Dislocation reactions with nanotwin boundaries presumably contribute to plastic dispersion during the fatigue crack growth. It is concluded that introducing nanotwin bundles into metastable austenitic stainless steels is an effective strategy to enhance the resistances to hydrogen embrittlement and fatigue crack growth via controlling the dynamic martensitic transformation.

Keywords : Austenitic stainless steels, Deformation induced martensitic transformation, Fatigue crack growth, Hydrogen embrittlement, Micromechanical testing, Nanotwin bundles

392. Peltier-Induced Thermal Fatigue Testing for Reliability Evaluation of Thermoelectric Devices

Han Seungwoo¹, Seungik Shin ², Seong-Jae Jeon ¹, Jung Yup Kim ¹

1 - Korea Institute of Machinery and Materials (South Korea), 2 - University of Science and Technology (South Korea)

Thermoelectric devices undergo repeated thermal loads, causing cracks at interfacial joints, which increases resistance and leads to failure. To enhance performance and reliability, thermal fatigue data for these joints are essential. A testing system was developed for thermal fatigue testing, comprising a temperature sensor, power supply, data acquisition unit, load cell, and cooling unit. Specimens were prepared by dicing thermoelectric devices without one side substrate, consisting of ceramic substrates with electrodes, bonding materials, and p-type or n-type thermoelectric legs. Thermal fatigue loading utilized the Peltier effect, enabling faster testing compared to conventional heater and cooling systems. Current was applied to generate heat at the specimen's upper part until the maximum target temperature was reached, then reversed to cool it. This cycle continued until failure. Resistance changes were measured to evaluate failure, and the life of interfacial joints was determined for various temperature differences. Using this data, a temperature difference-life curve was derived and converted into a stress-life curve through finite element analysis. The results provide valuable data on the life characteristics of interfacial joints under different thermal conditions. This data can be used to predict the life of thermoelectric devices, thermoelectric power generators and coolers under varying operational temperatures. It enables deeper understanding of the performance and reliability of thermoelectric devices in practical applications, offering a way to optimize design and extend the life of thermoelectric systems.

Keywords : Thermal fatigue, Peltier effect, Reliability, Thermoelectric device, Testing equipment

393. Lead-free KNN-based piezoelectric ceramics: Design and mechanical characterization

Clement Jade¹, Bah Micka¹, Monot-Laffez Isabelle², Richard Caroline¹

1 - GREMAN (matériaux, microélectronique, acoustique et nanotechnologies) (France), 2 - GREMAN (matériaux, microélectronique, acoustique et nanotechnologies) (France)

Piezoelectric materials for electromechanical devices such as lead zirconate titanate based ceramics (PZT), have nowadays dominated the industrial market thanks to their piezoelectric properties. However, the lead contained in these ceramics known for its toxicity, has become an issue for their use in the European Union following its banishment in electronic devices in 2003. Therefore, research in alternative lead-free piezoelectric materials have been investigated while still not being introduced at an industrial scale on account of manufacturing processes or inequivalent response values of PZT. Among lead-free ceramics composition, the (K,Na)NbO₃ system has been one of the most investigated and promising candidate that needs to be further investigated in order to introduce it at an industrial scale. For producing high quality ceramics, chemical modification such as doping is used, in addition to Spark Plasma Sintering (SPS) to limit alkali volatilization or excessive grain growth. It also allows a faster sintering step that gives time and energy consumption gain. However, it remains a lack of data on the mechanical behaviour to scale-up this material and to push forward its introduction at an industrial scale to fulfil European directives. The aim of this study is to study the design of lead-free piezoelectric ceramics in order to obtain highly dense and homogeneous materials with different grains sizes and ferroelectric performances, using conventional sintering and spark plasma sintering. Microstructure and mechanical characterizations have shown the high potential of spark plasma sintering technique in addition to the effect of tantalum doping in KNN-based ceramics for the strengthening of KNN which is important for applications. Ferroelectric domain structure has also been investigated by using Piezoresponse Force Microscopy (PFM) to understand the domain structure-property relationship in these materials.

Keywords : Mechanical properties, Spark Plasma Sintering, lead, free piezoelectrics, PFM

394. Relationship between Maximum Bending Stress and Surface Roughness of AZ31 Magnesium Alloy Fully Corroded in Salt-water Environment

Iizuka Keishi¹, Taro Kato², Yamada Kentaro³, Mitsuaki Furui⁴

1 - Tokyo University of Technology, Department of Mechanical Engineering, (Japan), 2 - Department of Mechanical Engineering, and Sustainable Engineering Program, Graduate school of Engineering (Japan), 3 - Tokyo Metropolitan Industrial Technology Research Institute (Japan), 4 - Department of Mechanical Engineering, and Sustainable Engineering Program, Graduate school of Engineering (Japan)

Owing to their light weight and strength, magnesium alloys are garnering attention for their ability to reduce the weight of automobile components, mobile phones and aircraft. Among these, AZ31 magnesium alloy is a representative magnesium alloy with well-balanced mechanical properties and castability. However, AZ31 magnesium alloy also has the disadvantage of poor corrosion resistance due to its low aluminium content. In previous research, we clarified the corrosion and tensile properties of AZ31 magnesium alloy. It is also known that the corrosion mechanism is such that filamentous corrosion is generated and then changes to full-scale corrosion. However, their corrosion and bending properties have not been revealed. In this study, AZ31 magnesium alloy was immersed in salt water with a concentration of 5%, and three-point bending test were conducted to confirm changes in bending stress and strain due to strength loss caused by corrosion. Then, investigated which parameters, the arithmetic mean roughness, Ra and the maximum height roughness, Rz, which are indicators of surface roughness, are related to the maximum bending stress of the fully corroded AZ31 magnesium alloy. As a result, it was found that the longer the immersion time, the lower the maximum bending stress. In addition, when evaluating the relationship between maximum bending stress and corrosion, it was found that it is better to evaluate by the arithmetic mean roughness, Ra of the corroded surface rather than by the maximum height roughness, Rz.

Keywords : AZ31 magnesium alloy, full corrosion, saltwater, immersion test, three, point bending test, surface roughness

395. Prediction of Hardness in the Heat-Affected Zone of Multilayer Welded Stainless Steel Based on Dislocation Density Change Behavior

Yu Lina¹, Hirata Hiroyuki ¹, Saida Kazuyoshi ¹

¹ - Osaka University (Japan)

The effects of strain hardening and recovery/recrystallization on the hardness of the heat-affected zone (HAZ) in multilayer welded austenitic stainless steel SUS316 were investigated in this study. The results revealed that strain hardening due to welding strain and softening due to recovery/recrystallization were the dominant factors affecting the hardness change in the HAZ during multilayer welding process. Furthermore, the relationship between the strain and dislocation density and that between the recovery/recrystallization and dislocation density were quantitatively investigated using positron annihilation lifetime spectroscopy. Based on these results, a new hardness prediction method based on the change in dislocation density in the HAZ during multilayer welding was proposed. The hardness values in the HAZ after the multilayer welding were predicted based on the simulated strain and thermal history, and the calculated hardness values agreed well with the measured results. This indicates that the newly proposed hardness prediction method based on the dislocation density change behavior in the HAZ during multilayer welding is valuable and effective for selecting the appropriate welding conditions before actual welding.

Keywords : Hardness, Dislocation Density, Austenitic Stainless Steel, Multilayer Welding, FEM

396. Sintering Characteristics of Mo-Ta Alloys via Spark Plasma Sintering Process

Kim Geon¹, Oh Byungheon ¹, Lee Dongju ¹

¹ - Chungbuk National University (South Korea)

Molybdenum (Mo) is highly valued for its outstanding mechanical strength and rigidity at elevated temperatures, superior electrical and thermal conductivity, and minimal thermal expansion. These attributes make Mo-based thin films integral to advanced technological applications, including electronics, nanotechnology, and gate electrodes in thin-film transistor liquid crystal displays (TFT-LCDs). Incorporating tantalum (Ta) enhances these properties further, particularly improving thermal conductivity, reducing thermal expansion, increasing high-temperature strength, and providing excellent corrosion resistance. The performance of Mo and Mo-based thin films is largely dictated by the characteristics of the sputtering targets utilized in their deposition, making powder metallurgy (PM) a promising fabrication technique due to its ability to produce a uniform microstructure. Conventional melting and casting methods often struggle with microstructural control and homogeneity, reinforcing the advantages of PM. In this study, Mo-Ta alloy nanopowders were synthesized via hydrogen reduction and consolidated through spark plasma sintering (SPS) to develop magnetron sputtering targets. The microstructural evolution and sintering behavior of the sintered Mo-Ta alloy compacts were systematically investigated, followed by a comparative assessment of the properties of the thin films sputtered from these targets. Acknowledgement This work was supported by Korea Institute of Energy Technology Evaluation and Planning (KETEP) grant funded by the Korea government (MOTIE, 20217510100020, Development of platform process using common core and materialization technology for rare metal recovery from industrial low-grade waste liquid)

Keywords : Powder metallurgy, Molybdenum, Alloy, Spark plasma sintering (SPS)

397. An Innovative Grain Refinement Strategy on Biomedical Ti-6Al-4V Alloy for Texture Annihilation

Tukac Ozgun Umut^{1 2}, Browne David^{1 2}, Celikin Mert^{1 2}

1 - School of Mechanical and Materials Engineering, University College Dublin (Ireland), 2 - I-Form Advanced Manufacturing Research Centre, University College Dublin (Ireland)

In this study, the methodology, initial outcomes, and potential implications of a novel approach are discussed, offering a pathway toward enhanced microstructure and texture control in metal additive manufacturing (AM). The additive manufacturing (AM) of Ti-6Al-4V, a key alloy for biomedical applications, especially implants, is hindered by columnar grain growth and pronounced texture formation, leading to anisotropic mechanical properties. To overcome these challenges, a new alloy development approach, focusing on the design and application of novel grain refinement strategies, is employed to facilitate columnar-to-equiaxed transition (CET). This study leverages the Miedema model and CALPHAD (CALculation of PHase Diagrams) simulations for designing grain refiners tailored to Ti-6Al-4V. Alloying techniques and mixing methods are optimized to suppress columnar grain formation, aiming to achieve isotropic material properties and improved mechanical stability. Preliminary results of the as-cast alloys produced by the inert gas arc melting (IGAM) technique indicate promising improvement in microstructure uniformity and texture mitigation. These findings pave the way for the production of Ti-6Al-4V implants/components with refined microstructures and enhanced mechanical performances.

Keywords : Ti6Al4V, Grain Refinement, Alloy development, Solidification microstructure, Columnar to equiaxed transition

398. Synchrotron X-ray characterization of gradient microstructure and residual stress anisotropy in high-pressure torsion processed Inconel 718

Bhatta Laxman¹, Lee Isshu ¹, Liss Klaus-Dieter ², Kawasaki Megumi ¹

1 - School of Mechanical, Industrial and Manufacturing Engineering, Oregon State University, Corvallis, OR 97331 (United States), 2 - University of Tennessee Oak Ridge Innovation Institute, Knoxville, TN 37996 (United States)

This study examines the gradient nanostructure and residual stress anisotropy in Inconel 718 subjected to high-pressure torsion (HPT) processing. HPT is a severe plastic deformation technique that simultaneously applies hydrostatic pressure and torsional straining to produce nanostructured materials. A synchrotron X-ray diffraction experiment was conducted at 50 distinct locations with a step size of 0.2 mm along the near-diameter of the 10 mm diameter disk sample to comprehensively map the spatial distribution of microstructural features. The two-dimensional diffraction rings were analyzed for peak intensity, full width at half maximum, and lattice strain, resulting in detailed diffraction mosaics for the first five reflections of 111, 200, 220, 311, and 400. Strain ellipsoids were observed, implying the heterogeneous deformation across radial positions of the disk. The lattice strain within these mosaics revealed significant anisotropy, indicating directional stress variations. Gradient changes in the estimated residual stress were observed along the torsional shear and its transverse directions, with tensile stress and compressive stress near the disk edge and center, respectively. The modified Williamson-Hall analysis reveals location-dependent variations, indicating a significant influence of shear strain on crystallite size, dislocation density, and microstrain distribution. Moreover, the elastic modulus and Poisson's ratio were calculated for the five reflections, showing significant variations that contribute to explaining the anisotropic configuration. These findings establish a clear link between strain gradients and residual stress across different lattice planes, providing the processing-microstructure-property relationship in HPT-processed nanostructured alloys.

Keywords : Gradient Microstructure, High, Pressure Torsion (HPT), Inconel 718, Residual Stress, Synchrotron X, ray Diffraction (XRD)

399. Application of Digital Image Correlation (DIC) at Cryogenic temperature: Deformation and Fracture Behavior of Metallic Materials (Al, Welding)

Lee Jongwon¹, Han Heeju ¹, Heo Seongjun , Lee Unhae ², Lee Eunjin ³, Kim Hyomin ³, Park Nokeun ^{1 3}

1 - YEUNGNAM UNIVERSITY (South Korea), 2 - Kyung Sung University (South Korea), 3 - Material Solution Park (South Korea)

With the transition towards a hydrogen energy society, research on alloys used for hydrogen storage has become increasingly important. In particular, the storage of liquid hydrogen, which occurs at extremely low temperatures (~20K), necessitates the use of alloys that can withstand cryogenic environments where significant changes in mechanical properties may occur. Understanding the deformation and fracture behavior of materials under these conditions is critical for ensuring the stability of hydrogen storage systems, alongside advancements in analytical techniques. Aluminum alloys are known for their excellent resistance to hydrogen embrittlement. However, when tensile testing is conducted at room temperature, these alloys exhibit flow instability due to the Portevin–Le Chatelier (PLC) effect, which negatively impacts elongation. In contrast, at liquid nitrogen temperatures (77K), the occurrence of serration is significantly reduced, leading to increased strength and ductility. This suggests the potential applicability of aluminum alloys in cryogenic environments, including at 20K. Digital Image Correlation (DIC) is a powerful technique that accurately visualizes and analyzes deformation behavior by tracking the displacement of speckled patterns applied to the specimen's surface. However, in cryogenic environments, technical limitations arise due to phenomena such as adiabatic heating, which can generate bubbles that interfere with the precise tracking of these patterns. We designed cryogenic chamber capable of facilitating DIC analysis under extreme low-temperature conditions. Using liquid nitrogen, we performed DIC analysis and addressed technical challenges in cryogenic conditions through the integration of machine learning techniques. The deformation and fracture behavior of Al 5182 alloy was observed and analyzed across a temperature range from room temperature to cryogenic temperatures. We also conducted microstructural observations to elucidate the underlying mechanisms responsible for the changes in deformation and fracture behavior. The results of this study are expected to contribute to a deeper understanding of material behavior under extreme cryogenic conditions.

Keywords : Digital Image Correlation(DIC), Machine Learning, Aluminum Alloys, Cryogenic Atmosphere, Plastic Deformation, Welding

400. Development of a New Mn and N Alloyed Austenitic Stainless Steel and Its Weldability Evaluation for Cryogenic Applications

Jung Geunsu¹, Shin Jongho ¹, Cha Dojin ¹, Bang Seungkook ¹, Ma Younghwa ¹

¹ - Doosan Enerbility, Materials Technology Development Team (South Korea)

An alloy design for a new austenitic stainless steel using Mn and N as key alloying elements has been conducted, aimed at developing cryogenic materials for extreme low-temperature environments. By optimally balancing the chemical compositions, the developed alloy demonstrates excellent overall physical properties. Mechanical testing indicates that the new alloy is stronger than conventional 300 series stainless steels, while maintaining similar ductility. Additionally, the new alloy exhibits great low temperature toughness, with Charpy V-notch impact values exceeding 100J at -196°C, suggesting its suitability in cryogenic environments. Corrosion tests showed that the new alloy outperforms grade 304 and performs comparably to grade 316 in corrosive environments. Welding was performed on the new alloy, using standard arc welding methods with grade 316 welding fillers for weldability assessment, and the weldability (weld strength, toughness, and corrosion resistance) proved to be highly promising.

Keywords : Stainless Steel, Cryogenic Materials, Weldability, Corrosion Resistance

401. High pressure Spark Plasma Sintering of boron based nano-structured hard boron phosphide (BP, B₁₂P₂) for ballistic applications

Moutaabbid Hicham¹, Le Godec Yann², Mañžtre Alexandre³, Tahan Yves³, Pradeilles Nicolas³, Rapaud Olivier³, Fortrin Pascal⁴

1 - IMPMC/ Sorbonne University (France), 2 - IMPMC/ Sorbonne University (France), 3 - ircer (France), 4 - Laboratoire sols, solides, structures - risques [Grenoble] (France)

Until very recently, the two scientific fields€”high-pressure (HP) science and spark plasma Sintering (SPS) continued their separate developments without combining the two technologies. Spark Plasma Sintering (SPS, Maitre's team) combined with the high pressure (HP-SPS) is a powerful technique for sintering powder under moderate uniaxial pressure (max. 10 GPa) and high temperature (up to 2500 °C). It has been widely used over the last few years as it can achieve full densification of ceramic or metal powders with lower sintering temperature and shorter processing time compared to conventional processes, opening up new possibilities for nanomaterials densification and preservation of the nanoscale grain size to produce bulk nanostructured ceramics, for which grain growth control is one of the main issues. Yield strength σ varies with grain size according to Hall€”Petch equation $\sigma_y = \sigma_{y,0} + k/d^{1/2}$ k is a constant, d is the average grain diameter, and $\sigma_{y,0}$ is the original yield stress. Here, we present recent results on boron based nano-structured hard material (BP and B₁₂P₂) as a demonstrative material at comparatively lower temperatures. The initial nanosized grains are retained in the sintered and dense compact sample and the measured hard Vickers hardness (24 - 48 GPa). New frontiers of opportunities are now emerging by coupling SPS with large volume (~ cubic millimeters) HP technology (up to ~10 GPa), allowing the ballistic applications (Fortrin's team)

Keywords : Boron phosphides, high pressure (HP), Spark Plasma Sintering, Paris, Edinburgh press, superhard material

402. Correlation between microstrain and hydrogen embrittlement in high strength quenching and partitioning (QP) steel

Kim Hyogeon¹, Jeong Mun Sik², Han Jeongho²

1 - Hanyang University (South Korea), 2 - Hanyang University (South Korea)

Quenching and Partitioning (QP) steel, known for its high strength and good formability, is gaining attention as a 3rd generation advanced high-strength steel for automotive steel sheet. The QP process involves heating the steel to produce a fully or partially austenitic microstructure, followed by quenching to a temperature between the martensite start and finish temperatures to control the fractions of martensite and austenite. Subsequently, during the partitioning step, carbon in martensite diffuses into untransformed austenite. This process results in a complex microstructure including ferrite, retained austenite, bainite, tempered martensite, and fresh martensite formed during the final stages of processing. QP steel is a Transformation-Induced Plasticity (TRIP) steel, achieving high strength through the transformation of carbon-rich retained austenite. Generally, High-strength materials are often susceptible to hydrogen embrittlement. In TRIP steels, the boundaries of martensite are known to be susceptible sites for hydrogen embrittlement. However, there has been limited research on how the TRIP behavior of retained austenite influences hydrogen embrittlement. In this study, microstructural analysis was conducted to differentiate austenite surrounded by softer phases from austenite surrounded by harder phases, and their respective effects on hydrogen embrittlement were investigated. Neutron diffraction was employed to determine which phases accommodate higher stress, while micro-digital image correlation was used to examine localized deformation differences in austenite.

Keywords : QP steel, Hydrogen embrittlement, Neutron diffraction, Micro digital image correlation

403. Effects of alloying elements on marine corrosion resistance of structural steel

Pena Quintero Borja¹, Arribas Maribel ¹, Perez Inaki ¹, Merchan Mikel ¹, Garcia Jose Carlos ¹, Elvira Roberto ², San Jose Jose Tomas ³

1 - Tecnia R&I-Industry and Transport Division-Foundry and Steelmaking Area (Spain), 2 - Sidenor Investigacion y Desarrollo, S.A (Spain), 3 - UPV/EHU, Dept. of Engineering in Mining, Metallurgy and Materials Science, University of the Basque Country. Plaza Ingeniero Torres Quevedo 1, 48013, Bilbao (Spain)

In the global transition to green energy, offshore wind has a very important role to play. Offshore wind farms benefit from higher and more consistent wind speeds than onshore farms, resulting in greater efficiency in the generation of electricity. Offshore wind farms also have a lower visual impact. However, one of the main drawbacks is the harsh environment, including saltwater corrosion, which can reduce the service life of the components. The aim of this work is to develop new structural steels, based on the conventional S355 steel, with improved marine corrosion resistance while maintaining mechanical properties. Two different alloying strategies were investigated: the first with Cu and Ni, the second with Al and Cr. Samples of the conventional and new steels were produced in the laboratory and characterised from a microstructural, mechanical and corrosion point of view. The new steels were shown to give similar or even improved mechanical properties compared to conventional steel. The corrosion behaviour of the specimens was studied by potentiodynamic polarisation tests, observing the stabilisation of the oxidation process in the new steels. In addition, laboratory accelerated corrosion tests were performed to evaluate the painted corrosion resistance. It was shown that although corrosion and paint blistering occurred at the paint film defect on both the conventional and the new steels, the blistering was less on some of the new steels. Finally, painted specimens of the conventional and new steels are being investigated in an advanced floating laboratory for study in a real offshore environment.

Keywords : structural steel, corrosion, offshore, microstructure, mechanical properties

404. High Pressure Synthesis and Compression Behaviour of Multicomponent Transition metal Nitrides and Phosphides

Hasegawa Masashi^{1 2}

1 - Department of Materials Physics, Nagoya University (Nagoya 464-8603 Japan), 2 - Research Center for Crystalline Materials Engineering, Nagoya University (Japan)

Transition metal nitrides and phosphides are a class of inorganic compounds that have attracted significant attention due to their unique physical and chemical properties and promising applications in various fields, including catalysis, energy storage, and electronics. Another important recent interest in material science has spotlighted equimolar multicomponent materials that incorporate a lot of distinct element species within a single structure. This burgeoning area of research has yielded surprising and novel properties. The first multicomponent effects have been reported on a fcc alloy, and then there has been extensive exploration of new compounds within the multicomponent ceramic family, particularly oxides. Attempts to compound multiple transition metal species into a single nitride or phosphide are largely unexplored areas. The difficulty of synthesizing these compounds may lie in the fact that they decompose easily at high temperatures and ambient pressure and in the large differences in melting points among the constituent transition metals. High-pressure synthesis methods are so advantageous in overcoming these challenges. In this study, a multicomponent nitrides and phosphides have been synthesized using the high-pressure technique. The crystal structures, homogeneity, stability and compression behaviours have been investigated based on the TEM-EDX and synchrotron powder X-ray diffraction experiments.

Keywords : High Pressure, Multicomponent, Compression, Phosphide, Nitride

405. CALPHAD methodology for high-pressure synthesis: Phase diagram of Mg-C system by in-situ X-ray diffraction and phenomenological thermodynamics

Courac Alexandre ¹, Turkevich Vladimir ², Pietrucci Fabio ¹,
Hasegawa Masashi ³, Crichton Wilson ⁴, Yann Le Godec ⁵

1 - IMPMC, Physical department, Sorbonne universite, Paris, 75005, France (France), 2 - Institute for Superhard Materials, NAS Ukraine, Kiev, 04074, Ukraine (Ukraine), 3 - Department of Materials Physics, Nagoya University, Nagoya, Aichi 4620063, Japan (Japan), 4 - ESRF-The European Synchrotron, Grenoble, 38000, France (France), 5 - IMPMC, Institut de Chimie, CNRS, Paris, 75005, France (France)

The phase diagram of the Mg-C system has been constructed up to 20 GPa and 4000 K based on complementary Thermo-Calc simulations and experimental data obtained in both ex situ and in situ experiments using X-ray diffraction with synchrotron radiation. As a result of our in-situ and ex-situ studies of the Mg-C system, only two magnesium carbides of allyide type (in beta and gamma crystalline forms) and one methanide with antiferite structure participate in phase equilibria at HPHT conditions up to 20 GPa and melting temperatures. The existence of some previously suggested carbides has been disproven. Using this data, the Mg-C phase diagram has been revised by adjusting the observations to thermodynamic CALPHAD simulations. The domains of thermodynamic stabilities of magnesium carbides show satisfactory agreement with numerous experiments of magnesium carbides' syntheses at HPHT conditions, while the p-T range of possible growth of single crystal diamond agrees well with the calculated domain of diamond-liquid coexistence. Decomposition mechanism of carbides and formation of nanostructured materials will be discussed.

Keywords : High pressure, Diamond, Magnesium, Single crystal, Nanomaterials, CALPHAD

406. Damage evolution in nanostructured ferritic alloys produced via various methods under high dose ion irradiations

Aydogan Eda¹, Darsell Jen¹, Chen Wei-Ying², Yano Kayla¹, Li Xiao¹, Massey Caleb³, Shao Lin⁴, Lavender Curt¹, Rhodes Mark¹, Olson Justin¹, Zhang Dalong⁵, Anderson Iver⁶, Maloy Stuart¹

1 - Pacific Northwest National Laboratory (United States), 2 - Argonne national laboratory (United States), 3 - Oak Ridge National Laboratory (United States), 4 - Texas A&M University (United States), 5 - Baylor University (United States), 6 - Ames Laboratory (United States)

Nanostructured ferritic alloys (NFAs) having ultra-fine grain structure and a high concentration of nano-size (~2-5 nm) oxide particles are considered one of the best candidates for structural components in advanced nuclear reactors due to their excellent irradiation resistance, high strength and resistance to oxidation/corrosion under extreme conditions of temperature and pressure. However, they are produced by lengthy and costly multi-step powder metallurgical (PM) methods. Here, we have developed 14YWT NFAs produced by shear-based extrusion followed by pilger processing of gas atomized reaction synthesis (GARS) powders without ball milling. In parallel, 2nd generation of NFAs having controlled inclusions were developed by traditional PM methods. The samples having various types and number densities of nanoparticles were Fe ion irradiated up to 500 peak dpa at 450 °C. The results were correlated with nanoparticle distributions to determine their efficiency in annihilating the defects.

Keywords : Nanostructured Ferritic Alloys, Nanoparticles, Powder Metallurgy, Shear, based Extrusion, Ion Irradiation

407. Can accelerated neutron irradiations replicate historical microstructural characteristics in U-Zr fuels?

Okuniewski Maria¹, Rodra-Guez Perez Nicole ¹, Smith Morgan ¹

¹ - Purdue University, School of Materials Engineering (United States)

Uranium-10wt.% zirconium (U-10Zr) fuels are under consideration for use within fast reactors. Historically, thousands of U-10Zr fuel pins were irradiated within the United States (U.S.) reactors, including the Experimental Breeder Reactor-II (EBR-II) and the Fast Flux Test Facility (FFTF). However, U-10Zr fuels have never been qualified for use within nuclear reactors in the U.S. Currently, there is a renewed interest in implementing fast reactors, which have the advantage of recycling commercial UO₂ fuel. The implementation requires additional in-reactor testing, which can be time consuming, and fuel qualification can take over 20 years. Therefore, colleagues have recently proposed a new fuel geometry to expedite neutron exposure, known as the Fission Accelerated Steady-state Test (FAST) integral irradiation experiments. This talk will explore and compare the microstructural characteristics of historically irradiated U-Zr fuels and the new FAST irradiations. Advanced characterization techniques, such as electron microscopy and atom probe tomography, as well as stereology will be used to assess the similarities and differences between the microstructures.

Keywords : U, Zr, nuclear fuel, neutron irradiation, microstructure

408. Atomic cooperativity at deformation of metallic glasses

Egami Takeshi ¹

¹ - Shull Wollan Center, University of Tennessee and Oak Ridge National Laboratory (Knoxville, TN United States)

Deformation mechanism in metallic glass has long been thought to involve structural defects, in association from deformation mechanisms in crystalline solids, and various types of defects have been proposed. However, unlike crystalline solids metallic glasses are remarkably structure-insensitive; their yield strains are universal at 2.7 ± 0.2 % [Johnson and Samwer]. We argue that the mechanical strength of metallic glass is not controlled by defects, but by cooperative resistance through the medium-range order (MRO), driven by the collective force to form a density wave state. Defects may start deformation, but the MRO resistance determines the final outcome. The MRO also controls liquid fragility and glass ductility. On the other hand, defects are responsible for local structural relaxation (internal friction) down to $T = 0$. The glass transition is caused by the freezing of the MRO, but the local structures are partially defective (liquid-like) even in the glassy state, resulting in the small ripples at the bottom of the potential energy landscape.

Keywords : Greer Symposium, Metallic Glasses, Deformation Mechanism, Structural Defects, Medium, Range Order

409. Processing of a Zr-based bulk metallic glass

Bornand Manon ¹

1 - Univ. Grenoble Alpes, CNRS, Grenoble INP, SIMaP, Grenoble F-38000 (France)

Various aspects (choice of compositions, purity of elements, atmosphere, cooling rates, oxygen content etc.) during the production of metallic glasses can induce the presence of structural defects, such as isolated crystalline phases (spherulites for example) in the final part. For scientific studies, modifying the process or investigating locations of the sample free of defect is relatively easy to bypass such issue. In a context of industrialization of metallic glass products the whole process can be more constrained and should also ensure reliability, repeatability and final part without any defects. The PhD topic involves the SIMaP laboratory and the rising company VULKAM and investigates the life of the material (a Zr-based metallic glass) during the whole process, from the primary alloy to the final product, in order to ensure the reliability of the production. The microstructural evolution of the alloys as well as complementary work using thermodynamical calculation will be presented in order to better understand the mechanisms at the origin of the presence of undesirable crystalline phases such as spherulites. Keywords: Thermec'2025, Zr-based bulk metallic glasses, processing, defects

Keywords : Thermec'2025, Zr, based bulk metallic glasses, processing, defects

410. Development of Biocompatible, Toxic-Free Zr-Based Metallic Glass Alloys for Long-Term Biomedical Applications

Sourani Fereshteh¹, Ramasamy Parthiban¹, Sharifikolouei Elham²,
Eckert Jurgen^{1 3}

1 - Erich Schmid Institute of Materials Science, Austrian Academy of Sciences, Jahnstraße 12, A-8700, Leoben (Austria), 2 - Department of Health Sciences, Center for Translational Research on Autoimmune and Allergic Diseases-CAAD, Università Del Piemonte Orientale UPO, Corso Trieste 15/A, 28100, Novara, NO (Italy), 3 - Department of Materials Science, Materials Physics, Montanuniversität Leoben, Jahnstraße 12, A-8700, Leoben (Austria)

The demand for orthopaedic prostheses or dental implants is rising due to the increase in ageing population and mechanical injuries. Despite the considerable clinical success of current implant alloys, complexities, including ion release infection remain during their practical performances. To diminish these difficulties, the design of new biomedical alloys is directed toward toxic-free elements and simultaneous improvement in glass-forming ability (GFA) and, high corrosion in the harsh in-vitro environment, supports the potential utilisation of the alloys as long-lasting implant material. We introduce four new biocompatible toxic element-free Zr-based metallic glass (MG) compositions with constant metalloid (Zr_{66.5}Al₁₀Fe₅Ti₂) and precious metal (Pd, Pt, and Au) contents obtained in ribbon form using conventional single roller melt spinning technique. In this regard, their glass-forming abilities (GFA), and structural and thermal properties are comparatively investigated using X-ray diffraction (XRD), transmission electron microscopy (TEM), and differential scanning calorimetry (DSC). Zr-Pt-Al-Fe-Ti showed the highest thermal stability and mechanical strength, with the highest hardness and compressive yield strength, attributed to its dense atomic packing and strong atomic interactions. However, its relatively lower biocompatibility compared to Zr-Au-Al-Fe-Ti suggests potential trade-offs between strength and cytocompatibility. The electrochemical corrosion and metabolic activity of cells exposed to alloy supernatants revealed that Zr-Au-Al-Fe-Ti and Zr-Pd-Al-Fe-Ti alloys as promising candidates for biomedical implants. These findings contribute to the advancement of Ni-Cu-free Zr-based BMGs for long-term medical applications, underscoring the importance of optimising alloy compositions to achieve desired performance metrics.

Keywords : Zr, based metallic glasses, Structural properties, Mechanical properties, Glass, forming ability, Corrosion properties, Biocompatibility

411. Fabrication of Zr-based Bulk Metallic Glasses Lattice Structures by L-PBF process

Hatta Muhammad Fakhry¹, Pauzon Camille¹, Blandin Jean-Jacques¹
², Daudin Remi¹

1 - SIMaP laboratory (France), 2 - Science et Ingenierie des Materiaux et Procedes (France)

Zr-based bulk metallic glasses (BMGs) exhibit exceptional mechanical properties, including high elastic deformation (~2%) and high yield stress (1.6 GPa) compared to other structural metals. However, inherently, it has a limited (or no visible) ductility at room temperature and constrained maximum size (tens of mm). Therefore, fabricating large and complex geometries is challenging while retaining the amorphous phase. The laser powder bed fusion (LPBF) process offers a promising solution by enabling the fabrication of large, intricate and light structures, such as lattice structures, while preserving the amorphous phase due to the high cooling rate (103-108K/s), keeping in mind that the heat accumulation during construction can be an issue concerning devitrification. In this study, the commercial AMLOYZR01 (Zr59.3Cu28.8Al10.4Nb1.5, at%) powders are 3D-printed into three distinct lattice structures: Body-Centered (BC), Octet, and Gyroid. Each fabricated at different relative densities of 0.1, 0.15, and 0.2. The printing parameters (laser power, beam velocity, lasing strategies) are investigated in order to produce amorphous samples. Structural and mechanical characterizations are subsequently performed both on isolated strut and on the whole structure to evaluate the impact of the printing strategies as well as the soundness of LPBF for producing lattice structure of metallic glasses.

Keywords : Zr, based BMG, Laser powder bed fusion, bulk and lattice structure

412. Insights on the heterogeneous to homogenous flow transition in a Zr-based metallic glass

Kempf Merlin¹, Daudin Remi¹, Fivel Marc², Wilde Gerhard³,
Musiol Lukas³, B Jean-Jacques²

1 - Universite Grenoble Alpes, SIMaP-GPM2 CNRS UMR 5266, Grenoble France (France), 2 - Universite Grenoble Alpes, SIMaP-GPM2 CNRS UMR 5266, Grenoble France (France), 3 - University of Munster, Institute of Materials Physics, Wilhelm-Klemm-Str.10, 48149, Munster, Germany (Germany)

Mechanical behaviours of bulk metallic glasses are ambivalent: at room temperature, they show extraordinary strength with little to no plasticity and localisation of the deformation in shear bands; at temperatures close to that of the glass transition their strength drastically diminishes and show impressive ductility through homogenous viscous flow. The transition from the heterogeneous to the homogeneous regime is usually promoted by increasing the temperature and/or reducing the strain rate. Still, this transition remains poorly understood. The present work aims at investigating such transition by performing compression and tensile tests on a well-known Zr-based metallic glasses (Zr_{58,5}Cu_{15,6}Ni_{12,8}Al_{10,3}Nb_{2,8}, T_g=390°) and on a wide range of temperatures and strain rates. During compression tests at room temperature and slightly above, the alloy exhibits a certain capacity for plastic deformation. However, at intermediate temperatures (in regard to T_g), no plastic deformation was observed. As temperature approaches T_g, the yield strength decreases drastically and the plastic behaviour is unpredictable. Indeed, at 0,9T_g, the glass displays unstable mechanical behaviours: either strong strain localisation leading to apparent brittle behaviour or, on the contrary, homogeneous flow. When the strain rate is modified, this unpredictable behaviour can be observed for other ranges of temperature, revealing a temperature-strain rate equivalency playing a key role between potential failure or large ductility. In this presentation, the origin of such behaviours is discussed in the light of structural characterization before and after deformation. Comparisons are made with a more ductile Pd-based metallic glass.

Keywords : Bulk metallic glass, Shear, band, Homogenous flow, Temperature, Strain rate

413. From nano-patterned Pt-based metallic glass to copper oxide foam formation

Spieckermann Florian¹, Fei-Fan Cai^{1 2}, Sarac Baran², Akman Adnan³, GuMruKcu Selin⁴, Schweiger Lukas¹, Hantusch Martin³, Schroers Jan⁵, Blatter Andreas⁶, Gebert Annett³, Eckert JuRgen^{1 2}

1 - Department of Materials Science, Chair of Materials Physics, Montanuniversitat Leoben, Jahnstraße 12, 8700 Leoben, Austria (Austria), 2 - Erich Schmid Institute of Materials Science (Austria), 3 - Leibniz-Institut für Festkörperlager- und Werkstoffforschung Dresden (Germany), 4 - Department of Chemistry, Istanbul Technical University, 34469 Istanbul, Turkey (Turkey), 5 - Department of Mechanical Engineering and Materials Science, Yale University, New Haven (United States), 6 - Research and Development Department, PX Services, 2300 La Chaux-de-Fonds, Switzerland (Switzerland)

The current climate crises and the subsequent need to move to energy sources that are CO₂ neutral or CO₂ negative to replace carbon-based technologies demand for new infrastructures for energy storage and conversion. This also requires to change the used materials. For instance, moving to hydrogen as an energy carrier will require to revisit the corrosive environments, to consider hydrogen storage and hydrogen production solutions. An environmentally friendly hydrogen production option lies in the usage of electrocatalysts with low overpotentials and long-term stability during hydrogen evolution reaction (HER). A surface modified Pt_{57.5}Cu_{14.7}Ni_{5.3}P_{22.5} bulk metallic glass (BMG) has been thermoplastically net shaped to achieve three distinct surface morphologies with flat, micro-patterned, and nanopatterned surfaces and HER in 0.5 M H₂SO₄ was studied. While the catalytic performance of the material is reasonable surprisingly it improves throughout for the nanopatterned case demonstrating long-term stability and self-improving behaviour with a final overpotential of 150 mV and a Tafel slope of 42 mV dec⁻¹ after 1000 linear sweep voltammetry (LSV) cycles, which is respectively 42% and 37% lower than in the first LSV cycle. Characterization by X-ray photoelectron spectroscopy (XPS) and Auger electron spectroscopy (AES) reveal a complex process leading to the formation of a CuO/Cu₂O foam deposited on top of the nano-patterned surface during 1000 LSV cycles. A pathway involving hydrogen bubble templating (DHBT) electrodeposition from Cu dissolution of the Pt-BMG without using copper salt a potentially interesting route towards the production of electrodes consisting of Cu_xO nanostructured foams is proposed.

Keywords : Hydrogen, thermoplastic forming, metallic glass, HER

414. Identification of Deformation Elements in Metallic Glasses through Frozen Atom Analysis

Shiihara Yoshinori¹, Iwashita Takuya²

1 - Graduate School of Engineering, Toyota Technological Institute (Japan), 2 - Department of Integrated Science and Technology, Oita University (Japan)

Metallic glasses exhibit remarkable properties such as high strength and elasticity, making them a subject of considerable interest in material science. However, their amorphous structure complicates the understanding of plastic deformation mechanisms. Traditional metrics such as non-affine displacement and local stress drop analyses, provide limited clarity in identifying deformation elements due to their dependence on arbitrary thresholds. To address this challenge, we propose a novel approach called Frozen Atom Analysis, which identifies deformation elements based on cooperative atomic motion. Frozen Atom Analysis focuses on the disappearance of cooperative motion upon freezing individual atoms, allowing us to pinpoint the atoms contributing to deformation. Molecular dynamics (MD) simulations of Cu₅₀Zr₅₀ metallic glass under shear deformation were performed to validate this method. The D parameter, derived from displacement magnitudes after freezing, was used to quantify the involvement of atoms in cooperative motion. Unlike conventional metrics, the D parameter exhibited a distinct gap in histograms, enabling unambiguous identification of deformation elements. The key findings are: ¹ Deformation elements are defined as atomic groups exhibiting cooperative motion. This clear, physically meaningful definition surpasses the ambiguity of traditional metrics. ² Frozen Atom Analysis revealed that deformation elements have an average size of about 40 atoms, with no correlation to stress drop magnitudes or shear strain, suggesting intrinsic size characteristics. ³ Examination of Voronoi features, such as volume and face count, showed no significant correlation with deformation elements, emphasizing the limitations of structural descriptors in capturing these mechanisms. This study establishes Frozen Atom Analysis as a powerful tool for understanding plastic deformation in metallic glasses, providing insights into their mechanical behaviours. By identifying deformation elements without any ambiguities, this methodology offers a pathway for designing more resilient amorphous materials.

Keywords : Metallic glasses, Plastic Deformation, Molecular dynamics, Cooperative motion

415. Influence of Strain Rate on the Deformation Behavior of Pt-Cu-Ni-P Bulk Metallic Glass

Zhang Shuhan¹, Hay Jenny², Johanns Kurt², Stein Aaron³, Datye Amit¹, Schwarz Udo^{1 4}

1 - Department of Mechanical Engineering, Yale University, New Haven, CT 06511 (United States), 2 - KLA Inc, Milpitas, CA (United States), 3 - Brookhaven National Laboratory [Upton, NY] (United States), 4 - Department of Chemical and Environmental Engineering, Yale University, New Haven, CT 06511 (United States)

The deformation behavior of Pt_{57.5}Cu_{14.7}Ni_{5.3}P_{22.5} metallic glass was systematically investigated under micro-/nanopillar compression, where pillars were prepared using a novel method based on thermoplastic forming. This manufacturing method not only produces better-defined pillar geometries with lesser structural flaws, but it also enables the fabrication of a large number of identical pillars in a short time. Here, the critical load for the formation of shear transformation zones and pillar yielding behavior was analyzed when applying well-controlled strain rates, showing that more pop-ins occur with decreasing strain rates. In contrast, yielding happens at higher strain rates in the areas with biggest flaws without time to accommodate the external pressure, which leads to the distribution of yield points becoming more scattered. Interestingly, fracture stress exhibited a different pattern, showing no significant strain rate sensitivity, contrasting with previous studies that reported negative strain rate sensitivity during pillar compression tests. Additionally, annealed pillars displayed closely clustered fracture loads, consistent with the understanding that annealing-induced structural relaxation enhances atomic packing, reduces defects, and increases resistance to compression. Further nanoindentation experiments, using CSM, CSR and step load techniques, across strain rates from 0.5 to 105 /s on flat Pt-BMG samples revealed that hardness remained steady, in alignment with pillar compression test results, indicating that bulk behavior is insensitive to strain rate.

Keywords : Deformation of Bulk Metallic Glass, Mechanical Properties, Strain Rate and Size Dependence of Compression Behavior

416. Relevance of the Structure and Dynamics of High Temperature Metallic Liquids to Glass Formation

Kelton Ken ¹

1 - Washington University in St. Louis (United States)

How structural changes in liquids correlate with changes in the dynamical properties, and what role these processes play in glass formation and the glass transition remain outstanding questions. Although it is widely believed that the dynamical behaviour is linked to the atomic structure of the liquid, this has been difficult to demonstrate experimentally. While the viscosity of the liquid changes by orders of magnitude with temperature, changes in the structure static structure factor, $S(q)$, or pair correlation function, $g(r)$, are almost negligible. However, the recent development of containerless processing methods and the introduction of intense X-ray and neutron sources have now enabled these changes to be accurately measured in deeply supercooled liquids. Molecular dynamics (MD) and experimental studies of the viscosity in liquid metals have identified a crossover temperature near the liquidus temperature. The MD studies suggest that this marks the onset of cooperative atomic behaviour in shear flow. Inelastic neutron scattering data are presented that support this. Additional results are shown that confirm a general correlation between dynamics and structure in metallic liquids and point to a structural origin for liquid fragility. Fragility and the reduced glass transition temperature are widely believed to correlate with glass formability. It will be shown that both quantities can be accurately calculated from properties of the high temperature liquid.

Keywords : metallic liquids, structure, dynamics, glass formation, fragility

417. Cryogenic Thermal Cycling of Metallic Glasses: From Concept to Applications

Sun Yonghao ¹

¹ - Institute of Physics, Chinese Academy of Sciences (China)

Cryogenic thermal cycling (CTC) has emerged as a significant technique in the field of materials science, particularly for the rejuvenation of metallic glasses. This method, which contrasts with thermal annealing by enhancing thermal energy and compressive plasticity, has sparked considerable debate and research since its initial publication in *Nature*. The concept originated in the laboratory of Greer at the University of Cambridge, where the team observed that CTC could restore properties to a near-liquid state, effectively reversing the structural relaxation that occurs with conventional annealing. The subsequent surge in research, with over 500 papers published on the subject, has yielded a wealth of findings. While many studies have corroborated the original findings across various alloy compositions, others have challenged the universality of CTC's effectiveness, reporting contradictory results. Some studies have even suggested that CTC can lead to relaxation rather than rejuvenation, depending on the initial state of the specimen. This highlights the complexity of the technique and the need for a nuanced understanding of its effects on different materials. In the context of the present talk, after recounting the inception of CTC at Cambridge, I will delve into the controversial results from the literature. A particular focus will be on recent publications that have shed light on the underlying mechanisms of CTC, offering a more comprehensive understanding of how and why it works. Furthermore, the potential application of CTC in addressing residual stress in additively manufactured metallic glasses will be explored, a field that could significantly benefit from the technique's ability to enhance ductility and toughness. The future of CTC in this context looks promising, as it offers a non-destructive approach to improve the mechanical properties of these advanced materials.

Keywords : Cryogenic thermal cycling, metallic glass, residual stress, additive manufacturing

418. Surface designs to improve the biocompatibility of Ti-based bulk metallic glasses

Gebert Annett¹, Fernandez Navas Nora ¹, Shtefan Viktoriia ¹, Hempel Ute ², Calin Mariana ¹

1 - Leibniz Institute for Solid State and Materials Research - IFW Dresden (Dresden, Germany) (Germany), 2
- TU Dresden, Institute of Physiological Chemistry (Dresden, Germany (Germany)

Bulk metallic glasses (BMGs) on Ti-Cu basis are promising new materials for bone implants in orthopedics, trauma and dental surgery, mainly due to their high mechanical biofunctionality, i.e. high strength and low Young's modulus. But in comparison to clinically used materials their biocompatibility in terms of corrosion resistance and cytocompatibility is still insufficient. Due to their unusual compositions, established chemical surface treatments for implants are not applicable. Thus, a main goal of research is the development of new concepts for nanoscale surface modifications. For representative two prominent BMGs, firstly the criticality of their pitting corrosion susceptibility in physiological solution will be discussed and fundamental corrosion mechanisms will be presented. Further, new strategies for electrochemical treatments aiming at strengthening their surface state by the generation of oxide layers with nanoporous morphology and the reduction of critical elements from near-surface regions will be demonstrated. The impact of those modified surfaces on suppressing pitting and on improving the response of bone-forming cells (human mesenchymal stroma cells, hBMSC) will be demonstrated. The potential of those surface designed BMGs for perspective implant material use will be assessed in comparison to the competing class of beta-type Ti alloys. Funding is acknowledged by the German Research Foundation DFG (projects GE/1106/12-2, no 419952351 and GE/1106/15-1, no. 458057521) and by the European Commission, H2020-MSCA grant agreement No. 861046 (BIOREMIA-ITN).

Keywords : Metallic Glass, Ti alloys, Biocompatibility, Implant Applications

419. Rapidly Annealed High-Bs Soft Magnetic FeCo-Based Amorphous and Nanocrystalline Ribbons for High Temperature Applications

Skorvanek Ivan¹, Kunca Branislav¹, Marcin Jozef¹, Svec Peter²

1 - Institute of Experimental Physics, Slovak Academy of Sciences (Watsonova 47, Kosice Slovakia), 2 - Institute of Physics, Slovak Academy of Science (Slovakia)

Technological demand for soft magnetic materials, which offer a large magnetic induction and at the same time are capable of operation at high temperatures has led to an increased interest in FeCo-based amorphous and nanocrystalline alloys. A further improvement of magnetic performance in these alloys is possible by using a careful compositional tuning as well as by employing special processing techniques. Particular attention of our work is focused on ultra-rapid annealing technique that utilizes a compression of thin ribbons between pre-heated massive Cu blocks [1]. Here, very high heating rates and short processing times result in a formation of smaller nanocrystalline grains as compared to conventional furnace annealing. Selected results showing the impact of elevated temperatures on soft magnetic properties will be presented for series of high-Bs Fe-Co-B-(Cu) alloys with reduced metalloids content.. A deeper knowledge on thermal stability of the ultra-rapidly annealed ribbons is important for estimation of their application potential because their exposure to high temperature environments can eventually degrade their functional properties. Our experiments revealed that rapidly annealed high-Bs Fe-Co-B-(Cu) ribbons exhibit very good thermal stability of soft magnetic characteristics up to 623K, which makes them promising soft magnetic materials for operation at elevated temperatures [2, 3]. [1] K. Suzuki et al., Appl. Phys. Lett. 110 (2017) 012407 [2] B. Kunca et al., J. Alloys Compd. 911 (2022) 165033 [3] B. Kunca et al., J. Magn. Mater. 591 (2024) 171679 Acknowledgement: This work was supported by the projects APVV-23-0281, VEGA 2/0148/23 and JRP NOMAGRAD

Keywords : nanocrystalline alloys, metallic glasses, heat treatment, microstructure, magnetic properties

420. The Crystal-Melt Interface in the Hard Sphere System

Spaepen Frans ¹

1 - Harvard University, School of Engineering and Applied Sciences (United States)

The interface between a crystal and its melt plays an important role in many aspects of materials processing. To study its structure and thermodynamic properties, the hard-sphere system is appealing because of the simplicity of its potential, which allows insight into the purely configurational aspects of the problem. Hard spheres are used in experiments (static models, dynamic colloidal systems), as well as in a range of computer simulations. Of particular interest is the interfacial (free) energy, γ , which has its origin in the entropy loss in the liquid near the crystal surface, as can be shown by simple static modeling. Direct experimental measurement of γ , however, is difficult. Confocal microscopy on colloidal systems presents three options: (i) measuring the positional fluctuations of the interface, which yields the interfacial stiffness (which equals γ plus its orientational second derivative); (ii) measuring the homogeneous nucleation frequency of crystals in an overcompressed liquid, and using classical nucleation theory to extract γ ; and (iii) measuring the size distribution of the crystalline fluctuations in a liquid in equilibrium with a crystal, and extracting γ from the Boltzmann distribution. A caveat for the latter two methods is the small size of the crystals. The results from these experiments are in broad agreement with those from various types of computer simulations. One exception is crystal nucleation, for which direct simulation strongly underpredicts the rate at the lower liquid densities, even when allowance is made for a small amount of softening and polydispersity of the spheres in the experiments interface, colloids, crystallization, nucleation

Keywords : interface, colloids, crystallization, nucleation

421. Formation of gradient rejuvenation structure in Zr-based bulk metallic glass and its effect on ductility improvement

Saida Junji¹, Ryu Wookha², Sugisawa Masaki³, Tabaru Keisuke³, Yamada Rui⁴

1 - Frontier Research Institute for Interdisciplinary Sciences (FRIS), Tohoku University (Japan), 2 - Department of Materials Science and Engineering, Research Institute of Advanced Materials & Institute of Engineering Research, Seoul National University (South Korea), 3 - Graduate School of Engineering, Tohoku University (Japan), 4 - Institute for Materials Research, Tohoku University (Japan)

Bulk Metallic glasses (BMGs) have continuously attracted great interest due to their unique and excellent mechanical properties resulting from the random atomic configuration. However, it is well known that an embrittlement occurs drastically by structural relaxation via low temperature annealing and/or mechanical processing. The authors have been investigating novel method to recover the less relaxed state (rejuvenation) as a relaxation control using a conventional annealing treatment [1-3]. Recently, we have developed a method to control the relaxation state precisely through a rejuvenation process. As a result, the unique BMG with 2D and/or 3D gradient rejuvenation structure can be fabricated [4,5] and it is found that they exhibit improved ductility. In this presentation, we report recent results on the control of the relaxation state and excellent ductility in Zr-based BMGs. We believe that these results will bring a new evolution to BMGs and beneficial advances in their application. [1] J. Saida et al., Appl. Phys. Lett., 103 (2013) 221910.

[2] J. Saida et al., Sci. Tech. Adv. Mater., 18 (2017) 152-162

[3] W. Guo et al., J. Phys.: Condensed Matter, 35 (2023) 154004.

[4] W.H. Ryu et al., NPG Asia Mater., 12 (2020) 52.

[5] R. Yamada et al., Adv. Eng. Mater., 26 (2024) 2401517.

Keywords : Bulk Metallic Glass, Rejuvenation, Gradient Glassy Structure, Mechanical Properties, Thermal Process

422. SPD as a tool to improve the plasticity of Bulk Metallic Glasses

Ebner Christian¹, Escher Benjamin², Pauly Simon³, Gammer Christoph⁴, Denis Pierre⁵, Meylan Caroline M⁶, Rentenberger Christian¹, Eckert Jurgen⁴, Fecht Hans-Joerg⁵, Greer A. Lindsay⁶, Zehetbauer Michael¹

1 - Faculty of Physics, University of Vienna (Austria), 2 - Bosch Sensortec Gmbh, Reutlingen (Germany), 3 - University of Applied Sciences Aschaffenburg (Germany), 4 - Erich Schmid Institute of Materials Science, Leoben (Austria), 5 - Institute of Micro- and Nanomaterials, Univ. Ulm (Germany), 6 - Department of Materials Science & Metallurgy, University of Cambridge (United Kingdom)

Broad application of Bulk Metallic Glasses (BMGs) suffers from their lack in plasticity. Mechanical treatment by Severe Plastic Deformation (SPD), e.g. high-pressure torsion (HPT) or cold rolling (CR) provides a solution of this problem. In addition to XRD, DSC, AFM, and TEM, the lecture reports nanoindentation tests on Pt- and CuZr-based BMGs, which e.g. allowed to monitor the velocity of shear band sliding governing the plasticity of BMGs. The velocity decreased after SPD, and increased after annealing: SPD is found to increase the mean atomic volume, of the amorphous structure, a process being called rejuvenation. A clear correlation between elastic and plastic softening on the one hand, and between softening and excess mean atomic volume on the other, has been established. The SPD-induced rejuvenation also implies some structural heterogeneity represented by highly strain-softened regions next to less-deformed ones. This is due to the enhancement of elastic fluctuations in the rejuvenated material on different length scales down to the atomic one. In case of CuZr-based metallic glasses, drops of hardness occur by up to 20% which are associated with an estimated increase of the mean atomic volume of up to 0.75%. It can be concluded that rejuvenation by SPD leads to structural and dynamical heterogeneities, increased atomic mobility, and an improved plastic deformation response.

Keywords : Bulk Metallic Glasses, Rejuvenation, Severe Plastic Deformation, High Pressure Torsion, Shear Bands, Plasticity

423. On the design of biocompatible β -Ti-based alloys for bone implants by ab initio and cellular potts model

Lekka Christina¹, Gebert Annett², Calin Mariana²

1 - Department of Materials Science & Engineering, University of Ioannina, Ioannina, 45110, Greece and University Research Center of Ioannina (URCI), Institute of Materials Science and Computing, Ioannina 45110, Greece (Greece), 2 - $\ddot{\text{I}}\text{I}$ – Institute for Complex Materials, Leibniz Institute for Solid State and Materials Research (IFW) Dresden (Germany)

Beta-type Ti-based alloys has been promising for bone implants due to their low Young moduli, high corrosion resistance and minimal cytotoxicity while their enrichment with well-known antibacterial elements like Ga, Cu and Ag causes antibiofilm activity. This work presents Density Functional Theory calculations using Siesta or Vasp software on Ti-based alloys aiming to reveal the electronic origin of the structural and mechanical properties, for the design of materials with predefined properties, even antibacterial, suitable for hard tissue implant applications. Ab-initio results reveal the suitable electronic properties while the calculated mechanical stability conditions and the elastic constants predict the α' -TiNb stabilization only for Nb-rich compositions and the known w-shape Young modulus curve in agreement with the experimental data. The enrichment of beta-TiNb with selective elements like In and Sn might decrease the Young modulus while Ga and Ag provide antibacterial characteristics. Furthermore, metallic implants require surface treatment which would be friendly for the adsorption and growth of human mesenchymal stem cells (hMSCs) promoting therefore the bone formation. To this end the simulation of adhesion and migration of hMSCs on β -Ti -based surfaces using large scale simulations with the Hybrid Cellular Potts model aims to mimic the experimental data. The diffusion coefficient and the hMSC- surface pattered sizes are directly correlated while the elongation and lamellipodium behaviour is simulated in line with experimental data. These results could be used for the design of a micropatterned biocompatible and antibacterial surface suitable for hMSCs adsorption, proliferation, and osteogenic differentiation for orthopedic and dental implants. Acknowledgement This work is supported by the Biorema (H2020-MSCA-ITN-2019, No 861046, 2020-2024). The authors would like to thank Prof.J.Eckert and DrF.Spieckermann Montanuniversitat Leoben, Prof.K.S.Lips Univ.Giessen, Mr Y.Fortouna UoI, Ms M.E.Nousia-Prof. M.P.Rizzi Univ. Torino, Dr.Banti, Prof.Chatzikacou, Dr.Moschovas, Prof.Avgeropoulos UoI

Keywords : Ti, based alloys, Density functional Theory, Large scale models, Implants

424. Neutralization of impurity elements of Cu and Ni in Mg-Zn alloy by dissolution into MgZn_2 phase

Uruchida Kaito¹, Kadota Naoki¹, Morishige Taiki¹

¹ - Kansai University (Japan)

Mg alloys are the lightest alloys in practical metal materials with high specific strength, and their demand is increasing for the purpose of energy saving and weight reduction. For sustainable use of Mg resources, recycling from used scrap, including industrial metal materials is desirable. However, even sorted Mg scrap may contain impurity elements from these industrial metal materials, among which Fe, Cu and Ni are known as harmful impurities that reduce the corrosion resistance of Mg alloys. In previous study, Mg-6 mass% Zn alloys containing Cu and Ni had enough low corrosion rate up to 1.4 mass% Cu and 0.25 mass% Ni. The result might be achieved by substitutional dissolution of Cu and Ni into MgZn_2 phase formed in the Mg-6mass%Zn alloy, which inhibits the formation of the Mg_2Cu and Mg_2Ni phases that deteriorate corrosion resistance. The solubility of Cu and Ni in the MgZn_2 phase is about 20 at. % for Cu and 10 at. % for Ni, and the difference in solubility may attribute difference in atomic radius with Zn. In alloys containing both Cu and Ni, neutralize of detrimental effect by impurities for corrosion resistance is achieved to the same degree of impurity content as in the case of individual impurities, while the solid solution limit to the MgZn_2 phase is not clarified. In this study, the solubility of Cu and Ni into MgZn_2 phase when they contain simultaneously was investigated by preparing the intermetallic compounds and the crystal structure evaluation.

Keywords : Mg alloys, Mg, Zn alloy, MgZn_2 , Impurity elements, Corrosion

425. Effect of Grain Size on the Behavior of Exfoliation Corrosion in Cold-rolled Mg-14mass%Li-3mass%Al alloy.

Kawahara Yuta, Morishige Taiki

1 - Kansai University (Japan)

Mg-Li alloys, the lightest alloys of practical metal materials, are expected to be applied to transport equipment components. More than 11 mass% of lithium addition to Mg becomes bcc-structured solid-solution alloy, and results in excellent cold workability. However, these alloys have poor corrosion resistance due to the high lithium concentration. As a result of progression of corrosion, the exfoliation corrosion appears in cold-rolled materials and causes a significant loss of the sample. Previous studies have shown that filiform corrosion progresses along elongated grains by cold rolling. The passive film formed on the corrosion surface at the initial stage of immersion test and the film thickness on the grain boundary was smaller than that on matrix grains. As a result, pitting corrosion and subsequent filiform corrosion appeared on this fragile area of passive film. Exfoliation corrosion eventually develops as progression of filiform corrosion. As the elongated microstructure tends to form inhomogeneous passive film, cold-rolled Mg-Li alloy has more sensitive to exfoliation corrosion. The grain size may also affect the behavior of occurrence of exfoliation corrosion due to above reason. In this study, the initial grain size of Mg-14mass%Li-3mass%Al alloy was varied by severe plastic deformation and subsequent annealing. The effect of grain size on the behavior of exfoliation corrosion is investigated under the same grain aspect ratio.

Keywords : Mg, Li alloy, Grain size, Corrosion, Exfoliation corrosion, passive film

426. Anisotropy in Microstructural Evolution in Pre-deformed AZ31 under directional EPT: A quasi in situ EBSD Analysis

Cheon Seho¹, Yu Jinyeong ¹, Lee Seong Ho ¹, Park Sung Hyuk ², Lee Taekyung ¹

1 - Pusan National University (South Korea), 2 - Kyungpook National University (South Korea)

Electropulsing treatment (EPT) offers an efficient method for refining and controlling microstructure, making it a promising approach for tailoring material properties. Investigating the athermal effects of EPT provides insights for optimizing materials for industrial applications. In this study, pre-deformed AZ31 rolled alloys were subjected to EPT along both rolling direction (RD) and transverse direction (TD) to explore the anisotropy of athermal effect and mechanisms underlying microstructural evolution. Microstructural changes were observed using a quasi in situ EBSD technique, providing high-resolution insights into the evolution dynamics. EPT was applied for 0.8 seconds in the RD and 0.7 seconds in the TD. The microstructure exhibited changes due to strain-induced boundary migration, predominantly driven by the movement of high-angle grain boundaries. Compared to conventional furnace heat treatment, microstructural evolution under EPT occurred at a significantly faster rate, highlighting the efficiency of EPT in accelerating grain boundary dynamics. However, the microstructural changes were observed to proceed faster along the RD than along the TD. This directional dependence of the microstructural evolution is attributed to an athermal effect induced by twin boundaries, leading to anisotropic responses under EPT. This work suggests that twin boundary may play a significant role in the microstructural evolution under EPT.

Keywords : electropulsing, athermal effect, anisotropy, strain induced boundary migration

427. Enhancing Energy-Based Fatigue Life Model for Wrought Mg Alloys through Machine Learning Integration

Yu Jinyeong¹, Cheon Seho ¹, Lee Seong Ho ¹, Park Sung Hyuk ², Lee Taekyung ¹

1 - Pusan National University (South Korea), 2 - Kyungpook National University (South Korea)

Magnesium (Mg) alloys, characterized by lower mechanical properties compared to other structural materials, are typically used in wrought forms. Consequently, they develop strong crystallographic textures and exhibit pronounced deformation anisotropy due to limited deformation mechanisms. Structural materials are rarely subjected to direct fatigue life analyses during their service life, making accurate fatigue life prediction essential. Mg's inherent anisotropy results in asymmetric hysteresis loops during fatigue testing, introducing non-zero mean stresses that complicate fatigue life estimation. To address this, a deformation energy-based modeling approach was employed instead of conventional strain-life or stress-life prediction methods. However, energy-based prediction models face a paradox wherein hysteresis loop energy values are unknown prior to actual experiments. This limitation was resolved by introducing machine learning (ML). ML techniques enabled the generation of hysteresis loops for wrought magnesium alloys under various processing and loading conditions. Furthermore, leveraging the decrease in plastic deformation energy€”attributed to increased symmetry in hysteresis loops induced by residual twinning€”facilitated successful fatigue life predictions. Ultimately, the integration of machine learning allowed the energy-based approach to be fully realized, providing a comprehensive framework for accurate and efficient fatigue life analysis.

Keywords : magnesium, low cycle fatigue, machine learning

428. Microstructure changes due to additional elements and processability at room temperature in Mg-In alloy systems

Nagata Ryota¹, Murakami Ryuta¹, Tomura Yoshiki¹, Yamagata Ryosuke¹, Itoi Takaomi¹

¹ - Department of Mechanical Engineering, Chiba University (Japan)

Since the Mg-In and Mg-Al-In alloys have the Mg_{0.1}In_{0.9} phase which is an FCC structure with more slip systems than HCP-Mg, we can expect to develop Mg alloys with excellent processability at room temperature. Actually, the LCR (Limiting Cold-Rolling ratio) at room temperature tended to increase with increasing area fraction of the Mg_{0.1}In_{0.9} phase, and the LCR achieved 80% for the single Mg_{0.1}In_{0.9} phase in both alloys. The hardness value of the Mg_{0.1}In_{0.9} phase in the Mg-In binary alloys increased after rolling originated from grain-refinement by recrystallization and precipitation hardening due to processing heat generated by rolling at room temperature. On the other hand, the Mg_{0.1}In_{0.9} phase formed in the Mg-Al-In ternary alloys was stable at room temperature and work hardened after rolling. Since the Mg_{0.1}In_{0.9} phase dissolves about 5 mol% of Al, substituting Al for In in the Mg-In alloy was effective in reducing density. The density of the Mg₈₀Al₁₇In₁₃ (mol%) alloy is 2.60 Mg/m³, which is lower than that of Al, and the LCR showed 49%. In Mg-In alloys, the substitution of Al is effective in developing alloys that are easy to process at room temperature and have low density, because the Mg_{0.1}In_{0.9} phase has a solid solution of Al and contributes to phase stabilization at room temperature.

Keywords : FCC structure, Microstructure, Mg alloy, Processability, Mg_{0.1}In_{0.9} phase

429. Atomistic Insights into Grain Boundary-Solute Interactions and Texture Formation in Mg Alloys

Al-Samman Talal

1 - Institute of Physical Metallurgy and Metal Physics [RWTH Aachen University] (Germany)

Modern alloys consist of multiple alloying elements that are crucial for enhancing performance. However, these elements also introduce complex microstructural interactions across different length scales. Understanding these interactions, especially at interfaces, is vital for designing and optimizing advanced structural materials that offer greater strength and ductility. This research focuses on the influence of chemical binding and solute distribution on grain boundary segregation and the subsequent changes in annealing texture in lean Mg-RE/Ca-Zn alloys. By combining atomic-scale experiments with ab initio predictions, the study provides strong evidence that selective texture development in Mg alloys is closely linked to heterogeneous solute-boundary interactions. In this context, the sensitivity of binding energy to volumetric strain affects solute segregation at grain boundaries, resulting in variations in grain boundary mobility and the growth of specific texture components. Furthermore, the research highlights that solute behavior related to clustering and segregation is influenced not only by atomic size but also by the chemical binding strength with vacancies or co-added Zn. This understanding is critical for advancing alloy design strategies through segregation engineering.

Keywords : Magnesium Alloys, Microstructure Characterization, Texture Evolution, Solute Segregation

430. Development of corrosion resistance Mg alloy for Die casting component

Bae Jun Ho, You Bong Sun, Kim Jae Yeon, Kim Young-Min

1 - Korea Institute of Materials Science (South Korea)

In the rapid shift of transportation vehicle drive systems from internal combustion engines to electric motor, lightweight design remains a key technology and is becoming even more critical for next-generation transportation, including advanced personal mobility and future air mobility. Magnesium alloys have garnered attention as a promising alternative due to their high specific strength and low density. However, the application of conventional magnesium alloys has been very limited because they lack essential characteristics required for using environments, such as adequate strength and corrosion resistance. To address these challenges, this study developed a high-corrosion-resistant magnesium alloy and introduced a technology that enhances both performance and weight reduction of transportation components by applying the alloy to the die-casting process.

Keywords : Magnesium, corrosion resistance, die, casting, transportation

431. Towards Green Magnesium - Environmental Aspects of Magnesium Materials for the Transportation Industry

Kainer Karl Ulrich ¹

¹ - Privat (Germany)

Magnesium alloys have proven their performance as lightweight materials for the transportation industry but have not achieved the desired breakthrough. The dominant technology to produce magnesium components is still die-casting. Wrought alloys have so far played only a minor role. Alloy and process development in the die-casting sector aimed to improve the performance of Mg alloy for powertrain application. Due to the discussion about the future of combustion engines, further optimization of such alloys is no longer of interest. Of increasing importance is the improvement of crashworthiness. Successes in these developments would also secure the future of Mg alloys in advanced vehicle concepts. Of particular interest here is the development of extremely large cast components for applications in electric cars. Another potential application requires the development of low-cost, non-flammable alloys: Application in civil aviation and public transport (rail and bus). The development of Mg nanocomposites or modified rare earth free alloys can lead to further improvement of the property profile by providing economical solutions to the problem of flammability of magnesium alloys, which is a key issue for such application. Another issue that needs to be addressed is the availability of green magnesium with a balanced eco-balance in production. In addition, there is lack of a circular market for Mg end-of-life scrap and secondary magnesium alloys. This lack has a corresponding impact on the carbon footprint of magnesium applications. This presentation attempts to provide an overview of the status and future of the development of advanced castings and wrought alloys to produce magnesium components for automotive and public transportation applications. Some examples will be used to discuss the problem of changes to the requirements depending on the market and applications of Mg alloys.

Keywords : Magnesium Alloys, Die, casting, Eco, balance, Processing, Applications

432. Ignition characteristics and mechanical properties of Mg-Al-Ca-X alloys for electric vehicle applications

Kim Jonghyun¹, Cao Yu ¹, Zhou Shuai ¹, Jiang Bin ¹, Pan Fusheng ²

1 - College of Materials Science & Engineering, Chongqing University (China), 2 - National Engineering Research Center for Magnesium Alloys, Chongqing University (China)

Magnesium alloys have low strength and are easy to oxidize and burn at high temperatures. In the process of using magnesium alloys, the study of magnesium alloys with high ignition points is very important to ensure the safety of magnesium alloys. In particular, non-combustible magnesium alloys have low ductility and are difficult to apply in industry. Mg-Al-Ca alloys have very low elongation, which limits their application in industry. We studied the mechanism of the effect of adding small amounts of additive elements to Mg-Al-Ca magnesium alloy on the microstructure, mechanical properties, and ignition properties. The addition of X element makes the grains finer, improves the strength and elongation of Mg-Al-Ca-X alloy, and increases the ignition point of the alloy, which can be applied to the battery case of electric vehicles.

Keywords : Mg, Al, Ca, mechanical properties, ignition characteristics, non, combustible magnesium alloy

433. Electropulsing Treatment for Mg alloys: Acceleration and Anisotropy

Lee Taekyung ¹

1 - Pusan National University (South Korea)

Traditional heat treatment of lightweight metals, including Mg alloys, typically involves furnace heat treatment (FHT). This presentation introduces electropulsing treatment (EPT) as an alternative heat treatment method, specifically focusing on Mg alloys. The study compares the microstructural kinetics of α -Mg alloys treated by both EPT and FHT, suggesting that EPT enhances various microstructural evolution processes such as recrystallization, recovery, and grain growth due to the promoted atomic diffusion resulting from the athermal effects of electropulses. The presentation further explores the phenomenon of 'electropulsing anisotropy,' which refers to directional differences in static recrystallization and precipitation kinetics under EPT. When EPT was applied along the extrusion direction, static recrystallization was completed faster compared to treatment along the transverse direction, and precipitates dissolved more rapidly. These observations suggest that EPT's athermal effects play a dominant role in enhancing microstructural evolution along the extrusion direction. The EPT-induced charge imbalance improved dislocation mobility and increased atomic diffusion flux, with these effects being more pronounced along the extrusion direction, thereby accelerating static recrystallization and precipitate dissolution. Such a microstructural evolution is not even limited to Mg alloys. Lastly, this presentation discusses the influence of EPT on long-period stacking-ordered Mg alloys, emphasizing the advantages of using EPT as an effective alternative heat treatment method for wrought Mg alloys.

Keywords : magnesium, electropulsing, recrystallization, anisotropy

434. Research on the microstructural evolution of injection molded AZ91 and ultralight LAZ561Ca magnesium alloys during solidification and heat treatment: multiscale characterizations and multiphase field modeling

Su Te-Cheng¹, Hu Si-Yuan ¹, Wu Ming-Hung ¹, I-An Chen ¹, Wu Lee-Han ¹, Huang Hao-Chuan ¹, Liang Kai-Yu ¹

¹ - National Taiwan University [Taiwan] (Taiwan)

AZ91 magnesium injection molding is suitable for manufacturing complex-shaped electronic product frames or thin plates. However, the strengthening effect of the Mg₁₇Al₁₂ precipitate in AZ91 is limited, and it tends to dissolve during heat treatment, leading to a lack of particles that can pin grain boundaries and prevent grain growth. To address these challenges, the LAZ561Ca alloy has been developed, offering a reduced density (83% of AZ91), AlLi nano-precipitates with strong strengthening capabilities, and thermally stable Ca-bearing intermetallics that effectively pin grain boundaries, maintaining fine-grained structure (~8 μm) even after heat treatment. Experimental results demonstrate that AZ91 undergoes abnormal grain growth after solution treatment at 400°C for 1 hour due to a significant reduction in Zener pinning forces. In contrast, the LAZ561Ca alloy, with stable Al₂Ca precipitates, resists such growth during two-stage heat treatment at 370°C-425°C. It achieves an impressive specific yield strength of 126.8 MPa/(g/cm³) and a total elongation of 5.2% after natural aging. Through the coupling between Thermo-Calc and MICRESS software, multiphase field modeling reasonably reproduced the microstructure evolution during injection molding and heat treatment processes, highlighting its value in establishing digital physical metallurgy models. This study reveals the microstructural mechanisms of magnesium alloys, confirming the critical role of Ca-bearing precipitates in grain growth suppression. It provides a foundation for further optimization of alloy compositions and heat treatment conditions, paving the way for advanced magnesium alloys with enhanced performance in injection molding applications.

Keywords : Magnesium injection molding, CALPHAD, Electron microscopy, Multiphase field method, Heat treatment

435. Combined 3DATP and HADDF studies of the microstructures of new generation magnesium alloys developed Magnesium Research Centre, Kumamoto

Chattopadhyay Kamanio^{1 2}, Makineni Sureandra Kumar³, Kumar Dipanjan⁴, Kumar Hemant⁵

1 - Indian Institute of Science [Bangalore] (Bangalore 560 012 India), 2 - National Science Chair (India), 3 - Department of Materials Engineering, Indian Institute of Science, Bangalore (India), 4 - Monash University (Australia), 5 - Department of Materials Engineering, Indian Institute of Science, Bangalore (India)

Professor Y. Kawamura, for the last 20 years, has contributed significantly to the development of new magnesium alloys for high performance applications and enabled global collaboration. Our group at the Indian Institute of Science have explored the structure and distribution of composition of phases that develop in these new alloys using aberration corrected STEM imaging and 3D Atom Probe Tomography. We will present the results of two class of alloys, Mg-Al-Ca and Mg-Zn-Y. Through these studies we could develop a comprehensive understanding of the phase evolution at multiple scales including at nanoscale that are often not revealed during normal studies. We will also discuss the importance of these microstructural features on the evolution of the properties in these alloys.

Keywords : Magnesium Alloys

436. A Comparative Investigation of the Formation Mechanism and Corrosion Behavior of Micro-Arc Oxidation-Treated AZ31 and AC84 Kumadai Magnesium Alloys

Chiu Chi-Hua¹, Huang Shih-Yen ¹, Chu Yu-Ren ¹, Lee Yuehlien ¹

¹ - National Taiwan University (Taiwan)

This study provides a comparative analysis of the formation mechanisms and corrosion behavior of micro-arc oxidation (MAO) coatings on AZ31 and AC84 Kumadai magnesium alloys. Magnesium alloys, renowned for their lightweight and high specific strength, are increasingly used in advanced industries but suffer from poor corrosion resistance. The MAO process is an effective surface modification technique that enhances corrosion protection by forming a dense ceramic-like oxide layer. In this work, AZ31 and AC84 Kumadai alloys were subjected to identical MAO treatment conditions. The microstructure, phase composition, and surface morphology of the MAO coatings were analyzed using scanning electron microscopy (SEM), energy-dispersive X-ray spectroscopy (EDS), and X-ray diffraction (XRD). Electrochemical impedance spectroscopy (EIS) and was employed to evaluate corrosion resistance. The preliminary results revealed that the presence of the second phase significantly influences the formation and corrosion resistance of MAO coatings. The growth kinetics and discharge behavior of MAO coatings on AZ31 and AC84 magnesium alloys differ under constant voltage conditions during the MAO process, resulting in variations in coating thickness and porosity between the two alloys. Specifically, AZ31 consistently exhibited a thicker oxide layer when anodized at voltages of 150V, 200V, and 250V. Despite this, the MAO coating on AC84 demonstrated comparable corrosion resistance. These findings highlight the critical role of the second phase in tailoring the properties of MAO coatings, underscoring its potential for optimizing performance.

Keywords : Kumadai magnesium alloys, micro, arc oxidation, constant voltage mode, formation mechanism, corrosion resistance

437. Development of Advanced Magnesium Alloys

Kawamura Yoshihito ¹

¹ - MRC, Kumamoto University (Japan)

The Magnesium Research Center (MRC) at Kumamoto University has been conducting research to improve the strength, heat resistance, corrosion resistance, toughness, non-flammability, and thermal conductivity of magnesium alloys from both the alloy design and process design perspectives.

As a result, we have developed advanced magnesium alloys such as LPSO-type Mg-M-RE (M=Al, Zn, Cu, Ni or Co, RE=Y, Sm, Gd, Tb, Dy, Ho, Er or Tm) alloys with high heat resistance, Mg-Al-Ca alloys with non-flammability, Mg-Al-Ca-Mn alloys and Mg-Zn-Y alloys with high thermal conductivity, and Mg-Ca-Zn-Y-Mn alloys for biomedical applications alloys.

In LPSO-type Mg-M-RE alloys, we discovered a new LPSO structure and kink strengthening, and we also clarified that kink strengthening occurs in the mill-feuille structured Mg-Zn-Y alloys. Furthermore, in non-flammable magnesium alloys, we demonstrated for the first time in the world that they do not ignite even when the boiling point of pure magnesium is exceeded, and we discovered several additive elements for non-flammability. In addition, we have established a material design guideline for high-strength, high-thermal-conductivity magnesium alloys. Meanwhile, we have developed manufacturing technology for the large-scale magnesium alloys we have developed, and are promoting the development of applied products such as parts for transportation and industrial equipment, and medical devices to be implanted in the human body.

In this lecture, I will give an overview of the basic and applied research on magnesium alloys over the past 26 years.

Keywords : Magnesium alloys, Kink strengthening, Non, flammability, High thermal conductivity, High corrosion resistance

438. Effects of strain states induced by different wrought processes on microstructure evolution of AZ31 magnesium alloy

Yoshizumi Hiromasa¹, Maeda Satoru ¹, Yuasa Motohiro ¹, Miyamoto Hiroyuki ¹, Somekawa Hidetoshi ²

1 - Doshisha University [Kyoto] (Japan), 2 - National Institute for Materials Science (Japan)

Magnesium (Mg) alloy, the lightest in structural materials, is attractive for weight reduction of transportation equipment. However, Mg alloy exhibits poor strength, ductility, and formability. Microstructure control by dynamic recrystallization (DRX) has been studied to improve mechanical properties, and various wrought processes have been invented to refine grain size further. Many studies have focused on the effects of processing conditions (e.g., processing speed and processing temperature) on microstructure evolution in an individual wrought process. On the other hand, the relationship between the difference in wrought processes and microstructure development has not been revealed. Thus, this study aims to investigate this relationship quantitatively in terms of induced strain state. AZ31 (Mg-3.0 Al-0.8 Zn-0.31 Mn, wt. %) Mg alloy was annealed for an hour at 673 K, then processed by three wrought processes (forging, rolling, and caliber rolling) at 573 K. The conditions of these processes were designed to induce approximately the same equivalent strains, 0.38, 0.75, and 1.5 in the center of the processed materials. The introduced strain states were computed with finite element method (FEM), and microstructures were observed by optical microscope (OM) and electron back-scattering diffraction (EBSD). FEM shows that forging and rolling apply a large compressive strain in one direction with little shear strain. Conversely, caliber rolling introduces a strain distribution with compressive strains in multi-direction and a large shear strain. Combining FEM results with OM and EBSD observations, the strain states corresponding to multidirectional deformation develop a weak basal texture and a homogenized and refined grain structure.

Keywords : Magnesium alloys, Dynamic recrystallization, Microstructure, Texture, Finite element method

439. Plastic deformation of fine-grained pure magnesium and AZ series Mg alloys between 298K and 4K

Kula Anna¹, Walag Michal , Tokarski Tomasz , Noga Piotr , Niewczas Marek

1 - AGH University of Science and Technology [Pologne] (30 Mickiewicza Av. 30-059 Krakow Poland)

Plastic deformation and work-hardening behaviour of fine-grained commercially pure magnesium (CP-Mg) and Mg-Al-Zn alloys have been studied by a combination of measurements of mechanical response, texture analysis and microstructural observations. The grain size strongly affects the mechanical properties of CP-Mg, but its influence is different at room than at cryogenic temperatures. At room temperature, Mg samples with grain sizes above 3 μm deform through a combination of slip and twinning mechanisms. In contrast, specimens with grain sizes below 3 μm , in addition to slip, undergo deformation by grain boundary sliding (GBS). Below the critical grain size of 3 μm , one observes the inverse Hall-Petch behaviour reflected in the decreasing yield stress and increasing ductility with grain refinement. At cryogenic deformation temperatures of 4K and 78K, Mg samples demonstrate conventional behaviour manifested in the increased yield stress and reduced ductility that accompany the grain refinement. In Mg-Al-Zn alloys, a reduction of grain size even far below 3 μm , does not induce GBS and alloy softening. The Hall-Petch relationship maintains conventional behaviour across the tested grain size range between 298K and 4K. The mechanical response of the studied materials will be analysed in relation to the microstructure and texture evolution during deformation, as investigated using XRD and EBSD techniques, strain rate sensitivity measurements, and in situ deformation experiments.

Keywords : Magnesium alloys, Deformation mechanisms, Grain refinement, Cryogenic temperatures, Grain boundary sliding

440. Synergistic effects of Rolling and Mixed rare earth (Er+Yb) additions on mechanical, corrosion and biocompatibility properties of Mg-Zn-Ca alloys for orthopedic applications

Aggarwal Divyanshu¹, Pakki Vamsi Krishna ², Latiyan Sachin ², Suwas Satyam ², Chatterjee Kaushik ², Shabadi Rajashekara ¹

1 - Universite de Lille - Faculte des sciences et technologies (France), 2 - Indian Institute of Science [Bangalore] (India)

The study focuses on enhancing the mechanical, corrosion, and microstructural properties of Mg-1.5Zn-0.5Ca alloys through the incorporation of a mixed rare-earth (RE) system comprising Erbium (Er) and Ytterbium (Yb) at varying concentrations (0.75, 2, and 5 wt%). The performance of these alloys was further elevated by employing symmetric rolling as a secondary thermomechanical processing technique using a multi-pass approach. The dual RE additions facilitated the formation of RE-based secondary phases, significantly enhancing mechanical properties and providing remarkable corrosion resistance. Rolling proved transformative, improving the mechanical properties and reducing corrosion rates by 45% as confirmed by electrochemical and immersion testing in simulated body fluid (SBF) at 37°C. Microstructural analysis attributed the improvements to mechanisms such as fine grain strengthening, twin formation, and dislocation strengthening induced by rolling. Additionally, in-vitro cell culture studies using MC3T3-E2 cells demonstrated superior biocompatibility, positioning the rolled Mg-Zn-Ca-RE based alloys as highly promising candidates for biomedical implants. This work underscores the critical role of rolling in unlocking the full potential of rare-earth-modified Mg-Zn-Ca alloys, offering a robust framework for designing next-generation biodegradable materials with exceptional mechanical, corrosion, and biological performance.

Keywords : Mg, Zn, Ca alloys, rare earth, rolling, corrosion, mechanical properties, biocompatibility

441. Development of biodegradable magnesium implants from an engineer's perspective

Hort Norbert^{1 2}, Wiese Bjoern¹, Maier Petra^{3 4}, Orlov Dmytro⁴,
Tolnai Domonkos¹

1 - Helmholtz- Zentrum Hereon (Germany), 2 - Leuphana Universitat Luneburg (Germany), 3 - Hochschule Stralsund - University of Applied Sciences (Germany), 4 - Lund University (Sweden)

Prostheses/Implants for humans are exciting, modern, and ever evolving topic despite millennia-long history. The oldest prostheses/implant found to date comes from Egypt and is more than 2500 years old. Since then, prosthesis/implants have been developed and used again and again. Magnesium as a material is comparatively new. It was first introduced as an element around 200 years ago. It was first used in photography as a flashlight, then structural components were developed, including implants, as first reported by E.C. Huse in 1878. Further Mg-based implants were introduced in the following decades. Subsequently, however, Mg implants were practically replaced by the newly developed stainless steels, titanium and Co-Cr alloys as metallic implant materials. However, a renaissance for implants made of magnesium and its alloys has been observed since the beginning of the 21st century. In this context, it has often been discussed whether implant-specific production is necessary or advantageous. This article will take a closer look at this topic, considering the alloying elements used, the various process routes, the design of the implants and various other influencing factors regarding the application profile.

Keywords : magnesium alloy, degradable implant, design, property profile, processing

442. Specific resistance measurements for the development of Mg based alloys

Wiese Bjoern¹, Hort Norbert ^{1 2}

1 - Helmholtz- Zentrum Hereon (Germany), 2 - Leuphana Universitat Luneburg (Germany)

Magnesium (Mg) materials are a promising group of metallic materials for medical and lightweight applications. New materials are developed based on specific requirements, allowing composition or processing adjustments to tailor properties. The processing of these new or established alloys must be optimised. This applies, for example, to heat treatments such as ageing or recrystallisation treatments. When we look for a process parameter, we have multiple parameters such as temperature and time to optimise the material, resulting in a huge variety of samples. A common method is to study the microstructure of a range of parameter combinations using microscopy, X-ray diffraction and other standard techniques to follow the evolution of the microstructure, which is a time-consuming approach. Resistance measurements in a furnace offer the possibility of an in situ measurement, which provides an insight into the process and reduces the number of attempts to select a useful parameter combination. We will present some initial investigations with these measurements on different Mg materials. The results of resistivity during heating and cooling as well as a temperature over time during ageing and recrystallisation will be presented. The change in resistivity can then be related to microstructural features such as the degree of recrystallisation as well as the precipitation phase during ageing. If the signals, the specific resistance, stabilise, this is an indicator of a fully recrystallised structure or the peak ageing state. This type of information reduces the parameter space and can accelerate material development to a certain extent.

Keywords : Mg alloys, alloy development, biodegradable, specific resistance, heat treatment, recrystallization

443. A deep-learning based surrogate model for the numerical simulation of casting process

Kang Jinwu¹, Zhao Qichao , Wang Jiwu , Yahui Yang

1 - School of Materials Science and Engineering, Tsinghua University (A236, Lee Shau Kee Building, School of Materials Science and Engineering, Tsinghua University, Beijing, 100084, China China)

Numerical simulation of casting process is of great significance to unveil the solidification process of castings, predict defects formation and provide the process optimization guidelines. However, the numerical method require constitutive models, thermal and mechanical properties of materials and boundary conditions which are hard to be clarified due to the complexity of casting process. And the numerical simulations usually take long time, which results into its limited operations in labs, isolated from production lines. In recent years, the sprouting of artificial intelligence shows a new possible method to address the numerical simulation problems. In this paper, a deep learning method was adopted to deal with the simulation of the casting process. Modified U-net models were established, incorporating the convolutional block attention and inception modules. There are two branches for the input of geometrical model of casting-mold-chill and the ith step results. After training, the models can predict the three-dimensional temperature fields of an arbitrary shaped casting during the casting process. As the temperature error for each mesh is set as 5oC, the accuracy reaches 90%. The prediction for each time step takes just few seconds and the time interval can be adjusted, therefore it is fast to obtain the temperature fields during the whole solidification process, which is greatly different from the time consuming numerical simulation method. Thus, the deep learning method provides a possibility to integrate the simulation of the casting process into production lines.

Keywords : Deep Learning, Casting Process, Simulation, Solidification, Temperature Field

444. Multiscale Modeling and Simulation of Manufacturing Process for Ni-Based Single-Crystal Superalloys

Xu Qingyan, Hu Yeyuan

1 - School of Materials Science and Engineering, Tsinghua University (China)

Ni-based single-crystal superalloys have complex elemental compositions which makes it challenging to control their microstructure during manufacturing. Defects such as freckles and stray grains often form in the manufacturing process. Traditional experimental study method is usually a long cycle and high cost process. In this study, a combined approach of numerical simulation and experiments was used to investigate single crystal superalloys. The process from changes in the large-scale temperature field to dendrite growth and defect formation at smaller scales was simulated. On the macroscopic scale, finite difference method were used to study how processing parameters, such as pulling speed, affect the temperature distribution. The temperature data was then applied to mesoscopic simulations. At this scale, a phase-field method combined with lattice Boltzmann techniques was adopted which helped simulate dendrite growth and solutal flow under different process conditions. By linking the macroscopic and mesoscopic scales, this multiscale approach offered a model for the manufacturing process of Ni-based single-crystal superalloys. This study provides insights to help improve process design and reduce defect formation.

Keywords : Multiscale Modeling and Simulation, finite difference method, phase field method, Single Crystal Superalloy, Manufacturing Processing

445. Stochastic scaling of time step in a full-scale Monte Carlo Potts model

Oh Sang-Ho¹, Lim Chan ², Lee Byeong-Joo ^{3 4}

1 - Center for Advanced Aerospace Materials, Pohang University of Science and Technology (POSTECH) (South Korea), 2 - Department of Physics, Pohang University of Science and Technology (POSTECH) (South Korea), 3 - Center for High Entropy Alloys, Pohang University of Science and Technology (Pohang 790-784 South Korea), 4 - Department of Materials Science and Engineering, Pohang University of Science and Technology (POSTECH) (South Korea)

Grain growth is a fundamental reaction in polycrystalline solid materials that significantly influences various material properties. The Monte Carlo Potts model is notable for its simple algorithm and low computational cost, effectively capturing fundamental grain growth kinetics and providing quantitative predictions. Its realistic time assignment scheme relies on experimental information and simulation resolution. This can result in too short simulation time step, far increasing the required simulation time and limiting its practical use in real-world materials design. Here, we propose a novel scheme to control the actual length of a Monte Carlo step based on the fundamental physics principles underlying the Monte Carlo algorithm and confirm that simulation results remain consistent. It additionally enables a reasonable way to determine the length of a Monte Carlo step in a complex simulation where Monte Carlo Potts models for different reaction kinetics are included. Consequently, the proposed scheme is expected to broaden the applicability of the Monte Carlo Potts model on practical processes in the real world.

Keywords : Monte Carlo Potts Model, Real Scale, Stochastic Scaling of Time Step, Grain Growth Simulation, Micro, structure Evolution

446. Application of Thermodynamic Extremal Principle to the Sintering of Irregular Powder Particles

Weiner Max¹, Schmidtchen Matthias¹, Prahl Ulrich¹

1 - Institute for Metal Forming, Technische Universität Bergakademie Freiberg (Germany)

The field of modelling sintering processes is currently highly dominated by the application of phase-field methods. Although these methods provide a concise and flexible formulation for dissipative processes, they suffer from high computational effort due to fine spatial discretization and unphysical diffuse interfaces. The current work proposes a different approach by applying the thermodynamic extremal principle (TEP) to a sharp interface description providing a similarly concise and flexible formulation but circumventing the mentioned drawbacks. The solution of the diffusion problem reduces hereby to the solution of a multi-dimensional linear constrained optimization problem per time step. Computational effort is drastically reduced by lowering the need for fine discretization. The discretization width, and therefore the count of unknowns, in this approach is dependent on the size of particle surface features, rather than on numerical requirements of the diffuse interface description. By using a sharp interface, the thermodynamic interface properties like interface energies can directly be applied with no need for diffuse energy density mappings and so reducing systematic model error. Rigid body motion, often a problem in phase-field formulations, can be regarded directly. The proposed model is able to describe the sintering process of 2D particles of arbitrary shape and asymmetric contacts between them (regarding geometry and material properties). This enables efficient studying of the influence of irregular powder geometries and multi-material contacts, while usual low-effort models often rely on heavy symmetry assumptions.

Keywords : Sintering, Simulation, Modelling, Thermodynamic Extremal Principle, Refractories

447. Simple flow rules for three-phase viscoplastic materials

Montheillet Frank¹, Piot David¹

¹ - Mines Saint-Etienne, IMT, Centre SMS, Laboratoire Georges Friedel UMR CNRS 5307, Departement PMM, 158 cours Fauriel, 42023 Saint-Etienne Cedex 2, France (France)

The stress-strain rate dependence of 2-phase viscoplastic materials has been the subject of a number of investigations in the past. Lower and upper bounds as well as estimations are now widely used for the viscosity-like parameter of the mixture, especially in the isotropic case. However in some situations three phases are present, for example in two-phase metal alloys like alpha-beta brasses containing a dispersion of hard (e.g. oxides) or soft (e.g. lead) particles. The case of metal alloys or composites containing three phases in roughly equal proportions can also be conceived. Noting that there is very little literature on the topic, a first analytical approach is proposed in this work. In a first part, the conditions of application and the consequences of the three "macrohomogeneity" Hill equations are reviewed for 2-phase mixtures and extended to three phases. The classical static and Taylor bounds as well as the heuristic "iso-strain rate" assumption are analyzed. An extension of the Mori-Tanaka estimation to the 3-phase case is then proposed for viscoplastic linear constituents, which satisfies all three Hill equations and provides reasonable predictions. These are illustrated and discussed in various cases. If the volume fraction of one of the phases is very low, in particular when its viscosity tends towards zero or infinity, fully analytical results are presented, which is an extension of the classical dilute model. Numerous perspectives need now to be considered, first of all comparing the present results with any available numerical or experimental data.

Keywords : continuum mechanics, multiphase materials, viscoplasticity, rules of mixture, modeling

448. Verification of a novel mathematical model for determination of the biomass specific growth rate in bioprocesses.

Kraus Mirjam¹, Verona-Rinati Gianluca², Boehme Andrea³

1 - Technical University of Applied Sciences, Wildau, 15745 Wildau, Germany (Germany), 2 - Tor Vergata University, Rome, 00133 Rome, Italy (Italy), 3 - Technical University of Applied Sciences, Wildau, 15745 Wildau, Germany (Germany)

This study presents a new mathematical model for determining the specific growth rate of biomass in biotechnological production processes, which aims to optimize the production of biotechnological products such as the advanced material polyhydroxyalkanoates. The specific growth rate is classified by the FDA as a critical process parameter that affects product quality and quantity, but is difficult for laboratory personnel to determine. Therefore, a simple and robust method for real-time monitoring and control is crucial. According to the current state of the art, the established Luedeking-Piret model for determining the specific growth rate requires the determination of the biomass as an absolute value to initialize the model and to determine two further model parameters. However, determining the biomass is time-consuming and error-prone. The new relative model replaces this value with the relative change in biomass, which can be easily recorded using standard laboratory methods such as optical density measurement. This eliminates the need for time-consuming and resource-intensive preliminary work. Despite this simplification, simulation tests have shown that the new model delivers identical results to the established model. It represents an independent, precise alternative and offers advantages in terms of handling. The results underline the model's potential to make bioprocesses more sustainable and efficient. Especially in research, material consumption, laboratory time and costs can be reduced compared to the established model. Future experiments will further investigate the performance of the new approach compared to the established model.

Keywords : Biomass specific Growth Rate, Real Time Monitoring, sustainable Bioprocesses

449. Generalized stacking fault energy in multi-component Co-based L12 precipitates

Tang Yingchun^{1 2}, Lu Song³, Vitos Levente^{4 5 6}, Pyczak Florian^{1 2}

1 - Institute Materials Physics, Helmholtz-Zentrum Hereon (Germany), 2 - Brandenburgische Technische Universität Cottbus-Senftenberg (Germany), 3 - Integrated Computational Materials Engineering, VTT Technical Research Centre of Finland Ltd. (Finland), 4 - Applied Materials Physics, Department of Materials Science and Engineering, KTH Royal Institute of Technology (Sweden), 5 - Department of Physics and Astronomy, Division of Materials Theory, Uppsala University (Sweden), 6 - Research Institute for Solid State Physics and Optics, Wigner Research Center for Physics (Hungary)

For novel Co-based superalloys, it is important to form gamma prime-precipitates with good mechanical properties. The generalized stacking fault energies (SFEs) determine plastic deformation and have to be controlled. To achieve this, the chemical composition and temperature dependence of SFEs in different types of gamma prime-precipitates are systematically analyzed using ab initio calculations. This includes Co₃(Al₅₀,TM₅₀) (M=Ti, Cr, Nb, Mo, Ta) precipitates in ferromagnetic (FM) and paramagnetic (PM) states, and a series of Co-based precipitates found in experimental Co-9Al-9W, Co-xNi-12Al-9W-2Ta, and Co-7Al-8W-yTa-4Ti alloys. The SFEs of Co-Al-W based precipitates are sensitive to chemical composition and magnetic state. Ni increases the antiphase boundary energy, indicating that it improves mechanical properties, while Ta has a similar effect as Ni, consistent with experimental observations of improved creep strength. The temperature dependence (via considering the thermal lattice expansion) of the SFEs in PM state was studied for Co-9Al-9W and Co-7Al-8W-1Ta-4Ti alloys. The results show that the antiphase boundary (APB) energy decreases with increasing temperature, and the ratio of antiphase boundary energy to super intrinsic stacking fault energy exhibits the same trend in the paramagnetic state for both alloys. Finally, effective energy barriers (EEBs) were used to investigate the plastic deformation behavior, and the predicted deformation modes matched well with experimental observations in a Co-7Al-8W-1Ta-4Ti alloy. This shows that favorable plastic deformation mechanisms of Co-based precipitates in superalloys can be predicted reliably by calculating GSFEs with ab initio methods, which can support and accelerate the design of future advanced superalloys.

Keywords : generalized stacking fault energies, Co, based superalloys, deformation mechanisms, ab initio calculations

450. Thermodynamics properties of Ti₂Al-M-ternary V-VIB groups O-phase alloys from first-principles calculations

Heidaripebdani Zeinab^{1 2}, Janisch Rebecca³, Pyzcak Florian^{2 4}

1 - Helmholtz-Zentrum Hereon, Geesthacht (Germany), 2 - Brandenburgische Technische Universität Cottbus-Senftenberg (Germany), 3 - Interdisciplinary Centre for Advanced Materials Simulation (Ruhr-University Bochum 44780 Bochum Germany), 4 - Helmholtz-Zentrum Hereon, Geesthacht (Germany)

Based on first-principles calculations within the projector augmented wave method and the Perdew-Burke-Ernzerhof version of the generalized gradient correction (PBE-GGA), the structural, thermodynamic, as well as phonon properties of orthorhombic Ti₂AlM compounds (M = V, Nb, Ta, Mo, or W) have been investigated. Besides phonon calculations, the Debye model is also used to evaluate the thermodynamic properties at elevated temperatures, which are compared with available data from experiments and thermodynamic modelling. A good agreement is found between first-principles calculations and experimental values or thermodynamic modelling. Also, it is observed that for all Ti₂AlM compounds, (i) the equilibrium volume decreases roughly linearly while the bulk modulus increases roughly linearly when changing M from group VB to VIB with the detailed trend of Mo > W > Ta > Nb > V; (ii) the bonding strength follows the trend of Ti-M > Ti-Al > Al-M; and (iii) roughly the higher the strength of the Ti-M bond in the Ti₂AlM compound, the smaller the vibrational contribution to entropy and, in turn, to Gibbs energy. The demonstrated methodology herein, along with the predicted thermodynamic properties, provides helpful insights into the stability of O-phases at both zero Kelvin and finite temperatures, especially for systems where the experimental information is lacking or less reliable.

Keywords : TiAl compounds, Thermodynamics, Phonon, Debye model, First principles calculations

451. The effect of precipitate chemistry on hydrogen-enhanced decohesion in Ni-based alloys: An ab initio study

Damm Nina¹, Scheiber Daniel ¹, Romaner Lorenz ², Razumovskiy Vsevolod ¹

1 - Materials Center Leoben Forschung GmbH (Austria), 2 - Montanuniversitat Leoben (Austria)

Precipitation hardened Ni-based alloys have been initially deemed to be immune to hydrogen embrittlement. However, many studies have shown significant ductility losses of these alloys due to hydrogen. It is believed that two mechanisms cause this behaviour: hydrogen-enhanced localised plasticity (HELP) and hydrogen-enhanced decohesion (HEDE). In this study, we employ density functional theory methods to determine the effect of the gamma-prime and gamma-double-prime precipitate chemistry (Ni₃X, with X=Al, Ti, Nb) on their hydrogen segregation and trapping behaviour. In addition, we investigate the combined effect of precipitate chemistry and hydrogen segregation on the work of separation of the formed interfaces, precisely gamma/gamma-prime, gamma/gamma-double-prime and gamma-prime/gamma-double-prime, and relate it to the HEDE mechanism. Finally, the effect of hydrogen trapping at these interfaces on the amount of diffusible hydrogen content is discussed. We use these results alongside with available literature data to define trends with regard to hydrogen embrittlement resistance in precipitation hardened Ni-based alloys.

Keywords : H, HEDE, DFT, PH Ni, based alloys, Interface segregation

452. Generation of morphology-controlled three-dimensional microstructures in dual-phase steels using SliceGAN-AdaIN

Sakakibara Toshiki, Chen Ta-Te, Sun Fei, Yoshitaka Adachi

Nagoya University (Japan)

The mechanical properties of steel are strongly influenced by their microstructures. Therefore, understanding the mechanisms of deformation and fracture is essential for identifying the optimal microstructural features to control, to improve mechanical properties. For example, the tensile properties of dual-phase (DP) steel, composed of ferrite and martensite, depend on phase fraction, grain size, and spatial distribution, in addition to the mechanical properties of each phase. To elucidate the relationship between microstructure and mechanical properties, analyzing three-dimensional (3D) microstructures across diverse patterns is essential. However, obtaining 3D microstructures through conventional methods like tomography or serial sectioning requires specialized equipment and significant effort. SliceGAN, a generative AI model based on generative adversarial networks (GAN), addresses this challenge by reconstructing 3D microstructures from 2D images. SliceGAN can generate 3D structures using one cross-sectional image for isotropic materials or three for anisotropic cases. Watanabe et al. validated SliceGAN by comparing its results with real 3D DP steel microstructures, showing close agreement in morphology and tensile properties. While SliceGAN excels at reconstructing one-to-one representations that capture the features of learned 2D images, it is less suitable for generating diverse microstructures. To enhance the diversity of generated 3D microstructures, the application of adaptive instance normalization (AdaIN) has shown promise. AdaIN adjusts statistical image features, such as mean and standard deviation, enabling systematic manipulation of diversity by controlling morphological features. In this study, SliceGAN-AdaIN was applied to real DP steel microstructures, generating diverse 3D structures based on 2D images of DP steels with different morphologies.

Keywords : Dual phase steel, Generative adversarial networks, three dimensional microstructures, morphological features

453. Data-driven estimation of tensile properties of alloys using instrumented indentation method

Chen Ta-Te¹, Watanabe Ikumu², Yoshitaka Adachi¹

1 - Nagoya University (Japan), 2 - National Institute for Materials Science (1-2-1 Sengen, Tsukuba, Ibaraki Japan)

This study introduces a data-driven approach for estimating the tensile properties of alloys using an instrumented indentation method. Traditional methods relying on simple power-law hardening models often fail to characterize high work-hardening alloys accurately due to limited functional expressiveness. A modified constitutive model combining power-law and linear hardening is proposed to address this. The additional material constants in this model are determined without requiring further experimental data, utilizing response surfaces derived from the loading curvature of load-depth curves and the pile-up height of indentation impressions. Finite element simulations are employed to generate high-throughput material databases, enabling the estimation of material constants through interpolation without iterative calculations. The proposed model improves expressiveness, capturing intermediate material responses between power-law and linear hardening while ensuring consistency with experimental data. This method highlights the potential for efficient and accurate estimation of plastic properties, supporting advancements in materials research and high-throughput material characterization. By leveraging the instrumented indentation technique and computational simulations, the study provides an efficient pathway for determining stress-strain relationships in materials, significantly reducing experimental complexity and enhancing precision. This approach is particularly valuable for applications with essential high-throughput experimental data, offering a practical solution for material property estimation and constitutive model refinement.

Keywords : Instrumented Indentation, High, throughput Characterization, Tensile Properties, Finite Element Simulation

454. Finite element modelling of electromagnetic heating

Lehtola Katariina¹, Ilmola Joonas ¹, Larkiola Jari ¹

¹ - Materials and Mechanical Engineering, Centre for Advanced Steels Research, University of Oulu, 90570 (Finland)

In this work, electromagnetic heating was modeled using Abaqus software, which is based on the finite element method. The model was developed based on Linseis DIL L78 DQT/RITA Quenching & Deformation dilatometer where the heating process is carried out with an induction coil. The model incorporates the dimensions, current and frequency measured by the dilatometer. The material properties of the test material were also integrated into the model. The goal of this study was to replicate the behavior of the induction coil in the dilatometer as accurately as possible. During the model development, it became evident that the material properties have a significant impact on the performance of induction heating. Key material properties for effective induction heating include electrical conductivity and magnetism, specifically magnetic permeability. For electromagnetic heating to work, the material must be electrically conductive, allowing the induction heating process to occur. Material properties, which vary with temperature, were defined in the model as a function of temperature to ensure realistic thermophysical behavior of the simulated part. Two different analysis solvers were used for electromagnetic and heat transfer analysis. Abaqus Co-simulation feature was used to transfer relevant data between the two solvers. The model's accuracy was validated using data measured from the dilatometer coil.

Keywords : modeling, electromagnetic heating, steel, FEM

455. Numerical modelling of precipitation kinetics in Al alloys during solid-state processing

Chafle Rupesh¹, Henninger Susanne², Staron Peter², Klusemann Benjamin^{1 3}

1 - Institute of Material and Process Design, Helmholtz-Zentrum Hereon, 21502 Geesthacht, Germany (Germany), 2 - Institute of Materials Physics, Helmholtz-Zentrum Hereon, 21502 Geesthacht, Germany (Germany), 3 - Institute of Production Technology and Systems, Leuphana University Luneburg, 21335 Luneburg, Germany (Germany)

The precipitation behaviour plays a vital role in enhancing the mechanical properties of aluminum (Al) alloys such as the theta precipitation in Al-Cu alloys and eta precipitation in AA7xxx series alloys. The precipitation behaviour for a particular alloy composition is governed by nucleation and growth which depend on the processing conditions. Friction-based solid-state techniques offer a more efficient processing route by reducing the number of steps and avoiding the need for external heating. This study aims at demonstrating a model for predicting the precipitation kinetics in Al alloys undergoing heat treatment similar to that occurring in solid-state processes. The work employs the PanPrecipitation module of the commercial Pandat software supported by the relevant thermodynamic, kinetic, and thermophysical databases. The KWN model is used to describe the precipitation kinetics and the classical nucleation theory is applied for nucleation. The diffusion-controlled growth theory ensures that precipitate growth and coarsening are accurately captured. Through a series of calibrations, the fitting parameters governing the solubility of alloying elements, interfacial energy of the precipitate-matrix interface and diffusion constants are determined. This is complemented by validation against experimental results from the literature. Finally, the applicability of the model to predict precipitation behaviour during different heat treatments in Al alloys is presented.

Keywords : Precipitation kinetics, Numerical modelling, Pandat, Al alloys, Solid state processing

456. Experimental Studies and Simulation of TRIP-TWIP Roll Bonding

Mantel Jennifer¹, Schmidtchen Matthias¹, Seleznev Mikhail²,
Weidner Anja², Biermann Horst², Prahl Ulrich¹

1 - Institute of Metal Forming, TU Bergakademie Freiberg (Germany), 2 - Institute of Materials Engineering, TU Bergakademie Freiberg (Germany)

For the production of lightweight components with high strength and good formability, optimized materials are needed. Metallic laminates offer the opportunity for application-oriented material properties. Roll bonding of two- and four-layered materials was used to produce high-alloy steel laminates with improved ductility at a higher tensile strength. The monolithic materials were a X3CrMnNi-16-7-6 and a X3CrMnNi-16-7-9 steel. In order to ensure a good bond strength after roll bonding, a special role is attributed to the surface properties and the rolling parameters. To achieve these goals, experiments with and without an intermediate layer of nickel foil were conducted. Different foil thicknesses between 10 and 150 µm were used to determine an optimum layer ratio with a fixed rolling temperature of 440 °C. To further improve the understanding of the roll bonding process and the development of the bond strength, a fast rigid-plastic analytical simulation for material flow and bond strength development was adopted, which is based on the work of Schmidtchen [1]. The collection of further experimental data aimed at refining and further validation of the simulation, especially in the context of different materials, is an ongoing task.

Keywords : Thermec'2025, Roll Bonding, Steel, Simulation, Analytical Solutions

457. Finite element simulation strategies for cold pilgering process

Marir Anes¹, Mocellin Katia ¹, Pierre Montmitonnet ¹, Florian Lyonnet ², Jean-Luc Doudoux ²

1 - Centre de Mise en Forme des Matériaux (France), 2 - FRAMATOME (France)

Cold pilgering is a material forming process widely used for the production of seamless tubes requiring precise control of dimensions and texture. This process is cyclic and incremental: the thermomechanical history of a material point involves 50 to 100 elementary plastic deformations. Finite element simulations, essential for optimizing the process parameters, are computationally expensive due to the large number of cycles needed to reach the system's mechanical steady state. To address this challenge, two acceleration strategies are being evaluated: - Starting the simulation with a configuration close to the steady state, requiring only a few corrective cycles. Current efforts are focused on refining the initialization hypotheses. - Dual Simulation: First, a coarse-mesh simulation to quickly reach the steady state, followed by a refined-mesh simulation of a few steady state cycles. This method relies on optimizing both meshes and effective interpolation between them. Additionally, thermal stabilization requires even more cycles due to the thermal inertia of the tools. A similar strategy to the mechanical approach is being developed to accelerate convergence to the thermal steady state. It involves a precise initialization of the tube and tool temperatures, which are corrected during the simulation using well-calibrated Heat Transfer Coefficients (HTC). The calibration procedures are based on experimental temperature measurements.

Keywords : Cold pilgering, Finite Element Method, Forge® NxT, Simulation Strategies, Thermal Modelling

458. Identification of the stochastic hot forming model based on the inverse analysis for the four types of compression tests

Szeliga Danuta¹, Jazdzewska Natalia , Kusiak Jan ², Oprocha Piotr ¹,
Pietrzyk Maciej ¹, Potorski Pawel, ¹, Przybylowicz, Owicz Pawel ¹

1 - AGH University of Krakow, PL (Poland), 2 - AGH University of Krakow, PL (Poland)

A need for prediction of the microstructure heterogeneity was the motivation for this project. Deterministic model of hot deformation was replaced by a stochastic model, which accounts for the random character of the recrystallization. The probability equation was proposed on the basis of the metallurgical knowledge. In consequence, instead of the average values, histograms of the dislocation density and the grain size could be calculated. In the stochastic model the evolution equation for dislocation populations the time for the beginning of the recrystallization was substituted by the probability function. This function combines the probability that the material point recrystallizes in a current time step and the present state of the material [1]. Problem of the identification of this model was considered. The following hot compression tests were applied: uniaxial compression, plane strain compression for the two sizes of the samples and ring compression. The parameters of the tests are given in [3]. Identification of the models was performed using inverse analysis with the objective function composed of two parts. The first was the mean square root error (MSRE) between measured and calculated dislocation density and the second was the distance between measured and calculated histograms of the austenite grain size. The results for different tests were consistent. The identified stochastic model was implemented in the FE program and hot rolling process was simulated.

[1] Szeliga D., et. al., Formulation, identification and validation of a stochastic internal variables model describing the evolution of metallic materials microstructure during hot forming, Int. J. Mat. Forming, 15, 2022, 53.

[2] K. Huang, R.E. Loge, A review of dynamic recrystallization phenomena in metallic materials, Materials & Design, 111, 2016, 548.

[3] D. Szeliga, et. al. , Identification of rheological parameters on the basis of various types of plastometric tests, J. Mat. Proc. Techn., 125-126, 2002,150.

Keywords : dislocation density, stochastic model, identification, compression tests

459. Dissecting physics of carbon ordering in bcc iron

Waseda Osamu¹, Hickel Tilmann, Chantrenne Patrice, Morthomas Julien, Perez Michel, Neugebauer Joerg

¹ - Max-Planck-Institute for sustainable materials (Germany)

Zener ordering is a phenomenon that octahedral interstitial atoms such as carbon occupy the same sublattice inside bcc matrix such as iron. The original formulation relies on a mean field theory, which is still most in use today. We employ multiple methods, such as Molecular Dynamics, Metropolis Monte Carlo, Mean Field Theory with chemical interactions and finite temperature effects to show that the Zener ordering for iron carbon systems is governed by local chemical interactions and finite temperature effects and less of mean field nature as described originally by Zener.

Keywords : Zener ordering, carbon ordering, martensitic transformation, iron, carbon steel

460. Representing texture in surrogate models of crystal plasticity to predict material behaviour and quantify uncertainty

Peel Matthew¹, Dorward Hugh¹, Safari Sina¹, Mostafavi Mahmoud²

1 - School of Electrical, Electronic and Mechanical Engineering, University of Bristol, Bristol, BS8 1TR (United Kingdom), 2 - Department of Mechanical and Aerospace Engineering, Monash University, Clayton, Victoria 3800 (Australia)

The mechanical behaviour of materials is influenced by processing and thermomechanical exposure. In safety-sensitive industries there is a need to make predictions on the envelope of safe use beyond proven constitutive equations. Microstructural simulations, such as crystal plasticity modelling, can model features like grain size, morphology and texture. However, they are computationally demanding and it can be hard to translate measured microstructures into meaningful or representative statistical distributions. Surrogate models incorporate machine learning regression and statistical methods to emulate the response of a complex model. As they are much faster, they can model the response over a wide range of material parameters, permitting sensitivity analysis and uncertainty quantification. Preferred orientation (texture) can be challenging to incorporate into surrogate models as accurate methods can require a lot of parameters. In this study, reduced-order representations of crystallographic texture are presented to describe the bulk response of a polycrystal volume element. These representations are used as inputs to a gaussian process regression (GPR) model that is used to predict the macroscopic stress-strain response of a polycrystal for different crystallographic textures. The GPR acts as a surrogate model of the underlying crystal plasticity model and allows an inherent quantification of the model epistemic uncertainty and the uncertainty related to unobserved effects not captured by the texture parameterisation. Incorporation of the surrogate model into finite element coding will be used as an application of the method.

Keywords : Mechanical behaviour, surrogate modelling, texture, crystal plasticity

461. Utilizing Automated Workflows and Thermodynamic Models to Compute Ab Initio Bulk and Defect Phase Diagrams

Neugebauer Joerg¹, Poul Marvin, Tehranchi Ali, Yang Jing, Todorova Mira, Janssen Jan, Hickel Tilmann

¹ - Max-Planck-Institut for Sustainable Materials (MPI-SusMat) (Germany)

Ab initio calculations have proven to provide highly accurate predictions of materials properties without any experimental input. While $T=0K$ properties can nowadays be routinely studied for tens of thousands of potential materials compositions in high-throughput simulations the accurate inclusion of finite temperature phenomena related to electronic, vibrational or magnetic excitations is still challenging. Accurate DFT datasets [1] together with advanced machine learning approaches provide a powerful approach to systematically include such entropic contributions while requiring only a fraction of the computational effort. This boost in computational efficiency - when coupled with our latest advancements in parametrizing free energies [2], integrating nuclear quantum effects [3], and implementing automated workflows spanning from electronic reference structure calculations through to phase diagram construction [4] - yields a robust and comprehensive framework for predicting properties of real-world materials. [1] M. Poul, L. Huber, E. Bitzek, J. Neugebauer, Phys. Rev. B 107 (2023) 104103. [2] J. Yang, K.B. Sravan Kumar, M. Todorova, J. Neugebauer, Phys. Rev. Mater. 7 (2023) 095802. [3] R. Dsouza, L. Huber, B. Grabowski, J. Neugebauer, Phys. Rev. B 105 (2022) 184111. [4] S. Menon, Y. Lysogorskiy, A. Knoll, N. Leimeroth, M. Poul, M. Qamar, J. Janssen, M. Mrovec, J. Rohrer, K. Albe, J. Behler, R. Drautz, J. Neugebauer, npj Comput. Mater. 10 (2024) 261.

462. Deep Generative Model to extract process-structure-property linkage in low-carbon steel

Inoue Junya ¹

¹ - Research Center for Advanced Science and Technology, The University of Tokyo (Meguro, Tokyo 153-8904 Japan)

Establishing the process-structure-property linkage is essential for designing new materials with desired properties. Based on the concept, the discovery of new materials has been accelerated in functional and bio-materials by combining quantum and molecular modeling tools with efficient machine learning methods. However, in the case of structural materials, even with the development of Integrated Computational Materials Engineering (ICME), it is still difficult to efficiently design new materials because of the uncertainties within models and experimental data. In the present paper, our recent development of a general methodology for extracting the linkage between hierarchical microstructure and process conditions, as well as properties, will be reviewed. In the proposed method, the uncertainties will be captured in the form of probability density functions using deep learning methods. The framework comprises two different functional components: one is for extracting geometrical features of material microstructures necessary to decompose each different microstructure, and the other is for clarifying spatial orders among the extracted characteristic components. The method was applied for generating virtual steel microstructures obtained after a certain continuous cooling process and those for desired mechanical properties. The obtained results show that the proposed methodology not only generates realistic microstructural images comparable to real experimental images but also clarifies a part of microstructures critically affecting the target property.

Keywords : Deep generative model, process, structure, property linkage

463. Multiscale Finite Element Simulation on Effect of Groove Shape on Strain Distribution in Caliber Rolling

Aoyagi Yoshiteru¹, Ohashi Haruki¹, Watanabe Chihiro², Miura Hiromi³

1 - Department of Finemechanics, Tohoku University (Japan), 2 - Kanazawa University (Japan), 3 - Toyohashi University of Technology (Japan)

New materials produced by plastic deformation processing, such as caliber rolling, outperform conventional materials in strength and ductility. In the case of plastic deformation processing, the performance of a material depends on how efficiently strain is introduced into the material. The strength of the caliber rolled bars depends on the shape of the roll grooves, which can be attributed to the fact that the strain introduced during the caliber rolling is non-uniform in the bar cross-section. However, when materials are subjected to non-uniform deformation, as in the case of caliber rolling, there is a limit to the cost and time required to improve material properties by determining the cross-sectional shape using conventional empirical rules. Therefore, this study conducted elasto-plasticity simulations to reproduce the deformation caused by the caliber rolling using different rolling dies: rhombic, hexagonal, elliptical, and circular. The simulation predicts the strain distribution within the cross-section of caliber rolled bars. Crystal plasticity simulations are performed using a unit cell model, assuming local strain in the cross-section of the caliber rolled bar, and the effect of macroscopic strain on microstructure formation is investigated. The mechanism of strength enhancement induced by groove geometry is discussed by comparing the results of the simulations with experimental results for caliber rolled bars produced using rolling dies with the same geometry as above.

Keywords : Caliber rolling, Finite element analysis, Crystal plasticity, Multiscale simulation, Strain distribution

464. Phase field model of modification of microstructure of Novel Al-15Mg2Si-4.5Si composite by addition of Strontium during semi-solid processing

Mukherjee Indrani¹, Das Prosenjit ²

1 - Advanced Manufacturing and Materials Processing Laboratory, Department of Materials Engineering, Indian Institute of Science (India), 2 - Advanced Manufacturing and Materials Processing Laboratory, Department of Materials Engineering, Indian Institute of Science (India)

Semi-solid processing over cooling slope emerges as an efficient technique for producing near spherical grain structure in the cast light alloys. The novel, in-situ Al-15Mg₂Si-4.5Si composite, processed by semi-solid processing over cooling slope, contains globular Mg₂Si grains, surrounded by α -Al phase. The size of the Mg₂Si particles is further reduced by addition of 0.01% Sr within the composite melt, which acts as grain refiner element for primary Mg₂Si grains. A two-dimensional phase field model has been developed in the present study to grab insight into the effect of Sr addition on the microstructure evolution of Al-15Mg₂Si-4.5Si composite during semi-solid processing. Instead of considering nucleation of any Sr based phase, the effect of Sr addition is realized by adjusting the phase field parameters. The phase field study predicts the grain size, sphericity, weight fraction of the evolving phases as well as the phase field parameters such as interfacial free energy, mobility, anisotropy parameters, nucleation parameters for the base composite as well as for the Sr added composite. The phase field results are found to be in close agreement with the experimental findings.

Keywords : Semi, solid, Magnesium silicide, Phase field, Grain refinement

465. Testing Theories and Simulations on Phase Coarsening by Experiments

Wang Kegang ¹

¹ - Mechanical and Civil Engineering Department, Florida Institute of Technology (United States)

Microgravity experiments on phase coarsening in solid-liquid mixtures provided an ideal tool to closely and accurately explore the kinetics of phase coarsening because the sedimentation and convective melt flow are eliminated in the International Space Station. In this presentation, we will show phase-field simulations for the investigation of the microstructure evolution during phase coarsening at various volume fractions. Simulated microstructure evolution during phase coarsening are compared quantitatively with the microstructure evolution archived from microgravity experiments. Furthermore, kinetics of phase coarsening in Pb-Sn solid-liquid mixtures at various volume fractions is studied theoretically and numerically, which is compared with microgravity experiments. In particular, particle size distribution, relative coarsening rate constants, and scaled maximum particle radii, are quantitatively compared among the predictions from theories, microgravity experiments, and phase-field simulations. This systematic and quantitative study of phase coarsening confirms the consistency to the results from phase-field simulation, microgravity experiments and theories at lower volume fractions.

Keywords : Phase coarsening, Phase, field simulations, Microgravity experiment.

466. Microstructure-Based Fatigue Life Prediction Approaches for Hypo-Eutectoid Steels: Uniaxial and Non-Uniaxial Fatigues Lives, and Their Variabilities

Choi Yoon Suk¹, Shin Jonghoon¹, Nam Dae-Geun²

1 - School of Materials Science and Engineering, Pusan National University (South Korea), 2 - Korea Institute of Industrial Technology (South Korea)

The talk consists of the following topics aiming for building a comprehensive fatigue life prediction methodology based on microstructures for 44MnSiVS6 hypo-eutectoid steels: - Microstructure-based uniaxial fatigue life prediction - Microstructure-based non-uniaxial fatigue life prediction using the uniaxial fatigue life data - Microstructure-based fatigue life variability prediction As a first step, a statistically equivalent synthetic microstructure generation algorithm was developed by applying the cellular automata under the multi-level microstructure generation approach, and verified by comparing to the real microstructure. A second step involved the development of crystal plasticity-based elasto-viscoplastic constitutive models for the primary ferrite and pearlite of the hypo-eutectoid steel, and the calibration of major constitutive parameters using uniaxial and incremental step fatigue test results. For a third step, synthetic microstructure-based crystal plasticity finite element method (CP-FEM) simulations were performed for stress-controlled uniaxial, torsional, and in-phase and out-of-phase axial plus torsional fatigue loading conditions, and cyclic increments of fatigue indicator parameters (DFIPs) were extracted from fatigue-simulated microstructures for the local fatigue damage quantification. Four different fatigue indicator parameters, Smith-Watson-Topper, Brown-Miller, Fatemi-Socie and Garud parameters, were adopted for the DFIP quantification. As a final step, four different simulated DFIPs were coupled with the power law-based model to predict fatigue lives, and their fatigue life predictability was assessed. In particular, simulated DFIP hot spots were used to predict the fatigue life variability under the framework of the extreme value analysis.

Keywords : Fatigue life, Modeling, Microstructures, Steels

467. A computational framework for modeling and predicting the mechanical behavior of materials applied to martensitic steels.

Jansson Ake¹, Kaplan Bartek ¹, Barkar Thomas , Salmasi Armin

1 - Thermo-Calc Software AB (Sweden)

A computational framework for modeling and predicting the mechanical behavior of materials applied to martensitic steels. We here introduce a computational framework for modelling and predicting the mechanical behaviour of materials during plastic deformation, focusing on the phenomenon of strain hardening. The framework provides tools to estimate the stress-strain relationships of materials, including models for stress beyond the ultimate tensile strength and fracture properties. The framework combines theoretical approximations, such as the Ramberg-good relationship, with numerical methods and machine learning models. Inputs include alloy compositions and thermal history, while outputs include engineering and true stress-strain curves, yield strength, ultimate tensile strength, fracture strength and elongation. Approximations are made using empirical relationships, analytical elastic and plastic response equations, and parameter estimates based on material data. The current implementation is directed towards predicting the mechanical properties of martensitic steels but the framework supports modularity and allows for integration of additional material classes and strain-hardening models. Results and validation will be presented in several graphs.

468. A meso-scale model to predict flow stress and microstructure during hot deformation of IN718WP

Kumar Nilesh¹, Ferraz Franz Miller Branco Ferraz², Buzolin Ricardo², Shahryari Esmaeil Shahryari², Poletti Maria Cecilia², Yadav Surya¹

1 - Indian Institute of Technology [BHU Varanasi] (India), 2 - Institute of Materials Science, Joining and Forming, TU Graz (Austria)

This research presents a dislocation-based hot deformation model to address a nickel-based superalloy's flow stress response and discontinuous dynamic recrystallization (DDRX) behavior. The developed model can predict the flow curves and subsequent microstructure evolutions during the hot deformation. The evolution of microstructure-reliant internal variables was predicted and validated thoroughly. Furthermore, the influence of strain rate and temperature on the glide and climb velocities have also been discussed to reveal more insights into the microstructural development. Dislocation density and DDRX fraction predicted from the model was compared with dislocation density and DDRX fraction obtained from electron backscattered diffraction (EBSD) measurements with reasonable matching. Higher temperatures and slower strain rates provide favorable conditions for DDRX in this alloy. The importance of this model relies on its prediction capability in terms of flow curve, mobile and immobile dislocation densities, DDRX fraction, grain size and dislocation velocities. Single set of parameters were obtained from twelve experimental curves and rest of the eleven curves were predicted by the model using those parameters. The present research approach is helpful to predict the multiple flow curves along with the corresponding microstructure evolution in LSFE materials.

Keywords : IN718WP, Flow stress, Dislocation density, Glide velocity, Climb velocity, EBSD, DDRX

469. Modelling combined hardening mechanisms in alloys through the analysis of dislocation percolation.

Schouwenaars Rafael ^{1 2}

1 - Departamento de Materiales y Manufactura, Universidad Nacional Autonoma de Mexico (Mexico), 2 - Department of Electromechanical, Systems and Metals Engineering, Ghent university (Belgium)

The critical resolved shear strength of pure metals is given by the Peierls-Nabarro equation; impurities or alloying elements will significantly increase . Additional strength is introduced by strain hardening (SH), the grain size effect (GSE), precipitates and particle dispersion. The combination of these mechanisms is generally described in an additive manner, which can be justified by the Taylor expansion of a multivariate function. This approach is highly empirical and involves extensive parameter fitting. The Kocks-Mecking model (KM) and discrete dislocation dynamics show that SH is mainly due to forest effects (latent hardening). More than 90% of the mechanical work during plastic deformation is dissipated as heat. This means that less than 10% is stored in the form of the self-energy (line tension) and interaction energy between dislocations. Consequently, the main explanation for alloy strength must be sought in the resistance against dislocation percolation through a field of obstacles with different strengths, with the slip length limited by the grain diameter. This hypothesis is explored by reviving early graphical simulations to the percolation problem by introducing a grain boundary and variable obstacle strength in an efficient computer program. Large scale statistical simulations and theoretical considerations demonstrate the limitations of the additive description of combined hardening. An alternative approximation is proposed, based on a theoretical analysis of the statistical micromechanics of dislocation percolation, dislocation junctions and dislocation-grain boundary interaction. Its success is demonstrated by the analysis of the GSE in Cu, Ni and Al.

Keywords : Micromechanics, Statistical modelling, Alloy strength, Strain hardening, Grain size effect

470. Application of an Activation-function modified Norton law to predict the two-step minima creep deformation observed in Incoloy 800H

Rojas-Ulloa Carlos¹, Chen Fan ¹, Tuninetti Vã-Ctor ^{2 3}, Di Giovanni Amedeo ⁴, Pensis Olivier ⁴, Vendramini Alexandre ⁴, Duchane Laurent ¹, Habraken Anne ^{1 5}

1 - Departement Architecture, Geologie, Environnement et Constructions - ArGEnCo (Liege, Belgium) (Belgium), 2 - University of La Frontera (Chile), 3 - Department of Mechanical Engineering, University of La Frontera (Chile), 4 - Drever international (Belgium), 5 - Fonds National de la Recherche Scientifique [Bruxelles] (Belgium)

For some temperature-stress loading combinations, the steady-state creep stage exhibited by alloy UNS N08810 is preceded by an initial viscoplastic hardening regime. This results in two-step creep rate minima that conventional creep models fail to reproduce. In this work, we address this issue by coupling the well-known Norton creep law with an activation function. The Activation Function \times Norton (AFN) model is implemented as a viscosity function within a Chaboche-type unified viscoplastic constitutive model in the Lagamine finite element software. The implementation follows an implicit integration algorithm. The parameter identification procedure follows a direct methodology. The creep data used was generated after a thorough in-house experimental campaign combined with a comprehensive postprocessing of results, where both creep minima are correctly identified from. Finite element simulations allow to accurately recover the experimental data, thus validating the Chaboche-type constitutive law coupled with the AFN viscosity function to model the non-classical creep regime of the alloy. The explanation of the two-step creep rate phenomenon can be found in the microstructure. The first creep rate minimum is attributed to the pinning of dislocations induced by a combination of solid solution and precipitate hardening. The second one corresponds to the conventional steady-state creep rate. Creep micromechanical approaches are being implemented to explore this behavior from a physical perspective.

Keywords : Incoloy 800H, Creep, modified Norton law, finite elements, viscoplasticity, damage

471. Concept of a module for water treatment with plasmonically active nanoparticles, to extend a multivalent modular prototype system for adaptable water treatment and analysis

Heinrich Moritz, Bald Ilko, Boehme Andrea, Krenz-Baath Rene

1 - Technical University of Applied Science Wildau (Hochschulring 1 15745 Wildau Germany)

This study introduces a concept for a specific new module for water purification through plasmon-induced photocatalysis, which addresses the urgent need for advanced treatment of industrial and hospital wastewater. The emergence of new pollutants, including a range of toxic molecules produced by modern processes, has highlighted the need for innovative solutions to effectively remove these substances. One principle of water treatment is plasmonic photocatalysis, which uses silver nanoparticles activated by 450 nm blue light to generate a plasmonic reactive reaction for contaminant degradation. In this study, we conceptualize the integration of this principle into a specific new module designed for a recently developed unified modular system. This modular system consists of customizable 3D-printed purification, infrastructural and analytical units, which allow adaptive configurations and expansions. The reactor's design is based on the modular system's architecture and incorporates a continuous sample flow principle with immobilized nanoparticles on cellulose matrices. The initial tests, which used methylene blue as a model compound, demonstrated rapid degradation rates, which serve to underscore the potential effectiveness of this approach. Subsequent experiments will target the degradation of complex antibiotic residues, such as vancomycin, in order to further validate the module's efficacy in real-world applications.

Keywords : Water Purification, Additive Manufacturing, Modular System, Plasmonic Nanoparticle Process

472. Control of osteoblast cell behavior by titanium alloys' microstructure

Kobayashi Sengo¹, Okano Satoshi

¹ - Department of Materials Science and Biotechnology, Ehime University (3 Bunkyo-cho, Matsuyama 790-8577 Japan)

Titanium alloys are widely used as biomaterials, e.g., artificial bone and bone plates. One of the problems with titanium alloys for artificial bone is that there are cases where the artificial bone and the living bone are not firmly joined. In order to contact the artificial bone with the living bone firmly, the osteoblasts must activate and create living bone on the artificial bone. Therefore, control of osteoblasts on the titanium alloys is critical. This study aims to reveal the effects of the titanium alloys' microstructure on the behavior of osteoblasts. Ti-6Al-4V ELI (Ti64) and Ti-15Zr-4Nb-4Ta (TZNT) alloy plates were mechanically mirror-polished. Some of them were chemically etched. A part of them was heat-treated at 500 °C. After sterilization, MC3T3-E1 osteoblast-like cells were cultured. The morphology and number of cells were evaluated using a fluorescence microscope. The microstructures of the Ti64 and TZNT alloys consisted of alpha (hcp phase) and beta (bcc phase) phases. The concentration of aluminum in the alpha phase and vanadium in the beta phase was confirmed in the Ti64 alloy. On the other hand, condensation of niobium and tantalum in beta phase was detected in the TZNT alloy. It should be noted that osteoblasts preferentially adhered to alpha phase in the Ti64 alloy, while they were likely to attach to beta phase in the TZNT alloy. The difference in osteoblast adhesion on the two titanium alloys can be explained by the release of ions from the alloys and the variation of oxides on the microstructure.

Keywords : Titanium, Osteoblast cell, Microstructure, Etching, Oxidation

473. Argon plasma etching process to fabricate the antibacterial nanopillar on stainless steel surface

Hirano Mitsuhiro, Miura Koyo, Ohtsu Naofumi

1 - Kitami Institute of Technology (Japan)

The fabrication of nanotextured surfaces inspired to insect wings is attracted as a novel strategy to enhance the antibacterial activity. In previous study, plasma etching using fluoride gas enables the formation of nanopillars on silicon substrates. However, in case of stainless steels, the process can't be applicable due to corrosivity of fluorine atoms. Therefore, we attempted to fabricate the nanopillars on AISI 316 stainless steel (SS316) substrates using plasma etching with Ar gas as alternative process; furthermore, the antibacterial activity was investigated. Ar plasma etching of 316SS was performed for 60 min with a constant current ranging from 0.05 to 0.15 A, which affected drastically dimensions of the nanopillars. Pillars with several hundred nanometers in size were observed on the entire surface plasma-etched at 0.05 A, of which the height, cap and base diameters increased with increasing applied current. Furthermore, the nanopillars fabricated on 316SS substrate functioned as an antibacterial surface. The survival rates against *Escherichia coli* were reduced below 10%, regardless of applied current. Observing bacterial morphology, the bacteria adhered on plasma-etched surface were stretched and stabbed by nanopillars. Therefore, it is suggested that these morphological variations are physically damage induced by nanopillars, which are a principal factor of antibacterial activity. Based on these results, Ar plasma etching is expected to apply as a technique enhancing antibacterial activity for stainless steel surface.

Keywords : Plasma etching, Nanopillar, Antibacterial activity, Stainless steel

474. Safe-by-design conception and synthesis of metallic nanoparticles for biomedical applications

Patrizio Benzo¹, Trillot Salome¹, Kaur Ramanpreet¹, Tarrat Nathalie¹, Benoit Magali¹, Makasheva Kremena², Casanove Marie-Jose¹, Bonafos Caroline¹

1 - CEMES-CNRS and Universite de Toulouse, 29 rue J. Marvig, 31055 Toulouse, France (France), 2 - LAPLACE, Universite de Toulouse; UT3, INPT, CNRS; 118 route de Narbonne, F-31062 Toulouse cedex 9, France. (France)

Metal nanoparticles (NPs) are highly valued in biomedical fields due to their unique physicochemical properties, making them promising for diverse applications. However, large-scale implementation requires strategies to mitigate impacts on human health and environmental safety. Beyond optimizing NP properties, "safer by design" approaches are essential. This work introduces two "nano-safe by design" systems. The first involves trimetallic (Fe, Rh, Au) nanoparticles synthesized by magnetron sputtering with controlled composition, crystalline quality, and chemical distribution. The FeRh core, exhibiting a magnetic transition near physiological temperatures (~310K), has significant biomedical potential (e.g., as a contrast agent or for drug delivery). A gold shell, grown epitaxially, ensures biocompatibility. The second example features antibacterial Ag-NPs embedded in dielectric matrices for controlled Ag⁺ release, providing antimicrobial effects over adjustable periods (from days to months) while minimizing environmental toxicity. The synthesis involves two steps within an ultra-high-vacuum system: i) Ag-NPs are vapor-phase synthesized by magnetron sputtering, size-selected with a quadrupole mass filter (QMF), and deposited onto a silica substrate; ii) a silica layer is added via radio-frequency magnetron sputtering. This approach allows precise control of NP density, balancing effective Ag⁺ reservoirs for antibacterial action below toxicity thresholds, and positioning NPs to finely tune Ag⁺ release rates. For both systems, synthesis processes and nanoparticle characteristics (size, density, crystalline structure, composition, and morphology) will be examined using transmission electron microscopy at atomic resolution. These properties will be correlated with synthesis parameters, and potential nucleation and growth mechanisms for each system will be discussed.

Keywords : nano, safe by design, metallic nanoparticles, nucleation and growth

475. Self-Assembled Growth of 3D Nanostructures for High Electrochemical Performance by RF Magnetron Sputtering

Kim Ki-Chul ¹

¹ - Department of Intelligent Information Convergence, Graduate School of Mokwon University (South Korea)

As microelectronic devices are developed, the development of micro-batteries and highly sensitive electrochemical sensors using on-chip processes are requested. Three-dimensional (3D) nanostructures are effective in implementing high electrochemical responses because they have high effective surface area. In this study, 3D nanostructures of molybdenum oxide or vanadium oxide with high effective surface area were grown directly on substrates using a self-assembled growth mechanism by controlling of RF magnetron sputtering conditions. The surface morphology and cross-sectional growth patterns of the nanostructures were analysed by field emission scanning electron microscope. The crystallographic properties were characterized by XRD and Raman spectroscopy. The study results showed that either perfect 2D thin films were deposited or nano-platelets were grown vertically on the substrate with dense structure depending on the sputtering conditions. At RF power of 40 W and substrate temperature of RT, a perfect 2D alpha-MoO₃ thin film was deposited and RF power of 120 W and substrate temperature of 200 °C, 3D alpha-MoO₃ nanostructures were grown. In addition, in the case of vanadium oxide, perfect 2D alpha-V₂O₅ thin film was deposited at RF power of 100 W and substrate temperature of RT. 3D alpha -V₂O₅ nanostructures were grown at RF power of 200 W and substrate temperature of 200 °C. It is expected that 3D nanostructures with high effective surface area can exhibit high electrochemical performance and can be applied to the fabrication of high-performance gas sensors and lithium-ion batteries.

Keywords : Self, Assembled Growth, Three, Dimensional Nanostructure, Electrochemical Performance, RF Magnetron Sputtering

476. A Novel Understanding for Plastic Deformation and Mechanical Amorphization of Amorphous and Crystalline Silica under Electron-Beam Irradiation

Choi In-Suk ¹

¹ - Seoul National University [Seoul] (South Korea)

Amorphous silica, typically brittle, can undergo viscoplastic deformation at elevated temperatures. In this study, we highlight the possibility of achieving precise nanoscale mechanical shaping of amorphous silica through electron-matter interactions, without the need for heating. We found that ductile plastic deformation and densification can be induced athermally by focused scanning electron beams at low acceleration voltages. Our simulations indicate that the extent of deformation is governed by the interaction volume, where inelastic scattering occurs. Moreover, we demonstrated that electron beam irradiation can dramatically facilitate solid-state mechanical amorphization of crystalline α -quartz at room temperature, a process that usually demands high pressure. Microstructural examinations and atomic-scale simulations suggest that this is attributed to the uniformly distributed delocalized electrons, introduced by the electron beam excitation, collectively moving like anions situated between the positively charged silicon ions, effectively mitigating the repulsive forces within the distorted atomic structures. This research not only deepens our comprehension of electron-matter interactions but also unveils a new pathway for mechanical forming and processing of glass and ceramic materials.

Keywords : In, situ testing, Electron beam, Nanomechanics, Plastic Deformation, Amorphization

477. Employing Shear Punch Testing to Investigate Thermomechanical Properties of Nanocrystalline Brass

Petry Oliver¹, Durst Karsten ², Bruns Sebastian ³, Fakhar Naeimeh ⁴

1 - Technische Universität Darmstadt - Technical University of Darmstadt (Germany), 2 - Technical University Darmstadt (Technical University Darmstadt, Materials Science, Alarich-Weiss-Str. 2 64287 Darmstadt Germany), 3 - Technical University of Darmstadt (Germany), 4 - Hamedan University of Technology (Iran)

The shear-punch test can be used to evaluate the mechanical properties of materials with limited availability. The shear-punch test was used to evaluate ultimate shear strength and shear yield strength of nanocrystalline (nc) brass (Cu-30 wt% Zn) and a linear relation between ultimate strength and yield strength from uniaxial compression and tensile tests could be confirmed. A softening could be observed at high strains, and was investigated for different temperatures (RT, 100°C, 200°C, 300°C). The softening was related to a change in geometry and a method to evaluate an effective thickness from laser-microscopic images was established. Strain-rate-jump (SRJ) tests were employed using the shear punch method and the results were compared to uniaxial compression and nanoindentation SRJ tests. The results show the breakdown of the Hall-Patch effect in nc brass at elevated temperatures and good agreement of strain rate exponents calculated from tensile, compression and nanoindentation tests. Furthermore, the SPT allows the investigation of the microstructure in highly deformed area and undeformed area, showing stress assisted grain growth after testing at 200 °C.

Keywords : Shear punch test, Mechanical properties, Nanocrystalline, Strain Rate Jump, Brass, CuX

478. Optimization of Hydrogen Alarm Sensor on Semiconductor Basis

Werner Ronald¹, Proposito Paolo^{2 3}, Boehme Andrea⁴, Krenz-Baath Rene⁴

1 - Microsystem Engineering/Systemintegration, Technical University of Applied Sciences, Wildau, 15745, Germany. (Germany), 2 - Center for Regenerative Medicine, University of Rome Tor Vergata (Via Montpellier 1, Rome, 00133 Italy), 3 - Department of Industrial Engineering and INSTM, University of Rome Tor Vergata (Via del Politecnico 1, Rome, 00133 Italy), 4 - Technical University of Applied Sciences Wildau (Germany)

A semiconductor based sensor system was optimized by various modifications, which allow an improved detection of very low concentrations of hydrogen in air. The base for new investigations on the sensor base is a design for different chips on a single wafer, which allows to create different types and structures for sensor measurements. Fast and reliable sensor chips can be created by application of maskless lithography without limitations of wafer process lines. Also fragments can be processed. This is beneficial for effective and economical investigations of a variety of structures from a single wafer. Modifications were made to the insulator layers and the ion conductor layer, the gate material and the gate structures on it. To improve the sensor properties, variations of the sensor design and structural properties were required, which were achieved by different coating techniques and variable layer compositions. Sensor reference structures were used to reduce interference and enable reliable operation of the system. Many characterization measurements were employed to validate the effectiveness of modifications and structural changes of the sensor and additional functionalities.

Keywords : Hydrogen Sensor, Semiconductor Sensor, Alarm Sensor, optimized structures

479. Low-temperature synthesis of graphene usable in the harsh environment of liquids for energy applications

Tanemura Masaki¹, Ngatiman Muzzammil Bin ¹, Rohim Nur Sahiera Binti Abd ¹, Yoshida Naoko ¹, Yan Jiabin ², Chua Daniel ², Lin Wei Ming ¹, Asaka Toru ¹, Yaakob Yazid ³, Yang Yong ⁴, Yusop Mohd Zamri Mohd ⁵

1 - Nagoya Institute of Technology (Japan), 2 - National University of Singapore (Singapore), 3 - Universiti Putra Malaysia (Malaysia), 4 - Shanghai Institute of Ceramics, Chinese Academy of Sciences (China), 5 - Universiti Teknologi Malaysia (Malaysia)

Sustainable development goals (SDGs) are nowadays a global issue, and it is also the case for the synthesis of materials for energy- and environmental- related applications. Carbon-based nanomaterials, such as graphene, are promising for the energy device applications including lithium-ion batteries (LIBs) and fuel cells. So, it is essential to develop methods for their synthesis at lower temperatures with less energy consumption. The graphitized nanocarbon are usually synthesized from gas phase at elevated temperatures, sometimes at the temperature close to the melting point of catalyst metals, as exemplified by chemical vapor deposition (CVD) methods. An alternative approach to reduce the synthesis temperature of graphene will be the solid phase reaction method based on the solid-state transformation of segregated carbon. For Ni case, for example, which is the typical catalyst for the CVD graphene synthesis, the localized graphitization occurred around Ni nanoparticles even at room temperature (spontaneous graphitization) [1]. Well graphitized films were synthesized by simple vacuum annealing of Ni-C composite films at the temperature much lower than CVD, independent of the substrate material and shape. The multilayer graphene thus synthesized was usable as the electrode for the development of LIBs, and in-situ transmission electron microscopy observation clearly demonstrated the intercalation of Li into graphene interlayer to form LiC₆ [2]. Another successful example is the enhancement of the biofilm formation and current generation of *Geobacter* species for the microbial fuel cell application [3]. Thus, the graphene synthesized by this method can be used even in the harsh environment of liquid and is quite promising for a variety of applications. [1] S. Elnobi, et al., RSC Adv. 10 (2020) 914. [2] W. M. Lin, et al., Adv. Mater. Technol. 9 (2024) 2301564. [3] S. Giri, et al., submitted.

Keywords : nanocarbon, graphene, energy device, Li ion battery, in situ TEM, microbial fuel cell

480. Nanocomposites of reduced graphene oxide for 2D symmetric micro-supercapacitor with high energy storage performances

Debiemme-Chouvy Catherine¹, Bouzina Adnane ¹, Marzouq Nada ¹, Sel Ozlem, Perrot Hubert ¹

¹ - Laboratoire Interfaces et Systemes Electrochimiques (France)

In the domain of electrochemical storage of the energy, the simple and eco-friendly preparation of microsupercapacitor (MSC) remains a great challenge. In this communication, the preparation and the characterizations of symmetric MSCs based on graphene-polydopamine (PDA) composites and graphene-polyoxometalate (POM) will be presented. These composites were obtained either by an electrochemical route or by a hydrothermal route (HR). One composite was prepared by electroreduction of graphene oxide followed by the electrooxidation of dopamine that leads to PDA. This composite, ERGO-PDA, is formed of highly ordered graphene sheets. For the HR, graphene oxide suspension and dopamine solubilized in PBS were added together in an autoclave to obtain the composite, rGO-PDA. For the rGO-SiW₁₂O₄₀-composite, graphene oxide suspension and reduced POM solution obtained by an electrochemical route were mixed. In Na₂SO₄ solution pH 7 or 4 (addition of H₂SO₄), electrochemical characterizations of the composites using a three-electrode set-up show that the three composite materials exhibit excellent capacitance and stability even at a high scan rate (2 V/s) and a low relaxation time. In good agreement with the high transfer kinetic values of the ions implied in the charge storage process determined by ac-electrogravimetry (crystal microbalance coupled with electrochemical impedance spectroscopy). Finally, it is shown that the MSCs, 2D interdigitated electrodes obtained using a CO₂ laser and Na₂SO₄/PVA hydrogel, prepared with the composites with polydopamine deliver a remarkable energy density of 6.4 mWh/cm³ (electrochemical route) and 6.20 mWh/cm³ (HR, collector-free MSC) for a power density of 0.22 W/cm³ and exhibit excellent cycling stability after 10,000 cycles at 2 V/s.

Keywords : Graphene, Nanocomposite, Electrochemistry, Fabrication, Microsupercapacitor, Polydopamine, Polyoxometalate

481. Some Issues Related to the Formation of GaN-based Nanopillar LEDs on Multicrystalline Si Substrates

Sato Yuichi ¹

¹ - Akita University (Japan)

If good GaN-based light-emitting devices can be formed on non-single-crystal substrates that can be large-scale at low cost, it can be applied to low-cost large-area micro-LED displays and high-performance planar lighting devices. So far, the authors have attempted to form GaN-based nanopillar crystals and LED arrays by them on several non-single crystal substrates, and have shown that light-emitting devices with some performance can be obtained [1,2]. However, some problems have arisen with these devices. In order to further increase the brightness as a planar light emitting source, it is necessary to obtain a higher current density, but the resistance of the device as a whole is high and sufficient current density cannot be obtained. In addition, in order to apply it to a high-resolution display, the in-plane uniformity of the light emission characteristics must be high, but the distribution of the light emitting color and the unevenness of the light emitting location due to the crystal domain in the multicrystalline Si substrate occur. Although it has been possible to obtain the comparable light emission as single-crystal devices, such problems still remain, and it is necessary to analyze and overcome these factors. The author will focus on some of these issues, for example, electrical properties and structures of each part included in the LEDs and discuss measures to solve them. References [1] Y. Sato et.al., AIP Advances, 11⁷, 075110 (2021). [2] Y. Sato et.al., Key Engineering Materials, 967, 57 (2023).

Keywords : Nitride Semiconductor, Multicrystalline Si Substrate, Nanopillar, LED

482. Plasma Synthesis of 3D Graphene-Based Materials and their Applications

Hiramatsu Mineo¹, Takeda Keigo ¹

¹ - Meijo university (Japan)

Three-dimensional (3D) graphene-based materials contain interconnected graphene layers that form 3D porous structures. The high porosity, large surface area, and excellent electrical conductivity render these 3D graphene-based materials having potential applications in many fields. Besides graphene foams and sponges, vertical graphene network (VGN) can be also categorized as 3D graphene. VGN forms a 3D interconnected structure possessing intimate contact with substrate and exposed edges at its top, and easily accessible open surfaces of graphene nanosheets. We have fabricated VGNs by plasma-enhanced chemical vapor deposition employing methane and hydrogen mixtures. VGNs are self-supported architecture of few-layer graphene sheets standing almost vertically on the substrate. The morphology of VGNs depends on the growth condition. As the process pressure increases, interspaces between adjacent sheets decrease, then VGNs become dense and less-aligned. When adding Ar into gas mixtures, the increase of ion flux on the growing surface would induce secondary nucleation to form branched nanographene sheets. As a result, VGNs with sponge structure can be formed. Both VGNs with wall and sponge structures possess large specific surface area and spaces surrounded by nanographene sheets. As an application of VGNs, glucose oxidase (GOD) was selected as an oxidoreductase enzyme and the GOD was immobilized on the surface of VGN to be used as electrode materials for glucose fuel cell. Moreover, VGNs with wall and sponge structures were applied as electrodes of Li-ion and Li-S batteries. Electrochemical experiments demonstrate that 3D graphene-based materials can be promising electrode materials for energy conversion applications.

Keywords : 3D graphene, Vertical Graphene, glucose fuel cell, Li, S battery

483. Superatom Like b-FeSi₂ Core/Si Shell Quantum Dots via Self-Assembly and Self-Alignment Processes

Makihara Katsunori ¹

¹ - Nagoya University (Japan)

The monolithic integration of Si-based photonics with electronic processes on a single chip is considered a key advancement for beyond CMOS computing. In this paper, our achievements on fabrication of Si quantum dots (QD) with a b-FeSi₂ core by controlling self-aligned silicidation of the Si-QDs and subsequent selective Si-growth have been reviewed. First, uniformly sized Si-QDs with an areal density as high as $\sim 10^{11} \text{ cm}^{-2}$ were self assembled on an ultrathin SiO₂/p-Si(100) by LPCVD using SiH₄, where the average dot height was estimated to be $\sim 5.1 \text{ nm}$. After the Fe-film deposition, the surface morphology was slightly smeared, and the average dot height slightly decreased to $\sim 3.9 \text{ nm}$. However, after the HCl treatment, the dot height became the same size as that of the as-grown Si-QDs. Subsequent SiH₄ exposure, resulted in a slight increase up to $\sim 5.9 \text{ nm}$ with no change in the areal dot density. From the room-temperature PL characteristics, light emission from the sample after HCl treatment was hardly detected although a weak PL signal in the range from ~ 0.73 to 0.83 eV was observed immediately after the Fe deposition. It should be noted that, after SiH₄-exposure, the PL intensity drastically increased by a factor of five compared to that after Fe film deposition. The origin of this light emission is considered to be the radiative recombination between the quantized states in the conduction band of the b-FeSi₂ core and the valence band of the Si-shell.

Keywords : Si Nanodot, Core/Shell Dot, b-FeSi₂, Light Emission

484. Growth and Magnetic Characteristics of Iron-filled Carbon Nanotubes

Sato Hideki¹, Fujiwara Yuji²

1 - Graduate School of Engineering, Mie University (1577 Kurima-machiya-cho, Tsu, Mie, 514-8507 Japan),

2 - Graduate School of Engineering, Mie University (Japan)

Iron-filled carbon nanotubes (Fe@CNTs) are CNTs that encapsulate iron nanowires within their inner hollows, achieving a high filling rate of over 50%. Due to the encapsulation of ferromagnetic iron, Fe@CNTs exhibit ferromagnetic properties. The iron nanowires possess a high aspect ratio exceeding 10. This high aspect ratio enables CNTs to demonstrate a coercivity greater than 1.0 kOe. These characteristics suggest that Fe@CNTs are promising candidates for hard magnetic materials, such as those used in permanent magnets. We have examined the growth and magnetic characteristics of Fe@CNTs with the goal of obtaining Fe@CNTs with higher coercivities. To achieve this, we have developed a chemical vapor deposition (CVD) reactor that allows for the controlled introduction of ferrocene vapor [Fe(C₅H₅)₂], which serves as the precursor for Fe@CNT growth. Fe@CNTs are grown on silicon substrates through the thermal decomposition of ferrocene. We have found that catalyst thin films, which are pre-deposited on Si substrates, play a crucial role in improving both growth and magnetic characteristics. The use of an iron/platinum bilayer thin film significantly enhanced the coercivity to over 2.0 kOe. Furthermore, we recently discovered a growth condition that achieves a coercivity exceeding 2.0 kOe without the use of platinum. Additionally, we found that the number of graphitic layers in Fe@CNTs depends on the flow rate of ferrocene vapor into the CVD reactor. The growth of Fe@CNTs with several graphitic layers has been confirmed.

485. Data-driven analysis and control of plasma-enhanced deposition of functional carbon materials

Kondo Hiroki^{1 2}, Tsutsumi Takayoshi ², Ishikawa Kenji ², Sekine Makoto ², Hori Masaru ²

1 - Kyushu University (Japan), 2 - Nagoya University (Japan)

Plasma-enhanced techniques are widely used in academic research and industry as a powerful method for thin film deposition and nanomaterial synthesis. However, plasma processes are generally complicated, since they involve a variety of active species, making them difficult to elucidate the mechanism and control the process. Efforts have been made mainly in academic research to measure active species in process plasmas and elucidate their generation mechanisms. Recently, attempts have been made to control this complex plasma process using machine learning approaches. However, since learning models are black boxes, it is difficult to understand their mechanisms of plasma-excited reactions. Therefore, we quantitatively clarified the interactions between reactive species in plasma and their effects on film quality by contribution analysis using machine learning. Specifically, we clarified the mechanism behind the etching resistance of carbon hard masks used in high-aspect etching of 3D flash memory. Radical species generated during a plasma-enhanced chemical vapor deposition were quantitatively measured using a quadrupole mass spectrometer (QMAS). Deposition and etching rates by oxygen plasma were evaluated using in-situ ellipsometry. Combining these data and contribution analysis using machine learning, we have succeeded in quantitatively characterizing the correlation between the active species in the plasma and the physical properties of the amorphous carbon films. By utilizing informatics, we can quantitatively understand the interactions between reactive species. It allows us to scientifically interpret complicated plasma processes and lead to innovations in new processes and materials.

Keywords : Plasma, enhanced chemical vapor deposition, Radical, Amorphous carbon, Machine learning, SHAP

486. Amorphous Gallium Oxide Memristor for High-temperature Electronics

Sakai Akira ¹

¹ - Osaka University (Toyonaka, Osaka, 560-8531 Japan)

Memristors, which show non-volatile resistance changes under external bias voltage, have attracted significant interest for resistive memory and neuromorphic AI hardware applications. In metal-oxide memristors, the resistance state is determined by the distribution of oxygen vacancy ions within the metal oxide thin film. For memristors and neuromorphic devices to be deployed in extreme environments such as geothermal and underground resource development, automotive engine control, and aerospace industries, reliable high-temperature performance is crucial. While silicon metal-oxide-semiconductor field-effect transistor-based memory devices are competitive, they are limited by the material properties of Si (bandgap energy of ~1.1 eV) for high-temperature use. This talk discusses a memristor device developed for high-temperature operation. We focused on reduced amorphous gallium oxide (a-GaOx), which has a bandgap energy of approximately 4.1 eV. Using pulsed laser deposition, we fabricated a Pt/a-GaOx/ITO memristor and measured its current-voltage characteristics at various temperatures. The results demonstrated stable non-volatile resistance change even at 600 K. Hysteresis curves confirmed that the resistance change is due to oxygen vacancy ion distribution changes in a-GaOx, indicating non-filamentary behavior. Detailed analysis showed that the resistance change is caused by the transition between ohmic conduction and space-charge-limited current conduction. These results highlight a-GaOx as a promising memristor material capable of stable operation even at the record-high temperature of 600 K. Acknowledgements: This work was supported by JSPS KAKENHI Grant Numbers JP 24K00926, JP 24K21620.

Keywords : Memristor, High, temperature, Resistive memory, Electrical conduction, Oxygen vacancy ion

487. In situ XAFS study on chemical states of transition-metal catalyst during single-walled carbon nanotube growth under conventional CVD conditions with ethanol and C₂H₂ feedstock

Maruyama Takahiro¹, Horiuchi Jumpei¹, Mizuno Shinya¹, Sharma Kamal¹, Saida Takahiro¹

¹ - Meijo university (Japan)

Single-walled carbon nanotubes (SWCNTs) possess promising applications in wide range of fields such as electronics, flexible sensors, and energy materials. To realize SWCNT devices, selective growth of semiconducting SWCNTs is essential. The electronic state of a SWCNT is determined by its structure such as diameter and chirality. At present, chemical vapor deposition (CVD) is commonly used for SWCNT growth, where nanosized metal particles are used as catalysts. Therefore, it is important to clarify the physical and chemical states of catalyst particles during SWCNT growth because the diameters and chirality of SWCNTs depend on the property of catalyst particles. So far, several groups reported environmental transmission electron microscopy (ETEM) analysis for catalyst particles during SWCNT growth. However, they were performed under the low temperature with low feedstock gas pressure, compared with the typical growth condition of SWCNTs. In this study, we performed in situ X-ray absorption fine structure (XAFS) spectroscopy to investigate chemical states of transition metal catalysts during SWCNT growth under the conventional growth condition by CVD. Our result showed that the degree of carbonization was different between Fe, Co, and Ni catalysts. From transmission electron microscopy (TEM) and X-ray diffraction (XRD) results, we proposed a growth model of SWCNTs from iron-group metal catalysts. We will also discuss the difference in the growth mode. Part of this work was conducted at the Institute of Molecular Science (IMS), supported by ARIM. XAFS analysis was performed at Aichi SR in Japan.

Keywords : Carbon nanotube, XAFS, CVD, Catalyst

488. Hydrogen desorption from GeH nanosheets under ultrahigh vacuum ambient towards germanene synthesizing

Kurosawa Masashi¹, Matsumoto Kazuho¹, Araidai Masaaki²,
Shibayama Shigehisa¹, Sakashita Mitsuo¹, Nakatsuka Osamu^{1 2}

1 - Graduate School of Engineering, Nagoya University (Japan), 2 - Institute of Materials and Systems for Sustainability, Nagoya University (Japan)

Germanene, a 2D material in which the carbon in graphene is replaced by germanium, is listed as an innovative material in the International Roadmap for Devices and Systems (IRDS, 2022 Edition), a roadmap for silicon semiconductor integrated circuits. It is theoretically predicted to possess extremely high electron mobility and attractive characteristics (topological insulator and bandgap tuning by applying an electric field) originating from a significant spin-orbit interaction and the buckled structure. Many researchers successfully synthesized germanene using vapor deposition or surface segregation methods on metallic surfaces. However, graphene-analogous on the metallic surfaces is theoretically predicted that the Dirac cone is destroyed. Therefore, a new approach is strongly required to clarify the intrinsic properties of germanene experimentally. Under such a background, we have theoretically proposed a new method to synthesize germanene nanosheets from hydrogen-terminated germanene (GeH) and experimentally demonstrated it. This paper presents an experimental window that allows hydrogen desorption without destroying the crystal structure, which could be made possible by using heating under an ultrahigh vacuum ambient.

489. Monolithic Integration of Eu-doped GaN/InGaN Quantum Wells for Full-color Micro-LEDs with Enhanced Red Emission

Fujiwara Yasufumi^{1 2}

1 - Ritsumeikan University (Japan), 2 - Osaka University (Japan)

Monolithic integration of RGB primary colors is a crucial technology for achieving micro-LED displays with ultra-small size, full-color capability, and high definition. We have demonstrated a full-color LED utilizing Eu-doped GaN and InGaN quantum wells on a single sapphire substrate [1]. This LED exhibited an exceptionally wide color gamut, covering 105.5% of the area and 91.2% of the Rec. 2020 standards at its peak, while achieving a maximum luminance exceeding 10,000 cd/m². While this luminance is sufficient for VR applications, further enhancement of red LED luminance is essential for AR applications. Eu doping in GaN typically results in at least eight different local configurations that affect emission efficiency. Growth at a relatively low temperature, such as 960°C, allows for high Eu doping concentrations but also promotes Eu clustering due to its low diffusion coefficient, leading to the formation of inefficient luminescent sites. Post-growth thermal annealing at higher temperatures induces structural changes that convert inefficient sites into efficient ones. For example, annealing at 1100°C increased luminescence efficiency by up to 5.1 times compared to the as-grown sample [2]. Incorporating this annealing technique into LEDs resulted in a significant improvement in electroluminescence intensity. The substrate's surface orientation also plays a critical role in Eu center formation. On semipolar substrates, such as (20-21), efficient Eu centers preferentially form, resulting in sharper spectra and markedly improved emission intensity, as evidenced by enhanced output power in the LEDs. [1] S. Ichikawa, Y. Fujiwara et al., Appl. Phys. Express 14, 031008 (2021). [2] T. Iwaya, Y. Fujiwara et al., Appl. Phys. Lett. 122, 032102 (2023).

Keywords : Micro, LED, Display, Eu, doped GaN, Red LED

490. Precision metal patterning via femtosecond laser-induced thermochemical reaction without excessive precipitation from glyoxylic acid metal complex solution

Mizoshiri Mizue ¹

1 - Nagaoka University of Technology (Japan)

Direct writing using femtosecond laser pulse-induced multiphoton absorption has attracted significant attention in micro-additive manufacturing and printing. Initially, this technique enabled the fabrication of three-dimensional microstructures from photopolymer, organic/inorganic hybrid materials, and noble metals such as gold and silver through photochemical reactions. However, applying this method to common metals like copper and nickel remains challenging due to their low precipitation rates. To overcome this limitation, we developed a direct writing based on multiphoton absorption-induced thermochemical precipitation. Using glyoxylic acid metal complex solutions as raw materials, we successfully precipitated copper, nickel, cobalt, and their alloys to form patterned structures. However, thermal diffusion led to an expansion of the precipitation areas. In this presentation, we investigated the effects of surfactant and capping polymer additives on metal patterning. By introducing n-decanoyl sarcosine sodium salt, we controlled precipitation, ensuring that the diameter of the copper dots matched the laser spot size. In contrast, dots formed without the surfactant were more than three times larger due to excessive thermal diffusion. These findings suggest that the surfactant inhibited excessive copper precipitation by reducing the growth rate. These findings suggest that the surfactant inhibited excessive copper precipitation by reducing the growth rate. Furthermore, transient precipitation phenomena were analyzed using an open-aperture z-scan method with varying pulse numbers and a pump-probe technique. The z-scan curves revealed copper nanoparticle formation in the early precipitation stage, consistent with the pump-probe traces. These results demonstrated that surfactant-assisted thermochemical precipitation improved precision in direct metal writing using femtosecond laser pulses.

Keywords : Femtosecond laser, multiphoton absorption, thermochemical reaction, metal precipitation, direct writing

491. Robust high-capacity all-solid-state Lithium-ion batteries enabled with nanoparticulate anodes produced by plasma spraying

Kambara Makoto¹, Kyutoku Sora ¹, Hagiwara Tsubasa ¹, Tanaka Toshimi ², Dougakiuchi Masashi ³

1 - Osaka University (Japan), 2 - Takeuchi Electric. Co. Ltd. (Japan), 3 - Shimane Institute for Industrial Technology (Japan)

Silicon nanoparticle is the promising candidate for anode of high density lithium ion batteries (LiB) as it possesses high theoretical capacity and attains high cyclability. Its nanostructure, however, conversely contains high oxygen content per unit mass due to its high specific surface area and hence increases the irreversible phase amount deteriorating the initial coulombic efficiency and the cycle capacity eventually. Furthermore, the nanoparticle with oxidized surface in general tends to aggregate and hinders the homogeneous particle dispersion in the less-polar organic slurry electrodes which is necessary for stable mixture with sulfuric solid electrolyte. The resultant inhomogeneous electrode structure is considered as the main cause for the decrease in the battery cyclability. Therefore, these nanoparticles are to be produced with suppressed oxidation during synthesis while maintaining the nanosizing of the particles. Even so, from the production perspective, to meet the quantity demands from the ever-growing EV market, nanoparticles have to be produced by high throughput method using affordable raw materials. With these in mind, we have successfully produced silicon nanoparticles with suppressed oxidation by plasma spray from low-cost powder feedstock at throughputs, by introducing the retarded oxidation process after nanoparticle production. Furthermore, based on the thorough analysis of the surface free energies of nanoparticles and various organic regents, we have successfully produced homogeneous electrodes, which exhibit unique structural robustness after battery repeated reactions, resulting in higher capacity and better cyclability. Details of these structural formation and the battery performance will be discussed at the presentation.

Keywords : nanoparticles, lithium, ion batteries, plasma spray

492. Surface Chemical Modification of BaTiO₃ Nanocubes for Controlling Physical-Chemical Functions

Sekino Tohru¹, Cho Yonghyun¹, Kondo Yoshifumi¹, Seo Yeongjun¹, Cho Sunghun¹, Goto Tomoyo²

1 - SANKEN, Osaka University (Japan), 2 - Institute for Advanced Co-Creation Studies, Osaka University (Japan)

Nanostructured oxides have attracted much attention due to their various functions developed through the synergy of physical-chemical properties, nanoscale-size and morphology-driven functionalization. In addition, surface chemical structures are important characteristics and might act as an origin of unique and superior properties and functions, because of higher surface to volume ratio than large bulk materials. In this paper, surface modification of nanostructured oxides by small organic molecules for BaTiO₃ nanocube (BTNc) have been attempted to control, enhance and add properties to nanostructured oxides. BTNc was obtained by the controlled hydrothermal method in aqueous solution with an addition oleic acid and tert-butylamine. Size-controlled nanocube-shape with a size of around 25-35 nm were achieved. FT-IR analyses revealed that the oleic-acid (OA) was immobilized on the surface of the BTNcs. Our strategy in this study is to control chemical and/or physical properties of the BTNcs and to add self-assembling functions to the nanocubes using immobilized surface molecules. Thus, the surface OA ligands was replaced to the other molecules such as dihydroxybenzoic acid and dopamine by the ligand-exchange protocol. The dispersibility of modified BTNcs to water or toluene, and the powder colour was changed by the kinds of surface-immobilized molecules, which indicated the energy-transfer between the ligands and BTNcs due to the strong chemical bond formation. According to the surface modification as well as controlled-size of BTNcs, regularly-ordered nanocubes could be obtained when the suspension was dried. Detailed morphological, chemical and physical-chemical properties and their correlations for the surface-modified BT nanocubes will be discussed.

Keywords : BaTiO₃, Nanocubes, Surface Immobilization, Ligand Exchange, Ordering, Charge Transfer

493. Transient phenomena in additive manufacturing of Ni-base alloys investigated by synchrotron X-ray scattering

Wahlmann Benjamin ¹

¹ - Department of Materials Science and Engineering, Institute II: Materials Science and Engineering for Metals (WTM), Friedrich-Alexander-Universitat Erlangen-Nurnberg (FAU), Martensstr. 5, 91058, Erlangen (Germany)

Additive manufacturing (AM) by powder bed fusion is a highly non-equilibrium process due to the rapid local heating and cooling caused by a moving heat source. While laser (PBF-LB) and electron beam powder bed fusion (PBF-EB) have become established manufacturing methods, there are still challenges in the defect-free processing of several hard-to-weld alloys, such as Ni-base superalloys. These challenges are directly related to the extreme thermal conditions: high thermal gradients cause residual stresses, and repeated thermal cycling leads to solid-state metallurgical reactions. To control the properties of an AM part, it is therefore necessary to understand how the mechanical and metallurgical state evolves during the processing. In this contribution, we investigate the kinetics and dynamics of the gamma/gamma prime phase transformation in a Ni-base superalloy by small-angle X-ray scattering under near-PBF-EB conditions using physical simulations and in PBF-LB using a custom sample environment. Furthermore, the evolution of strains and texture is investigated using wide-angle X-ray scattering within the printing of a single layer and over multiple layers in PBF-LB. A method for separating thermal and elastic strains is introduced and verified using thermo-mechanical modeling of the PBF-LB process. Finally, the obtained insights inform a model for cracking in Ni-base superalloys in AM.

Keywords : Synchrotron X ray diffraction, Additive manufacturing, Ni base superalloys, Thermo mechanical modeling

494. Accuracy Study on X-ray Stress Measurement using Fourier Analysis of Debye-Scherrer Ring

Ejiri Shouichi¹, Ohba Hiroaki ², Sasaki Toshihiko ³

1 - Iwate Medical University (Japan), 2 - Kanagawa Institute of Technology (Japan), 3 - Kanazawa University (Japan)

Conventionally, the $\sin^2 \psi$ method has been used as X-ray stress measurement. However, in recent years, the 2D method and $\cos \alpha$ method have been put into practical use and spreading. In addition, Fourier analysis method that shares the same measurement principle of the $\cos \alpha$ method has been developed and is attracting attention.

Therefore, in this paper, the Fourier analysis method is examined from the measurement theory and the measurement accuracy is investigated. It is reviewed that the basic equation is a finite Fourier series, and that stress can be determined from the Fourier coefficient by using coordinate transformations. Then, while comparing it with other methods, the accuracy of the Fourier analysis method is discussed by using numerical calculations.

Keywords : X, ray stress measurement, Fourier analysis, Debye Scherrer ring, cos alfa method, Two dimensional Detector

495. Observation of Impact Fracture on Heterogeneous Nanostructured Stainless Steel and Titanium by Using Synchrotron Radiation

Kobayashi Masakazu¹, Oba Yojiro ¹, Miura Hiromi ¹, Watanabe Chihiro ², Furuta Shogo ¹

1 - Toyohashi University of Technology (Japan), 2 - Kanazawa University (Japan)

Impact testing machine for in-situ observation on the beam line in SPring-8 has been developed to investigate high-speed deformation and fracture in heterogeneous nanostructured stainless steel and titanium. The load was applied to a specimen by impact of dropping weight and was measured by strain gauge via signal conditioner. Synchrotron radiation (SR) experiment was carried out at beam lines 20B2 and 47XU with X-ray energy of 25 - 40 keV in SPring-8. 2D detector, which is visible-light conversion type consisting of scintillator, optics lens and high-speed camera, was utilized for high-speed X-ray imaging of 50000 fps. A set-up for taking X-ray computed tomography was also installed on the beam line to observe internal voids caused by deformation on failure samples. As an additional measurement instrument, X-ray diffraction (XRD) was tried to monitor by using 2D detector during impact fracture test. This study successfully employed a custom-built testing machine and an X-ray high-speed camera system for in-situ observation of the impact fracture of heterogeneous nanostructured materials through X-ray transmission. The impact tensile tests revealed distinct differences in fracture processes based on the direction of specimen extraction. Under impact loading conditions, it became evident that the current time resolution was insufficient to detect lattice strain changes within the rapid deformation and fracture times observed in the X-ray transmission in-situ measurements. To overcome this limitation, it is imperative to enhance the X-ray flux or improve the sensitivity of XRD detectors. Given the constraints of X-ray intensity, the development of more advanced local XRD measurement detectors is essential.

Keywords : Impact test, High speed, In situ observation, Synchrotron radiation, Stress measurement, X ray Tomography

496. How rapid quenching and reheating influences phase transformations in advanced gamma-TiAl alloys

Stark Andreas ¹

¹ - Helmholtz- Zentrum Hereon (Germany)

Intermetallic gamma-TiAl based alloys have been successfully introduced as structural materials for turbine blades in civil jet engines. Now additive manufacturing (AM) processes are considered as an additional manufacturing route to expand the range of their use. A challenge of AM processes are the very fast cooling and heating rates that enforce phase transformations far away from chemical and thermodynamic equilibrium. These transformation pathways are difficult to understand using conventional analysis methods solely based on the resulting microstructures. In contrast, in situ high-energy X-ray diffraction experiments, using synchrotron radiation, enable a highly time-resolved and direct observation of the evolution of phases during processing. We studied this dynamic process, using a quenching dilatometer (DIL805 A/D) modified for working in the Hereon run HEMS beamline of the Petra III synchrotron radiation source at DESY. Quenching rates in the range of -500 K/s result in massively transformed tetragonal gamma-TiAl phase or even freeze in the high temperature hexagonal alpha/alpha₂ phase. During reheating several reordering and transformation steps take place in different temperature ranges, like orthorhombic distortion of the supersaturated alpha₂, complete transformation of quenched alpha₂ to massively transformed gamma, or formation of new alpha₂ with different lattice parameters. Based on this results, special processing parameters can be recommended for AM processes to allow chemical equilibration in the produced gamma-TiAl parts.

Keywords : synchrotron radiation, X, ray diffraction, intermetallics, gamma, TiAl based alloys, additive manufacturing

497. In-Operando Analysis of Carbide Formation and Stress Generation during Low Pressure Carburizing by High-Energy Synchrotron X-ray Diffraction

Epp Jeremy^{1 2}, Tapar OguN Baris ¹, ZuRn Michael ³, Gibmeier Jens ³,
De F. Silveira Antonio Carlos ¹, Steinbacher Matthias ^{1 2}, Schell
Norbert ⁴

1 - Leibniz Institute for Materials Engineering - IWT (Germany), 2 - MAPEX Center for Materials and Processes (Germany), 3 - Karlsruhe Institute of Technology, Institute for Applied Materials (IAM) (Germany), 4 - Institute of Materials Physics, Helmholtz-Zentrum Hereon (Poland)

Low pressure carburizing (LPC) is a thermochemical process which modifies the chemical composition of the near-surface region of the material through carbon enrichment. While LPC is already used in industry, there are still aspects that offer opportunities for optimization. The present study aims to quantify the effect of LPC process parameters on the resulting material state of different steel grades. For this purpose, carburizing and quenching were examined spatially and timely-resolved using self-built process chamber specifically designed for in-operando synchrotron X-ray diffraction experiments. These investigations were conducted at the German Electron Synchrotron (DESY) facility in Hamburg, Germany. During the carbon enrichment phase, carbon saturation and subsequent carbide formation were observed experimentally, which slowed the acetylene decomposition at the surface. Carbides initially formed at the surface during the enrichment steps began to dissolve during subsequent diffusion steps. The kinetics of carbide formation and dissolution were found to depend significantly on the steel grade and the size of the carbides. Additionally, the evolution of phase-specific stresses during quenching was systematically analysed and experimentally tracked in both surface and subsurface regions. The effect of transformation temperature along the carbon gradient for different carbon depth profiles on the maximum stresses could be observed. Additionally, a direct correlation between the local amount of formed martensite and the generated stresses was identified within the carburized layer.

Keywords : Low Pressure Carburizing, Steel, Heat Treatment, In, situ, in, operando, X, ray Diffraction, Residual Stresses, Stress Generation

498. Structure and dynamics in densified silica glasses

Kohara Shinji ¹

1 - National Institute for Materials Science (1-1-1 Kouto, Sayo-cho, Sayo-gun 679-5148 Japan)

Silica (SiO₂) is a prototypical glass forming material on which numerous studies have been reported. Nevertheless, the mechanism of densification is still not well understood. We synthesized glasses by hot compression at 7.7 GPa and up to 1200 °C. Molecular dynamics and reverse Monte Carlo modelling based on neutron and X-ray diffraction data, followed by topological analyses, suggested that the glass exhibits inter-tetrahedral oxygen-oxygen correlations. Such correlations do not exist in the crystalline phase with a comparable density (α -cristobalite) but are observed in a higher density crystalline phase (coesite). Moreover, topological analyses indicated that silicon-silicon correlations, manifested by the first sharp diffraction peak, and the increased packing fraction of oxygen atoms associated with the ordering of inter-tetrahedral oxygen-oxygen correlations, manifested by the second principal peak, are the origin of densification by a hot compression. Specific heat and X-ray diffraction measurements, supported by inelastic neutron scattering measurements, suggested that the original glass transforms to a glass with a longer correlation length at temperatures greater than 800 °C at 7.7 GPa. The glass synthesized at 1200 °C at 7.7 GPa exhibits a correlation length of approximately 60% longer than the glass with a comparable density synthesized at room temperature at 20 GPa (cold compression).

Keywords : Densified glass, X, ray diffraction, Neutron diffraction, Inelastic neutron scattering, Structure, Dynamics

499. Per-Grain behaviour in polycrystalline alloys during stress induced phase transformations

Collins David¹, Ball James²

1 - Department of Materials Science and Metallurgy [Cambridge University] (United Kingdom), 2 - European Synchrotron Radiation Facility [Grenoble] (France)

To understand the response of a polycrystalline material to deformation, the factors that govern the onset of plasticity for individual grains must be explored. This is particularly true for alloys that possess a stress induced phase transformation, where the grain character and its neighbourhood influence its behaviour. Here, a complex-phase steel alloy is conceived with a deliberately unstable austenite phase that enables the deformation-induced martensitic transformations (DIMIT) to be explored at low levels of plastic strain. The DIMIT was studied, in-situ and non-destructively, using both far-field Three-Dimensional X-Ray Diffraction (3DXRD) and Electron Back-Scatter Diffraction (EBSD). Substantial alpha-martensite formation was observed at low strains with EBSD, and many epsilon grain formation events were captured with 3DXRD, indicative of the indirect transformation of austenite to an intermediary phase, epsilon martensite, before alpha-martensite forms. Using epsilon grain formation as a direct measurement of austenite grain stability, the influence of several microstructural properties, such as grain size, orientation and neighbourhood configuration, on austenite stability have been identified. Larger austenite grains were found to be less stable than smaller grains, and transformed at lower stresses if the {100} planes were parallel to the loading direction. Additionally, parent epsilon forming austenite grains possessed a neighbourhood with increased ferritic/martensitic volume fraction. This finding shows, unambiguously, that the nearby presence of ferrite and alpha-martensite promotes epsilon formation in neighbouring grains. The findings are considered key for the future design of alloys where the deformation response can be controlled by tailoring microstructure and local or macroscopic crystal orientations.

Keywords : 3DXRD, EBSD, stress induced phase transformation, steel, microstructure

500. Observation of a zirconium oxide crystal nucleus in the initial nucleation stage in aluminosilicate glass by X-ray multiscale analysis

Onodera Yohei¹, Takimoto Yasuyuki², Hijiya Hiroyuki³, Li Qing³,
Tajiri Hiroo⁴, Ina Toshiaki⁵, Kohara Shinji¹

1 - Center for Basic Research on Materials, National Institute for Materials Science (Japan), 2 - Innovative Technology Laboratories, AGC Inc. (Japan), 3 - Materials Integration Laboratories, AGC Inc. (Japan), 4 - Scattering and Imaging Division, Japan Synchrotron Radiation Research Institute (Japan), 5 - Spectroscopy Division, Japan Synchrotron Radiation Research Institute (Japan)

Glass-ceramics are composed of precipitated crystals and a glass matrix, which exhibit unique characteristics that are not observed in conventional glasses. To understand the structure of a commercially important glass-ceramic ZrO₂-doped lithium aluminosilicate system during its initial nucleation stage, we conducted an X-ray multiscale analysis by combining diffraction, small-angle scattering, absorption, and anomalous scattering techniques. Element-specific pair distribution function analysis using anomalous X-ray scattering (AXS) data showed the formation of edge-sharing structure between ZrO_x polyhedra and (Si/Al)O₄ tetrahedra during the initial nucleation stage. The edge-sharing polyhedral connection was not a typical structural feature of glass-forming materials; a corner-sharing polyhedral network is formed in typical glass-forming materials, e.g., silica glass. Furthermore, AXS data indicated that the local structure of the Zr⁴⁺ ions, which resembled a cubic or tetragonal ZrO₂ crystalline phase, formed after 2 h of annealing the pristine glass. Therefore, the Zr-centric periodic structure surrounded by the (Si/Al)O₄ tetrahedral network was potentially the initial crystal nucleus for the ZrO₂-doped lithium aluminosilicate glass-ceramic.

Glass ceramics, Pair distribution function analysis, Anomalous X, ray scattering, Nucleation

501. Quantitative Analysis of Complex Defect Structures created by Advanced Manufacturing using X-Ray Diffraction

Balogh Levente¹, Ravkov Lucas ¹, Brown Donald ², Muransky Ondrej³

1 - Queen's University, Kingston, ON, Canada (Canada), 2 - Los Alamos National Laboratory, Los Alamos, NM, USA (Canada), 3 - Australian Nuclear Science and Technology Organisation (Australia)

A variety of manufacturing processes, including novel and disruptive methods such as Additive Manufacturing, frequently yield samples with complex, often metastable features that are difficult to characterize. X-ray scattering data not only reveals the crystal structure but also allows the quantification of crystallographic defects, including dislocations, radiation-induced damage, grain and sub-grain boundaries, as well as twinning and stacking faults. These defects, collectively known as the microstructure, strongly influence the mechanical properties of materials.

This presentation will examine the capabilities of whole-pattern Diffraction Line Profile Analysis (DLPA), a modern approach to microstructure characterization based on first-principle physical models. It will also outline a synchrotron-based X-ray technique that enables precise spatial mapping of defect populations in specimens where these characteristics vary by location. Furthermore, the lecture will address the spatial variation of dislocation structures observed in as-printed Additively Manufactured materials.

Keywords : Additive Manufacturing, Microstructure, Line Profile Analysis, Xray Diffraction, Synchrotron

502. X-ray fluorescence Holography Study on Ferroelectric Materials under an Electric Field

Kimura Koji^{1 2 3}, Toyama Hiroshi¹, Nakashima Seiji⁴, Tajiri Hiroo²,
Iwata Makoto¹, Sekhar Halubai^{1 2}, Happo Naohisa⁵, Hayashi Koichi^{1 2}

1 - Nagoya Institute of Technology (Japan), 2 - Japan Synchrotron Radiation Research Institute [Hyogo] (Japan), 3 - National Institute for Materials Science (Japan), 4 - University of Hyogo (Japan), 5 - Hiroshima City University (Japan)

X-ray fluorescence holography (XFH) is a powerful method to elucidate the local structures of materials by visualizing three-dimensional atomic arrangements around a specific element. XFH has been widely applied to ferroelectric materials, such as $\text{Pb}(\text{Mg}_{1/3}\text{Nb}_{2/3})\text{O}_3$, $\text{Pb}(\text{Fe}_{1/2}\text{Nb}_{1/2})\text{O}_3$, and $(\text{Ba}_{0.9}\text{Ca}_{0.1})\text{TiO}_3$, because the positions, shapes, and intensities of atomic images sensitively reflect the ionic displacements, which are closely related to the ferroelectric properties. To obtain deeper insights into the origin of the ferroelectric properties, it is important to clarify how the constituent ions of ferroelectric materials response to the external electric field at atomic scale. In this study, we performed XFH experiments for $\text{Pb}(\text{Mg}_{1/3}\text{Nb}_{2/3})\text{O}_3$ - PbTiO_3 (PMN-PT) single crystal under an electric field in the SPring-8, Japan. The X-ray fluorescence holograms of Nb, Ti, and Pb were recorded using cylindrical graphite analyzer crystal and avalanche photodiode or silicon drift detector. From the obtained holograms, atomic images were reconstructed using Barton's algorithm. We found positional shifts of atomic images of the cations accompanied by the field-induced polarization inversion, which suggests the difference in the responses of each cation to the external field. Furthermore, we observed variations in the profiles of standing wave lines in the holograms caused by the application of the electric field. From these findings, we will discuss the displacements of the constituent cations in an element-specific manner.

Keywords : X ray Fluorescence Holography, Synchrotron Radiation, Ferroelectric Materials

503. Development of Acoustic Device using Giant Magnetostrictive Material: Consideration on Acoustic Characteristics of Sound Generated by Wall Surface Vibration

Taro Kato¹, Mitsuki Narita², Keishi Iizuka², Saneyuki Abe³, Ryusei Naganuma³, Koki Bando³, Mitsuaki Furui⁴

1 - Department of Mechanical Engineering, and Sustainable Engineering Program, Graduate school of Engineering (Japan), 2 - Department of Mechanical Engineering (Japan), 3 - Sustainable Engineering Program, Graduate school of Engineering (Japan), 4 - Department of Mechanical Engineering, and Sustainable Engineering Program, Graduate school of Engineering (Japan)

The giant magnetostrictive material (GMM) changes sharply due to the magnetic field from outside. The feature of the GMM is high-speed response and high-output energy more than other functional materials. Therefore, the sensors and actuators using GMM have been researched and actively developed in recent years. The author has been studying the interior sound control system for ultra-compact electric vehicles which is one-or two seat. In this study, the most important work is developing the acoustic device for controlling sound. Therefore, we focused on the giant magnetostrictive actuator (GMA) which is small and high output performance. In the previous study, we conducted fundamental consideration on output performance analysis of acoustic devices using GMM. In this paper, we conducted experimental study on sound characteristics by wall surface using manufactured GMA according to previous analytical study. In this experiment, the manufactured GMA was installed on the wall of the experimental equipment, and the output audio signal was analysed frequency of sound to evaluate its acoustic characteristics. In addition, we compared the results between experimental study and previous analytical study. From the result, manufactured GMA output wide range frequency sound. However, the sound quality of low frequency was not good due to the noise. In the design of the GMA, the natural frequency of each element is considered to affect the output characteristics. And we are changing material with higher magnetic permeability.

Keywords : Acoustic Device, Giant magnetostrictive Material, Wall surface Vibration, Output Sound characteristics, Frequency

504. Effect of grain size on shape memory properties of Cr₂₀Mn₂₀Fe₂₀Co₃₅Ni₅ high-entropy alloy

Jeong Hwiyeun¹, Lee Je In ¹

1 - School of Materials Science and Engineering, Pusan National University (South Korea)

Controlling grain size of FCC-based shape memory alloys (SMAs) is important for excellent shape memory effect. Recent findings show that linear relationship between recovery strain and logarithmic grain size, revealing weak dependence of shape recovery properties with grain size. However, very large recovery strain was obtained when the Fe-Mn-Si-Cr-Ni SMAs were cast and annealed to achieve their grain size up to 1000 μm . In the present study, we investigated the effect of grain size on the recovery strains in CrMnFeCoNi high-entropy alloy system. Alloy specimens with a wide range of grain size were fabricated by casting, rolling, and recrystallization annealing. The recovery strain of high-entropy SMAs increased with increasing the grain size due to the decrease of the density of total boundaries. It was found that cast-and-annealed alloy with the largest grain size of 730 μm shows a maximum recovery strain of 4.7 %. To understand the largest recovery strain in the cast-and-annealed alloy, stress-induced martensitic transformation in 5 % tensile-deformed alloys were analysed by EBSD technique. Tensile tests at different temperatures were performed to estimate the critical stress for the martensitic transformation and plastic yielding. We demonstrated that the compositional homogeneity is also an important factor for excellent shape memory effect in cast CrMnFeCoNi high-entropy alloys. These results suggest a guideline for designing optimal microstructure of FCC-based shape memory alloys in multi-principal element system.

Keywords : Shape memory alloys, High, entropy alloys, Casting, Grain size, Martensitic transformation

505. Microstructures and Properties of Diffusion Layer Formed at Laminated Interface of Alumina-Particle Dispersed Magnesium Laminated Compacts Fabricated by MM/SPS Method

Kawamori Shigehir¹, Nagai Yoshinori ¹, Fujiwara Hiroshi ²

1 - Tamagawa University (Japan), 2 - Ritsumeikan University (Japan)

20/0/20vol% Al₂O₃/Mg laminated spark plasma sintering compacts (20/0/20vol% laminated SPS compacts), which were fabricated by mechanical milling / SPS method, have proved to possess lightweight like that of general practical Mg alloys and higher surface hardness than them. Moreover, the diffusion layer formed at their 0/20vol% layer interface has been found to exhibit high adhesion to the 20 and 0 vol% layers. The microstructures and the characteristics of diffusion layer were investigated using EPMA, XRD and so on. From the results of XRD, the constitutive phases were identified as α Mg and MgO. From the results of microstructure observation and elemental analysis using EPMA at the cross section, the microstructures were presumed to be Al solid-solved α Mg, MgO and needle-like Mg₁₇Al₁₂ generated along the grain boundary of α Mg in the ring-shaped MgO. Furthermore, from the results of microstructural observation and qualitative analysis using TEM of the diffusion layer surface, the needle-like finely dispersed phase estimated to be Mg₁₇Al₁₂ is thought to be generated not only near the α Mg grain boundary but also at the α Mg grain/MgO fine particle interface. The cross-sectional hardness was 145 to 155 HV and was higher than that of the AZ91D Mg alloys. The width grew almost linearly rather than parabolic with the passage of sintering time. It is considered that the solid-state reaction of Mg and Al₂O₃ was promoted with the passage of the sintering time, and the amount of Al dissolved from Al₂O₃ increased, so that the diffusion amount of Al increased.

Keywords : 0vol% Al₂O₃/Mg laminated spark plasma sintering compacts, microstructures, diffusion layer, hardness of diffusion layer, growth behavior of diffusion layer width

506. Machine learning multi-objective optimization design multi performances of Zn alloys and Mg alloys

Gou Wei^{1 2}, Shi Zhang-Zhi^{1 2}, Wang Lu-Ning^{1 2}

1 - Beijing Advanced Innovation Center for Materials Genome Engineering, State Key Laboratory for Advance Metals and Materials, School of Materials Science and Engineering, University of Science and Technology Beijing, Beijing 100083, China (China), 2 - Institute of Materials Intelligent Technology, Liaoning Academy of Materials, Shenyang 110004, China (China)

Conventional trial-and-error method is usually time-consuming and expensive for multi-objective optimization of alloy design. Although machine learning exhibits the great potential to accelerate related researches, machine learning prediction is often a single prediction of different performances. To address this, we integrates NSGA III multi-objective optimization algorithm with traditional machine algorithm to simultaneously optimize multi performances of Zn alloys and Mg alloys. This machine learning method can simultaneously achieve multi-objective optimization with more than three target properties and interpretability analysis for alloy design. This method greatly reduces the cost of trial-and-error method and significantly accelerates development cycle, which directly provides guidance for the design of various properties based on the expected performance.

Keywords : Zn alloys, Mg alloys, machine learning, alloy design, multi, objective optimization

507. Relationship between deformability and crystalline system of martensite phase in Au-Cu-Al

Matsuoka Yuki¹, Yamamoto Wakana², Kubo Kyoko², Han Dong-Keun^{3 4}, Nohira Naoki^{4 3}, Hosoda Hideki^{4 5}

1 - Faculty, Division of Natural Science, Nara Women's University (Japan), 2 - Graduate school of Humanities and Science, Nara Women's University (Japan), 3 - Laboratory for Future Interdisciplinary Research of Science and Technology, Institute of Integrated Research, Institute of Science Tokyo (Japan), 4 - Laboratory for Materials and Structures, Institute of Integrated Research, Institute of Science Tokyo (Japan), 5 - Laboratory for Future Interdisciplinary Research of Science and Technology, Institute of Integrated Research, Institute of Science Tokyo (Japan)

We report the composition dependence of deformability for Au-Cu-Al martensitic alloy, in quasi 2D system; $\text{Au}_{50-x}\text{Cu}_{25}+\text{xAl}_{25}$. The ideal $L2_{11}$ structure of $\text{Au}_{50}\text{Cu}_{25}\text{Al}_{25}$ easily ruptured at the grain boundaries in tensile test, but as Au was replaced by Cu, it became less likely to rupture, while it was less likely to strain. However, the deformability does not monotonically decrease with substitution. In some cases there is a reversal with respect to the elemental composition ratio. This may be attributed to the effect of the crystalline system of the martensite phase. The specimen is easily distorted in compositional regions where the beta phase transforms to the single orthorhombic martensite phase, while less easily distorted in compositional regions where the beta phase transforms to the single monoclinic martensite phase. In compositional regions where orthorhombic and monoclinic martensite phases coexist, the higher the substitution ratio from Au for Cu, the higher the ratio of monoclinic martensite phase, and as a result, the less susceptible to distortion under stress. If we discuss only the relationship between the crystalline system of the martensite phase and the modulation of atomic positions, for the same crystalline system of the martensite phase, the higher the substitution ratio from Au to Cu, the greater the modulation tends to be. Therefore, modulation can be considered a factor that hinders deformability. However, in Au-Cu-Al, the compositional regions where the two martensite phases coexist are not clearly separated, so a final conclusion cannot be reached without clarifying this cause.

Keywords : martensite, Au based alloy, stress strain curve, modulation

508. Formulation of chitosan-based resists for an optimized eco-efficient photolithography process: focus on the ToF-SIMS characterization

Rani Dipti^{1 2}, Gablin Corinne¹, Ferrer Magin Benedict^{3 4}, Virieux Kylian⁵, Servin Isabelle⁶, Foscolos Angeliki Sofia⁷, Trombotto Stephane⁵, Soppera Olivier^{3 4}, Soultati Anastasia⁷, Vidali Veroniki P.⁷, Argitis Panagiotis⁷, Chevolot Yann², Leclercq Jean-Louis², Leonard Didier¹

1 : ISA - Surfaces

Université Claude Bernard Lyon 1, CNRS, ISA, UMR 5280, 5 rue de la Doua, F-69100 Villeurbanne, France

2 : INL - Dispositifs pour la Santé et l'Environnement

CNRS, Ecole Centrale de Lyon, INSA Lyon, Université Claude Bernard Lyon 1, CPE Lyon, INL, UMR5270, 69134 Ecully, France

3 : Institut de Science des Matériaux de Mulhouse

Université de Haute-Alsace, CNRS, IS2M UMR 7361, F-68100 Mulhouse, France

4 : Université de Strasbourg

Université de Strasbourg, Strasbourg F-67000, France

5 : Ingénierie des Matériaux Polymères

Ingénierie des Matériaux Polymères (IMP), UMR 5223, Université Claude Bernard Lyon 1, CNRS, INSA Lyon, Université Jean Monnet Saint-Etienne, F-69622 Villeurbanne, France

6 : Commissariat à l'énergie atomique et aux énergies alternatives - Laboratoire d'Électronique et de Technologie de l'Information

Univ. Grenoble Alpes, CEA, Leti, F-38000 Grenoble, France

7 : National Centre for Scientific Research "Demokritos" (NCSR "Demokritos"), Institute of Nanoscience and Nanotechnology, 15341 Agia Paraskevi, Athens, Greece

A leading research effort by co-authors has demonstrated the excellent potential of the polysaccharide chitosan as a bio-sourced resist in an eco-efficient photolithography process, one of the major techniques in manufacturing semiconductor devices [1-4]. However further optimization is needed to fully meet the requirements necessary for industrial transfer. This work focuses on the formulating resists with additives, including both commercial and lab-scale synthesized water-processable photo-acid generators (PAGs). Key optimisation parameters include film formation, (D)UV exposure doses and selectivity upon etching plasmas. The use of Time-of-Flight Secondary Ion Mass Spectrometry (ToF-SIMS) characterization (a top-surface mass spectroscopy technique providing molecular information) to support the optimization process is illustrated. This work was supported by the EU project Resist materials for transition to green processing in semiconductor industry (RESIN GREEN), funded from the European Union's Horizon Europe research and innovation program under Grant Agreement No. 101135783. [1] P. Durin et al., JVSTB, 2023, 41⁶, 062204, 10.1116/6.0002934 ; [2] I. Servin et al., Micro and Nano Engineering, 2023, 19, 100202, 10.1016/j.mne.2023.100202 ; [3] O. Sysova et al., Journal of Applied Polymer Science, 2023, 140 (32), e54244, 10.1002/app.54244 ; [4] O. Sysova et al., ACS Applied Polymer Materials, 2022, 4⁶, 4508-4519, 10.1021/acsapm.2c00475

Keywords : ToF, SIMS, Chitosan, Photoacid generator, Photolithography, Ecoefficiency

509. Thermal, Mechanical, and Materials Aspects of a Shape Memory Alloy Stirling Heat Engine

Chikhareva Maria¹, Vaidyanathan Raj ¹

1 - Materials Science and Engineering, University of Central Florida (United States)

Shape memory alloy (SMA) heat engines possess an inherent property of sensing a change in temperature, performing work, and rejecting heat through the shape memory effect resulting from a temperature-induced phase transformation. While SMA heat engines have previously been proposed and demonstrated, there has been a lack of a systematic approach in the comprehensive analysis of SMA heat engines combining materials, mechanical, and heat transfer aspects. Their ability to function in environments where they scavenge free heat that would nominally be wasted has not been utilized. Here a framework for the design and implementation of an SMA-based Stirling heat engine optimized for maximum torque or speed is presented. The framework presented here builds on a previous body of NASA funded work at UCF that has considered SMA thermal switches operating in a make or break contact mode. Mechanical aspects were addressed from force balances in the SMA element and focused on the resulting stress distribution. Thermal aspects considered heat transfer between the SMA element and both the heat source and the heat sink. Materials aspects considered the chemical, elastic, and frictional contributions to the enthalpy of the transformation. The roles of microstructure through composition, precipitates, variant interfaces, training, cycling, texture, defects, nucleation sites (bulk vs. surface), and multi-step transformations (e.g., a trigonal R-phase transformation) in NiTi based-alloys are highlighted. Emphasis is placed on examining the role of plasticity on the phase transformation in such engines and its implications on fatigue life.

Keywords : Shape Memory Alloys, Heat Engine, Stirling, NiTi

510. Mechanical Properties of Au-Cu-Al Dual Phase Alloys for Biomedical Applications

Hosoda Hideki^{1 2}, Goo Kang Wei, Nohira Naoki, Chiu Wang-Ting, Tahara Masaki

1 - Laboratory for Future Interdisciplinary Research of Science and Technology, Institute of Integrated Research, Institute of Science Tokyo (Japan), 2 - Laboratory for Materials and Structures, Institute of Integrated Research, Institute of Science Tokyo (Japan)

Au-Cu based alloys are fascinating not only for jewelries but also for industrial applications. Among the apparent phases in the Au-Cu based system, α (fcc) terminal solid solution (Au, Cu) is commonly used as gold alloys, and an intermetallic phase of β -type (L21 or its martensite phase) Au₂CuAl is attractive due to its shape memory effect and superelasticity, high corrosion resistance, high X-ray imaging, and MRI-artifact-free visibility. In order to develop Au-Cu based alloys, we have focused α and β dual phase Au-Cu-Al alloys. Then, the enhancement of mechanical properties towards biomedical applications is investigated by controlling phase fraction. As for α -phase based dual phase alloys, introduction of β phase is considered to enhance elongation from the viewpoint of "twin-induced plasticity (TWIP)" and/or "transformation induced plasticity (TRIP)". On the other hand, as for β -phase based dual alloys, introduction of soft fcc phase is considered to enhance ductility from the viewpoint of "ductile phase toughening (DPT)". Three series of alloys are systematically prepared: ¹ Au-(31~44)Cu-12Al, Au-(36~38)Cu (12~14)Al, and Au-30Cu-(13~14)Al (mol%). Mechanical properties are evaluated by tensile tests at room temperature. It is found that dual phase alloys exhibit good balance of tensile ductility and strength. For example, Au-30Cu-13Al (major phase is α fcc, minor phase is β martensite, and α/β ratio is 3.0) showed elongation of 25% and ultimate tensile strength of 680MPa, and Au-38Cu-12Al alloy (major phase is β martensite, minor phase is α fcc, and α/β ratio is 0.85) showed 34% and 674MPa, respectively

Keywords : mechanical properties, Au, Cu, Al, dual phase, martensite, fcc, tensile strength, elongation

511. Application of electron beam welding in the production of TEMPALLOY AA1 and T92 butt joints of pipes assigned for the energy industry

Krzysztof Kwiecinski *, Hanna Purzynskav, Michał Urzynicok, Adam Zieliński

Łukasiewicz – Upper Silesian Institute of Technology, ul. K. Miarki 12-14., 44-100 Gliwice, Poland. , V
Łukasiewicz – Upper Silesian Institute of Technology, ul. K. Miarki 12-1444-100 Gliwice, Poland. , +
ZELKOT, Nowy Dwór 8, 42-286 Koszęcin, POLAND. ++Łukasiewicz – Upper Silesian Institute of
Technology, ul. K. Miarki 12-1444-100 Gliwice, Poland.

One of the main problems with the use of steels for elevated temperatures is their limited weldability. This is mainly due to the fact that these materials may contain in their chemical composition. Due to the susceptibility to cold cracking, PWHT is necessary, especially in high-stiffness welded structures. In addition, depending on the condition after heat treatment or in the absence of heat treatment, precipitates may appear in the microstructure of the steel, affecting its mechanical properties. It is important in this case to ensure the high quality of welded joints, which means that the manufacturer has to demonstrate a very high technical culture. Currently, thin-walled pipe butt joints are welded manually using a tungsten electrode with solid wire material (TIG method). One of the solutions that can significantly speed up the welding process of components for work at elevated temperatures is the use of an electron beam welding. In addition, the ability to make welded joints without the use of filler material and to achieve narrow heat-affected zones may find application in the welding of modern materials used in the power industry. This paper presents the welding experience of materials assigned for the power industry (TEMPALLOY AA1 and T92) by use of electron beam. In this article authors present the results of tests gained during first steps of welding welded joints. The article also includes preliminary results on the service life of the fabricated joints.

512. Evaluation of Strain Distribution of Perforated Sheet in Circular Cup Deep Drawing

Yoshihara Shoichiro¹, Nakagawa Tomoki¹, Hasegawa Osamu²,
Nishimura Hisashi³

1 - Shibaura Institute of Technology (Japan), 2 - Tokyo Metropolitan College of Industrial Technology (Japan), 3 - Tokyo Metropolitan University (Japan)

Perforated sheets of metal with numerous holes made by the punching process are used for various purposes from automotive parts to daily kitchen products in terms of ventilation, soundproofing, sound and light shielding, and weight reduction. However, plastic forming of thin metal sheets has generally been limited to materials of uniform thickness and quality, and has not been the subject of technological development or research. Most of the current products have flat shapes or are bent, and there are few precedents of machining methods that apply strong forces to the hole edges. In the drawing process in which a strong force is applied to the hole edge, changes in tensile and compressive deformation are caused by a discontinuity in deformation resistance, resulting in non-uniform sheet thickness products due to a mixture of deformation in the hole and no deformation in the sheet. Therefore, clarification of the drawing processing characteristics of perforated sheets will lead to progress in plastic forming. In this report, deep drawing was performed using punching sheets with different hole diameters and pitches, and the effects of hole diameter and pitch on formability and thickness strain were investigated. Specifically, circular cup deep drawing was performed using punching sheets with different hole diameters and pitches in mild steel sheet SPCC and annealed aluminum sheet A1100-O to investigate formability and thickness strain. As a result, this suggests that there are optimal material conditions that can suppress wall thinning depending on the hole diameter and pitch of the punching sheet.

Keywords : Circular Cup Deep Drawing, Perforated Sheet, Strain Distribution, mild steel sheet SPCC, annealed aluminum sheet A1100, O

513. Enhancing Mechanical Properties of Mg-Zn-Ca Alloys via Texture Modification in Multi-Pass Constrained Friction Processing

Chen Ting¹, Fu Banglong ¹, Suhuddin Uceu ¹, Dos Santos Jorge ²,
Bergmann Jean Pierre ³, Klusemann Benjamin ^{1 4}

1 - Solid State Materials Processing, Institute of Material and Process Design, Helmholtz-Zentrum Hereon (Germany), 2 - Applied Materials and Manufacturing, Energy and Environment Division, Pacific Northwest National Laboratory (United States), 3 - Production Technology Group, Technische Universität Ilmenau (Germany), 4 - Institute for Production Technology and Systems, Leuphana University Lüneburg (Germany)

Constrained Friction Processing (CFP), an innovative friction-based technique, has been developed to efficiently fabricate fine-grained magnesium (Mg) rods, broadening the scope of biodegradable Mg alloys for medical implant applications. This study explores the enhancement of mechanical properties achieved through multiple-pass CFP (MP-CFP) compared to conventional single-pass CFP. The findings demonstrate significant improvements in compressive yield strength (CYS), ultimate compressive strength, and failure plastic strain, with increases of 11%, 28%, and 66%, respectively. A detailed investigation into the material evolution during processing revealed that the final plunge stage of MP-CFP induces intricate material flow, resulting in a notable reduction in the intensity of local basal texture and macrotexture. This texture weakening, combined with a reduced geometrical compatibility factor at the top of the rod, effectively hinders slip transfer across grain boundaries. The resulting local strain gradient along the compression direction is a key factor in the observed enhancement of mechanical properties. Following texture modification via MP-CFP, the ZX00 alloy exhibits a competitive SYS compared to traditional processing methods, underscoring the potential of MP-CFP for advancing the application of Mg alloys in biomedical engineering.

Keywords : Constrained friction processing, Magnesium alloys, Microstructure, Mechanical properties, Texture.

514. Microstructure evolution in two-step friction extrusion of aluminium alloys

Chan Chang Yin-Cheng¹, Suhuddin Uceu¹, Rana Harikrishnasinh², Klusemann Benjamin^{1 2}

1 - Solid State Materials Processing, Institute of Material and Process Design, Helmholtz-Zentrum Hereon (Germany), 2 - Institute for Production Technology and Systems, Leuphana University Luneburg (Germany)

Friction extrusion (FE) has gained considerable attention in the past decade as an energy-efficient alternative to conventional recycling methods, such as remelting. By utilizing the intrinsic frictional heating generated through the relative rotational motion between the die and feedstock, FE eliminates the need for external heat sources for both pre-heating and processing. Different types of feedstock materials, such as billet, chips and powder, as well as various extrudates, including wires, rods, tubes, and cell structures, have made FE intriguing to researchers. Additionally, the combination of severe plastic deformation coupled with the high-temperature exposure during FE introduces dynamic recrystallization, resulting in a refined microstructure. The refined microstructure offers the capability to achieve high strength while maintaining ductility. As demonstrated in the equal channel angular pressing (ECAP) process, where mechanical properties can be enhanced through multiple passes, a two-step FE experiment is proposed in this study. This approach aims to increase the strain level and further improve the mechanical properties. The evolution of the grain structure both in the material ahead of the die and within the extruded wire are analysed.

Keywords : Friction Extrusion, Solid State Processing, Aluminium, Dynamic Recrystallization

515. Low temperature sintering of ink-spray BST layers for fabrication of an electromagnetic shutter

LabarreRe Hugo¹, Penin Nicolas ¹, Pouliguen Philippe ², Heintz Jean-Marc ¹

1 - Institut de Chimie de la Matière Condensée de Bordeaux (France), 2 - Agence de l'innovation de defense (60 boulevard General-Martial-Valin75015 Paris France)

Ba_xSr_{1-x}TiO₃ (BST) presents excellent dielectric properties in its paraelectric phase, and is widely used in many microwave and RF devices. Furthermore, the dielectric constant can be modified by applying an electric field, making it an ideal material for use as an electromagnetic shutter. To achieve a significant tunable effect, it is essential to deposit the material in the form of thin ceramic layers on a metal circuit. The ink-spray deposition technique is ideally suited to the manufacture of these types of layers. In this process, ink formulation and deposition parameters play a decisive role. We have therefore studied and optimized these points in order to obtain homogeneous layers with a thickness of around 20 micrometers. Moreover, as the deposition is carried out on a metal electrode, the densification of the BST must occur at a temperature below the melting point of the metal used. We have therefore chosen to use a co-sintering additive that enables liquid phase sintering at low temperature and has little effect on dielectric properties. Several additives and compositions have been identified from the literature as suitable for this purpose. Their influence on the sintering behavior and dielectric properties of the BST thus prepared was compared using the same parameters, in order to identify the best additive.

Keywords : BST, ink, spray, aqueous suspension, deposition, liquid phase sintering, dielectric properties

516. Forming of Multifunctional Corrugated Cup using Roller Ball Die

Harada Yasunori¹, Okada Shota

1 - University of Hyogo (2167 Shosya, Himeji, Hyogo 6712280 Japan)

To produce functional cups by press forming, clad cups with a corrugated structure with voids like the cross section of corrugated cardboard were formed. Deep drawing, which is one type of press forming, is a plastic processing technology that forms thin sheets into three-dimensional containers. In the experiment, pure titanium TP270 and low carbon steel SPCC were used as test materials. The blank sheet thickness was 0.3 mm and the diameter was 80 mm to 90 mm. To form the corrugated cup, the roller ball die with steel balls installed on the shoulder of the die was prototyped. The steel balls were made of bearing steel SUJ2 and had diameters of 6.4 mm and 7.5 mm. The corrugated clad cup was formed by the composite die combined with a conventional die. Three conventional dies and two roller ball dies were used to obtain two corrugated layers with voids. The lubricant was a tool oil containing molybdenum disulfide powder. The sheet thickness strain distribution and residual stress distribution of the cup were evaluated. No destruction of the cup occurred during deep drawing. A regular wavy structure was observed in the cross section of the cup. The maximum reduction in the cup thickness was approximately 10 %. The residual stress on the outside of the cup was tensile stress from the bottom to the opening of the cup. The composite die made it possible to form a functional cup.

Keywords : Sheet Forming, Deep Drawing, Formability

517. In-situ observation and quantitative evaluation of dendritic silver precipitates growth inside borosilicate glass substrate

Kono Miyuka¹, Kawamura Hirofumi ², Matsusaka Souta ¹, Itoh Sho ¹,
Hidai Hirofumi ¹

1 - Chiba University (Japan), 2 - Nagaoka University of Technology (Japan)

The high-voltage application to silver ion-doped borosilicate glass induces the growth of silver dendritic crystals inside the substrate. As these precipitates exhibit high electrical conductivity, this phenomenon holds significant potential for applications such as buried electric circuits and fine-hole drilling. However, understanding the underlying mechanism of this unique phenomenon is essential for its practical utilization. In this study, we conducted in-situ observation and quantitative evaluation of the silver dendrite growth, focusing on the areal growth rate. Voltage application along the longitudinal direction of the silver ion doped region significantly enhanced growth of silver dendrites was achieved compared to conventional methods. This enhancement facilitated in-situ observation of their growth, enabling the evaluation based on the areal growth rate. The measurements revealed that the growth rate accelerated as the growth progressed and increased with higher temperatures and voltages. The model proposed here, which assumes the specimen as the combination of the variable electric resistors, explained the observed change in the silver growth rate over time and under different experimental conditions. These changes are attributed to the variations in the electrical resistances of the specimens and difference in the flux of the silver ions. This study provides valuable insights into the mechanism of silver dendritic precipitate growth inside glass, enabling the formation of arbitrary shapes of in-glass silver.

Keywords : Dendritic metal growth, Borosilicate glass, In situ observation, Silver, Glass processing

518. Eliminating the Need for Post-Forming Annealing: Advancements in NSF Technology for Austenitic Stainless Steels

Murillo Alberto¹, Damilola-Sunday John ¹, Krawec Phillip ², Garcia Eduardo ¹, Slater Carl ²

1 - Department of Mechanics, Design and Industrial Management, University of Deusto, Avda Universidades 24, 48007 Bilbao, Spain (Spain), 2 - WMG, University of Warwick, Coventry CV4 7AL, UK (United Kingdom)

Hot forging complex geometries typically requires multiple high-capacity press operations, diverse tooling, reheating, and post-process annealing. Near Solidus Forming (NSF) technology offers an innovative approach by raising material temperatures close to the liquid-solid transition. This hybrid extrusion-forging process reduces mechanical loads and enables precise single-stage, closed-die forging. NSF holds potential to achieve microstructural stability without subsequent annealing, especially in austenitic stainless steels such as AISI 316, which derive strength from dynamic recrystallization (DRX), grain boundary strengthening, and deformation mechanisms. In this study, NSF's feasibility through high-temperature compression tests near the liquidus temperature was analysed. Custom dies were designed for forming tests on a hydraulic press. Embedded thermocouples monitored thermal exchange, while deformation stages were analyzed through samples taken from central, intermediate, and die-contact regions. These samples were evaluated for grain size, distribution, and boundary orientation. Finite element simulations, validated by experimental results, were employed to predict microstructural evolution under varying conditions. Preliminary results indicate NSF produces distinct microstructural gradients influenced by thermal and mechanical loads, with DRX contributing to stress relief and grain refinement. Thermal data from dies provided critical insights into temperature distribution and cooling rates, essential for mapping microstructural changes and residual stress profiles. This work highlights NSF's potential to deliver homogeneous microstructures in single-stage forging, reducing process complexity and eliminating annealing. Findings could improve forging techniques for complex geometries, improving efficiency and material performance.

Keywords : Near solidus forming, Microstructure, Stainless steel, DRX, Post, forming Annealing

519. Development of advanced tool pin geometries for Friction Stir Spot Welding (FSSW) by means of Selective Laser Melting (SLM)

Garcia-Gil Eduardo¹, Varas InIgo ¹, Murillo-Marrodan Alberto ¹,
Achiaga Beatriz ¹

1 - Department of Mechanical, Design and Industrial Engineering, University of Deusto (Spain)

Friction Stir Spot Welding (FSSW) is a well-known solid-state joining technique that has had a significant impact on industries such as automotive and aerospace over the last decade. The quality and performance of FSSW joints depend on several factors, one of the most critical being the geometry of the pin tool, as it directly influences frictional heat generation and material stirring—both key aspects of the joining process. This work investigates the effect of tool pin geometry on the joining of polypropylene (PP) plates using FSSW, leveraging the flexibility of Additive Manufacturing technology. Various tool pin geometries were fabricated using Selective Laser Melting (SLM) with AISI 316L stainless steel. The versatility of SLM enabled the evaluation of multiple geometrical parameters, including pin length, pin design, shoulder dimensions and design, and shoulder surface shape. Throughout the study, the pin tool geometries evolved from simple designs to intricate combinations of shoulder and pin shapes. While the simpler geometries validated existing literature findings regarding the influence of pin length and shoulder diameter on heat generation and joint depth, the SLM process allowed for the creation of more complex pin designs—such as conical, fir-tree, and helical pins—integrated with convex winged shoulders. These new designs improved the control of heat generation, the allocation of the stirred material in the joining zone and the stirring effect of the pin, favouring, thus, the joining process

Keywords : Solid State Joining, FSSW, Additive Manufacturing, SLM, Tool Pin Geometry

520. Improving sintering ability of alumina through gel casting process

Heintz Jean-Marc¹, Gauzere Laurie ^{1 2}, Besnard-Pontoreau Clemence², Couillaud Samuel ²

1 - Institut de Chimie de la Matiere Condensee de Bordeaux (France), 2 - Galtenco Solutions (France)

In recent years, significant progress has been made in the production of dense ceramics with complex shapes. Research has primarily focused on thermal cycles and novel sintering techniques, including cold-sintering and additive manufacturing. However, ensuring the uniformity of the green parts remains a crucial aspect in controlling and reducing sintering temperatures. This presentation will outline the numerous advantages of gel casting as a cold shaping technique for the production of large or complex shaped ceramic pieces. It is possible to prepare ceramic suspensions with a minimal amount of organic additives and a high ceramic loading (> 50 vol%), which remain sufficiently fluid to be cast into moulds of any shape or size. More specifically, we will demonstrate how an understanding of both the rheological behaviour of the slurry and the polymerisation process affects the granular homogeneity of the green sample. This will be discussed through an investigation of the influence of the chemical composition of the monomer on the characteristics of granular packing in green alumina samples and their subsequent sintering behaviour. Three monomers from the same chemical family were selected for analysis: acrylamide, methacrylamide, and dimethylacrylamide. While minor discrepancies are visible in the green state, they are significantly amplified during sintering, resulting in final densities that differ by over 10%. Finally, it will be shown that by controlling the various stages of gel casting, dense and homogeneous ceramic parts can be obtained, including complex parts.

Keywords : alumina, gelcasting, sintering, microstructure, densification

521. Processing of Amorphous Oxide Semiconductors and Future Prospects

Ide Keisuke ¹

¹ - Institute of Science Tokyo (Japan)

Amorphous oxide semiconductors (AOSs), typically fabricated via magnetron sputtering, are high-performance semiconductors that can be deposited on glass substrates. As low-temperature processable materials, they hold great promise for applications in flat-panel displays (FPDs) and large-scale microelectronics. Among these, a-In-Ga-Zn-O (a-IGZO), a groundbreaking material for AOS thin-film transistors (TFTs), was introduced in 2004 as a channel material compatible with deposition on PET substrates. The following year, a monochrome e-paper employing a flexible TFT backplane made with a-IGZO was announced. Since then, companies around the world have developed prototypes of liquid crystal displays (LCDs) and organic electroluminescent (OLED) displays utilizing this material, leading to commercialization and mass production as early as 2012. This class of materials, also known as transparent amorphous oxide semiconductors (TAOSs), exhibits unique properties that continue to drive global research and development efforts, positioning them as key candidates for next-generation electronic devices. This presentation reviews the optimal processing techniques required for display applications, explores the future prospects of the field, and outlines the history and current status of a-IGZO, including the reasons for its widespread adoption in cutting-edge displays.

Keywords : Sputtering process, Amorphous oxide semiconductor, Electronic defect

522. Experimental Study on the Behavior and Emissions of Methane/Hydrogen Diffusion Flames Under DC Electric Field

Park Daegeun ¹

¹ - Korea Institute of Industrial Technology (South Korea)

The significance of hydrogen as a carbon-free fuel is increasingly emphasized in efforts to reduce greenhouse gas emissions. While the use of hydrogen in combustion processes eliminates CO and CO₂ emissions, it also results in increased thermal NO_x formation due to its high flame temperature. Additionally, blending hydrogen into fuel mixtures can cause instability due to its high diffusivity and rapid flame propagation speed. Such instabilities can decrease combustion efficiency and reduce the effectiveness of emissions control, thereby necessitating technologies for stabilizing methane/hydrogen co-combustion flames and managing exhaust gases. Research on the impact of electric fields on flame behavior and exhaust gas emissions has shown that the direction of the ionic wind is determined by electrode placement, and that ionic winds can enhance flame stabilization and reduce pollutants like soot. This study aims to experimentally investigate the behavior and exhaust gas emissions of methane/hydrogen diffusion flames under the application of a DC electric field. In this study, a coaxial burner was used to form a diffusion flame with methane and hydrogen as fuels and air as the oxidizer. To apply an electric field, high voltage was applied to the flame nozzle, while grounding was done using a mesh placed 10 cm above the nozzle. The results demonstrated that the addition of hydrogen effectively reduced CO and CO₂ emissions, while NO_x emissions varied depending on the presence of instabilities. Applying a negative voltage intensified flame instability and compression, whereas applying a positive voltage stabilized the previously unstable flame. Emissions of CO, CO₂, and NO_x decreased regardless of polarity. Acknowledgment This research was supported by the Ministry of Trade, Industry, and Energy (MOTIE) and the Korea Evaluation Institute of Industrial Technology (KEIT) under the research grant ('RS-2024-00430798')

Keywords : Methane hydrogen combustion, Diffusion flame, Electric field, Emissions control, instability

523. N₂O and NF₃ Reduction and NO_x Emission Characteristics in Methane/Hydrogen Diffusion Flames

Park Daegeun ¹

¹ - Korea Institute of Industrial Technology (South Korea)

Methane and hydrogen are representative fuels with distinct chemical and combustion characteristics. Methane diffusion flames primarily produce CO₂, a greenhouse gas that contributes significantly to global warming. While methane combustion is relatively stable and efficient, its environmental impact raises the need for alternative fuels and new emission reduction technologies. On the other hand, hydrogen diffusion flames are considered an environmentally friendly alternative because they do not produce CO₂ during combustion. However, hydrogen flames burn at high temperatures, which leads to the formation of significant amounts of NO_x, a major concern. NO_x contributes to air pollution and acid rain, making NO_x reduction technologies essential for the effective utilization of hydrogen combustion. N₂O is primarily employed as an oxidizer for nitrogen doping in semiconductor manufacturing, while NF₃ is utilized as a powerful fluorine source in plasma etching and cleaning processes in display manufacturing. Both gases have high global warming potential (GWP), with N₂O being approximately 310 times and NF₃ about 17,200 times more potent than CO₂ in terms of their greenhouse effect. Due to their strong greenhouse impact even at low emission levels, these gases are critical targets for greenhouse gas reduction policies. However, during the removal process of these gases, harmful by-products such as NO_x may be generated. This study aims to compare the NO_x reduction characteristics depending on the injection methods of N₂O and NF₃ in methane/hydrogen diffusion flames and analyze their impact on NO_x formation. The findings of this study will provide foundational data to address key environmental issues in the semiconductor and display industries and guide research toward optimal NO_x reduction methods. Acknowledgment This research was supported by the Ministry of Trade, Industry, and Energy (MOTIE) and the Korea Evaluation Institute of Industrial Technology (KEIT) under the research grant ('RS-2024-00430798')

Keywords : Methane/hydrogen diffusion flame, NF₃ and N₂O Reduction, NO_x Characteristics, Semiconductor and Display industries

524. Thermal Deformation Analysis and Flashback Prevention in Aluminum Body Portable Butane Gas Burners

Park Daegeun ¹

¹ - Korea Institute of Industrial Technology (South Korea)

Since the introduction of portable butane gas burners in the 1970s, numerous manufacturers have continued to develop and market various models. However, these burners intermittently experience thermal deformation and flashback phenomena in the burner body and head during operation, which can lead to serious risks to both human life and property. In response, manufacturers have made continuous efforts to mitigate these issues. The burner body of a portable butane gas burner is typically constructed with a venturi tube that allows ambient air intake, creating a premixed flame. Considering the characteristics of premixed butane flames, it is assumed that flashback can be prevented. In this study, CHEMKIN was used to calculate the propagation speed of butane flames under various conditions: initial temperatures of 20°C, 50°C, 100°C, 200°C, 400°C, and 600°C, with equivalence ratios ranging from 0.6 to 1.4. Additionally, the fuel and air flow rates were measured experimentally to determine the equivalence ratio and the exit velocity at the burner head for actual portable butane gas burners. Flashback occurs when the flame propagation speed exceeds the burner head exit velocity; hence, this study aimed to evaluate the potential for flashback by comparing these two speeds. To assess thermal deformation under overheating conditions, a thermocouple was used to measure and analyze temperatures at the burner head over time. Furthermore, the aluminum alloy of the burner body was qualitatively analyzed using Scanning Electron Microscopy (SEM) and Energy Dispersive Spectroscopy (EDS), and quantitatively analyzed using X-Ray Diffraction (XRD). Acknowledgment This research was supported by the Korea Institute for Advancement of Technology (KIAT) through the Assessment Infrastructure Development for Control Modules in Autonomous Collaborative Manufacturing Process, funded by the Ministry of Trade, Industry, and Energy (Project Number: RS-2024-00469885)

Keywords : Portable butane gas burner, Premixed flame, Flashback, Thermal deformation, Aluminum die casting

525. Phase diagram of Ni-Si-Mn precipitates in reactor pressure vessel steels

Matsukawa Yoshitaka ¹

¹ - Kumamoto University (Japan)

The primary cause of irradiation-induced embrittlement of the reactor pressure vessel (RPV) steel is precipitation of its alloying elements (Ni, Si and Mn) in the form of nano particles (~2 nm). The RPV embrittlement practically limits the service life of the whole reactor; in other words, reactor's lifetime prediction is achieved by predicting the precipitation. Although precipitation under irradiation is a thermodynamically non-equilibrium reaction, recent studies have revealed that precipitation of those elements does occur even without irradiation. Hence the phase diagram of Ni-Si-Mn precipitates in steels has become a subject of interest in nuclear materials research. In this talk we demonstrate that the calculation phase diagram is still incomplete due to absence of experimental data about Ni-Si-Mn ternary compounds; there exist 10 in the phase diagram. We synthesized an ingot of the G-phase Ni₁₆Si₇Mn₆, which is one of the most frequently observed precipitates in the RPV steel, by arc-melting and examined the melting point and the composition range. The experimentally-determined melting point was inconsistent with simulation results, e.g., an old database (2016 version) resulted in an overestimation greater than 700 °C. As for composition range, although off-stoichiometry is not considered in the calculation phase diagram, the G-phase certainly has it. The same thing happens to the Γ₂-phase Ni₃SiMn₂, which is another most frequently observed precipitates in the RPV steel.

Keywords : nuclear materials, light water reactors, reactor pressure vessel, embrittlement, precipitation

526. Phase diagram of Ni-Si-Mn precipitates causing irradiation-induced embrittlement of nuclear reactors

Matsukawa Yoshitaka¹, Fujieda Hideto¹, Terao Masayuki¹,
Tsurekawa Sadahiro¹, Muta Hiroaki², Nakamori Fumihiro², Yuya
Hideki³, Kasada Ryuta⁴, Yoshida Kenta⁴, Yabuuchi Kiyohiro⁵,
Yamaguchi Masatake⁶, Abad Nina^{1 7}

1 - Kumamoto University (Japan), 2 - Osaka University (Japan), 3 - Chubu Electric Power, Inc. (Japan), 4 - Tohoku University (Japan), 5 - Kyoto University (Japan), 6 - Japan Atomic Energy Agency (Japan), 7 - Ecole des Mines d'Albi-Carmaux (France)

The primary cause of irradiation-induced embrittlement of nuclear reactors is precipitation of alloying elements (Ni, Si and Mn) involved in the pressure vessel steel. Since material embrittlement practically limits the service life of reactors, the breakdown of reactor's lifetime prediction model is the analysis of precipitation kinetics. Precipitation is controlled by thermodynamics, in terms of not only precipitation amount but also kinetics; therefore, the accuracy of thermodynamic database associated with Ni-Si-Mn precipitates in steels is crucial for nuclear power industry. In this talk we demonstrate that the calculation phase diagram is not accurate enough, in terms of the melting point and composition range of Ni-Si-Mn ternary compounds. There exist 10 ternary compounds in the Ni-Si-Mn phase diagram.

We have synthesized single-phase ingots of ternary compounds by means of arc melting; so far, 7 out of 10 compounds have been successfully obtained. In the case of the G-phase Ni₁₆Si₇Mn₆, which is one of the most frequently observed precipitates in the pressure vessel steel, the melting point determined by DTA/DSC measurements was 1,177 °C, whereas calculation results were 1,324 °C (TCNI12, the latest version of the Thermo-calc database), 1,430 °C (TCFE13) and 1,915 °C (TCFE8+TCA14), respectively. As for composition range, although only the stoichiometric composition is allowed for the G-phase in Thermo-calc calculations, the G-phase does have a composition tolerance of roughly ± 2 at.% for Ni and Mn but

Keywords : nuclear materials, light water reactors, reactor pressure vessel, embrittlement, precipitation

527. Downselection of Cladding Materials for Hydride Moderators

Luther Erik¹, Kohnert Caitlin , O'Brien Mary ², Nizolek Thomas ²

1 - Los Alamos National Laboratory (P.O. Box 1663, Los Alamos, NM, 87545 United States), 2 - Los Alamos National Laboratory (United States)

Microreactors are a class of nuclear reactors intended for special purpose applications such as providing power in remote locations and for disaster relief. These reactors are intended to be factory built and sufficiently compact to fit on a variety of transport options including truck, plane or rail. Numerous reactor designs have been proposed some of which benefit from the use of high temperature moderators that help reduce both the size and the fuel enrichment requirements. High temperature moderators must survive in-pile conditions that lead to hydride decomposition. Proper selection of a cladding that will serve to mitigate decomposition results in longer life and higher performance in a given reactor design. This presentation will discuss the requirements for moderators to identify selection criteria for appropriate cladding to enable high performance moderated reactor designs. LA-UR-25-20633

Keywords : Microreactor, Moderator, Hydride, Hydrogen Permeation, Nuclear Energy

528. Thermo-mechanical properties evaluation in chromium-doped UO₂

Terricabras Adrien¹, Pena Miguel¹, Kosmidou Maria¹, Chauhan Rijul², Butler Christopher¹, Serrano Joseph¹, Van Veelen Arjen¹, Finkeldei Sarah³, White Joshua¹

1 - Los Alamos National Laboratory (United States), 2 - Texas A&M University [College Station] (United States), 3 - University of California [Irvine] (United States)

Doped UO₂ has been investigated as one of the most feasible systems for the near-term development of accident tolerant fuels (ATF). Metallic oxides dopants have been previously studied with varying amount of success. Chromia additions close to the solubility limit have demonstrated several advantages (improved sinterability, grain size increase, reduction of released fission gases), yet the operating mechanisms of those additives in UO₂ remain not fully understood. Despite work being published in such systems, there is a lack of information in the literature regarding behaviour of Cr at grain boundary, the mechanical behaviour of doped UO₂ and evolution during irradiation. This work focuses on Cr-doped UO₂ samples sintered through powder processing, where a variety of dopant concentration was targeted, both above and below the solubility limit. Comparisons will be made between as sintered materials and following proton and ion irradiation. Fundamental and mechanical properties of the sintered materials were determined using a combination of Resonant Ultrasound Spectroscopy, nanoindentation, and compression testing. Lattice impacts were evaluated using a combination of Grazing Incidence X-ray Diffraction and X-ray Absorption Spectroscopy techniques. It was also complemented with Transmission Electron Microscopy and modelling work. Thermal properties including specific heat capacity, thermal diffusivity and thermal conductivity will also be discussed. Generated data will provide information for current and future model developments.

Keywords : Cr, doped UO₂, accident tolerant fuels, ion irradiation, properties evolution

529. Electropulsing effects on microstructural evolution in cold-rolled Grade 2 titanium sheet

Lee Seong Ho¹, Yu Jinyeong¹, Cheon Seho¹, Won Jong Woo², Lee Jong Un², Lee Taekyung¹

1 - Pusan National University (South Korea), 2 - Korea Institute of Materials Science (South Korea)

This study examined the relationship between rolling reduction and electropulsing treatment (EPT), in cold-rolled commercially pure titanium (CP-Ti) sheets, considering the microstructural evolution under various reduction levels. At low reductions, twinning initiates, causing the c-axis to tilt slightly from perpendicular to the rolling direction (RD) toward the transverse direction (TD). Up to 40% reduction, extensive twinning forms a pronounced normal direction (ND)-TD split texture. At higher reductions (>60%), slip mechanisms dominate, increasing the fraction of grains with the c-axis perpendicular to the RD. The interaction between texture and current flux during EPT results in distinct microstructural changes. In the 30% reduction specimen, EPT along RD achieves 60.5% static recrystallization (SRX) by aligning the current flux perpendicular to the c-axis. In contrast, the 40% reduction specimen exhibits the lowest SRX (9.2%) during EPT along TD due to the reduced electrical conductivity and current flux. In the highest reduction of 70% specimen, EPT along RD achieved 95% SRX, driven by the combined effects of texture and increased dislocation density as the primary SRX driving force. This study highlights the role of texture in electropulsing anisotropy, offering insights into precise microstructural control of CP-Ti.

Keywords : Titanium, Cold rolling, Microstructure, Texture, Electropulsing

530. Fretting damage mechanisms mediated by α precipitates and β crystallographic textures in a metastable β titanium alloy

Hua Ke¹, Tong Yanlin ¹, Cao Yue ¹, Wang Haifeng ¹

¹ - Northwestern Polytechnical University (China)

The fretting damage behavior of high-strength titanium alloys are strongly dependent on the characteristics of microstructure, especially during the plastic deformation and wear crack initiation and propagation processing in the fretting behavior. Regarding that the interplay relationship between the resistance to crack initiation and propagation and the microstructure characteristics is still not clear. In this work, a thorough investigation on the fretting damage mechanisms mediated by α precipitates and β crystallographic textures in a metastable β titanium alloy (TB8) has been conducted. The various characters of α precipitates and β crystallographic textures have been obtained through thermomechanical process firstly. Then their fretting damage behavior is analyzed under various fretting conditions. The influence of microstructure on the fretting damage behavior is revealed. Meanwhile, the effect of fretting condition factors on the evolution of α precipitates is illustrated. The interplay relationship between the wear crack initiation and propagation and characters of α precipitates and β crystallographic textures have been established, and the fretting damage mechanisms are revealed based on the relationship. And the design criterion for the high strength titanium alloy resistance to the fretting damage behavior is obtained. This work is not only helpful for the enhance of the operation reliability in metastable β titanium alloys but also the investigation of fretting damage mechanisms in other engineering alloys.

Keywords : Metastable β titanium alloy, Fretting damage, α precipitates, β textures

531. Effects of heat treatments on the microstructure, phase development and mechanical properties of PMD additively manufactured ternary and quaternary Ti-Cu-based alloys with Fe and Cr additions

Edtmaier Christian¹, Staufer Ella ¹

¹ - TU Wien (Austria)

The aim of this study is to provide new Ti alloys suitable for wire-based (WAAM) or powder-based (PMD) AM processes. One of the main challenges in these AM processes is to sufficiently suppress columnar grain growth to avoid anisotropic mechanical properties. In addition, the materials should also exhibit sufficient ductility and high strength. Eutectoid Ti-Cu alloys tend to have an equiaxed microstructure but exhibit lower strength than Ti-6-4. In the ternary and quaternary Ti-Cu-Fe and Ti-Cu-Fe-Cr alloys, the use of 'sluggish' elements such as iron and chromium, both of which are known as beta stabilisers, results in microstructural stability and higher strength on the one hand, but also in low ductility on the other. The aim of the study was to evaluate the influence of suitable heat treatment schemes with variations in the solution heat treatment temperature, heating & cooling rates and ageing times on the properties.

532. Heterogeneous Beta structure significantly improves work hardening properties of metastable Beta titanium alloy

Wang Guodong¹, Yang Hao¹, Zhu Mingxiang¹, Xu Xiaoxuan¹, Xue Xiangyi¹, Kou Hongchao¹

1 - State Key Laboratory of Solidification Processing, Northwestern Polytechnical University (China)

Heterogeneous structures and hierarchal structures are effective methods for overcoming strength-ductility trade-off in metals. In current study, a heterogeneous beta structure, containing heterogeneity of grain size and defects (including dislocations and low-angle grain boundaries), was obtained through hot rolling and partial recrystallization processes in metastable beta titanium alloy Ti-7Mo-3Nb-3Cr-3Al. The heterogeneous beta lamellar structure formed by hot rolling followed by annealing in the beta single-phase zone consisted of recrystallized equiaxed grains and elongated deformed lamellar beta grains; while the heterogeneous bimodal beta structure formed by annealing after hot rolling in the alpha+beta two-phase region consisted of recrystallized large-sized (30-100 μm) equiaxed grains, smaller-sized (5-15 μm) equiaxed grains and sub-grains. Compared with the alloys in the fully recrystallized state, heterogeneous beta structures both showed an increase in strength without loss of ductility and the tensile curves exhibited obvious double yielding and very strong work hardening. Analysis of the deformation microstructures after fracture reveals that the deformation mechanism of heterogeneous beta-structure is SIM $\alpha\epsilon^3$ and dislocation slip. Among them, the deformation mechanism in the equiaxed grain region is dominated by SIM $\alpha\epsilon^3$ while the deformation mechanism in the deformed grain region is a mixture of SIM $\alpha\epsilon^3$ and dislocation slip. This strong interaction of dislocations, phase boundaries, grain boundaries, and sub-grain boundaries results in the metastable beta titanium alloy with an ultra-high work hardening rate of ~ 15 GPa.

Keywords : Metastable beta titanium alloys, Heterogeneous beta structure, Partial recrystallization, Mechanical properties, Deformation mechanisms

533. Stability and segregation study of alphagenic and betagenic addition elements in pure titanium by atomistic approach

Amitouche Ahcene¹, Iabbaden Djafar ², Lecomte Jean-Sebastien ¹,
Zhang Yudong ¹, Raulot Jean-Marc ¹

1 - Laboratoire d'Etude des Microstructures et de Mecanique des Materiaux (France), 2 - Laboratoire Hubert Curien (France)

Titanium is a lightweight and strong metal widely used in aeronautics, medicine, chemical industry, and energy. Its corrosion resistance, high strength-to-weight ratio, and biocompatibility make it ideal for demanding applications. However, shaping titanium, particularly during machining and casting, poses challenges due to its specific properties like low thermal conductivity, high resistance to deformation, and tendency to generate excessive heat during machining. Titanium crystallizes in a hexagonal close-packed (hcp) structure at room temperature, limiting its ductility and complicating its deformation. Additive elements can modify phase stability and mechanical behavior of the alloy, affecting its shaping process. Hydrogen incorporation (as dissolved atoms or interstitial phases like TiH_2) significantly impacts plasticity. This complex phenomenon depends on hydrogen concentration, temperature, and material microstructure. Microstructure is influenced by alphagenic addition elements (aluminum, boron, carbon, oxygen, nitrogen) that increase the phase stability range, while betagenic elements (fully soluble vanadium) extend the beta phase stability range. The alpha and beta phases of titanium have different crystalline structures and deformation modes. The beta phase's yield strength is higher than the alpha phase, distinguishing them as 'hard' and 'soft' phases, respectively. The hexagonal structure exhibits two main deformation mechanisms: slip (five modes) and twinning (four modes). Twinning, a crystallographic deformation, alters the crystal structure without changing its chemical composition, allowing deformation without fracture. Studies show cavity nucleation (crack initiation) occurs on microstructural heterogeneities like grain boundaries or twins. Since titanium twinning depends on alloy composition and environmental conditions, this work aims to understand the role of alphagenic and betagenic addition elements on the stability and segregation of interfaces (grain boundary or twin boundary) in pure titanium using atomistic approaches (molecular dynamics or ab initio).

534. Revealing the Mechanism Behind the Strength-Plasticity Dependence on Lamellar Orientation in Polycrystalline TiAl Alloys

Mengyu Jia¹, Kou Hongchao², Wang Yarong¹

1 - State Key Laboratory of Solidification Processing, Northwestern Polytechnical University (China), 2 - State Key Laboratory of Solidification Processing, Northwestern Polytechnical University (China)

TiAl alloys are widely used in aerospace applications due to their excellent high-temperature properties. Based on the dependence of deformation mechanisms on lamellar orientation, aligning the lamellae with the loading direction has been shown to further enhance the properties and remarkable balance of strength and plasticity have been achieved in PST crystals. However, controlling lamellar orientation does not show the same improvement in polycrystalline alloys. To investigate this effect, this study modulated the texture of the high-temperature alpha-phase to control the lamellar orientation. Two lamellar structures with distinct orientation characteristics were obtained and subsequently subjected to tensile testing. The results show that both the strengths at RT and 750 °C increase with the preferred orientation of lamellar colonies, while the plasticity does not exhibit significant improvement, especially at 750 °C, where plasticity tends to decrease. The increase in strength is attributed to the hindrance of dislocation motion and twin propagation at the semi-coherent alpha/gamma interfaces within the hard-oriented lamellar colonies. On the other hand, the unexpected plasticity is closely related to the grain boundary-mediated plastic deformation, which depends on the orientation of the lamellar colonies. In soft-oriented lamellar colonies, the active dislocation slip not only promotes the formation of shear bands, leading to localized structural destabilization but also necessitates GBs deformation to accommodate the relative motion between adjacent colonies. This results in an increase in lattice defects and dislocation density at the GBs, eventually triggering recrystallization, which alleviates stress concentration and improves plasticity. In contrast, in hard-oriented lamellar colonies, dislocations are restricted by the alpha/gamma interfaces, leading to limited plastic deformation and weakening the role of GBs in coordinating intergranular deformation. However, the absence of recrystallization due to the insufficient strain leads to stress concentration, which promotes crack propagation and early fracture of under low strain.

Keywords : TiAl alloys, hot extrusion, lamellar orientation, high, temperature properties

535. Enhancement of Mechanical Properties of Titanium Alloys through Innovative Thermomechanical Processing

Yeom Jong-Taek¹, Park Chan Hee ¹, Hong Jae Keun ¹

¹ - Korea Institute of Materials Science (South Korea)

Titanium is increasingly recognized as a key material for future industries due to its high specific strength, excellent corrosion resistance, and biocompatibility. However, as the industry advanced, demands for maximizing the properties of titanium materials have been steadily raised. One of the strategies to meet this demand has been the development of nanocrystalline titanium alloys through severe plastic deformation (SPD) techniques such as equal channel angular extrusion (ECAP), high pressure torsion (HPT), and asymmetric rolling (AR). Despite these efforts, commercialization of these methods has proven challenging. In this presentation, we will explore alternative approaches for producing nanostructured two-phase titanium alloys and shape memory alloys without relying on severe plastic deformation. Specifically, for two-phase titanium alloys, a nanostructure can be achieved by progressively lowering the processing temperature, based on the principle that formability improves as the nanocrystalline fraction increases during processing. Meanwhile, the NiTi alloy, which is a shape memory alloy, can generate nanostructures by the thermo-mechanical process considering phase transformation behavior of the alloy. In addition, as one of the application fields of nanocrystalline superelastic NiTi alloy, the manufacturing technology of nanocrystalline NiTi alloy fine tube for use in vascular stents will be discussed in detail in this conference.

Keywords : Titanium Alloys, Nanocrystalline, Innovative Thermomechanical Processing, Mechanical Properties

536. In situ assessment of the influence of omega on the properties of metastable beta Ti alloys

Jones Nick¹, Church N. L. ¹, Talbot C. E. P. ¹, Reed O. G. ¹

¹ - University of Cambridge (United Kingdom)

Metastable beta Ti alloys are of critical importance to the aerospace sector for high strength applications, such as in landing gear assemblies, and in vibration dampening systems. However, during processing and whilst in service these alloys are susceptible to the formation the omega phase, which is widely regarded as severely detrimental to alloy performance. Within the literature, there remains substantial debate around the formation and influence of the omega phase. The lack of clarity is compounded by the nanoscale nature of the phase and the fact that the influence of the compositionally indistinct athermal and the compositionally distinct isothermal forms of omega are often conflated. This situation has led to several contradictory conclusions, for example reports that the formation of the omega phase can strengthen with no loss of ductility countered by others that claim the omega phase embrittles. Consequently, gaining a more complete understanding of the formation and influence of the omega phase is crucial to the continued development of these alloys. Using high energy synchrotron diffraction, we have been able to characterise the athermal and isothermal formation of the omega phase in a number of systematic alloy series with a level of detail not previously reported. These data have been linked to mechanical performance and, where applicable, the stress induced formation of $\alpha\epsilon^3$ martensite. Here, we will provide an overview of these novel data, show how the two forms of omega have different influences on material properties and discuss the implications of these findings on alloy design.

Keywords : Ti alloys, Metastable beta alloys, Omega phase, synchrotron diffraction

537. Fabrication and Thermomechanical Processing of Titanium-Based Laminates for Enhanced Performance under High Dynamic Impact

Prikhodko Sergey

University of California Los Angeles (Department of Materials Science and Engineering, University of California Los Angeles, CA 90095 United States)

One of the major challenges in structural materials engineering is the inherent trade-off between strength and toughness, which are often mutually exclusive. To date, achieving a significant improvement in both properties, particularly in titanium, remains a difficult challenge. A promising approach to overcome this limitation involves the use of layered structures, where different materials with varying properties—such as high ductility and toughness—can be deliberately combined. This enables the laminate to exhibit critical properties in specific regions, optimizing overall performance. Recent studies have shown that sintering elemental powder blends with corresponding compositions, in combination with post-sintering hot isostatic pressing (HIP), can effectively produce titanium-based composite laminates with enhanced properties. Furthermore, it has been suggested that these two technologies are complementary, working together to optimize the material's performance. The aim of current study was to explore the possibility of laminates fabrication using HIP treatment alone, employing prealloyed Ti-6Al-4V (Ti64) powders, with the addition of reinforcing powders. Two different three-layer plates were fabricated. Each plate contained an alloy layer and two composite layers reinforced with 20% and 40% (vol.) hardening additions. One plate incorporated TiC particles, while the other TiB. Both plates measured 100x100x36 mm. Each layer of powder was hot compacted in the die and then transferred to a stainless steel can for HIP processing at 900 °C for 3 hours under 100 MPa. The structures obtained after fabrication were analysed and tested ballistically. It was shown that the thermomechanical treatment used was crucial for complete structure consolidation, contributing to superior mechanical properties. The results were compared with those of homogeneous titanium alloys and layered alloy/composite structures produced using other techniques

Keywords : Titanium Alloy, Composite, Laminate, Powder Metallurgy, Ballistic Response

538. Fabrication and Thermomechanical Processing of Titanium-Based Laminates for Enhanced Performance under High Dynamic Impact

Prikhodko Sergey¹, Samarov Victor ², Eyerman Eric ³, Melnyk Chris ³, Ramos Evander ³, Savvakín Dmytro ⁴, Markovsky Pavlo ⁴

1 - University of California Los Angeles (Department of Materials Science and Engineering, University of California Los Angeles, CA 90095 United States), 2 - Synertech PM Inc. (United States), 3 - California Nanotechnologies (United States), 4 - G.V. Kurdyumov Institute for Metal Physics NASU (Ukraine)

One of the major challenges in structural materials engineering is the inherent trade-off between strength and toughness, which are often mutually exclusive. To date, achieving a significant improvement in both properties, particularly in titanium, remains a difficult challenge. A promising approach to overcome this limitation involves the use of layered structures, where different materials with varying properties—such as high ductility and toughness—can be deliberately combined. This enables the laminate to exhibit critical properties in specific regions, optimizing overall performance. Recent studies have shown that sintering elemental powder blends with corresponding compositions, in combination with post-sintering hot isostatic pressing (HIP), can effectively produce titanium-based composite laminates with enhanced properties. Furthermore, it has been suggested that these two technologies are complementary, working together to optimize the material's performance. The aim of current study was to explore the possibility of laminates fabrication using HIP treatment alone, employing prealloyed Ti-6Al-4V (Ti64) powders, with the addition of reinforcing powders. Two different three-layer plates were fabricated. Each plate contained an alloy layer and two composite layers reinforced with 20% and 40% (vol.) hardening additions. One plate incorporated TiC particles, while the other TiB. Both plates measured 100x100x36 mm. Each layer of powder was hot compacted in the die and then transferred to a stainless steel can for HIP processing at 900 °C for 3 hours under 100 MPa. The structures obtained after fabrication were analysed and tested ballistically. It was shown that the thermomechanical treatment used was crucial for complete structure consolidation, contributing to superior mechanical properties. The results were compared with those of homogeneous titanium alloys and layered alloy/composite structures produced using other techniques.

Keywords : Titanium Alloy, Composite, Laminate, Powder Metallurgy, Ballistic Response

539. High temperature oxidation behavior of lightweight and formable high entropy alloys

Balpande Aditya, Deshmukh Sanika, Nene Saurabh

Indian Institute of Technology Jodhpur (India)

Conventional Ti-alloys in multiple instances have effectively addressed their importance for a broad range of lightweight applications primarily focusing on automotive and aerospace sectors. Underlying the fact that the pre-existing Ti-alloys such as Ti-6Al-4V and Ti-5553 have excellent specific strength display limited applications in the space and defense sector due to their poor high-temperature response in terms of strength and oxidation resistance. Complex alloys like high entropy alloys (HEAs) for this instance hold the potential of retaining strength and high-temperature oxidation resistance by shifting the temperature range of operation to relatively higher temperatures although with a substantial increase in density. Our earlier work on the design of lightweight Ti-rich HEAs showed excellent synergy of specific strength and room temperature formability. Considering this, the present work focuses on studying the improvement in isothermal oxidation resistance of those Ti-rich lightweight HEAs inheriting excellent strength ductility synergy in as-cast conditions at room temperature in comparison with commercially preferred Ti-6Al-4V alloy.

Keywords : Lightweight, high entropy alloy, isothermal oxidation

540. Effect of Subgrain Boundary Distributions on Extra-Hardening of SPD-processed Al-3%Mg alloy

Morishige Taiki¹, Kozaki Atsushi², Tanaka Tsutomu³

1 - Department of Chemistry and Materials Engineering, Kansai University (Japan), 2 - Graduate School of Science and Technology, Kansai University (Japan), 3 - Osaka Research Institute of Industrial Science and Technology (Japan)

Severe plastic deformation (SPD) processing is an effective method to obtain ultrafine-grained microstructure (UFG) for metallic materials. SPD-processed Al alloys has extremely high strength than the extrapolated from Hall-Petch relationship due to their microstructure with residual excess strain after dynamic recrystallization. Especially, on account of Al alloys have high stacking fault energy, the dislocation rearrangement in the dynamically recrystallized grain is difficult to form high angle grain boundary. As a result, there are substantial dislocation wall and low-angle grain boundary after SPD processing. These dislocations remain in the grain after recrystallization and partially form low-angle grain boundaries and subgrain boundaries. Consequently, the strength increases from Hall-Petch relationship, which is the degree of extra-hardening, was measured up to 200 MPa in as-SPD processed Al-3%Mg alloy. The authors previously reported that the low-angle grain boundaries distributed in the microstructure after the repetitive equal-channel angular extrusion processing. The strength difference calculated by Bailey-Hirsch equations was not in accord with measured extra-hardened strength. In this study, the effect of grain boundary distributions on the extra-hardening was investigated by changing SPD-processing and subsequent annealing conditions. As a result of EBSD analysis, the fraction of subgrain boundary, which has

Keywords : Al alloys, Severe plastic deformation, extra hardening, low angle grain boundary, subgrain boundary, kernel average misorientation

541. Strengthening Mechanisms of Heterogeneous Nano-Structured Stainless Steels and Copper Alloys

Miura Hiromi¹, Kobayashi Masakazu ¹, Aoyagi Yoshiteru ², Watanabe Chihiro ³

1 - Toyohashi University of Technology (Japan), 2 - Department of Finemechanics, Tohoku University (Japan), 3 - Faculty of Mechanical Engineering, Kanazawa University (Japan)

Commercial austenitic stainless steels and Cu alloys with low-stacking energy were heavily cold-rolled to develop complicated heterogeneous nano-(HN-)structures, which were fragmented mainly by mechanical twins and shear bands. While the flat-rolled plates were composed of eye-shaped twin domains, shear bands and conventional low-angle lamellae, those groove-rolled did not possess the eye-shaped twin domains. Even while the evolved microstructures were somewhat changed depending on the fabrication procedure, all the samples exhibited ultrafine-grained structures with twin grain-boundary spacings and low-angle lamellae roughly about 25 nm and 40 nm in average, respectively. The shear bands with an average width of about 40 nm were composed of finer grains. Therefore, ultrafine-grained structures, so-called HN-structure, could be easily developed by means of conventional rolling processes employing deformation-induced microstructures. All the stainless steels and Cu alloys showed extraordinarily high tensile strength over 2 GPa and close to 1 GPa, respectively without spoiling ductility, showing better mechanical properties attained by severe plastic deformation. Tensile strengths were further raised by low-temperature annealing. Even while precipitation was not detected by TEM observation, 3D atom probe analyses revealed large amount of grain-boundary segregation of solute elements and their increment by annealing. Multiscale simulation confirmed obstruction of dislocation motion by grain-boundary segregation to increase tensile strength. Finally, it was found that strengthening mechanisms in the HN-structures were complicatedly combined ones of nano-ordered grains, strain hardening, dense distribution of high-strength grain boundaries such as twins and grain-boundary segregation.

Keywords : heterogeneous nano, structure, ultrafine grain, rolling, grain subdivision, mechanical twinning, grain, boundary segregation

542. Suppressing diffusion with the Schwarz crystal structure in Al alloys

Li Xiuyan

Institute of Metal Research, CAS, Shenyang 110015; Liaoning Academy of Materials, Shenyang 110167, China. (China)

High diffusivity of solutes in Al alloys enables age-hardening at relatively low temperatures, but causing rapid degradation of strength at moderate temperatures. In this study we discovered that the Schwarz crystal structure in Al alloys with extremely fine grains is effective in suppressing atomic diffusion in a supersaturated Al-Mg alloy and an Al-Zn alloy. In the Al-Mg alloy with the stable structures, diffusion-controlled intermetallic precipitation from the nano-sized grains and their coarsening are inhibited up to the equilibrium melting temperature, around which the apparent diffusivity is reduced by about 7 orders of magnitude. Melting temperature of the nanograined alloy is increased by 69 K with the suppressed diffusivity. In the Al-Zn alloy with Schwarz crystal structure, spinodal decomposition which occurs via chemical fluctuations without energy barriers to nucleation is also inhibited due to the suppression of diffusion.

Keywords : Al alloys, Schwarz crystal, diffusion

543. Prevention of hydrogen embrittlement of HPT-processed ultra-high strength aluminium alloys by hydrogen-absorbing nanoparticles

Toda Hiroyuki, Wang Yafei , Fujihara Hiro , Adachi Nozomu, Todaka Yoshitaka

Kyushu University (Japan)

Ultrahigh strengthening of structural materials is a relentless metallurgical pursuit, because of the cost savings, emission abatement, and enhanced structural performance. However, these ultrastrong materials encounter persistent usability challenges due to hydrogen embrittlement, an insidious phenomenon that unpredictably causes fractures by initiating cracks and exacerbates as strength increases. Here, to trailblaze the mitigation strategy against hydrogen-imposed barriers in ultrastrong alloys, we show that hydrogen-vulnerable ultrafine-grain-hardened Al-Zn-Mg-Cu alloys, with strengths nearing one gigapascal, can be made ductile via a thermal modification that induces energetically stable hydrogen-absorbing nanoprecipitates. In contrast to the intuitively downgraded contribution of second phases in nanocrystalline alloys caused by hardening-induced coarsening and dissolution and thus excluded nuanced exploration for their potential in enhancing mechanical properties we demonstrate, via comprehensive high-resolution, three-dimensional morphological and chemical analyses, that nanoprecipitates within aluminum nanograins can be maintained even under ultrahigh shear strains of up to one thousand during strengthening. These persistent precipitates prove to be exploitable and essential for achieving exceptional resistance to hydrogen embrittlement. This strategy, through thermal aging-based modification of precipitates in nanograins, may inspire the design of hydrogen-resistant ultrastrong metallic alloys across a broad strength-composition space.

Keywords : Aluminium Alloys, High Pressure Torsion, Hydrogen Embrittlement, T phase, Synchrotron X, ray Tomography

544. Advancing High-Entropy Alloys Through Nanostructuring: Enhancing Mechanical Properties and Thermomechanical Behavior

Kawasaki Megumi, Liss Klaus-Dieter

School of Mechanical, Industrial and Manufacturing Engineering, Oregon State University (Corvallis, OR 97331-6001 United States)

Multi-principal alloys (MPA) represent a novel class of metallic materials recognized for their excellent mechanical properties, which remain superior across diverse environments, including high temperatures and radiation-intensive conditions. This presentation explores the significance of nanostructuring in enhancing the properties of single-phase solid solution high entropy alloys (HEA), specifically focusing on conventional CoCrFeNi and CoCrFeNiMn HEA. Nanostructuring, achieved through severe plastic deformation using the high-pressure torsion technique, significantly enhances mechanical performance, both strength and plasticity, by altering microstructure by introducing an excess number of defects. These defects include grain boundaries, dislocations, and vacancies. A further increase in hardness through recrystallization of the nanostructured CoCrFeNi alloy is observed through in-situ heating neutron diffraction and hardness observations. The total stored energies from these defects in nanostructured MPA was estimated to be approximately 8,500 J/kg, highlighting the significant role of defects as a driving force behind the microstructural changes. High-temperature laser-scanning confocal microscopy visualizes the large-scale relaxation of the non-homogeneously strained nanostructure during heating. Additionally, nanostructured CoCrFeNiMn alloy demonstrated improved radiation resistance, while radiation-induced grain growth was observed at Ni ion irradiation at 500 °C. This study underscores the potential of nanostructuring to advance MPA microstructure design.

Keywords : Mechanical property, Neutron diffraction, Severe plastic deformation, Recrystallization, X ray diffraction

545. Applying ultra-high shear strains to aluminium-graphene composites to achieve an exceptional strength-ductility combination

Huang Yi¹, Bazarnik Piotr², Lewandowska Malgorzata², Langdon Terence G.³

1 - Department of Design and Engineering, Faculty of Science and Technology, Bournemouth University, Poole, Dorset BH12 5BB, UK (United Kingdom), 2 - Warsaw University of Technology [Warsaw] (Poland), 3 - University of Southampton (United Kingdom)

High-pressure torsion (HPT) can introduce large shear strains to refine the grain structure in metallic materials and make the reinforcements redistribute within the metal matrix through the flow of turbulent eddy currents. Aluminium-graphene composites with 5% graphene nanoplates (GNPs) as reinforcement were successfully processed at room temperature to 20 turns with significant microstructure refinement and hardness improvement. Agglomerated GNPs were fragmented during HPT processing and tended to become more dispersed in the aluminium matrix. The composites display excellent tensile strength (345 MPa) and very limited ductility (1.6%). Further HPT processing to 100 turns on the aluminium-graphene composites showed that the materials achieve not only higher strength (more than 405 MPa) but also excellent elongation (15.5%). There was no post-HPT heat treatment applied to the tensile specimens of 100 turns aluminium-graphene composites. The extra-large shear strains applied on aluminium-graphene composites through HPT processing produced an exceptional strength-ductility combination.

Keywords : graphene, aluminium composites, high, pressure torsion, strength, ductility relationship

546. Fabrication and Characterization of Insulation-Type Thermal Interface Materials Using Conformal SiO₂-Coated Copper Dendritic Particles

Lee Jong-Hyun¹, Jung Sang-Hoon¹

¹ - Seoul National University of Science and Technology (South Korea)

High-performance thermal interface materials (TIMs) are vital for advanced electronic systems requiring efficient heat dissipation and electrical insulation. This study explores the fabrication of copper (Cu) dendritic particles, synthesized via a wet chemical method and coated with silicon dioxide (SiO₂) using tetraethyl orthosilicate (TEOS). These SiO₂-coated Cu particles (Cu@SiO₂) were specifically developed for insulation-type TIM applications. Dendritic Cu particles were synthesized and coated with SiO₂ using TEOS, involving multiple iterative steps to ensure uniform and high-quality coverage. The coating process optimized the particles for insulation purposes. A TIM paste was then formulated by dispersing the Cu@SiO₂ particles in a solvent, creating a TIM layer through a sintering procedure. The resulting bulk material showed high thermal conductivity, suitable for thermal management in electronic systems. The Cu@SiO₂ material exhibited a thermal conductivity of 4.87 W/m·K, indicating its suitability for efficient heat transfer. The film sintered at 300 °C demonstrated electrical resistivity above 2.0 Å—108 Ω·cm, confirming its insulating properties. Compression sintering at 300 °C for 30 min produced a dense microstructure with minimal voids, achieving complete densification and a shear strength of 22.7 MPa. SiO₂-coated Cu dendritic particles effectively serve as insulation-type TIMs, combining enhanced thermal conductivity and reliable electrical insulation. These properties are crucial for the performance of electronic systems requiring efficient thermal dissipation and electrical isolation.

Keywords : Insulation, Thermal Interface Material, SiO₂, Coated Cu, Sintering, Thermal conductivity

547. Effect of friction between bonding tool and workpiece on bond microstructure in ultrasonic bonding of Aluminum alloys

Kitahara Masanori¹, Yamada Takuya, Sasaki Tomohiro , Eguchi Yuki, Maeda Yuto

1 - Graduate School of Engineering, [Niigata] , Niigata city, 950-2181, Japan. (Japan)

The effect of friction between an ultrasonic bonding tool and workpiece on the formation of bond microstructure in the ultrasonic bonding of Aluminum alloys including Al-Mg-Si wrought and die-cast alloys is investigated. The ultrasonic bonding tests two metal sheets performed under the condition where the interfacial friction of the bonding sheets is constrained, focussing on the application of ultrasonic bonding for joining autobody panels. The relative motion between the boning tool and the workpiece, as well as the bonding interface during the bonding are measured using a displacement sensor. The experiment showed that ultrasonic bonding was capable under the constrained condition. The result suggests that the frictional heat generation at the interface ultrasonic tool and the workpiece causes temperature increase around the bonding tool, resulting in of bonding area. The bond microstructure develops with the shear deformation induced by the relative motion of the bonding tools.

Ultrasonic bonding, Aluminum alloy, 6000 series, Solid state bonding, Weld microstructure

548. Development of Advanced Orbital TIG welding for Utility pipe in Semiconductor factory

Ham Hyosik¹, Y Hunsung ¹, Choi Doojin ¹

¹ - Samsung Heavy industries (South Korea)

In semiconductor factories, there are many utility pipes for semiconductor manufacturing. These pipes are welded. Because semiconductor utility piping supplies hazardous toxic chemicals, confidentiality and corrosion resistance are important. And fine dust through utility piping affects the quality of semiconductor wafers, the quality of welding parts is very demanding. Therefore, automatic welding with excellent and stable quality is applied to satisfy difficult welding quality specifications. Currently, tubes with little misalignment of welding joints are being applied to automatic welding. However, most pipes with a large diameter and a thick thickness are manually welded due to misalignment and equipment mounting problems. Therefore, it is necessary to develop automatic welding for manual welding part to improve the welding quality of utility piping. This study is to develop the V groove root pass automatic welding method for pipes of 100A over in semiconductor factories. It was verified through fluid and stress analysis and physical tests in all position orbital TIG welding, and applied to the site.

Keywords : Orbital welding, Semiconductor factory, V groove, Root pass welding

549. Ultrasonic Bonding of Aluminum alloys to carbon fiber reinforced thermoplastic

Zhang Zheyuan¹, Tomohiro Sasaki , Yamada Takuya, Maeda Yuto, Hisamori Hayao

1 - Graduate School of Science and Technology, Niigata University, Niigata, 9502181, Japan. (Japan)

Ultrasonic bonding of Al-Mg alloys used for automotive body panel and carbon fiber reinforced thermoplastic (CFRTP) is attempted focusing on the various bonding parameter including normal force and vibration amplitude. The dissimilar bonding of the Al alloy and the CFRTP is achieved in a short time within 1.0 second. The maximum tensile shear strength in this study reached up to 1600 N. The bonded interface is categorized into two types from cross sectional observation: fusion bonding of resin to Al alloy, and the mechanical bonding of the carbon fibers and Al alloy. The displacement measurements for the bonding tool and the bonding sheets showed that the friction of the bonding tool on the workpiece contributed to the heat generation of bonding area, resulting in fusion of resin, while the friction caused adhesion of Al alloy to the bonding tool. To reduce the adhesion issue, the effect of the shape of bonding tool surface is investigated. The experiments showed that by a bonding tool without knurled edges on the surface significantly reduces the adhesion, as well as the surface damage on the bonding sheet.

Keywords : Ultrasonic bonding, Carbon fiber, Aluminum alloy, CFRTP

550. Friction Behaviour and Microstructure in Ultrasonic Bonding using Complex Vibrations

Sasaki Tomohiro¹, Yamagishi Shunri², Nakagawa Tomoaki², Saito Shigeki³, Mitsuyuki Jun³

1 - Department of Mechanical Engineering, Niigata University (Japan), 2 - Graduate School of Science and Technology, Niigata University (Japan), 3 - LINK-US Co. LTD (Japan)

The effect of complex vibrations in the ultrasonic bonding on the bond microstructure is investigated focussing on friction behaviours between the bonding materials and the bonding tool. The motions bonding tool and bonding materials, and the friction force at their interfaces during the bonding process of Aluminum sheets are simultaneously measured with laser displacement sensors and a three-components force sensor. In addition, two-dimensional motions in the normal force and the vibration direction is visualized using a high speed camera observation and digital image correlation. The transitional stages in the ultrasonic bonding process are evaluated based on the changes in the relative motion between the materials and the friction coefficient, as well as the evolution of microstructure. The resistance force of bonding tool rises at the bonding time within 10ms, implying the fast formation of initial bond at the bonding interface. The microstructure observation suggests that shear force arise from the complex vibrations in the vibration direction and the normal direction has a significant effect on the formation of initial bond microstructure. The elliptical motion with the shear deformation enhances development of the initial bond, leading to the increase of interfacial strength. In particular, the effect of vibration in the normal force direction on the microstructure is discussed in comparison with the microstructure using the in-plane vibration bonding.

Keywords : Ultrasonic bonding, Complex vibration, Aluminum alloy, motion analysis, bond microstructure.

551. Microstructure and Property of Aluminum/Iron Non-Uniform Heat Input Laser Welded Joints

Luo Shuncun¹, Mu Honglin¹, Nagaumi Hiromi¹, Wang Xiaonan¹,
Hu Zengrong¹

¹ - Soochow University (China)

This study proposes a novel laser welding process scheme for dissimilar steel/aluminum materials: the non-uniform heat input welding process scheme. The Al-Si coated 22MnB5 steel and 6061-T6 aluminum alloy were lap-welded using the non-uniform heat input welding process scheme and compared with traditional welding process schemes. As the laser power increases, the mechanical performance of the welded joint initially increases and then decreases. Experimental results indicate that, under identical thermal input conditions, the novel welding process achieved high-quality weld joints, the samples exhibiting excellent performance in mechanical tests, surpassing the mechanical properties of joints produced using the traditional uniform thermal input welding process by 64%, and the average elongation increases by about 113%. Due to the significant differences in the morphology of the weld seams under two different welding processes, the nail-shaped weld seam altered the fracture path of the welded joint in the tensile test. The fracture mode transitioned from brittle fracture to a combination of crispy and ductile fractures. FEM (Finite Element Modeling) simulations were conducted to analyze the reason for the enhancement in the mechanical performance of the weld seam: the nail-shaped weld seam shifted the region of stress concentration in the mechanical tests.

Keywords : Aluminum/Iron joint, Laser welding, W shaped weld seam, Finite Element Analysis

552. Finite Element Modelling and Microstructural Analysis of Laser-Welded AM Inconel 718 Joints

Khosravi Ali¹, Hamada Atef², Ghosh Sumit³, Khedr Mahmoud²

1 - Department of Materials and Metallurgical Engineering, Abadeh Higher Education Centre, Shiraz University (Iran), 2 - Future Manufacturing Technologies (FMT), Kerttu Saalasti Institute, University of Oulu, Pajatie 5, 85500 Nivala (Finland), 3 - Materials and Mechanical Engineering, Centre for Advanced Steels Research (CASR), University of Oulu, P.O. Box 4200, 90014 Oulu, Finland (Finland)

Additively manufactured Inconel 718 (IN718) plates, valued for their high-temperature performance in various industrial applications, were laser welded using three distinct processing regimes: ¹ direct welding of the as-built material (built-LW), ² double aging heat treatment of the as-built material prior to laser welding (DAT-LW), and ³ post-welding double aging heat treatment (LW-DAT). This study offers a detailed characterization of the microstructural evolution within the fusion zones (FZs) of these welds, employing advanced techniques such as Electron Backscattered Diffraction (EBSD), scanning electron microscopy (SEM) with secondary electron imaging, and Transmission Electron Microscopy (TEM) for nanoscale analysis. The investigation highlights significant differences in grain morphology, phase distribution, and precipitate formation across the three regimes, elucidating their influence on mechanical performance. Tensile tests were conducted to evaluate the mechanical strength of the welded joints, with fracture locations and modes analyzed to determine weld integrity. Finite Element Modelling (FEM) of the tensile behaviour of IN718 joints provided insights into stress distribution and localized plastic deformation within the FZs, correlating with observed fracture behaviour. The results demonstrate the critical role of the presence of welding cracking on the fracture of the joints. The FEM results offer valuable guidance for optimizing welding protocols in these joints.

Keywords : Additively manufacturing, Inconel 718, laser welding, heat treatment, finite element analysis.

553. Impact of post-weld heat treatment on microstructure, mechanical properties, and corrosion behavior of laser-welded Nb-microalloyed ferritic stainless steel

Newishy Mohamed¹, Abdelghany Ahmed W.^{2 3}, Ali Mohammed^{4 5}, Soliman Hanaa⁶, Jaskari Matias², JaRvenpaa Antti², Hamada Atef²

1 - Welding Technology and NDT department, Central Metallurgical Research and Development Institute, Helwan, Cairo 11421 (Egypt), 2 - Future Manufacturing Technologies (FMT), Kerttu Saalasti Institute, University of Oulu, Pajatie 5, Nivala 85500 (Finland), 3 - Design and Production Engineering Department, Faculty of Engineering, Ain Shams University, Cairo 11535 (Egypt), 4 - Materials and Mechanical Engineering, Centre for Advanced Steels Research, University of Oulu, Oulu 90014 (Finland), 5 - Steel Technology Department, Central Metallurgical Research and Development Institute, Helwan, Cairo 11421 (Egypt), 6 - Surface treatment and corrosion control department, Central Metallurgical Research and Development Institute, Helwan, Cairo 11421 (Egypt)

In this study, butt joints of Nb-microalloyed ferritic stainless steel, base metal (BM), were welded using a disk laser with an energy input of 20 J/mm. The microstructure, mechanical properties, and corrosion behavior of the joints were analyzed, with a particular focus on the effects of post-weld heat treatments (PWHT) at 400 °C and 500 °C for 24 hours. Microstructural evaluation of the weldments and PWHTed joints was conducted using electron backscatter diffraction (EBSD) and laser scanning confocal microscopy. Hardness profiles across the weldments were measured using microhardness testing, and uniaxial tensile tests were performed to determine mechanical properties. The weld microstructures revealed a fusion zone (FZ) with elongated columnar ferritic grains, indicative of directional solidification during laser welding. PWHT promoted the formation of secondary-phase particles, including $\hat{\text{I}}$ -phase (Cr-rich) carbides and Laves-phase precipitates at 400 °C. At a higher temperature of 500 °C, the precipitation of σ -phase, Laves-phase, and M₂₃C₆ carbides were induced. These particles improved mechanical properties. For instance, the tensile strength increased from 525 MPa for the BM to 560 MPa and 570 MPa for joints treated at 400 °C and 500 °C, respectively. However, the presence of secondary-phase particles negatively impacted the corrosion behaviour of the material. The BM displayed superior corrosion resistance compared to the heat-treated samples at 400 °C and 500 °C, highlighting the detrimental effect of the precipitated phases on the corrosion behaviour of the BM.

Keywords : Laser welding, Ferritic stainless steel, post, weld heat treatment, microstructure, mechanical properties, corrosion resistance

554. Application of electron beam welding in the production of TEMPALLOY AA1 and T92 butt joints of pipes assigned for the energy industry

Kwiecinski Krzysztof¹, Purzynska Hanna ¹, Urzynicok Michal, ², Zielinski Adam ¹

1 - Ąukaszewicz Upper Silesian Institute of Technology, ul. K. Miarki 12-14 44-100 Gliwice. (Poland), 2 - ZELKOT, Nowy Dwor 8, 42-286 KoszÄ™cin (Poland)

One of the main problems with the use of steels for elevated temperatures is their limited weldability. This is mainly due to the fact that these materials may contain in their chemical composition. Due to the susceptibility to cold cracking, PWHT is necessary, especially in high-stiffness welded structures. In addition, depending on the condition after heat treatment or in the absence of heat treatment, precipitates may appear in the microstructure of the steel, affecting its mechanical properties. It is important in this case to ensure the high quality of welded joints, which means that the manufacturer has to demonstrate a very high technical culture. Currently, thin-walled pipe butt joints are welded manually using a tungsten electrode with solid wire material (TIG method). One of the solutions that can significantly speed up the welding process of components for work at elevated temperatures is the use of an electron beam welding. In addition, the ability to make welded joints without the use of filler material and to achieve narrow heat-affected zones may find application in the welding of modern materials used in the power industry. This paper presents the welding experience of materials assigned for the power industry (TEMPALLOY AA1 and T92) by use of electron beam. In this article authors present the results of tests gained during first steps of welding welded joints. The article also includes preliminary results on the service life of the fabricated joints.

Keywords : Welding, Electron Beam Welding, EBW, Creep Test, Pipes, Butt joints, Advance Manufacturing, Processing, Fabrication, TEMPALLOY AA1, T92

555. Effects of Factors on Deformation-Induced Martensitic Transformation of Metastable Austenitic Weld Metals at Cryogenic Temperature

Uranaka Shohei¹, Tochigi Eita¹, Hatano Masaharu², Kawabata Tomoya¹

1 - The University of Tokyo (Japan), 2 - NIPPON STEEL Stainless Steel Corporation (Japan)

Austenitic stainless steels are widely used as a material for liquefied hydrogen storage tanks, although, in order to increase the size of storage tanks for cost reduction, it is necessary to improve the toughness of welds, which have lower toughness than the base metal. Stress concentration on the welds due to large earthquakes can reduce the low-temperature toughness through deformation-induced martensitic transformation at 20 K of the liquefied hydrogen storage temperature, therefore, the control of deformation-induced martensitic transformation is an important point. However, there have been few investigations of deformation-induced martensitic transformation of weld metals at cryogenic temperatures. In this study, Type 316L welds were fabricated by three different arc welding methods to investigate the deformation-induced martensitic transformation behavior of metastable austenitic weld metals at cryogenic temperature. Tensile specimens were taken from the welds to apply pre-strain at 4 K. Since it is known that stress triaxiality affects deformation-induced martensitic transformation behavior, specimens designed for high stress triaxiality were prepared in addition to the normal round bar specimens. The microstructure of the specimens subjected to various pre-strain were analyzed by XRD, SEM-EBSD, and magnetic techniques. It was found that the specimens with higher stress triaxiality were more prone to deformation-induced martensitic transformation. Moreover, it was revealed that deformation-induced martensite tended to precipitate at the ferrite/austenite interface via SEM-EBSD observation, and FE-EPMA suggested that solidification segregation affected martensite precipitation sites.

Keywords : Metastable Austenitic Weld Metals, Deformation, Induced Martensitic Transformation, Cryogenic Temperature, Stress Triaxiality, Segregation

556. Improved mechanical properties of Al-Cu laser lap joints by optimization of laser beam wobbling

Seong Min Yun¹, Chae Eun Yun¹, Yong Kim², Je In Lee¹

1 - School of Materials Science and Engineering, Pusan National University (South Korea), 2 - AI & Mechanical System Center, Institute for Advanced Engineering (South Korea)

Electrical Vehicles (EV), using lithium-ion batteries as a power source, are one of the most promising replacements of the inter combustion engine cars. EVs contain a battery pack which has numerous cell connections between Al and Cu tabs joined by laser welding technique. Dissimilar welding of Al and Cu is difficult due to the formation of brittle intermetallic compounds (IMCs); thus, the formation of IMCs must be controlled to prevent the degradation of the laser welds. In this research, laser welding was performed with different wobbling amplitude ($a = 0.1, 0.4$ and 0.5 mm). As the wobbling amplitude increases, the area where Cu-rich IMCs formed changed from Al fusion zone to the fusion line between Cu fusion zone and heat affected zone. This result was attributed to the increase in the wobbling amplitude which significantly suppressed the upward flow of molten Cu. Because the Cu-rich IMCs were extremely brittle, the welds with low amplitude suddenly fractured at Al fusion zone which led to the low tensile shear strength and fatigue life. We demonstrated that suppressing the upward flow of molten Cu by increasing the wobbling amplitude was effective to control the distribution of Cu-rich IMCs in the fusion zone and increase the mechanical properties of the welds.

Keywords : laser welding, Al, Cu dissimilar welding, Intermetallic compounds, Laser beam wobbling, Fatigue

557. Effect of atmospheric condition in Electron beam welding of advanced high strength steel

Areskoug Magnus, Dadbakhsh Sasan , Rashid Amir

KTH Royal Institute of Technology (Sweden)

Critical applications of advanced high strength steels has inspired electron beam welding (EBW) process as a powerful tool for joining thick steel components. The EBW process can be applied in vacuum (VAC) and non-vacuum (NON-VAC) conditions, which the latter enables more manufacturing processability and hence less cost for high throughput industries. Accordingly, in this study, we focus on comparison between the characteristics of a weld performed by VAC and NON-VAC EBW on a high strength steel (with over 1300 MPa Yield strength and 8% elongation) with different plate thicknesses. The results are supported by investigating the changes in composition, melt pool shape/morphology, microstructure, and mechanical properties (including hardness, toughness, and tensile properties). The findings reveal that VAC EBW leads to higher mechanical properties than NON-VAC process, although NON-VAC welds can still be acceptable compared to reference virgin steel plates. The causes behind these findings are well analysed and discussed in the material level.

Keywords : Welding & Joining of Advanced and Specialty Materials, electron beam

558. Reinforcing FSW joints with mechanical interlock utilizing stamping holes

Ohashi Takahiro, Mofidi Tabatabaei Hamed , Nishihara Tadashi

Kokushikan University (3-4-1 Setagaya, Setagaya-ku, Tokyo Japan)

It is well known that adding a mechanical joining technique during FSW can effectively increase joint strength. However, the preparation of the source structure for mechanical interlocking is undesirable from the point of view of cost and processing time, as it increases the number of steps required for joining. On the other hand, parts to be joined are often prepared by the press working in the industry. Stamping holes are naturally given a diagonal structure owing to the stamping punch-die clearance, and can be utilized as a source structure for mechanical interlocking. Hence, stamping holes in press working parts can offer sources of mechanical interlocking during FSW without substantially adding actual production steps. This paper introduces three examples of stamping holes in steel sheets fabricated by single straight punches, single chamfering punches, and multiple punches generating perforated steel sheets for joining aluminum alloy plates. In the joining using a single hole pierced by a straight punch in the steel sheet, larger punch die clearance in stamping resulted in larger cross tensile strength of the mechanical interlocking after joining, because it developed sheer droop at the rim of the holes more. However, when a single hole pierced by a chamfering punch in the steel sheet was used, the pressed steel material tended to escape into the gap between the punch and die when clearance was excessive. Consequently, the formation of an oblique structure at the rim of the holes was insufficient, and the cross-tensile strength was reduced. In joining using high-density multiple holes, friction stirring with tool traveling enabled us to generate a pseudo linear weld line and join a wide area mechanically, as in linear joining. The above mechanical joints are expected as the reinforcement when combined with FSW joints.

Keywords : Friction stir welding(FSW), Mechanical interlock, Stamping, Dissimilar materials joining

559. Effect of Magnesium and Silicon on the Temperature Evolution and Mechanical Properties in Refill Friction Stir Spot Welding of Aluminum to Titanium

Malaske Lasse¹, Suhuddin Uceu², Klusemann Benjamin^{1 2}

1 - Leuphana University Luneburg, Institute for Production Technology and Systems, 21335 Luneburg, Germany (Germany), 2 - Helmholtz-Zentrum Hereon, Institute of Material and Process Design, Solid State Materials Processing, 21502 Geesthacht, Germany (Germany)

Optimizing the mechanical properties of aluminum to titanium welds is one crucial factor to establish applications for dissimilar lightweight hybrid structures in aerospace industry. In this context, solid-state welding technologies have proven effective in terms of short joining cycles allowing the combination of cost-effective production and structural weight optimization. Besides enhancing the joining efficiency, typical temperature related effects as high residual stresses, cracks, microporosity and severe formation of intermetallic compounds at the interface can be reduced due to lower temperature evolution during solid-state welding compared to fusion welding techniques [1]. However, metallurgical effects between aluminum and titanium in the joint interface are still not completely understood due to differences in physical as well as chemical characteristics. In this study, aluminum alloy 6013 was welded to Ti6Al4V by refill Friction Stir Spot Welding [2], including systematic variations of Mg and Si alloying element contents. Generally alloying elements as Mg, Si and V were found to retard the intermetallic compound formation [3]. In total five different alloys were welded to the titanium to further investigate the influence during processing. Apart from the material selection, the weld strength is mainly influenced by the intermetallic compound thickness at the interface, which in turn primarily depends on the exposed temperature cycle. Consequently, major interest during this study was given on the temperature evolution, interfacial features and the global mechanical properties.

Keywords : Aluminum, Titanium, solid, state, Magnesium, Silicon, refill Friction Stir Spot Welding, dissimilar, temperature evolution, interface, mechanical properties

560. Prediction and control of welding distortion in the aluminium basic element of vehicle structures

Song Jia, Chen Xiaming, Zhang Jiajie, Nagaumi Hiromi

Weiqiao Lightweight Research Center at Soochow (China)

The study is based on the hot plasticity method, and it numerically simulates the welding of the "T"-shaped structure of 6061-T4 aluminum alloy profiles. The research focuses on the angular joint of the "T"-shaped structure, investigating the effects of different fixture positions, the number of fixtures, and applied loads on the welding deformation of the joint. The results indicate that applying fixtures in the opposite direction of the maximum deformation of the angular joint, with a distance of 10mm from the weld seam, and applying a load of approximately $0.5-0.9\sigma_s$, can alter the residual stress distribution after welding and reduce the magnitude of residual stress. Compared to the welding method with two fixtures, this approach effectively controls the welding deformation of the "T"-shaped structure, reducing the maximum post-weld deformation from 4.5mm to 1.46mm, a decrease of approximately 67.6%.

Keywords : Numerical simulation, Aluminum alloy, Residual stress, Welding deformation

561. Porosity suppression Using a Combination of Quasi-continuous and Oscillating Lasers in HPDC Al-Si Alloy Welds

Chen Xiaming¹, Zhang Luzhong¹, Qin Kunlun¹, Song Jia¹, Hiromi Nagaumi²

1 - Weiqiao Lightweight Research Center at Soochow (China), 2 - Soochow University (China)

The high porosity in the laser welds of the high hydrogen aluminum alloy had been solved by combining the quasi-continuous laser and beam oscillation. Compared to continuous laser, the high temperature gradient at the alternation of troughs and peaks of quasi-continuous laser enhances the molten pool flow. Moreover, the keyhole and molten pool are enlarged by the high peak laser power. By combining the oscillating laser, the keyhole's stability and molten pool flow are both further enhanced. As a result, the keyhole-induced are suppressed because of the high keyhole stability. Meanwhile, the bubbles are encouraged to escape from the molten pool by the strong convection, leading to no dense-type pores in the weld seam. Thereby, the porosity of the weld seam is 0.3%, which is only $\sim 1/40$ of the continuous laser weld seam (10.8%). At this moment, the resistance to crack initiating and expanding has been enhanced, which increases the strength and elongation of weld seam. Its strength-ductility reaches to 2.3GPa%, which is ~ 14 times higher than that of the continuous laser welded joints.

Keywords : Quasi, continuous laser, oscillating laser, Al, Si alloys, porosity, mechanical property

562. Lap friction stir welding of a TRIP steel grade with a Ni filler

Avettand-Fenoel Marie-Noelle¹, Nagaoka Toru², Taillard Roland¹

1 - Univ. Lille, CNRS, INRAE, Centrale Lille, UMR 8207 UMET Unite Materiaux et Transformations, F-59000 Lille (France), 2 - Osaka Research Institute of Industrial Science and Technology, Osaka 5368553 (Japan)

Two 1.1 mm thick sheets of a TRIP steel were friction stir lap welded with a 0.1 mm thick Ni interlayer by varying the Si3N4 pin length (0, 0.5, 1.2 or 1.5 mm) [1]. The joints microstructure, namely the material flow, the recrystallization and the phase transformations during processing were investigated by complementary multiscale techniques (light microscopy, scanning electron microscopy, energy dispersive spectroscopy, electron back scattered diffraction). Globally, the nuggets microstructure was essentially a' martensitic whatever the pin length. A poor diffusion bonding occurred, without Ni stirring, at the interlayer interfaces with the two shorter pin lengths. With the longest probe, the reduced malleability of nickel, which played the role of a material flow marker, was inadequate for obtaining sound welds. However, in this case Ni stirring led to the formation, inside the nugget, of some areas locally graded in both chemical composition and thus phase nature. A nickel gradation was even faced in some grains. A marked diffusion of Ni in the nugget stabilized austenite with a few micrometers grain size. In addition, microhardness and tensile tests were performed on the joints. A thorough study of the fracture pattern of the tensile shear samples enabled to correlate the mechanical resistance of the various joints with their microstructure. Some ways of optimization are finally proposed. [1] M.-N. Avettand-Fenoel, T. Nagaoka, R. Taillard, Met. Mat. Trans. A 55⁹ (2024) 3724-3736

Keywords : Friction stir welding, TRIP steel, Ni interlayer, Microstructure, Mechanical properties

563. Friction Stir Technologies Evolution of a Disruptive Process over 30 Years

Mishra Rajiv ¹

¹ - University of North Texas (United States)

The invention of friction stir welding in 1995 was the onset of a disruptive joining technology. In the beginning, it enabled solid-state joining of unweldable high strength aluminum alloys. The first evolution of this technology by Mishra et al. (1999) was given a generic name of friction stir processing. The friction stir processing broadened the scope of this solid-state technology as a microstructural refinement technique with first application to superplasticity. From that time, it has been a continuous emergence of new technologies based on the principles of friction stir process. In this overview, the pace of evolution will be presented including the most recent variants of additive friction stir deposition (AFSD) and SolidStir additive manufacturing (AM). These solid-state additive manufacturing technologies have the highest deposit rate among all the AM technologies. In addition, being solid-state process, these result in wrought microstructure and are best suited for replacing of large-scale castings and forgings. Highlights of mechanical properties using these friction stir AM processes will be presented. Both these processes are also very suitable for recycling and upcycling of metallic materials. Examples of recent progress of recycling and repair will be presented to provide guidance for emerging directions. Even after 30 years of its first application, emergence of new concepts provides exciting opportunities.

Keywords : Friction Stir Welding, Friction Stir Technologies, Additive Manufacturing, Technology Innovation, Recycling, Repair

564. Corrosion Fatigue Property of Steel/Aluminum Alloy Weld-Bonded Lap Joint in High Temperature and High Humidity

Hisahi Serizawa

Joining and Welding Research Institute, The University of Osaka, 11-1 Mihogaoka, Ibaraki, Osaka 567-0047, Japan., Email: serizawa.hisashi.jwri@osaka-u.ac.jp

In order to evaluate the corrosion fatigue property of dissimilar joint by the simultaneous fatigue-corrosion test, an original compact shear fatigue test machine has been developed and installed in the combined cycle corrosion equipment. The material used were an innovative ultra-high strength steel (i-UHSS) with the ultimate strength of 1.5 GPa & large elongation of 20 % and an innovative Al-Mg alloy with high ductility. The dissimilar lap joints were fabricated by resistance spot welding (RSW) or refill friction stir spot welding (RFSSW). An innovative adhesive was also employed for producing the weld-bonded (WB) joints. An accelerated corrosion condition conducted in this research was the climate of high temperature & high humidity. In addition, the natural corrosion fatigue tests were performed outdoor on Miyakojima Island in Japan and indoor in an air-conditioned room. The accelerated corrosion fatigue tests suggest that the corrosion fatigue property of the dissimilar WB joint joined by RSW seems to be better than that of the WB joint joined by RFSSW because of the difference in the area of adhesive interface. In addition, it is considered that the crack would propagate in the adhesive interface and then lap joint might break suddenly after achieving the crack to the circumference of joint interface produced by RSW or RFSSW. Moreover, it can be concluded that the accelerated corrosion condition employed in the research seems to be an appropriate condition for examining the corrosion fatigue property of lap joint in the climate of high temperature and high humidity.

Keywords : Dissimilar Joint, Galvanic Corrosion, Corrosion Fatigue Property, Resistance Spot Welding, Friction Stir Spot Welding

565. Microstructure and Mechanical Properties in Al-Cu Lap Joint by Dual Beam Laser Welding

You Chaeun¹, Yun Seong Min ¹, Kim Yong ², Lee Je In ¹

1 - Pusan National University (South Korea), 2 - AI & Mechanical System Center, Institute for Advanced Engineering (South Korea)

A battery pack for an electric vehicle consists of thousands of battery cells that need electrical connection between Al cathode and Cu anode tabs. Because Al and Cu have high thermal conductivity, they are usually joined using laser beam with high energy density. However, dissimilar laser welding of Al and Cu leads to the formation of brittle intermetallic compounds and degradation of weld properties. Recently, a dual-beam laser promotes laser absorption and reduce spattering due to the introduction of a ring beam. In this study, a dual- beam laser with different power ratio from core to ring beams was applied with the power of core beam of 900, 1100, 1300 W. As the power ratio increases, the bead width increases and the tensile shear strength increases. If the power ratio exceeds 1.5, an increase in the mixing of Al and Cu leads to reduction in tensile shear strength. With an appropriate power ratio and power of core beam, fracture mode changed from brittle to ductile fracture. Furthermore, a fatigue test was conducted to evaluate the fatigue strength and life. This study aims to correlate the microstructure and mechanical properties of laser welds because the brittleness of the lap joints is closely related to the formation and distribution of intermetallic compounds.

Keywords : laser welding, Al Cu dissimilar welding, Intermetallic compounds, Dual beam laser

566. TLP Bonding of dissimilar materials

I. López-Ferreno*, L. Sanchez-Del Rio*, G. Cofrev, M. Saugov, S. Sommadossiv, B. Straumal+, M. C. Poletti§, G.A. Lopez*

Physics Department, University of the Basque Country UPV/EHU, Leioa, 48940, Spain. V Research Institute of Engineering Sciences and Technologies IITCI CONICET-UNCo, Comahue National University, 8300-Neuquén, Argentina. + Institute Osipyan Institute of Solid State Physics, Russian Academy of Sciences, 142432-Chernogolovka, Russia. § Institute of Materials Science, Joining and Forming, Graz University of Technology, 8010-Graz, Austria.

Transient Liquid Phase bonding (TLP) is an innovative technique used to join materials, identical or dissimilar. This method is based on the formation of a liquid interfacial layer promoting diffusion-reaction process to produce the formation of a thin high-quality bond using a filler layer between both substrates. The interest in this process lies in its possibility to improve the mechanical properties and corrosion resistance of the joints, which are crucial in industrial high-temperature applications or in medical field, i.e. the energy related industry or medical implants. The quality of the bonds relies on the different phases and/or intermetallics formed in the joint zone. Usually, it can be divided into three regions, namely, the isothermally solidified zone (ISZ), the athermally solidified zone (ASZ) and the diffusion-affected zone (DAZ). Using Al and Nickelbrazes HTN2 as thin filler materials, dissimilar substrates, like stainless steel SS316, Ti-Al6-V4 and Inconel 718, were bonded at high temperature using a Gleebe machine. In order to optimize the process variables and to ensure the integrity of the joints, microstructural and phase identification of the phases present is essential. Since the interfacial diffusion-reaction should be characterized, high resolution techniques play a fundamental role, i.e. TEM and SEM-EDS-EBSD. Therefore, the preparation of selected lamellas by Focused Ion Beam (FIB) will be mandatory. The results obtained with all of these techniques will be discussed with the purpose of comprehensively understanding the behaviour of TLP junctions, contributing to the advance in the design and manufacture of more efficient bonding technologies.

Keywords : Transient Liquid Phase Bonding, Bonding of dissimilar materials, FIB, TEM, SEM

567. Thermodynamical and experimental verification on the enhancement of tensile and impact properties of high strength low alloys steels and their welds

Kang Namhyun¹, Yoo Seonghoon¹, Lee Yoona¹, Moon Byungrok¹, Choi Junghyun¹, Park Hyunjoon¹, Nam Dae-Geun²

1 - Pusan National University (South Korea), 2 - Korea Institute of Industrial Technology (South Korea)

Heavy plates for megastructure need high-strength low-alloy (HSLA) steels manufactured through the thermomechanical controlling (TMC) process. Specifically, HSLA steels have a superior weldability compared to conventional steels due to their low carbon equivalent. Furthermore, remarkable mechanical properties can be achieved by adding microalloying elements such as Ti and Nb and/or replacing Ni to Mn, which contribute to precipitation hardening and/or saving the cost, respectively. However, the heat input during the welding process forms a local brittle zone (LBZ) with MA constituents degrading the impact toughness, and this phenomenon is known to be controlled by microalloying elements and solute segregation along the prior austenite grain boundary (PAGB). The formation of LBZ renders several beneficial strengthening mechanisms meaningless in as-rolled plates and coarse-grained heat affected zone (CGHAZ). Therefore, this study investigated the sophisticated control of the microstructure in obtaining the desired mechanical properties with a variation of alloying components such as C, Ni, Mn, Cu, Ti, and Nb. The calculated thermal profile of CGHAZ was employed in Gleeble machine to fabricate the simulated CGHAZ specimens. The study propose the optimum composition in HSLA steels to enhance the impact toughness of CGHAZ without sacrificing the tensile property.

Keywords : High strength low alloy steels, Welding, Heat affected zone, Impact toughness, Tensile strength, Microstructure

568. The Role of Interstitials on Phase Metastability and Dislocation Pathways in BCC Refractory Multi-Principal Element Alloys

Daniel S. Gianola

Materials Department, University of California Santa Barbara, 93106, United States of America.

BCC refractory multi-principal element alloys (MPEAs) are promising candidates for structural applications demanding temperatures exceeding the capacity of state-of-the-art superalloys. While excellent high temperature strength has been demonstrated in many refractory MPEAs, a fundamental understanding of the nature of dislocation pathways and their temperature dependence in these chemically complex alloys, and the role of interstitial species such as oxygen is still in its infancy. We use in-situ deformation to elucidate the pathways for dislocation slip in several BCC MPEAs, where defect dynamics can be linked to the mechanical response. We also demonstrate a metastability approach using oxygen interstitials to drive a hierarchical microstructure in Ti-Nb alloys with tensile strength exceeding 2 GPa while retaining good damage tolerance. These properties are linked to phase decomposition pathways arising from oxygen-induced immiscibility, including spinodal decomposition with nanoscale compositional undulations and an emergent dual-phase lamellar structure co-existing with the spinodal features. The role of phase decomposition during elevated temperature testing and service in other refractory alloys, as well as the evolution of experimental tools to study defect dynamics, will be highlighted.

569. Amorphous Materials Examined with a Multifaceted Approach

Hirokazu Masai

Department of Materials and Chemistry, National Institute of Advanced Industrial Science and Technology (AIST), 1-8-31 Midorigaoka, Ikeda, Osaka 563-8577, JAPAN

The conventional non-crystalline material is a solidified liquid; it neither has an ordered structure nor grain boundaries. Glass exhibiting the glass transition behavior possesses various excellent characteristics such as transparency, chemical durability, thermal stability, hardness, and a wide chemical composition range. Although the chemical composition is fixed, the thermodynamically metastable structure has a wide diversity. This diversity of glass is both an advantage and a disadvantage in science. Because glasses have no clear Bragg plane, collaborations among material scientists, theorists, and specialists in analysis and evaluation with their own areas of expertise are important. In particular, a shift in perspective from a local (atomistic) to an average (bulk) perspective is needed for deeper understanding. In this study, recent several topics on amorphous materials and glasses with a combination of measurement techniques are presented. By using synchrotron X-rays, structures of not only dopants (by X-ray Absorption Fine Structure), but also network (by X-ray diffraction and small angle X-ray diffraction) can be examined. Since physical properties of glasses are affected by many preparation parameters in addition to the chemical composition of glasses, various characterization techniques are important to discuss the structure-property relationships. The details are presented on the day.

570. Spintronic technologies for room-temperature germanium devices

Kohei Hamaya

Center for Spintronics Research Network, Graduate School of Engineering Science, Osaka University, 1-3 Machikaneyama, Toyonaka 560-8531, Japan, ., V Spintronics Research Network Division, Institute for Open and Transdisciplinary Research Initiatives, Osaka University, Yamadaoka 2-1, Suita, Osaka 565-0871, Japan

Semiconductor (SC) spintronic technologies are expected for novel logic and memory architectures with low power consumption in future electronics [1]. Thus far, we have developed highly efficient electrical spin injection and detection technologies in germanium (Ge) [2] at room temperature for CMOS- and Si-photonics compatible spintronics. In this talk, we show an original technique for growing high-quality ferromagnetic Heusler alloys on Ge and for detecting large spin signals in Ge-based lateral spin-valve devices [3,4]. For getting the highest magnetoresistance (MR) ratio, we can reduce the resistance area (RA) product down to $\sim 0.1 \text{ k}\Omega\text{cm}^2$, several order of magnitude lower than that in Si-based devices with MgO tunnel barriers. Also, by using a strained $\text{Si}_{0.1}\text{Ge}_{0.9}$ layer as a spin transport layer, we observe a long spin diffusion length of $\sim 0.9 \text{ }\mu\text{m}$ [5], comparable to Si, at room temperature. The present Ge spintronics technologies will be paving the way to achieve high-performance electron-photon-spin integrated devices on the Si platform at room temperature. This work was supported in part by JSPS KAKENHI (Grant No. 19H05616, 24H00034), and MEXT X-NICS (Grant No. JPJ011438), and the Spintronics Re-search Network of Japan (Spin-RNJ). [1]

M. Tanaka and S. Sugahara, IEEE Trans. Electron Devices 54, 961 (2007)., 2. K. Hamaya et al., J. Phys. D: Appl. Phys. 51, 393001 (2018)., 3. M. Yamada, KH et al., NPG Asia Mater. 12, 47 (2020)., 4. K. Kudo, KH et al., Appl. Phys. Lett. 118, 162404 (2021)., 5. T. Naito, KH et al., Phys. Rev. Applied 18, 024005 (2022).

571. Effect of friction stir welding on the microstructure and precipitation behaviour of new generation cast (Al-Zn-Mg)-Fe alloys

Ranjit Bauri¹, Manish N. Borse²

¹ - Department of Metallurgical and Materials Engineering, Indian Institute of Technology Madras, Chennai 600036, India. ²Department of Metallurgical and Materials Engineering, Indian Institute of Technology Madras, Chennai 600036, India.

Newly developed (Al-Zn-Mg)-Fe (HE700) alloys have shown the potential to fulfill the requirements for lightweight automotive components over conventionally used cast aluminium alloys. Near net shape HE700 alloy plates were processed by high vacuum high pressure die casting (HVHPDC) route. Friction stir welding (FSW), a solid-state joining technique, was used to join the plates. The microstructure evolution was thoroughly investigated to elucidate the effect of FSW. Micro-segregated Zn/Mg-based phases and Al-Fe-based eutectic phases were present in the intergranular regions in the as-cast HE700 alloy. The Al-Fe-based phases were refined to particulate form and distributed uniformly in the welded region during FSW. Finer grain size, refined Al-Fe particles, and microstructural homogeneity made the stir zone (SZ) significantly stronger than the as-cast base metal and the heat affected zone (HAZ). The study also provided insights into the aging behavior of the alloy, using advanced characterization tools like high-resolution transmission electron microscopy (HRTEM), atom probe tomography (APT), and high-angle annular dark field (HAADF) imaging. The SZ and HAZ exhibited different aging kinetics during long-term natural aging. Two types of precipitates, Zn-rich solute nanoclusters ($Zn/Mg > 3$) and Zn/Mg-based GP zones ($Zn/Mg < 2$), were observed in the SZ, while the HAZ exhibited accelerated growth of η -type precipitates with development of precipitate-free zones (PFZ) after 300 days natural aging. This comprehensive understanding gained from the study on microstructure evolution and precipitation behavior will help designing an optimal process window for joining and a suitable post-weld heat treatment (PWHT) process for developing components for structural light-weight applications.

Keywords: Advance Manufacturing, Light-weighting, Friction stir welding (FSW), Microstructure evolution, Precipitation.

572. Impact of Grain Size on Strain-Induced Phase Transformation in a CrCoNi Multi-Principal Element Alloy

Francisco Coury¹, , Gustavo Bertoli^{1,2}, Amy Clarke³ , Claudio Kiminami¹ , Michael Kaufman²

1 : Universidade Federal de São Carlos [São Carlos], **2** : Colorado School of Mines, **3** : Los Alamos National Laboratory

A Cr40Co40Ni20 (at.%) alloy with varying grain/crystallite sizes was examined using in-situ synchrotron X-ray diffraction during tensile testing. The FCC initial structure partially transformed to HCP via a strain-induced transformation (TRIP effect), and the extent of transformation was quantified throughout deformation. The critical stress required for a specific HCP fraction followed a Hall-Petch relationship ($\sigma_{\text{TRIP}} = \sigma_{\text{TRIP},0} + k_{\text{TRIP}}d^{-0.5}$), with the Hall-Petch slope being approximately equal for yield stress and the TRIP effect ($k_y \approx k_{\text{TRIP}}$). Additionally, a Hall-Petch-based model was developed to correlate applied stress, transformed phase fraction, and initial FCC grain/crystallite size. The model predicts the stress required for a given HCP fraction or the resulting fraction under a specific stress for different grain/crystallite sizes. A mechanism is proposed to explain the grain/crystallite size dependence of the TRIP effect, emphasizing how the TRIP effect and its early activation in the Cr40Co40Ni20 alloy enhance work-hardening capacity, thereby improving ductility and toughness. A refined FCC grain size ($d = 1.3$; $c = 0.7 \mu\text{m}$) increased yield stress by over 100% ($417 \rightarrow 834 \text{ MPa}$) compared to a coarser grain material (17 ; $6.8 \mu\text{m}$), while maintaining high ductility of 41%. This study advances the understanding of deformation mechanisms, particularly strain-induced phase transformation (TRIP), and underscores their critical role in enhancing mechanical properties.

Keywords : TRIP ; Mechanical properties ; Synchrotron XRD ; Strain ; hardening

573. Experimental and computational studies on delamination-induced loosening behavior of acetabular cup by cyclic load

Yuichi Otsuka

1 - Nagaoka university of Tehcnology (NUT) *Japan*.

We aimed to clarify the interaction effect between interface damage and bone damage on the loosening behavior of the acetabular cup. The interfacial damage near the edge of the acetabular cup was measured using the AE method, the temperature change at the loading point of the acetabular cup was measured using the IR method, and the interaction mechanism between the simulated bone damage and interface damage, which can induce loosening of the acetabular cup, was discussed. This study also aimed to analyze the loosening mechanism of the acetabular cup subjected to cyclic loading by the interactive effects of delamination behavior during the bone remodeling process. The mechanostat model for bone remodeling was introduced for a three-dimensional finite element simulation of loosening behavior based on a user subroutine. Delamination at the interface decreases the load transmission between the acetabular cup and the surrounding bone under cyclic loading, which may exaggerate the reduction in BMDs at the delamination area, such as in the case of stress shielding. The growth of reduced BMDs areas in the surrounding bone corresponding to the propagation of delamination was comprehensively analyzed. The interactive effects of delamination and bone remodeling on exaggerating the loosening behavior of the acetabular cup under various loading and fixation conditions were systematically analyzed.

Keywords : Aceptic loosening. Hydroxyapatite coating ; Fatigue ; Wear ; Interface fracture mechanics

574. Biomimetic 3D printed polymer-ceramic composite scaffold for vascularized bone defect repair

Yuyao Liu^{1, 2}, Marko Dobricic^{3, 4}, Claudio Intini^{3, 4, 5}, Fergal J. O'brien^{3, 4}, Javier Llorca^{1, 2}, Mónica Echeverry-Rendón¹

1 : Institute IMDEA Materials [Madrid], **2** : Universidad Politécnica de Madrid, **3** : Royal College of Surgeons in Ireland, **4** : Advanced Materials and Bioengineering Research (AMBER) Centre, **5** : University of Cagliari

Complicated environments involving osteogenesis, mineralization and angiogenesis in large bone defect repair lead to the urgent need for advanced tissue-engineered scaffolds with optimal mechanical properties, controlled degradation rates, and the ability to promote efficient tissue regeneration, while maintain dynamic compatibility under the native motive environment. To address this challenge, a novel biomimetic polymer-ceramic composite scaffold was designed and fabricated through a multi-step process. A rigid, 3D-printed porous framework was first manufactured from a biodegradable poly(ϵ -caprolactone)–poly(ethylene glycol)20k–poly(ϵ -caprolactone) (PCE20kC) triblock polymer through a pellet-based 3D printer equipped with a screw-assisted extrusion system. Then a porous bioactive matrix composed of key bone components—type I collagen and nanohydroxyapatite (CI-nHA)—was incorporated to obtain biomimetic hierarchical porosity. The composite scaffold showed a compressive modulus of 37.0 MPa comparable to native cancellous bone. Additionally, it effectively sustained mineralization and osteogenesis of mouse preosteoblast cells (MC3T3) up to 28 days, and promoted tube formation and angiogenesis of human endothelial cells (EA.hy 926) after 5 days. Notably, a novel bioreactor with a dynamic compression system was employed to simulate physiological mechanical condition in vitro, where enhanced early mineralization was found in cell-seeded composite scaffold after 7 days of intermittent mechanical stimulation. Overall, this work proposes a biomimetic composite scaffold with desirable mechanical properties, degradation rate, osteogenesis, angiogenesis and dynamic compatibility under stimulated motive environment, which showed great potential to be used as an off-the-shelf candidate for vascularized bone defect repair.

Keywords : 3D printing ; Composite scaffold ; Osteogenesis ; Angiogenesis ; Bioreactor

575. Internal Friction and Hydrogen Embrittlement of Steel

Sanjay Manda, Ajay S Panwar, Indradev Samajdar

Department of Metallurgical Engineering and Materials Science, Indian Institute of Technology Bombay

Internal friction in metallic materials reflects mechanical energy dissipation through various microstructural relaxations. This study used tailored microstructures and mechanical spectroscopy (bulk plus local dynamic mechanical analyzer (DMA) measurements) to establish a clear experimental linkage between various microstructural features and corresponding internal friction responses. Since experimental microstructures have the simultaneous presence of multiple defects, the resultant internal spectra are complex, and their interpretation becomes non-trivial. The decoupling of various contributions was achieved through a multiscale modeling approach combining kinetic Monte Carlo (KMC) and molecular dynamics (MD) simulations. In particular, the role of carbon/nitrogen content, crystallographic orientation, residual stress, and dislocation density was investigated. The simulations provided atomistic insights into defect migration and relaxation mechanisms. Particular focus was given to dislocation relaxation in hydrogen-rich Cottrell atmospheres, leading to the Snoek–Köster (SK) peak, which showed strong dependence on hydrogen type and concentration. The study also investigates hydrogen embrittlement in ferrite–martensite dual-phase steel through electrochemical charging, microstructural characterization, and MD-KMC simulations. Especially, a correlation was developed between internal friction and hydrogen embrittlement, demonstrating the potential of internal frictional measurements for hydrogen detection. Moreover, potential future applications of internal friction have been explored.

Keywords : Internal Friction ; Hydrogen ; Mechanical Spectroscopy ; Microstructure ; Molecular Dynamics ; Kinetic Monte Carlo.

576. Modification by heat treatment of powders for the cold spray process

Francesco Delloro, Mehend Tebib

Mines Paris – PSL, Brno University of Technology, Czech Republic

Numerous metallic alloys are still challenging to be deposited by cold spray, despite the technological advances of the technology in the past decade. The reason for that lies in the properties of the powder materials, rather than intrinsic limitations of the process. This presentation explores the reasons behind the challenges in cold spraying those atomized powders and how powder heat treatment can represent an effective way to overcome these issues. In particular, this will be illustrated through some examples. First, two carbon steel powders used for railway and pipeline applications, respectively, have been heat-treated to obtain thick and dense cold spray deposits. Then, an aluminum alloy powder for aerospace applications has been modified by various heat-treatments and cold sprayed.

577. Unraveling the Dynamics of Eutectic Melting an Insitu Study of CBr₄-C₂Cl₆ Microstructures

R. Kumari Rajendran, S. Bottin-Rousseau, K. Sbagoud, B. Raka, S. Akamatsu

INSP- Institut des NanoSciences de Paris- Sorbonne University, Paris, France

Multiphase melting/solidification processes are essential in novel material elaboration, yet eutectic melting dynamics remain poorly understood. We present an in situ experimental study of directional melting in the CBr₄-C₂Cl₆ eutectic, a transparent alloy that follows physical laws governing metallic eutectics while enabling direct visualization. Building upon previous work on this model system, we examine pre-solidified lamellar microstructures with controlled morphologies through real-time optical observation of the solid-liquid interface. Our research reveals complex melting behavior highly dependent on parameters including melting velocity, imposed lamellar spacing, and alloy concentration. We observe distinct asymmetries between solidification and melting kinetics that challenge current theoretical frameworks, with particular sensitivity noted in compositions away from the eutectic point. These findings address a significant knowledge gap in the materials elaboration literature and offer insights into processing techniques such as zone melting and additive manufacturing where controlled partial melting is essential for microstructural development.

578. Design and development of a novel Mg-Zn-Ca bulk metallic glass for biomedical applications

R. kumari Rajendran, Divyanshu Aggarwal, Cosmin Gruescu, Raj Shabadi

UMET - University of Lille, Villeneuve d'Ascq , France

Being amorphous, bulk metallic glasses (BMGs) exhibit superior properties compared to their crystalline alloy counterparts. Amorphous materials are preferred for their excellent mechanical and degradation behavior. Among the various elemental combinations, MgZnCa has shown the most promising results, as evidenced by the literature. However, the maximum achievable size of the metallic glasses remains a bottleneck. The current work aims to address this challenge and achieve it splendidly with a systematic methodology by developing larger diameter MgZnCa BMGs through vacuum induction casting using a specially designed copper mold. The optimal composition was formalized for glass formation of the Mg 65 Zn 31 Ca 4 system using the CALPHAD technique. As a result, a 6.5 mm diameter glassy alloy was successfully obtained. The XRD and TEM analysis experiments demonstrated a perfect amorphous structure of the developed sample. The anti-corrosion properties of the as-cast glass increased, followed by enhancement in the yield strength and hardness in contrast to the properties of the human bone. Furthermore, the surface wettability analysis showed an adequate surface obtained to promote fibroblast adhesion. In conclusion, the current work represents a notable progress in the fabrication of larger-diameter MgZnCa BMG for biomedical applications, considering that the biggest diameter ever reported in the MgZnCa system was more than a decade ago.

Keywords: Bulk metallic glasses, MgZnCa, casting, microstructure, corrosion

579. Anti-oxidation UHTC coatings obtained by plasma spraying.

Arthur Charrue¹, Marianne Balat-Pichelin², Aurelie Quet¹, Charlotte Gregis³

¹CEA – DAM Le Ripault, F-37260 Monts, France, ²Laboratoire PROcédés, Matériaux et Energie Solaire, PROMES-CNRS UPR 8521, 7 rue du four solaire, 66120 Font-Romeu-Odeillo, France, ³ArianeGroup, 3 Rue de Touban, 33185 Le Haillan, France UMET - University of Lille, Villeneuve d'Ascq, France

The plasma spray process is particularly well suited to produce protective coatings. The coatings are built through the successive layering, in the form of lamellae, of melted particles. Due to the energy available within the plasma jet, it is possible to shape any material with a melting point, including those with the highest melting temperatures. Therefore, the process is well suited to shape ultra-refractory materials (UHTCs, Ultra High Temperature Ceramics). This study focuses on four UHTC-based coatings as ZrB_2 , ZrC , HfB_2 and HfC obtained by plasma spraying under an inert atmosphere. It is conducted in the context of new space applications where carbon/carbon composites need protection against oxidation at temperatures above 2000°C for several minutes. The samples were evaluated at high temperatures and under an oxidizing atmosphere using the MESOX facility (air plasma), located at the focal point of the 6 kW solar furnace in Odeillo, and under an oxidizing plasma jet with Vulcain set-up. Different oxidation mechanisms, ablation phenomena and interactions with the substrate will be discussed based on SEM, XRD, EDS and SXES analyses.

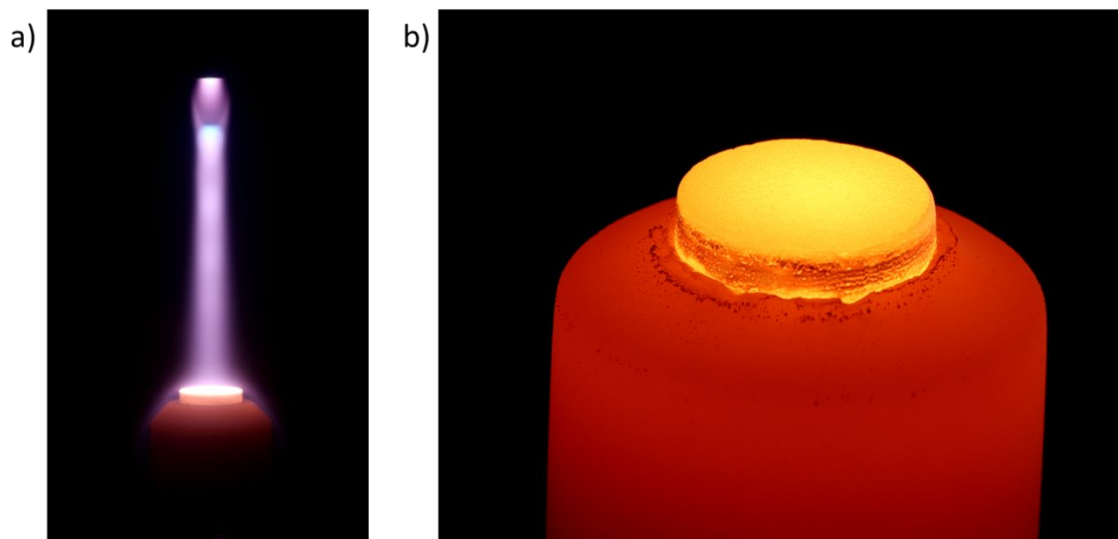


Figure 1 : Pictures of a) ZrC sample during oxidizing test on Vulcain set up and b) 5 seconds after test.

580. Multi-Physics, Multi-Scale Modeling Of A Plasma Jet Facility With Dsmc Technique: Methods For Continuous To Transitional Regimes And Evaluation Results

Lionel Jaouen, Aurelie Quet, Arthur Charrue, Vincent Genissel,
Benjamin Bernard

CEA, DAM, Le Ripault, F-37260 Monts, France

The plasma jet facility at the CEA Le Ripault, named Vulcain, can be used for the analysis of material behavior when exposed to high heat fluxes in order to sort materials for re-entry atmospheric applications, for example. The facility uses a continuous direct current plasma torch, mounted on a 6-axis robot and operating at chamber pressures ranging from a few millibars to atmospheric pressure. This allows for the thermal stressing of materials with heat fluxes reaching up to about 30 MW.m⁻² and supersonic gas velocities (Mach 3 to 5). In addition to the experimental works carried out, numerical simulations are performed to better understand the process and optimize the experimental conditions. The present work is related to the modeling of the Vulcain plasma jet facility, using the DSMC method (Direct Simulation Monte Carlo) with the open-source software SPARTA (Stochastic Parallel Rarefied Time-Analyzer).

581. Instrumented indentation studies on the hydrogenated high- and medium-entropy alloys

Jae-il Jang

Hanyang University, South Korea

Influences of hydrogen on multi-scale mechanical behavior of additively and conventionally manufactured medium- and high-entropy alloy (MEA and HEA) samples were explored through instrumented indentation tests. A series of indentation experiments at both macro- and nano-scale were performed on the samples that were hydrogenated in either electrochemical or gaseous manner. The results are discussed in terms of the hydrogen trapping sites and their roles under different hydrogen-charging conditions.

582. High strength and high elongation of die-casting aluminium alloys

Jiwook Park¹, Miyoung Lee², Sara Song³, Seonghyun Park⁴, Seokjae Lee⁴, Jaehwang Kim^{5,*}

1 : Korea Institute of Industrial Technology, University of Science & Technology

2 : Korea Institute of Industrial Technology, Jeonbuk National University, Korea Institute of Science and Technology

3 : Korea Institute of Industrial Technology

4 : Jeonbuk National University

5 : Korea Institute of Industrial Technology, University of Science & Technology, Korea Institute of Science and Technology

Die-casting process has been widely applied for manufacturing the automobile parts due to its good productivity. In order to increase the number of applied parts, it is necessary to develop a material that exhibits high mechanical properties. Several types of aluminium alloys were designed for obtaining high strength and high elongation die-casting material. Alloys were designed for obtaining high strength without solution heat treatment since the deformation occurs during quenching process. On the other hands, the heat treatable alloys were also designed for obtaining high strength and high elongation die-casted aluminium alloys. Differential scanning calorimetry (DSC) was utilized to investigate the heat treatment range. Heat treatment histories were designed for obtaining strengthening precipitates. Also, effect of cooling method after die-casting such as air-cooling and rapid quenching on mechanical property will be also introduced at the conference.

583. High strength and high elongation of die-casting aluminium alloys

Miyoung Lee², Jiwook Park¹, Sara Song³, Dieter Icheim⁴, David Siedman⁴, Seokjae Lee⁵, Jaehwang Kim^{6,*}

1 : Korea Institute of Industrial Technology, University of Science & Technology

2 : Korea Institute of Industrial Technology, Jeonbuk National University, Korea Institute of Science and Technology

3 : Korea Institute of Industrial Technology

4 : Jeonbuk National University

5 : Korea Institute of Industrial Technology, University of Science & Technology, Korea Institute of Science and Technology

This study investigates the cluster analysis of aluminum alloys using atom probe tomography (APT). Analyses excluding pole regions from the outset minimize distortion caused by Si-segregation. Fixed parameters such as D_{max} and N_{min} derived from random labelling process (RLP) were compared using the maximum separation method (MS) algorithm. There was limitation in detecting cluster in the case of fixed parameter. But, the parameters set by RLP more accurately reflected the atomic distribution inside cluster. The normalization method was applied to clarify whether or not Cu and Sn were included inside clusters. Results showed that Cu is incorporated into clusters, while Sn is excluded. Detail of cluster analysis using APT will be introduced.

584. Functionally graded materials by multi-layer friction stir (MLFS) deposition

Khodabakhshi Farzad¹, Sina Vaghefi¹, Aude Simar²

1: University of Tehran, 2 : Université Catholique de Louvain

An innovative approach was used to create functionally graded nanocomposite materials by employing multi-layer friction stir (MLFS) additive manufacturing (AM) technology. This involved drilling different holes of the same size but with varying designs in the AA7075 alloy consumable rods and pre-placing reinforcing Al₂O₃ nanoparticles. Following this, the MLFS deposition process was conducted, resulting in the production of functionally graded AA7075/Al₂O₃ nanocomposites. In this process, the volume fraction of alumina nanoparticles varied along the building direction (BD) for the consolidated wall. Subsequently, the microstructure and mechanical properties of the created AA7075/Al₂O₃ nanocomposite were examined in different sections of the additively manufactured wall. An increase in the fraction of Al₂O₃ nanoparticles along the BD led to significant microstructural refinement, which in turn resulted in enhanced indentation hardness and tensile strength.

Keywords : *Functionally graded ; Nanocomposite ; MLFS additive manufacturing ; Microstructure.*

585. Microstructure and mechanical properties of Mg and Mg / Nb alloys after severe plastic deformation by accumulative fold-forging

Khodabakhshi Farzad¹, Gerhard Wilde²

1: University of Tehran, 2 : University of Munster

Magnesium and magnesium/niobium foil structures were subjected to severe plastic deformation (SPD) based on the concepts of the accumulative fold-forging (AFF) method for the creation of ultra-fine grained (UFG) and nanostructured (NS) alloys. Afterwards, the microstructural characteristics and mechanical properties of the processed materials were assessed. To this end, microstructural refinement and the formation of sub-grains or nano-scale grains were studied using electron channeling contrast imaging (ECCI) and scanning transmission electron microscopy (STEM) alongside indirect observations based on the peak broadening in X-ray diffraction (XRD) analysis. In addition, metallurgical bonding at the interface of nano-layers, as well as the strain distribution around the dispersed Nb-nanoparticles, were studied using high-resolution STEM and nano-beam diffraction (NBD) mapping. Furthermore, the mechanical properties of the AFF consolidated Mg and Mg/Nb alloys were evaluated across two surfaces and across the thickness cross-section using nanoindentation hardness mapping and miniaturized tensile testing. Also, field emission-scanning electron microscopy (FE-SEM) imaging was accomplished on the surface of tensile failed specimens to reveal the contributing fractography mechanisms for two different AFF-treated Mg and Mg/Nb designs.

Keywords : Severe plastic deformation (SPD) ; Magnesium ; niobium ; Microstructure ; Mechanical property

586. Deformation behavior of a 3D-printed high-entropy alloy

Dhruv Bajaj¹, Aihan Feng^{2,3}, Shoujiang Qu^{2,3}, Dongyang Li⁴, Daolun Chen¹

¹ Department of Mechanical, Industrial and Mechatronics Engineering, Toronto Metropolitan University, Toronto, Ontario M5B 2K3, Canada

² School of Materials Science and Engineering, Tongji University, Shanghai 201804, China

³ Shanghai Key Laboratory of D&A for Metal-Functional Materials, Tongji University, Shanghai 201804, China

⁴ Department of Chemical and Materials Engineering, University of Alberta, Edmonton, Alberta T6G 2H5, Canada

High-entropy alloys and additive manufacturing (or 3D-printing) have been two of the hot areas in the field of materials science and engineering in recent years. The 3D-printed high-entropy alloys have attracted great interest from researchers worldwide due to their multi-faceted deformation mechanisms. The low stacking-fault energy in the 3D-printed CrMnFeCoNi high-entropy Cantor alloy allows the activation of deformation twinning and transformation-induced plasticity, while its face-centred cubic crystal structure permits the activation of multiple slip systems. Although several studies on the sequential and simultaneous activation of deformation mechanisms of the 3D-printed high-entropy alloys are available in the literature, further analysis is required to look into other key aspects such as orientation dependence and cyclic plasticity. Therefore, the monotonic and cyclic deformation behavior of the high-entropy Cantor alloy manufactured via laser beam powder bed fusion was investigated in this study. The microstructural characteristics of the as-printed and deformed Cantor alloy were scrutinized in detail via electron backscatter diffraction (EBSD). Upon monotonic deformation, the grain rotation paths were revealed for the first time for the 3D-printed Cantor alloy, while the effect of lattice orientation on FCC-to-HCP transformation was also investigated. A lattice rotation factor and two new parameters based on the Schmid factor were proposed to predict the grain rotation behavior and FCC-to-HCP transformation. After cyclic deformation, multiple slip bands were observed near surface cracks, indicating the activation of different slip systems in the regions of stress concentration, thus retarding the fatigue-crack growth. Details of this work will be presented at the conference.

Keywords: High-entropy alloys, Cantor alloy, additive manufacturing, EBSD, deformation.

587. Grains ain't misbehaving or going wild? A spontaneous activation of grain boundaries initiating abnormal grain growth!

Klaus-Dieter Liss¹, Pingguang Xu², Ayumi Shiro³, Shuoyuan Zhang⁴, Eitaro Yukutake⁵, Takahisa Shobu², Koichi Akita⁶,

1 : University of Tennessee – Oak Ridge Innovation Institute

2 : Japan Atomic Energy Agency

3 : Synchrotron Radiation Research Center, National Institutes for Quantum Science and Technology

4 : Comprehensive Research Organization for Science and Society

5 : Industrial Technology Innovation Center of Ibaraki Prefecture

6 : Faculty of Science and Engineering, Tokyo City University

Unconventional white-beam Laue synchrotron X-ray diffraction was used on fine-grained, rolled magnesium alloys during in-situ heating experiments. At high temperatures, reflections of single grains are superimposed on the halo stemming from matrix grains. Some unique grain reflections spontaneously move, indicating grain rotations in response to torque expedited at grain boundaries. When a grain boundary spontaneously activates, the grain can begin to reorient, necessitating diffusive mass transport and activating the boundaries of its other neighbors. Now the given grain can freely rotate towards coalescence; however, the multitude of grain boundaries compete in torque orientation and magnitude, resulting in zigzag rotations. After coalescence, the boundaries of the larger grain are still active and continue this scenario of growth, while the majority of the matrix grains remain inactive. The first-time experimental observation of such erratic grain behavior supplies the missing puzzle stone leading to anomalous grain growth, long postulated in literature.

Keywords : Abnormal Grain Growth ; Coalescence ; Diffusion ; Grain Boundary ; Microstructure ; Grain Rotation ; Phase Transformation ; In Situ ; High ; Temperature ; Creep ; Kinetics ; Diffraction ; Synchrotron ; White ; Beam Laue ; Magnesium ; Metals

588. Asymmetric Rolling To Improve Sheet Formability of AM30 Mg Alloy

Vamsi Krishna Pakki, Subodh Kumar, Satyam Suwas

Department of Materials Engineering, Indian Institute of Science, C. V. Raman Road, Bangalore - 560012 - India.

Mg alloys have hcp crystal structure and develop a strong basal texture on rolling, in which basal planes lie parallel to rolling planes, leading to poor formability. Asymmetric rolling (ASR) is a process in which the two rolls rotate at different speeds and the additional shear strain weakens the basal texture, thus increasing the ductility and formability of the alloy. Extrusion (E) before ASR further weakens the basal texture. When ASR is accompanied with cross rolling (CR) and reverse rolling (RR), a process in which the rolled sheet is rotated 90° and 180° respectively around normal direction of the sheet in each pass, it helps in further weakening the basal texture.

In the present investigation, as cast AM30 Mg alloy was hot rolled from 5 mm to 1 mm thickness by three different processing routes. In route 1, the alloy was processed by ASR+RR. In route 2, it was processed by E+CR+ASR. In route 3, it was processed by E+CR+ASR+RR. For ASR, speed ratio of 1:5 was used in all the routes. The alloy was examined in hot rolled as well as hot rolled and annealed conditions. The evolution of microstructure and texture was examined on ND-RD plane of the sheet by OM, SEM, EBSD and XRD pole figures. Tensile properties were evaluated in RD, TD and 45° directions. For annealed sheets, Erichsen cupping test was carried out to examine the formability. It is found that route 3 yields the weakest basal texture and best formability.

Keywords : Thermec'2025 ; Mg alloy ; Asymmetric rolling ; Extrusion ; Microstructure ; Texture ; Tensile properties ; Formability

589. Overlap-Bonding between Aluminium and Copper through Friction Stir Processing

Abdulrahaman Aljabri

1 – Department of Mechanical Engineering, Islamic University of Madinah, Medina 42351 Saudi Arabia

The demand for hybrid welded joints is increasing in industrial sectors due to their advantageous properties, such as improved conductivity and strength-to-weight ratios. Our study examines the effect of friction stir welding (FSW) parameters on the microstructure and mechanical properties of aluminum-copper lap joints. We evaluated various process conditions by using a tool inserted from the copper side, with traveling speeds of 0.83 mm/s and 1.66 mm/s, and rotational speeds ranging from 500 to 1500 rpm.

Results indicated that FSW at rotational speeds above 500 rpm effectively formed a nugget zone with minimal interface flaws, benefiting from improved thermal and mechanical mixing. A traveling speed of 1.66 mm/s produced a defect-free interface, highlighting its suitability for high-stress applications. Conversely, lower traveling speeds and higher rotational speeds resulted in interface defects, potentially compromising weld quality.

Mechanical tests revealed that the combination of a 1.66 mm/s travel speed and 1500 rpm rotational speed yielded the highest tensile shear force. This improvement is due to enhanced mixing and metallurgical bonding at the interface, as observed in the fine-grained microstructure of the nugget zone.

These findings emphasize the critical role of optimizing travel and rotational speeds to enhance the performance of hybrid joints, which are integral to sectors like automotive and aerospace. This research will focus on assessing fatigue properties and long-term performance and exploring additional alloy compositions to expand the applicability of hybrid joints.

Keywords : *Hybrid welded joints ; Friction stir welding (FSW) ; Processing ; Fabrication ; Metallurgical bonding*

<i>Abad Nina</i>	547
<i>Abdelaal Walaa</i>	131
<i>Abdelghany Ahmed</i>	58, 62, 147, 161, 574
<i>Abdeljawad Fadi</i>	330
<i>Abdulrahaman Aljabri</i>	610
<i>Abe Eiji</i>	75, 83, 360, 361, 366
<i>Achiaga Beatriz</i>	540
<i>Adachi Nozomu</i>	564
<i>Adachi Yoshitaka</i>	67, 139, 158
<i>Adam Zielinski</i>	406, 575
<i>Adams Claire</i>	356
<i>Addad Ahmed</i>	29
<i>Afonso Conrado</i>	224
<i>Ahmed Abrar</i>	192
<i>Aida Tetsuo</i>	370
<i>Aihan Feng</i>	607
<i>Ajay S Panwar</i>	596
<i>Akhtar Junaid</i>	142
<i>Akman Adnan</i>	81, 434
<i>Alatarvas Tuomas</i>	131, 174, 176
<i>Albizuri Joseba</i>	290
<i>Ali Mohammed</i>	176, 574
<i>Allam Tarek</i>	131
<i>Allix Mathieu</i>	266
<i>Al-Samman Talal</i>	334, 450
<i>Altinok Sertac</i>	82
<i>Alves Eduardo</i>	117
<i>Amemiya Hitoshi</i>	336
<i>Ameyama Kei</i>	291, 292, 395, 397, 405
<i>Anderson Iver</i>	427
<i>Andrieux Jerome</i>	237, 238
<i>Aoyagi Yoshiteru</i>	484, 562
<i>Apruzzese Gerarda</i>	372
<i>Araidai Masaaki</i>	509
<i>Aramendi Iosu</i>	167
<i>Araya Miguel</i>	105
<i>Ardid Renaud</i>	122
<i>Arkipov Serguei</i>	227
<i>Aron Loic</i>	185
<i>Arrabal Raul</i>	201
<i>Arribas Maribel</i>	424
<i>Arruabarrena Gurutze</i>	290
<i>Arthur Charrue</i>	600, 601
<i>Asaka Toru</i>	500
<i>Asci Atacan</i>	61
<i>Asta Mark</i>	330

<i>Atabay Sila</i>	40
<i>Aude Simar</i>	605, 608
<i>Audurier Valerie</i>	247
<i>Aumayr Christin</i>	61
<i>Aurelie Quet</i>	600, 601
<i>Autio Laura</i>	150
<i>Ayumi Shiro</i>	608
<i>B Jean-Jacques</i>	433
<i>B. Raka</i>	598
<i>B. Straumal</i>	587
<i>Baek Ju-Hyun</i>	314
<i>Baek Michelle</i>	56
<i>Baffie Thierry</i>	237
<i>Bah Micka</i>	414
<i>Bahari-Sambran Farid</i>	35, 87
<i>Bald Ilko</i>	492
<i>Ball James</i>	520
<i>Balog Martin</i>	94, 101
<i>Banait Shruti</i>	92
<i>Bang Seungkook</i>	151, 421
<i>Banks Kevin Mark</i>	154
<i>Baqeri Gholam</i>	137
<i>Barbaro Katia</i>	223
<i>Barkar Thomas</i>	488
<i>Barkia Bassem</i>	36
<i>Barradas Nuno</i>	117
<i>Bartunek Vilem</i>	106
<i>Basu Somanth</i>	351
<i>Baustert Eric</i>	53
<i>Bazarnik Piotr</i>	566
<i>Bechade Jean-Luc</i>	129
<i>Bedekar Vikram</i>	169
<i>Belpane Andrea</i>	372
<i>Benedetti Matteo</i>	409
<i>Benjamin Bernard</i>	601
<i>Benoit Magali</i>	495
<i>BeRard Emilie</i>	378
<i>Bergmann Jean Pierre</i>	534
<i>Berrabah Mohammed</i>	278
<i>Besnard-Pontoreau Clemence</i>	541
<i>Betanda Yanick Ateba</i>	378
<i>Bhattacharjee Debarna</i>	351
<i>Bi Siyao</i>	149
<i>Biermann Horst</i>	477
<i>Bin Jiang C</i>	369, 453,
<i>Biswas Krishanu</i>	322

<i>Bitar-Nehme Elie</i>	51
<i>Bizana Gashaw</i>	345
<i>Blandin Jean-Jacques</i>	432
<i>Blatter Andreas</i>	434
<i>Bochenek Kamil</i>	248
<i>Bodner Sabine Carmen</i>	61
	42, 71, 222, 391, 392, 469,
<i>Boehme Andrea</i>	492, 499
<i>Boenisch Matthias</i>	81
<i>Bonafos Caroline</i>	495
<i>Boncagni Luca</i>	372
<i>Borvik Tore</i>	208
<i>Boukalova Anna</i>	404
<i>Boukhili Rachid</i>	51
<i>Bouobda Moladje Gabriel Frank</i>	399
<i>Bouquerel Jeremie</i>	53
<i>Bourahima Fazati</i>	122, 232
<i>Boutahari Said</i>	80
<i>Bouzina Adnane</i>	501
<i>Brabazon Dermot</i>	54, 69, 79, 112
<i>Brajer Jan</i>	103
<i>Brisset Francois</i>	122, 232
<i>Brown Donald</i>	522
<i>Browne David</i>	418
<i>Bruns Sebastian</i>	498
<i>BuHler-Paschen Silke</i>	258
<i>Busabok Chumphol</i>	259
<i>Butcher Daniel</i>	288
<i>Butler Christopher</i>	549
<i>Buzolin Ricardo</i>	489
<i>Cabioch Thierry</i>	278
<i>Cabrera Jose Maria</i>	157
<i>Calin Mariana</i>	81, 439, 444
<i>Cantergiani Elisa</i>	185
<i>Cao Yu</i>	116, 453, 551
<i>Cao Yue</i>	116, 551
<i>Capek Jaroslav</i>	103, 104, 106
<i>Caprio Leonardo</i>	36
<i>Cardey Pierre Francois</i>	168
<i>Carpenter John</i>	356
<i>Carpio Marcel</i>	157
<i>CarrenO Fernando</i>	35, 87
<i>Casanove Marie-Jose</i>	495
<i>Castany Philippe</i>	63
<i>Castillo-Hernandez Jorge A.</i>	242
<i>Cavojsky Miroslav</i>	368

<i>Cayetano-Castro Nicolas</i>	333
<i>Cayron Cyril</i>	185
<i>Celikin Mert</i>	89, 112, 418
<i>Cepeda-JimeNez Carmen M.</i>	35
<i>Cha Dojin</i>	151, 421
<i>Chae Eun Yun</i>	577
<i>Chaffron Laurent</i>	237
<i>Chahbouni Mouhssine</i>	80
<i>Chambrial CleMent</i>	251
<i>Chan Chang Yin-Cheng</i>	211, 535
<i>Chantrenne Patrice</i>	480
<i>Charlotte Gregis</i>	600
<i>Charteau MeLanie</i>	247
<i>Chartier Patrick</i>	278
<i>Chatterjee Kaushik</i>	461
<i>Chauhan Ankur</i>	304
<i>Chauhan Rijul</i>	549
<i>Chen Cheng-Lung</i>	257, 258
<i>Chen Fan</i>	491
<i>Chen Han</i>	83, 366
<i>Chen Jia-Jun</i>	315
<i>Chen Lai</i>	203
<i>Chen Po-Yu</i>	323
<i>Chen Ta-Te</i>	473, 474
<i>Chen Wei-Ying</i>	427
<i>Chen Xiaming</i>	581, 582
<i>Chen Yan-Ming</i>	168
<i>Chen Zhe</i>	29, 275, 303
<i>Chen Zhenghao</i>	275, 303
<i>Cheon Seho</i>	447, 448, 550
<i>Chevalier Jerome</i>	111
<i>Chiu Po-Han</i>	315
<i>Chiu Po-Kai</i>	283
<i>Chiu Wang-Ting</i>	531
<i>Cho Ken</i>	38, 66
<i>Cho Sunghun</i>	513
<i>Cho Yonghyun</i>	513
<i>Choi Doojin</i>	569
<i>Choi Hyunjoo</i>	65
<i>Choi Junghyun</i>	588
<i>Choi Pyuck-Pa</i>	319, 400
<i>Choi Shi-Hoon</i>	267
<i>Choi Yi-Jeong</i>	229
<i>Chou Shang-Wei</i>	257
<i>Chu Yu-Ren</i>	457
<i>Chua Daniel</i>	500

<i>Chung Hyun</i>	65
<i>Church N. L.</i>	306, 557
<i>Church Nicole</i>	321
<i>Ciftci Jakub</i>	226
<i>Claudio Intini</i>	595
<i>Claudio Verona</i>	222
<i>Coan Karine</i>	223
<i>Cofre Gonzalo</i>	269
<i>Contreras-Almengor Oscar</i>	99
<i>Cookson Peter</i>	288
<i>Copes Francesco</i>	100
<i>Cosmin Gruescu</i>	599
<i>Couillaud Samuel</i>	541
<i>Courtois Nicolas</i>	111
<i>Crichton Wilson</i>	426
<i>Cuenca-Ariza Mikel</i>	167
<i>Cura Ege</i>	230
<i>Curry John</i>	330
<i>Dadbakhsh Sasan</i>	578
<i>D'Agostino Valentina</i>	372
<i>Dalibor Vojtech</i>	104, 368
<i>Damilola-Sunday John</i>	539
<i>Daolun Chen</i>	607
<i>Darsell Jen</i>	427
<i>Das Prosenjit</i>	246, 485
<i>Dasaradha Ramarao S</i>	261
<i>Datye Amit</i>	436
<i>Daudin Remi</i>	432, 433
<i>David Piot</i>	355
<i>David Siedman</i>	603, 608
<i>Davut Kemal</i>	69
<i>De F. Silveira Antonio Carlos</i>	518
<i>De Kloe Rene</i>	353
<i>Delhote Nicolas</i>	28
<i>Demir Ali Gokhan</i>	36
<i>Denis Pierre</i>	443
<i>Depond Philip</i>	84
<i>Deshmukh Sanika</i>	560
<i>Desrayaud Christophe</i>	354
<i>Dezellus Olivier</i>	237
<i>Dhruv Bajaj</i>	607
<i>Di Giovanni Amedeo</i>	491
<i>Diego Correa</i>	223, 224
<i>Dienwiebel Martin</i>	398
<i>Dieter Icheim</i>	603, 607
<i>Ding Lipeng</i>	184, 186, 187

<i>Djenizian Thierry</i>	251
<i>Dmitry Albov</i>	120
<i>Doehler Torsten</i>	71
<i>Dogu Merve Nur</i>	69, 112
<i>Dong Xianping</i>	347
<i>Dongyang Li</i>	607
<i>Donoghue Jack</i>	133, 160
<i>Dorantes-Rosales Hector J.</i>	242
<i>Dorward Hugh</i>	481
<i>Dos Santos Jorge</i>	534
<i>Dougakiuchi Masashi</i>	512
<i>Dowling Denis</i>	89
<i>Drahokoupil Jan</i>	106
<i>Duchane Laurent</i>	491
<i>Duchon Jan</i>	368
<i>Ducommun Nadege</i>	168
<i>Dumitraschkewitz Phillip</i>	191
<i>Durand Olivier</i>	266
<i>Durst Karsten</i>	498
<i>Dutta Akshit</i>	280, 326
<i>Dvorsky Drahomir</i>	368, 404
<i>Ebel Thomas</i>	91
<i>Ebihara Kaito</i>	50
<i>Eckert Jurgen</i>	431, 434, 443
<i>Eguchi Yuki</i>	568
<i>Egusa Daisuke</i>	75, 83, 366
<i>Eichlseder Marlene</i>	207
<i>Eiichi Wakai</i>	373
<i>Eissa Mamdouh</i>	176
<i>Eitaro Yukutake</i>	608
<i>El Bouzidi Zineb</i>	238
<i>Elkot Mohamed N.</i>	162
<i>Elvira Roberto</i>	424
<i>Enzlberger Ludwig</i>	258
<i>Escauriza Borja</i>	290
<i>Escher Benjamin</i>	443
<i>Esmaeilzadeh Reza</i>	92
<i>Euh Kwangjun</i>	189
<i>Eyerman Eric</i>	559
<i>Fabregue Damien</i>	111
<i>Fakhar Naeimeh</i>	498
<i>Fang Haixing</i>	156, 194
<i>Farhadi Ahmad</i>	89
<i>Favre Julien</i>	354, 355
<i>Fecht Hans-Joerg</i>	443
<i>Fei-Fan Cai</i>	434

<i>Fergal J. O'brien</i>	595
<i>Fernandez Navas Nora</i>	439
<i>Fernandez-Sanchez Sergio</i>	167
<i>Ferraz Franz Miller Branco</i>	489
<i>Ferraz</i>	
<i>Ferreira Armando</i>	117
<i>Ferrer Magin Benedict</i>	529
<i>Fiantok Tomas</i>	120
<i>Field David</i>	356
<i>Figueiredo Roberto</i>	101
<i>Finel Alphonse</i>	399
<i>Finkeldei Sarah</i>	549
<i>Fitrianni Sukma</i>	121
<i>Fivel Marc</i>	433
<i>Flament Camille</i>	237
<i>Flemming Ehlers</i>	184
<i>Florian Lyonnet</i>	478
<i>Foitzik Andreas</i>	222, 227
<i>Fojt Jaroslav</i>	106
<i>Fontanari Vigilio</i>	409
<i>Forget Baptiste</i>	237
<i>FortmuLler Stefan</i>	201
<i>Fortrin Pascal</i>	422
<i>Fosca Marco</i>	223
<i>Foscolos Angeliki Sofia</i>	529
<i>Francesco Delloro</i>	597
<i>Frank Montheillet</i>	355
<i>Friedli Jonathan</i>	185
<i>Friedo Maria Helene</i>	391, 392
<i>Fu Banglong</i>	534
<i>Fu Chu-Chun</i>	129
<i>Fujieda Hideto</i>	547
<i>Fujihara Hiro</i>	564
	291, 292, 395, 397, 405,
<i>Fujiwara Hiroshi</i>	526
<i>Fujiwara Yuji</i>	505
<i>Fukumoto Ken-Ichi</i>	371
<i>Funatomi Fumiya</i>	335, 338
<i>Furushima Tsuyoshi</i>	386
<i>Furuta Shogo</i>	516
<i>Fusheng Pan D</i>	369, 453
<i>G. Cofrev</i>	587
<i>G.A. Lopez</i>	587
<i>Gabelleri Lori</i>	372
<i>Gablin Corinne</i>	529
<i>Gabor Camelia</i>	117
<i>Gaertner Frank</i>	52

<i>Galbusera Francesco</i>	36
<i>Galindo-Nava Enrique</i>	169
<i>Gammer Christoph</i>	443
<i>GamsjaGer Ernst</i>	178
<i>Gao Kang</i>	202
<i>Gao Kunyuan</i>	183
<i>Garca Omar</i>	157
<i>Garcia Eduardo</i>	539
<i>Garcia Jose Carlos</i>	424
<i>Gardiola Bruno</i>	237
<i>Gaspar Marcell</i>	174
<i>Gaudio Pasquale</i>	372
<i>Gault Baptiste</i>	314
<i>Gautam Jaiprakash</i>	407
<i>Gauthier-Brunet Veronique</i>	247, 278
<i>Gauzere Laurie</i>	541
<i>Gebert Annett</i>	81, 434, 439, 444
<i>Geissler Ute</i>	392
<i>Genevois CeCile</i>	266
<i>Gerhard Wilde</i>	605, 609
<i>Germain Lionel</i>	376
<i>Gervasyev Alexey</i>	407
<i>Gey Nathalie</i>	376
<i>Gharzouni Ameni</i>	124
<i>Ghassemali Ehsan</i>	176
<i>Gholipour Javad</i>	40
<i>Ghosh Sumit</i>	161, 164, 573
<i>Gibmeier Jens</i>	518
<i>Gigmes Didier</i>	251
<i>Girish S.</i>	351
<i>Gloriant Thierry</i>	63, 68
<i>Goddard Caroline</i>	288
<i>Gollapudi Srikant</i>	199, 403
<i>Goo Kang Wei</i>	531
<i>Gorny Marcin</i>	352
<i>Gorsse StePhane</i>	299
<i>Goto Tomoyo</i>	513
<i>Gottschalk Josefina</i>	227
<i>Govercin Betul</i>	112
<i>Grabowski Blazej</i>	319
<i>Gramlich Alexander</i>	166
<i>Grandini Carlos</i>	223, 224
<i>Grandini Carlos Roberto</i>	223
<i>Greer A. Lindsay</i>	443
<i>Grosjean Christophe</i>	53
<i>Gruber Martin</i>	179

<i>Gu Hengfeng</i>	69
<i>Guangjie Huang</i>	181, 193
<i>Guillaume Kermouche</i>	355
<i>GuilleN Teodolito</i>	105
<i>Gulbay Oguz</i>	166
<i>GuLletutan Umut Can</i>	82
<i>GuMruKcu Selin</i>	434
<i>GuNaydiN Ahmet Can</i>	82
<i>GuNther Fabian</i>	81
<i>Guo Wenheng</i>	50
<i>Gurao Nilesch Prakash</i>	322
<i>Guraya Maria Teresa</i>	290
<i>Guss Gabe</i>	84
<i>Gutierrez-Urrutia Ivan</i>	155, 402
<i>Guyon Julien</i>	376
<i>Ha Jeonghong</i>	30, 31, 44
<i>Habraken Anne</i>	491
<i>Hackenberg Robert</i>	356
<i>Hagihara Koji</i>	45, 180
<i>Hagiwara Tsubasa</i>	512
<i>Haifeng Wang</i>	116
<i>Haiko Oskari</i>	152
<i>Haitao Zhang</i>	198
<i>Hamada Atef</i>	58, 62, 131, 573, 574
<i>Han Dong-Keun</i>	528
<i>Han Heeju</i>	420
<i>Han Jeongho</i>	153, 301, 316, 400, 423
<i>Han Jieun</i>	228
<i>Han Jung Hun</i>	314
<i>Hanna Purzynskav</i>	532
<i>Hantusch Martin</i>	434
<i>Happo Naohisa</i>	523
<i>Hara Toru</i>	349
<i>Harada Hiroshi</i>	268
<i>Hasegawa Masashi</i>	425, 426
<i>Hasegawa Osamu</i>	533
<i>Hatano Masaharu</i>	389, 576
<i>Hauschultz Mike Thomas</i>	391, 392
<i>Hawk Cheryl</i>	356
<i>Hay Jenny</i>	436
<i>Hayashi Koichi</i>	523
<i>Hayashi Yoshikazu</i>	241
<i>He Lei</i>	291, 292
<i>He Qian</i>	311
<i>Hebrard Pierre</i>	36
<i>Hee Yeon Jeon</i>	279

<i>Heilmaier Martin</i>	304, 305
<i>Heintz Jean-Marc</i>	536, 541
<i>Heinz Mayrhofer Paul</i>	258
<i>Helbert Anne-Laure</i>	378
<i>Heller Ludek</i>	368
<i>Helstroffer AureLien</i>	354
<i>Hempel Ute</i>	439
<i>Henninger Susanne</i>	476
<i>Heo Seongjun</i>	420
<i>Hernandez-Demesa Yuri S.</i>	242
<i>Herwan Jonny</i>	262
<i>Hickel Tilmann</i>	480, 482
<i>Hidai Hirofumi</i>	538
<i>Higashino Shota</i>	37
<i>Hijiya Hiroyuki</i>	521
<i>Hirano Mitsuhiro</i>	216, 494
<i>Hirasawa Koichi</i>	336
<i>Hirata Hiroyuki</i>	416
<i>Hiromi Nagaumi</i>	582
<i>Hisamori Hayao</i>	570
<i>Hishinuma Yoshimitsu</i>	370
<i>Hoebenreich Philipp</i>	61
<i>Hoffmann Frank</i>	147, 161
<i>Hohmann Brian</i>	375
<i>Holmedal Bjorn</i>	204
<i>Honda Ryota</i>	291, 292
<i>Hong Jae Keun</i>	556
<i>Honma Yuki</i>	386
<i>Hopperstad Odd Sture</i>	204, 208
<i>Hori Masaru</i>	506
<i>Horiuchi Jumpei</i>	508
<i>Hort Norbert</i>	462, 463
<i>Hoshino Tomohisa</i>	331
<i>Hosoda Hideki</i>	528, 531
<i>Hosova Klara</i>	104
<i>Hou Sen-You</i>	323
<i>Hsiao Chien-Nan</i>	283
<i>Hsieh P.C.</i>	132
<i>Hu Si-Yuan</i>	455
<i>Hu Yeyuan</i>	465
<i>Hu Zengrong</i>	572
<i>Hua Ke</i>	116, 551
<i>Huang Hao-Chuan</i>	455
<i>Huang Hui</i>	183
<i>Huang Shih-Yen</i>	457
<i>Hussein Abdelrahman</i>	156

<i>Hutchinson Christopher</i>	133, 160
<i>Hutsch Thomas</i>	248
<i>Huuki Juha</i>	394
<i>Hybasek Vojtech</i>	94
<i>Iabbaden Djafar</i>	554
<i>I-An Chen</i>	455
<i>Ichikawa Satoshi</i>	41
<i>Ichikawa Takayuki</i>	254
<i>Ii Seiichiro</i>	340, 349
<i>Ikada Kizuku</i>	114
<i>Ikeda Ken-Ichi</i>	358, 365
<i>Ikeda Yuji</i>	319
<i>Ikeno Susumu</i>	192, 370
<i>Ikuo Shohji</i>	384
<i>Ilmola Joonas</i>	475
<i>Im Youngroc</i>	171
<i>Ina Toshiaki</i>	521
<i>Inacio Da Rosa Gregory</i>	354
<i>Inamura Tomonari</i>	359, 360
<i>Indradev Samajdar</i>	596
<i>Inoue Daiki</i>	187
<i>Inoue Schin-Ichi</i>	368
<i>Inoue Shinichi</i>	221
<i>Inui Haruyuki</i>	273, 275, 303
<i>Irokawa Yoshihiro</i>	341
<i>Ishikawa Kenji</i>	506
<i>Ishimoto Takuya</i>	37, 41, 67, 70, 83, 158
<i>Itagaki Naho</i>	121
<i>Ito Taishi</i>	300
<i>Itoh Sho</i>	538
<i>Itoh Takamoto</i>	291, 292
<i>Itoi Takaomi</i>	449
<i>Ivanisenko Julia</i>	211
<i>Iwashita Takuya</i>	435
<i>Iwata Makoto</i>	523
<i>Jablonska Eva</i>	104
<i>Jablosnka Eva</i>	404
<i>Jacobs Hannes</i>	42
<i>Jaehwang Kim</i>	603, 610
<i>Jae-il Jang</i>	602
<i>Jain Amrita</i>	248
<i>Janebova Barbora</i>	104
<i>Jang Tae Jin</i>	314, 319
<i>Janisch Rebecca</i>	471
<i>Janssen Jan</i>	482
<i>JaRvenpaa Antti</i>	58, 62, 105, 131, 574

<i>Jaskari Matias</i>	58, 62, 131, 394, 574
<i>Jason M. Harp</i>	177
<i>Javaheri Vahid</i>	164, 165, 174, 176
<i>Javier Llorca</i>	595
<i>Jazdzewska Natalia</i>	479
<i>Je In Lee</i>	577
<i>Jean-Louis Leclercq</i>	529
<i>Jean-Luc Doudoux</i>	478
<i>Jeon Seung-Min</i>	284
<i>Jeong Dea-Han</i>	189
<i>Jeong Heechan</i>	65
<i>Jeong Hwiyun</i>	318, 325, 525
<i>Jeong Mun Sik</i>	153, 400, 423
<i>Jeppsson Johan</i>	77
<i>Jhabvala Jamasp</i>	92
<i>Ji Gang</i>	29, 53, 239
<i>Ji Vincent</i>	378
<i>Jia Zhihong</i>	186, 187
<i>Jiang Bin</i>	453
<i>Jiang Weiguo</i>	136
<i>Jinno Yusuke</i>	235
<i>Jinsoo Lee</i>	219
<i>Jiwook Park</i>	603, 605
<i>Johanns Kurt</i>	436
<i>Joly Pierre</i>	354
<i>Jones Nicholas</i>	321
<i>Jongmin Byun</i>	279
<i>Jorge-Badiola Denis</i>	167
<i>Jothi Sudagar</i>	261
<i>Joulain Anne</i>	247
<i>Ju Song Hyeon</i>	57
<i>Jung Geunsu</i>	151, 421
<i>Jung Jiwon</i>	57
<i>Jung Sang-Hoon</i>	567
<i>Jung Yup Kim</i>	413
<i>Juvin Manon</i>	238
<i>K Chattopadhyay</i>	55
<i>K. Sbargoud</i>	598
<i>Kaar-Schickinger Simone</i>	179
<i>Kabbouri Ikram</i>	80
<i>Kadota Naoki</i>	445
<i>Kaijalainen Antti</i>	134, 150, 152, 174, 394
<i>Kallabis Conrad</i>	391
<i>Kallien Zina</i>	196
<i>Kamataki Kunihiro</i>	114, 121
<i>Kang Jee-Hyun</i>	135

<i>Kang Minwoo</i>	400
<i>Kang Seung-Kyun</i>	218, 228, 229
<i>Kantanen Pekka</i>	134
<i>Kaplan Bartek</i>	488
<i>Karjalaine Pentti</i>	176
<i>Karjalainen Pentti</i>	131, 165
<i>Kasada Ryuta</i>	547
<i>Kashaev Nikolai</i>	408
<i>Kassaye Firew Tullu</i>	166
<i>Kataoka Keisuke</i>	253, 259
<i>Katayama Kazunari</i>	371
<i>Kato Takanori</i>	381
<i>Kato Takeharu</i>	300
<i>Katsuhiko Sawaizumi</i>	66
<i>Kauffmann Alexander</i>	304, 305
<i>Kaufman Jan</i>	103
<i>Kaur Ramanpreet</i>	495
<i>Kawabata Mie</i>	291, 292, 395, 397, 405
<i>Kawabata Tomoya</i>	389, 576
<i>Kawagishi Kyoko</i>	264, 268
<i>Kawagoe Norino</i>	390
<i>Kawaguchi Kenta</i>	336, 338
<i>Kawaguchi Kurumi</i>	398, 412
<i>Kawakami Ryota</i>	216
<i>Kawamura Hirofumi</i>	538
<i>Kawamura Yoshihito</i>	221, 368, 458
<i>Kawasaki Akira</i>	300
<i>Kawasaki Megumi</i>	419, 565
<i>Kawashima Naoki</i>	300
<i>Ke Hua</i>	116
<i>Keaveney Shane</i>	89
<i>Keckes Jozef</i>	61
<i>Keishi Iizuka</i>	524
<i>Kermouche Guillaume</i>	354
<i>Kestens Leo A.I.</i>	407
<i>Khedr Mahmoud</i>	573
<i>Khodabakshi Farzad</i>	605, 606
<i>Killmore Chris</i>	137
<i>Kim Chaerin</i>	34
<i>Kim Du-Hyun</i>	267
<i>Kim Hyomin</i>	420
<i>Kim Jae Yeon</i>	451
<i>Kim Kyung Il</i>	32, 44
<i>Kim Se-Ho</i>	314
<i>Kim Sungil</i>	171
<i>Kim Won-Kyeong</i>	189

<i>Kim Yong</i>	39, 586
<i>Kim Yong Seong</i>	39
<i>Kim Young-Kyun</i>	284
<i>Kim Young-Min</i>	451
<i>Kimura Ken</i>	380
<i>Kishida Kyosuke</i>	273, 275, 303
<i>Kishimoto Takuma</i>	386
<i>Klassen Thomas</i>	52
	196, 211, 408, 476, 534,
<i>Klusemann Benjamin</i>	535, 580
<i>Ko Won-Seok</i>	314
<i>Kobayashi Masakazu</i>	516, 562
<i>Kobayashi Ryo</i>	329
<i>Kobayashi Shunsuke</i>	331
	331, 335, 336, 337, 338,
<i>Kobayashi Tatsuya</i>	339, 387
<i>Kobori Daiju</i>	342
	164, 165, 170, 174, 175,
<i>Koemi Jukka</i>	176
<i>Koermann Fritz</i>	319
<i>Koga Kazunori</i>	121
<i>Koga Norimitsu</i>	388
<i>Kohara Shinji</i>	519, 521
<i>Kohnert Caitlin</i>	548
<i>Koichi Akita</i>	608
<i>Koide Yasuo</i>	341
<i>Koizumi Yuichiro</i>	48, 67, 72, 76, 158
<i>Koki Bando</i>	524
<i>Komatsu Masayuki</i>	390
<i>Kondo Yoshifumi</i>	513
<i>Kooi Bart J.</i>	173
<i>Korbinian Högerv</i>	143
<i>Korla Rajesh</i>	407
<i>Kosmidou Maria</i>	549
<i>Kostenov Jovan</i>	51
<i>Kostryzhev Andrii</i>	137
<i>Kou Hongchao</i>	276, 553, 555
<i>Kovacs Judit</i>	174
<i>Kozaki Atsushi</i>	561
<i>Krawec Phillip</i>	539
<i>Kremmer Thomas</i>	191
<i>Krenz-Baath Rene</i>	42, 391, 392, 492, 499
<i>Kreyca Johannes</i>	178
<i>Krizik Peter</i>	94
<i>Krumnow Erik</i>	227
<i>Krupp Ulrich</i>	166

<i>Krzik Peter</i>	101
	94, 101, 103, 104, 106, 368, 404
<i>Kubasek Jiri</i>	528
<i>Kubo Kyoko</i>	366
<i>Kubota Kakeru</i>	456
<i>Kumar Dipanjan</i>	456
<i>Kumar Hemant</i>	142
<i>Kumar Saurabh</i>	440
<i>Kunca Branislav</i>	351
<i>Kundu Saurabh</i>	61
<i>Kunnas Peter</i>	291, 292, 397
<i>Kuno Tomoko</i>	121
<i>Kurosaki Yosei</i>	479
<i>Kusiak Jan</i>	61
<i>Kutlesa Kevin</i>	104
<i>Kutova Anna</i>	120
<i>Kvetkova Lenka</i>	512
<i>Kyutoku Sora</i>	379
<i>L. O. Goulart Livia</i>	587
<i>L. Sanchez-Del Rio</i>	122
<i>Lafarge Christophe</i>	566
<i>Langdon Terence G.</i>	94
<i>Lapinova Jana</i>	475
<i>Larkiola Jari</i>	461
<i>Latiyan Sachin</i>	304
<i>Laube Stephan</i>	355
<i>Laurence Latu-Romain</i>	427
<i>Lavender Curt</i>	288
<i>Lavery Nicholas</i>	399
<i>Le Bouar Yann</i>	266, 422
<i>Le Godec Yann</i>	106
<i>Lebeda Miroslav</i>	554
<i>Lecomte Jean-Sebastien</i>	319, 466
<i>Lee Byeong-Joo</i>	314
<i>Lee Chang-Gi</i>	382, 383, 385
<i>Lee Dong-Geun</i>	417
<i>Lee Dongju</i>	420
<i>Lee Eunjin</i>	267
<i>Lee Geun Woo</i>	314, 319
<i>Lee Gunjick</i>	419
<i>Lee Isshu</i>	284
<i>Lee Jae-Ho</i>	249, 277, 318, 325, 525, 586
<i>Lee Je In</i>	550
<i>Lee Jong Un</i>	309, 323
<i>Lee Jyh-Wei</i>	

<i>Lee Seong Ho</i>	447, 448, 550
<i>Lee Seung-Cheol</i>	267
<i>Lee Seungmin</i>	44, 78
<i>Lee Seungwon</i>	192, 370
<i>Lee Sungho</i>	212, 213
<i>Lee Sunghun</i>	119
<i>Lee Taekyung</i>	447, 448, 454, 550
<i>Lee Unhae</i>	420
<i>Lee Yoona</i>	588
<i>Lee Young-In</i>	279
<i>Lee Yuehlien</i>	457
<i>Leguen Emilie</i>	36
<i>Lei Xiao-Wen</i>	377
<i>Lenthe William</i>	353
<i>Leonard Didier</i>	529
<i>Letofsky-Papst Ilse</i>	201
<i>Lewandowska Malgorzata</i>	566
<i>Lhuissier Pierre</i>	194
<i>Li Bolong</i>	183
<i>Li Chang-Jiu</i>	231
<i>Li Hang</i>	116
<i>Li Junpeng</i>	136
<i>Li Meng</i>	108, 109
<i>Li Qing</i>	521
<i>Li Xiang-Min</i>	109
<i>Li Xiao</i>	427
<i>Li Ya</i>	209, 239
<i>Liang Kai-Yu</i>	455
<i>Liang Shangshang</i>	183
<i>Liang Zeqin</i>	185
<i>Lietzau Kai-Henning</i>	227
<i>Lim Chan</i>	466
<i>Lim Jinsurang</i>	318, 325
<i>Limberg Wolfgang</i>	91
<i>Lin Wei Ming</i>	500
<i>Lingfei Cao</i>	193
<i>Lionel Jaouen</i>	601
<i>Lison-Pick Michael</i>	274
<i>Liss Klaus-Dieter</i>	419, 565, 608
<i>Liu Liyuan</i>	294
<i>Liu P. H.</i>	132
<i>Liu Yuheng</i>	48, 72, 76
<i>Llorca Javier</i>	99
<i>Loge Roland</i>	84, 92, 185
<i>Lopes Claudia</i>	117
<i>Lopez Gabriel A.</i>	269

<i>Lopez-Hirata Victor M.</i>	242, 333
<i>Lou Bih-Show</i>	309, 323
<i>LoubeRe Emmanuel</i>	244
<i>Louis Hennocque</i>	355
<i>Lu Guang-Hong</i>	374
<i>Lu Song</i>	470
<i>Lu Yongfeng</i>	244
<i>Ludwig Wolfgang</i>	156
<i>Luo Xiao-Tao</i>	231
<i>Luthuli Nonkululeko Tracy</i>	154
<i>Lyon Ashton</i>	233
<i>M. C. Poletti</i>	587
<i>M. Lasmar Ronaldo</i>	379
<i>M. Saugov</i>	587
<i>Ma Siming</i>	29
<i>Ma Tianze</i>	148
<i>Ma Younghwa</i>	421
<i>Ma Youngwha</i>	151
<i>Macedo Francisco</i>	117
<i>Maeda Satoru</i>	459
<i>Maeda Taiyo</i>	264
<i>Maeda Takuya</i>	145
<i>Maeda Yuto</i>	568, 570
<i>Mahmood Yasir</i>	330
<i>Maier Petra</i>	462
<i>Maitre Alexandre</i>	28, 266
<i>Makasheva Kremena</i>	495
<i>Makineni Sureandra Kumar</i>	456
<i>Makoto Kosaka</i>	141
<i>Malik Amer</i>	77
<i>Maloy Stuart</i>	427
<i>Manik Tomas</i>	204, 210
<i>Mantovani Diego</i>	100
<i>Marcin Jozef</i>	440
<i>Marianne Balat-Pichelin</i>	600
<i>Marioara Calin D.</i>	208
<i>Markmann JuRgen</i>	211
<i>Marko Dobricic</i>	595
<i>Markovsky Pavlo</i>	559
<i>Markstroem Andreas</i>	77
<i>Marosz Jan</i>	352
<i>Marques De Castro Moara</i>	94, 101
<i>Marthinsen Knut</i>	204, 210
<i>Martin Arndt</i>	143
<i>Martin Etienne</i>	51, 90
<i>Martin Gruber</i>	143

<i>Martinez Diana</i>	221
<i>Martinez-de Guereanu Ane</i>	167
<i>Martinez-Perez Armando I.</i>	242
<i>Marzouq Nada</i>	501
<i>Massey Caleb</i>	427
<i>Masumura Takuro</i>	128, 130, 146, 148
<i>Matsuda Kenji</i>	182, 192, 370
<i>Matsugaki Aira</i>	46, 225, 320
<i>Matsumoto Kazuho</i>	509
<i>Matsumura Ryutaro</i>	359, 360
<i>Matsusaka Souta</i>	538
<i>Matthias Wallner</i>	143
<i>Maubane Dannis</i>	102, 154
<i>Mayama Tsuyoshi</i>	70, 180
<i>Meena Anil</i>	73
<i>Mehand Tebib</i>	597
<i>Mehraban Shahin</i>	288
<i>Meindlhumer Michael</i>	61
<i>Mellor R. F. L.</i>	306
<i>Melnyk Chris</i>	559
<i>Merchan Mikel</i>	424
<i>Meyer Ryan</i>	375
<i>Meylan Caroline M</i>	443
<i>Miao Hongyan</i>	90
<i>Michael T. Benson</i>	177
<i>Michal Urzynicok</i>	532, 575
<i>Mikula Marian</i>	120
<i>Min Zhu</i>	159
<i>Minarik Peter</i>	404
<i>Mine Yoji</i>	398, 412
<i>Minh Do Quang</i>	77
<i>Minsu Park V</i>	328
<i>Mitome Riku</i>	386
<i>Mitsuaki Furui</i>	393, 415, 524
<i>Mitsuki Narita</i>	524
<i>Mitsuyuki Jun</i>	571
<i>Miura Hiromi</i>	341, 388, 484, 516, 562
<i>Miura Koyo</i>	494
<i>Miura Seiji</i>	358, 365
<i>Miyamoto Hiroyuki</i>	364, 459
<i>Miyamoto Manami</i>	341
<i>Miyazawa Tomotaka</i>	377
<i>Miyoshi Eisuke</i>	37
<i>Miyoung Lee</i>	603, 604
<i>Mizuno Shinya</i>	508
<i>Mizuta Kazuhiro</i>	263

<i>Moallemi Mohammad</i>	170
<i>Mocellin Katia</i>	478
<i>Mofidi Tabatabaei Hamed</i>	579
<i>Molina-Aldareguia Jon</i>	99
<i>Mollaei Nafiseh</i>	99
<i>Molodov Dmitri</i>	334, 340
<i>Molodov Konstantin</i>	334
<i>Mónica Echeverry-Rendón</i>	595
<i>Monot-Laffez Isabelle</i>	414
<i>Monroy-Sanchez Ixchel</i>	333
<i>Montes De Oca Zapiain David</i>	330
<i>Moon Byungrok</i>	588
<i>Moreno-Martinez Jesus D.</i>	333
<i>Moreno-Rios Marisa</i>	333
<i>Morishige Taiki</i>	445, 446, 561
<i>Morita Koji</i>	358, 365
<i>Morthomas Julien</i>	480
<i>Mostafavi Mahmoud</i>	481
<i>Moutaabbid Hicham</i>	266, 422
<i>Mozumder Yahya H.</i>	86, 160
<i>Mu Honglin</i>	572
<i>Muniyandi Muneeswaran</i>	261
<i>Murakami Hideyuki</i>	327
<i>Murakami Ryuta</i>	449
<i>Muransky Ondrej</i>	522
<i>Muraoka Johtaro</i>	365
<i>Muratori Marta</i>	147, 161
<i>Murillo-Marrodan Alberto</i>	540
<i>Musiol Lukas</i>	433
<i>Muta Hiroaki</i>	547
<i>Nag Samik</i>	351
<i>Nagai Yoshinori</i>	526
<i>Nagaoka Toru</i>	583
<i>Nagase Takeshi</i>	320
<i>Nagashima Ryota</i>	163, 350
<i>Nagata Fukue</i>	213
	197, 198, 202, 203, 572,
<i>Nagaumi Hiromi</i>	581
<i>Nakada Nobuo</i>	141, 163, 350
<i>Nakagawa Tomoaki</i>	571
<i>Nakagawa Tomoki</i>	533
<i>Nakai Masaaki</i>	214
<i>Nakajima Tomoki</i>	214
<i>Nakamori Fumihito</i>	547
<i>Nakamura Keishi</i>	336
<i>Nakamura Shuichi</i>	145

<i>Nakano Takayashi</i>	83
	37, 38, 39, 41, 45, 46, 48, 49, 66, 67, 70, 75, 76, 158, 225, 320
<i>Nakano Takayoshi</i>	
<i>Nakashima Seiji</i>	523
<i>Nakatsuka Osamu</i>	509
<i>Nakayama Kei</i>	300
<i>Nam Dae-Geun</i>	487, 588
<i>Nam Jungsoo</i>	44, 57
<i>Nam Seungjin</i>	65
<i>Narducci Riccardo</i>	250
<i>Narushima Takayuki</i>	214
<i>Natarajan Arunkumar</i>	90
<i>Necas David</i>	404
<i>Nene Saurabh</i>	280, 326, 560
<i>Netshilema Muthoiwa</i>	102
<i>Neugebauer Joerg</i>	319, 480, 482
<i>Ngatiman Muzzammil Bin</i>	500
<i>Nicolas Meyer</i>	355
<i>Nie Zuoren</i>	183
<i>Niewczas Marek</i>	460
<i>Nishihara Tadashi</i>	579
<i>Nishimoto Soya</i>	368
<i>Nishimura Hisashi</i>	533
<i>Nivet Eric</i>	53
<i>Nizolek Thomas</i>	548
<i>Nobufumi Ueshima</i>	271
<i>Noce Simone</i>	372
<i>Noga Piotr</i>	460
<i>Nohira Naoki</i>	528, 531
<i>Nowell Matthew</i>	353
<i>Nyo Tun Tun</i>	58, 150
<i>Oba Yojiro</i>	516
<i>Obata Akiko</i>	212, 213
<i>Obeidi Muhannad Ahmed</i>	79
<i>O'Brien Mary</i>	548
<i>Ochiai Yuto</i>	128
<i>Odani Naohito</i>	331
<i>Offerman Sven Erik</i>	127, 144
<i>Ogawa Takafumi</i>	300
<i>Ogawa Yuhei</i>	155
<i>Ogura Ichiro</i>	262
<i>Oh Byungheon</i>	417
<i>Oh Sang-Ho</i>	319, 466
<i>Ohashi Haruki</i>	484
<i>Ohashi Kyohei</i>	335, 338

<i>Ohba Hiroaki</i>	515
<i>Ohtsu Naofumi</i>	216, 494
<i>Okada Kazuho</i>	402
<i>Okada Shota</i>	537
<i>Okajyo Shinji</i>	311
<i>Okano Hiroshi</i>	128
<i>Okano Satoshi</i>	493
<i>O'Kelly Paraic</i>	310
<i>Okugawa Masayuki</i>	48, 66, 72, 76, 83
<i>Okumura Takamasa</i>	121
<i>Olson Justin</i>	427
<i>Ono Yoshinori</i>	390
<i>Onoue Shuki</i>	405
<i>Oprocha Piotr</i>	479
<i>OrdonO Jesus</i>	99
<i>Orlov Dmytro</i>	462
<i>Orozco Alberto</i>	87
<i>Orozco-Caballero Alberto</i>	35
<i>Osada Toshio</i>	47, 264
<i>Ouyang Fan-Yi</i>	296, 327
<i>Ovri Henry</i>	211
<i>Oyama Marina</i>	336
<i>Ozaki Shingo</i>	264
<i>Ozasa Ryosuke</i>	45, 70, 75, 83
<i>Ozer Seren</i>	69
<i>P Nageena</i>	261
<i>Paavola Jussi</i>	175
<i>Pai Namit</i>	142, 351
<i>Pakki Vamsi Krishna</i>	461
<i>Palomba Silvia</i>	372
<i>Palombi Alessandra</i>	392
<i>Pan Fusheng</i>	453
<i>Panagiotis Argitis</i>	529
<i>Panetta Paul</i>	375
<i>Pang Hon Tong</i>	321
<i>Pankov Vladimir</i>	119
<i>Pantawane Mangesh Vyankat</i>	169
<i>Panwar Ajay</i>	351
<i>Papaefthymiou Spyros</i>	205
<i>Park Chan Hee</i>	556
<i>Park Daegeun</i>	44, 543, 544, 545
<i>Park Hyunjoon</i>	588
<i>Park Ihho</i>	119
<i>Park Jini</i>	293
<i>Park Jiyong</i>	44, 59, 60
<i>Park Jiyu</i>	78

<i>Park Joon Sik</i>	293
<i>Park Nokeun</i>	420
<i>Park So-Yeon</i>	56
<i>Park Sung Hyuk</i>	447, 448
<i>Parnell Steven R.</i>	127
<i>Patel Maulik</i>	296
<i>Paternoster Carlo</i>	100
<i>Pauly Simon</i>	443
<i>Pauzon Camille</i>	432
<i>Pedraza Juan Pablo</i>	157
<i>Pena Miguel</i>	549
<i>Pendurti Srinivas</i>	90
<i>Peng Jiaguan</i>	374
<i>Penin Nicolas</i>	536
<i>Pensis Olivier</i>	491
<i>Perez Inaki</i>	424
<i>Perez Michel</i>	480
<i>Perrot Hubert</i>	501
<i>Petra Hviscova</i>	120
<i>Pickering Ed</i>	86, 133, 160
<i>Pickering Ed J.</i>	86
<i>Pierre Montmitonnet</i>	478
<i>Pietrucci Fabio</i>	426
<i>Pietrzyk Maciej</i>	479
<i>Pilz Stefan</i>	81
<i>Pinc Jan</i>	101, 103, 104, 106
<i>Pingguang Xu</i>	608
<i>Piot David</i>	468
<i>Pizhi Zhao</i>	200
<i>Plancher Emeric</i>	354
<i>Pokka Aki-Petteri</i>	394
<i>Poletti Cecilia</i>	207, 269
<i>Poletti Maria Cecilia</i>	201, 489
<i>Polishetty Ashwin</i>	73
<i>Potorski Pawel</i>	479
<i>Poul Marvin</i>	482
<i>Pouliguen Philippe</i>	536
<i>Povoden-Karadeniz Erwin</i>	201
<i>Pradeilles Nicolas</i>	28, 266, 422
<i>Prado Esther De</i>	368
<i>Prahl Ulrich</i>	367, 467, 477
<i>Pramanik Aparajita</i>	304
<i>Prangnell Phil</i>	86, 133, 160
<i>Prangnell Philip</i>	86, 133
<i>Prangnell Philip B.</i>	86
<i>Preminger Daniel</i>	210

<i>Prosposito Paolo</i>	499
<i>Prum Sovannara FreDeRic</i>	238
<i>Przybylowicz, Owicz Pawel</i>	479
<i>Punera Devesh</i>	199, 403
<i>Purzynska Hanna</i>	406, 575
<i>Pyczak Florian</i>	91, 470
<i>Pyzcak Florian</i>	471
<i>Qi Peng</i>	183
<i>Qin Jian</i>	202
<i>Qin Kunlun</i>	582
<i>R. Kumari Rajendran</i>	598, 599
<i>R. Pavan Kumar</i>	55
<i>Raabe Dierk</i>	162
<i>Rackel Marcus</i>	91
<i>Raj Shabadi</i>	599
<i>Raja Vikram</i>	305
<i>Ramasamy Parthiban</i>	431
<i>Ramos Evander</i>	559
<i>Ramuz Marc</i>	251
<i>Rana Harikrishnasinh</i>	535
<i>Rapaud Olivier</i>	266, 422
<i>Rashid Amir</i>	578
<i>Rath Lars</i>	196
<i>Rau Julietta</i>	223
<i>Raulot Jean-Marc</i>	554
<i>Rautio Timo</i>	58, 105
<i>Ravkov Lucas</i>	522
<i>Razaz Ghadir</i>	190
<i>Razumovskiy Vsevolod</i>	472
<i>Reed O. G.</i>	557
<i>Regnaud William</i>	51
<i>Reiji Hirono</i>	180
<i>Reinhold Schneiderv</i>	143
<i>Rentenberger Christian</i>	443
<i>Resendiz-Hernandez Jose E.</i>	333
<i>Reynaud Pascal</i>	238
<i>Rhodes Mark</i>	427
<i>Richard Caroline</i>	168, 260, 414
<i>Richetta Maria</i>	391, 392
<i>Rizzi Paola</i>	111
<i>Robert Kahlenberg</i>	209
<i>Roch Tomas</i>	120
<i>RodraGuez Perez Nicole</i>	428
<i>Rodrigues Marco</i>	117
<i>Rohim Nur Sahiera Binti Abd</i>	500
<i>Rojas Oscar</i>	266

<i>Rollet Marion</i>	251
<i>Romaine Alexandre</i>	168
<i>Romaner Lorenz</i>	207, 472
<i>Rossignol Sylvie</i>	124
<i>Rostom Aya</i>	232
<i>Ru Hangyeol</i>	57
<i>Ryou Kenhee</i>	319, 400
<i>Ryu Ho Jin</i>	34
<i>Ryu Wookha</i>	442
<i>Ryusei Naganuma</i>	524
<i>S. Akamatsu</i>	598
<i>S. Bottin-Rousseau</i>	598
<i>S. Carvalho Marcelo</i>	379
<i>S. Sommadossiv</i>	587
<i>Safari Sina</i>	481
<i>Saida Kazuyoshi</i>	416
<i>Saida Takahiro</i>	508
<i>Sainio Johannes</i>	174
<i>Saito Shigeki</i>	571
<i>Saito Takuma</i>	66
<i>Sakai Ryuki</i>	335, 338
<i>Sakashita Mitsuo</i>	509
<i>Sakka Yoshio</i>	358, 365
<i>Saksena Aparna</i>	314
<i>Sakurai Makoto</i>	213
<i>Sakurai Seiji</i>	371
<i>Salmasi Armin</i>	488
<i>Salvo Luc</i>	194
<i>Samajdar Indradev</i>	142, 351
<i>Samarov Victor</i>	559
<i>San Jose Jose Tomas</i>	424
<i>Sanchez-Camacho Lizeth Johana</i>	169
<i>Sanchez-Del Rio Laura</i>	269
<i>Saneyuki Abe</i>	524
<i>Sanjay Manda</i>	596
<i>Santofimia Navarro Maria</i>	144
<i>Sara Song</i>	603, 606
<i>Sarac Baran</i>	434
<i>Sarkissian Andranik</i>	100
<i>Sasaki Gen</i>	241, 245
<i>Sasaki Taisuke</i>	66, 83
<i>Sasaki Tomohiro</i>	568, 571
<i>Sasaki Tomoko</i>	253
<i>Sasaki Toshihiko</i>	515
<i>Sato Kazuhisa</i>	41, 48, 67, 76, 158
<i>Sato Kenichi</i>	331

<i>Sato Tsubasa</i>	48
<i>Sato Yushi</i>	121
<i>Sato Yutaka S.</i>	313
<i>Saugo Melisa</i>	269
<i>Savvakin Dmytro</i>	559
<i>Sawada Tomomi</i>	341
<i>Scenini Fabio</i>	86, 133, 160
<i>Scheiber Daniel</i>	472
<i>Schell Norbert</i>	518
<i>Schlegel Volker</i>	42
<i>Schlenger Lucas</i>	84, 92
<i>Schliephake Daniel</i>	304, 305
<i>Schmidtchen Matthias</i>	467, 477
<i>Schneider Reinhold</i>	138, 179
<i>Schreiber Marcel</i>	334
<i>Schroers Jan</i>	434
<i>Schumann Melanie</i>	93
<i>Schwarz Udo</i>	436
<i>Schweiger Lukas</i>	434
<i>Seabra Francisca M.</i>	94, 101
<i>Sei Eiichi</i>	358, 365
<i>Sekhar Halubai</i>	523
<i>Sekine Makoto</i>	506
<i>Sel Ozlem</i>	501
<i>Seleznev Mikhail</i>	477
<i>Sen Sandipan</i>	304, 305
<i>Seo Yeongjun</i>	513
<i>Seokjae Lee</i>	603, 609
<i>Seong-Jae Jeon</i>	413
<i>Sequeira Anil</i>	248
<i>Serrano Joseph</i>	549
<i>Servin Isabelle</i>	529
<i>Seth Malobi</i>	110
<i>Seungik Shin</i>	413
<i>Sha Wei</i>	261
<i>Shabadi Rajashekhara</i>	461
<i>Shahryari Esmaeil Shahryari</i>	489
<i>Shakeri Mohsen</i>	62
<i>Shao Lin</i>	427
<i>Sharifikolouei Elham</i>	431
<i>Sharma Kamal</i>	508
<i>Sheng-Chi Chen</i>	257, 258
<i>Shi Junqin</i>	116
<i>Shi Zhang-Zhi</i>	108, 109, 527
<i>Shibata Akinobu</i>	155, 402
<i>Shibata Haruo</i>	300

<i>Shibayama Shigehisa</i>	509
<i>Shiga Shinya</i>	235
<i>Shigesato Genichi</i>	145
<i>Shim Jae-Hyeok</i>	267
<i>Shimoda Eriko</i>	130
<i>Shin Jongho</i>	151, 421, 487
<i>Shin Jonghoon</i>	487
<i>Shinohara Yuuki</i>	241
<i>Shinohra Yuri</i>	360
<i>Shiratani Masaharu</i>	114, 121
	331, 335, 336, 337, 338,
<i>Shohji Ikuo</i>	339, 387
<i>Shoujiang Qu</i>	607
<i>Shreyasi Vasu</i>	55
<i>Shtefan Viktoriia</i>	439
<i>Shu Qingsong</i>	347
<i>Shuai Zhou B</i>	369, 401
<i>Shuaibo Zhang</i>	181
<i>Shuoyuan Zhang</i>	608
<i>Silvain Jean-Francois</i>	243, 244, 247
<i>Simone Kaar-Schickinger</i>	143
<i>Sina Vaghefi</i>	605, 607
<i>Singh Navjeet</i>	137
<i>Sixt Willi</i>	227
<i>Sket Federico</i>	99
<i>Skolakova Andrea</i>	101, 104, 106
<i>Skolakova Tereza</i>	104
<i>Skowronek Adam</i>	166
<i>Slater Carl</i>	539
<i>Smith Albert</i>	133, 160
<i>Smith Ali</i>	147, 161
<i>Smith Morgan</i>	428
<i>Smola Vojtech</i>	106
<i>Sohn Seok Su</i>	65, 267
<i>Soisson Frederic</i>	129
<i>Soliman Hanaa</i>	574
<i>Somani Mahesh</i>	147, 161
<i>Somekawa Hidetoshi</i>	364, 459
<i>Sommadosi Silvana</i>	269
<i>Sommitsch Christof</i>	138, 179
<i>Song Geon Ho</i>	153, 316
<i>Song Jia</i>	581, 582
<i>Song Renbo</i>	126, 149, 172, 401
<i>Song Sang Yoon</i>	314, 319
<i>Song Taejin</i>	171
<i>Soost Josh</i>	40

<i>Soppera Olivier</i>	529
<i>Sornin Denis</i>	376
<i>Soule Samantha</i>	110
<i>Soulier Mathieu</i>	237
<i>Soultati Anastasia</i>	529
<i>Speck Sandy</i>	42, 222
<i>Sroka Marek</i>	406
<i>Stark Andreas</i>	61, 517
<i>Staron Peter</i>	211, 476
<i>Stauder Bernhard</i>	201
<i>Staufer Ella</i>	552
<i>Steggo Jacob</i>	176
<i>Stein Aaron</i>	436
<i>Steinbacher Matthias</i>	518
<i>Steineder Katharina</i>	138, 179
<i>Stollfuss Carsten</i>	227
<i>Stone H. J.</i>	306
<i>Stone Howard</i>	321
<i>Straumal Boris</i>	269
<i>Street Steven</i>	274
<i>Studecky Tomas</i>	103
<i>Subodh Kumar</i>	609
<i>Sugawara Takamasa</i>	371
<i>Sugisawa Masaki</i>	442
<i>Sugiura Natsuko</i>	380
<i>Suh Jin-Yoo</i>	267, 314
<i>Suhuddin Uceu</i>	196, 211, 534, 535, 580
<i>Suhuddin Uceu Fuad Hasan</i>	211
<i>Suman Ravisankar</i>	199
<i>Suman Ravishankar</i>	403
<i>Sun Binhan</i>	162
<i>Sun Fei</i>	67, 158, 473
<i>Sun Hui</i>	257
<i>Sun Lican</i>	401
<i>Sung Min Young</i>	314
<i>Suwas Satyam</i>	461, 609
<i>Suzuki Hiroaki</i>	300
<i>Suzuki Hirose</i>	339
<i>Suzuki Kohtaku</i>	253
<i>Suzuki Shinsuke</i>	264, 268
<i>Suzuki Tohru</i>	358, 365
<i>Suzuki Tohru S.</i>	365
<i>Svastova Eliska</i>	94
<i>Svec Peter</i>	440
<i>Sven P. Rudin</i>	177
<i>Sven Vogel</i>	177

<i>Swieszkowski Wojciech</i>	221, 226
<i>Tabaru Keisuke</i>	442
<i>Tabata Chihiro</i>	264, 268
<i>Tahan Yves</i>	266, 422
<i>Tahara Masaki</i>	531
<i>Taiki Tsuchiya</i>	192
<i>Taillard Roland</i>	583
<i>Tajiri Hiroo</i>	521, 523
<i>Takacova Martina</i>	94
<i>Takagi Shunya</i>	41
<i>Takahashi Minori</i>	213
<i>Takahashi Nagi</i>	320
<i>Takahisa Shobu</i>	608
<i>Takashima Kazuki</i>	412
<i>Takebe Hiromichi</i>	235
<i>Takeda Keigo</i>	503
<i>Takenaka Hiroto</i>	339
<i>Takenouchi Yushi</i>	128
<i>Takeyama Masao</i>	38
<i>Takimoto Yasuyuki</i>	521
<i>Talbot C. E. P.</i>	557
<i>Tamura Tomoyuki</i>	329
<i>Tanaka Daisuke</i>	320
<i>Tanaka Makoto</i>	300
<i>Tanaka Masaki</i>	311
<i>Tanaka Neiro</i>	320
<i>Tanaka Toshimi</i>	512
<i>Tanaka Tsutomu</i>	561
<i>Tane Masakazu</i>	37, 75
<i>Tangestani Reza</i>	90
<i>Tapar OguN Baris</i>	518
<i>Taro Kato</i>	393, 415, 524
<i>Tarrat Nathalie</i>	495
<i>Tatsuya Kobayashi</i>	384
<i>Taylor Mark</i>	86, 133, 160
<i>Tehranchi Ali</i>	482
<i>Teramoto Takeshi</i>	272
<i>Terao Masayuki</i>	547
<i>Terasawa Ryosuke</i>	253, 259
<i>Ter-Ovanessian Benoit</i>	81, 111
<i>Tervo Henri</i>	174, 175, 176
<i>Thekkepat Krishnamohan</i>	267
<i>Theska Felix</i>	274
<i>Thomas Rhys</i>	133, 160
<i>Thomas Sourisseau</i>	355
<i>Thompson R. P.</i>	306

<i>Thompson Robert</i>	321
<i>Tiwari Kirti</i>	111
<i>Tochigi Eita</i>	576
<i>Todaka Yoshitaka</i>	564
<i>Todorova Mira</i>	482
<i>Tokarski Tomasz</i>	352, 460
<i>Toko Tokunaga</i>	363
<i>Tolnai Domonkos</i>	462
<i>Tomohiro Sasaki</i>	570
<i>Tomstad Asle J.</i>	208
<i>Vamsi Krishna Pakki</i>	609
<i>Veroniki P Vidali</i>	529
<i>Vincent Genissel</i>	601
<i>Yann Chevolot</i>	529
<i>Yi Xie</i>	177
<i>Yuyao Liu</i>	595
<i>Zrodowski Lukasz</i>	226

Conference Secretariat

Catherine Mausion
University of Lille
Lille
Email: secretariat-thermec2025@univ-lille.fr